

---

# Environmental Survey of Potential Sand Resource Sites Offshore Delaware and Maryland

---

Final Report

OCS Study 2000-055

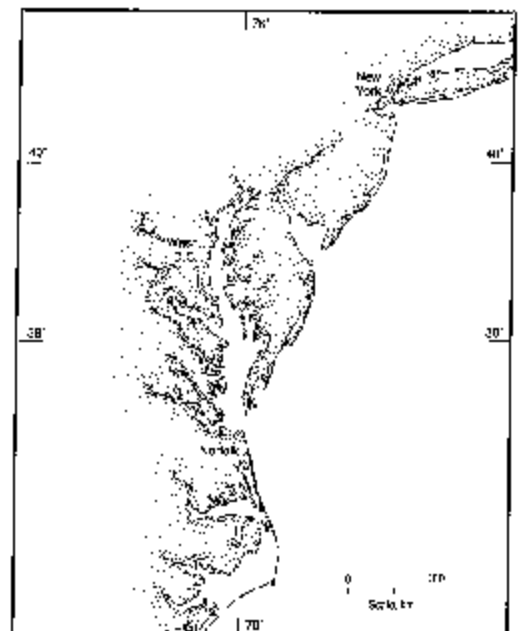
August 2000

Authors:

G. R. Cutter, Jr.  
R. J. Diaz  
John A. Musick  
John Olney, Sr.  
Donna M. Bilkovic  
Jerome P.-Y. Maa  
Sung-Chan Kim  
C. Scott Hardaway, Jr.  
D. A. Milligan  
Rebecca Brindley  
Carl H. Hobbs, III  
Virginia Institute of Marine Science

Project Manager:

Carl H. Hobbs, III  
Virginia Institute of Marine Science



Prepared under MMS contract 1435-01-97-CT-30853 to the  
Virginia Institute of Marine Science  
College of William & Mary

**MMS** U.S. Department of the Interior  
Minerals Management Service

College of William and Mary  
**MMS**  
Virginia Institute of Marine Science  
School of Marine Science

International Activities and Marine Minerals Division

## DISCLAIMER

This report has been reviewed by the Minerals Management Service and approved for publication. Approval does not signify that the contents necessarily reflect the views and policies of the Service, nor does mention of trade names or commercial products constitute endorsement or recommendation for use.

Final Report  
Environmental Survey of Potential Sand Resource Sites

By

G. R. Cutter, Jr.  
R. J. Diaz  
John A. Musick  
John Olney, Sr.  
Donna M. Bilkovic  
Jerome P.-Y. Maa  
Sung-Chan Kim  
C. Scott Hardaway, Jr.  
D. A. Milligan  
Rebecca Brindley  
Carl H. Hobbs, III

Virginia Institute of Marine Science

Carl H. Hobbs, III, Project Manger  
Virginia Institute of Marine Science

for

U. S. Department of the Interior  
Minerals Management Service  
International Activities and Marine Minerals Division

Contract 1435-01-97-CT-30853

OCS Study 2000-055

August 2000

## CONTENTS

Technical Summary

Non-Technical Summary

Part 1: Benthic Habitat Mapping and Resource Evaluation of Potential Sand Mining Sites Offshore Delaware and Maryland

Part 2: Transitory Species (Vertebrate Nekton)

Part 3: Literature Survey of Reproductive Finfish and Ichthyoplankton Present in Proposed Sand Mining Locations

Part 4: Potential Modifications to Waves Due to Dredging and Other Oceanographic Considerations

Part 5: Maryland-Delaware Shoreline: Long Term Trends versus Short Term Variability

---

# Environmental Survey of Potential Sand Resource Sites Offshore Delaware and Maryland

## Technical Summary

---

Final Report

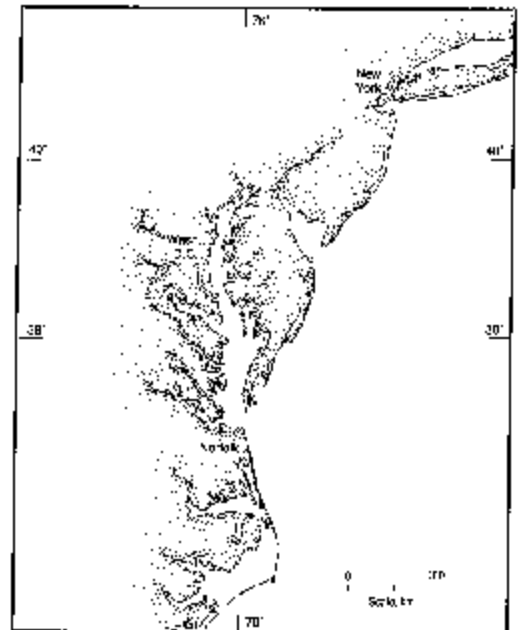
OCS Study 2000-055

August 2000

Project Manager:

Carl H. Hobbs, III  
Virginia Institute of Marine Science

Prepared under MMS contract 1435-01-97-CT-30853 to  
the  
Virginia Institute of Marine Science  
College of William & Mary



**MMS** U.S. Department of the Interior  
Minerals Management Service

International Activities and Marine Minerals Division

College of William and Mary  
**MMS**  
Virginia Institute of Marine Science  
School of Marine Science

## DISCLAIMER

This report has been reviewed by the Minerals Management Service and approved for publication. Approval does not signify that the contents necessarily reflect the views and policies of the Service, nor does mention of trade names or commercial products constitute endorsement or recommendation for use.

Final Report  
Environmental Survey of Potential Sand Resource Sites

Technical Summary

Carl H. Hobbs, III, Project Manger  
Virginia Institute of Marine Science

for

U. S. Department of the Interior  
Minerals Management Service  
International Activities and Marine Minerals Division  
Contract 1435-01-97-CT-30853  
OCS Study 2000-055

August 2000

**STUDY TITLE:** Environmental Survey of Potential Sand Resource Sites Offshore Delaware and Maryland

**REPORT TITLE:** Environmental Survey of Potential Sand Resource Sites Offshore Delaware and Maryland

**CONTRACT NUMBER:** MMS 1435-01-97-CT-30853

**SPONSORING OCS REGION:** International Activities and Marine Minerals Division

**APPLICABLE PLANNING AREA:** N/A

**FISCAL YEARS OF PROJECT FUNDING:** 1997, 1998, 1999, 2000

**COMPLETION DATE OF REPORT:** August 2000

**COSTS:** FY 1997: \$ 4,635, FY 1998: \$ 173,482, FY 1999: \$ 169,239, FY 2000: \$ 36,885  
Cumulative Cost: \$ 384,241

**PROJECT MANAGER:** Carl H. Hobbs, III

**AFFILIATION:** Virginia Institute of Marine Science, College of William & Mary

**ADDRESS:** P. O. Box 1346, Gloucester Point, Virginia, 23062

**PRINCIPAL INVESTIGATORS:** G. R. Cutter, Jr., R. J. Diaz, J. A. Musick, J. Olney, Sr., D. M. Bilkovic, J. P.-Y. Maa, S. C. Kim, C. S. Hardaway, Jr., D. A. Milligan, R. Brindley, and C.H. Hobbs, III

**KEY WORDS:** Maryland, Delaware, continental shelf, sand mining, benthic habitats, fisheries, wave refraction, storm surge, beach nourishment, shoreline, erosion, sand, shoreline.

**BACKGROUND:** The shore between Ocean City Inlet, Maryland and Cape Henlopen, Delaware is a burgeoning recreational area that experiences chronic shoreline erosion and retreat. In order to maintain the economic viability of the region and to limit losses to physical processes various governmental agencies, local, state, and federal, have taken actions to stabilize the shoreline. Paramount among these is beach nourishment. Increasingly the sand used in the nourishment projects is likely to be taken from beneath federal waters. Over the next two decades, the demand for sand from the continental shelf offshore of Maryland and Delaware could be on the order of ten to twenty millions of cubic meters. Consequently the U.S. Department of the Interior, Minerals Management Service initiated the Environmental Survey of Potential Sand Resource Sites Offshore Delaware and Maryland in order to assess potential physical and biological environmental consequences of mining sand.

**OBJECTIVES:** To examine the present conditions of transitory vertebrate nekton including fishes, sea turtles, and marine mammals, of reproductive finfish and ichthyoplankton, benthic fauna and infauna, of physical oceanographic phenomena such as waves, currents, and storm surge, and of shoreline stability; to develop interpretations of how offshore sand mining might affect those conditions; and, where reasonable, to issue recommendations as to how potential adverse consequences of sand mining could be minimized.

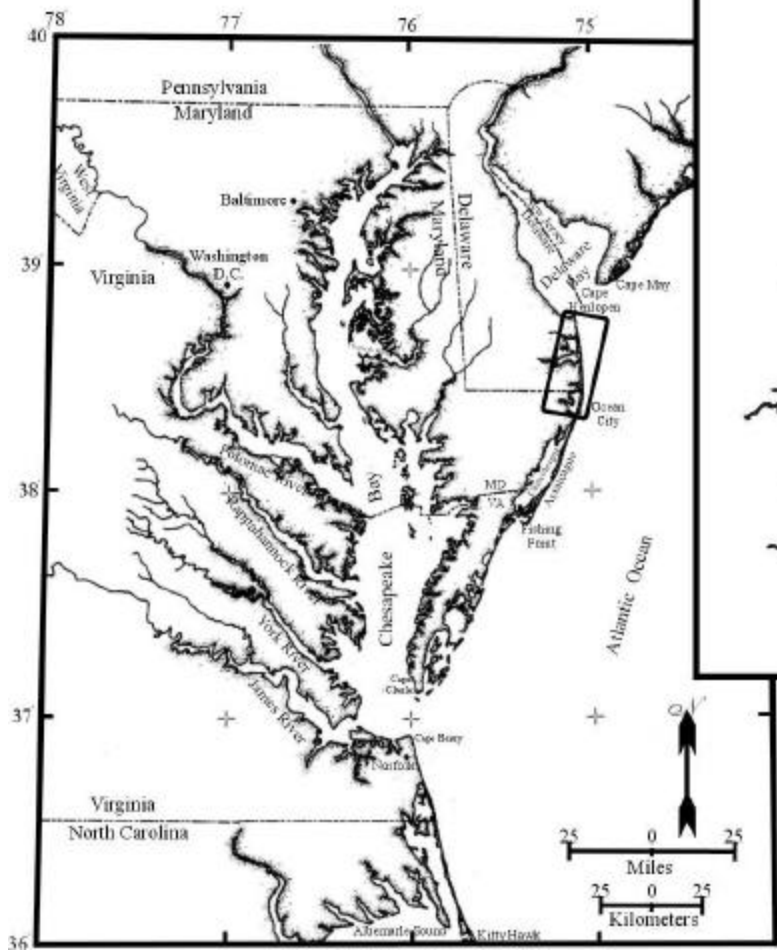
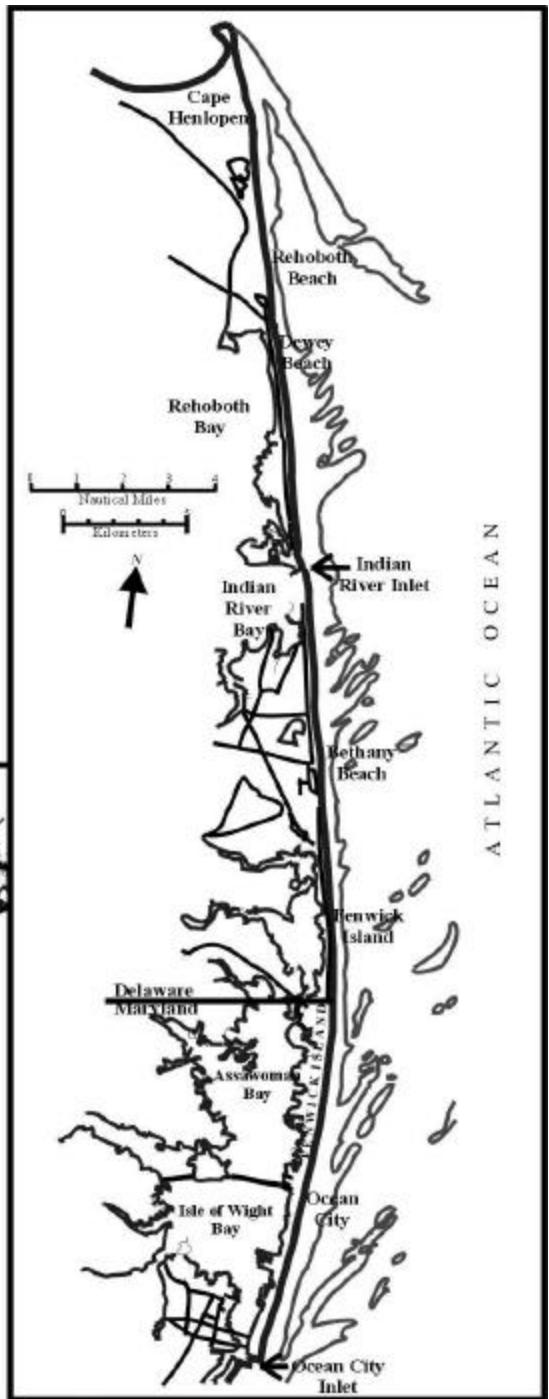
**DESCRIPTION:** The study area includes the inner continental shelf generally out to approximately the 20 m isobath and shore of the region between Cape Henlopen, Delaware and Ocean City Inlet, Maryland. The study was conducted and is presented in five parts: 1) benthic habitat mapping and resource evaluation of potential sand mining areas, 2) a review of transitory species of fishes, sea turtles, and marine mammals

that visit the study area, 3) a review of reproductive finfish and ichthyoplankton that utilize the area, 4) a study of the potential modifications to waves due to dredging and other oceanographic considerations, and 5) an analysis of the long term trends and short term variability of the Maryland-Delaware shoreline. Part 1 required a substantial field effort including two cruises with collection and subsequent analysis of myriad samples and photographic or similar images of the bottom. Parts 2 and 3 primarily were reviews of the appropriate literature. Part 4 involved acquisition and analysis of historical wave and current information, reformatting of existing bathymetric data, and substantial computer modeling and analysis. Part 5 is a synthesis and interpretation of a varied suite of generally unpublished data.

**SIGNIFICANT CONCLUSIONS:** Although there are potentially adverse consequences to sand mining in the offshore regions of Delaware and Maryland, they likely are not substantial and actions can be taken to eliminate or minimize them. Obviously dredging the bottom destroys all the organisms that had lived within the dredged area, but the best sands for beach nourishment have a comparatively low resource value. The benthic fauna of those areas are likely to recolonize fairly rapidly especially if small "islands" are left untouched within the otherwise dredged area. Care should be taken to minimize disturbance of the substrate between the shoals that will be the targets for dredging. The very small size of the areas likely to be dredged relative to the large geographic ranges of transitory fishes indicates that sand mining would have very little impact on the fish populations. The species occurrence of fishes in spawning, egg, and larvae stages is least from October through March and peak in the late spring and summer. The potential threat to sea turtles can be avoided by mining from mid-November to mid-April when these sub-tropical animals are absent from the area. Sand mining poses no foreseeable threat to the migratory and highly mobile marine mammals. Analysis of existing wave conditions demonstrates that modern shoreline stability is related to areas of concentration and dispersion of wave energy near the zone of breaking waves. The relatively stable area around the Maryland-Delaware border is one of relatively low waves whereas the various erosional "hot spots," especially along Fenwick Island, appear coincident with zones of wave energy concentration. Wave transformation modeling indicates that removal of  $10^6$  m<sup>3</sup> of sand from the top of Fenwick and Isle of Wight Shoals will result in very small changes from present conditions. Removal of  $10^7$  m<sup>3</sup> might cause more noticeable changes in the regions between the dredged areas and the shore. Modeling also predicts that dredging will have an extremely small impact on ambient tidal currents and potential storm surges. The Maryland-Delaware shore is experiencing increasing pressure from expanding recreational and residential uses and the associated commercial developments. The form of the shoreline results from interactions amongst the local geology and stratigraphy, the history of Holocene sea-level rise, and the contemporary wave climate. Although rising sea level drives a general marine transgression/shoreline retreat through the area, the rate of retreat and apparent local stability vary along the shore. Shoreline engineering, most noticeably sand bypassing at Indian River Inlet and repetitive beach nourishment at several sites, has been employed to control shoreline retreat and enhance the recreational value and use of the beach. The cumulative impact of the many beach nourishment projects that already have been performed appears to be more beneficial than any individual project.

**STUDY RESULTS:** See Significant Conclusions, above.

**STUDY PRODUCTS:** Virginia Institute of Marine Science, 2000. Environmental Survey of Potential Sand Resource Sites Offshore Delaware and Maryland. Final Report to the U.S. Department of the Interior, Minerals Management Service, International Activities and Marine Minerals Division, Herndon, VA. Contract No. 1435-01-97-CT-30853. Printed Copy and CD.



## The Department of the Interior



As the Nation's principal conservation agency, the Department of the Interior has responsibility for most of our nationally owned public lands and natural resources. This includes fostering sound use of our land and water resources, protecting our fish, wildlife, and biological diversity, preserving the environmental and cultural values of our national parks and historic places; and providing for the enjoyment of life through outdoor recreation. The Department assesses our energy and mineral resources and works to ensure that their development is in the best interests of all our people by encouraging stewardship and citizen participation in their care. The Department also has a major responsibility for American Indian reservation communities and for people who live in island territories under U.S. Administration.

## The Minerals Management Service Mission



As a bureau of the Department of the Interior, the Minerals Management Service's (MMS) primary responsibilities are to manage the mineral resources located on the Nation's Outer Continental Shelf (OCS), collect revenue from the Federal OCS and onshore federal and Indian lands, and distribute those revenues.

Moreover, in working to meet its responsibilities, the Offshore Minerals Management Program administers the OCS competitive leasing program and oversees the safe and environmentally sound exploration and production of our Nation's offshore natural gas, oil and other mineral resources. The MMS Royalty Management Program meets its responsibilities by entrusting the efficient, timely and accurate collection and distribution of revenue from mineral leasing and production due to Indian tribes and allottees, States and the U. S. Treasury

The MMS strives to fulfill its responsibilities through the general guiding principles of: (1) being responsive to the public's concerns and interests by maintaining a dialog with all potentially affected parties and (2) carrying out its programs with an emphasis on working to enhance the quality of life for all Americans by lending MMS assistance and expertise to economic development and environmental protection.

---

# Environmental Survey of Potential Sand Resource Sites Offshore Delaware and Maryland

## Non-Technical Summary

---

Final Report

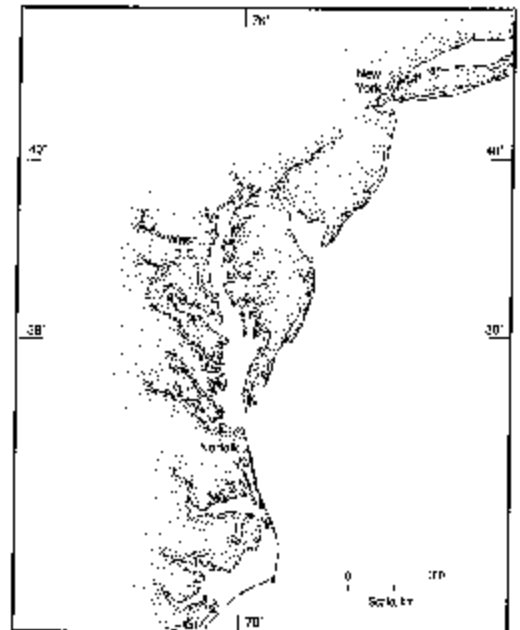
OCS Study 2000-055

August 2000

Project Manager:

Carl H. Hobbs, III  
Virginia Institute of Marine Science

Prepared under MMS contract 1435-01-97-CT-30853 to  
the  
Virginia Institute of Marine Science  
College of William & Mary



**MMS** U.S. Department of the Interior  
Minerals Management Service

College of William and Mary  
**MMS**  
Virginia Institute of Marine Science  
School of Marine Science

International Activities and Marine Minerals Division

## DISCLAIMER

This report has been reviewed by the Minerals Management Service and approved for publication. Approval does not signify that the contents necessarily reflect the views and policies of the Service, nor does mention of trade names or commercial products constitute endorsement or recommendation for use.

Final Report  
Environmental Survey of Potential Sand Resource Sites  
Offshore Delaware and Maryland

Non-Technical Summary

Carl H. Hobbs, III, Project Manger  
Virginia Institute of Marine Science

for

U. S. Department of the Interior  
Minerals Management Service  
International Activities and Marine Minerals Division  
Contract 1435-01-97-CT-30853  
OCS Study 2000-055

August 2000

## **BACKGROUND**

The shore between Ocean City Inlet, Maryland and Cape Henlopen, Delaware is a burgeoning recreational area that experiences chronic shoreline erosion and retreat. In order to maintain the economic viability of the region and to limit losses to physical processes, various governmental agencies, local, state, and federal, have taken actions to stabilize the shoreline. Paramount among these is beach nourishment. Increasingly the sand used in the nourishment projects is likely to be taken from beneath federal waters, *i.e.* from more than 3 nautical miles offshore. Over the next two decades, the demand for sand from the continental shelf offshore of Maryland and Delaware could be on the order of ten to twenty millions of cubic meters. Consequently the U.S. Department of the Interior, Minerals Management Service initiated the Environmental Survey of Potential Sand Resource Sites Offshore Delaware and Maryland in order to assess potential physical and biological environmental consequences of mining sand. Three shoals, Fenwick, Weaver, and Isle of Wight, roughly 5 km offshore are considered likely sights for future sand mining.

## **OBJECTIVES**

To examine the present conditions of transitory vertebrate nekton including fishes, sea turtles, and marine mammals, of reproductive finfish and ichthyoplankton, benthic fauna and infauna, of physical oceanographic phenomena such as waves, currents, and storm surge, and of shoreline stability; to develop interpretations of how offshore sand mining might affect those conditions; and, where reasonable, to issue recommendations as to how potential adverse consequences of sand mining could be minimized.

## **DESCRIPTION**

The study area includes the inner continental shelf generally out to approximately the 20 m isobath and shore of the region between Cape Henlopen, Delaware and Ocean City Inlet, Maryland. The study was conducted and is presented in five parts: 1) benthic habitat mapping and resource evaluation of potential sand mining areas, 2) a review of transitory species of fishes, sea turtles, and

marine mammals that visit the study area, 3) a review of reproductive finfish and ichthyoplankton that utilize the area, 4) a study of the potential modifications to waves due to dredging and other oceanographic considerations, and 5) an analysis of the long term trends and short term variability of the Maryland-Delaware shoreline. Part 1 required a substantial field effort including two cruises with collection and subsequent analysis of myriad samples and photographic or similar images of the bottom. Parts 2 and 3 primarily were reviews of the appropriate literature. Part 4 involved acquisition and analysis of historical wave and current information, reformatting of existing bathymetric data, and substantial computer modeling and analysis. Part 5 is a synthesis and interpretation of a varied suite of generally unpublished data.

**Part 1** presents an assessment of the existing community structures, spatial distributions, substrate dependencies, productivity, and trophic linkages in order to anticipate the consequences of sandmining upon the biological resources of the area. These subjects should be considered with respect to the scales and magnitudes of normal environmental stressors and the potential for interference with these dynamics.

The primary data on which to base this set of studies were obtained during the course of a research cruise in 1998 and a second cruise in 1999. Instruments used on either or both cruises included a standard “Young” grab with a 0.044 m<sup>2</sup> surface area for sediment samples, a Hulcher model Minnie Sediment profile camera (SPI), a standard bottom imaging sled which carried video cameras and water quality sensors, a Burrow-Cutter-Diaz Plowing Sediment Profile Camera System, a 600kHz high resolution side-scan sonar, and a 2.4 m (8 ft) beam trawl to collect juvenile fish, epibenthos, and macrobenthos. In addition to analyses of the samples and images, the data were coded for display in a Geographic Information System (GIS).

Calculated indices reflect that the quality of the benthic habitats is relatively low on the shoals and relatively high in the valleys between the shoals, although the distribution of microhabitats is more complex than suggested by that simple statement. Biological associations with individual microhabitats are functions of substrate (primarily grain size distribution) and energy regime. The characteristics of

specific areas may vary through time in response to physical changes in the shoals. Thus anthropogenic modification of the shoals, as would result from sand mining, would alter the benthic habitats. Also the season(s) in which sand mining took place would affect recolonization as function of the life history stage of the benthic organisms. Recruitment of larvae and juvenile stages of animals likely would be better in spring-summer while recruitment of adults likely would be regulated by factors that affect passive transport, such as storms.

In order to ensure that the biological assemblage that recolonizes a mined area resembles that prior to mining, it would be beneficial to avoid total stripping of the surface. By leaving small “islands,” or refuge patches, within the sand mining area, local resident species would more easily be able to recolonize the near by disturbed sections resulting in a post-mining assemblage that should be generally like the earlier condition.

The alteration and recovery of a benthic biological community from a disturbance such as sand mining likely will be dependent upon waves, currents, and bottom stresses in the period subsequent to mining. Therefore the consequences of sand mining could be substantially different if a long period of calm or a major storm followed the dredging.

**Parts 2 and 3** should be considered together as they address the major biota of the water of the study area. The work must be taken in the context of the relatively very small size of the potential mining area as compared to the inner continental shelf offshore of Maryland and Delaware and as compared to the inner continental shelf of the entire mid-Atlantic region. There are three broad groups of vertebrate animals that are to be expected in the area: fishes, sea turtles, and marine mammals. Because of the substantial seasonal variation in water temperature, most of the fishes and all of the sea turtles and marine mammals migrate with the seasons. Warm-temperature, sub-tropical species are present in the summer and boreal species during the winter.

The area is used by a wide variety of fishes, many of which are valuable to either or both the commercial or recreational fisheries. Sea herring and Atlantic mackerel, among others, are common

during the winter while croaker, drum, sea trout, menhaden, and large coastal sharks are summer residents. The area is an important migration corridor for striped bass and bluefish. But, as noted above, the relatively limited size of potential dredging operations compared to the very large geographic ranges and populations of the fishes suggests that sand mining would have little effect on the fish populations.

The consideration of spatial scale also should hold true for the spawning, egg, and larval fishes within the area. These conditions peak in terms of number of species during the summer months and fall to a low during the winter.

Of the several species of sea turtles which use the mid-Atlantic Bight, the loggerhead and Kemp's ridley are vulnerable to entrapment by hopper dredges. The Kemp's ridley is the most endangered of the sea turtles and is the second most abundant sea turtle in the mid-Atlantic during the summer. As all sea turtles are considered threatened or endangered, the National Marine Fisheries Service (NMFS) takes an active role in the regulation of dredging activities.

The marine mammals that migrate through the area include boreal harbor porpoise, bottlenose dolphin, juvenile humpback whales, and right whales. Although the right whale which is vulnerable to collision with moving ships, all of the marine mammals are highly mobile and migratory and easily can avoid dredges.

**Part 4** both analyzes a set of existing physical oceanographic aspects and models how conditions might change following sand mining. The work addressed changes in waves, storm surge, tidal currents, and bottom stress resulting from dredging on Fenwick and Isle of Wight Shoals. The wave analyses considered two dredging scenarios: mining of approximately  $2 \times 10^6$  m<sup>3</sup> (two million cubic meters) from each shoal and a total removal of  $20 \times 10^6$  m<sup>3</sup> (twenty million cubic meters). The model was run using an unmodified bathymetry to establish base conditions then run again using a post-dredging bathymetric scenario.

For driving conditions and calibration, the study uses wave data from an wave buoy located about 40 km offshore of Ocean City maintained by the National Data Buoy Center and from two nearshore stations maintained by the U.S. Army Corps of Engineers. During 13 years of observations at the offshore station, the maximum significant wave was 7.6 m with a period of 16.7 s which occurred during a January storm, or northeaster, and not during a hurricane. Review of the data resulted in selection of 60 waves from among four wave heights (2, 4, 6, and 8m), five periods (10, 12, 14, 16, and 20s) from seven general directions (NNE, NE, ENE, E, ESE, SE, and SSE). Because short period waves (less than 10s) do not affect the shoals, they were not considered even though they have a relatively high frequency of occurrence. The bathymetry input to the model was taken from NOAA sources.

The REF/DIF-1 wave transformation model was selected over several other models following a comparison of the different model's strengths and weaknesses. The wave model was calibrated by comparing conditions synoptically observed at the offshore and inshore wave stations with calculated or modeled data for the inshore stations using the observed offshore data as input. The variable model parameter estimating bottom friction was adjusted so that the model's output most closely resembled the observed conditions.

In addition to providing base-line information, running the wave transformation model with a unmodified bathymetric input provided an ability to compare the present distribution of wave energy with the condition of the shoreline. In general the relatively stable region of the shoreline around the Maryland-Delaware boundary coincides with an area of diminished wave energy and the more erosive sections near Ocean City appear related to local concentrations of wave energy.

Comparisons of results from model runs with the unmodified bathymetry with runs in which the removal of approximately  $2 \times 10^6 \text{ m}^3$  from each shoal indicates that there would be relatively little change in the wave environment. However a total mining of  $20 \times 10^6 \text{ m}^3$  would result in an increase in wave height in the area between the dredge sites and the shoreline. Evaluation of the impact of this increase on the shore is difficult.

The potential impact of dredging on storm surge was assessed with a standard computer model (SLOSH – Sea, Lake, and Overland Surges from Hurricanes). The model was run with the unmodified bathymetry and the bathymetry after the  $20 \times 10^6 \text{ m}^3$  mining scenario. Using a modeled category 4 hurricane and two storm tracks, one generally shore parallel, the other shore normal, there were negligible, almost non-existent, difference between the pre and post dredging outputs.

The natural tidal currents in the area are fairly small, approximately 20 cm/s at the surface decreasing at the bottom to around 5 cm/s except slightly greater, 5-10 cm/s, over the shoals. Modeling indicates that the cumulative dredging scenario would result in an increase of approximately 10 percent in the bottom currents. As this translates to an overall increase on the order of 1 cm/s, the impact of dredging on bottom currents is considered to be very small.

Finally, yet another computer model was used to assess changes in the combined wave and current generated bottom disturbing forces. Again, the impacts of dredging appear minimal.

**Part 5** reviews the recent geologic history of the coast with emphases on changes in shoreline position and possible influences of works intended to stabilize the shore. The approximately 100 km long coastal region between Ocean City, Maryland and Cape Henlopen, Delaware is the product the sea rising across a young, sedimentary substrate. The recently eroded, underlying, and presently eroding strata were formed in very similar environments as the ocean had moved back and forth across the coastal plain in response to sea level changes during the Quaternary resulting from global changes in glaciation. The shoreline is a wave (or storm) dominated, micro-tidal (mean tide range about 1.1m) system that has experienced approximately 30 cm of sea-level rise over the past century. Although natural process operating along an open coast tend to straighten the shoreline, the actual form of the shoreline depends, in part, on the geology of strata both being and recently eroded. Bluffs, dunes, barrier spits, marshes, and inlet associated areas all respond differently and leave different physical remnants on the post-erosion, flooded sea floor. Modern “hot spots,” sites of chronically greater erosion, appear to be related to patterns of wave refraction which is a function of the overall wave climate and the location of offshore shoals.

The jetties at Ocean City Inlet, the southern limit of the study area, and Indian River Inlet have had substantial local impact since their construction and indicate a spatial change in condition along the coast. The net longshore current near Ocean City flows southward and has built a substantial fillet of sand against the north jetty whereas the net drift at Indian River Inlet is toward the north. A permanent sand-bypassing plant serves to feed the longshore drift to the north of the inlet. The nodal zone, or region of current reversal, appears to be around the Delaware-Maryland border. Many sections of the shore have been modified with sea walls or bulkheads and groins. During the past two decades there have been several substantial episodes of beach nourishment.

The long term history of the shore is one of retreat. Comparisons of maps and charts from 1850 with modern map, chart, and photographic data document a receding shoreline and a transgressing sea. The rate of retreat shows both spatial and temporal variability. Analysis of recent beach profiles suggests that although the actual shoreline (*i.e.* the intersection of the physical shoreface and a tidal datum such as mean high water or mean sea level) may be retreating, sand eroded from landward portions of the beach might be accumulating in the shallow nearshore, especially in the vicinity of sections that have been nourished. If this is so, even though the sand has been lost from the accessible, recreational beach, it still is part of the beach-shoreface system and might be serving to protect the inshore portions from larger waves.

## **SIGNIFICANT CONCLUSIONS**

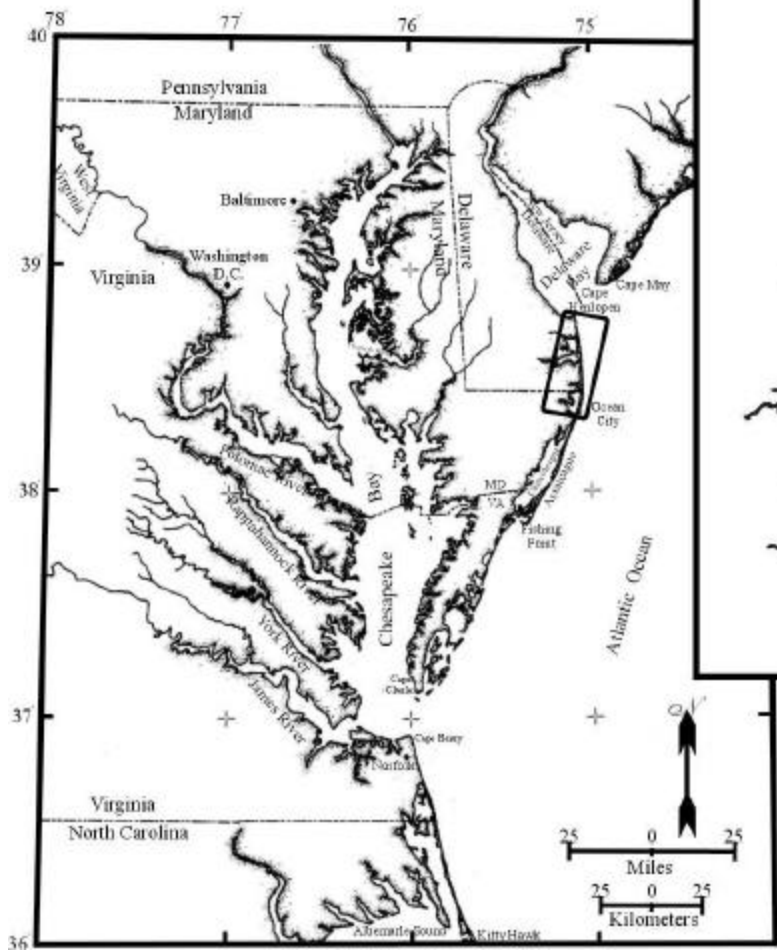
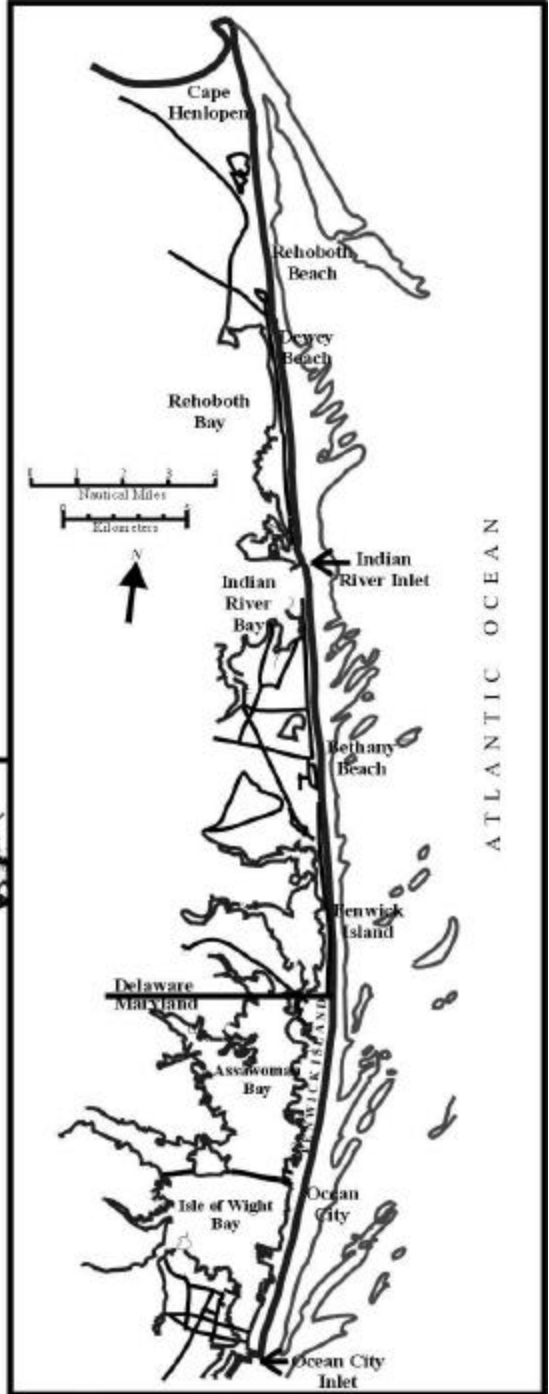
Although there are potentially adverse consequences to sand mining in the offshore regions of Delaware and Maryland, they likely are not substantial and actions can be taken to eliminate or minimize them. Obviously dredging the bottom destroys all the organisms that had lived within the dredged area, but the best sands for beach nourishment have a comparatively low resource value. The benthic fauna of those areas are likely to recolonize fairly rapidly especially if small “islands” are left untouched within the otherwise dredged area. Care should be taken to minimize disturbance of the substrate between the shoals that will be the targets for dredging. The very small size of the areas likely to be dredged relative to the large geographic ranges of transitory fishes indicates that sand mining would have very little impact on the fish populations. The species occurrence of fishes in spawning,

egg, and larvae stages is least from October through March and peak in the late spring and summer. The potential threat to sea turtles can be avoided by mining from mid-November to mid-April when these sub-tropical animals are absent from the area. Sand mining poses no foreseeable threat to the migratory and highly mobile marine mammals.

Analysis of existing wave conditions demonstrates that modern shoreline stability is related to areas of concentration and dispersion of wave energy near the zone of breaking waves. The relatively stable area around the Maryland-Delaware border is one of relatively low waves whereas the various erosional “hot spots,” especially along Fenwick Island, appear coincident with zones of wave energy concentration. Wave transformation modeling indicates that removal of  $10^6$  m<sup>3</sup> of sand from the top of Fenwick and Isle of Wight Shoals will result in very small changes from present conditions. Removal of  $10^7$  m<sup>3</sup> might cause more noticeable changes in the regions between the dredged areas and the shore. Modeling also predicts that dredging will have an extremely small impact on ambient tidal currents and potential storm surges.

The Maryland-Delaware shore is experiencing increasing pressure from expanding recreational and residential uses and the associated commercial developments. The form of the shoreline results from interactions amongst the local geology and stratigraphy, the history of Holocene sea-level rise, and the contemporary wave climate. Although rising sea level drives a general marine transgression/shoreline retreat through the area, the rate of retreat and apparent local stability vary along the shore. Shoreline engineering, most noticeably sand bypassing at Indian River Inlet and repetitive beach nourishment at several sites, has been employed to control shoreline retreat and enhance the recreational value and use of the beach. The cumulative impact of the many beach nourishment projects that already have been performed appears to be more beneficial than any individual project.

**STUDY PRODUCTS:** Virginia Institute of Marine Science, 2000. Environmental Survey of Potential Sand Resource Sites Offshore Delaware and Maryland. Final Report to the U.S. Department of the Interior, Minerals Management Service, International Activities and Marine Minerals Division, Herndon, VA. Contract No. 1435-01-97-CT-30853. Printed Copy and CD.



## The Department of the Interior



As the Nation's principal conservation agency, the Department of the Interior has responsibility for most of our nationally owned public lands and natural resources. This includes fostering sound use of our land and water resources, protecting our fish, wildlife, and biological diversity, preserving the environmental and cultural values of our national parks and historic places; and providing for the enjoyment of life through outdoor recreation. The Department assesses our energy and mineral resources and works to ensure that their development is in the best interests of all our people by encouraging stewardship and citizen participation in their care. The Department also has a major responsibility for American Indian reservation communities and for people who live in island territories under U.S. Administration.

## The Minerals Management Service Mission



As a bureau of the Department of the Interior, the Minerals Management Service's (MMS) primary responsibilities are to manage the mineral resources located on the Nation's Outer Continental Shelf (OCS), collect revenue from the Federal OCS and onshore federal and Indian lands, and distribute those revenues.

Moreover, in working to meet its responsibilities, the Offshore Minerals Management Program administers the OCS competitive leasing program and oversees the safe and environmentally sound exploration and production of our Nation's offshore natural gas, oil and other mineral resources. The MMS Royalty Management Program meets its responsibilities by entrusting the efficient, timely and accurate collection and distribution of revenue from mineral leasing and production due to Indian tribes and allottees, States and the U. S. Treasury

The MMS strives to fulfill its responsibilities through the general guiding principles of: (1) being responsive to the public's concerns and interests by maintaining a dialog with all potentially affected parties and (2) carrying out its programs with an emphasis on working to enhance the quality of life for all Americans by lending MMS assistance and expertise to economic development and environmental protection.

---

# Environmental Survey of Potential Sand Resource Sites Offshore Delaware and Maryland

## Part 1: Benthic Habitat Mapping and Resource Evaluation of Potential Sand Mining Areas, 1998-1999

---

Final Report

OCS Study 2000-055

August 2000

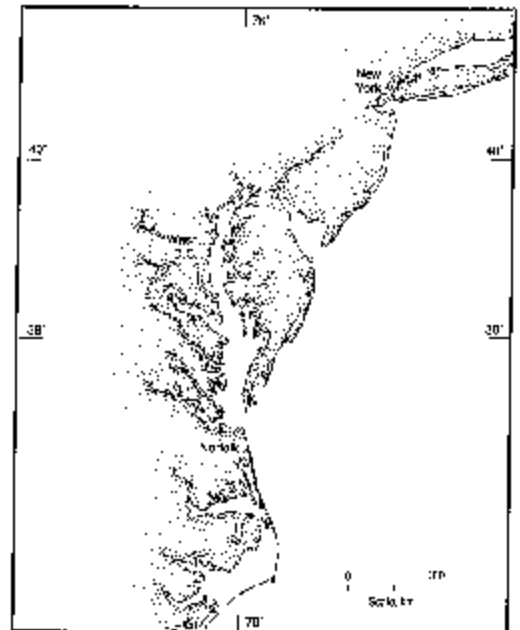
Authors:

G. R. Cutter Jr and R. J. Diaz  
Virginia Institute of Marine Science

Project Manager:

Carl H. Hobbs, III  
Virginia Institute of Marine Science

Prepared under MMS contract 1435-01-97-CT-30853 to  
the  
Virginia Institute of Marine Science  
College of William & Mary



**MMS** U.S. Department of the Interior  
Minerals Management Service

International Activities and Marine Minerals Division

College of William and Mary  
**MMS**  
Virginia Institute of Marine Science  
School of Marine Science

Final Report

Environmental Survey of Potential Sand Resource Sites

Offshore Delaware and Maryland

Part 1

Benthic Habitat Mapping and Resource Evaluation of Potential Sand Mining Areas  
Offshore Maryland and Delaware, 1998-1999

G. R. Cutter, Jr. and R. J. Diaz

Principal Investigators  
Virginia Institute of Marine Science

Carl H. Hobbs, III, Project Manger

Virginia Institute of Marine Science

for

U. S. Department of the Interior

Minerals Management Service

International Activities and Marine Minerals Division

Contract 1435-01-97-CT-30853

OCS Study 2000-055

August 2000

#### DISCLAIMER

This report has been reviewed by the Minerals Management Service and approved for publication. Approval does not signify that the contents necessarily reflect the views and policies of the Service, nor does mention of trade names or commercial products constitute endorsement or recommendation for use.

### The Department of the Interior



As the Nation's principal conservation agency, the Department of the Interior has responsibility for most of our nationally owned public lands and natural resources. This includes fostering sound use of our land and water resources, protecting our fish, wildlife, and biological diversity, preserving the environmental and cultural values of our national parks and historic places; and providing for the enjoyment of life through outdoor recreation. The Department assesses our energy and mineral resources and works to ensure that their development is in the best interests of all our people by encouraging stewardship and citizen participation in their care. The Department also has a major responsibility for American Indian reservation communities and for people who live in island territories under U.S. Administration.

### The Minerals Management Service Mission



As a bureau of the Department of the Interior, the Minerals Management Service's (MMS) primary responsibilities are to manage the mineral resources located on the Nation's Outer Continental Shelf (OCS), collect revenue from the Federal OCS and onshore federal and Indian lands, and distribute those revenues.

Moreover, in working to meet its responsibilities, the Offshore Minerals Management Program administers the OCS competitive leasing program and oversees the safe and environmentally sound exploration and production of our Nation's offshore natural gas, oil and other mineral resources. The MMS Royalty Management Program meets its responsibilities by entrusting the efficient, timely and accurate collection and distribution of revenue from mineral leasing and production due to Indian tribes and allottees, States and the U. S. Treasury

The MMS strives to fulfill its responsibilities through the general guiding principles of: (1) being responsive to the public's concerns and interests by maintaining a dialog with all potentially affected parties and (2) carrying out its programs with an emphasis on working to enhance the quality of life for all Americans by lending MMS assistance and expertise to economic development and environmental protection.

## TABLE OF CONTENTS

CHAPTER 1. INTRODUCTION .....	1
1.1. Overview and Objectives .....	1
1.2. Benthic Resources and Habitats .....	2
1.2.1. Scales of Variation .....	2
1.2.1.1. Spatial .....	2
1.2.1.2. Temporal .....	3
1.2.2. Assessment and Evaluation .....	4
1.2.2.1. Existing Tools .....	4
1.2.2.2. Relevance .....	6
1.2.2.3. Modification and Development .....	6
CHAPTER 2 STUDY AREA .....	9
2.1. Regions of Interest .....	9
2.2. Sample Locations .....	9
3. MATERIALS AND METHODS .....	11
3.1. Field Methods .....	11
3.1.1. Vessel .....	11
3.1.2. Grab .....	11
3.1.3. SPI .....	11
3.1.4. Sled .....	12
3.1.5. SPI-Plow .....	13
3.1.6. Sidescan Sonar .....	13
3.1.7. Trawl .....	13
3.2. Laboratory Methods .....	14
3.2.1. Grab .....	14
3.2.2. SPI .....	14
3.2.3. Sled .....	14
3.2.4. Video Image Analysis Data .....	16
3.2.4.1. SPI-Plow .....	17
3.2.5. Trawl .....	17
3.2.6. Sidescan Sonar .....	18
3.2.7. Position Data .....	18
3.2.8. Grab Sample Substrate Data .....	18
3.2.9. Grab Sample Biological Data .....	18
3.2.9.1. Preliminary Data Treatment .....	18
3.2.9.2. Community Analysis .....	19
3.2.10. Image Analysis: SPI and Sled Still .....	21
3.2.11. Regional Condition Data .....	25
3.2.11.1. NOAA Buoy Data .....	25
3.2.12. Habitat Classification and Biological Resource Information .....	25

3.2.12.1. Indices and Derived Statistics .....	25
3.2.12.2. Secondary Production .....	27
3.2.12.3. Mapping .....	28
CHAPTER 4. RESULTS .....	31
4.1. Grab Sample Substrate Data .....	31
4.2. Grab Sample Biological Data .....	31
4.2.1. Biological Data - Descriptive Summaries .....	31
4.2.1.1. 1998 .....	31
4.2.1.2. 1999 .....	33
4.2.2. Biological Data - Community Structure and Function .....	34
4.2.2.1. Diversity and Evenness .....	34
4.2.2.2. Numbers of Taxa and Species .....	35
4.2.2.3 Cluster Analysis .....	35
4.2.2.4. Dominant Species .....	37
4.2.2.5 Dominant Community Groups .....	39
4.2.2.6 Life History Attributes .....	39
4.3. Fish Trawls .....	41
4.3.1. Fish Assemblages .....	41
4.3.2. Fish Gut Content .....	43
4.4. SPI Image Analysis Data .....	44
4.4.1. Standard SPI Analysis Data .....	44
4.4.2. SPI Grain-size Analysis .....	46
4.4.3. Comparison of SPI and Grab Grain-size Determinations .....	46
4.5. Sled Still Image Analysis Data .....	47
4.6. Video Image Analysis Data .....	47
4.7. Regional Condition Data .....	47
4.7.1. NOAA Buoy Data .....	47
4.8. Biological Resource Information .....	48
4.8.1. Indices and Derived Statistics: SPI-based BHQ and SBHQ .....	48
4.9. Habitat Classification and Resource Value Results, Secondary Production .....	49
4.10. Prediction of Biology Using Substrate and Image Data .....	52
4.10.1. Secondary Production .....	52
4.10.2. Community Groups .....	53
CHAPTER 5. DISCUSSION, SUMMARY, AND CONCLUSIONS .....	55
5.1. Origins and Fate of Topographic Features .....	55
5.2. Benthic Habitat Characteristics .....	55
5.3. Perspectives on Former Organism-sediment Models and a New Model .....	58
5.4. Evaluating Biological Resource Potential .....	60
5.5. Relationship of Secondary Production to Habitat Value .....	62
5.6. Assessing Potential Sandmining Impacts .....	63
5.7. Minimizing Impacts to Biological Resources .....	66

CHAPTER 6. ACKNOWLEDGMENTS ..... 67

CHAPTER 7. REFERENCES CITED ..... 69

## LIST OF FIGURES

- Figure 2.1-1: General location of the Maryland/Delaware (MD/DE) study area.
- Figure 2.1-2: General location and boundaries of the Indian River (IR) and North Bethany Beach (NBB) regions of interest (ROI).
- Figure 2.1-3: General location and boundaries of the Fenwick Shoal (FS), Weaver Shoal (WS), and Isle of Wight Shoal (IWS) regions of interest (ROI).
- Figure 2.2-1: Location of grab samples in the Maryland and Delaware study area.
- Figure 2.2-2: Location of sediment profile camera stations in the Maryland and Delaware study area.
- Figure 3.1-1: Young grab used to collect benthic infauna and sediments.
- Figure 3.1-2: Sediment profile camera system used to collect images of the sediment-water interface.
- Figure 3.1-3: Standard video and still camera sled used to collect images of surface features over broad spatial scales.
- Figure 3.2-1: Relationship among sediment grain size, compaction (Cp), and prism penetration (Pen).
- Figure 4.1-1: Percent composition of sediments from the Maryland and Delaware study area.
- Figure 4.2-1: Distribution frequency of taxa occurrences for all grabs from the Maryland and Delaware study area for both May 1998 and June 1999.
- Figure 4.2-2: Dendrogram of all stations sampled in 1998 and 1999 in the Maryland and Delaware study area. Cluster groups, indicated by letters, are based on simultaneous double standardization of data, Bray-Curtis similarity, and flexible sorting. See text for details.
- Figure 4.2-3: Species cluster groups based on simultaneous double standardization of data from the Maryland and Delaware study area, Bray-Curtis similarity, and flexible sorting. See text for details.
- Figure 4.2-4: Dendrogram of Fenwick Shoals stations sampled both in 1998 and 1999. Cluster groups are based on simultaneous double standardization of data, Bray-Curtis similarity, and flexible sorting. See text for details.
- Figure 4.2-5: box plots of community structure statistics from the Maryland and Delaware study area by cluster analysis station group. Bar is median; box is interquartile range; tails are trimmed range; and dots are outliers (>2 times the interquartile range).

Figure 4.3-1: Locations of bottom trawls around the Fenwick Shoals ROI. Trawls were located in four benthic habitats.

Figure 4.3-2: Cluster analysis of demersal fish collected May 1999 at four benthic habitat types within the Maryland and Delaware study area. Based on Bray-Curtis similarity and flexible sorting.

Figure 4.3-3: Cluster analysis of fish data collected May 1999 at four benthic habitat types in the Maryland and Delaware study area. Based on Bray-Curtis similarity and flexible sorting. See text for a description of the habitat characteristics. See Figure 4.3-1 for the location of the habitats.

Figure 4.4-1: SPI (sediment profile images) from selected locations.

Figure 4.4-2: SPI (sediment profile images) from selected locations.

Figure 4.4-3: SPI (sediment profile images) from selected locations.

Figure 4.4-4: SPI (sediment profile images) from selected locations.

Figure 4.4-5: SPI (sediment profile images) from selected locations.

Figure 4.4-6: Examples of sediment grain-size determinations from sediment profile images. CS = coarse sand; FS = fine sand; GR = gravel; MS = medium sand; SH = shell; SI = silt; VCS = very coarse sand; VFS = very-fine sand.

Figure 4.4-7: Relationship between grain-size determinations from sediment profile images. Y-axis is grab mean grain-size in mm (MZMM). X-axis is image mean grain-size in mm.

Figure 4.5-1: Surface camera images from selected stations.

Figure 4.5-2: Surface camera images from selected stations.

Figure 4.7-1a: Water temperature (°C) and wave height (m) from NOAA Bouy 44009 for the year 1998.

Figure 4.7-1b: Water temperature (°C) from NOAA buoy 44099 for the 17 to 21 May 1998 cruise.

Figure 4.7-2: Water temperature (°C) and wave height (m) from NOAA Bouy 44009 for the first six months of 1999.

Figure 4.8-1a: Distribution of Benthic Habitat Quality index values for the Indian River ROI.

Figure 4.8-1b: Distribution of Scaled Benthic Habitat Quality index values for the Indian River ROI.

Figure 4.8-2a: Distribution of Benthic Habitat Quality index values for the Fenwick Shoal ROI.

Figure 4.8-2b: Distribution of Scaled Benthic Habitat Quality index values for the Fenwick Shoal ROI.

Figure 5.2-1: Benthic habitat map of Fenwick Shoal ROA showing SBHQ index surface generated with inverse distance weighting, secondary production, and surface biological features from video transects. The presence of *Ammodytes* spp. From the video is over-lain on the video transects.

Figure 5.4-1: Sediment grain-size (mm) map of the Fenwick Shoal ROI derived from sediment profile images. Surface was generated with inverse weighting interpolation. Coarser sediments tended to be on the crest of the shoals.

Figure 5.6-1: Sand-mining scenario for the Fenwick Shoal ROI. Benthic recolonization to the mined area (coarse stippling) would proceed from community groups in the buffer zone (fine stippling) and from outside the mined area. Letters refer to cluster groups and subgroups.

## LIST OF TABLES

- Table 4.1-1: Sediment grain-size distribution from grab samples collected in the Maryland and Delaware study area. Gravel is >2mm. Sand is between 2 and 0.063mm. Silt is between 0.063 and 0.039mm. Clay is <0.0039mm.
- Table 4.1-2: Sediment grain-size analysis of sand fraction grab samples collected in the Maryland and Delaware study area. All statistics are in mm.
- Table 4.2-1: Major taxa abundance (individuals/0.04 m<sup>2</sup>) of infauna collected in the Maryland and Delaware study area in May 1998 and June 1999.
- Table 4.2-2: Proportional contribution of major taxa to total infaunal abundance and species richness for samples collected in the Maryland and Delaware study area in May 1998 and June 1999.
- Table 4.2-3: Percentage of major taxa abundance (individuals/individuals/0.04 m<sup>2</sup>) of infauna collected in the Maryland and Delaware study area in May 1998 and June 1999.
- Table 4.2-4: Species richness (taxa/0.04 m<sup>2</sup>) by major taxa for infauna collected in the Maryland and Delaware study area in May 1998 and June 1999.
- Table 4.2-6: Percentage species by major taxa for infauna collected in the Maryland and Delaware study area in May 1998 and June 1999.
- Table 4.2-7: Percentage of biomass by major taxa for infauna collected in the Maryland and Delaware study area in May 1998 and June 1999.
- Table 4.2-8: Infaunal community structure in the Maryland and Delaware study area for May 1998 and June 1999.
- Table 4.2-9: Constancy and fidelity based on nodal analysis of all grab data from the Maryland and Delaware study area. See Figure 4.2-2 for stations and Figure 4.2-3 for species in each group.
- Table 4.2-10: Dominant taxa (present at >20% of stations, 15 of 70 stations) collected in the Maryland and Delaware study area.
- Table 4.2-11: Abundance dominants from the Maryland and Delaware study area. Includes all taxa that were at least one percent of total abundance in either May 1998 or September 1999 with and without the polychaete *Siophanes bombyx*.
- Table 4.2-12: Biomass dominants (>0.5 g wet weight/0.04 m<sup>2</sup>) collected in the Maryland and Delaware study area. Numerical or occurrence dominant species are also included.
- Table 4.2-13: Summary of overall dominants based on occurrence, abundance, and biomass collected

in the Maryland and Delaware study area.

Table 4.2-14: Average abundance of dominant taxa in the Maryland and Delaware study area by cluster analysis station group (see Figure 4.2-2). Dominance Types are: O = Occurrence (>20% of stations), A = Abundance (>1% of total abundance for May of September cruise), B = Biomass (>0.5% g total wet weight). \* = average abundance was <1. Blank = taxa did not occur in the station group.

Table 4.2-15: Life history characteristics and estimate of recruitment potential for dominant species from the Maryland and Delaware study area.

Table 4.3-1: Fish collected in May 1999 at four major benthic habitat types within the Maryland and Delaware study area. Data are summed occurrence of species caught in eight trawls from each habitat.

Table 4.3-2: Invertebrates collected in May 1999 at four major benthic types within the Maryland and Delaware study area. Data are the summed occurrence of selected species caught in eight trawls from each habitat. For most species only presence in the trawl was recorded (+).

Table 4.3-3: Summary of gut content by taxa for the three dominant demersal fish species trawled around Fenwick Shoal. Gut content for all individuals was summed for each species.

Table 4.4-1: Sediment size classes estimated from SPI images collected in the Maryland and Delaware study area.

Table 4.9-1: Estimated secondary production of macroinfauna for the 1998 grab data from the Maryland and Delaware study area.

Table 4.9-2: Estimated secondary production of macroinfauna for the 1999 grab data from the Maryland and Delaware study area.

Table 4.9-3: Averaged annual secondary production of macroinfauna from the Maryland and Delaware study area.

Table 4.9-4: Summary of gut content by major taxa for the three dominant demersal fish species trawled around Fenwick Shoal. All counts and weights (g wet) are for total stomachs analyzed. Mean Ind. Weight is the average weight (g wet) of an individual food item.

Table 4.9-5: Averaged annual P/B ratios of macroinfauna from the Maryland and Delaware study area.

Table 4.9-6: relationship between P/B ratio and sediment type for the May 1998 grab data. Based on discriminant analysis of sediment grain-size categories and major taxa P/B ratios. A total of 48 stations were classified; four stations did not have grain-size data. CS = coarse sand; FS = fine sand; GR = gravel; MU = mud.

Table 4.10-1: Averaged abundance (individuals/m<sup>2</sup>) of selected taxa (occurring at five or more stations) by cluster subgrouping for the Maryland and Delaware study area.

Table 5.3-1: Scenarios depicting the effect of season and climatology on infaunal recolonization trajectory. Faunal characteristics favored by the combinations of season and climate are listed in each cell of the table.

## CHAPTER 1. INTRODUCTION

### 1.1. Overview and Objectives

The removal of mineral resources, typically mining of sand for beach nourishment, from the continental shelf poses a threat of direct disturbance to benthic communities and trophically dependent pelagic species. In order to eventually predict the impacts of sandmining upon biological resources within a designated project area, it is necessary to first determine existing community structures, spatial distributions, substrate dependencies, productivity and trophic linkages. The natural dynamics of the biological assemblages should be assessed with respect to the scales and magnitudes of normal environmental stressors and the potential for some activities to interfere with these dynamics. For example, benthic community structure can sometimes be accurately inferred based upon sediment types, however sediment types is a function of the transport environment controlled by highly variable wave and current dynamics. The mid-Atlantic continental shelf is annually exposed to summer hurricanes and winter northeaster storms. Yet, primary topographic features, such as the shoals offshore Maryland and Delaware, and the predominant sediment distribution patterns persist. Persistent biological assemblages there reflect balance with system dynamics. However, apparent persistence may also result from continual population responses to disturbance, where eradication is quickly followed by recolonization dependent upon substrate changes and water column conditions subsequent to disturbance.

Disturbances associated with sandmining are not inconsequential because of existing highly dynamic conditions on the shelf. Sandmining will directly alter topographic features which in turn will influence how and to what degree water column dynamics will influence the substrate and hence the biology. Prediction of the short-term responses of the benthic community will be considerably more difficult than long-term because of asynchronous and variable natural short-term population fluctuations (Maurer *et al.*, 1976). Long-term responses however can be considered in terms of a spatial problem in that community structure should eventually reflect substrate components, and primary alterations to substrates should be limited to the general vicinity of the mined region.

Impacts of sandmining to the biological resources include removal of and extermination of

infauna, epifauna, and some benthic fish; alteration of bathymetry by reduction of topographic features; exposure of buried substrate; and potential dispersion of surrounding biological community constituents.

Regions of potential sandmining activities in U.S. Federal waters off Maryland and Delaware include the offshore ridges known as Fenwick, Weaver, and Isle of Wight Shoals, and nearshore gravel and sand sheets east of Indian River Inlet. Sediments in the region are primarily terrigenous quartz (subarkosic) sands (Milliman, 1972), however grain-sizes from clays to gravels exist in the area. The offshore ridges are topographic features initially thought by Shepard (1948) to be drowned barrier islands, but are now believed to be long-term accretional and erosional responses to storm-related hydraulic regimes in combination with sea-level rise since the last deglaciation (Swift and Field, 1981; Goff *et al.*, 1999). The ridges apparently form as shore-attached features produced during shoreline erosion induced by storm generated currents and vortices, and also dependent upon substrates composed of mixed sands with a coarse component (Swift *et al.*, 1973).

## **1.2. Benthic Resources and Habitats**

### **1.2.1. Scales of Variation**

#### **1.2.1.1. Spatial**

Spatial variability in water depth, topography, substrate characteristics and biological community attributes occurs at very small (cm) to regional (km) scales. Determinations of distributions, aerial coverages, and transitions will depend upon the scale(s) at which sampling occurs. Resolving spatial variations is important to delineation of impacts, however resolving power is inversely proportional to sampling effort. Therefore, in order to resolve both large and small-scale phenomena and their variability, the sampling support and design must provide sufficient coverage for both. Sampling regionally at very high densities is infeasible, therefore we chose to use varying spatial supports for our data collection. Point sampling provided large-scale coverage and gross approximations of habitat distributions, and transect sampling (with point and continuous devices) provided fine-scale coverage and estimates of rates of small-scale spatial change which could be combined with the large-scale data in order to better represent intermediate-scales without direct sampling. This approach utilized the concepts of geostatistics and varied support, reactive sampling

techniques in order to maximize the information return for the field efforts.

### **1.2.1.2. Temporal**

Temporal variability operates upon benthic habitats and communities at long and short time scales. Continental shelf communities vary seasonally but this temporal variation is confounded with distance off shore and depth (Maurer *et al.*, 1976). The farther offshore and deeper the area the less pronounced seasonality becomes and presumably interannually variation also declines (Boesch *et al.*, 1979). However, within our region of interest benthic community structure and function is primarily associated with substrate type and changes in substrate. Therefore, unless the bottom changes in substrate or hydrodynamics, variation from temporal change in the communities should be relatively small, and community structure and function should be relatively predictable, irrespective of when sampled during the year. Temporal dynamics in substrates and habitats that will have the most effect upon benthic communities operate in response to forcings with short temporal scales but broad spatial scales. Stresses incurred by the bottom are primarily associated with major storm events or dredging activities. Unless storms spawn tornadoes that would proceed along a discrete path across the study area, the storms' potential to induce bottom change would influence the entire study area. And, unless climatic dynamics change drastically, seasonal effects in a particular location should be predictable from year to year. Unpredictable changes that would be expected where there are combined effects induced by high-energy events occurring in transitional areas. Transitional areas are characterized by high rates of local variability in terms of physical structure (steep grades) or the induced effects of structural changes exhibited in water column physics and resultant effects on the substrate (shear, suspension, sedimentation) and biology (exposure, removal, burial). Thus determinations of rates of spatial changes in ecosystem components are more important than attempts at detecting seasonal patterns in dynamic environments, especially if the time series used to detect seasonality is short or the sampling interval infrequent.

## **1.2.2. Assessment and Evaluation**

### **1.2.2.1. Existing Tools**

The organism sediment index (OSI) was developed (Rhoads and Germano, 1986) in order to

provide a means to assess benthic habitat condition using sediment profile image data. Recently, Nilsson and Rosenberg (1997) developed a similar index, the benthic habitat quality (BHQ) index, also for applying profile image data to habitat assessment. Standard sediment profile image (SPI) analysis and the OSI and BHQ indices offer insights into habitat and microhabitats which other techniques do not (Rhoads and Germano, 1986), and provide complementary data (Bonsdorff *et al.*, 1996) to standard benthic community and substrate characterization.

Other survey tools and techniques provide habitat data at scales difficult to resolve by SPI sampling. Video and interval still imaging sleds, which provide continuous detailed transect data, equivalent to ROV-gathered data, but at lower cost and cover greater area in less time although with less directional control. Side-scan sonar devices provide wider swath coverage over transect lines, revealing substrate configurations and transitions. Additionally, sonar units can be deployed simultaneously with towed sleds, providing the acoustic swath view of the bottom about to be encountered by the sled. These techniques provide habitat and microhabitat information important to understanding biological community data from sediment grab samples and benthic trawl samples.

Data from benthic-grab sample analysis offer several resource assessment parameters including abundance, biomass, and diversity. These basic community structure parameters offer intuitively valuable resource information and have formed the basis of many impact assessments. Recently community structure parameters have been incorporated into numerical indices designed to measure the magnitude of response of the benthos to various forms of disturbance. For example, a benthic index of biotic integrity (B-IBI) was developed by Weisberg *et al.*, (1997) as a means of evaluating benthic community conditions based upon species' tolerances and sensitivities to environmental conditions and used data from “reference” areas as a calibration of the index. This approach focuses on community structure and does not account for energetic or ecosystem level responses, which should be the central issue in any assessment of potential impacts. To overcome the limited usefulness of community structure based assessments we have included an energy flow based approach to this study by estimating the secondary production of the infaunal communities.

Secondary production can be derived from the grab data and imparts more efficiency upon any assessment or characterization of resource value or potential than any of the community structure based approaches (Diaz and Schaffner, 1990). Secondary production estimates also benefit from mathematical models that have incorporated many datasets from around the world (for recent examples see Brey (1990) and Tumbiolo and Downing (1994), meaning that applicability and comparison are enhanced. The Benthic Resources Assessment Technique (BRAT) developed by Lunz and Kendall (1987) was an early attempt to add the concept of energy flow to resource assessment and ascribe resource value to subtidal estuarine and marine bottom habitats. BRAT utilizes data collected on both infaunal communities via grab and fish assemblages via trawl. Gut content analysis of the fishes is compared to existing benthic infaunal resources to estimate trophic transfer of benthic resources. However, BRAT is rather labor intensive and difficult to apply over large areas because sampling at frequent intervals over a year is needed to characterize energy transfer to transient fishes. In addition, BRAT relied on standing stock biomass of benthos and did not consider the productivity and turnover rate of the infauna.

If the goal is to assess benthic biological resources that will support fisheries species, high priority should be given to assessing resource potential of a bottom to provide fish food and the spatial distribution of these resources.

Evaluating sand-mining effects based upon benthic biological resources and habitat conditions requires a combination of the previously described tools and techniques for habitat valuation, and in addition predictions concerning community and system responses to disturbance events.

#### **1.2.2.2. Relevance**

Both of the profile image-derived indices (the OSI developed for northeast estuarine and marine bottoms and the BHQ developed for Scandinavian fjords systems) heavily weight the redox potential discontinuity (RPD) layer depth. Although appropriate for the systems within which these indices were developed, where variation in RPD layer depth could be related to variation in biological activity. RPD layer depth is also intimately linked to and correlated with geophysical and geotechnical

sediment properties. RPD layer depth is essentially the recent time-averaged depth below the sediment-water interface to which oxidized water penetrates, either by biogenic flushing induced by organismal activity (Aller and Aller, 1998) or by physical percolation induced by advection (Ziebis *et al.*, 1996). Unfortunately, both indices (OSI and BHQ) utilize RPD without compensating for confounding factors that control permeability and influence RPD, such as sediment grain-size, porosity, cohesivity, compaction, and sorting. In simple cases, sediment grain-size distributions can serve as a proxy for the others. As long as the sediments studied are similar, in that grain-size distributions and geotechnical properties are limited in variability, application of either index is valid. However, neither the OSI nor BHQ can accommodate the physical processes that structure surficial substrates in our study region, the inner continental shelf offshore Maryland and Delaware, or the east coast continental shelf in general. Coarse, highly permeable sediments cover much of the area as does steep topographic features that are often exposed to strong currents and high turbulence.

### **1.2.2.3. Modification and Development**

Since the OSI and BHQ suffer serious effects from confounded, correlated variables such as RPD and sediment grain-size, and have limited relevance to most continental shelf habitats, we developed a new SPI index based upon the BHQ. We used the BHQ index as a base because it relies upon discretely identifiable sediment and biological features. We do not present the OSI in this report because successional states were indeterminate for nearly all the images, therefore the OSI was undefined. Goals for the new index included simplicity, similarity to OSI and BHQ, adjustment for correlated variables, and accommodation for variables exceeding tool measurement capabilities, and of course utilization for mid-Atlantic continental shelf environments. We call the index SBHQ for Scaled Benthic Habitat Quality index. The design of the SBHQ should make it applicable to not only the mid-Atlantic shelf but to sedimentary environments in general.

## **CHAPTER 2 STUDY AREA**

### **2.1. Regions of Interest**

The study area was located on the inner continental shelf in the central portion of the mid-Atlantic bight (Figure 2.1-1). Minerals Management Service (MMS) specified five regions of interest (ROI). Two ROI's were located offshore Indian River Inlet, Delaware: the ROI to the north was called Indian River ROI (IR-ROI) and its southern neighbor was called North Bethany Beach ROI (NBB-ROI) (Figure 2.1-2). Three ROI's were located on the primary shoal features offshore northern Maryland and southern Delaware: from north to south, Fenwick Shoal (FS), Weaver Shoal (WS), and Isle of Wight Shoal (IWS) (Figure 2.1-3).

For general descriptions in this report, Indian River Regions refers to both the Indian River and North Bethany Beach ROI's. Likewise, Fenwick Shoals Regions refers to the three shoal ROI's (FS-ROI, WS-ROI, IWS-ROI).

### **2.2. Sample Locations**

Sampling in 1998 encompassed all ROI's, and some areas surrounding the ROI's. In 1999, sampling was concentrated in the FS Regions, primarily where major sedimentological and biological transitions were identified from the 1998 data. Several different sampling gear were deployed within and around the ROI's. In May 1998, point samples were acquired from stations on a regular lattice: SPI at all stations, sediment grabs at randomly selected stations within the lattice. Additional point samples were taken at intermediate positions along seven of the lattice axes. Transects were sampled using a towed sled system along three of the higher density point sample lines and also across areas within the overall lattice where point samples were not acquired. In June 1999 sediment grabs were acquired at a subset of the same grab stations from 1998 (Figure 2.2-1).

SPI samples were taken at some of the same stations visited in 1998. However, because of the sea-state, sampling efforts were reallocated, focusing upon collection of biological grab samples at the same stations as 1998, video sled tows, and high-density point SPI sampling, where SPI images were acquired at close intervals along transects by drift deployment. The high-density SPI transect samples

were acquired over and between much of Fenwick Shoal and Weaver Shoal (Figure 2.2-2).

### **3. MATERIALS AND METHODS**

#### **3.1. Field Methods**

##### **3.1.1. Vessel**

For the 1998 cruise we used the M/V Atlantic Surveyor from Toms Inlet, New Jersey used for this cruise. Oits overall length was 110 feet and accommodated berthing for 9 nine scientists. For the 1999 cruise we used the UNOLS vessel R/V Cape Henlopen of the University of Delaware its overall length was 120 feet and accommodated berthing for 12 scientists. On both cruises we conducted 24-hour operations to make the most efficient use of our shipboard time.

##### **3.1.2. Grab**

A Young grab, 0.044 m<sup>2</sup> surface area, was deployed to collect sediment grab samples for substrate and biological community data (Figure 3.1-1). This is the same sampler used by EPA in its EMAP and MAIA programs. The Young grab is similar to a van Veen grab that has been placed in a frame to hold it level with the sediment surface while a sample is collected. Grabs without frames tend to twist and collect uneven samples. Because of its frame, the Young grab functions well in both soft and hard sediment.

##### **3.1.3. SPI**

A Hulcher model Minnie Sediment profile camera was deployed attached to a Benthos profile camera frame (Figure 3.1-2). Fujichrome 100 ASA professional color slide film was used. Tests were done frequently onboard in order to ensure camera function and mark stations. In addition, a video camera was attached to the SPI camera frame in order to both monitor camera operation on bottom and to provide close-up video images of the sediment surface features and epifauna in front of the profile prism.

The sediment profile camera was developed to collect data on sediments at and below the sediment-water interface. Sediment profile cameras provide a unique in situ view of the sediment-water interface and subsurface sediments yielding both quantitative and qualitative data on the biological, chemical, and physical character of the sediments. The sediment profile camera is composed of two

parts; 1- the camera, encased in a pressure housing, and 2- a 45° prism, with an approximately 15 x 23 cm clear plexiglass face plate and mirror to reflect the image of the sediment up to the camera lens. The bottom edge of the prism is sharpened to neatly cut through the sediment. The prism is filled with clear fresh water to prevent hydrostatic pressure from distorting the faceplate as the prism is lowered below the sea surface. The lens and light source (strobe for still and incandescent bulbs for video) used to illuminate the sediment are both contained inside the clear water-filled prism. The camera is focused on the prism faceplate and records sediment features pressed against the faceplate. This configuration allows the camera to work in complete darkness with image clarity independent of turbidity. For deployment, the camera and prism are attached to a cradle held by a larger stabilizing frame to insure the prism enters the sediment at a 90° angle (Figure 3.1-2). The entire cradle and frame assembly is lowered to the bottom by winch. Once on the bottom a hydraulic piston regulates the rate of descent of the prism and camera cradle into the bottom. This prevents excessive disturbance of the sediment-water interface. The profile camera is externally triggered on contact with the bottom. Electronic circuits in the camera control the exposure timing to allow the prism to penetrate the sediment after contacting the bottom. Delay times usually range from 1 sec. in soft mud to 15 sec. in hard sand.

#### **3.1.4. Sled**

VIMS Standard Bottom Imaging Sled was deployed with video cameras, and water quality sensors. The sled was towed at <1 knot when possible. This sled system was also deployed with the SPI-Plow (BCD system, see below) attached after the plow-sled had been damaged (Figure 3.1-3). Sled still images had the following dimensions, based upon the camera lens angles and depth above the bottom. The length of the image was about 43 cm, the width of the image was 30 cm, the area was about 1300 cm<sup>2</sup>, or 0.13 m<sup>2</sup>. The sled was towed at 2 to 3 knots when the vessel was under power and as low as 0.8 knots when adrift in order to acquire close-up bottom video and water quality data. The video camera was set obliquely and about 15 cm from the bottom in order to resolve the smaller details of the surface and biological structures. The area viewed by the video camera was a trapezoid about 10 cm along the base line closest to the camera and 40 cm along the other baseline. The field of view was about 0.2 to 0.4 m<sup>2</sup> depending on sled orientation.

The camera was mounted so that the focal plane was 40 cm above the plane of the sled runners, meaning that each image represented an area of 0.13 m<sup>2</sup>, since the lens had been adjusted for close-up focus and the lens angles were 20.6° and 28.5°. Normal lens angles are 35° and 50°.

### **3.1.5. SPI-Plow**

The SPI-Plow, or Burrow-Cutter-Diaz Plowing Sediment Profile Camera System (Cutter and Diaz, 1998) was deployed, only on the 1999 cruise, to acquire continuous video profile images. It was towed at 0.1 to 1.5 knots and subbottom video was recorded onboard. However, the sled superstructure was broken during a tow, was recovered, and the system had to be modified onboard. The plow and camera encasement was then transferred to the standard sled.

### **3.1.6. Sidescan Sonar**

A Marine Sonic Technologies Inc. 600 KHz sidescan sonar towfish and digital acquisition unit were deployed during several of the sled tows and plow drags on the 1999 cruise. Sidescan records were stored on a PC hard drive, then transferred to removable magnetic disk, and archived on CD-ROM.

### **3.1.7. Trawl**

On the 1999 cruise, Rutgers University researchers deployed an eight-foot beam trawl to collect juvenile fish, epibenthos, and megabenthos. Four trawls locations were chosen based upon sled and plow video observations to cover a broad range of sedimentary and biological conditions. Two physically dominated sandy and gravel/shelly habitats with little evidence of biogenic structure were sampled along the northeastern and northwestern sides of Fenwick Shoal and two more biologically accommodated *Diopatra* and *Asabellides* tube field habitats along the southeastern and southwestern sides. At each location four trawls were collected during daylight and four trawls during the night. The trawl was fitted with a meter-wheel to measure the distance trawled so that fish abundance per unit area could be estimated.

## **3.2. Laboratory Methods**

### **3.2.1. Grab**

Samples were rinsed in freshwater over a 500-um sieve and sorted by placing a small amount of the sample in a plastic dish. All organisms, including fragments of worms, were removed and sorted to major taxonomic categories such as polychaetes, crustaceans, molluscs, echinoderms, and other. After samples were sorted, all organisms were identified and enumerated. Identifications were made at the lowest practical taxonomic level (LPTL), usually species. After identification and enumeration all organisms were grouped by LPTL and placed in 2% Formalin until wet weight measurements were completed.

### **3.2.2. SPI**

Slide images were reviewed on a light table, then digitized using a Polaroid Sprintscan 35Plus slide scanner. Images were stored as TIFF files, using no compression, and archived on CD-ROM for later computer image analysis.

### **3.2.3. Sled**

Still images collected from sled tows using the Benthos Deep-Sea Standard Camera were processed the same as SPI images (above). Sled video images were transferred from analog to digital video format. The digital video was then played back at 1/3 speed, and feature determinations, counts, and classifications were done by an observer every 3 seconds, providing 1 second real-speed interval data. Substrate configuration, biological feature occurrence, quantity and type were recorded for each record. Video times were translated to position using DGPS logs recorded onboard. Where position data were missing due to slowed DGPS data-logging, positions were estimated using an average of the two nearest neighbors.

Whereposition data between two images or video analysis sequences were too imprecise to detect a difference, latitude and longitude were adjusted between the two closest reliable points. Adjusted latitude and longitude for the sled and plow transects were estimated using one or two functions. If latitude and longitude values did not change between time intervals, then latitude was adjusted by a cosine function of heading that incorporated velocity, and longitude was adjusted by a sine function of heading that incorporated velocity. If one or more successive positions were missing,

latitude and longitude values from the previous time step were used with a random value added (on the order of 0.000001 degrees).

Still images collected at 15 sec and 60 sec intervals with the standard underwater camera attached to the sled in 1998 were analyzed for features pertinent to substrate and habitat characterization. Seventy-nine images from the 1-minute interval series and 83 images from the 15-second interval series were visually analyzed for habitat features. Most features were accounted for in terms of binary occurrence/absences (1 if present or 0 if absent), and more than one feature may have been present per set, they were not necessarily mutually exclusive. Counts of features in the table represent number per the 0.13 m<sup>2</sup> image area.

Several sets of parameters, listed below, were documented and are presented in the CD-ROM appendix. Maps of the features elucidate the small-scale spatial variation and zonation inherent to the regions studies (Map Atlas).

Set 1 - Sediment Type. Presence/Absence of:

- Silt (SI)
- Very Fine Sand to Fine Sand (VFSFS)
- Medium Sand to Coarse Sand (MSCS)
- Gravel (GR)
- Shell Fragments (SHFR)
- Large Shell Parts or Whole Shells (SHLG)

Set 2 - Bed Type. Presence/Absence or Predominance of:

- Bedforms; Wave or Current Ripples (Bedf)
- Burrowed
- Tracked
- Small Tubes
- Large Tubes (LgTubes)
- Tube Bed or Mat (TubeBed)

Set 3 - Surface Variance. Image brightness pattern properties induced by primary bottom features:

- Uniform
- Graded
- Split
- Periodic
- Heterogeneous (HETERO)

Set 4 - Roughness. Primary origins of roughness (equivalent contribution by more than one feature led to some cases where more than one parameter would be attributed responsibility):

- Small Ripples (SMALLRIPP)
- Large Ripples (LARGERIPP)
- Biogenic Structures, *e.g.* tubes (BIOSTRUCT)
- Evidence of Biogenic Activity, *e.g.* tracks (BIOACTIV)
- Sediment Grains or Shells (GRAINorSH)
- Unstructured; perhaps heterogeneous, or a surface in transition (UNSTRUCTURED)

Set 5 - Live Biology (LiveBiol); epifauna or structures attributable to certain infauna. Presence or Absence of:

- *Asabellides oculata* tubes (Asabellides)
- *Diopatra cuprea* tubes (Diopatra)
- Other Polychaete tubes (OtherPoly)
- Crustaceans, typically *Cancer* crabs (Crust)
- Hermit Crabs or Gastropods; shell inhabitants indiscernible (HermCrabORGast)
- Gastropods; discernible (Gast)
- Bivalves (Biv)
- Echinoderms; sea stars or sand dollars (Echin)
- Ascidiaceans; tunicates (Ascidiacean)
- Fish
- Other

#### **3.2.4. Video Image Analysis Data**

Expanding upon the analysis concept used for the 1998 still images, video acquired from sled tows during the 1998 and 1999 deployment were visually analyzed at one second intervals. Substrate, invertebrate fauna/biological features, and fish were classified into categories for each second of video, played at one-third speed. Substrates were classified in terms of visible physical characteristics:

Set 1 - Physical Characteristic Classes (SediHabi)

1. Sharp crested ripples, wavelength greater than video field of view, bedform crest

- straight, no secondary ripples.
2. Sharp crested ripples, wavelength greater than video field of view, bedform crest straight, secondary ripples asymmetrical.
  3. Sharp crested ripples, wavelength greater than video field of view, bedform asymmetric, secondary ripples asymmetrical.
  4. Smooth crested ripples, wavelength greater than video field of view, no secondary ripples.
  5. Smooth crested ripples, wavelength less than video field of view, no secondary ripples.
  6. Smooth crested ripples, wavelength less than video field of view, secondary ripples asymmetrical.
  7. Sandy bottom, bedforms not apparent
  8. Uneven bottom, likely biogenic; or outcrops.

#### Set 2 - Biogenic Structure Classes (BiogHabi)

1. No biology apparent.
2. Occasional single tube or organism.
3. Small patches of tubes or organisms.
4. Large patches or fields of tubes.
5. Dense tube beds or tube mats.

Maps of the physical and biological habitat feature classes can be found in the Map Atlas and on the CD-ROM as file “9899sledviddata-final.dbf” that can be accessed via the GIS projects.

In addition to habitat classifications, each fish observed in the video from 1999 was reviewed at slow speed until species, or lowest practical taxonomic level, identification could be determined by K. Able, Rutgers University. Maps for the dominant benthic fish species collected in trawls, and seen in video, are presented in the Map Atlas.

#### **3.2.4.1. SPI-Plow**

SPI-Plow videos were reviewed in the lab, transferred to digital videotape, and archived onto CD-ROM.

#### **3.2.5. Trawl**

Fish and invertebrates collected in trawls were emptied into large container on-deck, sorted to major taxa, counted and recorded, and preserved in formalin for laboratory processing and identification. In

the laboratory, preserved fish and invertebrates were identified to species or lowest practical taxonomic level, weighed, and measured. Gut content analysis was performed on the three most abundant fish; *Urophycis regia*, *Etropus microstomus*, and *Prionotus carolinus*. Guts were removed and stored in ethanol. Gut contents were sorted to major taxa, and where possible to the generic level. Contents were enumerated and wet weight biomass determined by major taxa.

### **3.2.6. Sidescan Sonar**

Sidescan records stored on magnetic disk were transferred to CD-ROM for archive along with the program for reviewing the sonar image records.

### **3.2.7. Position Data**

Position data for point and transect interval samples are provided in the and continuous transect logs are provided in digital form on the CD-ROM Appendix.

### **3.2.8. Grab Sample Substrate Data**

Sediment grain-size distributions and sand fraction distributions were determined by VIMS Analytical Services Laboratory. Sand:silt:clay ratios were using standard techniques and sand size fractions were measured using a Rapid Sediment Analyzer.

### **3.2.9. Grab Sample Biological Data**

#### **3.2.9.1. Preliminary Data Treatment**

Prior to performing any of the analyses of the 1998 and 1999 benthic data several modifications to the station by species matrix were made. The purpose of these modifications was to remove bias that would result in calculation of diversity and similarity indices from either inflated number of taxa, which in fact likely do not represent different species and represented identification problems, or species that were not representatively sampled by the Young grab, or species not properly sampled by the Young grab such as mobile epifauna. First, several non-infaunal mobile taxa were excluded, such as hermit crabs (genus *Paguras*) because of their potential ability to avoid capture by grab. Second, questionable taxa, such as Unidentified Bivalve, were excluded. Taxa in this group were either very

small or fragmented individuals. Third, data for some taxa were pooled. Usually this involved pooling data for a taxon identified to a level higher than species (*e.g.*, genus) with those data for a species within the higher taxon. This pooling was done only when a single species of the genus was identified. For example, *Lumbrinerides dayi* (a polychaete) was the only species of the genus found, so any polychaetes identified only to the genus *Lumbrinerides* were treated as if they were *L. dayi*. In most cases the species could not be determined on these organisms because they were small, immature individuals or key taxonomic structures, like antennae or palps, were missing. Fourth, data for some species were pooled to a higher level taxon, usually genus, because more than one species of a genus was identified and many small or immature individuals could not be identified beyond the genus level. For example, two species of the bivalve genus *Astarte* were found, *castanea* and *nana*, but about 25% of all *Astarte* could not be speciated. Therefore, *A. castanea* and *A. nana* were combined into the genus *Astarte*. This fourth data reduction strategy would bias diversity and similarity indices in the opposite direction of the first three and was only applied to six genera (*Ampelisca*, *Astarte*, *Nucula*, *Nephtys*, *Pseudeurythoe* and *Tellina*). Fifth, several species were not consistently sorted from the samples and were dropped. These included three species of small ascideans (sea squirts or grapes) that closely resembled grains of sand and one very small polychaete (*Spirorbis* sp.) that builds a thin calcareous tube on sand grains. One sorter did not recognize these four species.

### 3.2.9.2. Community Analysis

Diversity and community structure calculations were done with the program PRIMER (Carr, 1997). PRIMER (Plymouth Routines in Multivariate Ecological Research) is a series of programs developed at the Plymouth Marine Laboratory, United Kingdom, for analysis of benthic community data. Information on PRIMER can be found at <http://www1.npm.ac.uk/primer/>. Magurran (1991) describes all of the diversity indices used here. Shannon's  $H'$  was calculated by using  $\log_2$ :

$$H' = - \sum p_i (\log p_i)$$

Where  $p_i$  is the proportion of the total counts arising from the  $i^{\text{th}}$  species. Comparisons of  $H'$  with other studies must be done with caution, for two reasons; first,  $H'$  can also be calculated using Napierian logarithms or  $\log_{10}$  and, second, different sized samplers are affected by species-area relationships, larger grabs collect more species than smaller samplers.

Species richness was expressed at the total number of species in a sample (S) and Margalef's index (d):

$$d = (S-1) / \log N$$

which also incorporates that total number of species present for a given number of individuals (N).

Equitability of species distribution among individuals was expressed using two measures. Pielou's evenness index that expresses how evenly the individuals are distributed among the different species:

$$J' = H' / \log S$$

where  $\log S$  represents the maximal possible diversity that would be achieved if all species were equally abundant in a sample. Simpson's dominance index (SI) that expresses dominance of individual species in a sample, essentially the reverse of evenness:

$$SI = \sum p_i^2$$

Cluster analyses were performed with the program COMPAH96 (currently available on E. Gallagher's web page, <http://www.es.umb.edu/edgwebp.htm>) originally developed by at the Virginia Institute of Marine Science in the early 1970's. The sample and species clusters were generated using flexible sorting with  $\hat{\alpha}$  of -0.25 and Bray-Curtis similarity, also known as Pielou's (1984) percentage similarity, calculated from simultaneous standardization of abundance (Boesch 1977):

$$Y = X / \%(\text{sample total} * \text{species total})$$

where Y is the standardized value of abundance (X). Any taxa that was present in three or fewer grabs was eliminated from the cluster analysis. This resulted in a combined total of 73 of 166 total taxa being dropped for both years.

Results of the station and species clusters were compared using nodal analysis, which examines the original data matrix rearranged into a two-way table based on the cluster defined groups. Constancy, a measure of the association of species with stations (Fager 1963), was calculated from the nodal table based on the proportions of the number of occurrences of species in the station group to the total possible number of such occurrences (Boesch 1977):

$$C_{ij} = a_{ij} / (n_i n_j)$$

where  $a_{ij}$  is the actual number of occurrences of members of species group  $i$  in station group  $j$ ,  $n_i$  is the total number of species in group  $i$ , and  $n_j$  is the number of stations in group  $j$ . Constancy will range from 0.0 when none of the species in a species group occurred in a station group to 1.0 when all of the species in a species group occurred in all of the stations of a station group. Fidelity, a measure of the constancy of species in a station group compared to the constancy over all station groups (Fager 1963), was used to indicate the degree to which species prefer station groups (Boesch 1977):

$$F_{ij} = (a_{ij} n_j) / (n_j a_{ij})$$

where  $a_{ij}$  and  $n_j$  are the same as defined for the constancy index. Fidelity is 1.0 when the constancy of a species group in a station group is equal to its overall constancy,  $>1.0$  when its constancy in a station group is greater than that overall, and  $<1.0$  when its constancy is less than its overall constancy. Values of  $F >2.0$  suggest strong preference of species for a station group and values  $<0.7$  suggest avoidance of these species from the station group in question (Boesch 1977).

### 3.2.10. Image Analysis: SPI and Sled Still

Digitized images were analyzed visually on computer screen and digitally using NIH Image (*NIH*, public domain), Image Pro Plus® (*Media Cybernetics*), and Adobe® Photoshop® with the Image Processing Toolkit© (*Reindeer Games*). Feature counts were made visually and linear and areal feature measurements were made digitally, by direct application of measurement tools and by spatially calibrated grid overlays. A brief description of major image parameters follows:

**Prism Penetration** - This parameter provided a geotechnical estimate of sediment compaction with the profile camera prism acting as a dead weight penetrometer. The further the prism entered into the sediment the softer the sediments, and likely the higher the water content. Penetration was measured as the distance the sediment moved up the 23-cm length of the faceplate. The weight on the camera frame was kept constant at 341 kg (750 lbs.) so prism penetration provided a means for assessing the relative compaction between stations.

**Surface Relief** - Surface relief or boundary roughness was measured as the difference between the maximum and minimum distance the prism penetrated and provided qualitative and

quantitative data on habitat characteristics which can be used to evaluate existing conditions. This parameter also estimated small-scale bed roughness, on the order of the prism faceplate width (15 cm). The causes of roughness can often be inferred from visual analysis of the film images and video.

**Apparent Color Redox Potential Discontinuity (RPD) Layer** - This parameter has been determined to be an important estimator of benthic habitat quality (Rhoads and Germano 1986, Diaz and Schaffner 1988), providing an estimate of the depth to which sediments appear to be oxidized. The term apparent was used in describing this parameter because no actual measurement was made of the redox potential. An assumption was made that, given the complexities of iron and sulfate reduction-oxidation chemistry, reddish-brown sediment color tones (Diaz and Schaffner 1988), or in black and white images whiter or lighter areas of the image (Rhoads and Germano 1986), were indications that the sediments were oxic, or at least are not intensely reducing. This is in accordance with the classical concept of RPD depth, which associates it with sediment color (Fenchel 1969, Vismann 1991).

The depth of the apparent color RPD was defined as the area of all the pixels in the image discerned as being oxidized divided by the width of the digitized image. The area of the image with oxic sediment was obtained by digitally manipulating the image to enhance characteristics associated with oxic sediment (greenish-brown color tones). The enhanced area was then determined from a density slice of the image.

The apparent color RPD has been very useful in assessing the quality of estuarine and coastal embayment habitats for epifauna and infauna from both physical and biological points of view. Rhoads and Germano (1986), Diaz and Schaffner (1988), Valente *et al.* (1992), Nilsson and Rosenberg (1997) and Bonsdorff *et al.* (1996) all found the depth of the RPD from profile images to be directly correlated to the quality of the benthic habitat in polyhaline and mesohaline estuarine zones. Controlling for differences in sediment type, habitats with thinner RPD's (mm's) tend to be associated with some type of environmental stress. While, habitats with deeper RPD's (cm's) usually have flourishing epibenthic and infaunal communities.

**Sediment Grain-size** - Grain-size is an important parameter for determining the nature of the physical forces acting on a habitat and is a major factor in determining benthic community structure (Rhoads 1974). The sediment type descriptors used for image analysis follow the Wentworth classification as described in Folk (1974) and represent the major modal class for each image. Grain-size was determined by comparison of collected images with a set of standard images for which mean grain-size had been determined in the laboratory

**Surface Features** - These parameters included a wide variety of features. Each gives a bit of information on the type of habitat and its quality for supporting benthic species. The presence of certain surface features is indicative of the overall nature of a habitat. For example, bedforms are always associated with physically dominated habitats, whereas the presence of worm tubes or feeding pits would be indicative of a more biologically accommodated habitat (Rhoads and Germano 1986, Diaz and Schaffner 1988). Surface features were visually evaluated from each slide and compiled by type and frequency of occurrence.

**Subsurface Features** - These parameters included a wide variety of features and revealed a great deal about physical and biological processes influencing the bottom. Surface features were visually evaluated from each slide and compiled by type and frequency of occurrence.

**Successional Stage** - Sediment profile data have also been used to estimate successional stage of the fauna (Rhoads and Germano 1986). Characteristics associated with pioneering or colonizing (Stage I) assemblages (in the sense of Odum 1969), such as dense aggregations of small polychaete tubes at the surface and shallow apparent RPD layers, were easily seen in sediment profile images. Advanced or equilibrium (Stage III) assemblages also have characteristics that were easily seen in profile images, such as deep apparent RPD layers and subsurface feeding voids. Stage II is intermediate to I and III, and has characteristics of both (Rhoads and Germano 1986). A group of SPI parameters are evaluated to determine successional stage (- = not associated with, + = associated with, +++ = strongly associated):

Successional Stage

Parameter	I	II	III
Average RPD (cm)			<1 1-3 >2
Max depth RPD (cm)			<2 >2 >4
Small Tubes			+++ ++ +
Large Tubes			- ++ +++
Burrows			- ++ +++
Feeding Voids			- + +++
Small Infauna			+++ ++ +
Large Infauna			- + ++
Epifauna			+ ++ ++

**Organism-Sediment Index** - Rhoads and Germano (1982, 1986) developed the multi-parameter organism-sediment index (OSI), from data provided by the sediment profile images, to characterize benthic habitat quality. The OSI defines quality of benthic habitats by evaluating images for depth of the apparent RPD, successional stage of macrofauna, the presence of gas bubbles in the sediment (an indication of high rates of methanogenesis), and the presence of reduced sediment at the sediment-water interface. The following parameter ranges and scores are used in the calculation of the OSI (taken from Rhoads and Germano 1986):

Depth of the apparent color RPD:	Estimated successional stage:
0 cm	Azoic -4
>0-0.75	I 1
0.76-1.50	I-II 2
1.51-2.25	II 3
2.26-3.00	II-III 4
3.01-3.75	III 5
>3.75	I on III 5
	II on III 5
Methane voids present	-2
No/Low DO	-4

The OSI ranges from -10, poorest quality habitats, to +11, highest quality habitats. The OSI has been used in estuarine and coastal bay systems to map disturbance gradients (Valente *et al.*, 1992) and to follow ecosystem recovery after disturbance abatement (Rhoads and Germano 1986). OSI values >6 are generally associated with habitats that have well developed infaunal communities.

**BHQ** – The Benthic Habitat Quality index of Nilsson and Rosenberg (1996) was calculated

from the SPI data. The BHQ was developed to evaluate benthic habitat quality in Scandinavian fjords and is based on biogenic structures seen in the SPI images that relate to infaunal successional stage as described by Pearson and Rosenberg (1978). The BHQ is calculated from three basic groups of data derived from SPI images: surface structures, subsurface structures, and mean depth of apparent RPD (see Table 1 in Nilsson and Rosenberg, 1996). The BHQ ranges from 0 to 16 in its original formulation. Nilsson and Rosenberg (1996) related the BHQ to successional stage as follows:

Successional Stage	BHQ
0	<2
I	2 - 4
II	5 - 10
III	>10

BHQ values greater than or equal to 5 should then indicate good quality benthic habitat.

### **3.2.11. Regional Condition Data**

#### **3.2.11.1. NOAA Buoy Data**

Historical surface water temperatures from 1998 and 1999 were obtained from NOAA buoy 44009, through the website [http://www.ndbc.noaa.gov/station\\_history?\\$station=44009](http://www.ndbc.noaa.gov/station_history?$station=44009).

### **3.2.12. Habitat Classification and Biological Resource Information**

#### **3.2.12.1. Indices and Derived Statistics**

Calculation of the OSI index is based upon mean depth of the RPD layer, presence or absence of methane gas voids, evidence of hypoxia or anoxia, and successional stage (Rhoads and Germano, 1986). The OSI was abandoned because successional stages were indeterminate for most of the SPI images and because the RPD depths observed exceeded the range provided for calculation of the OSI was insufficient for most of the sediments sampled. The Benthic Habitat Quality index is based upon the RPD and upon surface and subsurface biogenic features (Nilsson and Rosenberg, 1997). Although the RPD scale designated by the BHQ discriminates levels as deep as 5 cm, it did not accommodate most RPD's observed from the SPI images collected. Since the BHQ is image feature-based, as opposed to estimation based OSI, it was calculated for the MD/DE SPI database. Although many of the biological features were sparse, enough were evident to justify use of the BHQ. Since the RPD parameterization did not support the range of RPD's observed in these shelf sediments, we modified the

BHQ to accommodate observed RPD variable ranges in order to provide a more generally applicable biological resource index based upon sediment profile image data.

We call the new index SBHQ, for Scaled Benthic Habitat Quality index. It is scaled in the sense that RPD values are parameterized after adjustment for generalized sediment class, consolidation and predicted permeability based upon compaction and compressibility. The other parameters involved in calculation were maintained. For the SBHQ, scaling of the RPD incorporated three related variables: gross sediment type (determined visually) and sediment compaction (derived from sediment type), and prism penetration. As part of the index calculation, certain criteria had to be met by variables involved. Prism penetration was compared to a threshold value determined by the value of the 75% quartile of all penetrations measured divided by the compaction rating. The compaction rating was determined from sediment type. Sediment type classes were grouped into the classes mud, muddy-fine, fine, muddy-coarse, and coarse. Sediment compaction (inversely related to prism penetration) is usually indicative of compressibility, and varies non-linearly with sediment type, tending to be low for mud, high for fine to medium sands, and moderate for coarse sediments (Figure 3.2-1).

Because of that, compaction ratings ( $C_p$ ) were applied as follows:

$$C_{p_{\text{mud}}} = 1, C_{p_{\text{muddy-fine}}} = 1.5, C_{p_{\text{fine}}} = 3, C_{p_{\text{muddy-coarse}}} = 2.5, \text{ and } C_{p_{\text{coarse}}} = 2$$

Then, the threshold penetration value ( $z$ ) was set at the overall 75% quartile value divided by  $C_p$ , for each sample based upon each sample's sediment class. For example, if the 75% quartile for penetration was 10 cm, and the sediments were coarse grained ( $C_p=2$ ), threshold penetration value would be 5 cm. If penetration exceeded the threshold value, in this example 5 cm, and if RPD was determinable, then the SBHQ index was calculated using the discrete feature count categories of the BHQ and a scaled RPD. Penetration thresholds were applied because RPD depth is related to the permeability, which is related to sediment compaction, consolidation, and sediment type, and therefore, without respect to biological effects, should be deeper in certain sediments. If prism penetration was insufficient in a particular case, then RPD depths could not be assessed quantitatively or qualitatively (*e.g.* observed RPD versus ideal RPD), therefore that case would not be considered.

The RPD was scaled using the following logic. If penetration exceeded threshold penetration, for each compaction rating, and if RPD exceeded 50% of the actual penetration, scaled RPD was calculated as  $(1/C_p)*RPD$ . If RPD was less than 50% of the actual penetration but greater than 10% of the actual penetration, scaled RPD was calculated as  $(1/3.3*C_p)*RPD$ . If RPD was less than 10% of the actual penetration but greater than zero, scaled RPD was calculated as  $(1/33*C_p)*RPD$ . If RPD was zero, scaled RPD was zero. Scaled RPD values are not restricted to an absolute range, nor are they categorized, therefore the SBHQ is also not restricted. However, since they are a function of penetration depth and adjusted by sediment type, scaled RPD values are more applicable across habitats and ecosystems, potentially facilitating system comparisons. Also, since Scaled RPD is adjusted for the effects of physical advection of porewater by accounting for sediment class and compaction, the parameter should reveal where biological influence upon RPD is relevant.

### 3.2.12.2. Secondary Production

Estimates of secondary production were made from the grab samples using the model developed by Tumbiolo and Downing (1994). This model incorporates basic life history information on the species and the influence of environmental parameters (temperature and depth) to predict the level of secondary production. Parameters in the model are:

$$\text{Log } P = 0.24 + 0.96\text{Log } B - 0.21\text{Log } W_m + 0.03 T_s - 0.16\text{Log } (Z+1)$$

were  $P$  is annual production in g Dry Weight (DW)  $\text{m}^{-2} \text{y}^{-1}$ ,  $B$  is average biomass in g DW  $\text{m}^{-2}$ ,  $W_m$  is the maximum individual body mass in mg DW,  $T_s$  is annual mean bottom temperature in  $^{\circ}\text{C}$ , and  $Z$  is depth in m.  $W_m$  should be interpreted as the maximum size reached by the populations in the study area and not the maximum size ever recorded. Because most individuals are small and published maximum body mass for shallow continental shelf fauna are few, we estimated  $W_m$  from the size of the individuals in the grab samples and applied conversion factors to taxonomic groups that most likely represented the maximum size for shallow shelf fauna in the study area. Polychaete maximum individual size was estimated to be a factor of five over the mean individual weight, bivalves and gastropods a factor of two, and all other groups were given a factor of one.

The wet weight biomass of each species from the grab samples was converted to dry weight

mass based on conversion constants in Waters (1977) and Rainer (1982):

$$\text{Dry Weight} = 0.16 \text{ Wet Weight}$$

In general, conversion of various units of biomass to energy is possible because production is primarily a physiological process that is similar for a broad range organisms from bacteria to mammals (Banse and Mosher, 1980). For example, organic carbon is related to other units as follows:

$$1 \text{ g C} = 10 \text{ g Live} = 12.5 \text{ g wet} = 2 \text{ g Dry} = 1.9 \text{ g AFDW} = 20 \text{ g N} = 0.004 \text{ g ATP} = 2.7 \text{ Kcal}$$

For calculation of production, 12 major taxonomic groups were considered. Species and taxa groups that were not quantitatively surveyed by the garb sampling were not considered, such as decapods and echinodrems, even though they contributed significantly to overall community production. Both sled video and trawl samples indicated decapods and to a lesser extent echinoderms were common throughout the study area. Thus our secondary production estimates should be considered total macroinfaunal production.

### **3.2.12.3. Mapping**

#### **3.2.12.3.1. Point Maps**

Point feature maps were produced using ESRI ArcView versions 3.1 and 3.2. Separate maps were produced for the three Fenwick Shoals ROI's and the two Indian River ROI's. Maps are at 1:45000 scale, unless otherwise specified.

#### **3.2.12.3.2. Spatial Interpolation**

IDW techniques - Two-dimensional interpolations of point feature data were mapped using inverse distance weighted squared technique with ArcView and the Spatial Analyst extension. Fenwick Shoals (FS) grid surfaces were created using 56 by 36 cell grid, with cell sizes of 0.0024 by 0.0024 degrees, and no correction for projection. Indian River (IR) grid surfaces were composed of 56 by 30 cells, with cell sizes of 0.0024 by 0.0024 degrees, and no correction for projection. Each cell is approximately 265 m north-south by 210 m east-west.

#### **3.2.12.3.3. Kriging**

Maps interpolated using ordinary kriging were produced using ArcView and the Avenue™ Script MB.View.SpatialKriging (Boeringa, 1998) available from the ESRI website. FS kriged surfaces were composed of 69 by 36 cells, with cell sizes of 216.13 \* 216.13 m, upon a Lambert Conformal Conic projection. IR data were not kriged.

#### **3.2.12.3.5. Cokriging**

Cokriging estimates were produced using WinGSLIB(c) and GSLIB(c) routines (*Staios* LLC: <http://www.staios.com>) (Deutsch and Journel, 1998). Model parameters used for cokriging varied and are included with the resultant maps.

## **CHAPTER 4. RESULTS**

### **4.1. Grab Sample Substrate Data**

Sediment grain-sizes determined from grab subsamples indicated that the IR regions contained larger grained sediments than the FS regions (Table 4.1-1). Sediments from 11 of the 14 IR grab stations for which grain-size analysis was done, consisted of over 10% gravel (grain diameter >2 mm), and six of those had over 20% gravel (Figure 4.1-1). Only four of the 36 FS grab stations for which grain-size analysis was done, had sediments composed of over 10% gravel, and all were less than 20% gravel. Seven of the FS grab stations had slightly muddy sediments (clay + silt > 1%), and four of those had muddy (>2%) sediments. Whereas, three of the IR grab stations had slightly muddy sediments, and only one had muddy sediments (Table 4.1-1 and Figure 4.1-1).

From the sand fraction only, FS grab stations had a mean sand grain-size of 0.42 mm (SD  $\pm$  0.19), and IR grab stations had a mean sand grain-size of 0.52 mm ( $\pm$  0.17) (Table 4.1-2).

### **4.2. Grab Sample Biological Data**

#### **4.2.1. Biological Data - Descriptive Summaries**

##### **4.2.1.1. 1998**

##### **4.2.1.1.1. Abundances**

Among the 52 samples collected in May 1998, a total of 10,634 infaunal individuals representing 152 taxa were found (1998 data appendix). Infaunal abundance varied about 780-fold, ranging from 4 to 3,108 individuals/0.04 m<sup>2</sup> (90 to 70,600/m<sup>2</sup>). Lowest abundance occurred at stations FS10.5D and FS12E, and highest at station FS01G (Table 4.2-1). Mean ( $\pm$ 95% confidence interval, CI) abundance from all samples collected in 1998 was 204 ( $\pm$ 129) individuals/0.04 m<sup>2</sup> and the median was 78 ( $\pm$ 42) individuals/0.04 m<sup>2</sup>. The large difference between the mean and median was a function of the underlying non-normal distribution of abundance and three outlier stations with high abundance (FS01G, HCS31, and FS04C).

Annelid worms were the most abundant major infaunal taxon among the May 1998 samples followed by molluscs and crustaceans (Table 4.2-2). Annelids accounted for >75% of the infauna at 19 stations, with highest percentages, >90%, at three stations (Table 4.2-3). Molluscs were the overall second

highest contributors to infaunal abundance and were >50% of the infauna at two stations. Crustaceans, the third most abundant major taxon, were only relatively important contributors, >50%, at seven stations with low total infaunal abundance, <40 individuals/0.04 m<sup>2</sup>. None of the other major taxa was an important contributor to abundance. At a slightly finer taxonomic scale, oligochaetes were 15% of the annelids and polychaetes 85%, gastropods were 3% of the molluscs and bivalves 97%, and amphipods were 60% of the crustaceans.

#### **4.2.1.1.2. Number of Species**

The total number of species per sample collected in May 1998 varied about 10-fold, ranging from 3 to 35 at station FS10.5D and IR04E, respectively (Table 4.2-4). Mean ( $\pm$ 95% CI) number of species from all samples collected in 1998 was 17.8 ( $\pm$ 4.4) and the median was 17 ( $\pm$ 5) species per sample.

Among the major taxa collected in May 1998, overall, annelid worms contributed the highest percentage of species (Table 4.2-5). Annelids accounted for from 0 to 85% of the species collected at each station. Crustaceans and molluscs accounted for about 22-23% of the species, overall, and 0 to about 50% of the species on an individual station bases. Within each of their respective major taxa, polychaetes, amphipods, and bivalves provided the greatest contribution to species numbers.

#### **4.2.1.1.3. Biomass**

Among the 52 samples collected in May 1998, representing 10,634 infaunal individuals, total wet weight biomass was 214.8 g (1998 biomass data appendix). Biomass varied by over 6,000-fold, ranging from 14 mg to 88.6 g wet/0.04 m<sup>2</sup> (0.3 to 2,000 g wet/m<sup>2</sup>). Lowest biomass occurred at station FS10.5D and highest at IR05D (Table 4.2-6). Mean ( $\pm$ 95% confidence interval, CI) biomass from all samples collected in 1998 was 4.1 ( $\pm$ 4.5) g wet/0.04 m<sup>2</sup> and the median was 0.2 ( $\pm$ 0.07) g wet/0.04 m<sup>2</sup>. The large difference between the mean and median was a function of the underlying non-normal distribution of biomass and outlier stations that contained large individuals, most of which were molluscs, such as stations IR05D and IR05.5C (Table 4.2-6).

Molluscs made up most of the biomass in the May 1998 samples accounting for about 87% of

the total biomass. The second highest contribution to biomass was from polychaetes, about 6%. Gastropods and amphipods were about 3% and 1%, respectively (Table 4.2-7). All other taxa contributed about 3% of the total biomass.

#### **4.2.1.2. 1999**

##### **4.2.1.2.1. Abundances**

Among the 20 samples collected in June 1999, a total of 6,145 infaunal individuals representing 108 taxa were found (1999 data appendix). Infaunal abundance varied about 130-fold, ranging from 10 to 1,336 individuals/0.04 m<sup>2</sup> (230 to 30,400/m<sup>2</sup>). Lowest abundance occurred at station FS12E, and highest at station FS04C (Table 4.2.1). Mean ( $\pm 95\%$  CI) abundance from all samples collected in 1999 was 307.2 ( $\pm 162.8$ ) individuals/0.04 m<sup>2</sup> and the median was 87.5 ( $\pm 75.4$ ) individuals/0.04 m<sup>2</sup>. The large difference between the mean and median was a function of the underlying non-normal distribution of abundance and outlier stations with high density.

Annelid worms were the most abundant major infaunal taxon among the June 1999 samples followed by crustaceans and molluscs (Table 4.2-2). Annelids accounted for >80% of the infauna at four stations, with highest percentage of about 87% at station FS07B2 (Table 4.2-3). Crustaceans and molluscs were about equal contributors to infaunal abundance and were >50% of the infauna at three and five stations, respectively. None of the other major taxa was an important contributor to abundance. At a slightly finer taxonomic scale, oligochaetes were 8% of the annelids and polychaetes 92%, gastropods were 8% of the molluscs and 92% bivalves, and amphipods were 92% of the crustaceans.

##### **4.2.1.2.2. Number of Species**

The total number of species per sample collected in June 1999 varied about 7-fold, ranging from 6 to 40 at station FS04E and FS07B2, respectively (Table 4.2-4). Mean ( $\pm 95\%$  CI) number of species from all samples collected in 1999 was 20.4 ( $\pm 4.6$ ) and the median was 18.5 ( $\pm 6$ ) species per sample.

Among the major taxa collected in June 1999, overall, annelid worms contributed the highest

percentage of species (Table 4.2-2). Annelids accounted for from 0 to 65% of the species collected at each station. Crustaceans and molluscs accounted for about 20-21% of the species, overall, and <5 to about 60% of the species at each station (Table 4.2-5). Within each of their respective major taxa, polychaetes, amphipods, and bivalves typically provided the greatest contribution to species numbers.

#### **4.2.1.2.3. Biomass**

Among the 20 samples collected in June 1999, representing 6,145 infaunal individuals, total wet weight biomass was 214.8 g (1998 biomass data appendix). Biomass varied by over 6,000-fold, ranging from 14 mg to 88.6 g wet/0.04 m<sup>2</sup> (0.3 to 2,000 g wet/m<sup>2</sup>). Lowest biomass occurred at station FS10.5D and highest at IR05D (Table 4.2.6). Mean ( $\pm 95\%$  confidence interval, CI) biomass from all samples collected in 1998 was 4.1 ( $\pm 4.5$ ) g wet/0.04 m<sup>2</sup> and the median was 0.2 ( $\pm 0.07$ ) g wet/0.04 m<sup>2</sup>. The large difference between the mean and median was a function of the underlying non-normal distribution of biomass and outlier stations that contained large individuals, most of which were molluscs, such as stations IR05D and IR05.5C (Table 4.2-6).

Molluscs made up most of the biomass in the June 1999 samples accounting for about 64% of the total biomass. The second highest contribution to biomass was from polychaetes, about 24%. Amphipods and gastropods were 6% and 3%, respectively (Table 4.2-7). Cephalochordates were about 1% of the biomass and all other taxa contributed about 2% of the total biomass.

### **4.2.2. Biological Data - Community Structure and Function**

#### **4.2.2.1. Diversity and Evenness**

As measured by the Shannon index ( $H'$ ), diversity among individual stations collected in May 1998 varied from 0.44 at station FS01G to 4.00 at station IR04B (Table 4.2-8). Species Richness (SR), Evenness ( $J'$ ), and Simpson Dominance ( $d$ ) among stations ranged widely from about 1.0 to 4.1, 0.1 to 1.0, and 0.1 to 0.9, respectively. As diversity increased, SR ( $r = 0.78$   $p = <0.001$ ) and  $J'$  ( $r = 0.51$   $p = <0.001$ ) also increased while  $d$  ( $r = -0.91$   $p = <0.001$ ) declined.

Diversity among individual stations collected in June 1999 varied from 1.70 at station FS10B to 4.00 at station FS08D (Table 4.2.8). Species Richness (SR), Evenness ( $J'$ ), and Simpson Dominance

(d) among stations ranged widely from about 1.0 to 4.1, 0.1 to 1.0, and 0.1 to 0.9, respectively. As in May 1998, diversity in June 1999 was correlated to SR ( $r = 0.68$   $p = 0.001$ ),  $J'$  ( $r = 0.54$   $p = 0.013$ ), and  $d$  ( $r = -0.89$   $p = <0.001$ ). At station FS07B the three replicate grabs, collected to evaluate within-station variation, had very consistent diversity values (Table 4.2.8).

#### **4.2.2.2. Numbers of Taxa and Species**

The total number of taxa from May 1998 and June 1999 included in the analysis of infauna was 166. Criteria for inclusion are described in the methods (Section 3.2.10.1 Preliminary Data Treatment). In May 1998, 152 taxa were collected and 102 in the June 1999 collections. The majority of taxa were identified to species level (141 species in the 166 taxa collected). Of the 25 non-species taxa 19 were at the generic level and the other 6 at higher taxonomic levels, such as Oligochaeta. The lower number of taxa in the June 1999 collections reflects the strong species-area relationship known to exist in marine systems (Sanders, 1968; Hurlbert 1971). In general, the larger the area sampled the more species encountered, up to an asymptotic level that would characterize the total species diversity for a system. The distribution of individuals among the species followed the classical log-normal distribution of species occurrence (Hurlbert, 1971). The majority of species, about 54%, occurred in fewer than five of the 72 stations occupied (Figure 4.2-1).

#### **4.2.2.3 Cluster Analysis**

Cluster analysis of the 1998 and 1999 infaunal data, all 72 grab stations, segregated the stations into five dissimilar groups, which were subdivided into a total of 11 subgroups (Figure 4.2-2), and species into six dissimilar groups (Figure 4.2-3).

The basic patterns in both cluster analyses appeared to be controlled by species-habitat or species-sediment preferences. Year to year difference among the stations was minimal with only a subset of station group D being exclusively composed of 1999 stations. Subgroup D' was composed of five stations from Fenwick Shoals that were all sampled in 1999. An analysis of only the 18 stations sampled both in 1998 and 1999, using the same methods, yielded four dissimilar groups none of which were composed of stations from a single year (Figure 4.2-4). For 15 of these 18 stations, both years

occurred within the same cluster group indicating a strong qualitative and quantitative similarity of fauna between years. Stations FS12F and FS13F split years between cluster groups primarily due to quantitative differences between species present, variation in numbers of the same species. Station FS08E split years due to qualitative differences with a doubling of species from 1998 to 1999.

Station group A, from the combined analysis of all data (Figure 4.2-2), was the largest group being composed of 28 stations from the BB, IR, and FS areas. Group A stations had high species richness (SR) but low total abundance. Median and mean Shannon diversity,  $H'$ , was highest for station group A (Figure 4.2-5). A posteriori contrast of richness, however, did not find station group A to be significantly different for other high species richness groups (groups B and E) but did find group A to be significantly higher than lower richness groups C and D. Three stations from group A (BB04, FS10B, and IR09C) had low  $H'$  due to low evenness,  $J'$ , and a high degree of dominance,  $d$ , of a few taxa such as oligochaetes and *Brania wellfleetensis*. These three stations consistently appear in Figure 4.2.5 as outliers in the  $H'$ ,  $J'$ , and  $d$  boxplots. The last two stations to join group A (FS10B and FS12B) were weakly associated with other stations in group A and had lower  $H'$ ,  $J'$ , and SR (Table 4.2.8).

Station group B was composed of eight FS stations similar in characteristics to group A, except group B while having similar total species occurrence had lower SR and  $H'$ . Group C was composed of three FS stations and represented areas with lowest total abundance and species occurrence, SR, and  $H'$ . Group C had high  $J'$  and highest  $d$  of all station groups. Station group D was composed of 11 stations (10 from FS and one from IR) with low abundance and intermediate values for most of the other community structure measures, including numbers of species, SR,  $H'$ , and  $d$ . The only exception was station FS04C, which was an outlier with higher abundance and lower  $J'$  (Figure 4.2-5). Average and median  $J'$  for group D was highest of all station groups. Group D also had the strongest year-to-year difference with subgroup D' composed of five FS stations from 1999. As explained above, this yearly signal was caused by within year similarity of stations not sampled both years.

Station group E was composed of 12 stations from FS, IR, and the single HCS station. Group

E represented station with highest abundance and species occurrences. A posteriori contrast of abundance and species, however, did not find station group E to be significantly different for other groups A and B which also had high abundance and species totals, but did find group E to be significantly higher than groups C and D for these parameters. Within group E, five stations from IR formed a separate subgroup (E'') that had higher H' and J' and much lower total abundance than group E' stations. Overall, stations from IR tended to have lower abundance than FS (Table 4.2.2).

Species groups formed primarily around subtle differences in sediment preference. Species groups I, II, and III tended to be representative of coarse sediment stations while groups IV, V, and VI represented finer sediment stations. Nodal analysis of the station/species data matrix indicated that species group I had a high constancy and fidelity to station group B (Table 4.2-9). Species group II was most associated with station group A. Species group III was not characteristic of any single station group, but occurred across all station groups with low constancy and fidelity. Species group IV, which contained the highest abundance species, such as *Spiophanes bombyx*, was strongly associated with all of station group E. Both species groups V and VI were highly associated with station group E'' (Table 4.2-9).

#### **4.2.2.4. Dominant Species**

While a total of 166 taxa were collected over both cruises, only 31 taxa occurred at >20% (at least 15 of 72) of the stations (Table 4.2-10). By comparison, the median number of station occurrences for a taxa was four and about 28% of the taxa occurred once. Of the top 31 taxa, oligochaete worms were most widely distributed and occurred at about 80% of the stations. This taxa represents at least two families of oligochaetes (Tubificidae and Enchytraeidae) and many species. As a group oligochaetes are diverse on the middle Atlantic continental shelf (Diaz et al., 1987) and difficult to identify. Two other major taxonomic groups, which could not be speciated, were among the occurrence dominants; anthozoans or sea anemonies (21%) and nemertean worms (76%). Thirteen polychaetes were among the top occurring taxa being found at about 55 to 21% of the stations. Of the six occurrence dominant bivalves, *Tellina* spp. was found at 65% of the stations while the rest occurred at 32 to 21%. Crustaceans were represented by eight taxa that occurred at from 42 to 21% of the

stations. The cephalochordate *Branchiostoma caribaeum*, or sand lance, occurred at 25% of the stations.

#### **4.2.2.4.1. By Abundances**

Total abundance of taxa was distributed in a similar manner as species with most taxa being rare. About 52% of all taxa had a total abundance of <10 individuals at all stations, combining both cruises (Table 4.2-11). One taxon dominated both cruises. The polychaete *Spiophanes bombyx* accounted for about 35% of all individuals collected. The next closest taxa was oligochaeta being about 10% of all individuals and no other taxa represented more than 5%. If the overwhelming dominance of *Spiophanes bombyx* was removed then three additional taxa were >5% of the individuals (Table 4.2-11). The top 26 taxa, each being at least 1% of individuals for one cruise, cumulatively represented 86% of all individuals. Of these taxa polychaetes represented 15, bivalves five, and crustaceans four. Oligochaeta and Nemertinea were also included.

#### **4.2.2.4.2. By Biomass**

Wet weight biomass was dominated by the bivalve *Spisula solidissima*, the surf clam, which composed about 65% of the total biomass for both cruises (Table 4.2-12). The next top 23 taxa with >0.5 g wet wt/0.04 m<sup>2</sup> were about 30% of the total biomass. Bivalves were the major contributors to biomass, eight being in the top 24 taxa, followed by eight polychaetes, two gastropods, nemerteans, one cephalochordate, three amphipods, and one isopod. The dominant biomass taxa also tended to have the largest mean individual weights, but there were another 14 taxa that while not dominant (>0.5 g wet wt/0.04 m<sup>2</sup>) had mean individual weights >20 mg wet wt (Table 4.2-12). This group included three bivalves, three amphipods, and eight polychaetes.

#### **4.2.2.5 Dominant Community Groups**

Ten taxa were considered to be overall dominants within the study site (Table 4.2-13). These overall dominants were defined as the taxa that appeared on all three lists of dominant taxa (occurrence Table 4.2-10, abundance Table 4.2-11, and biomass Table 4.2-12). The relationship between

dominant taxa (those that occurred at >20% of the stations, were >1% of the individuals for at least cruise, and had >0.5 g total wet weight biomass) and cluster analysis species groups was primarily related to sediment grain-size with *Nemertina*, *Astarte* spp., *Crenella glandula*, *Mytilus edulis*, and *Byblis serrata* characteristic of coarser grained sediments that had significant amounts of gravel or coarse-sands. *Asabellides oculata*, *Spio setosa*, *Spiophanes bombyx*, *Tellina* spp., and *Unciola irrorata* were all associated with finer grained sediments that had significant amounts of fine-sands or even silts. All of these top dominants were broadly distributed but the coarser sediment dominants had highest fidelity within cluster station groups A and B, which represented most of the coarse sediment stations, and finer sediment dominants had highest fidelity within cluster groups D and E (Table 4.2-14).

Similar preferences for sediment type were seen among other important taxa. The exception was the Oligochaeta taxon that likely represented a multispecies mix of at least 10 species. Diaz *et al.* (1987) found the species richness of oligochaetes to be high on the shallow Middle Atlantic continental shelf. Oligochaeta was an occurrence and abundance dominant at all cluster station groups, except C (Table 4.2-14). Group C was composed of three Fenwick Shoals stations (FS02.5 and FS13E from May and FS03E from September) that were depauperate relative to other station groups.

#### **4.2.2.6 Life History Attributes**

The dominant taxa represented a broad range of life history traits (Appendix B and summarized in Table 4.2-15). In general, the literature indicates that shallow continental shelf macrobenthic communities are controlled primarily by sediment grain-size and bottom topography. The life histories of the dominants reflect this physical processes control of species distributions with many of the taxa restricted to either coarse sands or fine sands. The feeding type of the majority of the dominants was either suspension feeders, common in high energy and high particulate habitats, or carnivorous. Deposit feeders played a less prominent role, a reflection of the lack of fine sediment depositional areas within the study area. The majority of the dominants had some ability to move being free-burrower like nemertean worms, tube builders with mobility like the amphipod *Ampelisca* spp., or mobile surface dwellers like the cumacean *Oxyurostylis smithi*. Overall, the predominance of mobile fauna reflects

the dynamic nature of shallow continental shelf habitats.

Dominants could be separated into two basic spawning modes, discrete spawners that have one or two spawns per year like the surf clam *Spisula solidissima* and multiple event spawners like the polychaete *Aphelochaeta* sp. (Table 4.2-15). Typically the spawning mode matches a species larval development mode and life span, with annual species (completes life cycle in a year or less) that have planktonic larvae spawning once during the year. Annual species that brood typically have multiple spawning events during the year. Longer-lived, greater than one year, species tend to spawn once or twice a year.

The potential of a species to recolonize an area that has been mined for its sand resources will primarily be a function of its life history traits. The traits summarized in Table 4.2-15 were evaluated and a recruitment or recolonization potential was determined for each species. Unfortunately, the life histories of many species are not well known. Of the 37 taxa and species considered, complete information the life history table was only found for 16 species. Three categories of recolonization potential were considered based on season; Year Round (YR), Spring/Summer (SS), and Fall/Winter (FW). A species was considered to be a good YR colonizer if it had a broad range of sediment preferences, spawned more than once a year over several seasons, and was an annual. Any species with good mobility or dispersal was considered a good colonizer. For example, oligochaetes while small and not able to move long distances on their own can recolonize a habitat as adults any time of the year by being carried along as part of the bed load transport. Thus storm conditions would aid in the dispersal of oligochaetes. Poor YR colonizers were considered those species that spawned once per year and recruited over a single season to a limited range of sediment types. Good SS or FW colonizers were those species that recruited during spring/summer or fall/winter, respectively, and had good mobility. A total of 15 species were considered to be good and 18 poor YR colonizers. Of the 18 poor YR colonizers, eight were good SS colonizers and seven good FW colonizers (Table 4.2-15). We had insufficient information to categorize four of the dominant taxa.

Taxonomically the best YR recolonizers were Nemertean, oligochaetes, gastropods,

cumaceans, and cephalochordates, each for a particular life history trait. Amphipods, in general, were poor YR recolonizers mainly because of limited reproductive periods, which made the five species good SS colonizers. Anemonies was the only taxonomic group considered to be a poor recolonizer for any season. Bivalves and polychaetes were split between good and poor YR recolonizers with half of the bivalves and about one-third of the polychaetes considered good YR colonizers. The three poor YR bivalve species were considered to be good FW colonizers. Among the poor YR polychaetes, three were good SS, three were good FW, and three could not be assigned a good recruitment season (Table 4.2-15).

### **4.3. Fish Trawls**

#### **4.3.1. Fish Assemblages**

On the May 1999 cruise a metered beam trawl was used to assess fish use in the four major habitat types delineated by the June 1998 data. The four habitats were the northeast seaward flank of the shoal (NE) primarily coarser sands with gravel and shell hash, the northwest shoreward face of the shoal (NW) primarily medium and fine sands with some shell hash, the southeast seaward trough (SE) where surface sediments medium and fine sands and dominated by *Diopatra* tubes, and the southwest shoreward trough (SW) where surface sediments were finer sands with some silt and dominated by *Asabellides* tubes. The first two habitats represent physically dominated bottom with little evidence of biological control over habitat characteristics. The last two habitats represent biologically dominated bottom and are named after the predominant biogenic structure present. Both species are polychaetes that construct large tubes, *Diopatra* uses fragments of organic debris and shell, *Asabellides* uses fine sand. Trawls were conducted during both day and night at two locations within each habitat type (Figure 4.3-1). Within each habitat four trawls were collected during the day and four at night to evaluate diurnal patterns of habitat use.

A total of 333 fish representing 20 species were collected at the four habitats along with 35 species of invertebrates (Table 4.3-1, 4.3-2). The most abundant fish was the hake, *Urophycis regia*, followed by the *Etropus microstomus*. Together they were about 70% of the fish caught and common members of the shallow continental shelf fish assemblages (Able and Fahay, 1998). Cluster analysis of

the fishes grouped by habitat and day/night trawls indicated that there were day/night differences in fish caught in the SW *Asabellides* tube and NW sand habitats. Two of the five species groups were associated with the SW *Asabellides* tube habitat. Species group D being six species mostly associated with day trawls in the SW *Asabellides* tube habitat. Group E was four species caught only at night in the SW *Asabellides* tube habitat (Figure 4.3-2). Group C was primarily a night time group of three species mostly associated with the NW sand habitat. Species group B were day/night species from the NW sand and SE *Diopatra* habitat. Group A was the numerically dominant species that occurred in all habitats both day and night (Table 4.3-1, Figure 4.3-2).

The association of fishes between habitats appeared to be related to sediment grain-size, bed roughness, and presence of biogenic structure. Cluster analysis indicated that both the NE coarser sand/gravel and SE *Diopatra* tube habitats had the similar fish assemblages (Cluster group I, Figure 4.3-3). The NW sand habitat (group II) fish assemblage was most similar to the more dynamic sandy habitats represented in group I (Figure 4.3-3). The SW *Asabellides* tube habitat (group III) was the most dissimilar of the four habitat types.

The trawl also collected many mobile and sessile invertebrates (Table 4.3-2) that were not collected quantitatively by the grab. The most abundant being *Pagurus* spp., *Libinia emarginata*, and *Cancer irroratus* crabs. Large gastropods *Busycon canaliculatum* and *Polinices* spp. were also collected. Other large collected were the infaunal bivalves *Spisula solidissima* and *Ensis directus* that are known to jump out of the sediment in response to a disturbance. *Astarte* spp. also a bivalve known to lie on the sediment surface was collected along with the echinoderms *Asterias* spp. and *Echinarachnius parma*. Overall, crabs were most abundant in the habitats with biogenic structure, SW *Asabellides* and SE *Diopatra* tube habitats, and appeared to be using these habitats as nursery areas since the most of the individuals were small (<5 cm). Other species were broadly distributed across all habitats such as Nudibranchs, *Pagurus* spp., *Crangon septemspinosa*, and *Asterias* sp. The two species that appeared to prefer the sandy more dynamic habitats were *Polinices* spp. and *Echinarachnius parma*.

### 4.3.2. Fish Gut Content

Gut content was analyzed for the three fish species that were dominants and occurred in all four trawled areas (Table 4.3.1). Overall, *Urophycis regia* was the most abundant species collected with 78 guts from fish that ranged from 43 to 215 mm were examined. A total of 36 guts from *Etropus microstomus* that were 42 to 125 mm and 22 guts from *Prionotus carolinus* that ranged from 47 to 200 mm were also examined. All these fish represented young of the year or year class +1 individuals. A total of 45 taxa were identified from the guts of these three fishes (Table 4.3-3). The most numerous food items were epifaunal or near surface infaunal species in the decapod, amphipod, and mysid taxonomic groups and accounted for over 90% of all gut items and biomass. Because the fish were all small, total range of 42 to 215 mm, the average size of the food items was also small being about 3 to 9 mg wet weight. Polychaetes and other soft bodied taxa were not well represented in the gut content likely because of rapid digestion. Only large individuals were recognizable in the guts. The average wet weight of the polychaetes found in the guts was 25 mg that was 16 mg larger than the grand average individual weight (9 mg) of all polychaetes collected in the grab samples.

Based on the gut content analysis, benthic habitats with high numbers of epifauna, particularly crustaceans, and amphipods would have higher resource value than habitats without epifauna. Epifaunal species, those that live on or near the sediment surface, were the most common food item in the stomachs of the fish examined. The presence of abundant epifauna, such as mysid shrimp and *Crangon septemspinosa*, in an area would then attract fishes and provide more resource value relative to areas with little to no epifauna. Unfortunately, the grab sampler did not quantify the abundance of many of the mobile epifaunal species, for example mysids or the small shrimp *Crangon septemspinosa* that turned out to be the most abundant species found in the guts. The second most abundant food item were the amphipods, which quantified with the grab. Most of the amphipods were either surface tube builders (*Ampelisca* and *Unciola*) or shallow free burrowing infaunal species like the haustoriids. The distribution of amphipods around Fenwick Shoal as characterized by grab samples corresponded well with their occurrence in fish guts.

### 4.4. SPI Image Analysis Data

#### 4.4.1. Standard SPI Analysis Data

Sediment profile image analysis produced measures of sediment type, sediment-water interface properties, and biogeochemical features, and counts of organisms and biogenic features. These data formed the bases for many of the benthic habitat maps in the Map appendix and are contained on the CD-ROM appendix. For all of the SPI parameters, their spatial variability is often more informative than the descriptive statistics described here, and the maps below have been included to synthesize the spatial patterns. Example images depicting the range of benthic habitats found can be found in Figures 4.4-1 to 4.4-5.

**RPD:** In the Fenwick Shoals Regions, 1998 apparent color redox potential discontinuity layer depth (RPD) averaged 7.8 cm (SD=3.2; SE=0.3). Along the SPI transects in the Fenwick Shoals Region, 1999 average RPD was 6.1 cm (3.0; 0.3). In the Indian River Regions, 1998 average RPD was 7.4 cm (3.3; 0.5). See Map appendix.

The lower average RPD in the FS Regions in 1999 was a result of sampling locations. The 1998 data represent broad coverage with samples taken at approximately 500 to 1000 m spacing. In 1999, SPI images were collected along several transects at short intervals, typically less than 50 m. Also, the 1999 transects were focused upon transition zones, where steep gradients in substrate properties occurred over short distances.

**Prism Penetration:** Average prism penetration into the substrate for Fenwick Shoals Regions, 1998 was 8.3 cm (3.2; 0.3). Along the SPI transects in the Fenwick Shoals Region, 1999 average penetration was 6.8 cm (3.4; 0.3). In the Indian River Regions, 1998 average was 7.2 cm (3.2; 0.4).

**Visible Infauna:** Infauna were observed in images at 13 stations in Fenwick Shoals Regions, 1998, at three stations along the SPI transects in the Fenwick Shoals Region, 1999, and at three stations in the Indian River Regions, 1998. Most of the infaunal organisms appeared to be free-burrowing polychaete or nemertean worms and associated with the more physically dominated habitats.

**Infaunal Feeding Voids:** Few voids were observed overall. Voids were present in images at 2 stations in Fenwick Shoals Regions, 1998, at 5 stations along the SPI transects in the Fenwick Shoals Region, 1999, and at two stations in the Indian River Regions, 1998. The development of voids is very much related to grain-size in particular the fine (silt-clay) content. Sediments with less than 10% fines typically do not support void structures (Diaz and Schaffner, 1988).

**Fecal Pellets:** Fecal pellets were present in images at 18 stations in the Fenwick Shoals Regions, 1998, at 21 stations along the SPI transects in the Fenwick Shoals Region, 1999, and at seven stations in the Indian River Regions, 1998.

**Sediment-Water Interface Relief:** In the Fenwick Shoals Regions, 1998 sediment-water interface (SWI) relief averaged 2.3 cm ( $SD = 1.5$ ;  $SE = 0.1$ ). The origins of SWI relief, or roughness, generally could be attributed to one or a combination of four factors: bedforms (wave and/or current-induced sand ripples), sediment grains, or biogenic structures, or shell (whole, fragments, or hash) (See Map Atlas). In the FS Regions, 1998 SWI relief was dominated by ripples at 126 of 154 SPI stations analyzed for relief. In the FS Regions, 1998 biogenic features or reworked bedforms were sometimes apparent, resulting in 33 of 154 stations where biogenic features were independently or co-responsible for SWI relief, typically in the deeper, muddier areas (See Map Atlas). Sediment grains, generally pebbles, dominated SWI relief at eight of the 154 stations in the FS Regions, 1998.

In the Indian River Regions, 1998 average SWI relief was 2.6 cm ( $SD = 1.4$ ;  $SE = 0.2$ ). In the IR Regions SWI relief was dominated by ripples at 35 of the 61 SPI stations analyzed for relief. Biogenic roughness dominated at only four of the 61 stations, and grain roughness dominated at 26 of the 61 station in the IR Regions.

#### **4.4.2. SPI Grain-size Analysis**

Sediment grain-size determinations made using SPI images were performed by visually classifying sediments into Wentworth size classes, including mixed classes, the range of observed classes are presented in Figure 4.4-6. Size classes were converted to millimeter size estimates using

Folk's (1974) scheme. The median value for the primary sediment class was taken as the initial value, then adjusted by the number of size steps larger or smaller dependent on the number of size class differences between the primary and secondary sediment components. For example, a sediment classification of medium sandy coarse sand (mscs) indicated coarse sand as the primary component and medium sand as the secondary component. The median size value for coarse sand was 0.71 mm, but since the secondary component was medium sand, the value from the next lower size step, 0.59 mm, would be used. Had the secondary component been fine sand, two size classes lower than coarse sand, the value of 0.5 mm that was two size steps smaller would have been used. The size classes and converted size estimates as well as more general descriptions of the sediment types and coarseness are presented in Table (4.4-1).

#### **4.4.3. Comparison of SPI and Grab Grain-size Determinations**

The agreement between grain-size estimates from SPI images and those from grab samples was good. SPI and grab grain-sizes were compared using paired t-test for stations where only sandy sediments were found; where zero percent or negligible amounts of clay, silt, or gravel were present. Direct comparison was made for samples containing only sandy sediments because the Rapid Sediment Analyzer (RSA) results characterized the entire grain-size distribution for those sediments only. Twenty-seven of the stations met these criteria. A paired t-test between square-root transformed mean grain-size from the RSA analysis and square-root transformed modal grain-size from SPI determinations showed no significant difference ( $p=0.70$ ).

A linear regression of the square-root transformed data, excluding an outlier from station FS09D, reveals the relationship for sandy sediments:

$$\begin{aligned} \%(\text{Mean Grab RSA Grain-size (mm)}) &= 0.284 + 0.506 * (\%(\text{Modal SPI Grain-size (mm)})) \\ &(\text{df} = 24, \text{R-square} = 0.53, p = 0.0001). \end{aligned}$$

The grain-size relationship is presented in Figure 4.4-7, after forcing the line through the origin. When sorting is accounted for by multiple linear regression of the square-root transformed grain-size data, the relationship is improved. The model for all grab station samples is:

$$\%(\text{Mean Grab RSA Grain-size (mm)}) = 0.906 + 0.224 * (\%(\text{Modal SPI Grain-size (mm)}))$$

-0.699\*(Sorting Value in mm from RSA, "SIMM")  
(R-square = 0.60, p = 0.0001).

#### **4.5. Sled Still Image Analysis Data**

Sled still image data were used to augment many of the benthic habitat maps contained in the Map appendix and also to confirm modeled surface sediment grain-size maps. A range of different benthic habitats were documented from physically dominated coarse sands (Figure 4.5-1) to biologically dominated very-fine to fine-sands (Figure 4.5-2).

#### **4.6. Video Image Analysis Data**

Video image data from the 1998 and 1999 sled tows produced detailed information on physical and biological characteristics of the bottom over broad-scales (> Km). These data were used to augment many of the benthic habitat maps contained in the Map appendix. The data files from the sled video analysis are contained in the CD-ROM appendix.

#### **4.7. Regional Condition Data**

##### **4.7.1. NOAA Buoy Data**

**1998:** Surface water temperature records from archived data from NOAA buoy 44009, for 1998 are summarized in the graph in Figure 4.7-1 a. Water temperature from the period during the 1998 sampling cruise are presented in Figure 4.7-1 b. Average surface water temperature during the 1998 cruise (May 17-21, 1998) was 14.3 EC (SD=1.5).

**1999:** Surface water temperature records from archived data from NOAA buoy 44009, for 1999 are summarized in the graph in Figure. Average surface water temperature during the 1999 cruise (June 12-17, 1999) was 18.8 EC (SD=0.3).

#### **4.8. Biological Resource Information**

##### **4.8.1. Indices and Derived Statistics: SPI-based BHQ and SBHQ**

Overall BHQ values for 1998 ranged from 1 to 13 and averaged 5.6 (SD= 1.76, CV= 31.19;

SD: Standard Deviation, CV: Coefficient of Variation). In the Indian River Regions, 1998 BHQ values ranged from 1 to 8 and averaged 5.0 (SD= 1.26, CV=25.09). In the Fenwick Shoals Regions, 1998 BHQ values ranged from 1 to 13 and averaged 5.8 (SD= 1.86, CV=31.77). While the overall range of the SBHQ for 1998 was the same as the BHQ, the averaged SBHQ was consistently lower being 3.2 (SD= 1.81, CV=55.79). In the Indian River Regions, 1998 SBHQ values ranged from 2 to 6 and averaged 2.8 (SD= 0.91, CV=32.40).

In the Fenwick Shoals Regions, 1998 SBHQ values ranged from 1 to 13 and averaged 3.4 (SD= 1.99, CV=58.97). For 1999, BHQ values ranged from 1 to 12 and averaged 5.6 (SD= 2.07, CV=36.66). The 1999 SBHQ values ranged from 1 to 11 and averaged 3.1 (SD= 2.07, CV=65.93) (Data on CD-ROM). Overall, for combined data from 1998 and 1999, BHQ ranged from 1 to 13 and averaged 5.6 (SD= 1.88, CV= 33.29). SBHQ ranged from 1 to 13, averaging 3.2 (SD= 1.90, CV= 59.14).

In general, within the IR Regions the BHQ and SBHQ were low and exhibited little spatial variation (Figures 4.8-1a and 4.8-1b). In the FS Regions both the BHQ and SBHQ were lower on the shoals, especially in the central area and on northwest faces of the shoals, and were higher in the valleys between and deeper regions just inshore and offshore from the shoals (Figures 4.8-2a and 4.8-2b). This basic pattern of lower BHQ and SBHQ values on the shallow shoals and higher values in the deeper less physically dynamic areas is related to the concentration of biogenic features in the deeper more protected areas and corresponds with the clines of lower bottom energy reflected in the grain-size distributions.

#### **4.9. Habitat Classification and Resource Value Results, Secondary Production**

To ascribe potential for disturbing ecosystem energy flow we have incorporated an estimate of secondary production into our assessment of impacts from sand mining on benthic resources. Benthic habitats are conspicuous sites for focusing and transformation of biological energy and are an integral part of ecosystem function. Consideration of energy flow is important because, in general, the annual income and outgo of energy to an ecosystem is in balance. This is most true for physical budgets (*i.e.*

Temperature). For biological budgets, a portion of the biomass of long-lived species is carried over to the next year, but since this occurs every year there is also a general balance in the biological budgets of an ecosystem. Lindeman (1942) was one of the first to consider this overall flow and balance of matter in an energetic sense. Thus in assessing impacts from disturbance, such as sand mining, it is the energetic transformations that occur between and within portions of an ecosystem through time that are most important for informed management of resources.

Measurements of biomass or standing stock while important in comparing immediately available energy are quite inadequate for purposes of predicting rates of predator cropping, yield, or growth. For example, without information on production it is not possible to predict if the food supply of benthic feeding fishes has been impacted.

The range in infaunal production estimated for all 1998 and 1999 grab stations was 0.2 to 159.0 and 1.3 to 59.1 g DW m<sup>-2</sup> y<sup>-1</sup>, respectively (Tables 4.9-1 and 4.9-2). However, the differences between years for the 18 stations sampled both years was less pronounced and indicated that broad scale spatial variation in production related to benthic habitat type was greater than both time and small scale variation within habitat types. The range for the 18 stations sampled both years was 0.3 to 86.5 g DW m<sup>-2</sup> y<sup>-1</sup> for 1998 and 1.3 to 58.0 g DW m<sup>-2</sup> y<sup>-1</sup> for 1999. Average production at these 18 stations indicated that overall secondary production in 1999 may have been slightly higher than in 1998 by about 1 g DW m<sup>-2</sup> y<sup>-1</sup>. While not a significant difference, 14 of the 18 stations may have had higher productivity in 1999 over 1998. Within station variation in production for both years (0.3 to 29.4 g DW m<sup>-2</sup> y<sup>-1</sup>) was smaller than between stations for either year. FS02 and FS04 had consistently high production both years. Other high production stations were FS01G, IR05, IR05.5, and HCS31 in 1998 and FS07B in 1999. Since interannual differences in production did not appear to be significant, we averaged the two years for the purposes of assessing regional and habitat productivity differences (Table 4.9-3).

Taxonomically, bivalves had the highest productivity in both years and accounted for 68% of the total production in 1998 and 49% in 1999. Polychaetes were second most productive with 21%

and 33% of the total in 1998 and 1999, respectively. All crustaceans combined accounted for 5% and 13% of the production for both years. The remaining seven taxonomic groups accounted for about 7 to 8% of the production. Since productivity by major taxa for both years was similar the data were combined and averaged to represent the basic macroinfaunal secondary productivity of the habitats within the study area. Overall, bivalves were about 65%, polychaetes and other worms about 24%, all crustacean taxa about 6%, gastropods about 3%, and anemonies and cephalochordates about 1% of the total secondary production within the study area (Table 4.9-3).

The high productivity of bivalves was due to rapid growth rates of large numbers of small young-of-the-year (YOY) individuals. For example, at stations FS02C and FS04C there were hundreds of small bivalves in the grab samples. Only at stations IR05C and IR05.5C was bivalve production due to growth of larger (+1 year old) individuals. It is likely that small YOY bivalves are a significant source of food for many invertebrate (crabs, nemerteans) and fish predators. Settlement of bivalves into a habitat would contribute significantly to higher habitat value from an energetic standpoint. Large bivalves, which were not sampled with the grab, would also contribute significantly to habitat value both ecologically and commercially. Some larger benthic predators, for example rays, whelks and starfish, feed directly on these larger bivalves.

Polychaetes and other worms, including oligochaetes, phoronids, sipunculids, and nemerteans, were the numerically dominant taxonomic groups (75 to 80% of all individuals) but their productivity was second to bivalves because of their smaller mean individual weight. Stations with highest worm productivity had large numbers of small individuals, over 25,000 individuals  $m^2$ . For example, FS01G with >76,000 individuals  $m^2$  and HCS31 with >26,000 had the highest worm productivity of 32.6 and 36.1 g DW  $m^2 y^{-1}$ , respectively (Table 4.9-3).

While crustaceans, including amphipods, isopods, mysids, cumaceans, and tanaids, were the third most productive group they were very important in the diet of bottom feeding fishes (Table 4.9-4). In part this was due to the slower digestion of their exoskeletons that made crustaceans more recognizable in the stomach contents. Worms and other soft-bodied fauna tend to be less obvious in

stomach content and consequently their importance in the diet of fishes is usually underestimated. Habitats high in crustacean numbers would then be more valuable habitat for bottom feeding fishes. In particular amphipods, which accounted for about 70% of the crustaceans production, were common prey. Mysids were also important food items but were not quantified by the grab samples.

The dynamic nature secondary production and its contribution to energy flow through an ecosystem can be expressed by the production to biomass ratio (P/B). The main attraction of the P/B or turnover ratio is its potential to characterize, for various species and habitats, the magnitude of production and express productivity independent of the standing stock (biomass). It is called turnover ratio because the number arrived at seems intuitively to be the number of times the population biomass turns over for a specific period. The units of P/B are  $y^{-1}$ . It expresses the number of times that the biomass could possibly change for the period studied relative to total biomass produced. In general, the higher the P/B ratio the higher the energy flow. A lower production but higher P/B taxa could be as important at the ecosystem level as quantitatively more productive but lower P/B taxa. On average oligochaetes had the highest P/B ratio of 8.9 (SD = 1.3), which basically means that over the period of a year the biomass of oligochaetes turns over about 9 times. Lowest P/B ratios were associated with areas dominated by larger longer-lived individuals such as IR05D and IR05.5C where the bivalve P/B ratio was 0.4. Overall, the bivalve P/B ratio was 3.9 (2.1) indicating the dominance of small YOY individuals (Table 4.9-5).

The magnitude of P/B is related to a combination of both life-history traits of the individual species and physical environmental conditions. This property of P/B makes it useful for expresses the relationship between habitat conditions and biological response. Discriminant analysis was used to test if the pattern in the distribution of P/B ratios corresponded to sediment type and cluster analysis groups, both of which are the major determinant and expression of benthic habitat conditions. For the sediment discrimination 48 stations were included, four stations were missing sediment data, and seven sediment type groups defined that ranged from coarse-sand to muddy-fine-sand. The pattern in the major taxa P/B ratios closely corresponded to sediment type with 92% of the stations remaining with their original grain-size group. Misclassification occurred four times among the coarser sediment stations (Table 4.9-

6). Of the 16 coarse-sand stations predicted group membership changed for two stations. Station FS07F was classified to the fine-sand group and BB04 to the gravel-coarse-sand group. One fine-sand station (FS07F) and one gravel-coarse-sand station (FS10A) were classified to the coarse-sand group.

#### **4.10. Prediction of Biology Using Substrate and Image Data**

##### **4.10.1. Secondary Production**

The relationship between energy flow within an ecosystem and substrate characteristics is not well understood. Using estimates of secondary production as a surrogate for energy flow we find that for infauna there is a no linear correlation between the secondary production and substrate grain-size. A quadratic model was significant ( $p = 0.029$ ) and did indicate that secondary production tended to be higher in sediments with mean  $\Phi > 2$  (coarse sands) and  $< 1$  (fine to very-fine sands):

$$\text{Log (Production)} = 0.98 - 0.98 (\text{Mean } \Phi) + 0.38 (\text{Mean } \Phi)^2$$

An examination of the variance structure of the data indicated that the silt content accounted for much of the variation between production and grain-size and that there was a strong relationship ( $p = 0.0004$ ) between secondary production and percent silt:

$$\text{Log (Production)} = 0.38 (\text{Arcsin } \% \text{ silt})$$

This is consistent with other production studies that found mixed (sand-silt-clay) sediments to have highest secondary production (see references in Diaz and Schaffner (1990) and Tumbiolo and Downing (1994)). However, the range in silt content with the study area was small (0 to 4.4%) relative to published production studies and indicates how important substrate characteristics are in shaping habitat value on the shallow continental shelf.

Therefore, any disturbance that would increase the silt-clay content of surface sediments would also likely increase secondary production of the infauna. This in turn would support higher utilization by demersal feeding fishes.

Spatial interpolation of secondary production to biomass ratios (P:B) were done using ordinary cokriging accomplished with GSLIB (Deutsch and Journel, 1998), with sediment grain size determined

from SPI as the covariate. Two realizations of that procedure are presented in the Map Atlas. The cokriged interpolations of P:B agree well with the spatial distributions for many of the other habitat parameters mapped for the FS regions. High P:B estimates occur in the biologically rich, deeper, finer sediment regions, and also on parts of the shoals.

#### **4.10.2. Community Groups**

If sandmining activities are planned for a certain location, potential impacts can be assessed based upon the community groups found at the point grab sample locations (Figure 2.2-1 and Table 4.10-1). Each community cluster group and subgroup (A, A', A'', B, B', C, D, D', D'', E, and E') represents a relatively unique species distribution. At the level of entire regions of interest (ROI), the following provides a summary of which communities were, and are likely to be, present in each ROI. In both IR-ROI and in NBB-ROI, three cluster subgroups, A, A', and E', were present. In FS-ROI, nine cluster subgroups, A, A', A'', B, B', C, D, D', and D'', were present. In WS-ROI, 4 cluster subgroups, A', B, D, and D'', were present. In IWS-ROI, 4 cluster subgroups, B, C, D, and D'', were present. In MKP-SMA-FS (Maa and Kim proposed Sand Mining Area - Fenwick Shoal), two cluster subgroups, D and D', were present. And in MKP-SMA-IWS (Maa and Kim proposed Sandmining Area - Isle of Wight Shoal), four cluster subgroups, B, C, D, and D'', were present. Determinations of the likely impacted constituents are based upon species composition and relative distributions by each cluster subgroup (Table 4.10-1).

## **CHAPTER 5. DISCUSSION, SUMMARY, AND CONCLUSIONS**

### **5.1. Origins and Fate of Topographic Features**

Although the shoals of interest are apparently storm-derived offshore ridges (Swift and Field, 1981; Goff *et al.*, 1999), their rate and process of formation suggest that they will not aggrade to prior form if they are subject to major loss of material to mining. The offshore ridges are believed to have initially originated as shore-attached ridges during a prior of lower sea level. As shoreface transgression has occurred, hydrodynamic processes, including storm waves and currents, have led to detachment and segmentation of the offshore ridges from the shore-attached ridges, and slight offshore and southward migration (Swift and Field, 1981). Since becoming offshore features, the ridge morphologies have changed, producing mildly concave northwest shoals with slope asymmetries, such that the seaward slopes are steeper, such as in the case of Fenwick Shoal, where the southeastern face has the steepest slope in the region (Swift and Field, 1981) (Figure 2.1-3).

### **5.2. Benthic Habitat Characteristics**

Preliminary habitat classifications, or habitat proxies, were made using SPI and sled images. The Benthic Habitat Quality (BHQ) index (Nilsson and Rosenberg, 1997) was used as SPI Habitat Proxy 1. Values of the BHQ ranged from 1 to 13, on a scale of 0 to 15, with mean value of 5.63 (SD = 1.75) overall, 5.83 (1.85) for the Fenwick Shoals Regions, and 5.04 (1.26) for the Indian River Regions. The BHQ index did distinguish between gross habitat types, such as physically structured versus biologically dominated. However, BHQ did not resolve finer scale differences well. The formulation of the BHQ relies heavily upon the thickness of the RPD layer, and also parameterizes RPD into specific, discrete value bounded bins, as does the OSI index (Rhoads and Germano, 1986). Both indices weight the RPD according to values representative of the ranges typically found in the ecosystems for which they were developed, estuaries and harbors of the northeast U.S. coast and Swedish fjords. In order to apply the BHQ to shelf habitats we decided to scale the influence of the RPD and to adjust for correlation between the RPD and properties of the sediment which affect porewater flow by substituting a variable derived from RPD, sediment grain-size, and sorting.

The OSI was undefined for nearly all cases because it depends upon determination of

successional stage for its calculation. Successional stage was indeterminate for most of the images from this study area. Although some images, like those from the valley to the south of Fenwick Shoal, resemble successional stage III, and could be classified, images from the shoal stations were often devoid of indicative features. Therefore, objective classification might apply the label azoic to those images, which would be misclassification due to sediment characteristics, and limitations in the images and the index. In the shoal crest sediments, lack of apparent biogenic features does not necessarily mean a paucity in biological resources. Rather, the biological constituents are adapted to the energetic conditions that maintain "clean sand" appearance and do not expend energy or resources in futile attempts to provide lasting structures, which are the bases for construction of both the BHQ and OSI indices. The biology common to those conditions were very small ascideans (tunicates or sea squirts) which often were only as large as the sand grains and were attached to the grains, and deep-burrowing amphipods. The ascideans were rarely visible when small.

The BHQ and the SBHQ would both indicate that benthic habitat quality in the vicinity of FS, WS, and IWS shoals was relatively low on the shoals and high in the valleys between and deeper water areas inshore of the shoals. That result is slightly deceiving because the indices are based upon biological and physical sediment features which are likely to occur and be preserved in finer, more cohesive sediments. The SBHQ does not indicate simply that habitat quality on the shelf increases with depth, rather it indicates that the local effects of topographic variability influence habitat conditions such that organism-sediment interactions are enhanced where finer-grained substrates occur. Because of the combined effects of topography, hydrodynamics, and climatological forcing, particle and sediment transport and deposition have resulted in patterns of substrate composition and biological community structure which resemble variations in bathymetric. In addition, scales of bathymetric variation are important to benthic communities. For example, infaunal communities can vary according to their position in relation to bedform crests or troughs. However, bedforms are dynamic features, and the material composing crests does not move all at once, there is rather a gradual diminishment and reformation of crests as feature migration occurs. It is unlikely that a particular community moves in unison with a particular crest feature. More reasonable is that the vertical distribution of the local community constituents reflects microhabitat condition preference. In broader terms, microhabitat

associations should be predictable based upon the substrate and energy regime.

SBHQ values should be calculated for archived SPI images or profile image analysis datasets from various systems in order to compare SBHQ values to BHQ and OSI. Once that has been done, it should be clear how values of SBHQ relate to particular habitat conditions and generalized states of ecosystem health, such as those specified by the BHQ and OSI. The SBHQ, should provide a measure of benthic ecosystem health that allows cross-system comparison, without the limitations of the indices developed specifically for sheltered systems and based upon a model with limited diagnostic capability offshore (Maurer *et al.*, 1993).

When sled transect image data are considered, there is greater support that the deeper regions surrounding and especially the valley between FS and WS is a more biologically active and productive area than the shoal crests and northwest faces. However, sled data also shows that fish, filter feeding epibenthos, and sand dollars are more prevalent on the shoals. In fact, what we observed is a functional community shift between the subenvironments. Biological community data from grabs and fish and epibenthic community data from the trawls demonstrate the same. In terms of production and resource value, none of the individual means of assessment (indices and statistics) provide a complete diagnostic. Therefore, combining them into a system assessment tool has become one of our priorities. Until a suitable combined measure can be reviewed, some of the methods may be applied with reasonable relevancy if they are used and interpreted with respect to the local environment. Transitions in the local environment occur over different scales in the vicinity of FS, and the spatial rate of change appears related also to the rate of change in bathymetry. The steepest faces of FS, WS, and IWS are to the southeast of each crest. In between FS and WS, bathymetric change is greatest, and habitat changes are most abrupt. Substrates changed from medium to coarse sand to clayey-silty mud in a very short distance, (tens of meters), with a limited zone of mixing. Instead, it appears that the transition follows the predominant, time varying sedimentation scheme which in most cases produces mud beds, but at times covers them with large, sand bedforms induced by storm transport of lower shoal sediments. Therefore, the lower parts of the SE face of FS can be found interbedded sand and mud and large relict bedforms colonized by dense mats of mud-tube-building infaunal polychaetes.

The biogenic structure classes identified in video corresponded well with the general spatial patterns determined by interpolation of point sample data from SPI and grab (Figure 5.2-1). In the Fenwick Shoal ROI, the regions of dense biological associations at or near the sediment surface occurred to the southwest and southeast of the shoal. In the southwest, the region was marked by fine sediments, diverse and numerous epifauna, and infauna which build tubes from fines, such as *Asabellides*. To the southeast, often large *Diopatra cuprea* tubes pervaded the shelly rippled sands. On the northeast and northwest shoal flanks, the surface oriented infauna and epifauna was sparser, and in some instances absent (Map Atlas).

On the northeast flank of Fenwick Shoal, where the fish *Ammodytes* occurred, surface oriented biology and biological features were absent (Figure 5.2-1). The behavior of *Ammodytes* was likely responsible, since *Ammodytes* buries into the surface sediments. It actually dives head-first into sandy ripples at high speed, as seen in the video records. Where these fish were abundant, the continued disturbance to the surface layer sediments apparently has affected the distribution of epifauna and infauna, which build surficial structures. These epifauna and infauna may have been absent solely because of the physical energy regime, however on other parts of the northeast shoal flank, sparse epifauna and infaunal tubes were present, whereas *Ammodytes* were absent. Disturbance was the likely exclusionary culprit because since *Ammodytes* feeds upon plankton (K. Able, pers. comm.), competition for resources with the epifauna and infauna was unlikely.

### **5.3. Perspectives on Former Organism-sediment Models and a New Model**

Organism-sediment interaction models can be useful for classifying habitat conditions based upon the appearance of the substrate. For example, Pearson and Rosenberg (1978) produced a model demonstrating how organic enrichment gradients could structure communities, organism-sediment interactions, and habitat condition. Rhoads and Germano (1986) later produced a model resembling that of Pearson and Rosenberg, but dealt with how physical disturbance effected community succession. Both models were developed for application in fjords, estuarine, harbor, and some river systems, however both lack validity in sandy open coastal systems such as the Atlantic coast of the U.S. We suggest that in continental shelf environments the transitions in community structure and

organism-substrate associations along dynamic energy edges (for example the transition from coarse to silty-fine sands) would resemble in part both of the former models. However, on the continental shelf, the structuring factors are principally space and energy regime and propose that a spatial-energetic benthic community structuring model is more applicable to shelf environments.

Both prior models of community-state succession, in space or time, are theoretically appropriate for disturbance cases such as sandmining. However, as previously discussed, a shelf habitat state may appear similar to late successional stage assemblage in intracoastal waters but may actually be the functional equivalent of an early stage condition. In addition, water column dynamics and topographic variability combine to confound the former models primarily because of material transport effects. For example, community alteration and recovery from disturbance effects on shoals will likely be highly dependent upon wave, current, and bottom stresses in the period subsequent to sandmining. Although it is possible to predict loss of and recolonization community structure based upon existing local populations and their spatial distributions, actual responses will be influenced by fluxes driven by the direction and magnitude of water mass motion. Therefore, the results of a sandmining operation could be totally different if a long period of calm followed or if a major storm followed the dredging. Prediction of recolonization and community development subsequent to sandmining disturbances therefore follows no simple formula, and may be simple or complicated dependent upon the occurrence of unpredictable influential conditions and interactions of climatological, topographic, and biological phenomena.

Several recolonization scenarios could be envisioned by considering just season and climatology subsequent to sandmining activities (Table 5.3-1). The primary effect of season would be related to temperature, which regulates primary productivity and thus availability of new food to the benthos. The primary effect of climatology would be sediment reworking and transport during storm events. Thus spring/summer stormless conditions would tend to favor the deposition of organic matter over the mined area that would tend to initially favor surface deposit feeders and then subsurface feeders. Fall/winter stormy conditions would tend to favor vigorous reworking and transport of sediments, including associated epifaunal and infaunal individuals, into the mined area. Fine sediments and organic matter

would also be transported out of the area. Summer storms and winter quite periods would be intermediate in effecting recolonization.

#### **5.4. Evaluating Biological Resource Potential**

Community measures such as abundance and biomass, numbers of species (diversity), diversity indices, and measures of dominance provide good indications of biological resource status for a particular time and place. Indices of biotic integrity provide a good consolidated measure of community attributes, however do not directly assess resource potential. Secondary production provides a time integrated measure of biological resource potential in terms of availability to trophic transfer, can be modeled using few measurement parameters, and is based upon world-wide data and theory. BRAT measures are intended to provide energy transfer data, but the technique is difficult to implement for large regions over time, especially if different subregional habitats exist which have different resident species as well as transients.

Production is probably the best means of assessing benthic biological resource potential, when used in combination with the spatial characteristics of the region of interest. Production essentially relates the rate of biomass change for a particular taxa or community. Predators feed upon prey biomass, whereupon energy changes trophic levels, and in turn affect prey production. Production estimates incorporate information about growth in terms of individuals and populations, including population dynamics, additions and losses, whereby information concerning the fate of biomass is unnecessary. Production estimates are robust to organism interactions and system dynamics because those variable influences are incorporated into the measure. Variations in community structure and function are important to production, and although those can change in time, certain communities or community types are characteristic of certain shelf habitats and regions. Therefore habitat characteristics are important to production because living modes are controlled and structured by habitat and microhabitat conditions. Spatial variation in habitat characteristics is more important on annual to decadal scales than seasonal changes in water column conditions because seasonal conditions recur with similar variability. Unless climatic changes occur rapidly, seasonality in an east-coast shelf environment will be predictable. Even extreme energetic events such as cyclonic summer and winter

storms can be expected, and they impact the region on a spatial scale much larger than the study area. Similarly, most weather and the related changes in water column conditions are larger than the scale of interest. Seasonal climatic conditions do influence habitats, and over long periods, even configure topography and substrates which help determine habitat distributions. However, the present distribution of habitats with respect to regional and topographic influences, including the substrate and the functional biological community, should have the greatest influence upon production and therefore resource potential.

Water column conditions induced by climatic events can alter the resource availability, however their likelihood may be estimated from features evident in the substrate. For example, storms with high winds and waves most often are easterly in the Fenwick Shoals Region (Maa, pers. comm.). From SPI and Sled images, surface relief and the largest bedforms, as well as larger grain-sized sediments were all found just to the west of the crests of the three shoals (FS, WS, IWS). The roughness configurations and their magnitudes apparently correspond to easterly waves peaking over the shoals. Although those features are ephemeral, they likely are maintained until similarly erosive conditions occur, thus elucidating where and to what extent the substrates were affected by the most recent disturbance. The larger roughness feature distributions and distributions of relatively larger grain-sized sediments extended over approximately 10, 8, and 6 square kilometers on FS, WS, and IWS (Figure 5.4-1) based upon IDW interpolations. Because the shoals themselves influence the behavior of the waves and currents, their lasting presence and configurations influence habitat-structuring conditions such as those, substrate type and configuration, on scales of influence to large biological populations. Therefore, changes to the shoals will influence both habitat distributions and biological resources. The extent to which either would be affected will depend upon the magnitude and distribution of the changes to the shoals.

## **5.5. Relationship of Secondary Production to Habitat Value**

Secondary production reflects the main energetic contribution to benthic habitat value that links primary production and detritus to higher trophic levels. There is, however, no simple connection between benthic secondary production and fisheries species. Not all benthic production is utilized by

or available to fisheries species (Moller *et al.*, 1985, Lunz and Kendall 1987). In addition to the stochastic element of predation, which allows for a certain level of prey survival, organisms avoid predators through quick escape responses, burrowing below the sediment surface, and to a lesser extent in large size. Benthic standing stock biomass at any given time then represents surviving prey available to be carried over from year to year. The percent biomass carryover tends to be higher in "mature" communities that exhibit successional advanced characteristics (Odum 1969, Wolff *et al.*, 1977, Wolff 1983). This results from the fact that organisms live longer and are larger, which increases biomass, in "mature" communities. Lower biomass and smaller individual size are characteristics associated with early successional stage communities or communities under stress. For the shallow continental shelf the stressor is primarily physical disturbance caused by wave induced sediment instability.

A portion of the secondary production is also cycled within the benthos by infaunal predators (Cederwall 1977, Ambrose 1984, McDermatt 1976, Virnstein 1979). Many infaunal species are predacious (particularly important are nemerteans and many polychaetes and gastropods) and influence the energetics of other infaunal species by preying on adult, juvenile, or larval stages (Ambrose 1984, Commito 1982, Oliver *et al.*, 1982). The production of infaunal predators is then potentially available to epifaunal predators and may actually be more available than nonpredacious infauna, because of the free burrowing and surface searching habits associated with a predacious life history (Ambrose 1984).

Overall, areas with higher secondary production would tend to have higher habitat value particularly if the production is transferred to fisheries species. Based on gut content analysis then areas with higher levels of crustacean production would have the highest habitat value. Crustaceans were found to constitute the majority of the food items eaten by demersal feeding fish in the Fenwick Shoals region.

## **5.6. Assessing Potential Sandmining Impacts**

Our assessment of potential sandmining impacts on biological resources is based upon observed and interpolated data from offshore Maryland and Delaware (MD/DE). Based upon the species associations derived from the cluster analysis, certain community groups would be impacted if

the ROI's represented regions where sandmining would occur (Figure 5.6-1). A different suite of species each with their own distribution pattern characterized each of the groups. Since each cluster subgroup represented a particular species distribution, the magnitude of impact upon particular species or sets of species by sandmining activities can be estimated directly from the lists in Tables 4.10-1 that provide proportions of species contributions to each group.

Assuming complete excavation and total removal of organisms within the posed sandmining ROI's, we predict potential recolonization communities based upon first, simply the occurrences and proximity of community groups observed in the vicinity of the mined region. First order predicted recolonization communities are based upon the neighboring community groups, species compositions and proportional abundances, and the distances between the samples and the border of the proposed ROI. As such, if we consider a scenario in which MKP-SMA-FS is completely mined to a depth below the vertical distribution extent of the infauna, on the order of 50 cm, and expect the nearby (within 1 km of the boundary) communities to provide recruits (Figure 5.6-1), then based upon within-group abundances the initial recolonizers should be from cluster subgroups A, A', A'', B', C, D, D', and D''. These are the subgroups within the the 1 km buffer zone. Therefore the initial recolonizers will likely be some or all of the following dominant taxa, and likely many of the less abundant taxa listed in Table 4.10-1:

Oligochaeta (A, A', B', D')	<i>Aricidea cerrutii</i> (A, B')
Nemertinea (A, A')	<i>Protodorvillea kefersteini</i> (A')
<i>Byblis serrata</i> (A'')	<i>Pseudunciola obliquua</i> (A'')
<i>Brania wellfleetensis</i> (A'')	<i>Hesionura elongata</i> (B')
<i>Chirodotea coeca</i> (C)	<i>Parahaustorius longimerus</i> (C)
<i>Tellina</i> spp. (C, D, D'')	<i>Nucula</i> spp. (D)
<i>Asabellides oculata</i> (D)	<i>Protohaustorius wigleyi</i> (D')
<i>Mytilus edulis</i> (D')	<i>Astarte</i> sp. (D'')
<i>Natica pusilla</i> (D'')	

The effect of seasonal sandmining, either spring/summer or fall/winter, on recolonization potential would be seen in species that have life history characteristics that would preclude their availability as recruits (Table 4.2-15). Five of the above listed dominants would likely recruit as well during any season after a sandmining event (oligochaetes, nemerteans, *Protodorvillea*, *Tellina*, and

*Asabellides*). The amphipods (*Bybilus*, *Pseudunciola*, and *Parahaustorius*) would all likely have better recruitment in the spring/summer than fall/winter. The polychaete *Brania* and the bivalve *Nucula* would both likely do better in the fall/winter. Overall, there would likely be slightly better larval and juvenile recruitment after spring/summer than after fall/winter sandmining activities. Recruitment by adults during any season would likely be regulated by factors that affect passive transport, such as storms. Active transport of mobile species, such as epifaunal mysids or *Crangon septemspinosa* may proceed more rapidly during warmer seasons, but would also occur in winter.

If we consider a similar scenario for MKP-SMA-IWS, then the initial recolonizers should be from cluster subgroups C and D (Tables 4.10-1). For any area to be mined, a disturbance-recolonization scenario can be constructed using the maps and tables provided. This approach ignores all of the substrate, hydrodynamic, timing, and biological interaction effects that will be important to the colonization process, however it does provide a reliable, data-based initial prediction. The life history attributes of the potential recolonizers should be examined to determine if the predicted assemblage is realistic based upon individual substrate preferences, reproductive timing, frequency and magnitude (relative to the time of disturbance), adult migration capabilities, and potential competition for resources with functionally similar species. Some of that information has been documented for some species (Table 4.2-15), but it can only be inferred for the majority of the species. Additionally, functional equivalents of occurring species may also be considered as potential recolonizers since community structure is likely to persist although individual species may differ (Maurer *et al.*, 1976). However the spatial extent of the disturbance is likely to control how variable the recolonization community will be relative to the prior assemblage. Therefore, errors in the prediction will increase as the impacted area grows.

As an example, we will consider a scenario that removes at least the top meter of sand from all of the Fenwick Shoals ROI (Figure 5.6-1) and that the grain-size of the sediment surface in the mined area remains unchanged. The area mined would be approximately 7.7 km<sup>2</sup> with a benthic infaunal community characterized by cluster subgroups D and D' (Table 4.10-1) in an areal ratio of about 1:2, respectively. Average infaunal density of the dominant and subdominant species, those included in the

cluster analysis, would then be about 1900 individuals/m<sup>2</sup>, based on data in Table 4.10-1. Average biomass would be about 3.8 g wet weight/m<sup>2</sup>, based on data in Table 4.2-6 for stations FS06B, FS09B, and FS10.5D, the three stations within the ROI mined. For this scenario acute impacts would be the loss of approximately 150 x 10<sup>6</sup> infaunal individuals and 300 kg of biomass that would be removed with the sand resource mined. If we further assume that recolonization would proceed with the dominant species listed above then a mining operation that ended in time for Spring/Summer recruiters would favor crustaceans and a Fall/Winter end would favor annelids (Table 4.2-15). After a single Spring/Summer recruitment season it is likely that some level of benthic resource value for demersal fishes would return, assuming no change in the character of surface sediments, or possibly even be enhanced by favorable conditions for crustacean recruitment. After a Fall/Winter recruitment event benthic resource value would likely not be as high as the Spring/Summer event because annelids may not be utilized by demersal feeders to the extent that crustaceans are.

Should the mining operation lead to fining of surface sediments annelids and bivalves would be favored which might in the long-term reduce resource value for demersal fishes. The accumulation of fines would be related to the hydrodynamics after mining. It is not certain that fining of surface sediments will occur. Jutte and VanDolah (1999) found that a year after sand mining of two areas offshore Hilton Head Island, South Carolina, the silt/clay content of surface sediments increased by 13% and that benthic resources had changed and not recovered to pre-mining community structure. However, Jutte *et al.* (1999) also found that after sand mining of the Cherry Grove borrow area offshore Myrtle Beach, South Carolina, the surface sediments did not become finer and the infaunal community recovery occurred after about two years.

## **5.7. Minimizing Impacts to Biological Resources**

In order to ensure that the biological assemblage that recolonizes a mined area resembles those present prior to mining, it would be beneficial to avoid total area removal of surficial substrates. Instead of mining an extensive continuous region, avoid certain small areas within the sandmining area so that local resident species remain as likely recolonizers. Retaining small refuges within a sandmining area should minimize potential alteration of community structure and function, and therefore reduce potential

effects upon trophically dependent species. Refuges from mining should be of higher priority when shoals are to be mined for two main reasons. First, shoal ridge communities differ from mid-shoal and trough communities; and second, potential recolonizers from similar communities on nearby shoals (if they exist) will likely suffer high mortality during migration, due to exposure to predators during open water transit, and therefore have limited success. Whereas, if local mining refuge patches (RP) are retained, distances and exposure times endured by migrating organisms will be minimized and therefore recolonization success should be greater. Retaining RP's is analogous to the silvicultural practice of retaining seed trees for natural regeneration of harvested forests (Zhou, 1998). Although the resultant recolonization community in the mined area may be different dependent upon whether adult migration or larval dispersal dominates, RP's should augment similar pre-mining and post-mining communities.

Determinations of impacts of sandmining on mobile fisheries resources is also connected to the rate and success of benthic recolonization. Many fishes utilize the shallow continental shelf as a nursery ground (Able and Fahay, 1998) and depending on when their demersal life history stages utilize a particular area, any impacts could be minimized by insuring that their cover or food base not be disrupted. For the most part this would primarily mean minimizing impacts to crustaceans and secondarily to other taxonomic groups. Conversely, any aspect of sandmining that would enhance the production of crustaceans would likely also improve habitat quality for demersal fishes.

## **CHAPTER 6. ACKNOWLEDGMENTS**

We thank the crews of the R/V Atlantic Surveyor and R/V Cape Henlopen for making our data collection so successful. We also thank the Benthic Ecology Group at VIMS for their assistance in conducting the fieldwork and laboratory processing of grab samples and profile camera images. Special thanks go to Barry Drucker, our contract monitor, for allowing us flexibility in data collection.

## CHAPTER 7. REFERENCES CITED

- Able, K. W. and M. P. Fahay. 1998. The first year in the life of estuarine fishes in the middle Atlantic Bight. Rutgers University Press New Brunswick, New Jersey, 343 p.
- Aller, R. C. and J. Y. Aller. 1998. The effect of biogenic irrigation intensity and solute exchange on diagenetic reaction rates in marine sediments. *Journal of Marine Research* 56:905-936.
- Ambrose, J. 1984. Role of predatory infauna in structuring marine soft-bottom communities. *Mar. Ecol. Prog. Ser.* 17:109-115.
- Banase, K. and S. Mosher. 1980. Adult body mass and annual production/biomass relationships of field populations. *Ecol. Monogr.* 50:355-379.
- Boeringa, M. 1998. MB.View.SpatialKriging Avenue script: interpolates values using the kriging method. Marco Boeringa, Gemeentewaterleidingen Amsterdam (Amsterdam Water Supply), Vogelenzangseweg 21, 2114 BA Vogelenzang, the Netherlands, poect8@gw.amsterdam.nl.
- Boesch, D. F. 1977. Application of numerical classification in ecological investigations of water pollution. Report prepared for US EPA Ecological Research Series (EPA-600/3-77-033). Available as PB269 604 from: National Technical Information Service. U.S. Dept. of Commerce. Springfield VA 22161.
- Boesch, D. F. 1979. Benthic ecological studies: Macrobenthos. Chapter 6. Middle Atlantic outer continental shelf environmental studies. Final Report to Bureau of Land Management, Washington, D. C.
- Bonsdorff, E., R.J. Diaz, R. Rosenberg, A. Norkko and G.R. Cutter. 1996. Characterization of soft-bottom benthic habitats of the Åland Islands, northern Baltic Sea. *Marine Ecology Progress Series* 142:235-245.
- Brey, T. 1990. Estimating productivity of macrobenthic invertebrates from biomass and mean individual weight. *Meeresforsch.* 32: 329-343.
- Carr, M.R. 1997. PRIMER user manual, Plymouth Routines In Multivariate Ecological Research. Plymouth Marine Laboratory, Plymouth, England, 44 pp.
- Cederwall, H. 1977. Annual macrofauna production of a soft bottom in the northern Baltic proper. pp. 155-164. In: Keegan, B.F.; Ceidigh, P.O.; Boaden, P.J.S. eds. *Biology of benthic organisms*. Pergamon Press, Oxford.
- Commito, J. A. 1982. Effects of *Lunatia heros* predation on the population dynamics of *Mya arenaria* and *Macoma balthica* in Maine, USA. *Mar. Biol.* 69:187-193.
- Cutter, G.R. and R.J. Diaz. 1998. Novel optical remote sensing and ground-truthing of benthic habitat using the Burrow-Cutter-Diaz plowing sediment profile camera system (BCD sled). *Journal of Shellfish Research*, 17: 1443-1444.
- Diaz, R.J. and L.C. Schaffner. 1988. Comparison of sediment landscapes in the Chesapeake Bay as seen by surface and profile imaging. p. 222-240. In: M. P. Lynch and E. C. Krome, eds. *Understanding the estuary; Advances in Chesapeake Bay research*. Chesapeake Res. Consort. Pub. 129, CBP/TRS 24/88.
- Diaz, R.J. & Schaffner, L.C. 1990. The functional role of estuarine benthos. In *Perspectives in the Chesapeake Bay, 1990: Advances in estuarine sciences*. M. Haire & E. C. Krome (eds.), Report No. CBP/TRS41/90, Chesapeake Research Consortium, Gloucester Pt., Virginia. pp. 25-56.

- Diaz, R.J., C. Erseus, and D.F. Boesch, 1987. Distribution and ecology of Middle Atlantic Bight Oligochaetes. *Hydrobiologia* 141: 215-225.
- Deutsch, C.V., and A.V. Journel. 1998. *GSLIB: geostatistical software library and user's guide*. New York, Oxford University Press, 1998.
- Fager, E.W. 1963. Communities of organisms. pp. 415-433. In: M. N. Hill (ed.) *The sea*. Wiley-Interscience, New York.
- Fenchel, T. 1969. The ecology of marine microbenthos. IV. Structure and function of the benthic ecosystem, its chemical and physical factors and microfauna communities with special reference to the ciliated Protozoa. *Ophelia* 6:1-182.
- Folk, R.L. 1974. *Petrology of sedimentary rocks*. Austin, Texas, Hemphill's. 170 pp.
- Gaston, G.R. 1987. Benthic polychaeta of the middle Atlantic bight: feeding and distribution. *Mar. Ecol. Prog. Ser.*, 36: 251-262.
- Goff, J.A., Swift, D.J.P, Duncan, C.S., Mayer, L.A, Hughes-Clarke, J., 1999. High-resolution swath sonar investigation of sand ridge, dune and ribbon morphology in the offshore environment of the New Jersey margin. *Marine Geology*, 161, 307-337.
- Hurlbert, S. M. 1971. The non-concept of species diversity: a critique and alternative parameters. *Ecology* 52: 577-586.
- Jutte, P.C. and R.F. VanDolah. 1999. An assessment of benthic infaunal assemblages and sediments in the Joiner Bank and Gaskin Banks borrow areas for the Hilton Head beach renourishment project, Final Report – Year 1. to: Town of Hilton Head Island, Hilton Head, South Carolina. 44 p.
- Jutte, P.C., R.F. VanDolah, M.V. Levisen, P. Donovan-Ealy, P.T. Gayes and W.E. Baldwin. 1999. An environmental monitoring study of the Myrtle Beach renourishment project: physical and biological assessment of offshore sand borrow sites, Phase I – Cherry Grove borrow area. Final Report to: U.S. Army Corps of Engineers, Charleston District, Charleston, South Carolina. 105 p.
- Lindeman, R.L. 1942. The trophic-dynamic aspect of ecology. *Ecology* 23:399-418.
- Lunz J.D. and D.R. Kendall. 1987. The Netherlands Meeting on Dredging and Related Technology 10-14 September, 1984, Charleston, SC. Final Report, *Mar.* 1987. p 84-95.)
- Magurran, A.E. 1991. *Ecological diversity and its measurement*. Academic Press, London.
- Maurer, D., P. Kinner, W. Leathem, and L. Watling. 1976. Benthic faunal assemblages off the Delmarva peninsula. *Estuarine and Coastal Mar. Sci.*, 4: 163-177.
- Maurer, D., Robertson, G., Gerlinger, T., 1993. San Pedro Shelf California: testing the Pearson-Rosenberg model. *Marine Environ. Res.* 35:303-321.
- McDermott, J.J. 1976. Observations on the food and feeding behavior of estuarine nemertean worms belonging to the order Hoplonemertea. *Biol. Bull.* 150:57-68.
- Milliman, J.D., 1972. Atlantic continental shelf and slope of the united states- petrology of the sand fraction of sediments, northern New Jersey to southern Florida. Geological survey professional paper 529-j, 40 pp., 9 plates.
- Moller, P., L. Pihl and R. Rosenberg. 1985. Benthic faunal energy flow and biological interaction in some shallow marine soft bottom habitats. *Mar. Ecol. Prog. Ser.* 27:109-121.
- Nilsson, H.C. and R. Rosenberg. 1997. Benthic habitat quality assessment of an oxygen stressed fjord by surface and sediment profile images. *J.Mar. Syst.* 11:249-264.

- Odum, E.P. 1969. The strategy of ecosystem development: An understanding of ecological succession provides a basis for resolving man's conflict with nature. *Science* 164:262-270.
- Oliver, J. S., Oakden, J. M.; Slattery, P. N. 1982. Phoxocephalid amphipod crustaceans as predators on larvae and juveniles in marine soft-bottom communities. *Mar. Ecol. Prog. Ser.* 7:179-184.
- Pearson, T.H. and R. Rosenberg. 1978. Macrobenthic succession in relation to organic enrichment and pollution of the marine environment. *Oceanogr. Mar. Biol. Annu. Rev.*, 16: 229-311.
- Pielou, E.C. 1984. The interpretation of ecological data. A primer on classification and ordination. John Wiley, New York.
- Rainer, S.F. 1982. Trophic structure and production in the macrobenthos of a temperate Australian estuary. *Estuar. Coast. Shelf Sci.* 15:423-441.
- Rainer, S.F. 1984. Polychaeta as a representative taxon: their role in function and secondary production of benthic communities in three estuaries. In: Hutchings, P.A. (ed.). *Proc. First Internat. Polychaete Conf.*, Sydney. The Linnean Society of New South Wales. p. 370-382.
- Rhoads, D.C. 1974. Organism sediment relations on the muddy sea floor. *Oceanography and Marine Biology Annual Review* 12:263-300.
- Rhoads, D.C. and J.D. Germano. 1982. Characterization of organism-sediment relations using sediment profile imaging: an efficient method of remote ecological monitoring of the seafloor (REMOTS system). *Mar. Ecol. Prog. Ser.* 8:115-128.
- Rhoads, D.C. and J.D. Germano. 1986. Interpreting long-term changes in benthic community structure: a new protocol. *Hydrobiologia*, 142: 291-308.
- Sanders, H. L. 1968. Marine benthic diversity: A comparative study. *Amer. Natur.* 102: 243-282.
- Shepard, F.P., 1948. *Submarine Geology*. Harper and Row, New York, 348 pp.
- Swift, D.J., Field, M.E., 1981. Evolution of a classic sand ridge field: Maryland sector, North American inner shelf. *Sedimentology*, 28, 461-482.
- Swift, D.J.P., Duane, D.B., McKinney, T.F., 1973. Ridge and swale topography of the Middle Atlantic Bight, North America: secular response to the Holocene hydraulic regime. *Marine Geology*, 15, 227-247.
- Tumbiolo, M.L. and J.A. Downing. 1994. Empirical model for the prediction of secondary production in marine benthic invertebrate populations. *Mar. Ecol. Prog. Ser.*, 114: 165-174.
- Valente, R.M., D.C. Rhoads, J.D. Germano and V.J. Cabelli. 1992. Mapping of benthic enrichment patterns in Narragansett Bay, Rhode Island. *Estuaries* 15:1-17.
- Vismann, B. 1991. Sulfide tolerance: Physiological mechanisms and ecological implications. *Ophelia* 34:1-27.
- Virnstein, R.W. 1979. Predation on estuarine infauna: Response patterns of component species. *Estuaries* 2:69-86.
- Waters, T.F. 1977. Secondary production in inland waters. *Adv. Ecol. Res.* 14:91-164.
- Weisberg, S.B., J.A. Ransinghe, L.C. Schaffner, R.J. Diaz, D.M. Dauer, and J.B. Frithsen. 1997. An estuarine benthic index of biotic integrity (B-IBI) for Chesapeake Bay. *Estuaries*, 20: 149-158.
- Wolff, W.J. 1983. A benthic food budget for the Grevelingen Estuary, The Netherlands, and a consideration of the mechanisms causing high benthic secondary production in estuaries. p. 267-280 In: B.C. Coull (ed.), *Ecology of marine benthos*. U. of S. Carolina Press, Columbia, SC.

- Wolff, W.J., A.J.J. Sandee and L. deWolf. 1977. The development of a benthic ecosystem. *Hydrobiologia* 52:107-115.
- Zhou, W. 1998. Optimal natural regeneration of Scots pine with seed trees. *Journal of Environmental Management*, 53:263-271.
- Ziebis, W., Huettel, M., Forster, S. 1996. Impact of biogenic sediment topography on oxygen fluxes in permeable seabeds. *Mar. Ecol. Prog. Ser.* 140: 227-237.

# FIGURES



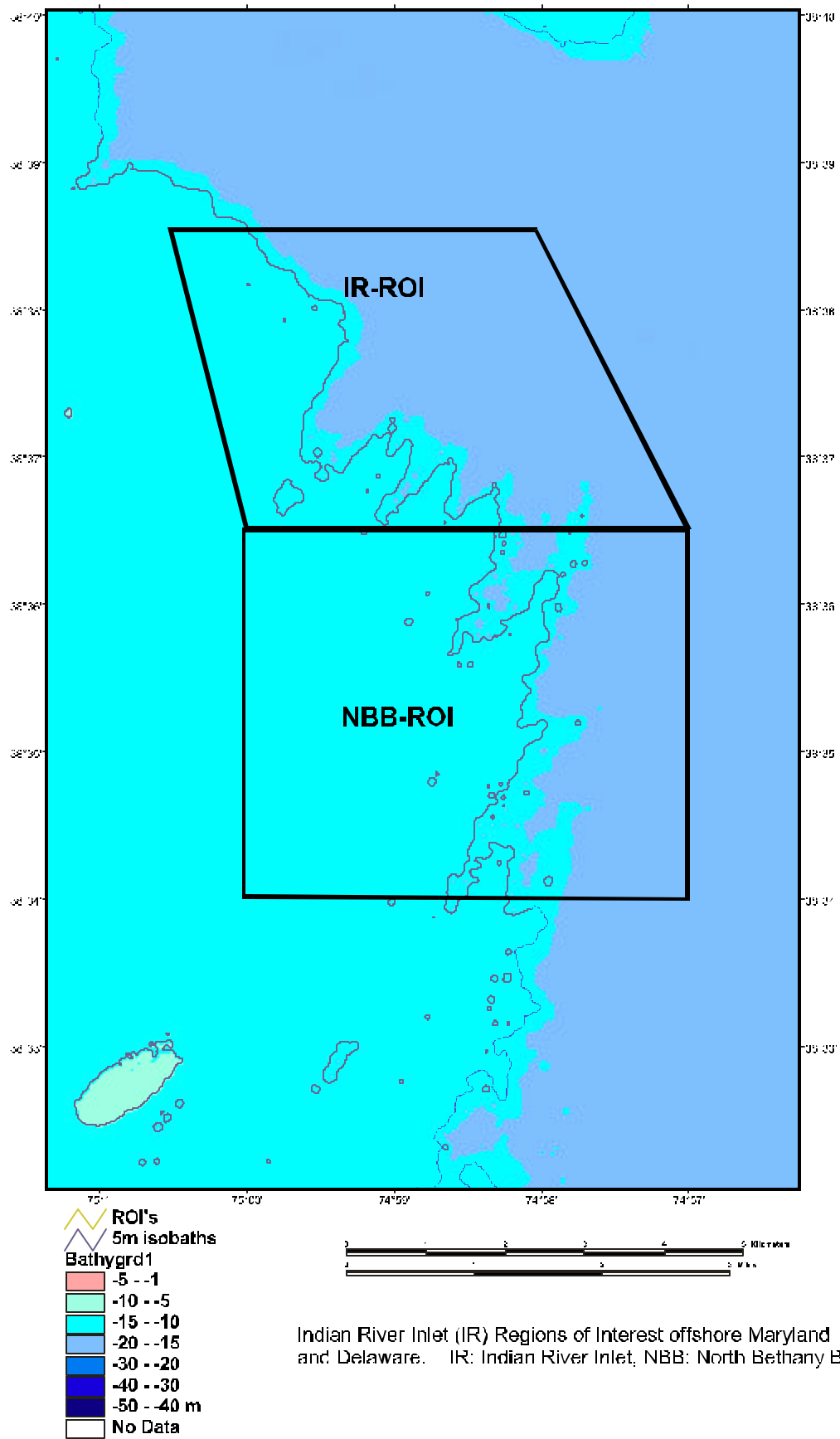


Figure2.1-2: General location and boundaries of the Fenwick Shoal (FS) and North Bethany Beach regions of interest (ROI).

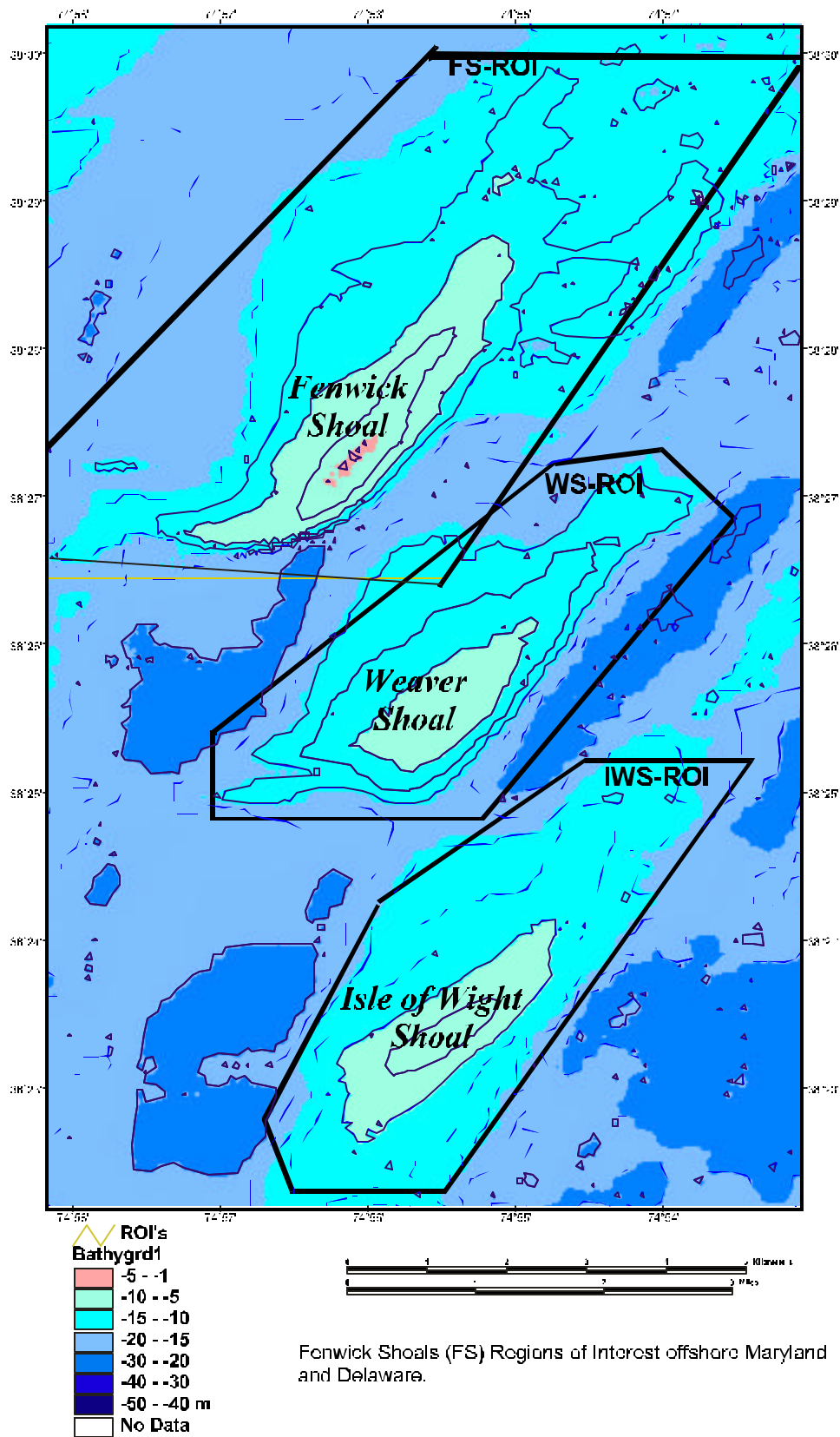


Figure 2.1-3: General location and boundaries of the Fenwick Shoal (FS), Weaver Shoal (WS), and Isle of Wight Shoal (IWS) regions of interest.

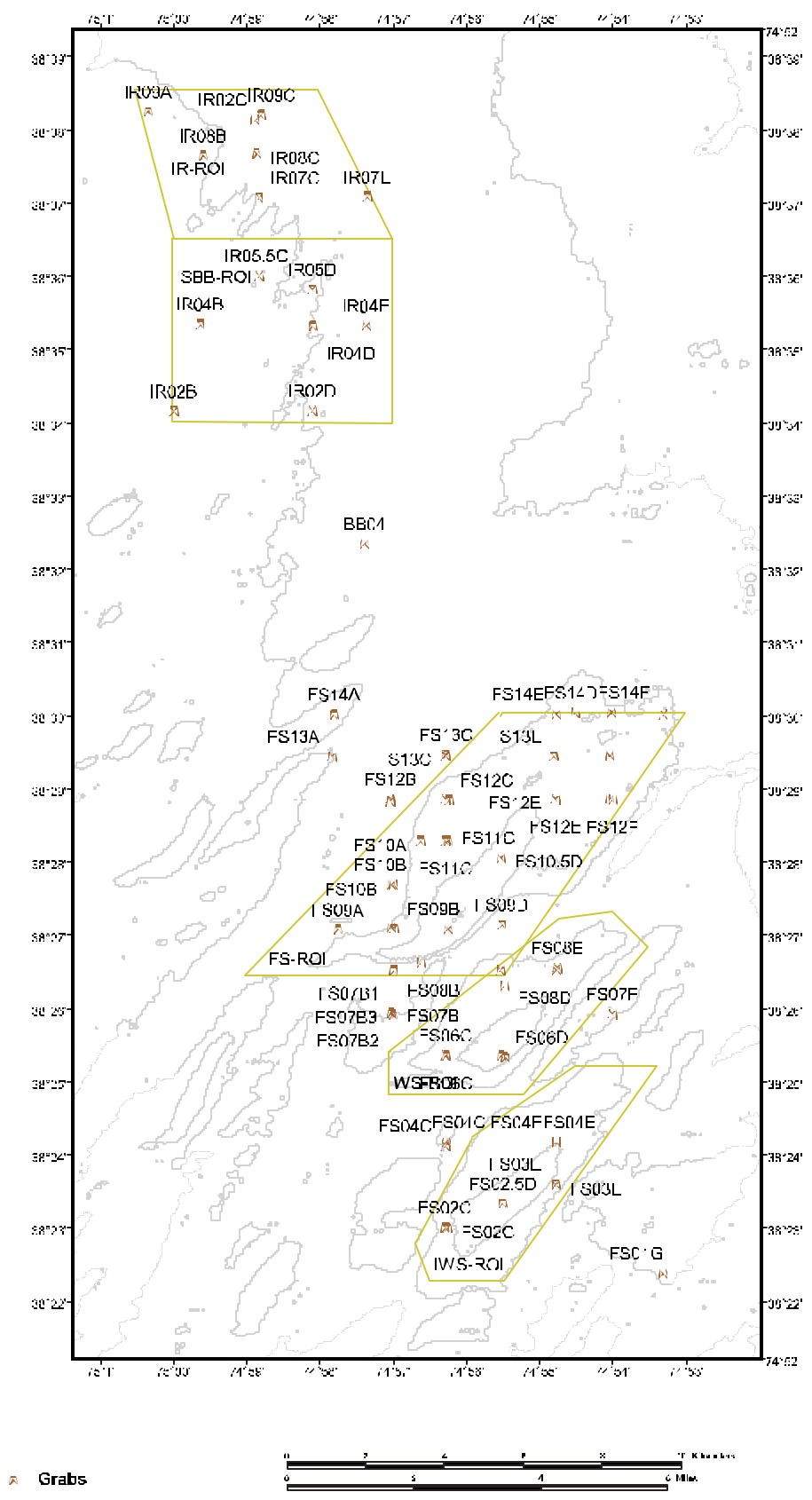


Figure 2.2-1: Location of grab stations in the Maryland and Delaware study area.

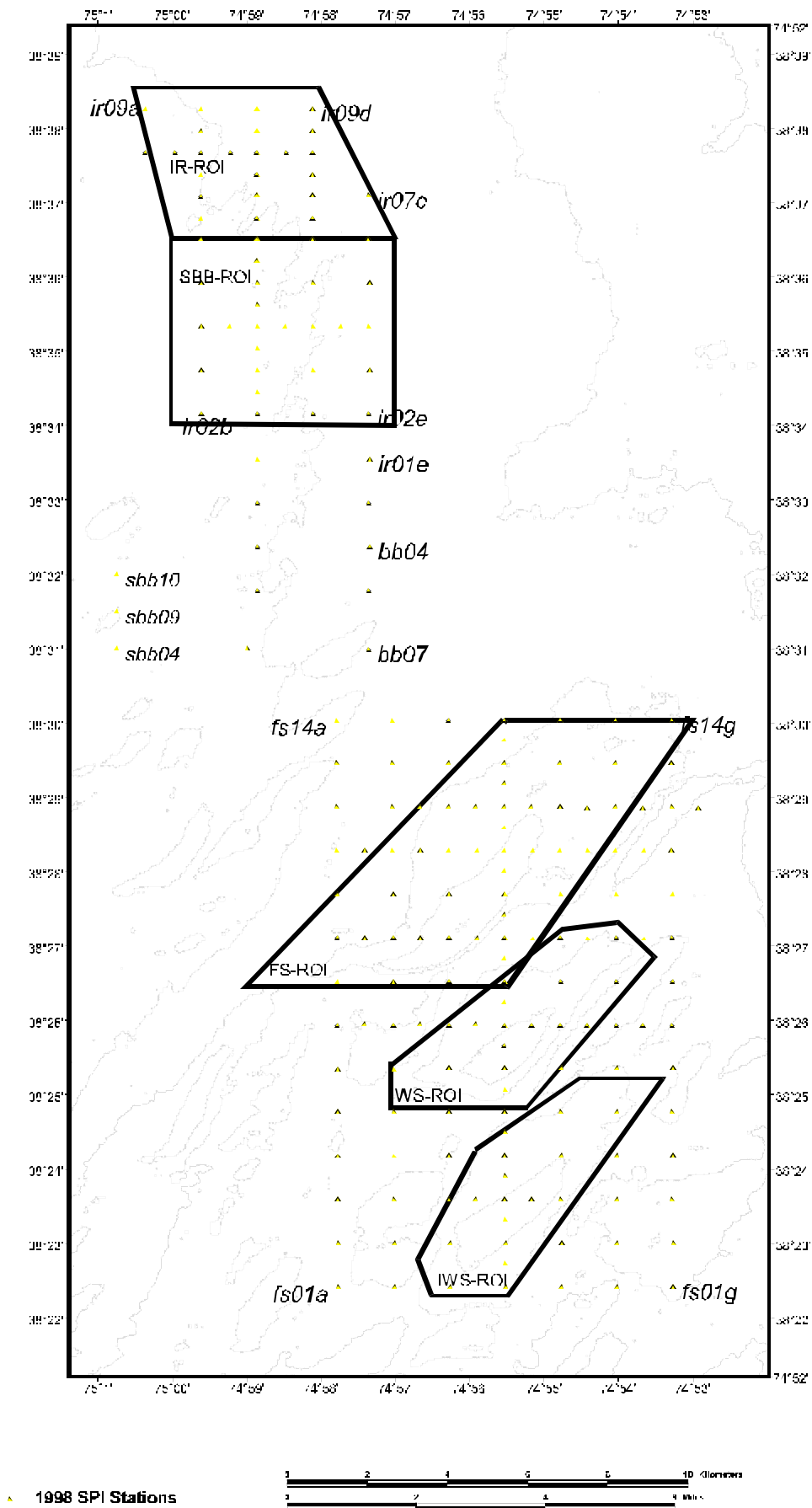


Figure 2.2-2: Location of sediment profile camera stations in the Maryland and Delaware study area.



Figure 3.1-1: Young grab used to collect benthic infauna and sediments.

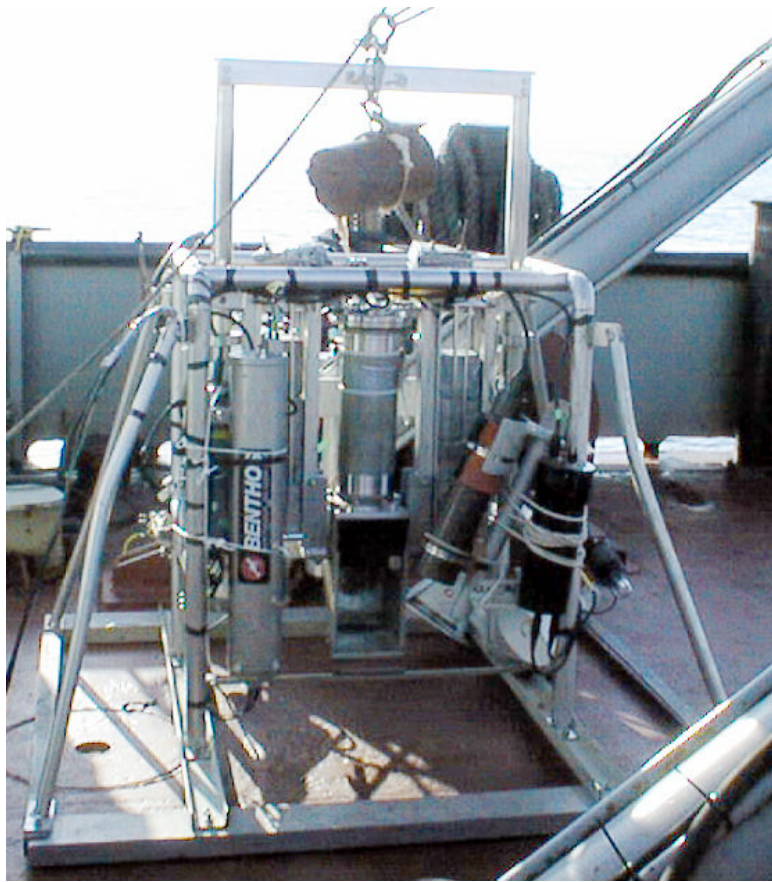


Figure 3.1-2: Sediment profile camera system used to collect images of the sediment-water interface. The camera system includes a Hyulcher profile camera, a Benthos still camera, and a Panasonic video camera within a Benthos deep-sea camera frame. The SPI prism window is in the center of the image.



Figure 3.1-3: Standard video and still camera sled used to collect images of surface features over broad spatial scales.

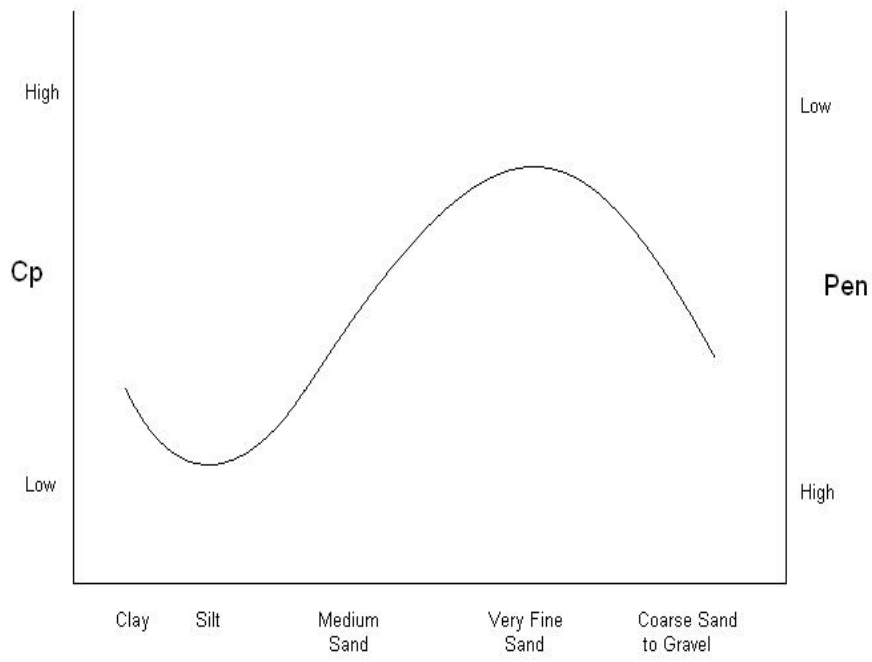


Figure 3.2-1: Relationship among sediment grain-size, compaction (Cp), and prism penetration (pen).



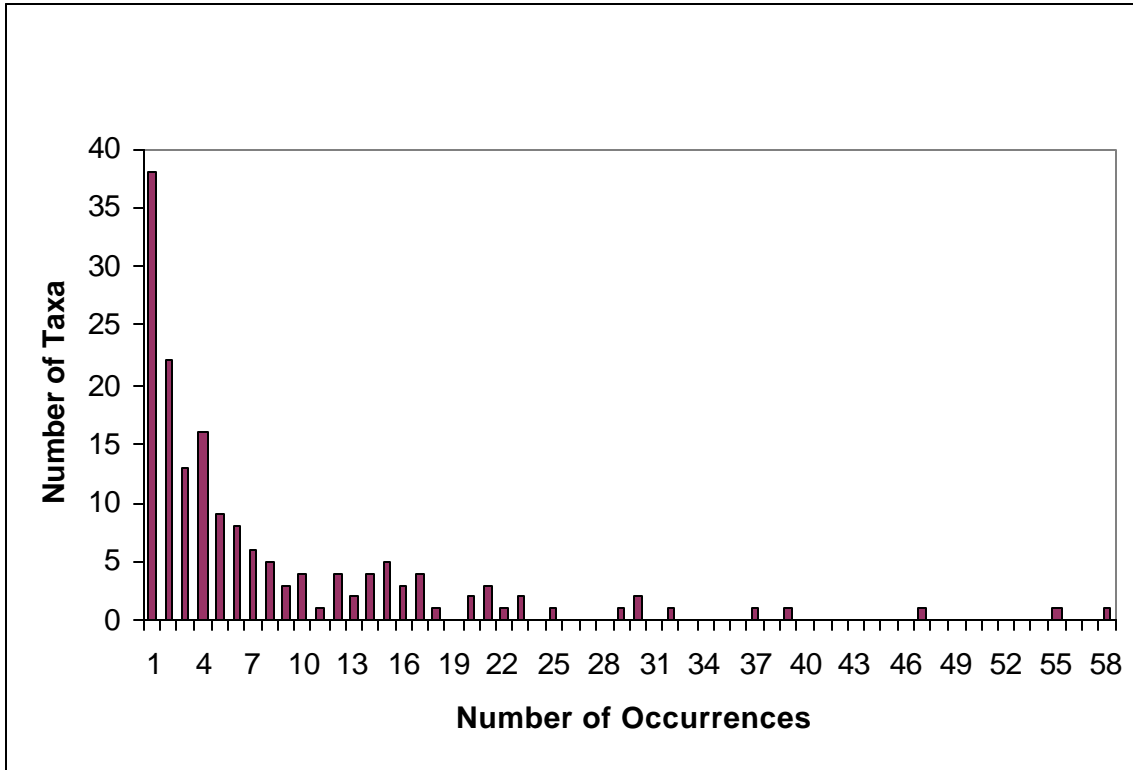


Figure 4.2-1: Distribution frequency of taxa occurrences for all stations, both May 1998 and June 1999.

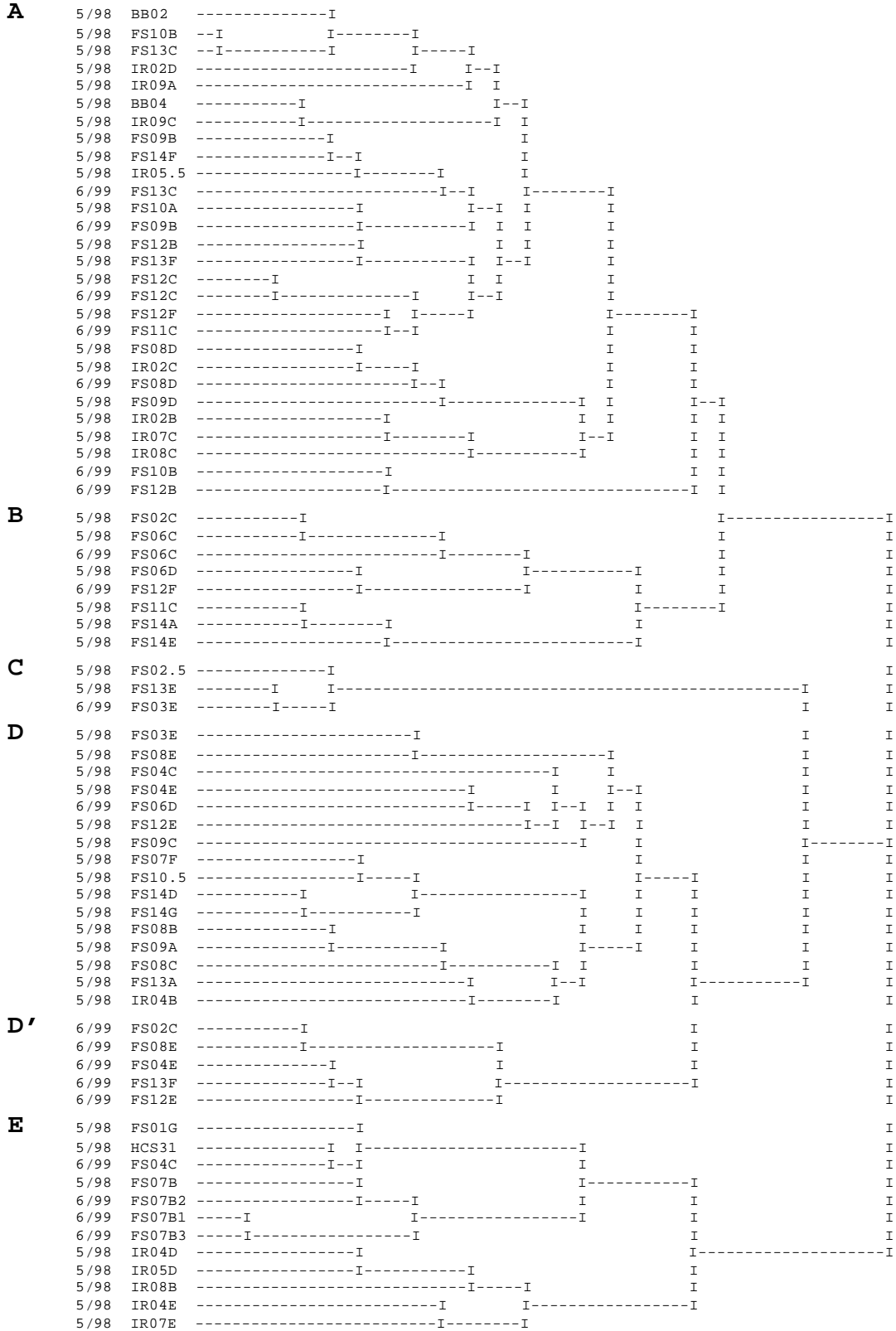


Figure 4.2-2: Dendrogram of all stations sampled in 1998 and 1999. Cluster groups, indicated by letters, are based on simultaneous double standardization of data, Bray-Curtis similarity, and flexible sorting. For details see text.



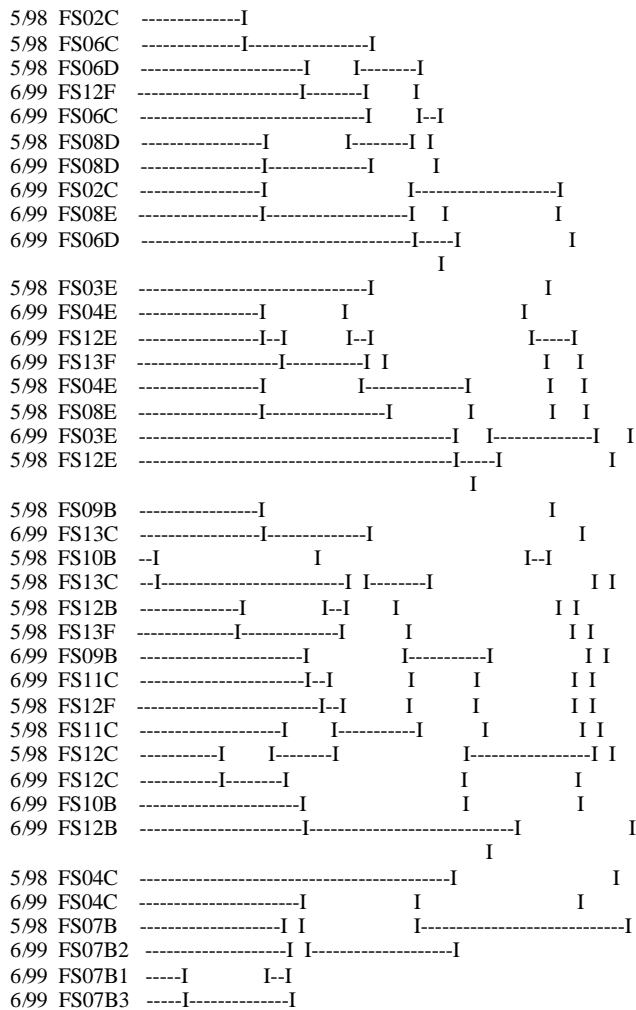


Figure 4.2-4: Dendrogram of Fenwick Shoals stations sampled both in 1998 and 1999. Cluster groups are based on simultaneous double standardization of data, Bray-Curtis similarity, and flexible sorting. For details see text.

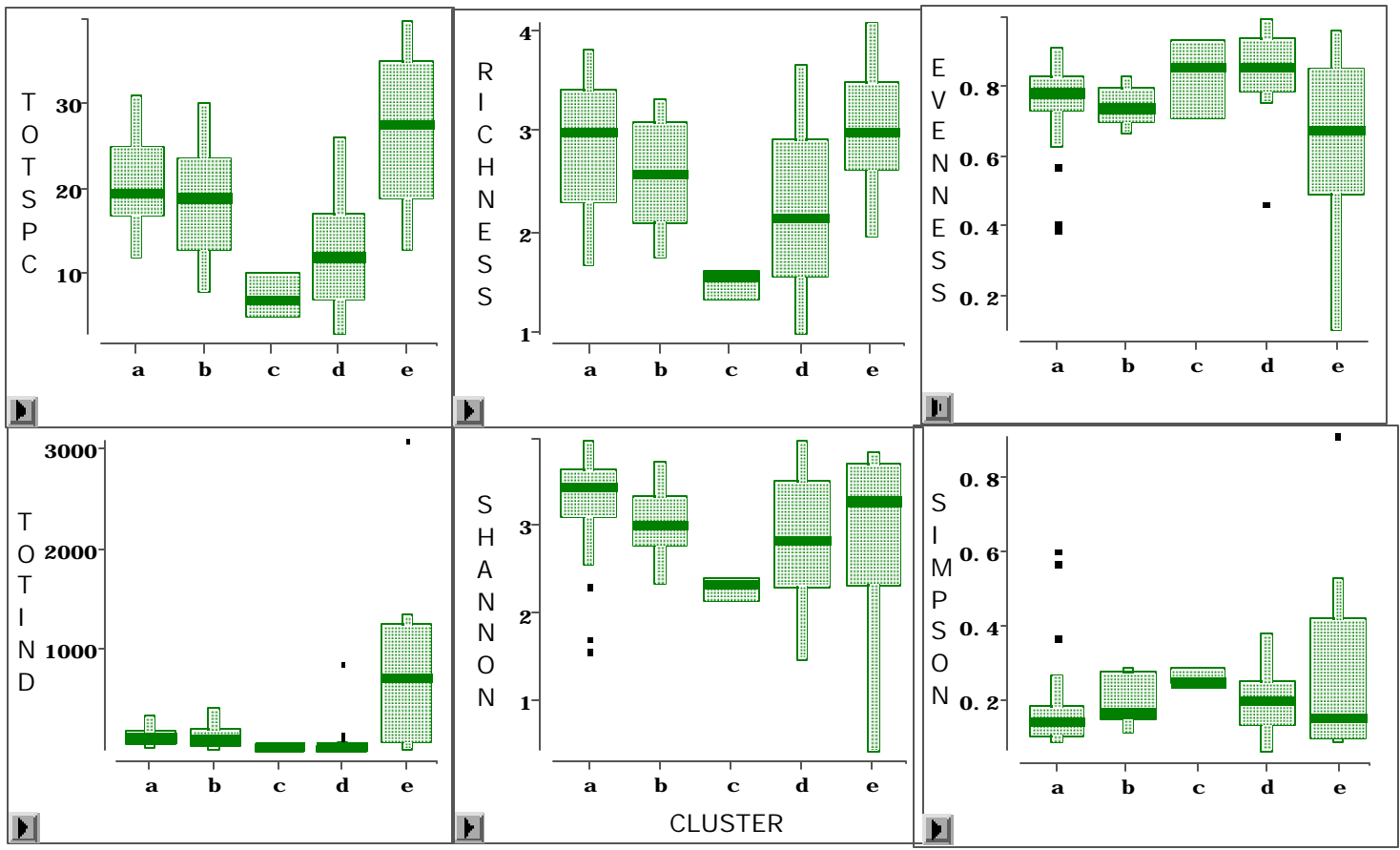


Figure 4.2-5. Box plots of community structure statistics from MD/DE study area by cluster analysis station group. Bar is median, box is interquartile range, tails are trimmed range, and dots are outliers (>2 times interquartile range).

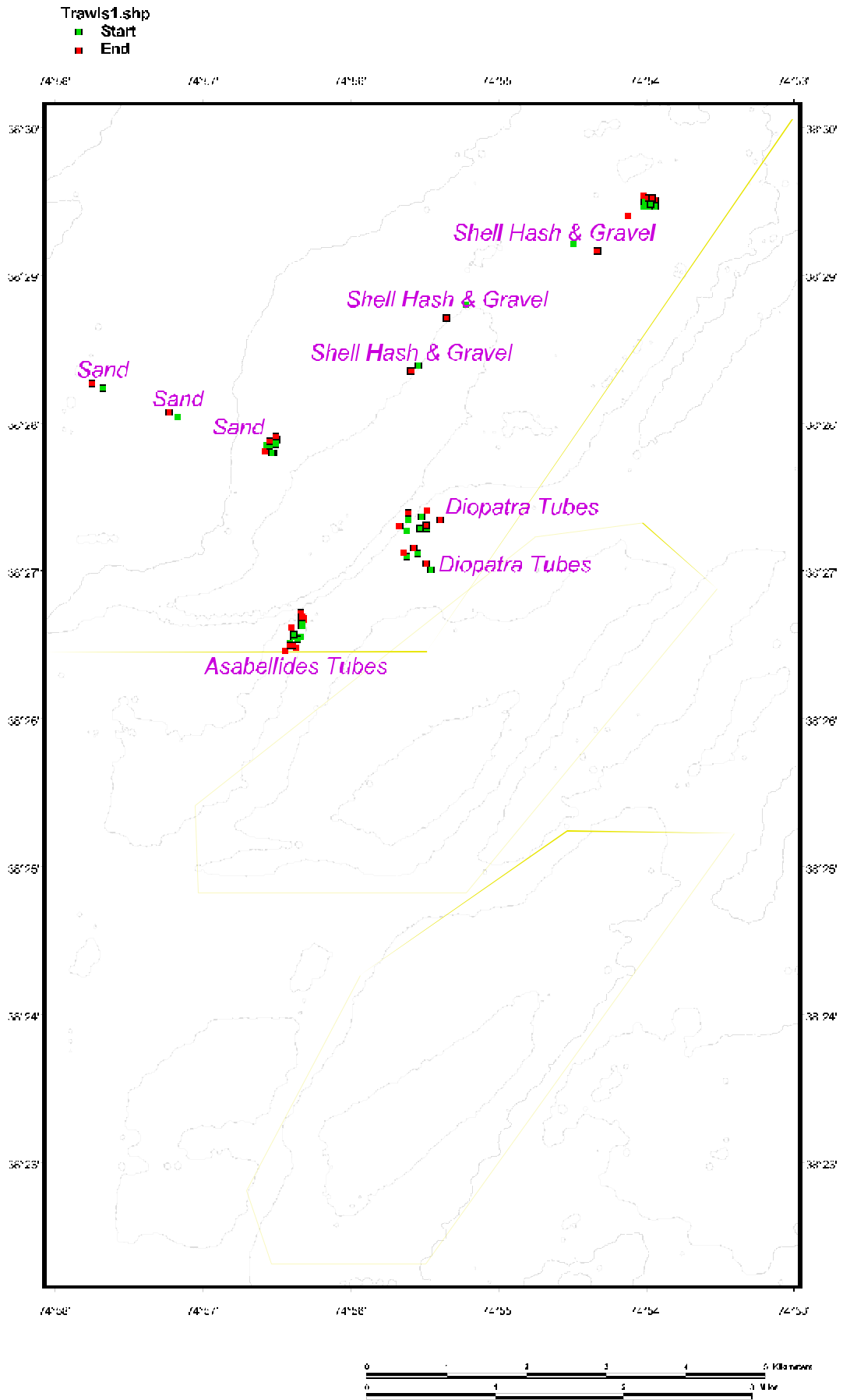


Figure 4.3-1: Location of bottom trawls around the Fenwick Shoal ROI trawls were located in four benthic habitats.

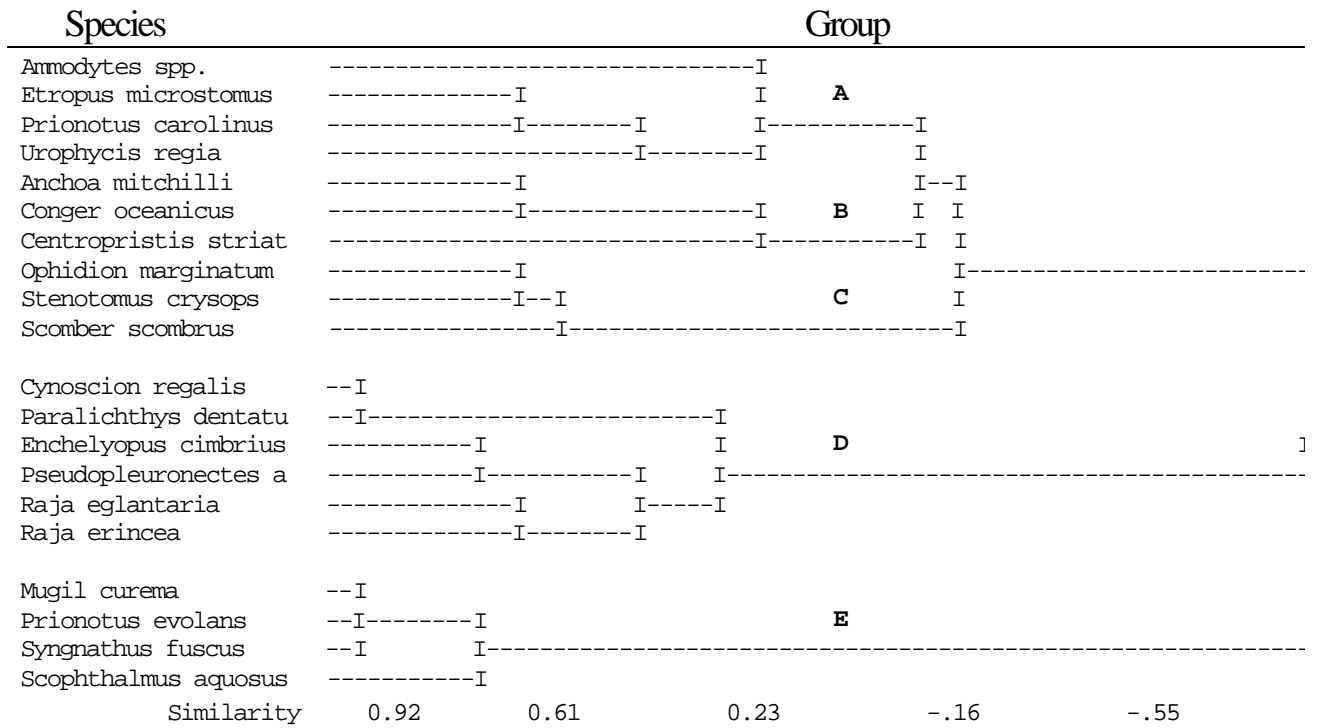


Figure 4.3-2: Cluster analysis of demersal fish collected May 1999 at four benthic habitat types within the MD/DE study area. Based on Bray-Curtis similarity and flexible sorting.





Figure 4.4-1: Selected Sediment Profile Images (SPI).

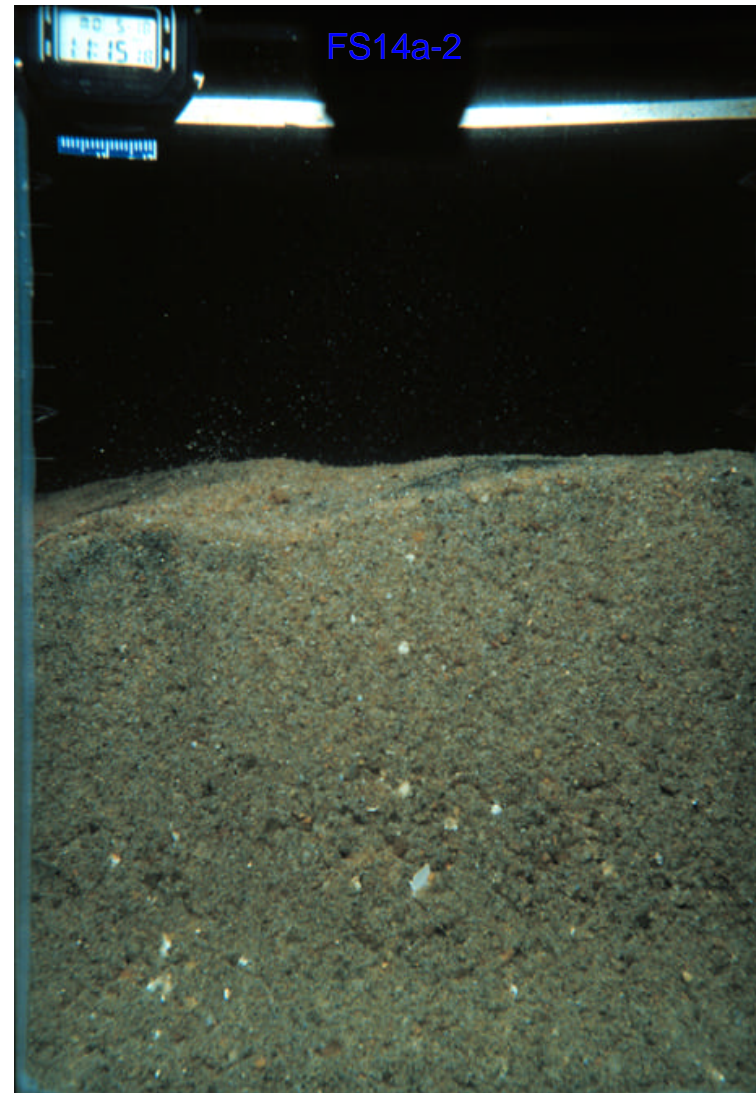


Figure 4.4-2: Selected Sediment Profile Images (SPI).

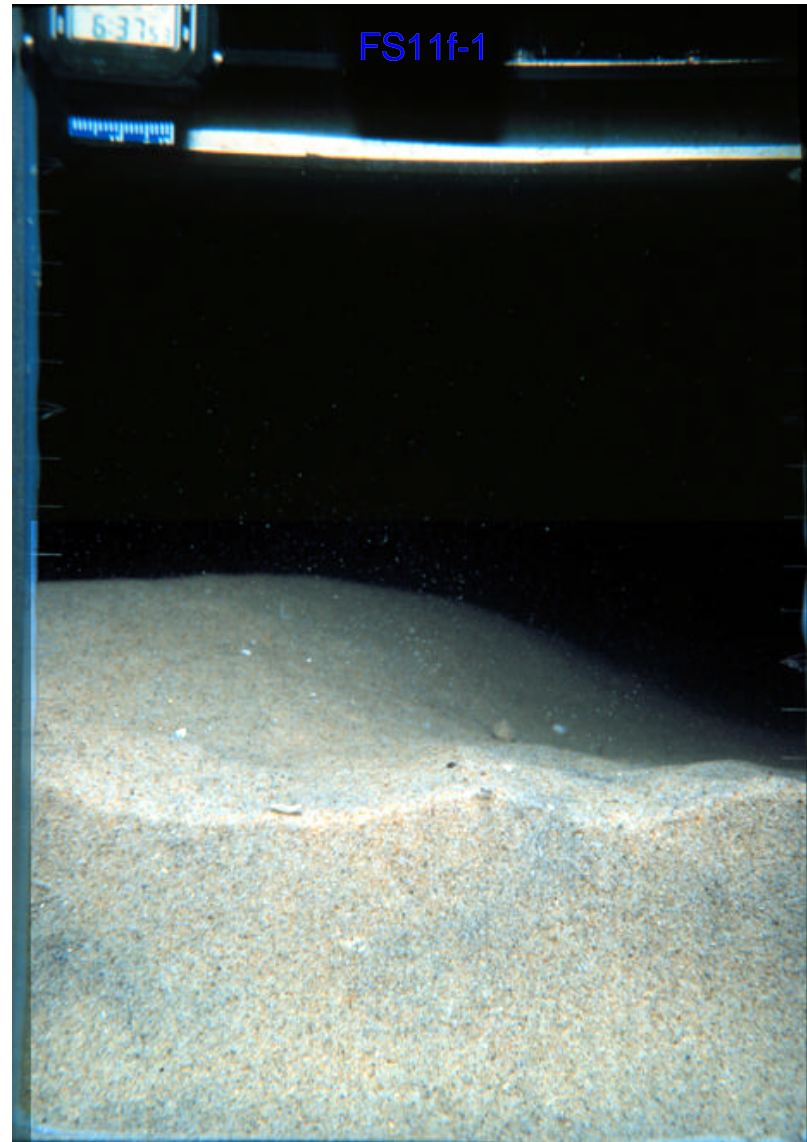
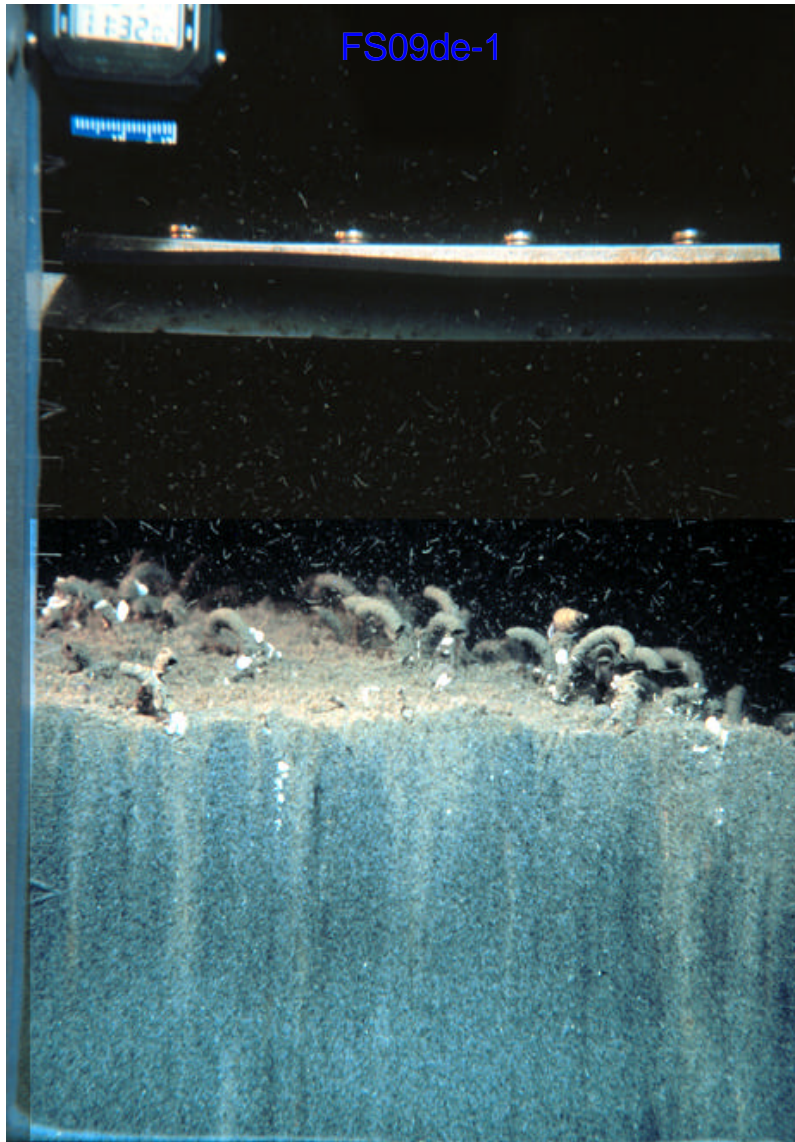


Figure 4.4-3: Selected Sediment Profile Images (SPI).

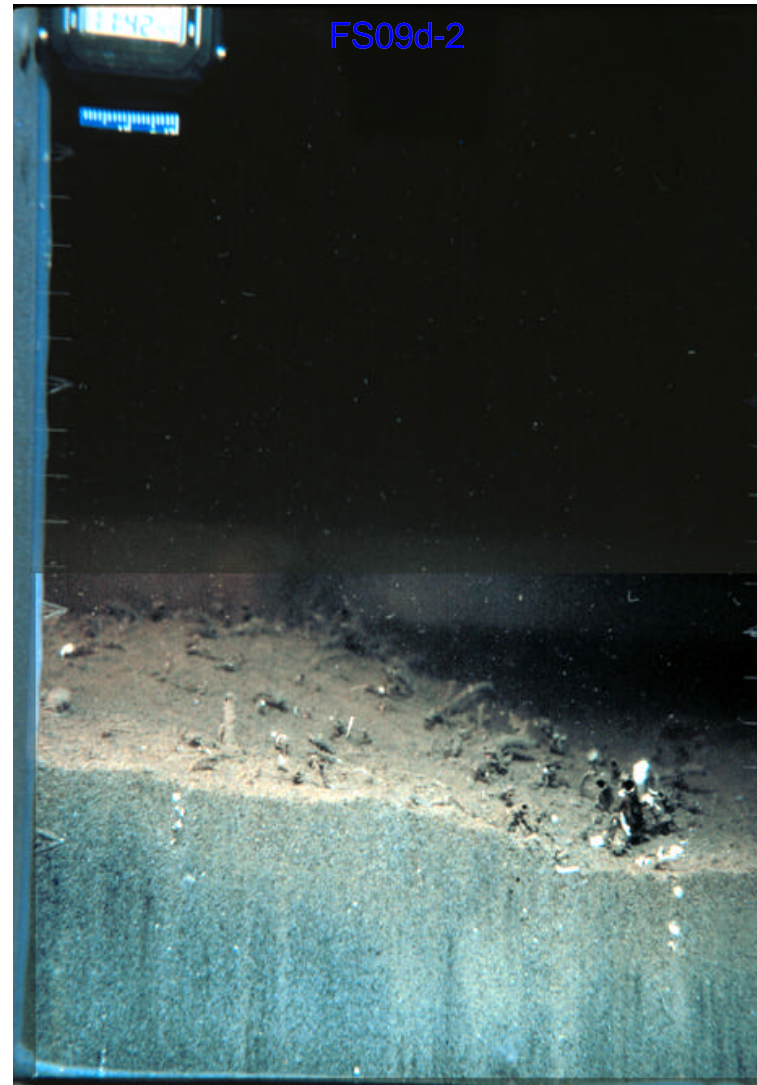


Figure 4.4-4: Selected Sediment Profile Images (SPI).

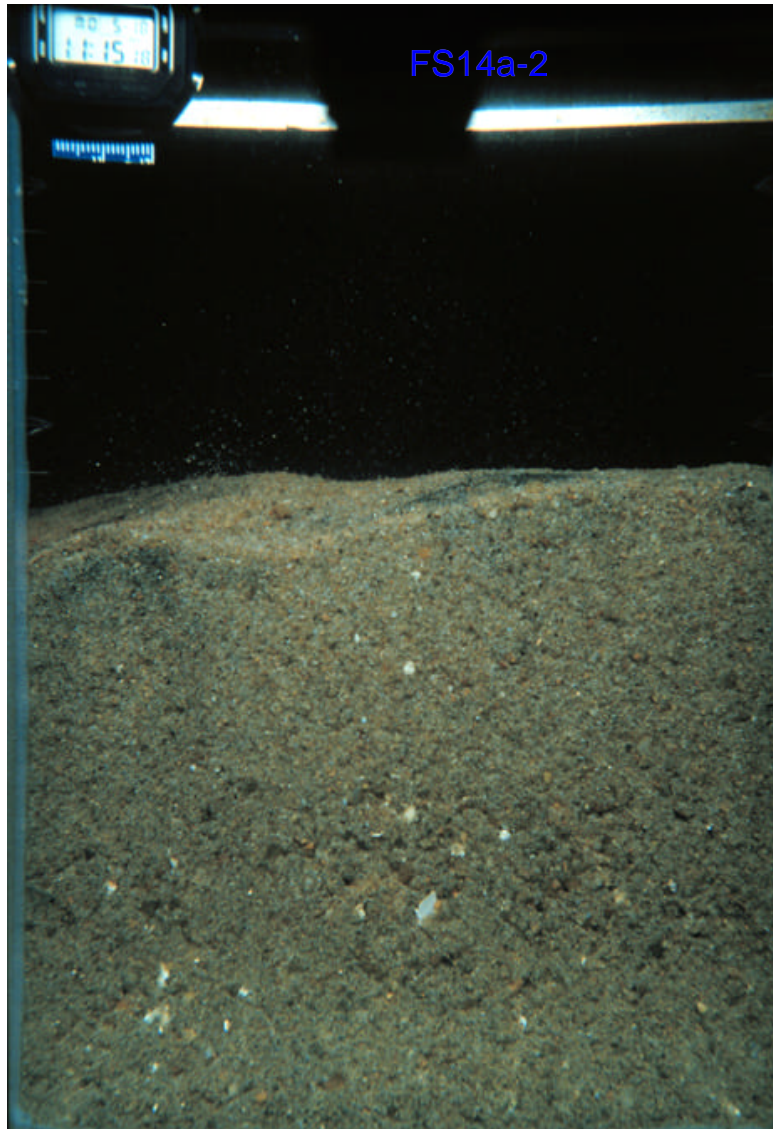


Figure 4.4-5: Selected Sediment Profile Images (SPI).

# MDDE 1998 SPI: Examples of Sediment Grain Size Determinations

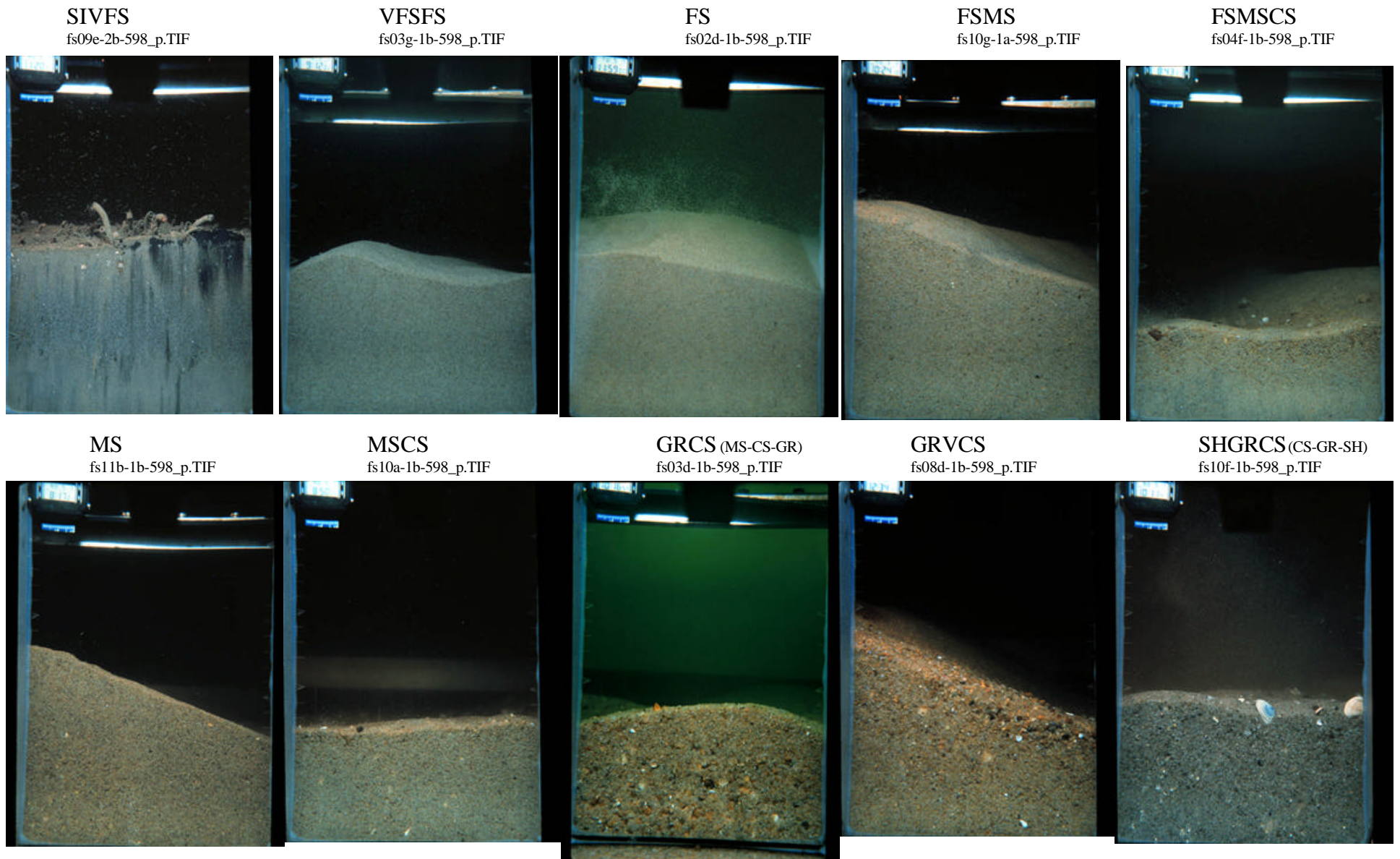


Figure 4.4-6: Examples of sediment grain-size determinations from sediment profile images. CS = coarse sand, FS = fine sand, GR = gravel, MS = medium sand, SH = shell, SI = Silt, VCS = very coarse sand, VFS = very fine sand.

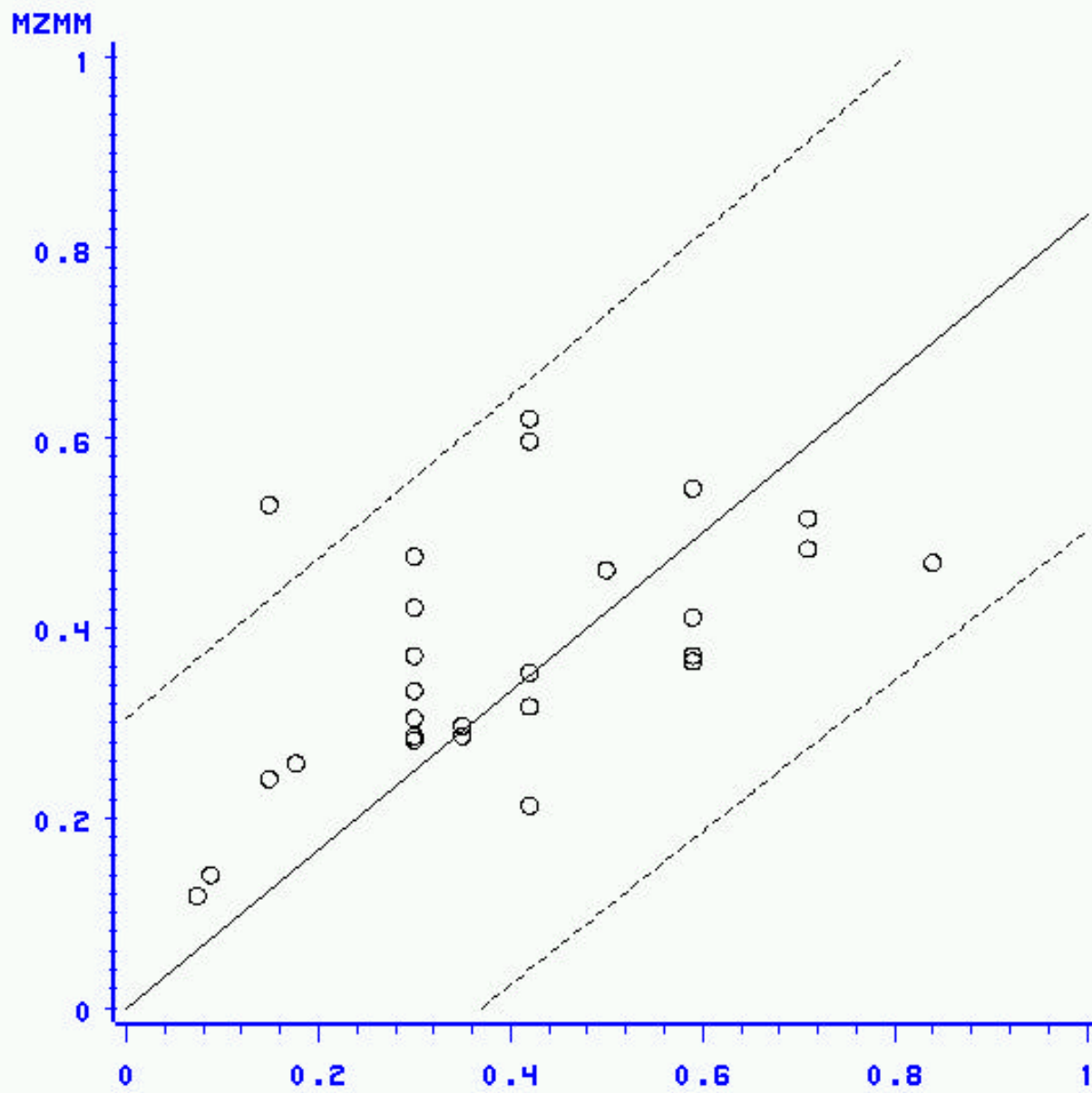


Figure 4.4-7: Relationship between grain-size as determined from grab samples and sediment profile images. Y-axis is mean grain-size in mm of grab samples. X-axis is the mean grain-size in mm as determined from images.

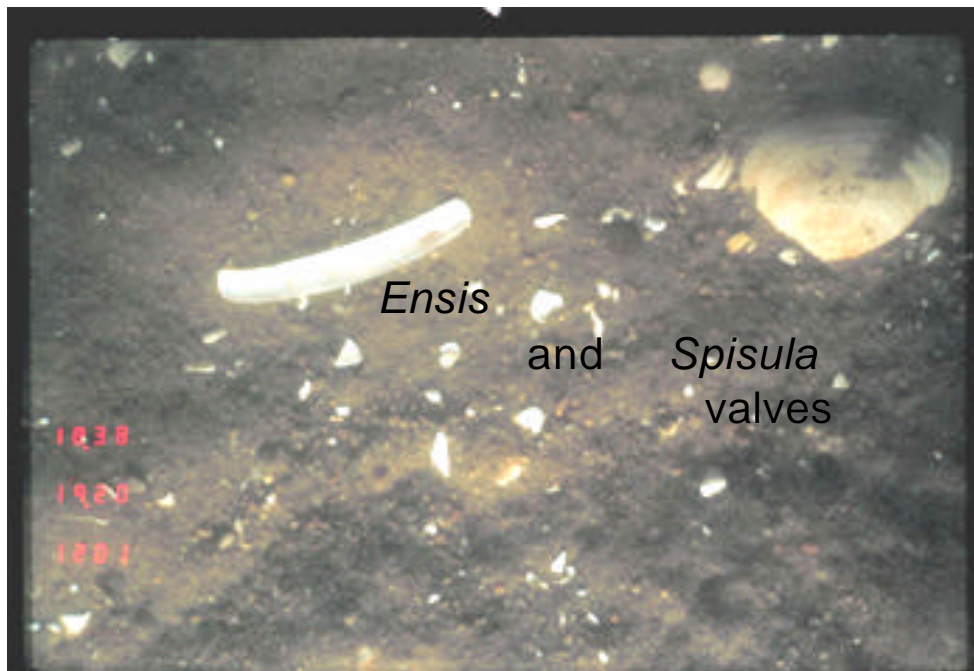
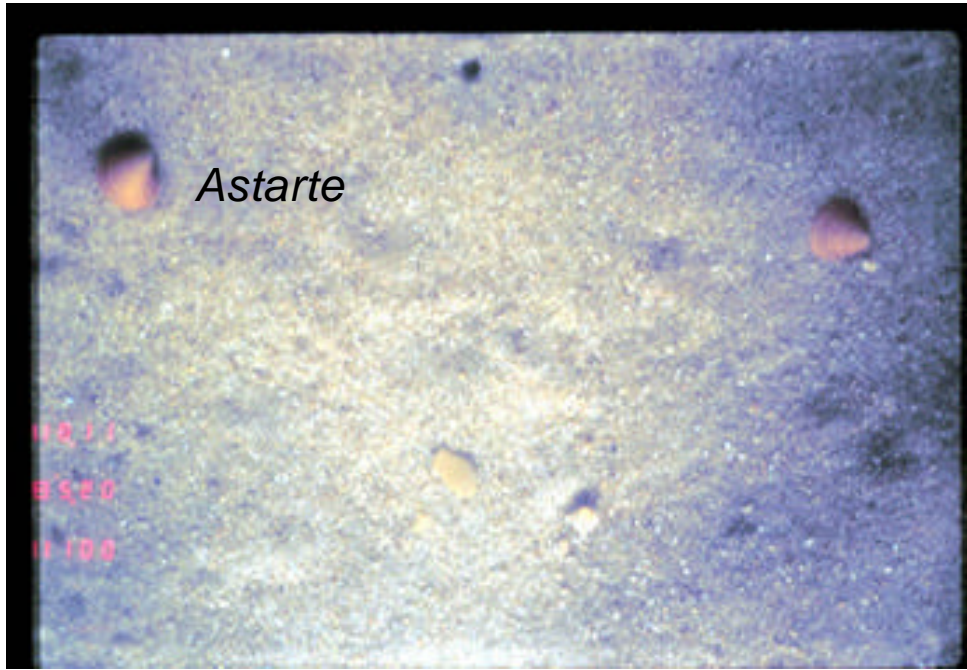


Figure 4.5-1. Selected surface camera images, coarser environments.

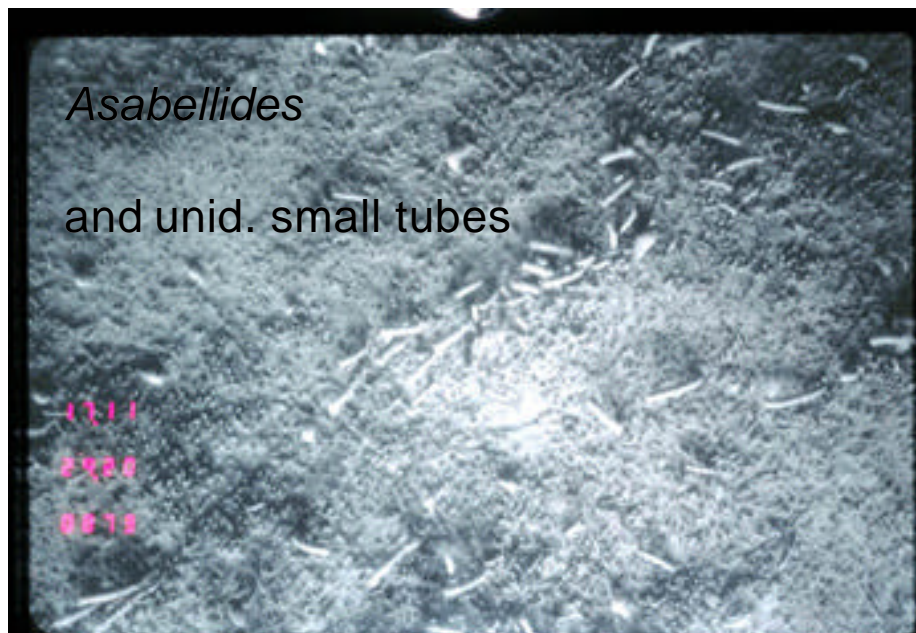
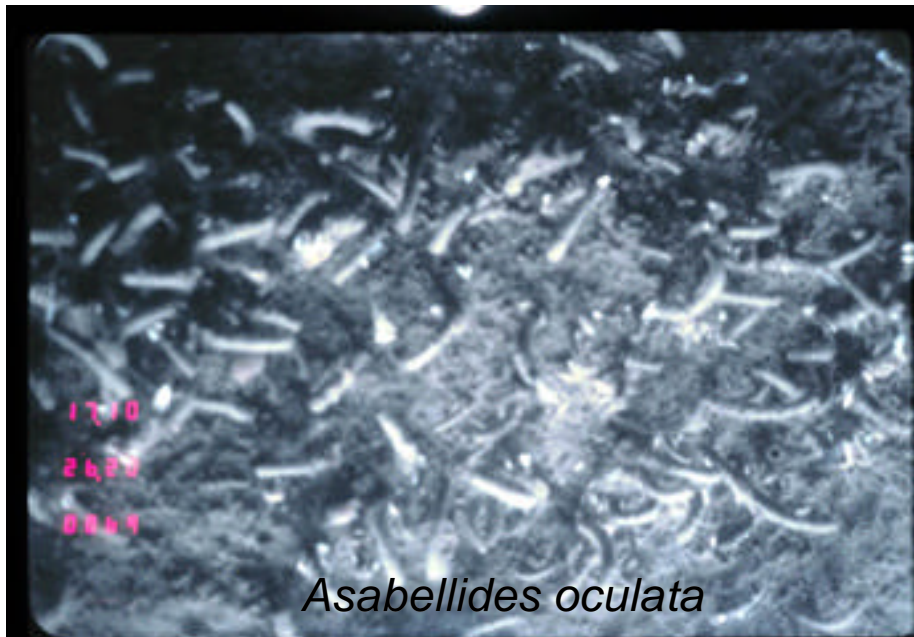


Figure 4.5-2: Selected surface camera images, finer-grained environments.

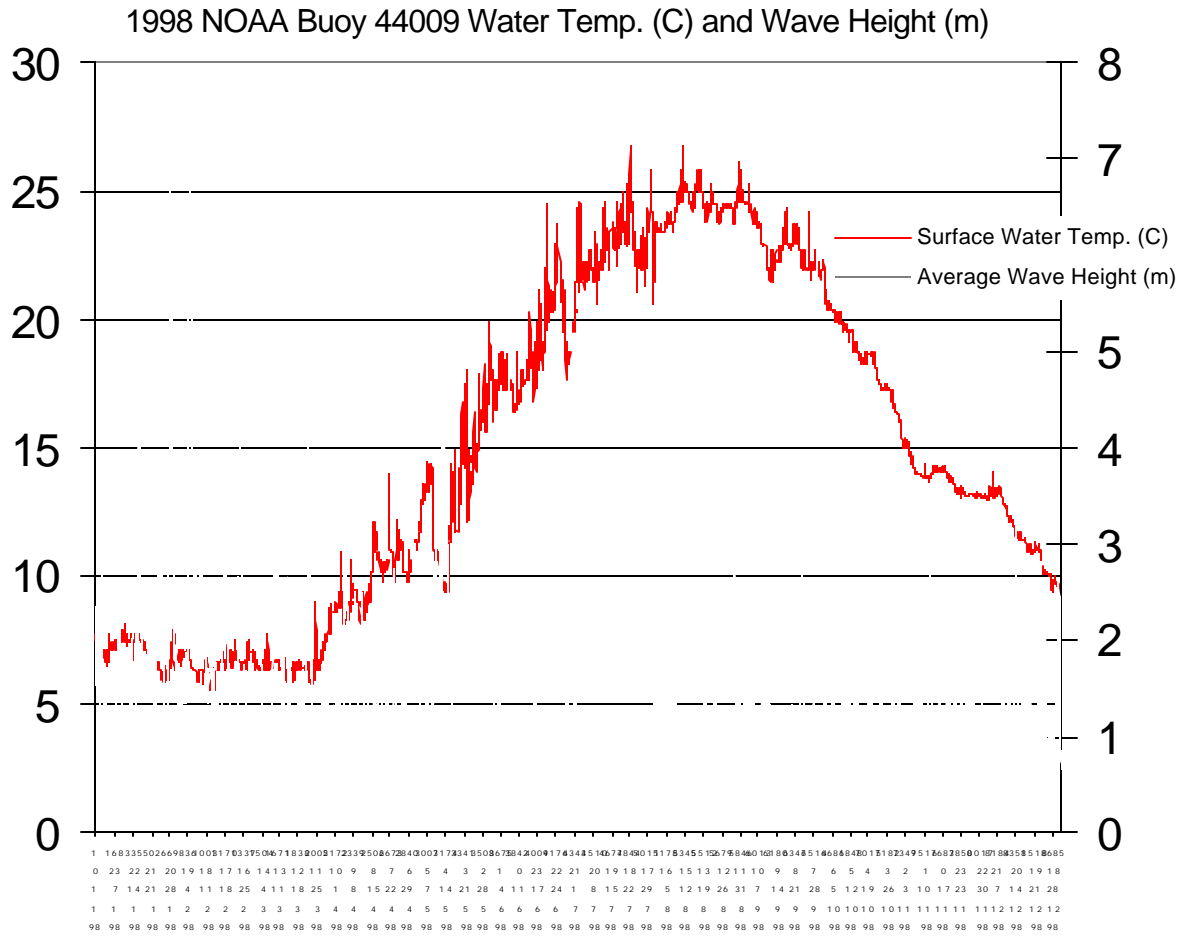


Figure 4.7-1a: Water temperature (°C) and wave height (m) from NOAA Buoy 44009 for the year 1998.

Surf. Water Temp (C)  
 May 17 - 21, 1998, During VIMS MDDE Benthic Cruise

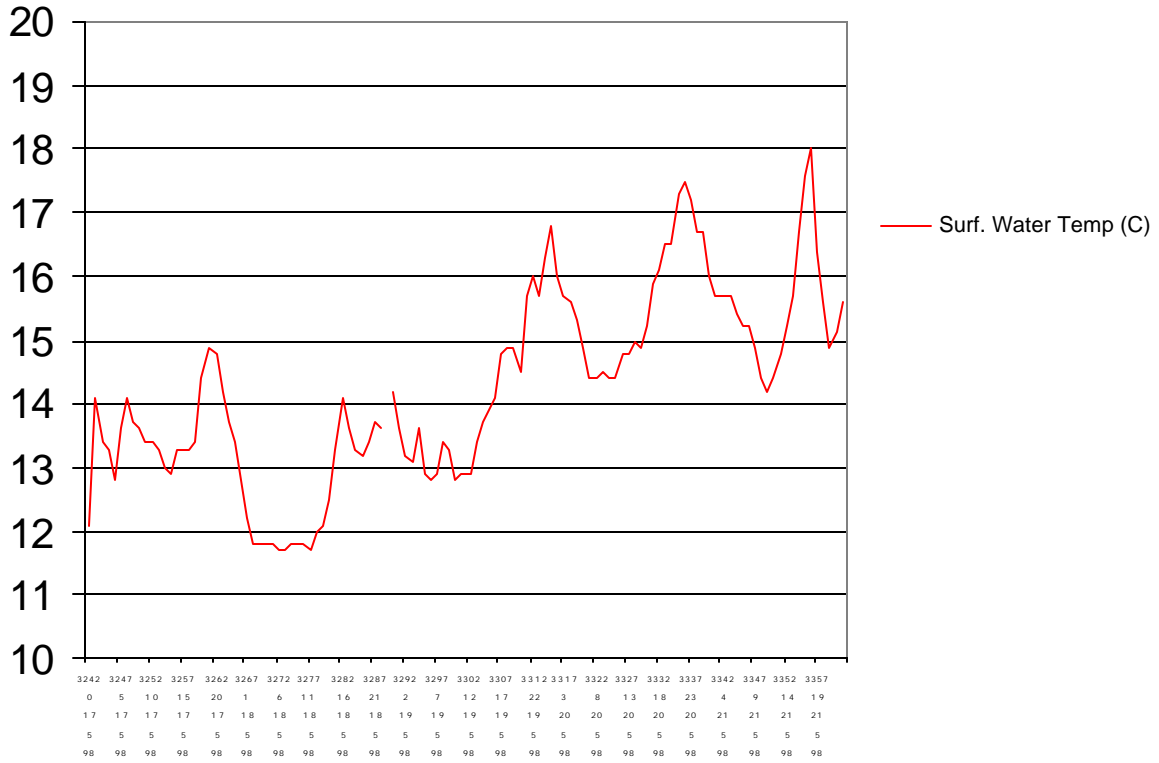


Figure 4.7.1-b: Water temperature (°C) data from NOAA Bouy 44009 during the 17 to 21 May, 1998 cruise.

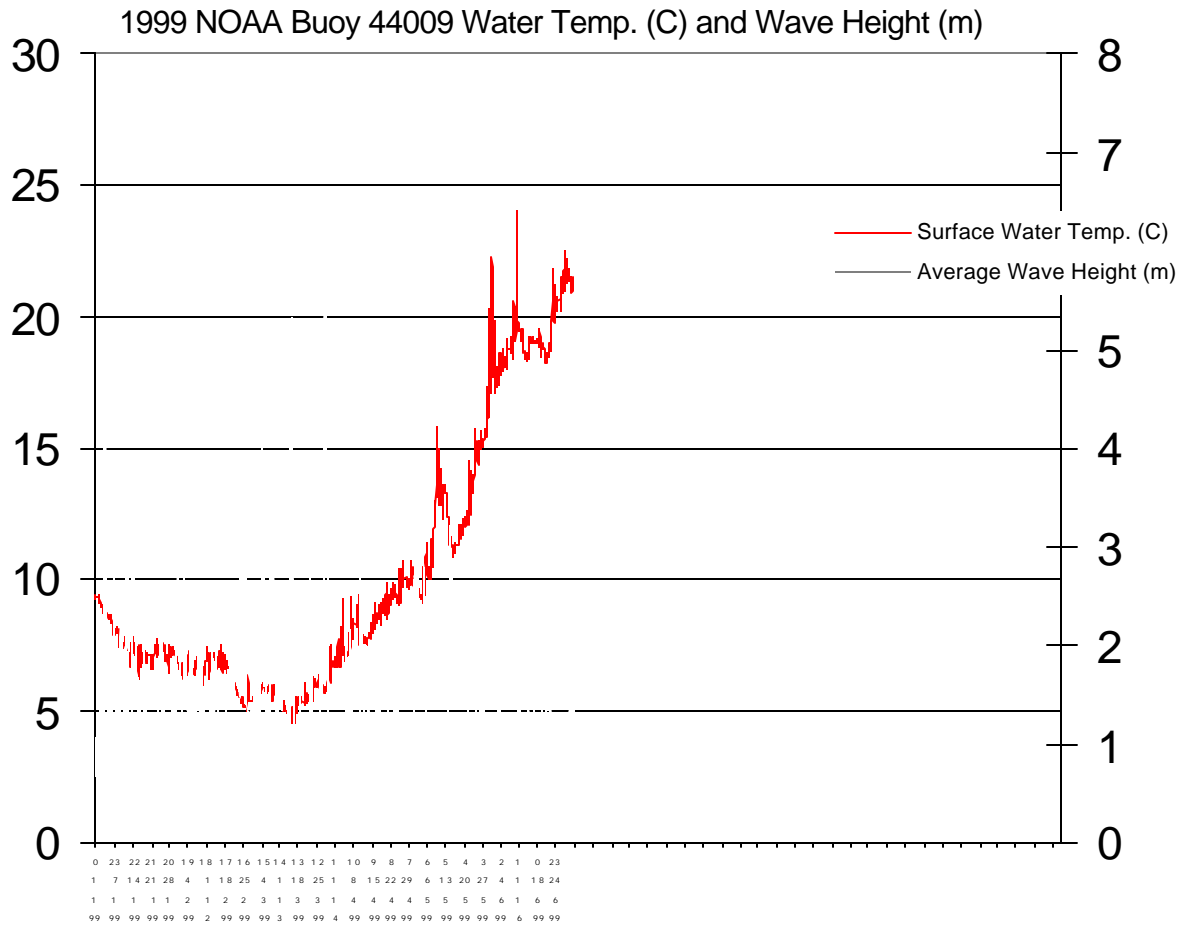


Figure 4.7-2: Water temperature (°C) and wave height (m) from NOAA Buoy 44009 for the first six months of 1999.

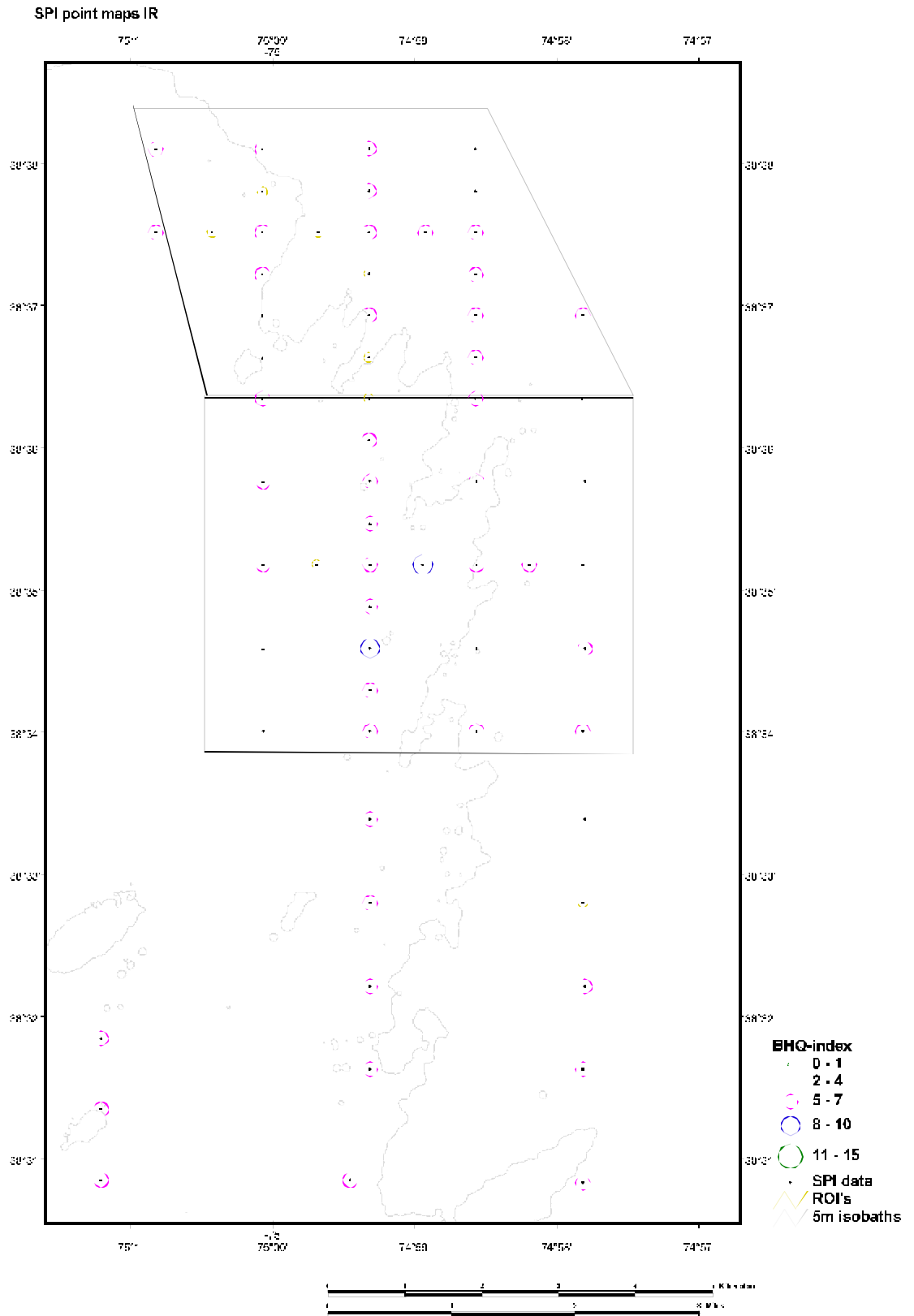


Figure 4.8-1a: Distribution of Benthic Habitat Quality index values for the Indian River ROI.

SPI point maps IR

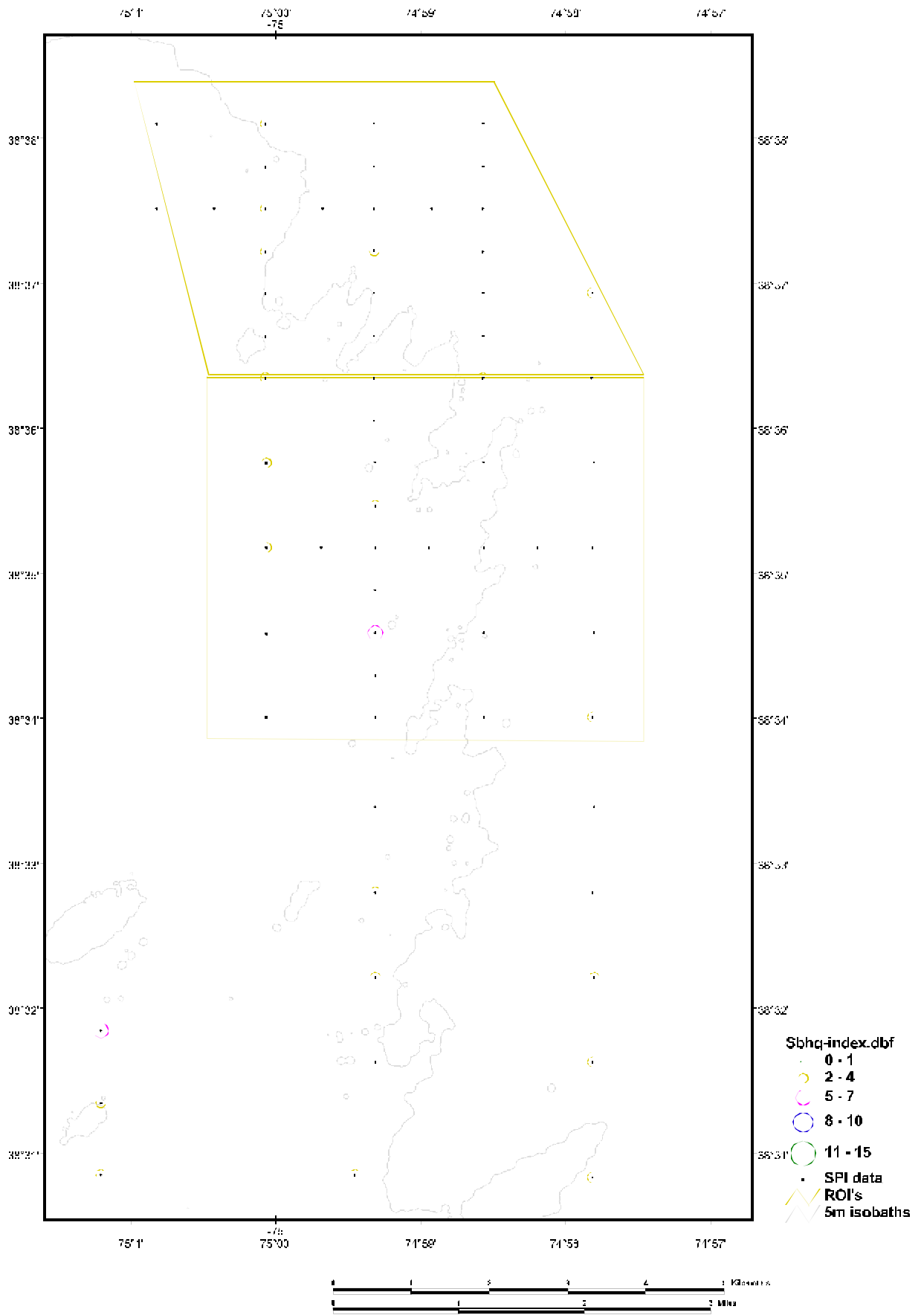


Figure 4.8-1b: Distribution of Scaled Benthic Habitat Quality index value for the Indian River ROI.

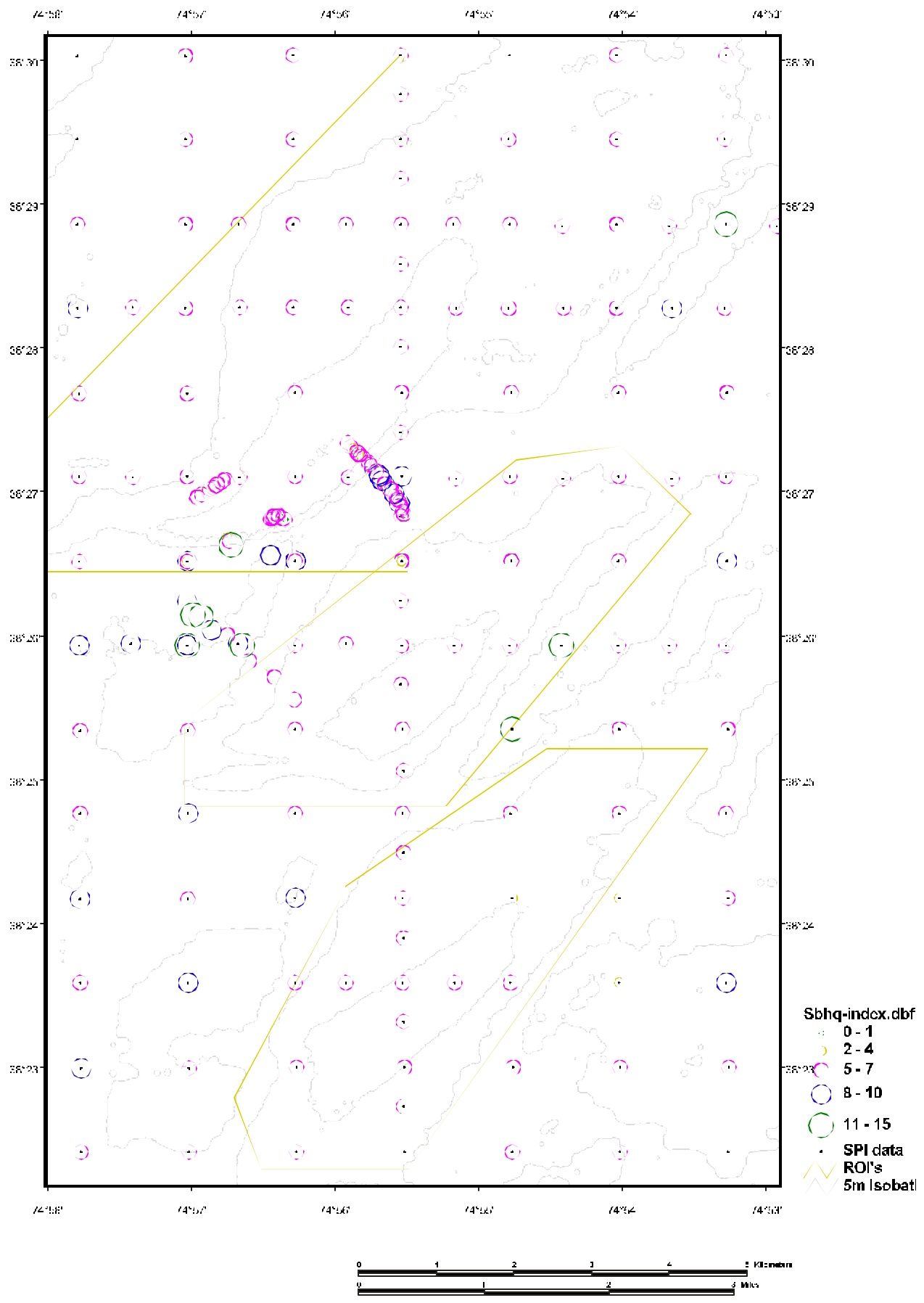


Figure 4.8-2a: Distribution of Benthic Habitat Quality index values for the Fenwick Shoal ROI.

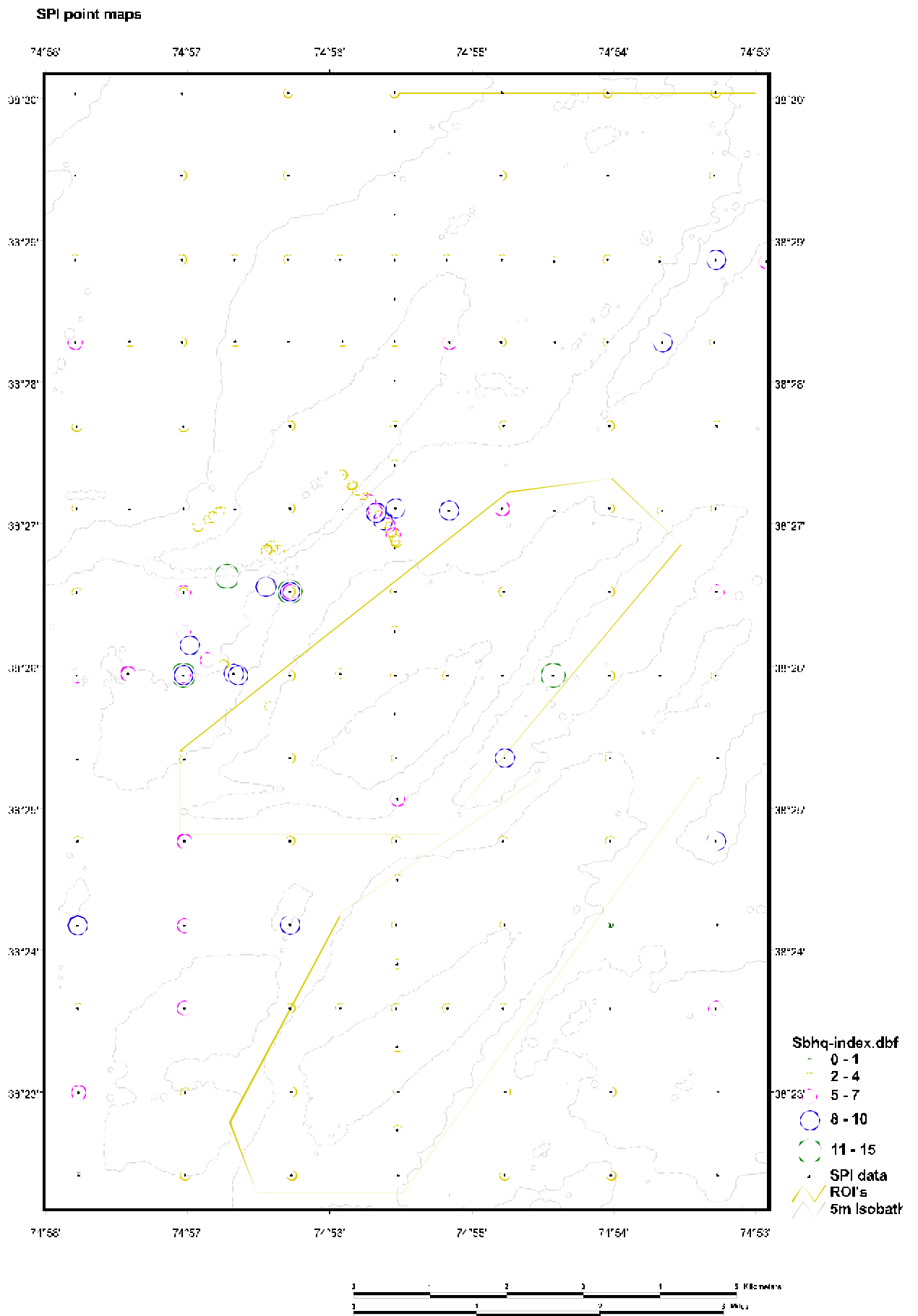


Figure4.8-2b: Distribution of Scaled Benthic Habitat Quality index values for the Fenwick Shoal ROI.

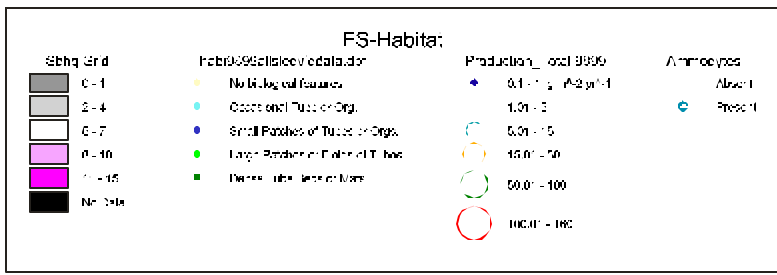
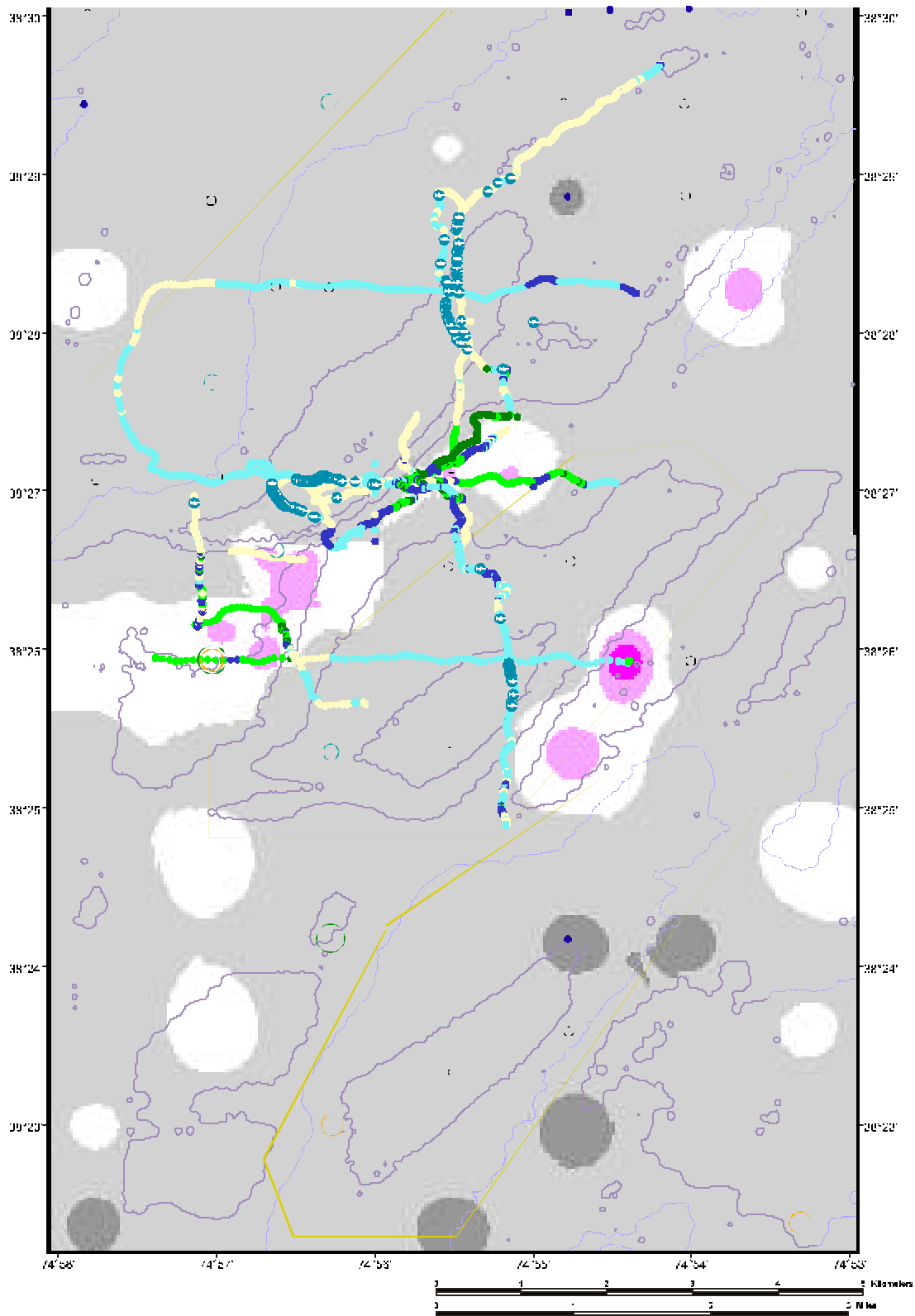


Figure 5.2-1: Benthic habitat map of Fenwick Shoals ROI showing SBHQ index surface generated with inverse distance weighting, secondary production, and surface biological features from video transects. The presence of *Ammodytes* spp. from the video over-lain on the video transects.

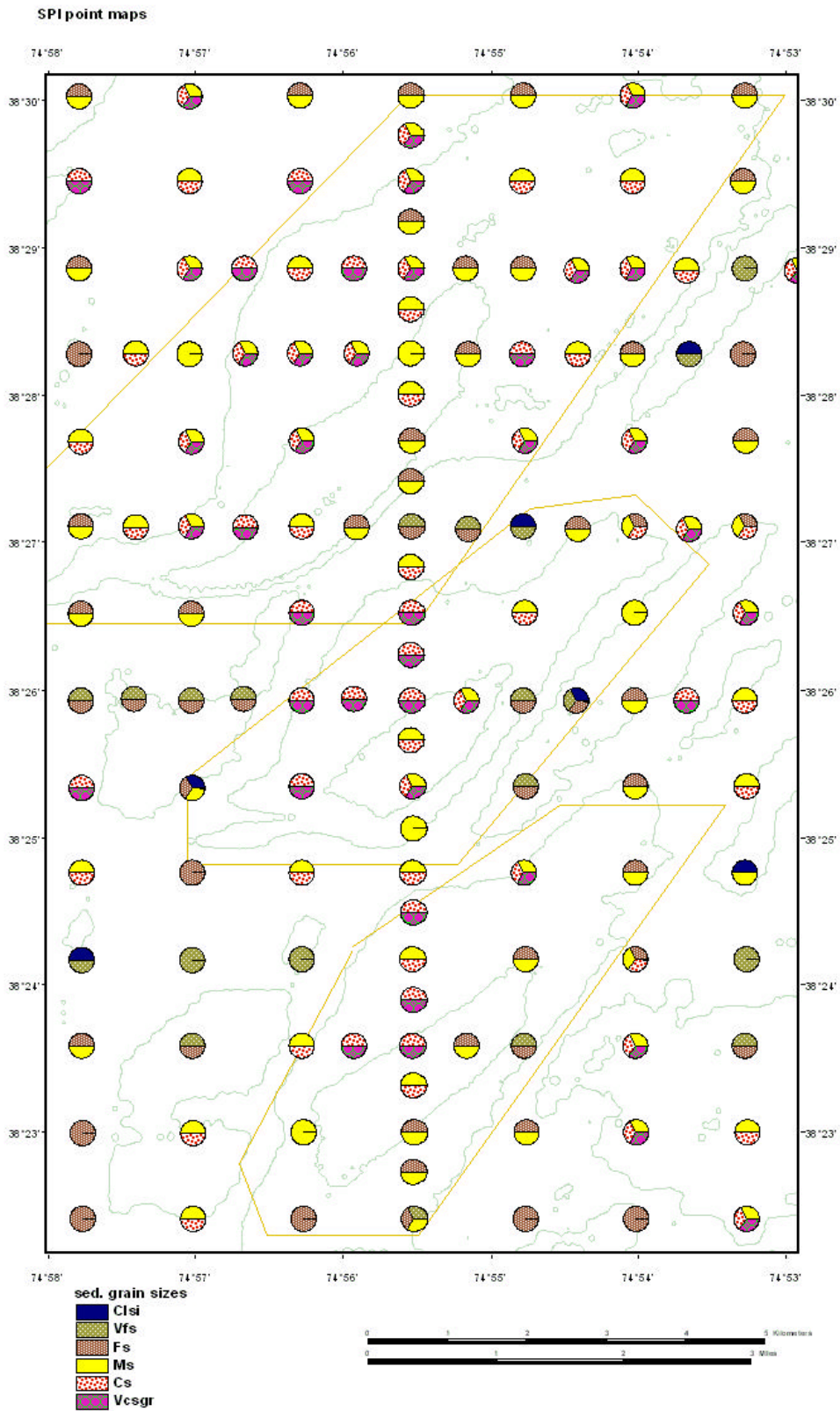


Figure 5.4-1: Sediment grain-size (mm) map of the Fenwick Shoal ROI derived from sediment profile images. Surface was generated with inverse distance weighting interpolation. Coarser sediments tend to be on the crests of the shoals.

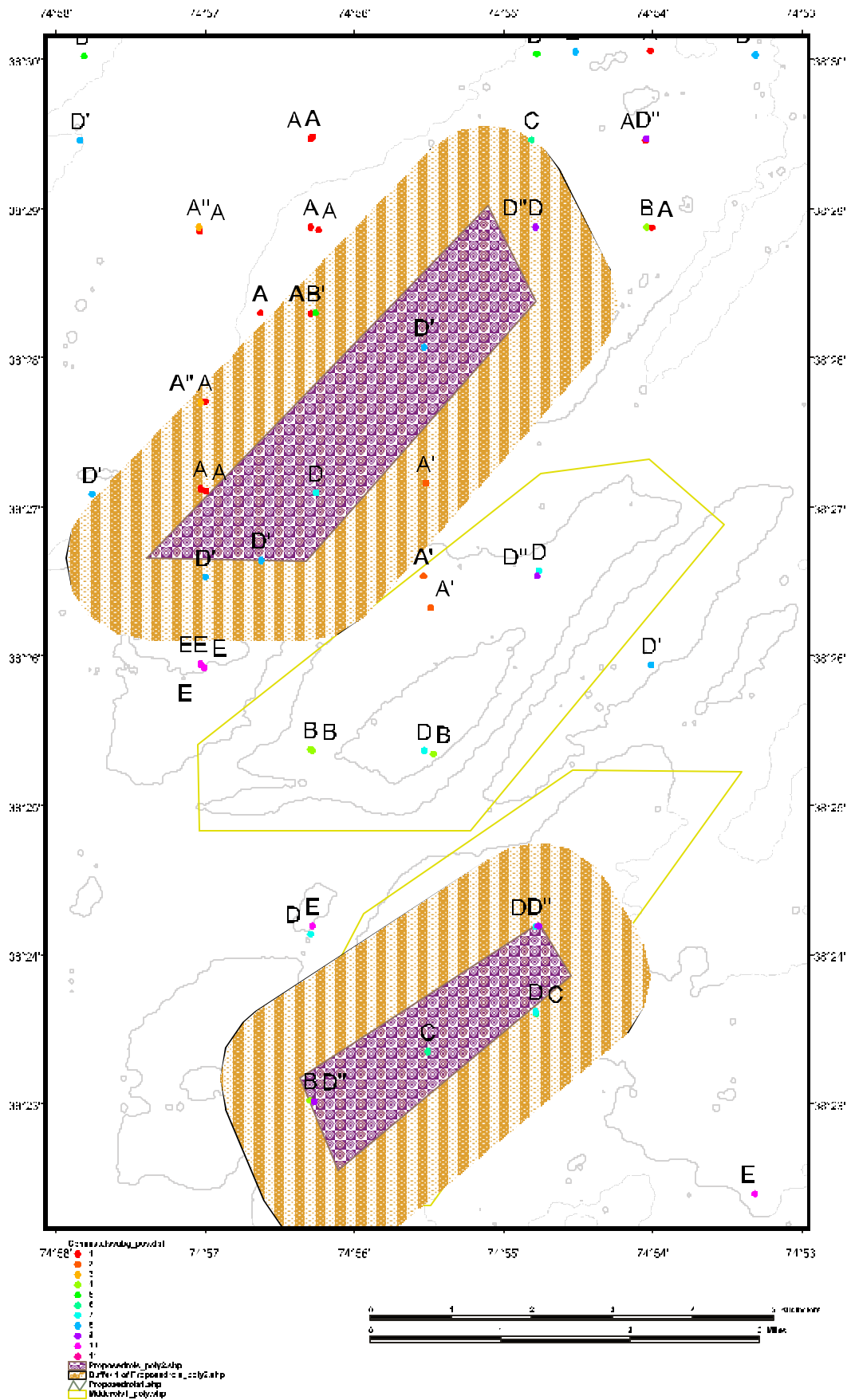


Figure 5.6-1: Sand-mining scenario for the Fenwick Shoal ROA. Benthic recolonization of the mined area (coarse stippling) would proceed from community groups in the buffer zone (fine stippling) and from outside the mined area. Letters refer to cluster groups and subgroups.



# TABLES

Table 4.1-1

Sediment grain-size distribution from grab samples collected in the MD/DE study area.

Gravel is >2mm. Sand is between 2 and 0.063 mm. Silt is between 0.063 mm and 0.0039 mm.

Clay is <0.0039 mm.

STN	% Gravel	%Sand	% Silt	% Clay
BB04	13.8	85.6	0.1	0.5
FS01G	0.6	88.7	4.4	6.3
FS02.5D	0.0	99.6	0.1	0.3
FS02C	2.7	96.8	0.0	0.5
FS02C	12.3	86.9	0.1	0.7
FS03E	0.0	99.2	0.2	0.6
FS04C	0.0	95.7	2.9	1.4
FS04E	0.0	99.6	0.0	0.4
FS06C	14.7	85.0	0.0	0.3
FS06D	0.3	99.2	0.1	0.4
FS07B	0.0	91.2	6.0	2.8
FS07F	0.2	99.0	0.1	0.7
FS08B	0.0	98.8	0.4	0.8
FS08C	0.3	97.9	0.7	1.1
FS08D	2.2	97.5	0.1	0.2
FS08E	0.0	99.5	0.1	0.4
FS09A	2.1	96.8	0.3	0.8
FS09B	0.9	98.1	0.3	0.7
FS09C	0.0	99.5	0.1	0.4
FS09D	3.3	94.6	0.7	1.4
FS10.5D	0.0	99.4	0.1	0.5
FS10A	2.4	96.7	0.3	0.6
FS10B	5.5	93.8	0.1	0.6
FS11C	3.7	96.0	0.1	0.2
FS12B	16.7	82.8	0.1	0.4
FS12C	15.2	84.5	0.0	0.3
FS12E	1.0	98.8	0.0	0.2
FS12F	2.3	97.3	0.1	0.4
FS13A	4.5	94.5	0.2	0.8
FS13C	7.5	91.9	0.1	0.5
FS13E	0.0	99.1	0.2	0.7
FS13F	1.5	97.9	0.1	0.5
FS14A	3.2	96.2	0.1	0.5
FS14D	1.9	97.5	0.2	0.4
FS14D	0.0	99.2	0.1	0.7
FS14E	1.4	98.0	0.1	0.5
FS14G	0.0	99.1	0.1	0.8
HCS31	0.0	74.0	7.7	18.3
IR02B	66.4	33.5	0.1	0.1
IR02D	18.5	80.6	0.2	0.7
IR04B	4.5	94.8	0.1	0.6
IR04D	56.7	42.3	0.3	0.7
IR04E	61.1	36.1	1.2	1.6
IR05.5C	4.3	95.1	0.1	0.5
IR05D	34.1	65.1	0.2	0.6
IR07C	1.7	97.6	0.1	0.6
IR08B	21.9	77.3	0.1	0.7
IR08C	36.0	62.8	0.4	0.8
IR09A	11.2	88.2	0.1	0.5
IR09C	16.1	83.2	0.1	0.6
SBB32	14.7	84.1	0.2	1.0

Table 4.1-2  
Sediment grain-size analysis of sand fraction from grab samples  
collected in the MD/DE study area. All statistics are in mm.

---

Station	Mean	Median	Sorting	Skewness	Kurtosis
BB04	0.47	0.49	0.59	0.94	0.57
FS01G	0.18	0.18	0.70	1.04	0.74
FS02.5D	0.37	0.39	0.70	0.82	0.59
FS03E	0.24	0.24	0.78	0.96	0.77
FS04C	0.14	0.14	0.67	1.27	0.72
FS04E	0.37	0.39	0.70	0.82	0.63
FS06C	1.07	1.11	0.58	0.83	0.13
FS06D	0.60	0.61	0.66	0.87	0.45
FS07B.2	0.12	0.11	0.82	1.19	0.88
FS07F	0.31	0.27	0.53	1.19	0.60
FS08B	0.26	0.26	0.76	1.12	0.71
FS08C	0.28	0.29	0.65	0.91	0.69
FS08D	0.76	0.74	0.68	0.96	0.39
FS08E	0.32	0.33	0.62	0.88	0.60
FS09A	0.29	0.28	0.61	1.02	0.63
FS09B	0.46	0.43	0.57	1.13	0.61
FS09C	0.37	0.37	0.77	0.92	0.67
FS09D	0.53	0.86	0.39	0.65	0.66
FS10.5D	0.35	0.37	0.71	0.79	0.62
FS10A	0.41	0.40	0.58	1.08	0.61
FS10B	0.41	0.38	0.55	1.21	0.59
FS11C	0.65	0.65	0.55	0.92	0.53
FS12B	0.52	0.47	0.53	1.11	0.56
FS12C	0.55	0.54	0.55	0.97	0.56
FS12E	0.33	0.33	0.65	1.02	0.63
FS12F	0.57	0.57	0.49	0.94	0.46
FS13A	0.49	0.43	0.54	1.21	0.56
FS13C	0.52	0.51	0.54	1.00	0.62
FS13E	0.21	0.21	0.76	0.97	0.77
FS13F	0.62	0.63	0.49	0.94	0.58
FS14A	0.48	0.44	0.51	1.06	0.54
FS14D	0.29	0.29	0.67	0.95	0.68
FS14E	0.42	0.41	0.61	1.02	0.63
FS14F	0.44	0.44	0.53	0.98	0.58
FS14G	0.28	0.28	0.76	1.07	0.75
HCS31	0.45	0.44	0.56	0.94	0.55
IR02B	0.97	1.11	0.57	0.77	0.39
IR02D	0.64	0.60	0.52	1.05	0.52
IR04B	0.42	0.41	0.65	1.06	0.60
IR04D	0.27	0.26	0.73	1.08	0.74
IR04E	0.41	0.41	0.50	0.98	0.58
IR05.5C	0.61	0.61	0.58	0.96	0.49
IR05D	0.30	0.29	0.73	1.10	0.71
IR07C	0.56	0.52	0.62	1.10	0.52
IR08B	0.51	0.50	0.59	1.05	0.59
IR08C	0.48	0.47	0.54	1.04	0.51
IR09A	0.67	0.72	0.55	0.89	0.47
IR09C	0.52	0.52	0.53	0.93	0.53
SBB32	0.47	0.44	0.54	1.09	0.57

Table 4.2-1.

Major taxa abundance (individuals/0.04 m<sup>2</sup>) of infauna collected off Maryland and Delaware in May 1998 and June 1999.

-----  
 May 1998

Station	Anthozoa		Annelida		Crustacea		Phoronida		Cephalochordata		Totals
		Nemertinea		Bivalvia		Sipuncula		Echinodermata			
BB02	1	20	293	6	28	0	0	0	0	348	
BB04	1	14	243	1	12	0	0	0	0	271	
FS01G	0	1	3066	13	26	0	2	0	0	3108	
FS02.5D	0	1	9	1	37	0	0	0	0	48	
FS02C	4	13	53	61	15	0	0	2	2	150	
FS03E	0	0	0	0	20	0	0	0	1	21	
FS04C	0	0	82	734	56	0	0	0	0	872	
FS04E	0	1	1	3	2	0	0	0	0	7	
FS06C	19	7	206	166	5	0	0	11	2	416	
FS06D	0	0	21	33	3	0	0	0	0	57	
FS07B	0	0	283	102	68	0	8	0	0	461	
FS07F	0	2	9	13	10	0	0	0	0	34	
FS08B	0	3	29	2	42	0	2	0	0	78	
FS08C	0	1	98	65	2	2	0	0	0	168	
FS08D	5	13	143	4	2	0	0	0	1	168	
FS08E	0	0	2	4	3	0	2	0	0	11	
FS09A	0	0	56	23	38	0	0	0	1	118	
FS09B	0	5	44	6	37	0	0	0	0	92	
FS09C	0	0	3	1	12	0	0	0	0	16	
FS09D	0	3	72	0	3	0	0	0	0	78	
FS10.5D	0	0	1	0	3	0	0	0	0	4	
FS10A	0	12	159	0	27	0	0	2	0	200	
FS10B	1	13	149	4	14	0	0	0	0	181	
FS11C	0	2	81	12	2	0	0	0	0	97	
FS12B	0	9	58	1	15	0	0	0	0	83	
FS12C	0	5	49	1	3	0	0	0	1	59	
FS12E	0	0	1	1	2	0	0	0	0	4	
FS12F	0	4	25	2	3	0	0	1	0	35	
FS13A	0	3	20	0	6	0	6	0	0	35	
FS13C	2	15	153	4	12	0	0	0	1	187	
FS13E	0	0	0	2	6	0	0	0	0	8	
FS13F	2	38	52	16	15	0	0	0	0	123	
FS14A	0	26	233	5	7	0	0	0	0	271	
FS14D	0	0	3	2	4	0	0	0	0	9	
FS14E	0	1	12	0	3	0	0	0	0	16	
FS14F	0	6	50	5	12	0	0	0	0	73	
FS14G	0	1	0	2	13	0	0	0	0	16	
HCS31	0	11	1123	68	22	0	7	0	0	1231	

Table 4.2.1. Continued.

May 1998

Station	Anthozoa		Annelida		Crustacea		Phoronida		Cephalochordata		Totals
		Nemertinea		Bivalvia		Sipuncula		Echinodermata			
IR02B	0	12	62	16	2	0	0	0	1	93	
IR02C	0	21	201	15	6	0	0	0	0	243	
IR02D	0	10	119	18	2	0	0	0	0	149	
IR04B	0	1	14	4	6	0	0	0	0	25	
IR04D	0	0	12	5	4	0	0	0	0	21	
IR04E	0	1	257	20	32	2	0	0	0	312	
IR05.5C	0	4	47	5	4	0	0	0	0	60	
IR05D	0	0	145	6	11	1	2	0	0	165	
IR07C	0	5	41	1	8	0	0	1	0	56	
IR07E	0	0	19	0	4	2	1	0	0	26	
IR08B	0	0	14	2	5	0	0	0	0	21	
IR08C	0	4	41	2	14	0	0	0	0	61	
IR09A	1	1	29	5	5	0	0	0	0	41	
IR09C	0	12	192	2	1	0	0	0	0	207	
Totals	36	301	8075	1464	694	7	30	17	10	10634	

June 1999

	Anthozoa		Annelida		Crustacea		Phoronida		Cephalochordata		Totals
		Nemertinea		Bivalvia		Sipuncula		Echinodermata			
FS02C	4	3	1	38	21	0	0	1	0	68	
FS03E	0	0	0	2	11	0	0	0	1	14	
FS04C	0	3	1136	157	40	0	0	0	0	1336	
FS04E	0	0	0	8	4	0	0	0	1	13	
FS06C	3	6	73	13	2	0	0	1	3	101	
FS06D	0	11	10	10	4	0	0	0	0	35	
FS07B1	0	16	1034	187	53	0	0	0	0	1290	
FS07B2	0	3	1007	86	39	0	27	0	0	1162	
FS07B3	1	2	711	110	181	1	0	0	0	1006	
FS08D	7	13	131	13	1	0	0	2	1	168	
FS08E	1	1	7	28	6	0	0	0	0	43	
FS09B	0	8	159	7	56	0	0	0	0	230	
FS10B	0	1	25	7	170	0	0	0	0	203	
FS11C	0	4	52	4	5	0	0	0	0	65	
FS12B	0	5	20	0	103	0	0	0	2	130	
FS12C	1	14	43	7	7	0	0	0	2	74	
FS12E	0	1	1	4	3	0	0	0	1	10	
FS12F	0	5	6	32	3	0	0	0	1	47	
FS13C	0	16	39	13	52	0	0	0	2	122	
FS13F	0	1	3	14	9	0	0	0	1	28	
Totals	17	113	4458	740	770	1	27	4	15	6145	

Table 4.2-2.

Proportional contribution of major taxa to total infaunal abundance and species richness for samples collected off Maryland and Delaware in May 1998 and June 1999.

---

May 1998

Major Taxon	Percentage of Individuals	Percentage of Taxa
Anthozoa	0.3	0.7
Nemertinea	2.8	0.7
Annelida	75.9	50.7
Mollusca	13.8	23.0
Crustacea	6.5	22.4
Sipuncula	0.1	0.7
Phoronida	0.3	0.7
Echinodermata	0.2	0.7
Cephalochordata	0.1	0.7

June 1999

Major Taxon	Percentage of Individuals	Percentage of Taxa
Anthozoa	0.3	0.9
Nemertinea	1.8	0.9
Annelida	72.5	52.8
Mollusca	12.0	21.3
Crustacea	12.5	20.4
Sipuncula	0.02	0.9
Phoronida	0.4	0.9
Echinodermata	0.1	0.9
Cephalochordata	0.2	0.9

Table 4.2-3.

Percentage of major taxa abundance (individuals/0.04 m<sup>2</sup>) of infauna collected in the Maryland and Delaware study area in May 1998 and June 1999.

May 1998									
Station	Anthozoa	Annelida		Crustacea		Phoronida	Cephalochordata		
	Nemertinea		Bivalvia		Sipuncula	Echinodermata			
BB02	0.3	5.7	84.2	1.7	8.0	0.0	0.0	0.0	0.0
BB04	0.4	5.2	89.7	0.4	4.4	0.0	0.0	0.0	0.0
FS01G	0.0	0.0	98.6	0.4	0.8	0.0	0.1	0.0	0.0
FS02.5D	0.0	2.1	18.8	2.1	77.1	0.0	0.0	0.0	0.0
FS02C	2.7	8.7	35.3	40.7	10.0	0.0	0.0	1.3	1.3
FS03E	0.0	0.0	0.0	0.0	95.2	0.0	0.0	0.0	4.8
FS04C	0.0	0.0	9.4	84.2	6.4	0.0	0.0	0.0	0.0
FS04E	0.0	14.3	14.3	42.9	28.6	0.0	0.0	0.0	0.0
FS06C	4.6	1.7	49.5	39.9	1.2	0.0	0.0	2.6	0.5
FS06D	0.0	0.0	36.8	57.9	5.3	0.0	0.0	0.0	0.0
FS07B	0.0	0.0	61.4	22.1	14.8	0.0	1.7	0.0	0.0
FS07F	0.0	5.9	26.5	38.2	29.4	0.0	0.0	0.0	0.0
FS08B	0.0	3.8	37.2	2.6	53.8	0.0	2.6	0.0	0.0
FS08C	0.0	0.6	58.3	38.7	1.2	1.2	0.0	0.0	0.0
FS08D	3.0	7.7	85.1	2.4	1.2	0.0	0.0	0.0	0.6
FS08E	0.0	0.0	18.2	36.4	27.3	0.0	18.2	0.0	0.0
FS09A	0.0	0.0	47.5	19.5	32.2	0.0	0.0	0.0	0.8
FS09B	0.0	5.4	47.8	6.5	40.2	0.0	0.0	0.0	0.0
FS09C	0.0	0.0	18.8	6.3	75.0	0.0	0.0	0.0	0.0
FS09D	0.0	3.8	92.3	0.0	3.8	0.0	0.0	0.0	0.0
FS10.5D	0.0	0.0	25.0	0.0	75.0	0.0	0.0	0.0	0.0
FS10A	0.0	6.0	79.5	0.0	13.5	0.0	0.0	1.0	0.0
FS10B	0.6	7.2	82.3	2.2	7.7	0.0	0.0	0.0	0.0
FS11C	0.0	2.1	83.5	12.4	2.1	0.0	0.0	0.0	0.0
FS12B	0.0	10.8	69.9	1.2	18.1	0.0	0.0	0.0	0.0
FS12C	0.0	8.5	83.1	1.7	5.1	0.0	0.0	0.0	1.7
FS12E	0.0	0.0	25.0	25.0	50.0	0.0	0.0	0.0	0.0
FS12F	0.0	11.4	71.4	5.7	8.6	0.0	0.0	2.9	0.0
FS13A	0.0	8.6	57.1	0.0	17.1	0.0	17.1	0.0	0.0
FS13C	1.1	8.0	81.8	2.1	6.4	0.0	0.0	0.0	0.5
FS13E	0.0	0.0	0.0	25.0	75.0	0.0	0.0	0.0	0.0
FS13F	1.6	30.9	42.3	13.0	12.2	0.0	0.0	0.0	0.0
FS14A	0.0	9.6	86.0	1.8	2.6	0.0	0.0	0.0	0.0
FS14D	0.0	0.0	33.3	22.2	44.4	0.0	0.0	0.0	0.0
FS14E	0.0	6.3	75.0	0.0	18.8	0.0	0.0	0.0	0.0
FS14F	0.0	8.2	68.5	6.8	16.4	0.0	0.0	0.0	0.0
FS14G	0.0	6.3	0.0	12.5	81.3	0.0	0.0	0.0	0.0
HCS31	0.0	0.9	91.2	5.5	1.8	0.0	0.6	0.0	0.0

Table 4.2-3. Continued.

May 1998

Station	Anthozoa		Annelida		Crustacea		Phoronida	Cephalochordata	
	Nemertinea		Bivalvia		Sipuncula		Echinodermata		
IR02B	0.0	12.9	66.7	17.2	2.2	0.0	0.0	0.0	1.1
IR02C	0.0	8.6	82.7	6.2	2.5	0.0	0.0	0.0	0.0
IR02D	0.0	6.7	79.9	12.1	1.3	0.0	0.0	0.0	0.0
IR04B	0.0	4.0	56.0	16.0	24.0	0.0	0.0	0.0	0.0
IR04D	0.0	0.0	57.1	23.8	19.0	0.0	0.0	0.0	0.0
IR04E	0.0	0.3	82.4	6.4	10.3	0.6	0.0	0.0	0.0
IR05.5C	0.0	6.7	78.3	8.3	6.7	0.0	0.0	0.0	0.0
IR05D	0.0	0.0	87.9	3.6	6.7	0.6	1.2	0.0	0.0
IR07C	0.0	8.9	73.2	1.8	14.3	0.0	0.0	1.8	0.0
IR07E	0.0	0.0	73.1	0.0	15.4	7.7	3.8	0.0	0.0
IR08B	0.0	0.0	66.7	9.5	23.8	0.0	0.0	0.0	0.0
IR08C	0.0	6.6	67.2	3.3	23.0	0.0	0.0	0.0	0.0
IR09A	2.4	2.4	70.7	12.2	12.2	0.0	0.0	0.0	0.0
IR09C	0.0	5.8	92.8	1.0	0.5	0.0	0.0	0.0	0.0

June 1999

Station	Anthozoa		Annelida		Crustacea		Phoronida	Cephalochordata	
	Nemertinea		Bivalvia		Sipuncula		Echinodermata		
FS02C	5.9	4.4	1.5	55.9	30.9	0.0	0.0	1.5	0.0
FS03E	0.0	0.0	0.0	14.3	78.6	0.0	0.0	0.0	7.1
FS04C	0.0	0.2	85.0	11.8	3.0	0.0	0.0	0.0	0.0
FS04E	0.0	0.0	0.0	61.5	30.8	0.0	0.0	0.0	7.7
FS06C	3.0	5.9	72.3	12.9	2.0	0.0	0.0	1.0	3.0
FS06D	0.0	31.4	28.6	28.6	11.4	0.0	0.0	0.0	0.0
FS07B1	0.0	1.2	80.2	14.5	4.1	0.0	0.0	0.0	0.0
FS07B2	0.0	0.3	86.7	7.4	3.4	0.0	2.3	0.0	0.0
FS07B3	0.1	0.2	70.7	10.9	18.0	0.1	0.0	0.0	0.0
FS08D	4.2	7.7	78.0	7.7	0.6	0.0	0.0	1.2	0.6
FS08E	2.3	2.3	16.3	65.1	14.0	0.0	0.0	0.0	0.0
FS09B	0.0	3.5	69.1	3.0	24.3	0.0	0.0	0.0	0.0
FS10B	0.0	0.5	12.3	3.4	83.7	0.0	0.0	0.0	0.0
FS11C	0.0	6.2	80.0	6.2	7.7	0.0	0.0	0.0	0.0
FS12B	0.0	3.8	15.4	0.0	79.2	0.0	0.0	0.0	1.5
FS12C	1.4	18.9	58.1	9.5	9.5	0.0	0.0	0.0	2.7
FS12E	0.0	10.0	10.0	40.0	30.0	0.0	0.0	0.0	10.0
FS12F	0.0	10.6	12.8	68.1	6.4	0.0	0.0	0.0	2.1
FS13C	0.0	13.1	32.0	10.7	42.6	0.0	0.0	0.0	1.6
FS13F	0.0	3.6	10.7	50.0	32.1	0.0	0.0	0.0	3.6

Table 4.2-4

Species richness (taxons/0.04 m<sup>2</sup>) by major taxa for infauna collected in the Maryland and Delaware study area in May 1998 and June 1999.

---

May 1998

	Nemertinea		Bivalvia		Sipuncula		Echinodermata		Total
	Anthozoa	Annelida		Crustacea		Phoronida	Cephalochordata		
SBB32	1	1	18	6	4	0	0	0	30
BB04	1	1	11	1	3	0	0	0	17
FS01G	0	1	15	2	5	0	1	0	24
FS02.5D	0	1	3	1	5	0	0	0	10
FS02C	1	1	7	7	7	0	0	1	25
FS03E	0	0	0	0	6	0	0	0	7
FS04C	0	0	10	7	4	0	0	0	21
FS04E	0	1	1	3	2	0	0	0	7
FS06C	1	1	11	11	4	0	0	1	30
FS06D	0	0	4	6	3	0	0	0	13
FS07B	0	0	10	11	6	0	1	0	28
FS07F	0	1	5	1	5	0	0	0	12
FS08B	0	1	10	1	10	0	1	0	23
FS08C	0	1	14	8	2	1	0	0	26
FS08D	1	1	10	2	2	0	0	0	17
FS08E	0	0	2	1	3	0	1	0	7
FS09A	0	0	11	4	7	0	0	0	23
FS09B	0	1	9	5	9	0	0	0	24
FS09C	0	0	2	1	3	0	0	0	6
FS09D	0	1	17	0	2	0	0	0	20
FS10.5D	0	0	1	0	2	0	0	0	3
FS10A	0	1	18	0	6	0	0	1	26
FS10B	1	1	18	2	7	0	0	0	29
FS11C	0	1	10	6	1	0	0	0	18
FS12B	0	1	10	1	3	0	0	0	15
FS12C	0	1	11	1	2	0	0	0	16
FS12E	0	0	1	1	2	0	0	0	4
FS12F	0	1	6	2	2	0	0	1	12
FS13A	0	1	11	0	3	0	1	0	16
FS13C	1	1	16	4	4	0	0	0	27
FS13E	0	0	0	1	4	0	0	0	5
FS13F	1	1	7	2	6	0	0	0	17
FS14A	0	1	15	2	4	0	0	0	22
FS14D	0	0	3	1	2	0	0	0	6
FS14E	0	1	5	0	2	0	0	0	8
FS14F	0	1	9	2	5	0	0	0	17
FS14G	0	1	0	1	6	0	0	0	8
HCS31	0	1	17	5	6	0	1	0	30

---

Table 4.2.4. Continued.

May 1998

	Nemertinea		Bivalvia		Sipuncula		Echinodermata		Total	
	Anthozoa	Annelida	Crustacea	Phoronida	Cephalochordata					
IR02B	0	1	18	3	2	0	0	0	1	25
IR02C	0	1	13	4	2	0	0	0	0	20
IR02D	0	1	15	7	2	0	0	0	0	25
IR04B	0	1	11	3	3	0	0	0	0	18
IR04D	0	0	8	2	4	0	0	0	0	14
IR04E	0	1	22	7	4	1	0	0	0	35
IR05.5C	0	1	10	4	4	0	0	0	0	19
IR05D	0	0	13	6	5	1	1	0	0	26
IR07C	0	1	12	1	4	0	0	1	0	19
IR07E	0	0	9	0	2	1	1	0	0	13
IR08B	0	0	7	2	4	0	0	0	0	13
IR08C	0	1	11	2	3	0	0	0	0	17
IR09A	1	1	8	4	3	0	0	0	0	17
IR09C	0	1	10	2	1	0	0	0	0	14
Totals	1	1	77	35	34	1	1	1	1	152

June 1999

	Nemertinea		Bivalvia		Sipuncula		Echinodermata		Total	
	Anthozoa	Annelida	Crustacea	Phoronida	Cephalochordata					
FS02C	1	1	1	7	3	0	0	1	0	14
FS03E	0	0	0	1	5	0	0	0	1	7
FS04C	0	1	16	6	4	0	0	0	0	27
FS04E	0	0	0	2	3	0	0	0	1	6
FS06C	1	1	8	6	2	0	0	1	1	20
FS06D	0	1	7	5	4	0	0	0	0	17
FS07B1	0	1	20	9	5	0	0	0	0	35
FS07B2	0	1	24	11	3	0	1	0	0	40
FS07B3	1	1	21	8	5	1	0	0	0	37
FS08D	1	1	17	5	1	0	0	1	1	27
FS08E	1	1	4	6	3	0	0	0	0	15
FS09B	0	1	14	3	13	0	0	0	0	31
FS10B	0	1	10	3	7	0	0	0	0	21
FS11C	0	1	9	2	3	0	0	0	0	15
FS12B	0	1	11	0	4	0	0	0	1	17
FS12C	1	1	13	2	4	0	0	0	1	22
FS12E	0	1	1	2	3	0	0	0	1	8
FS12F	0	1	4	5	2	0	0	0	1	13
FS13C	0	1	9	6	7	0	0	0	1	24
FS13F	0	1	3	3	4	0	0	0	1	12
Totals	1	1	57	23	22	1	1	1	1	108

Table 4.2-5

Percentage species by major taxa for infauna collected off Maryland and Delaware in May 1998 and June 1999.

---

May 1998

Station	Nemertinea		Mollusca		Sipuncula	Echinodermata			
	Anthozoa	Annelida		Crustacea		Phoronida		Cephalochordata	
BB02	3.3	3.3	60.0	20.0	13.3	0.0	0.0	0.0	0.0
BB04	5.9	5.9	64.7	5.9	17.6	0.0	0.0	0.0	0.0
FS01G	0.0	4.2	62.5	8.3	20.8	0.0	4.2	0.0	0.0
FS02.5D	0.0	10.0	30.0	10.0	50.0	0.0	0.0	0.0	0.0
FS02C	4.0	4.0	28.0	28.0	28.0	0.0	0.0	4.0	4.0
FS03E	0.0	0.0	0.0	0.0	85.7	0.0	0.0	0.0	14.3
FS04C	0.0	0.0	47.6	33.3	19.0	0.0	0.0	0.0	0.0
FS04E	0.0	14.3	14.3	42.9	28.6	0.0	0.0	0.0	0.0
FS06C	3.3	3.3	36.7	36.7	13.3	0.0	0.0	3.3	3.3
FS06D	0.0	0.0	30.8	46.2	23.1	0.0	0.0	0.0	0.0
FS07B	0.0	0.0	35.7	39.3	21.4	0.0	3.6	0.0	0.0
FS07F	0.0	8.3	41.7	8.3	41.7	0.0	0.0	0.0	0.0
FS08B	0.0	4.3	43.5	4.3	43.5	0.0	4.3	0.0	0.0
FS08C	0.0	3.8	53.8	30.8	7.7	3.8	0.0	0.0	0.0
FS08D	5.9	5.9	58.8	11.8	11.8	0.0	0.0	0.0	5.9
FS08E	0.0	0.0	28.6	14.3	42.9	0.0	14.3	0.0	0.0
FS09A	0.0	0.0	47.8	17.4	30.4	0.0	0.0	0.0	4.3
FS09B	0.0	4.2	37.5	20.8	37.5	0.0	0.0	0.0	0.0
FS09C	0.0	0.0	33.3	16.7	50.0	0.0	0.0	0.0	0.0
FS09D	0.0	5.0	85.0	0.0	10.0	0.0	0.0	0.0	0.0
FS10.5D	0.0	0.0	33.3	0.0	66.7	0.0	0.0	0.0	0.0
FS10A	0.0	3.8	69.2	0.0	23.1	0.0	0.0	3.8	0.0
FS10B	3.4	3.4	62.1	6.9	24.1	0.0	0.0	0.0	0.0
FS11C	0.0	5.6	55.6	33.3	5.6	0.0	0.0	0.0	0.0
FS12B	0.0	6.7	66.7	6.7	20.0	0.0	0.0	0.0	0.0
FS12C	0.0	6.3	68.8	6.3	12.5	0.0	0.0	0.0	6.3
FS12E	0.0	0.0	25.0	25.0	50.0	0.0	0.0	0.0	0.0
FS12F	0.0	8.3	50.0	16.7	16.7	0.0	0.0	8.3	0.0
FS13A	0.0	6.3	68.8	0.0	18.8	0.0	6.3	0.0	0.0
FS13C	3.7	3.7	59.3	14.8	14.8	0.0	0.0	0.0	3.7
FS13E	0.0	0.0	0.0	20.0	80.0	0.0	0.0	0.0	0.0
FS13F	5.9	5.9	41.2	11.8	35.3	0.0	0.0	0.0	0.0
FS14A	0.0	4.5	68.2	9.1	18.2	0.0	0.0	0.0	0.0
FS14D	0.0	0.0	50.0	16.7	33.3	0.0	0.0	0.0	0.0
FS14E	0.0	12.5	62.5	0.0	25.0	0.0	0.0	0.0	0.0
FS14F	0.0	5.9	52.9	11.8	29.4	0.0	0.0	0.0	0.0
FS14G	0.0	12.5	0.0	12.5	75.0	0.0	0.0	0.0	0.0
HCS31	0.0	3.3	56.7	16.7	20.0	0.0	3.3	0.0	0.0

Table 4.2.5. Continued.

May 1998

Station	Nemertinea		Bivalvia	Sipuncula		Echinodermata			
	Anthozoa	Annelida	Crustacea	Phoronida	Cephalochordata				
IR02B	0.0	4.0	72.0	12.0	8.0	0.0	0.0	0.0	4.0
IR02C	0.0	5.0	65.0	20.0	10.0	0.0	0.0	0.0	0.0
IR02D	0.0	4.0	60.0	28.0	8.0	0.0	0.0	0.0	0.0
IR04B	0.0	5.6	61.1	16.7	16.7	0.0	0.0	0.0	0.0
IR04D	0.0	0.0	57.1	14.3	28.6	0.0	0.0	0.0	0.0
IR04E	0.0	2.9	62.9	20.0	11.4	2.9	0.0	0.0	0.0
IR05.5C	0.0	5.3	52.6	21.1	21.1	0.0	0.0	0.0	0.0
IR05D	0.0	0.0	50.0	23.1	19.2	3.8	3.8	0.0	0.0
IR07C	0.0	5.3	63.2	5.3	21.1	0.0	0.0	5.3	0.0
IR07E	0.0	0.0	69.2	0.0	15.4	7.7	7.7	0.0	0.0
IR08B	0.0	0.0	53.8	15.4	30.8	0.0	0.0	0.0	0.0
IR08C	0.0	5.9	64.7	11.8	17.6	0.0	0.0	0.0	0.0
IR09A	5.9	5.9	47.1	23.5	17.6	0.0	0.0	0.0	0.0
IR09C	0.0	7.1	71.4	14.3	7.1	0.0	0.0	0.0	0.0

June 1999

Station	Nemertinea		Mollusca	Sipuncula		Echinodermata			
	Anthozoa	Annelida	Crustacea	Phoronida	Cephalochordata				
FS02C	7.1	7.1	7.1	50.0	21.4	0.0	0.0	7.1	0.0
FS03E	0.0	0.0	0.0	14.3	71.4	0.0	0.0	0.0	14.3
FS04C	0.0	3.7	59.3	22.2	14.8	0.0	0.0	0.0	0.0
FS04E	0.0	0.0	0.0	33.3	50.0	0.0	0.0	0.0	16.7
FS06C	5.0	5.0	40.0	30.0	10.0	0.0	0.0	5.0	5.0
FS06D	0.0	5.9	41.2	29.4	23.5	0.0	0.0	0.0	0.0
FS07B1	0.0	2.9	57.1	25.7	14.3	0.0	0.0	0.0	0.0
FS07B2	0.0	2.5	60.0	27.5	7.5	0.0	2.5	0.0	0.0
FS07B3	2.7	2.7	56.8	21.6	13.5	2.7	0.0	0.0	0.0
FS08D	3.7	3.7	63.0	18.5	3.7	0.0	0.0	3.7	3.7
FS08E	6.7	6.7	26.7	40.0	20.0	0.0	0.0	0.0	0.0
FS09B	0.0	3.2	45.2	9.7	41.9	0.0	0.0	0.0	0.0
FS10B	0.0	4.8	47.6	14.3	33.3	0.0	0.0	0.0	0.0
FS11C	0.0	6.7	60.0	13.3	20.0	0.0	0.0	0.0	0.0
FS12B	0.0	5.9	64.7	0.0	23.5	0.0	0.0	0.0	5.9
FS12C	4.5	4.5	59.1	9.1	18.2	0.0	0.0	0.0	4.5
FS12E	0.0	12.5	12.5	25.0	37.5	0.0	0.0	0.0	12.5
FS12F	0.0	7.7	30.8	38.5	15.4	0.0	0.0	0.0	7.7
FS13C	0.0	4.2	37.5	25.0	29.2	0.0	0.0	0.0	4.2
FS13F	0.0	8.3	25.0	25.0	33.3	0.0	0.0	0.0	8.3

Table 4.2.6.

Biomass (mg wet/0.04 m<sup>2</sup>) by major taxa for infauna collected off Maryland and Delaware in May 1998 and June 1999.

-----  
 May 1998

Station	Anthozoa		Polychaetes		Gastropods		Isopods		Other Crustaceans		Phoronida		Cephalochordata		Total
		Nemertinea		Oligochaetes		Bivalves		Amphipods		Sipuncula		Echinodermata			
BB02	1	5	80	9	0	14	0.5	8	0.5	0	0	0	0	118	
BB04	0.5	2	54.5	15	0	1	0	17	2	0	0	0	0	92	
FS01G	0	5	2387.5	0.5	4893	1	62	17	0.5	0	0.5	0	0	7367	
FS02.5D	0	0.5	4.5	0	0	0.5	32.5	87	0.5	0	0	0	0	125.5	
FS02C	2	679	5	1	1	6798	282	69	1	0	0	7	123	7968	
FS03E	0	0	0	0	0	0	18	117	0.5	0	0	0	6	141.5	
FS04C	0	0	645	4	1143	8176	9	4	0	0	0	0	0	9981	
FS04E	0	1	0	0.5	3	4.5	0	6.5	0	0	0	0	0	15.5	
FS06C	7	7	291.5	30	28	700.5	0.5	1.5	0.5	0	0	4	285	1355.5	
FS06D	0	0	2.5	2	1	502	6.5	18	0	0	0	0	0	532	
FS07B	0	0	715	7	48.5	155.5	16	173.5	2	0	0.5	0	0	1118	
FS07F	0	1	4.5	0.5	0	445	0.5	26.5	0	0	0	0	0	478	
FS08B	0	2	348.5	0	0	0.5	1.5	16	5	0	0.5	0	0	374	
FS08C	0	1	322.5	1	46	719	0	1	0	3	0	0	0	1093.5	
FS08D	1	6	34.5	8	0	120	0.5	1	0	0	0	0	10	181	
FS08E	0	0	0.5	0.5	0	0.5	4	52	0	0	0.5	0	0	58	
FS09A	0	0	25.5	2	0	11	0	114	1	0	0	0	111	264.5	
FS09B	0	3	15	2	0	3.5	13	27	3	0	0	0	0	66.5	
FS09C	0	0	0.5	0.5	0	1	42	54	0	0	0	0	0	98	
FS09D	0	5	113.5	3	0	0	0	2	0	0	0	0	0	123.5	
FS10.5D	0	0	1	0	0	0	4	9	0	0	0	0	0	14	
FS10A	0	3	113.5	0.5	0	0	0	52.5	0.5	0	0	13	0	183	
FS10B	0.5	8	35.5	5	0	4	0	77	2	0	0	0	0	132	
FS11C	0	4	32.5	3	3	68	0	124	0	0	0	0	0	234.5	
FS12B	0	15	119.5	1	0	0.5	0	0.5	1	0	0	0	0	137.5	
FS12C	0	1	5	3	0	1	0	2	0.5	0	0	0	6	18.5	
FS12E	0	0	0.5	0	0	39	0	12	0	0	0	0	0	51.5	
FS12F	0	3	25.5	2	0	90	0.5	115	0	0	0	0.5	0	236.5	
FS13A	0	3	15.5	0.5	0	0	0	0	7.5	0	3	0	0	29.5	
FS13C	2	5	596	3	5	2.5	0	19	1	0	0	0	9	642.5	
FS13E	0	0	0	0	0	25	147	13.5	0	0	0	0	0	185.5	
FS13F	0.5	10	3	4	0	1	8.5	9.5	1	0	0	0	0	37.5	
FS14A	0	8	119	14	0	48	9	14	4	0	0	0	0	216	
FS14D	0	0	1.5	0	0	30	0	12	0.5	0	0	0	0	44	
FS14E	0	0.5	2.5	0.5	0	0	87	11	0	0	0	0	0	101.5	
FS14F	0	20	23.5	3	0	1	0	1.5	4	0	0	0	0	53	
FS14G	0	0.5	0	0	0	55	4	43	1	0	0	0	0	103.5	

Table 4.2-6 Continued

May 1998

Station	Anthozoa		Polychaetes		Gastropods		Isopods		Other Crustaceans		Phoronida		Cephalochordata		Total
	Nemertinea		Oligochaetes		Bivalves		Amphipods		Sipuncula		Echinodermata				
HCS31	0	182	3633.5	2	0	1459	6	36	4	0	30	0	0	5352.5	
IR02B	0	6	101	2	0.5	4.5	0	0.5	0.5	0	0	0	18	133	
IR02C	0	9	83	7	0	56.5	0.5	0.5	0	0	0	0	0	156.5	
IR02D	0	5	147.5	2	0	1438.5	0	1	1	0	0	0	0	1595	
IR04B	0	1	210	0.5	0	47	0	24	1	0	0	0	0	283.5	
IR04D	0	0	154	0.5	0.5	0.5	3	4	2	0	0	0	0	164.5	
IR04E	0	0.5	906.5	6	71	3	11	82	0	1	0	0	0	1081	
IR05_5C	0	50	97.5	2	0	78386	86	20	0	0	0	0	0	78641.5	
IR05D	0	0	425	0.5	0.5	88136	11	1.5	0.5	0.5	0.5	0	0	88576	
IR07C	0	1	1108	0.5	0	3	0	11	1	0	0	4	0	1128.5	
IR07E	0	0	22.5	0.5	0	0	0	1	0.5	15	0.5	0	0	40	
IR08B	0	0	9.5	0.5	0	55	67	11	0.5	0	0	0	0	143.5	
IR08C	0	0.5	105	0	541	0.5	0	13.5	0	0	0	0	0	660.5	
IR09A	30	2	46	0.5	0	3.5	0.5	2.5	0	0	0	0	0	85	
IR09C	0	6	23	18	0	2741.5	0	0	12	0	0	0	0	2800.5	

June 1999

Station	Anthozoa		Polychaetes		Gastropods		Isopods		Other Crustaceans		Phoronida		Cephalochordata		Total
	Nemertinea		Oligochaetes		Bivalves		Amphipods		Sipuncula		Echinodermata				
FS02C	0.5	89	67	0	11	12855	2	41	0	0	0	72	0	13137.5	
FS03E	0	0	0	0	0	71	0.5	17	0.5	0	0	0	330	419	
FS04C	0	23	2650	1	2	3457	0	74	0	0	0	0	0	6207	
FS04E	0	0	0	0	8	49	0	49	0	0	0	0	10	116	
FS06C	0.5	8	28.5	1	0	60	6.5	0	0	0	0	12	13	129.5	
FS06D	0	0.5	4	0.5	0	69	0.5	79	0	0	0	0	0	153.5	
FS07B1	0	8	1817	23	342	3406	0	582.5	14	0	0	0	0	6192.5	
FS07B2	0	4	1554	7	502	259.5	0	235	6	0	19	0	0	2586.5	
FS07B3	6	1	2204.5	13	40	1155	0	436.5	1	0.5	0	0	0	3857.5	
FS08D	18	12	233	6	9	186.5	1	0	0	0	0	2	5	472.5	
FS08E	0.5	1	4	0.5	14	227.5	1	19	0	0	0	0	0	267.5	
FS09B	0	15	55.5	28	3	166	9	146	5	0	0	0	0	427.5	
FS10B	0	4	188	0.5	0	849	0	402	16.5	0	0	0	0	1460	
FS11C	0	4	47	4	0	14.5	98	13.5	0	0	0	0	0	181	
FS12B	0	5	22	0.5	0	0	0	165	1	0	0	0	21	214.5	
FS12C	1	6	12	2	0	224	0	12	1	0	0	0	16	274	
FS12E	0	0.5	0.5	0	3	95	7	9.5	0	0	0	0	9	124.5	
FS12F	0	3	8	0.5	6.5	170.5	0	33	0	0	0	0	10	231.5	
FS13C	0	8	19	1	14	549.5	0	128	3	0	0	0	40	762.5	
FS13F	0	0.5	164.5	0	4	133	0	14.5	0	0	0	0	40	356.5	

Table 4.2-7

Percentage of biomass by major taxa for infauna collected off Maryland and Delaware in May 1998 and June 1999.

-----													
May 1998													
Station	Anthozoa	Polychaetes		Gastropods		Isopods	Other Crustaceans		Phoronida	Cephalochordata			
	Nemertinea	Oligochaetes	Bivalves	Amphipods	Sipuncula	Echinodermata							
BB02	0.8	4.2	67.8	7.6	0.0	11.9	0.4	6.8	0.4	0.0	0.0	0.0	0.0
BB04	0.5	2.2	59.2	16.3	0.0	1.1	0.0	18.5	2.2	0.0	0.0	0.0	0.0
FS01G	0.0	0.1	32.4	0.0	66.4	0.0	0.8	0.2	0.0	0.0	0.0	0.0	0.0
FS02.5D	0.0	0.4	3.6	0.0	0.0	0.4	25.9	69.3	0.4	0.0	0.0	0.0	0.0
FS02C	0.0	8.5	0.1	0.0	0.0	85.3	3.5	0.9	0.0	0.0	0.0	0.1	1.5
FS03E	0.0	0.0	0.0	0.0	0.0	0.0	12.7	82.7	0.4	0.0	0.0	0.0	4.2
FS04C	0.0	0.0	6.5	0.0	11.5	81.9	0.1	0.0	0.0	0.0	0.0	0.0	0.0
FS04E	0.0	6.5	0.0	3.2	19.4	29.0	0.0	41.9	0.0	0.0	0.0	0.0	0.0
FS06C	0.5	0.5	21.5	2.2	2.1	51.7	0.0	0.1	0.0	0.0	0.0	0.3	21.0
FS06D	0.0	0.0	0.5	0.4	0.2	94.4	1.2	3.4	0.0	0.0	0.0	0.0	0.0
FS07B	0.0	0.0	64.0	0.6	4.3	13.9	1.4	15.5	0.2	0.0	0.0	0.0	0.0
FS07F	0.0	0.2	0.9	0.1	0.0	93.1	0.1	5.5	0.0	0.0	0.0	0.0	0.0
FS08B	0.0	0.5	93.2	0.0	0.0	0.1	0.4	4.3	1.3	0.0	0.1	0.0	0.0
FS08C	0.0	0.1	29.5	0.1	4.2	65.8	0.0	0.1	0.0	0.3	0.0	0.0	0.0
FS08D	0.6	3.3	19.1	4.4	0.0	66.3	0.3	0.6	0.0	0.0	0.0	0.0	5.5
FS08E	0.0	0.0	0.9	0.9	0.0	0.9	6.9	89.7	0.0	0.0	0.9	0.0	0.0
FS09A	0.0	0.0	9.6	0.8	0.0	4.2	0.0	43.1	0.4	0.0	0.0	0.0	42.0
FS09B	0.0	4.5	22.6	3.0	0.0	5.3	19.5	40.6	4.5	0.0	0.0	0.0	0.0
FS09C	0.0	0.0	0.5	0.5	0.0	1.0	42.9	55.1	0.0	0.0	0.0	0.0	0.0
FS09D	0.0	4.0	91.9	2.4	0.0	0.0	0.0	1.6	0.0	0.0	0.0	0.0	0.0
FS10.5D	0.0	0.0	7.1	0.0	0.0	0.0	28.6	64.3	0.0	0.0	0.0	0.0	0.0
FS10A	0.0	1.6	62.0	0.3	0.0	0.0	0.0	28.7	0.3	0.0	0.0	7.1	0.0
FS10B	0.4	6.1	26.9	3.8	0.0	3.0	0.0	58.3	1.5	0.0	0.0	0.0	0.0
FS11C	0.0	1.7	13.9	1.3	1.3	29.0	0.0	52.9	0.0	0.0	0.0	0.0	0.0
FS12B	0.0	10.9	86.9	0.7	0.0	0.4	0.0	0.4	0.7	0.0	0.0	0.0	0.0
FS12C	0.0	5.4	27.0	16.2	0.0	5.4	0.0	10.8	2.7	0.0	0.0	0.0	32.4
FS12E	0.0	0.0	1.0	0.0	0.0	75.7	0.0	23.3	0.0	0.0	0.0	0.0	0.0
FS12F	0.0	1.3	10.8	0.8	0.0	38.1	0.2	48.6	0.0	0.0	0.0	0.2	0.0
FS13A	0.0	10.2	52.5	1.7	0.0	0.0	0.0	0.0	25.4	0.0	10.2	0.0	0.0
FS13C	0.3	0.8	92.8	0.5	0.8	0.4	0.0	3.0	0.2	0.0	0.0	0.0	1.4
FS13E	0.0	0.0	0.0	0.0	0.0	13.5	79.2	7.3	0.0	0.0	0.0	0.0	0.0
FS13F	1.3	26.7	8.0	10.7	0.0	2.7	22.7	25.3	2.7	0.0	0.0	0.0	0.0
FS14A	0.0	3.7	55.1	6.5	0.0	22.2	4.2	6.5	1.9	0.0	0.0	0.0	0.0
FS14D	0.0	0.0	3.4	0.0	0.0	68.2	0.0	27.3	1.1	0.0	0.0	0.0	0.0
FS14E	0.0	0.5	2.5	0.5	0.0	0.0	85.7	10.8	0.0	0.0	0.0	0.0	0.0
FS14F	0.0	37.7	44.3	5.7	0.0	1.9	0.0	2.8	7.5	0.0	0.0	0.0	0.0
FS14G	0.0	0.5	0.0	0.0	0.0	53.1	3.9	41.5	1.0	0.0	0.0	0.0	0.0

Table 4.2-7 Continued

May 1998

Station	Anthozoa	Polychaetes		Gastropods		Isopods	Other Crustaceans			Phoronida	Cephalochordata		
	Nemertinea	Oligochaetes	Bivalves	Amphipods	Sipuncula	Echinodermata							
HCS31	0.0	3.4	67.9	0.0	0.0	27.3	0.1	0.7	0.1	0.0	0.6	0.0	0.0
IR02B	0.0	4.5	75.9	1.5	0.4	3.4	0.0	0.4	0.4	0.0	0.0	0.0	13.5
IR02C	0.0	5.8	53.0	4.5	0.0	36.1	0.3	0.3	0.0	0.0	0.0	0.0	0.0
IR02D	0.0	0.3	9.2	0.1	0.0	90.2	0.0	0.1	0.1	0.0	0.0	0.0	0.0
IR04B	0.0	0.4	74.1	0.2	0.0	16.6	0.0	8.5	0.4	0.0	0.0	0.0	0.0
IR04D	0.0	0.0	93.6	0.3	0.3	0.3	1.8	2.4	1.2	0.0	0.0	0.0	0.0
IR04E	0.0	0.0	83.9	0.6	6.6	0.3	1.0	7.6	0.0	0.1	0.0	0.0	0.0
IR05_5C	0.0	0.1	0.1	0.0	0.0	99.7	0.1	0.0	0.0	0.0	0.0	0.0	0.0
IR05D	0.0	0.0	0.5	0.0	0.0	99.5	0.0	0.0	0.0	0.0	0.0	0.0	0.0
IR07C	0.0	0.1	98.2	0.0	0.0	0.3	0.0	1.0	0.1	0.0	0.0	0.4	0.0
IR07E	0.0	0.0	56.3	1.3	0.0	0.0	0.0	2.5	1.3	37.5	1.3	0.0	0.0
IR08B	0.0	0.0	6.6	0.3	0.0	38.3	46.7	7.7	0.3	0.0	0.0	0.0	0.0
IR08C	0.0	0.1	15.9	0.0	81.9	0.1	0.0	2.0	0.0	0.0	0.0	0.0	0.0
IR09A	35.3	2.4	54.1	0.6	0.0	4.1	0.6	2.9	0.0	0.0	0.0	0.0	0.0
IR09C	0.0	0.2	0.8	0.6	0.0	97.9	0.0	0.0	0.4	0.0	0.0	0.0	0.0

June 1999

Station	Anthozoa	Polychaetes		Gastropods		Isopods	Other Crustaceans			Phoronida	Cephalochordata		
	Nemertinea	Oligochaetes	Bivalves	Amphipods	Sipuncula	Echinodermata							
FS02C	0.0	0.7	0.5	0.0	0.1	97.8	0.0	0.3	0.0	0.0	0.0	0.5	0.0
FS03E	0.0	0.0	0.0	0.0	0.0	16.9	0.1	4.1	0.1	0.0	0.0	0.0	78.8
FS04C	0.0	0.4	42.7	0.0	0.0	55.7	0.0	1.2	0.0	0.0	0.0	0.0	0.0
FS04E	0.0	0.0	0.0	0.0	6.9	42.2	0.0	42.2	0.0	0.0	0.0	0.0	8.6
FS06C	0.4	6.2	22.0	0.8	0.0	46.3	5.0	0.0	0.0	0.0	0.0	9.3	10.0
FS06D	0.0	0.3	2.6	0.3	0.0	45.0	0.3	51.5	0.0	0.0	0.0	0.0	0.0
FS07B1	0.0	0.1	29.3	0.4	5.5	55.0	0.0	9.4	0.2	0.0	0.0	0.0	0.0
FS07B2	0.0	0.2	60.1	0.3	19.4	10.0	0.0	9.1	0.2	0.0	0.7	0.0	0.0
FS07B3	0.2	0.0	57.1	0.3	1.0	29.9	0.0	11.3	0.0	0.0	0.0	0.0	0.0
FS08D	3.8	2.5	49.3	1.3	1.9	39.5	0.2	0.0	0.0	0.0	0.0	0.4	1.1
FS08E	0.2	0.4	1.5	0.2	5.2	85.0	0.4	7.1	0.0	0.0	0.0	0.0	0.0
FS09B	0.0	3.5	13.0	6.5	0.7	38.8	2.1	34.2	1.2	0.0	0.0	0.0	0.0
FS10B	0.0	0.3	12.9	0.0	0.0	58.2	0.0	27.5	1.1	0.0	0.0	0.0	0.0
FS11C	0.0	2.2	26.0	2.2	0.0	8.0	54.1	7.5	0.0	0.0	0.0	0.0	0.0
FS12B	0.0	2.3	10.3	0.2	0.0	0.0	0.0	76.9	0.5	0.0	0.0	0.0	9.8
FS12C	0.4	2.2	4.4	0.7	0.0	81.8	0.0	4.4	0.4	0.0	0.0	0.0	5.8
FS12E	0.0	0.4	0.4	0.0	2.4	76.3	5.6	7.6	0.0	0.0	0.0	0.0	7.2
FS12F	0.0	1.3	3.5	0.2	2.8	73.7	0.0	14.3	0.0	0.0	0.0	0.0	4.3
FS13C	0.0	1.0	2.5	0.1	1.8	72.1	0.0	16.8	0.4	0.0	0.0	0.0	5.2
FS13F	0.0	0.1	46.1	0.0	1.1	37.3	0.0	4.1	0.0	0.0	0.0	0.0	11.2

Table 4.2.8.  
Community Structure

-----  
May 1998

Station	Total Species	Total Individuals	Species Richness	Shannon Diversity	Evenness	Simpson Dominance
BB02	30	348	3.43	3.65	0.74	0.11
BB04	17	271	1.98	2.31	0.57	0.37
FS01G	24	3108	1.98	0.44	0.10	0.91
FS02.5D	10	48	1.61	2.35	0.71	0.29
FS02C	25	150	3.32	3.72	0.80	0.12
FS03E	7	21	1.37	2.33	0.83	0.26
FS04C	21	872	2.05	2.03	0.46	0.37
FS04E	7	7	2.14	2.81	1.00	0.14
FS06C	30	416	3.33	3.47	0.71	0.15
FS06D	13	57	2.06	3.07	0.83	0.16
FS07B	28	461	3.05	3.75	0.78	0.10
FS07F	12	34	2.16	2.90	0.81	0.20
FS08B	23	78	3.50	3.89	0.86	0.10
FS08C	26	168	3.38	3.65	0.78	0.12
FS08D	17	168	2.16	2.81	0.69	0.20
FS08E	7	11	1.73	2.55	0.91	0.21
FS09A	23	118	3.20	3.55	0.79	0.12
FS09B	24	92	3.53	3.64	0.79	0.12
FS09C	6	16	1.25	1.97	0.76	0.36
FS09D	20	78	3.02	3.15	0.73	0.20
FS10.5D	3	4	1.00	1.50	0.95	0.38
FS10A	26	200	3.27	3.16	0.67	0.23
FS10B	29	181	3.73	3.76	0.77	0.12
FS11C	18	97	2.58	3.20	0.77	0.16
FS12B	15	83	2.20	3.54	0.91	0.10
FS12C	16	59	2.55	3.10	0.78	0.17
FS12E	4	4	1.50	2.00	1.00	0.25
FS12F	12	35	2.14	3.08	0.86	0.15
FS13A	16	35	2.92	3.73	0.93	0.09
FS13C	27	187	3.45	3.65	0.77	0.13
FS13E	5	8	1.33	2.16	0.93	0.25
FS13F	17	123	2.30	3.20	0.78	0.16
FS14A	22	271	2.60	3.00	0.67	0.18
FS14D	6	9	1.58	2.42	0.94	0.21
FS14E	8	16	1.75	2.38	0.79	0.29
FS14F	17	73	2.58	3.25	0.80	0.15
FS14G	8	16	1.75	2.38	0.79	0.29
HCS31	30	1231	2.82	1.82	0.37	0.53
IR02B	25	93	3.67	3.78	0.81	0.11
IR02C	20	243	2.40	3.45	0.80	0.12
IR02D	25	149	3.32	3.60	0.78	0.14
IR04B	18	25	3.66	4.00	0.96	0.07
IR04D	14	21	2.96	3.65	0.96	0.09
IR04E	35	312	4.10	3.79	0.74	0.11
IR05.5C	19	60	3.05	3.38	0.80	0.15
IR05D	26	165	3.39	2.78	0.59	0.33
IR07C	19	56	3.10	3.60	0.85	0.11
IR07E	13	26	2.55	3.47	0.94	0.10
IR08B	13	21	2.73	3.42	0.93	0.12

Table 4.2-8 Continued

Station	Species	Total Individuals	Total Richness	Species Diversity	Shannon Evenness	Simpson Dominance
IR08C	17	61	2.70	3.48	0.85	0.12
IR09A	17	41	2.99	3.34	0.82	0.16
IR09C	14	207	1.69	1.56	0.41	0.57

Community structure 1999

Station	Total Species	Total Individuals	Species Richness	Shannon Diversity	Evenness	Simpson Dominance
FS02C	14	68	2.14	2.92	0.77	0.20
FS03E	7	14	1.58	2.41	0.86	0.25
FS04C	27	1336	2.50	1.90	0.40	0.51
FS04E	6	13	1.35	2.29	0.89	0.24
FS06C	20	101	2.85	2.97	0.69	0.27
FS06D	17	35	3.12	3.51	0.86	0.14
FS07B1	35	1290	3.29	3.15	0.61	0.19
FS07B2	40	1162	3.83	3.17	0.60	0.21
FS07B3	37	1006	3.61	3.84	0.74	0.10
FS08D	27	168	3.52	4.00	0.84	0.09
FS08E	15	43	2.58	3.29	0.84	0.14
FS09B	31	230	3.82	3.73	0.75	0.15
FS10B	21	203	2.61	1.70	0.39	0.60
FS11C	15	65	2.32	3.52	0.90	0.11
FS12B	17	130	2.28	2.58	0.63	0.27
FS12C	22	74	3.38	3.79	0.85	0.10
FS12E	8	10	2.11	2.85	0.95	0.16
FS12F	13	47	2.16	2.63	0.71	0.29
FS13C	24	122	3.32	3.69	0.81	0.11
FS13F	12	28	2.29	2.99	0.84	0.18

Table 4.2.9

Constancy and fidelity based on nodal analysis of all grab data.  
 See Figure 4.2.x for stations and species in each group.

---

Constancy

Species Group	Station Group				
	A	B	C	D	E
I	0.2	0.4	0.0	0.1	0.1
II	0.5	0.3	0.0	0.1	0.2
III	0.2	0.3	0.2	0.2	0.1
IV	0.1	0.1	0.1	0.2	0.4
V	0.0	0.0	0.0	0.0	0.3
VI	0.1	0.0	0.0	0.0	0.5

Fidelity

Species Group	Station Group				
	A	B	C	D	E
I	1.0	2.8	0.0	0.6	0.7
II	1.7	1.0	0.1	0.4	0.7
III	1.2	1.5	1.1	0.9	0.4
IV	0.7	0.4	0.6	0.9	2.4
V	0.4	0.1	0.0	0.4	4.1
VI	0.5	0.3	0.0	0.4	4.1

Table 4.2-10  
Dominant taxa (present at >20% of the stations, 15 of 70 stations) collected  
in the MD/DE study area.

---

Taxa	MajorTaxa	Total Occurences	Total Abundance
Oligochaeta	Annelida	58	1610
Nemertinea	Nemertinea	55	414
Tellina spp.	Bivalvia	47	732
Spiophanes bombyx	Annelida	39	5902
Aricidea (Acmira) cerrutii	Annelida	37	426
Aricidea (Acmira) catherinae	Annelida	32	244
Parapionosyllis longicirrata	Annelida	30	109
Unciola irrorata	Crustacea	30	279
Protohaustorius wigleyi	Crustacea	29	110
Aphelochaeta sp.	Annelida	25	165
Brania wellfleetensis	Annelida	23	222
Crenella glandula	Bivalvia	23	128
Tanaissus psammophilus	Crustacea	22	101
Hesionura elongata	Annelida	21	115
Hemipodus roseus	Annelida	21	54
Astarte spp.	Bivalvia	21	166
Nephtys spp.	Annelida	20	53
Asabellides oculata	Annelida	20	342
Branchiostoma caribaeum	Cephalochordata	18	25
Mytilus edulis	Bivalvia	17	130
Chiridotea coeca	Crustacea	17	57
Byblis serrata	Crustacea	17	250
Pseudunciola obliquua	Crustacea	17	231
Spio setosa	Annelida	16	788
Caulleriella sp. B	Annelida	16	84
Pseudoleptocuma minor	Crustacea	16	25
Anthozoa	Cnidaria	15	53
Streptosyllis pettiboneae	Annelida	15	54
Spisula solidissima	Bivalvia	15	27
Lyonsia hyalina	Bivalvia	15	27
Oxyurostylis smithi	Crustacea	15	19

---

Table 4.2-11

Abundance dominants from MD/DE. Includes all taxa that were at least one percent of the total abundance in either May 1998 or September 1999 with and without the polychaete *Spiophanes bombyx*.

Major Taxa	Taxa	Taxa Abundance			Percent of Total Abundance			Percentages No <i>S. bombyx</i>		
		98&99	98	99	98&99	98	99	98&99	98	99
Annelida	<i>Spiophanes bombyx</i>	5902	4240	1662	35.2	39.9	27.0	.	.	.
Annelida	Oligochaeta	1610	1218	392	9.6	11.5	6.4	14.8	9.7	2.6
Annelida	<i>Spio setosa</i>	788	73	715	4.7	0.7	11.6	7.2	0.6	4.7
Bivalvia	<i>Tellina</i> spp.	732	388	344	4.4	3.6	5.6	6.7	3.1	2.3
Bivalvia	<i>Nucula</i> spp.	624	550	74	3.7	5.2	1.2	5.7	4.4	0.5
Annelida	<i>Apoprionospio pygmaea</i>	478	50	428	2.8	0.5	7.0	4.4	0.4	2.8
Annelida	<i>Aricidea (Acmira) cerrutii</i>	426	388	38	2.5	3.6	0.6	3.9	3.1	0.3
Nemertinea	Nemertinea	414	301	113	2.5	2.8	1.8	3.8	2.4	0.7
Annelida	<i>Asabellides oculata</i>	342	242	100	2.0	2.3	1.6	3.1	1.9	0.7
Annelida	<i>Mediomastus ambiseta</i>	326	132	194	1.9	1.2	3.2	3.0	1.1	1.3
Annelida	<i>Macroclymene zonalis</i>	281	2	279	1.7	0.0	4.5	2.6	0.0	1.8
Crustacea	<i>Unciola irrorata</i>	279	125	154	1.7	1.2	2.5	2.6	1.0	1.0
Crustacea	<i>Byblis serrata</i>	250	15	235	1.5	0.1	3.8	2.3	0.1	1.6
Annelida	<i>Aricidea (Acmira) catherinae</i>	244	149	95	1.5	1.4	1.5	2.2	1.2	0.6
Crustacea	<i>Pseudunciola obliquua</i>	231	73	158	1.4	0.7	2.6	2.1	0.6	1.0
Annelida	<i>Brania wellfleetensis</i>	222	193	29	1.3	1.8	0.5	2.0	1.5	0.2
Bivalvia	<i>Astarte</i> spp.	166	122	44	1.0	1.1	0.7	1.5	1.0	0.3
Annelida	<i>Aphelochaeta</i> sp.	165	137	28	1.0	1.3	0.5	1.5	1.1	0.2
Annelida	<i>Paradoneis</i> sp. B	133	133	0	0.8	1.3	0.0	1.2	1.1	0.0
Bivalvia	<i>Mytilus edulis</i>	130	121	9	0.8	1.1	0.1	1.2	1.0	0.1
Bivalvia	<i>Crenella glandula</i>	128	79	49	0.8	0.7	0.8	1.2	0.6	0.3
Annelida	<i>Hesionura elongata</i>	115	100	15	0.7	0.9	0.2	1.1	0.8	0.1
Crustacea	<i>Protohaustorius wigleyi</i>	110	88	22	0.7	0.8	0.4	1.0	0.7	0.1
Annelida	<i>Protodorvillea kefersteini</i>	110	85	25	0.7	0.8	0.4	1.0	0.7	0.2
Annelida	<i>Parapionosyllis longicirrata</i>	109	99	10	0.6	0.9	0.2	1.0	0.8	0.1
Annelida	<i>Clymenella torquata</i>	104	1	103	0.6	0.0	1.7	1.0	0.0	0.7

Table 4.2-12

Biomass dominants (>0.5 g wet weight/0.04 m<sup>2</sup>) collected in the MD/DE study area.  
Numerical or occurrence dominant species are also included.

Taxa	Major Taxa	Total Taxa Biomass (g wet wt/0.04 m <sup>2</sup> )			Percent Taxa Biomass (%)			Mean Individual Biomass (mg/individual)		
		98&99	98	99	98&99	98	99	98&99	98	99
<i>Spisula solidissima</i>	Bivalvia	166.2	165.8	0.5	65.9	77.2	1.3	6157.1	7206.9	121.0
<i>Astarte</i> spp.	Bivalvia	21.0	7.3	13.7	8.3	3.4	36.5	126.8	60.2	311.6
<i>Nucula</i> spp.	Bivalvia	11.3	9.6	1.7	4.5	4.5	4.5	18.1	17.4	23.1
<i>Spiophanes bombyx</i>	Polychaeta	7.2	4.5	2.7	2.9	2.1	7.1	1.2	1.1	1.6
<i>Busycon canaliculata</i>	Gastropoda	4.9	4.9	*	1.9	2.3	.	4893.0	4893.0	.
<i>Ensis directus</i>	Bivalvia	4.7	0.1	4.6	1.9	0.0	12.2	53.3	25.8	54.6
<i>Pitar morrhuanus</i>	Bivalvia	4.5	4.5	0.0	1.8	2.1	0.1	104.8	1118.6	0.8
<i>Asabellides oculata</i>	Polychaeta	4.3	2.6	1.6	1.7	1.2	4.3	12.4	10.9	16.0
<i>Tellina</i> spp.	Bivalvia	3.9	0.9	3.0	1.6	0.4	8.1	5.4	2.3	8.8
<i>Nassarius trivittatus</i>	Gastropoda	2.6	1.8	0.8	1.0	0.8	2.1	257.0	254.7	262.3
<i>Lumbrineris fragilis</i>	Polychaeta	1.7	1.7	.	0.7	0.8	.	191.8	191.8	.
Nemertinea	Nemertinea	1.3	1.1	0.2	0.5	0.5	0.5	3.0	3.5	1.7
<i>Branchiostoma caribaeum</i>	Cephalochordata	1.1	0.6	0.5	0.4	0.3	1.3	42.5	56.8	32.9
<i>Spio setosa</i>	Polychaeta	1.0	0.5	0.6	0.4	0.2	1.5	1.3	6.4	0.8
<i>Ampelisca</i> spp.	Amphipoda	1.0	0.2	0.9	0.4	0.1	2.3	10.2	10.9	10.1
<i>Crenella glandula</i>	Bivalvia	0.9	0.6	0.3	0.4	0.3	0.7	7.0	7.9	5.5
<i>Byblis serrata</i>	Amphipoda	0.9	0.1	0.7	0.3	0.1	1.9	3.5	9.9	3.1
<i>Politolana concharum</i>	Isopoda	0.8	0.7	0.1	0.3	0.3	0.3	30.7	30.9	29.5
<i>Mytilus edulis</i>	Bivalvia	0.7	0.7	0.0	0.3	0.3	0.0	5.8	6.1	1.0
<i>Uniola irrorata</i>	Amphipoda	0.7	0.2	0.5	0.3	0.1	1.3	2.4	1.4	3.2
<i>Glycera americana</i>	Polychaeta	0.6	0.5	0.2	0.3	0.2	0.4	20.4	19.0	26.3
<i>Notocirrus spiniferus</i>	Polychaeta	0.6	0.1	0.5	0.2	0.0	1.3	97.7	40.5	126.3
<i>Sigalion arenicola</i>	Polychaeta	0.5	0.3	0.3	0.2	0.1	0.7	78.1	67.5	92.3
<i>Macroclymene zonalis</i>	Polychaeta	0.5	0.0	0.5	0.2	0.0	1.4	1.9	7.0	1.9
Subdominant Species:										
<i>Acanthohaustorius bousfieldi</i>	Amphipoda	0.1	.	0.1	0.0	.	0.2	31.5	.	31.5
<i>Parahaustorius holmesi</i>	Amphipoda	0.3	0.2	0.1	0.1	0.1	0.2	28.5	32.4	21.8
<i>Parahaustorius attenuatus</i>	Amphipoda	0.1	0.1	.	0.1	0.1	.	26.0	26.0	.
<i>Periploma papyratium</i>	Bivalvia	0.3	0.3	.	0.1	0.1	.	262.0	262.0	.
<i>Pandora trilineata</i>	Bivalvia	0.2	0.2	.	0.1	0.1	.	224.0	224.0	.
<i>Siliqua costata</i>	Bivalvia	0.1	0.1	.	0.0	0.0	.	59.0	59.0	.
<i>Scoletoma acicularum</i>	Polychaeta	0.3	0.0	0.3	0.1	0.0	0.7	72.8	9.0	264.0
<i>Leitoscoloplos</i> spp.	Polychaeta	0.4	0.0	0.4	0.2	0.0	1.2	72.5	0.5	108.5
<i>Onuphis eremita</i>	Polychaeta	0.1	0.1	.	0.0	0.0	.	58.0	58.0	.
<i>Glycera dibranchiata</i>	Polychaeta	0.4	0.1	0.3	0.2	0.0	0.9	43.1	12.6	165.0
<i>Ophelia denticulata</i>	Polychaeta	0.5	0.5	0.0	0.2	0.2	0.0	25.2	159.2	0.1
<i>Sthenelais limicola</i>	Polychaeta	0.2	0.2	0.0	0.1	0.1	0.0	22.5	24.1	8.0
<i>Lumbrinerides dayi</i>	Polychaeta	0.3	0.0	0.3	0.1	0.0	0.8	21.6	3.5	61.5
<i>Scoletoma tenuis</i>	Polychaeta	0.2	0.0	0.2	0.1	0.0	0.4	20.7	5.4	33.0

Table 4.2-13

Summary of overall dominants based on occurrence, abundance, and biomass collected in the MD/DE study area.

---

MajorTaxa	Taxa	Occurrences		Abundance		Biomass		Mean Individual
		Number	%	ind./0.04 m <sup>2</sup>	%	g wet/0.04 m <sup>2</sup>	%	Weight (mg)
Nemertiena	Nemertinea	55	76	414	2	1.3	0.5	3.0
Polychaeta	<i>Asabellides oculata</i>	20	28	342	2	4.3	1.7	12.4
Polychaeta	<i>Spio setosa</i>	16	22	788	5	1.0	0.4	1.3
Polychaeta	<i>Spiophanes bombyx</i>	39	54	5902	35	7.2	2.9	1.2
Bivalvia	<i>Astarte</i> spp.	21	29	166	1	21.0	8.3	126.8
Bivalvia	<i>Crenella glandula</i>	23	32	128	1	0.9	0.4	7.0
Bivalvia	<i>Mytilus edulis</i>	17	24	130	1	0.7	0.3	5.8
Bivalvia	<i>Tellina</i> spp.	47	65	732	4	3.9	1.6	5.4
Amphipoda	<i>Byblis serrata</i>	17	24	250	1	0.9	0.3	3.5
Amphipoda	<i>Unciola irrorata</i>	30	42	279	2	0.7	0.3	2.4

---

Table 4.2-14.

Average abundance of dominant taxa (those that were important contributors to either occurrence, abundance, or biomass) by cluster analysis station group (see Fig. 4.2-2). Dominance Type are: O = occurrence (>20% of stations), A = Abundance (>1% of total abundance for May or September cruise), B = Biomass (>0.5 g total wet weight).

\* = average abundance was <1. Blank = taxa did not occur in station group.

Dominance Type	Major Taxa	Species or Taxa	Average Abundance (individuals/0.04 m <sup>2</sup> )											
			Cluster Analysis Station Group											
			A	A'	A''	B	B'	C	D	D'	D''	E	E'	
O,A,B	Nemertinea	Nemertinea	11	10	3	6	10	*	2	1	1	5	*	
O	Cnidaria	Anthozoa	1	2		5					1	*		
O,A	Oligochaeta	Oligochaeta	38	25	2	38	26		4	5	1	42	16	
O,A	Polychaeta	<i>Aphelochaeta</i> sp.	8	1	1		1		*	*		2	*	
A	Polychaeta	<i>Apoprionospio pygmaea</i>							*		*	68		
O,A	Polychaeta	<i>Aricidea (Acmira) catherinae</i>	4	10	1		2			1		10	2	
O,A	Polychaeta	<i>Aricidea (Acmira) cerrutii</i>	12	6	3	*	34		*	2		2	1	
O,A,B	Polychaeta	<i>Asabellides oculata</i>	*	*	2				6	2		33	8	
O,A	Polychaeta	<i>Brania wellfleetensis</i>	10	3	5		*			*			*	
O	Polychaeta	<i>Caulleriella</i> sp. B	1	*			*		*	4		3	2	
A	Polychaeta	<i>Clymenella torquata</i>		*					*			15		
O	Polychaeta	<i>Hemipodus roseus</i>	1	3	2	*	3			*				
O,A	Polychaeta	<i>Hesionura elongata</i>	1	1	1	3	24			*	*			
B	Polychaeta	<i>Lumbrineris fragilis</i>		*						1			*	
A,B	Polychaeta	<i>Macroclymene zonalis</i>				*			*			40		
A	Polychaeta	<i>Mediomastus ambiseta</i>		*		*			1			44	3	
O	Polychaeta	<i>Nephtys</i> spp.	*	*	2				*	2		3	*	
B	Polychaeta	<i>Notocirrus spiniferus</i>										1		
A	Polychaeta	<i>Paradoneis</i> sp. B	7	*		*	*							
O,A	Polychaeta	<i>Parapionosyllis longicirrata</i>	4	3	1	1	1			*		*	2	
A	Polychaeta	<i>Protodorvillea kefersteini</i>	1	11	1	1								
B	Polychaeta	<i>Sigalion arenicola</i>	*							*	*	*		
O,A,B	Polychaeta	<i>Spio setosa</i>	*	3	1							104	7	
O,A,B	Polychaeta	<i>Spiophanes bombyx</i>	7	2	1	1	*	1	1	4	*	797	26	
O	Polychaeta	<i>Streptosyllis pettiboneae</i>	2	1	2	*	3			*				
B	Gastropoda	<i>Busycon canaliculata</i>										*		
B	Gastropoda	<i>Nassarius trivittatus</i>		*					*	*		1	*	
O,A,B	Bivalvia	<i>Astarte</i> spp.	1	2	1	17				*	7	1		
O,A,B	Bivalvia	<i>Crenella glandula</i>	1	1		16	3		*		1	2	*	
B	Bivalvia	<i>Ensis directus</i>			2					*		12	*	
O	Bivalvia	<i>Lyonsia hyalina</i>	1	*		*				*		1		
O,A,B	Bivalvia	<i>Mytilus edulis</i>	*	2		10	*		*	4	*	2	1	
A,B	Bivalvia	<i>Nucula</i> spp.	*						67	2		19		
B	Bivalvia	<i>Pitar morrhuanus</i>		*								6	*	
O,A,B	Bivalvia	<i>Tellina</i> spp.	2	1	2	1	1	2	36	4	5	52	1	
O,B	Bivalvia	<i>Spisula solidissima</i>	1			2	*		*	1			*	
O	Tanaidacea	<i>Tanaissus psammophilus</i>	5	*	4	1		*	*				*	
O	Cumacea	<i>Oxyurostylis smithi</i>	*	*		*	*			1		1	*	
O	Cumacea	<i>Pseudoleptocuma minor</i>	1			*	1			1		1	*	
O	Isopoda	<i>Chiridotea coeca</i>	*	*		1	1	8	*	*	3			
B	Isopoda	<i>Politolana concharum</i>	*			1	*	1	1	*	*		*	
B	Amphipoda	<i>Ampelisca</i> spp.								*	*	14	*	
O,A,B	Amphipoda	<i>Byblis serrata</i>	2	*	100	*				*	1			
O,A	Amphipoda	<i>Protohaustorius wigleyi</i>	1	*		*	1		*	7	3	*	1	
O,A	Amphipoda	<i>Pseudunciola obliquua</i>	5	1	28					1		11		
O,A,B	Amphipoda	<i>Unciola irrorata</i>	1	2	3	*		*	2	*	1	29	6	
O,B	Cephalochordata	<i>Branchiostoma caribaеum</i>	*	*	1	2		*	*	*	1			

Table 4.2.15. Life history attribute summary for dominant taxa from the inner continental shelf off MD and DE.

Major Group	Species Name	Preferred Substrate	Feeding Mode	Mobility	Size (cm)	Spawns/Year	Larval Mode	Spawning Times	LifeSpan	Year Round Recruitment Potential	Spring/Summer Recruitment Potential	Fall/Winter Recruitment Potential
Amphipoda	Ampelisca spp.	Medium to Coarse Sand	Suspension	Tube Builder	<1	Twice	Brooding	Spring/Summer	Annual	Poor	Good	Poor
Amphipoda	Byblis serrata	Medium to Coarse Sand	Suspension	Tube Builder	<1	Multiple Events	Brooding	Late Spring/Summer	Annual	Poor	Good	Poor
Amphipoda	Protohastorius wigleyi	Fine Sand	Suspension	Burrower	<1	Multiple Events	Brooding	Late Spring/Summer	Annual	Poor	Good	Poor
Amphipoda	Pseudounciola obliqua	Medium to Coarse Sand	Suspension	Tube Builder	<1	Multiple Events	Brooding	Late Spring/Summer	Annual	Poor	Good	Poor
Amphipoda	Unciola irrorata	Coarse to medium Sand	Deposit/Suspension	Lives in tubes of other organisms	<1	Once	Brooding	Spring/Early Summer	Annual	Poor	Good	Poor
Bivalvia	Astarte spp.	Muddy Fine Sand	Deposit/Suspension	Limited Mobility	3	Once	Lecithotrophic (eggs attached to substratum)	Fall	20 years	Poor	Poor	Good
Bivalvia	Crenella glandula	Fine Sand	Suspension	Sessile	2	?	?	?	>1	?	?	?
Bivalvia	Ensis directus	Medium to Fine Sand, Muddy Sand	Suspension	Limited Mobility	24	Multiple Events	Planktonic	?	>1	Good	Good	Good
Bivalvia	Mytilus edulis	Hard Substrates, Coarse Sand, Gravel	Suspension	Sessile	8	Once or Twice	Planktonic	Late Fall/Winter	7 years	Poor	Poor	Good
Bivalvia	Nucula proxima	Muddy	Deposit	Limited Mobility	<1	?	Planktonic	Late Summer/Early Fall	>1	Poor	Poor	Good
Bivalvia	Pitar morrhuanus	Coarse to medium Sand	Suspension	Sessile	4	?	Planktonic	?	>7 years	?	?	?
Bivalvia	Spisula solidissima	Coarse Sand	Suspension	Limited Mobility	18	Twice	Planktonic	Late Summer/Fall	20 to 35 Years	Good	Good	Good
Bivalvia	Tellina agilis	Medium to Fine Sand, Muddy Sand	Surface Deposit	Limited Mobility	2	Twice	Planktonic	Spring/Fall	2 Years	Good	Good	Good
Cephalochordata	Branchiostoma caribaeum	Coarse to Fine Silty Sand	Suspension	Mobile	5	?	Planktonic	?	?	Good	Good	Good
Cnidaria	Anthozoa	Coarse to Fine Sand	Carnivore/Suspension	Sessile	15	?	Asexual/Planktonic	?	Annual?	Poor	Poor	Poor
Cumacean	Oxyurostylis smithi	Fine Sand	Suspension	Burrower/Limited Mobility	<1	Continuous	Brooding	Early Winter	Annual	Good	Good	Good
Cumacean	Pseudoleptocuma minor	Fine Sand	Suspension	Burrower/Limited Mobility	<1	Continuous	Brooding	?	Annual	Good	Good	Good
Gastropoda	Busycon canaliculata	Coarse to Muddy Fine Sand	Carnivore	Mobile	19	Once	Direct Development	?	>5 years	Good	Good	Good
Gastropoda	Nassarius trivittatus	Coarse to Fine Sand	Scavenger	Mobile	2	?	Direct Development	?	>1	Good	Good	Good
Isopoda	Chironotea coeca	Coarse to medium Sand	?	Limited Mobility	2	?	Brooding	?	?	?	?	?
Isopoda	Politolana concharum	?	?	Limited Mobility	<1	?	Brooding	Winter/Early Spring	?	Good	Good	Good
Nemertinea	Nemertinea	Coarse to Muds	Carnivore	Burrower	20	?	Direct Development/Planktonic	?	Annual?	Good	Good	Good
Oligochaeta	Oligochaeta	Coarse to Fine Sand, Muds	Deposit	Burrower/Interstitial	<1	Continuous	Direct Development	Spring/Summer/Fall	Annual	Good	Good	Good
Polychaeta	Aphelochaeta sp.	?	Surface Deposit	Tube Builder	2	Multiple Events	Lecithotrophic eggs	Spring/Summer	?	Poor	Good	Poor
Polychaeta	Aricidea spp.	Muddy, Silty-Fine Sand	Subsurface Deposit	Burrower	<1	?	Brooding	?	?	Poor	?	?
Polychaeta	Asabellides oculata	Sand, Silty Sand	Surface Deposit	Tube Builder	1	Once	Brooding	Winter, Early Spring	Annual	Good	Good	Good
Polychaeta	Brania wellfleetensis	Muddy, Muddy Sandy	Deposit	Burrower	1	Once	Brooding	Fall	?	Poor	Poor	Good
Polychaeta	Hemipodus roseus	Coarse Sand	Carnivore	Burrower	1	Once	Planktonic	?	?	Poor	?	?
Polychaeta	Hesionura elongata	Medium to Coarse Sand	Carnivore	Burrower	1	Once	Planktonic	?	?	Poor	?	?
Polychaeta	Mediomastus ambiseta	Muddy Fine Sand	Deposit	Tube Builder	3	Once	Planktonic, Non-Feeding	Late summer/fall	Annual	Poor	Poor	Good
Polychaeta	Nephtys spp.	Coarse to Very Fine Sand	Carnivore/Omnivore	Burrower	8	Twice	Planktonic	Spring/Fall	4 Years	Good	Good	Good
Polychaeta	Paradoneis sp. B.	Clean Sand, Muddy Sand	Subsurface Deposit	Burrower	<1	?	Direct Development	?	?	?	?	?
Polychaeta	Parapionosyllis longicirrata	Muddy Sand, Shells	?	Burrower	<1	?	Brooding	Fall	?	Poor	Poor	Good
Polychaeta	Protodorvillea kefersteini	Coarse to Fine Sand	Carnivore	Burrower	<1	Once	Direct Development	Summer/Late Fall	?	Good	Good	Good
Polychaeta	Spio Setosa	Muddy Fine Sand	Deposit/Suspension	Tube Builder	1	Twice	Broods Spring/Planktonic Fall	Spring/Fall	Annual	Good	Good	Good
Polychaeta	Spiophanes bombyx	Fine Sand, Muddy	Deposit/Suspension	Tube Builder	1	Once	Planktonic	Late Summer	Annual	Poor	Good	Poor
Polychaeta	Streptosyllis pettiboneae	Medium Fine Sand	Carnivore	?	<1	Once	Brooding	Spring/Early Summer	Annual	Poor	Good	Poor

Table 4.3-1

Fish collected in May 1999 at the four major benthic habitat types.  
Data are the summed occurrence of species caught in eight trawls from each habitat.

Fish	Habitat				Total
	NE*	NW	SE	SW	
Ammodytes spp.	9	1	0	0	10
Anchoa mitchilli	0	1	1	0	2
Centropristis striata	0	0	1	0	1
Conger oceanicus	0	1	0	1	2
Cynoscion regalis	0	0	0	1	1
Enchelyopus cimbrius	0	0	0	6	6
Etropus microstomus	22	23	30	10	85
Mugil curema	0	0	0	1	1
Ophidion marginatum	0	3	1	0	4
Paralichthys dentatus	0	0	0	1	1
Prionotus carolinus	4	14	8	0	26
Prionotus evolans	0	0	0	1	1
Pseudopleuronectes americanus	0	0	1	4	5
Raja eglantaria	0	2	2	15	19
Raja erinacea	0	0	0	6	6
Scomber scombrus	0	1	0	0	1
Scophthalmus aquosus	0	0	0	2	2
Stenotomus crysops	0	4	0	0	4
Syngnathus fuscus	0	0	0	1	1
Urophycis regia	21	2	37	95	155

\* NE – Northeast seaward flank of shoal

NW – Northwest shoreward face of shoal,

SE – Southeast seaward trough, surface dominated by *Diopatra* tubes

SW – Southwest shoreward trough, surface dominated by *Asabellides* tubes

Table 4.3-2

Invertebrates collected in May 1999 at the four major benthic habitat types.  
 Data are the summed occurrence of selected species caught in eight trawls from each habitat.  
 For most species only presence in the trawl was recorded (+).

---

Invertebrate Taxa	Benthic Habitat Type				Total
	Shell&Gravel	<i>Diopatra</i>	Sand	<i>Asabellides</i>	
Hydroids		+			
Molluscs	+	+	+	+	
Loliginidae				+	
Nudibranchs	+	+	+	+	
<i>Littorina</i> spp.		+		+	
<i>Busycon canaliculatum</i>		+	+	+	
<i>Polinices</i> spp.	+	+	+		
<i>Astarte</i> spp.	+		+		
<i>Ensis directus</i>		+			
<i>Spisula solidissima</i>			+		
Crustaceans	+	+	+	+	
Amphipods	+			+	
Isopoda		+	+		
<i>Limulus polyphemus</i>	0	1	0	8	9
<i>Euceramus</i> sp.				1	1
<i>Pagurus</i> spp.	+	+	+	+	
<i>Crangon septemspinosa</i>	+	+	+	+	
Crab, Unknown	0	3	0	9	12
<i>Libinia emarginata</i>	8	93	8	92	201
<i>Cancer irroratus</i>	2	70	9	136	217
<i>Ovalipes ocellatus</i>	1	0	0	0	1
<i>Dissidactylus mellitae</i>	1	0	0	0	1
<i>Pinnixa lunzi</i>	0	0	1	0	1
<i>Pinnixa</i> sp.	0	2	0	0	2
<i>Hexanpanobeus angustifrons</i>	0	0	0	3	3
<i>Rhithropanopeus harrisi</i>	0	3	1	3	7
Echinoderms	+	+	+	+	
<i>Asterias</i> spp.	+	+	+	+	
<i>Echinarachnius parma</i>	+	+	+		

---

Table 4.3-3

Summary of gut content by taxa for the three dominant demersal fish species trawled around Fenwick Shoals. Gut content of all individual fish was summed for each species.

Major Taxa	Species	Number of guts	Fish Species			Total
			<i>E. microstomus</i> 36	<i>P. carolinus</i> 22	<i>U. Regia</i> 80	
Nemertean	Nemertinea	Abundance	1		3	4
		Wet Weight (g)	0.012		0.006	0.018
Polychaetes	Ampharetidae	Abundance	5			5
		Wet Weight (g)	0.241			0.241
	<i>Nephtys</i> sp.	Abundance	2			2
		Wet Weight (g)	0.033			0.033
	Polychaeta	Abundance	2		5	7
		Wet Weight (g)	0.023		0.107	0.130
	<i>Spio setosa</i>	Abundance	1			1
		Wet Weight (g)	0.019			0.019
	Spionidae	Abundance			1	1
		Wet Weight (g)			0.006	0.006
Bivalves	Bivalvia	Abundance			2	2
		Wet Weight (g)			0.025	0.025
	<i>Ensis directus</i>	Abundance		2		2
		Wet Weight (g)		0.069		0.069
Gastropods	Nudibranch	Abundance	1			1
		Wet Weight (g)	0.001			0.001
Cumacean	Cumacea	Abundance		1		1
		Wet Weight (g)		0.001		0.001
	<i>Cyclapsis varians</i>	Abundance		1		1
		Wet Weight (g)		0.003		0.003
	<i>Oxyurostylus smithi</i>	Abundance	3	6		9
		Wet Weight (g)	0.002	0.009		0.011
<i>Pseudoleptocuma minor</i>	Abundance	5	18	1	24	
	Wet Weight (g)	0.009	0.029	0.002	0.040	
Mysids	Mysidacea	Abundance			4	4
		Wet Weight (g)			0.009	0.009
	<i>Neomysis americana</i>	Abundance	9	2	203	214
		Wet Weight (g)	0.016	0.003	0.527	0.546
Isopods	<i>Politolana concharum</i>	Abundance			41	41
		Wet Weight (g)			0.735	0.735
Amphipods	<i>Ampelisca</i> sp.	Abundance	20	12	33	65
		Wet Weight (g)	0.324	0.085	0.268	0.677
	Amphipoda	Abundance		3	2	5
		Wet Weight (g)		0.068	0.001	0.069
	<i>Byblis serrata</i>	Abundance	12	44	50	106
		Wet Weight (g)	0.056	0.334	0.448	0.838
	<i>Corophium</i> sp.	Abundance			3	3
		Wet Weight (g)			0.006	0.006
	<i>Erichthonius rubricornis</i>	Abundance			1	1
		Wet Weight (g)			0.006	0.006
Haustoriidae	Abundance		4	1	5	
	Wet Weight (g)		0.007	0.007	0.014	
<i>Listriella barnardi</i>	Abundance		2		2	
	Wet Weight (g)		0.001		0.001	

Table 4.3-3 Continued.

Major Taxa	Species	Fish Species			Total	
		<i>E. microstomus</i>	<i>P. carolinus</i>	<i>U. Regia</i>		
Decapods	<i>Melita dentata</i>	Abundance		1	1	2
		Wet Weight (g)		0.001	0.002	0.003
	<i>Melita</i> sp.	Abundance			1	1
		Wet Weight (g)			0.002	0.002
	<i>Microdeutopus anomalus</i>	Abundance			1	1
		Wet Weight (g)			0.001	0.001
	<i>Monoculodes intermedius</i>	Abundance	1			1
		Wet Weight (g)	0.004			0.004
	<i>Monoculodes</i> sp.	Abundance		1		1
		Wet Weight (g)		0.001		0.001
	Photidae	Abundance			1	1
		Wet Weight (g)			0.005	0.005
	<i>Pseudounciola obliquua</i>	Abundance	1	2	2	5
		Wet Weight (g)	0.001	0.003	0.011	0.015
	<i>Rhepoxynus hudsoni</i>	Abundance		1		1
		Wet Weight (g)		0.001		0.001
	<i>Synchelidium americanum</i>	Abundance	4		1	5
		Wet Weight (g)	0.002		0.001	0.003
	<i>Unciola irrorata</i>	Abundance	62	35	142	239
		Wet Weight (g)	0.055	0.118	0.657	0.829
	<i>Cancer irroratus</i>	Abundance	8	48	3	59
		Wet Weight (g)	0.036	0.242	0.012	0.290
	Crab megalopae	Abundance	17	27	37	81
		Wet Weight (g)	0.043	0.058	0.075	0.176
	<i>Cragnon septemspinosa</i>	Abundance	42	38	2097	2177
		Wet Weight (g)	0.105	0.768	11.230	12.102
	Decapoda	Abundance	1			1
		Wet Weight (g)	0.006			0.006
	<i>Eucерamus praelongus</i>	Abundance			1	1
		Wet Weight (g)			0.150	0.150
	Hermit crab megalopae	Abundance	1			1
		Wet Weight (g)	0.001			0.001
	<i>Pagarus longicarpus</i>	Abundance			2	2
Wet Weight (g)				0.182	0.182	
<i>Pagarus</i> sp.	Abundance	2	1		3	
	Wet Weight (g)	0.032	0.031		0.063	
Spider Crab	Abundance			1	1	
	Wet Weight (g)			0.086	0.086	
Unknown Shrimp	Abundance			2	2	
	Wet Weight (g)			0.002	0.002	
Echinoderms	Holothroidae	Abundance	1		1	
		Wet Weight (g)	0.003		0.003	
Cephalochordate	<i>Branchiostoma caribieum</i>	Abundance	1		1	
		Wet Weight (g)	0.046		0.046	
		Total Abundance	202	249	2642	3093
		Total Wet Weight (g)	1.068	1.830	14.568	17.465

Table 4.4-1.  
Sediment size classes estimated from SPI images collected in the MD/DE study area.

Year	Station	Grain Size		Sorting	Interface	Class	Size		
		(mm)	Phi				Class	Type	Grade
98	BB01	2.00	-1.0			csgr	GR	GR	COARSE
98	BB02	2.00				csgr	GR	GR	COARSE
98	BB03	2.00				csgr	GR	GR	COARSE
98	BB04	1.00				grcs	VCS	SAND	COARSE
98	BB05	0.71				msgrcs	CS	SAND	COARSE
98	BB06	1.00				grcs	VCS	SAND	COARSE
98	BB07	1.00				grcs	VCS	SAND	COARSE
98	FS01.5D	0.30				fsms	MS	SAND	MED
98	FS01A	0.18	2.5	W	P	fs	FS	SAND	FINE
98	FS01B	0.59	2.0	P	P	mscs	CS	SAND	COARSE
98	FS01C	0.18	2.5	VW	P	fs	FS	SAND	FINE
98	FS01D	0.30	3.0	VW	P	fsms	MS	SAND	MED
98	FS01E	0.30	2.5	W	P	fsms	MS	SAND	MED
98	FS01F	0.30	2.5	M	P	fsms	MS	SAND	MED
98	FS01G	0.84	1.5	P	P	grmscs	CS	SAND	COARSE
98	FS02.5D	0.59	1.5	W	P	mscs	CS	SAND	COARSE
98	FS02A	0.18	3.0	VW	P	fs	FS	SAND	FINE
98	FS02B	0.59	2.0	M	P	mscs	CS	SAND	COARSE
98	FS02C	0.35	1.5	M	P	ms	MS	SAND	MED
98	FS02D	0.18	2.5	W	P	fs	FS	SAND	FINE
98	FS02E	0.30	2.5	W	P	fsms	MS	SAND	MED
98	FS02F	1.00	0.0	P	P	shgrcs	VCS	SAND	COARSE
98	FS02G	0.59	1.0	P	P	mscs	CS	SAND	COARSE
98	FS03.5D	2.00	-1.0	VP	P	csgr	GR	GR	COARSE
98	FS03A	0.35	2.0	M	P	ms	MS	SAND	MED
98	FS03B	0.15	3.0	VW	B	vfsfs	FS	SAND	FINE
98	FS03C	0.59	1.5	M	P	mscs	CS	SAND	COARSE
98	FS03CD	1.19	1.0	M	P	csvcs	VCS	SAND	COARSE
98	FS03D	1.68	0.0	P	P	grvcs	VCS	SAND	COARSE
98	FS03DE	0.30	2.0	W	P	fsms	MS	SAND	MED
98	FS03E	0.15	3.0	VW	P	vfsfs	FS	SAND	FINE
98	FS03F	0.59		M-P	P	shgrms-cs	CS	SAND	COARSE
98	FS03G	0.15	3.0	W	P	vfsfs	FS	SAND	FINE
98	FS04.5D	1.00	-1.0	P	P	grcs	VCS	SAND	COARSE
98	FS04A	0.07	3.0	W	B	sivfs	VFS	SAND	FINE
98	FS04B	0.09	3.0	VW	B	vfs	VFS	SAND	FINE
98	FS04C	0.09	3.0	W	B	vfs	VFS	SAND	FINE
98	FS04D	0.59	1.0	M	P	mscs	CS	SAND	COARSE
98	FS04E	0.30	1.0	M	P	fsms	MS	SAND	MED
98	FS04F		1.5	P	P	cs/fs		SAND	MED
98	FS04G	0.09	2.5	W	P	vfs	VFS	SAND	FINE
98	FS05.5D	0.35	1.5	W	P	ms	MS	SAND	MED
98	FS05A	0.42	1.0	M-P	P	csms	MS	SAND	MED
98	FS05B	0.18	2.5	W	B	fs	FS	SAND	FINE
98	FS05C	0.42	1.5	P-M	P	csms	MS	SAND	MED
98	FS05D	0.42	1.5	M-W	P	csms	MS	SAND	MED
98	FS05E	0.84	1.0	M	P	vcscs	CS	SAND	COARSE

Table 4.4-1. Continued.

Year	Station	Grain Size		Sorting	Interface	Class	Size		Type	Grade
		(mm)	Phi				Class	Class		
98	FS05F	0.21	2.0	VW	P	msfs	FS	SAND	FINE	
98	FS05G		4.0	M/VW	I	ms/si		MIXSM	FINE	
98	FS06.5D	0.84	1.0	M	P	grms-cs	CS	SAND	COARSE	
98	FS06A	1.00	-1.0	P-M	P	shgrcs	VCS	SAND	COARSE	
98	FS06B		2.0	M-W	P	ms/sicl		MIXSM	FINE	
98	FS06C	1.68	-1.0	M	P	grvcs	VCS	SAND	COARSE	
98	FS06D	0.42	0.0	M-W	P	csms	MS	SAND	MED	
98	FS06E	0.15	3.0	W	B	vfsfs	FS	SAND	FINE	
98	FS06F	0.30	2.0	M-W	P/I	fsms	MS	SAND	MED	
98	FS06G	0.42	0.0	M	P	csms	MS	SAND	MED	
98	FS07.5D	1.00	0.5	P-M	P	grcs	VCS	SAND	COARSE	
98	FS07A	0.15	3.0	W	B/I	vfsfs	FS	SAND	FINE	
98	FS07AB	0.11	3.0	W-VW	B/I	fsvfs	VFS	SAND	FINE	
98	FS07B	0.11	3.0	VW	B/I	fsvfs	VFS	SAND	FINE	
98	FS07BC	0.11		W-VW	B	fsvfs	VFS	SAND	FINE	
98	FS07C	1.00	0.5	P-M	P	grcs	VCS	SAND	COARSE	
98	FS07CD	1.00	0.5	P	P	grcs	VCS	SAND	COARSE	
98	FS07D	0.84	0.5	M	P	vcscs	CS	SAND	COARSE	
98	FS07DE	0.50	1.0	M-W	P	vcscs	MSCS	SAND	COARSE	
98	FS07E	0.11	2.5	W-VW	P	fsvfs	VFS	SAND	FINE	
98	FS07EF		3.5	W	B	fsvfs/si		MUD	FINE	
98	FS07F	0.30	2.0	M-W	P	fsms	MS	SAND	MED	
98	FS07FG	1.00	-1.0	M	P	grcs	VCS	SAND	COARSE	
98	FS07G	0.42	1.0	W-VW	P	csms	MS	SAND	MED	
98	FS08.5D	0.59	1.0	M	P	mcs	CS	SAND	COARSE	
98	FS08A	0.30	2.0	M-W	I	fsms	MS	SAND	MED	
98	FS08B	0.18	1.5	W	I	fs	FS	SAND	FINE	
98	FS08C	1.41	0.5	VP-P	P	grcs-vcs	VCS	SAND	COARSE	
98	FS08D	1.00	-1.0	P-M	P	grcs	VCS	SAND	COARSE	
98	FS08E	0.42	1.5	W	P	csms	MS	SAND	MED	
98	FS08F	0.35	1.5	M-W	P	ms	MS	SAND	MED	
98	FS08G		0.0	P/M	I	shgr/ms		MIXGS	CF	
98	FS09.5D	0.21	2.0	W-VW	I	msfs	FS	SAND	FINE	
98	FS09A	0.30	2.0	M	I	fsms	MS	SAND	MED	
98	FS09AB	0.50	1.5	P-M	P	shms-cs	MSCS	SAND	COARSE	
98	FS09B	0.50	0.0	M	I	shms-cs	MSCS	SAND	COARSE	
98	FS09BC	1.00	-1.0	M-W	P	grcs	VCS	SAND	COARSE	
98	FS09C	0.59	1.0	W-VW	P	mcs	CS	SAND	COARSE	
98	FS09CD	0.30	2.0	W-VW	P	fsms	MS	SAND	MED	
98	FS09D	0.15	3.0	W-VW	B	vfsfs	FS	SAND	FINE	
98	FS09DE	0.15	3.0	VW	B	vfsfs	FS	SAND	FINE	
98	FS09E	0.06	4.0	W-VW	B	clsivfs	SIFS	MUD	FINE	
98	FS09EF	0.21	2.0	M-W	P	msfs	FS	SAND	FINE	
98	FS09F	0.25	2.0	P-M	P	fs-cs	MS	SAND	MED	
98	FS09FG	1.19	1.0	P	P	grms-vcs	VCS	SAND	COARSE	
98	FS09G	0.42	1.5	M-W	P	csms	MS	SAND	MED	
98	FS10.5D	0.42	1.5	M	P	csms	MS	SAND	MED	

Table 4.4-1. Continued.

Year	Station	Grain Size		Sorting	Interface	Class	Size	Type	Grade
		(mm)	Phi				Class		
98	FS10A	0.59	1.0	P	P	mscs	CS	SAND	COARSE
98	FS10B	0.59	0.0	P	P	shgrms-cs	CS	SAND	COARSE
98	FS10C	0.84	1.0	P	P	grms-cs	CS	SAND	COARSE
98	FS10D	0.30	2.0	W	P	fsms	MS	SAND	MED
98	FS10E	0.84	1.5	P-M	P	grms-cs	CS	SAND	COARSE
98	FS10F	0.59	-1.0	P-M	P	mscs	CS	SAND	COARSE
98	FS10G	0.30	2.0	M	P	fsms	MS	SAND	MED
98	FS11.5D	0.59	1.0	M	P	mscs	CS	SAND	COARSE
98	FS11A	0.18	2.5	M	B	shfs	FS	SAND	FINE
98	FS11AB	0.42	1.0	M	P	csms	MS	SAND	MED
98	FS11B	0.35	1.5	P-M	P	ms	MS	SAND	MED
98	FS11BC	0.84	1.5	P	P	grms-cs	CS	SAND	COARSE
98	FS11C	0.84	1.0	P-M	P	grms-cs	CS	SAND	COARSE
98	FS11CD	0.50	1.5	M	P	vcms	MSCS	SAND	COARSE
98	FS11D	0.35	1.5	M-W	P	ms	MS	SAND	MED
98	FS11DE	0.30	2.0	M-W	P	fsms	MS	SAND	MED
98	FS11E	1.00	-1.0	P	P	grcs	VCS	SAND	COARSE
98	FS11EF	0.59	1.0	M	P	mscs	CS	SAND	COARSE
98	FS11F	0.21	2.5	W-VW	P	msfs	FS	SAND	FINE
98	FS11FG	0.07	4.0	W	B	sivfs	VFS	SAND	FINE
98	FS11G	0.18	2.5	VW	P	fs	FS	SAND	FINE
98	FS12.5D	0.30	2.5	M	P	fsms	MS	SAND	MED
98	FS12A	0.35	2.0	P-M	P	ms	MS	SAND	MED
98	FS12B	0.71	1.5	M	P	ms-vc	CS	SAND	COARSE
98	FS12BC	1.00	-0.5	VP-P	P	grcs	VCS	SAND	COARSE
98	FS12C	0.59	2.0	M	P	mscs	CS	SAND	COARSE
98	FS12CD	1.00	1.0	P-M	P	grcs	VCS	SAND	COARSE
98	FS12D	0.59	2.0	M-W	P	mscs	CS	SAND	COARSE
98	FS12DE	0.30		W	P	fsms	MS	SAND	MED
98	FS12E	0.30		M-W	P	fsms	MS	SAND	MED
98	FS12EF	0.71	1.0	M	P	ms-vc	CS	SAND	COARSE
98	FS12F	0.84	1.0	P-M	P	grms-cs	CS	SAND	COARSE
98	FS12FG	0.42	2.0	M	P	csms	MS	SAND	MED
98	FS12G	0.09	3.5	W	B	vfs	VFS	SAND	FINE
98	FS12GG	0.71	1.0			ms-vc	CS	SAND	COARSE
98	FS13.5D	0.71	1.0	P	P	cs	CS	SAND	COARSE
98	FS13A	0.35	1.0			ms	MS	SAND	MED
98	FS13B		0.5	M	P	ms-cs		SAND	COARSE
98	FS13C	1.00	-1.0	VP-P	P	shgrcs	VCS	SAND	COARSE
98	FS13D		1.0	P-M	P	cs/ms		SAND	MED
98	FS13E	0.42		M	P	csms	MS	SAND	MED
98	FS13F	0.42		M	P	csms	MS	SAND	MED
98	FS13G	0.30		M-W	P	fsms	MS	SAND	MED
98	FS14A	0.30	1.0	M-W	P	fsms	MS	SAND	MED
98	FS14B	0.84	1.5	VP-P	I	grms-cs	CS	SAND	COARSE
98	FS14C	0.35		M-W	P	ms	MS	SAND	MED
98	FS14D	0.35	1.5	M-W	P	ms	MS	SAND	MED
98	FS14E	0.30		VW	P	fsms	MS	SAND	MED
98	FS14F	0.84	1.0	P-M	P	grms-cs	CS	SAND	COARSE
98	FS14G	0.30	2.0	M-W	P	fsms	MS	SAND	MED

Table 4.4-1. Continued.

Year	Station	Grain Size (mm)	Phi	Sorting Interface	Class	Size Class	Type	Grade
98	HCS31				fssi/cl		MUD	FINE
98	IR01C	1.68			grvcs	VCS	SAND	COARSE
98	IR01E							
98	IR02.5C	2.00			csgr	GR	GR	COARSE
98	IR02B	2.38			vcsg	GR	GR	COARSE
98	IR02C	0.71			cs	CS	SAND	COARSE
98	IR02D	1.68			grvcs	VCS	SAND	COARSE
98	IR02E	1.68			grvcs	VCS	SAND	COARSE
98	IR03.5C	0.59			mcs	CS	SAND	COARSE
98	IR03B				gr(si)		MIXGM	CF
98	IR03C	2.38			vcsg	GR	GR	COARSE
98	IR03D				gr/cs		GR	COARSE
98	IR03E	2.38			vcsg	GR	GR	COARSE
98	IR04.5C	2.38			vcsg	GR	GR	COARSE
98	IR04B	1.00			grcs	VCS	SAND	COARSE
98	IR04BC	1.68			grvcs	VCS	SAND	COARSE
98	IR04C	2.83			gr	GR	GR	COARSE
98	IR04CD	1.68			grvcs	VCS	SAND	COARSE
98	IR04D	2.00			csgr	GR	GR	COARSE
98	IR04DE	1.68			grvcs	VCS	SAND	COARSE
98	IR04E	1.00			grcs	VCS	SAND	COARSE
98	IR05.5C	1.00			grcs	VCS	SAND	COARSE
98	IR05B	2.00			csgr	GR	GR	COARSE
98	IR05C	1.00			grcs	VCS	SAND	COARSE
98	IR05D	0.35			ms	MS	SAND	MED
98	IR05E							
98	IR06.5B				gr/sics		MIXGM	CF
98	IR06.5C	0.59			mcs	CS	SAND	COARSE
98	IR06.5D	1.00			grcs	VCS	SAND	COARSE
98	IR06B	2.38			vcsg	GR	GR	COARSE
98	IR06C				gr(si)		MIXGM	CF
98	IR06D				gr/csvcs		GR	COARSE
98	IR06E	0.30			shfms	MS	SAND	MED
98	IR07.5B	0.59			mcs	CS	SAND	COARSE
98	IR07.5C	0.59			mcs	CS	SAND	COARSE
98	IR07.5D	2.38			vcsg	GR	GR	COARSE
98	IR07B				gr/mcs		GR	COARSE
98	IR07C	2.83			gr	GR	GR	COARSE
98	IR07D	0.59			mcs	CS	SAND	COARSE
98	IR07E				gr/csvcs		GR	COARSE
98	IR08.5B	1.00			grcs	VCS	SAND	COARSE
98	IR08.5C	2.00			csgr	GR	GR	COARSE
98	IR08.5D				gr(si)		GR	COARSE
98	IR08A	2.00			csgr	GR	GR	COARSE
98	IR08AB				gr/csvcs		GR	COARSE
98	IR08B	1.00			grcs	VCS	SAND	COARSE
98	IR08BC	1.41			grsvcs	VCS	SAND	COARSE
98	IR08C	0.71			cs	CS	SAND	COARSE

Table 4.4-1. Continued.

Year	Station	Grain Size (mm)	Phi	Sorting	Interface	Class	Size Class	Type	Grade
98	IR08CD	0.71				cs	CS	SAND	COARSE
98	IR08D	0.84				vcscs	CS	SAND	COARSE
98	IR09A	1.00				vcsgres	VCS	SAND	COARSE
98	IR09B	0.84				grvcscs	CS	SAND	COARSE
98	IR09C	0.84				grvcscs	CS	SAND	COARSE
98	IR09D					vcs(si)		MIXGM	CF
98	SBB04	0.21				msfs	FS	SAND	FINE
98	SBB09	2.00				csgr	GR	GR	COARSE
98	SBB10	0.42				csms	MS	SAND	MED
98	SBB32	0.84				vcscs	CS	SAND	COARSE

Table 4.9-1  
Estimated secondary production of macroinfaunal for 1998 grab data.

Station	Nemerteaans		Polychaete		Gastropods		Isopods		Crustaceans		Phoronids		Total
	Anemonies		Oligochaeta		Bivalves		Amphipods		Sipunculids		Cepholo.		
BB02	0.16	0.02	1.47	0.32			0.23	0.01	0.23	0.02			2.46
BB04	0.07		0.90	0.55			0.02		0.24	0.07			1.78
FS01G	0.08		32.65	0.01	12.56		0.04	0.97	0.33	0.02	0.02		46.60
FS02.5D	0.01		0.09				0.01	0.67	1.15	0.01			1.93
FS02C	0.91	0.02	0.11	0.05	0.02	37.85	2.65	0.80	0.03			1.06	42.57
FS03E							0.29	1.54	0.02			0.10	1.94
FS04C	0.33		5.30	0.14	7.11	73.55	0.28	0.12					86.51
FS04E	0.02			0.01	0.05	0.08		0.12					0.26
FS06C	0.16	0.02	3.09	0.89	0.33	8.52	0.02	0.04	0.01			1.99	14.89
FS06D	0.02		0.05	0.07	0.02	4.72	0.12	0.22					5.20
FS07B			7.65	0.25	0.63	2.45	0.30	2.79	0.05		0.02		14.14
FS07F	0.03		0.08	0.02		3.57	0.01	0.46					4.14
FS08B	0.05		2.90			0.01	0.04	0.42	0.10		0.02		3.49
FS08C	0.02		3.40	0.04	0.38	7.14		0.03		0.07			11.06
FS08D	0.16	0.03	0.65	0.27		1.04	0.01	0.02				0.14	2.14
FS08E	0.02	0.01	0.01	0.01		0.02	0.07	0.56			0.02		0.69
FS09A			0.41	0.08		0.25		1.85	0.02			0.85	3.47
FS09B	0.08		0.28	0.07		0.08	0.20	0.52	0.11				1.25
FS09C			0.01	0.02		0.02	0.65	0.62					1.32
FS09D	0.10		1.34	0.12				0.05					1.51
FS10.5D			0.02				0.07	0.15					0.24
FS10A	0.10		1.77	0.02				0.94	0.02				2.75
FS10B	0.20	0.01	0.69	0.18		0.08		1.09	0.05				2.09
FS11C	0.09		0.58	0.10	0.05	0.84		1.07					2.64
FS12B	0.12		1.46	0.04		0.01		0.02	0.04				1.57
FS12C	0.03	0.02	0.12	0.10		0.02		0.04	0.02			0.10	0.40
FS12E	0.01		0.01			0.34		0.19					0.53
FS12F	0.08		0.36	0.06		0.73	0.01	1.01					2.18
FS13A	0.07		0.26	0.01					0.16		0.08		0.52
FS13C	0.15	0.05	5.83	0.12	0.07	0.05		0.32	0.04			0.13	6.56
FS13E						0.28	1.21	0.23					1.72
FS13F	0.30	0.02	0.08	0.13		0.04	0.14	0.17	0.04				0.61
FS14A	0.23		1.88	0.42		0.55	0.15	0.21	0.09				3.30
FS14D			0.03			0.32		0.20	0.01				0.57
FS14E	0.01		0.06	0.01			0.71	0.17					0.95
FS14F	0.34		0.39	0.11		0.03		0.04	0.11				0.68
FS14G	0.01					0.50	0.07	0.68	0.03				1.28
HCS31	2.04		36.13	0.07		12.30	0.15	0.59	0.09		0.48		49.81
IR02B	0.16		1.24	0.08	0.01	0.12		0.01	0.01			0.22	1.70
IR02C	0.24		1.40	0.24		0.78	0.02	0.02					2.46
IR02D	0.13		2.02	0.06		9.20		0.02	0.02				11.33
IR04B	0.02		1.65	0.02		0.52		0.36	0.03				2.57
IR04D			1.28	0.01	0.01	0.02	0.06	0.08	0.04				1.51
IR04E	0.01		8.85	0.23	0.89	0.08	0.20	1.36		0.03			11.63
IR05.5C	0.62		1.12	0.08		141.05	0.81	0.27					143.33
IR05D			4.68	0.02	0.01	154.01	0.20	0.05	0.01	0.01	0.02		159.02
IR07C	0.03		7.38	0.01		0.05		0.22	0.03				7.69
IR07E			0.32	0.02				0.03	0.01	0.22	0.01		0.62
IR08B			0.15	0.02		0.50	0.67	0.15	0.02				1.51
IR08C	0.02		1.27		2.41	0.01		0.30					3.99
IR09A	0.04	0.32	0.62	0.02		0.08	0.02	0.06					0.79
IR09C	0.16		0.40	0.63		9.41			0.16				10.59
Total	7.5	0.5	142.4	5.8	24.6	471.5	10.8	22.2	1.5	0.3	0.7	4.6	692.3
% Total	1.1	0.1	20.6	0.8	3.5	68.1	1.6	3.2	0.2	0.0	0.1	0.7	100.0

Table 4.9-2  
Estimated secondary production for 1999

---

Station	Nemertieans		Polychaete		Gastropods		Isopods		Crustaceans		Phoronids		Total
	Anemonies		Oligochaeta		Bivalves		Amphipods		Sipunculids		Cephalo.		
FS02C	5.66	0.06	0.41		0.20	52.95	0.07	0.61					54.25
FS03E						0.61	0.01	0.33	0.01			1.92	2.89
FS04C			28.60	0.04	0.04	27.92		1.36					57.96
FS04E					0.13	0.56		0.62				0.14	1.44
FS06C	0.17	0.20	0.53	0.04		0.79	0.12					0.21	1.69
FS06D			0.08	0.02		0.83	0.01	0.83					1.77
FS07B1	0.21		20.76	0.68	2.15	28.62		6.72	0.21				59.14
FS07B2	0.09		18.50	0.25	3.77	3.44		3.18	0.11		0.45		29.70
FS07B3	0.03	0.10	22.24	0.40	0.43	11.35		7.06	0.02	0.01			41.51
FS08D	0.27	0.33	2.81	0.19	0.15	1.72	0.02					0.08	4.97
FS08E			0.07	0.02	0.23	2.38	0.02	0.32					3.05
FS09B	0.29		0.90	0.76	0.05	1.45	0.16	2.34	0.12				5.78
FS10B	0.07		1.74	0.02		5.08		6.52	0.29				13.64
FS11C	0.08		0.69	0.12		0.21	0.77	0.23					2.03
FS12B	0.30		0.33	0.01				2.99	0.04			0.28	3.66
FS12C	0.17		0.23	0.07		1.87		0.21	0.03			0.23	2.65
FS12E			0.01		0.05	0.82	0.11	0.16				0.13	1.27
FS12F	0.08		0.12	0.01	0.12	2.02		0.43				0.14	2.85
FS13C	0.21		0.28	0.05	0.23	3.67		2.05	0.10			0.46	6.83
FS13F	0.01		1.02		0.08	1.39		0.29				0.40	3.18
Total	7.6	0.7	99.3	2.7	7.6	147.7	1.3	36.2	0.9	0.0	0.5	4.0	308.6
% Total	2.5	0.2	32.2	0.9	2.5	47.9	0.4	11.7	0.3	0.0	0.1	1.3	100.0

---

Table 4.9-3

Average annual secondary production of macroinfaunal for 1998 grab data production.

Station	Nemertean		Gastropods		Oligochaeta		Isopods		Crustaceans		Sipunculids		Total
	Anemonies		Bivalves		Polychaete		Amphipods		Phoronids		Cephalochord.		
BB02	0.16	0.02		0.23	0.32	1.47	0.01	0.23	0.02				2.46
BB04	0.07			0.02	0.55	0.90		0.24	0.07				1.85
FS01G	0.08		12.56	0.04	0.01	32.65	0.97	0.33	0.02	0.02			46.68
FS02.5D	0.01			0.01		0.09	0.67	1.15	0.01				1.95
FS02C	3.28	0.04	0.11	45.40	0.05	0.26	1.36	0.70	0.03			1.06	52.30
FS03E				0.61			0.15	0.93	0.02			1.01	2.72
FS04C	0.33		3.58	50.74	0.09	16.95	0.28	0.74					72.70
FS04E	0.02		0.09	0.32	0.01			0.37				0.14	0.95
FS06C	0.17	0.11	0.33	4.66	0.46	1.81	0.07	0.04	0.01			1.10	8.75
FS06D	0.02		0.02	2.77	0.04	0.07	0.07	0.52					3.52
FS07B	0.11	0.10	1.37	8.46	0.35	14.08	0.30	4.22	0.08	0.24	0.01		29.31
FS07F	0.03			3.57	0.02	0.08	0.01	0.46					4.17
FS08B	0.05			0.01		2.90	0.04	0.42	0.10	0.02			3.54
FS08C	0.02		0.38	7.14	0.04	3.40		0.03			0.07		11.08
FS08D	0.22	0.18	0.15	1.38	0.23	1.73	0.02	0.02				0.11	4.04
FS08E	0.02	0.01	0.23	1.20	0.02	0.04	0.05	0.44		0.02			2.03
FS09A				0.25	0.08	0.41		1.85	0.02			0.85	3.47
FS09B	0.19		0.05	0.76	0.42	0.59	0.18	1.43	0.11				3.73
FS09C				0.02	0.02	0.01	0.65	0.62					1.32
FS09D	0.10				0.12	1.34		0.05					1.62
FS10.5D						0.02	0.07	0.15					0.24
FS10A	0.10				0.02	1.77		0.94	0.02				2.84
FS10B	0.14	0.01		2.58	0.10	1.22		3.80	0.17				8.01
FS11C	0.09		0.05	0.53	0.11	0.64	0.77	0.65					2.83
FS12B	0.21			0.01	0.03	0.90		1.51	0.04			0.28	2.97
FS12C	0.10	0.02		0.95	0.09	0.18		0.13	0.02			0.16	1.65
FS12E	0.01		0.05	0.58		0.01	0.11	0.17				0.13	1.06
FS12F	0.08		0.12	1.38	0.04	0.24	0.01	0.72				0.14	2.73
FS13A	0.07				0.01	0.26			0.16	0.08			0.59
FS13C	0.18	0.05	0.15	1.86	0.08	3.06		1.18	0.07			0.29	6.92
FS13E				0.28			1.21	0.23					1.72
FS13F	0.16	0.02	0.08	0.71	0.13	0.55	0.14	0.23	0.04			0.40	2.46
FS14A	0.23			0.55	0.42	1.88	0.15	0.21	0.09				3.54
FS14D				0.32				0.20	0.01				0.57
FS14E	0.01				0.01	0.06	0.71	0.17					0.97
FS14F	0.34			0.03	0.11	0.39		0.04	0.11				1.02
FS14G	0.01			0.50			0.07	0.68	0.03				1.29
HCS31	2.04			12.30	0.07	36.13	0.15	0.59	0.09	0.48			51.85
IR02B	0.16		0.01	0.12	0.08	1.24		0.01	0.01			0.22	1.86
IR02C	0.24			0.78	0.24	1.40	0.02	0.02					2.71
IR02D	0.13			9.20	0.06	2.02		0.02	0.02				11.47
IR04B	0.02			0.52	0.02	1.65		0.36	0.03				2.59
IR04D			0.01	0.02	0.01	1.28	0.06	0.08	0.04				1.51
IR04E	0.01		0.89	0.08	0.23	8.85	0.20	1.36			0.03		11.64
IR05.5C	0.62			141.05	0.08	1.12	0.81	0.27					143.95
IR05D			0.01	154.01	0.02	4.68	0.20	0.05	0.01	0.02	0.01		159.02
IR07C	0.03			0.05	0.01	7.38		0.22	0.03				7.73
IR07E					0.02	0.32		0.03	0.01	0.01	0.22		0.62
IR08B				0.50	0.02	0.15	0.67	0.15	0.02				1.51
IR08C	0.02		2.41	0.01		1.27		0.30					4.01
IR09A	0.04	0.32		0.08	0.02	0.62	0.02	0.06					1.15
IR09C	0.16			9.41	0.63	0.40			0.16				10.76
Total	10.1	0.9	22.6	466.0	5.5	158.5	10.2	29.4	1.7	0.9	0.3	5.9	712.0
% Total	1.4	0.1	3.2	65.4	0.8	22.3	1.4	4.1	0.2	0.1	0.05	0.8	100.0

Table 4.9-4

Gut content by major taxonomic group for fishes trawled at the four habitat areas around Fenwick Shoal. Areas around Fenwick Shoal are: NE – northeast seaward flank of shoal, NW – northwest shoreward face of shoal, SE – southeast seaward trough, surface dominated by *Diopatra* tubes, and SW – southwest shoreward trough, surface dominated by *Asabellides* tubes.

Area*	Fish Species	Fish Length (mm)	Major Group	Total Number	Wet Weight (g)	
NE	<i>Etropus microstomus</i>	52.4	Amphipod	2	0.001	
			Decapod	2	0.002	
			Mysid	1	0.003	
					Total	0.006
		57.7	Amphipod	14	0.007	
			Decapod	7	0.009	
			Total	0.016		
		64.8	Amphipod	4	0.003	
			Decapod	1	0.001	
			Total	0.004		
	50.7	Empty				
	55.0	Empty				
	56.0	Empty				
	62.0	Empty				
	62.5	Empty				
	65.2	Empty				
	71.7	Empty				
	82.2	Empty				
	<i>Prionotus carolinus</i>	55.5	Amphipod	10	0.034	
			Decapod	2	0.007	
			Total	0.041		
	<i>Urophycis regia</i>	55.2	Empty			
		45.0	Mysid	4	0.005	
			Total	0.005		
		48.1	Mysid	1	0.006	
			Nemertean	1	0.001	
			Total	0.007		
		56.0	Mysid	1	0.004	
			Total	0.004		
		57.8	Mysid	1	0.001	
		Total	0.001			
61.8		Decapod	1	0.001		
		Total	0.001			
62.6		Amphipod	2	0.006		
		Decapod	1	0.003		
		Mysid	2	0.005		
	Total	0.014				
65.0	Amphipod	1	0.008			
	Decapod	6	0.012			
	Mysid	4	0.014			
	Total	0.034				
67.1	Amphipod	3	0.013			
	Cumacean	1	0.002			
	Decapod	7	0.017			
	Total	0.032				

Table 4.9-4. Continued.

Area*	Fish Species	Fish Length (mm)	Major Group	Total Number	Wet Weight (g)
NE	<i>U. regia</i>	70.3	Amphipod	3	0.016
				Total	0.016
		71.2	Amphipod	2	0.003
			Polychaete	1	0.006
				Total	0.009
		72.2	Decapod	1	0.004
			Mysid	1	0.001
				Total	0.005
		76.3	Amphipod	2	0.011
				Total	0.011
			Amphipod	1	0.005
			Decapod	2	0.023
			Mysid	2	0.006
				Total	0.034
		78.7	Decapod	2	0.003
			Mysid	2	0.009
				Total	0.012
		96.3	Amphipod	1	0.001
			Decapod	6	0.046
			Mysid	3	0.013
		Total	0.060		
34.0	Empty				
73.4	Empty				
NW	<i>E. microstomus</i>	41.6	Amphipod	3	0.002
			Cumacean	1	0.003
			Decapod	1	0.003
				Total	0.008
		49.8	Empty		
		51.2	Empty		
		54.4	Empty		
		54.5	Empty		
		55.0	Empty		
		56.2	Empty		
	60.8	Empty			
	61.5	Empty			
	67.4	Empty			
	71.5	Empty			
	<i>P. carolinus</i>	47.0	Decapod	1	0.001
				Total	0.001
		51.5	Amphipod	1	0.001
				Total	0.001
		56.6	Amphipod	1	0.003
				Total	0.003
62.1		Amphipod	2	0.010	
		Decapod	4	0.009	
		Mysid	1	0.001	
62.1		Unknown	.	0.004	
		Total	0.024		
65.6	Amphipod	3	0.031		
		Total	0.031		

Table 4.9-4. Continued.

Area*	Fish Species	Fish Length (mm)	Major Group	Total Number	Wet Weight (g)	
NW	<i>P. carolinus</i>	74.8	Amphipod	1	0.008	
			Decapod	4	0.021	
				Total		0.029
		200.0	Amphipod	45	0.371	
			Bivalve	1	0.015	
			Cumacean	1	0.003	
			Decapod	15	0.035	
				Total		0.424
		52.5	Empty			
		57.0	Empty			
	66.3	Empty				
	66.5	Empty				
	<i>U. Regia</i>	67.5	Decapod	1	0.002	
			Mysid	20	0.056	
				Total		0.058
		68.3	Mysid	12	0.038	
			Unknown	.	0.004	
		Total		0.042		
SE	<i>E. microstomus</i>	68.5	Amphipod	5	0.002	
			Cumacean	5	0.006	
			Decapod	13	0.011	
			Unknown	.	0.001	
				Total		0.019
		69.8	Amphipod	1	0.001	
			Decapod	4	0.011	
			Polychaete	1	0.009	
				Total		0.021
		72.8	Amphipod	3	0.002	
			Cephalochordate	1	0.046	
			Decapod	10	0.020	
			Mysid	1	0.005	
			Unknown	.	0.001	
				Total		0.074
		77.5	Amphipod	2	0.005	
			Decapod	2	0.019	
			Mysid	1	0.003	
				Total		0.027
		86.0	Amphipod	25	0.020	
			Decapod	19	0.071	
			Gastropod	1	0.001	
			Mysid	6	0.005	
				Total		0.097
		98.0	Amphipod	9	0.060	
			Cumacean	1	0.001	
			Decapod	2	0.002	
Polychaete	3		0.049			
			Total		0.111	

Table 4.9-4. Continued.

Area*	Fish Species	Fish Length (mm)	Major Group	Total Number	Wet Weight (g)
SE	<i>E. microstomus</i>	103.8	Amphipod	13	0.130
			Decapod	3	0.013
			Polychaete	1	0.019
			Total		0.162
		105.0	Amphipod	10	0.064
			Decapod	1	0.004
			Echinoderm	1	0.003
			Nemertean	1	0.012
			Polychaete	1	0.044
			Total		0.127
		117.3	Amphipod	3	0.053
			Cumacean	1	0.001
			Polychaete	1	0.065
			Unknown	.	0.008
			Total		0.127
	124.9	Amphipod	5	0.089	
		Decapod	6	0.057	
		Polychaete	2	0.123	
		Unknown	.	0.048	
		Total		0.317	
	<i>P. carolinus</i>	50.3	Decapod	2	0.002
			Mysid	1	0.002
			Total		0.004
		56.5	Decapod	2	0.005
			Total		0.005
		66.0	Amphipod	2	0.002
			Decapod	5	0.008
Unknown			.	0.008	
		Total		0.017	
67.5		Amphipod	4	0.007	
		Cumacean	8	0.009	
		Decapod	7	0.026	
	Total		0.042		
130.0	Amphipod	6	0.028		
	Cumacean	13	0.025		
	Decapod	6	0.017		
	Unknown	.	0.033		
	Total		0.103		
140.0	Amphipod	1	0.001		
	Decapod	7	0.130		
	Total		0.131		
200.1	Amphipod	18	0.073		
	Bivalve	1	0.054		
	Cumacean	2	0.003		
	Decapod	23	0.165		
	Unknown	.	0.041		
	Total		0.336		
200.2	Amphipod	11	0.050		
	Cumacean	2	0.002		
	Decapod	26	0.226		
	Total		0.278		

Table 4.9-4. Continued.

Area*	Fish Species	Fish Length (mm)	Major Group	Total Number	Wet Weight (g)
SE	<i>U. Regia</i>	42.6	Decapod	1	0.001
				Total	0.001
		50.3	Amphipod	1	0.002
				Total	0.002
		50.7	Amphipod	1	0.006
			Mysid	8	0.023
				Total	0.029
		51.1	Mysid	4	0.007
				Total	0.007
		57.3	Amphipod	1	0.001
				Total	0.001
		59.1	Decapod	1	0.003
			Mysid	1	0.006
				Total	0.009
		64.5	Decapod	2	0.001
			Mysid	1	0.003
				Total	0.004
		68.0	Amphipod	20	0.186
			Decapod	84	0.340
			Mysid	16	0.042
				Total	0.568
		72.5	Decapod	1	0.020
				Total	0.020
		76.6	Decapod	3	0.017
				Total	0.017
		77.0	Amphipod	1	0.010
			Decapod	2	0.013
			Mysid	4	0.014
				Total	0.037
		84.5	Amphipod	2	0.016
	Decapod	8	0.035		
	Mysid	2	0.018		
		Total	0.069		
107.0	Amphipod	4	0.003		
	Decapod	6	0.059		
	Polychaete	1	0.072		
		Total	0.134		
110.2	Decapod	1	0.011		
		Total	0.011		
119.0	Amphipod	2	0.002		
	Decapod	40	0.115		
	Mysid	13	0.016		
		Total	0.133		
155.2	Decapod	6	0.226		
	Isopod	7	0.023		
		Total	0.249		

Table 4.9-4. Continued.

Area*	Fish Species	Fish Length (mm)	Major Group	Total Number	Wet Weight (g)	
SW	<i>E. microstomus</i>	90.0	Amphipod	1	0.004	
			Polychaete	1	0.007	
		Total		0.011		
			68.0	Empty		
			118.0	Empty		
			120.0	Empty		
	<i>P. carolinus</i>	160.0	Decapod	10	0.447	
				Total	0.447	
	<i>U. Regia</i>	46.0	Decapod	1	0.008	
				Total	0.008	
			Decapod	21	0.019	
				48.0	Mysid	1
			Total		0.021	
				50.0	Decapod	9
			Mysid	2	0.006	
				Total	0.025	
		59.0	Decapod	8	0.013	
				Mysid	8	0.019
			Total		0.032	
				60.0	Decapod	16
			Total		0.050	
				67.0	Amphipod	3
			Decapod	40	0.116	
				Total	0.129	
		67.6	Amphipod	1	0.005	
				Total	0.005	
		69.0	Decapod	2	0.001	
				Mysid	6	0.007
			Total		0.008	
				70.0	Decapod	4
			Mysid	2	0.003	
				Total	0.068	
		70.1	Amphipod	2	0.006	
Decapod				22	0.050	
		Total		0.056		
			72.0	Amphipod	2	0.001
		Decapod	1	0.005		
			Mysid	1	0.001	
		Nemertean	1	0.001		
			Total	0.007		
	73.0	Amphipod	2	0.004		
			Decapod	3	0.009	
		Mysid	10	0.038		
			Total	0.051		
	75.0	Decapod	6	0.006		
			Mysid	1	0.002	
		Unknown	.	0.013		
			Total	0.021		

Table 4.9-4. Continued.

Area*	Fish Species	Fish Length (mm)	Major Group	Total Number	Wet Weight (g)	
SW	<i>U. Regia</i>	75.1	Amphipod	2	0.004	
			Decapod	46	0.108	
			Mysid	2	0.009	
					Total	0.121
		80.0	Amphipod	1	0.001	
			Decapod	5	0.036	
			Mysid	3	0.004	
					Total	0.041
		80.1	Decapod	21	0.036	
			Mysid	3	0.010	
					Total	0.046
		82.0	Mysid	6	0.020	
			Unknown	.	0.008	
					Total	0.028
		82.3	Amphipod	6	0.013	
			Decapod	128	0.411	
			Mysid	3	0.007	
			Unknown	.	0.008	
					Total	0.439
		83.0	Amphipod	3	0.009	
			Decapod	24	0.107	
			Mysid	4	0.005	
					Total	0.121
		85.0	Decapod	14	0.027	
			Unknown	.	0.019	
					Total	0.046
		85.1	Decapod	1	0.008	
					Total	0.008
		106.5	Amphipod	6	0.018	
			Decapod	97	0.351	
			Mysid	6	0.025	
					Total	0.394
110.0	Amphipod	2	0.002			
	Decapod	26	0.076			
			Total	0.078		
110.1	Amphipod	2	0.003			
	Decapod	16	0.135			
			Total	0.138		
120.0	Decapod	9	0.016			
	Mysid	4	0.009			
	Unknown	.	0.012			
			Total	0.037		
145.0	Amphipod	1	0.012			
	Decapod	40	0.155			
			Total	0.167		
150.0	Amphipod	1	0.004			
	Decapod	12	0.185			
			Total	0.189		

Table 4.9-4. Continued.

Area*	Fish Species	Fish Length (mm)	Major Group	Total Number	Wet Weight (g)
SW	<i>U. Regia</i>	150.1	Amphipod	9	0.063
			Decapod	85	0.377
			Isopod	1	0.003
			Mysid	18	0.036
			Total		0.479
		160.0	Amphipod	46	0.403
			Decapod	110	0.588
			Isopod	6	0.023
			Mysid	13	0.023
			Total		1.037
		160.1	Amphipod	10	0.095
			Decapod	193	1.070
			Total		1.165
		165.0	Amphipod	3	0.028
			Decapod	26	0.042
			Isopod	1	0.002
			Mysid	1	0.001
			Total		0.073
		170.0	Amphipod	20	0.077
			Decapod	53	0.573
			Isopod	2	0.044
			Total		0.694
		170.1	Decapod	111	0.755
			Isopod	2	0.057
			Total		0.812
		170.2	Amphipod	13	0.058
			Decapod	169	1.015
			Isopod	3	0.070
			Polychaete	1	0.004
			Total		1.147
		170.3	Amphipod	5	0.018
			Decapod	4	0.058
			Polychaete	1	0.002
			Total		0.078
		175.0	Amphipod	8	0.050
			Decapod	112	0.664
			Isopod	1	0.035
			Mysid	3	0.008
Total			0.757		
180.0	Amphipod	1	0.009		
	Decapod	14	0.041		
	Mysid	1	0.001		
	Nemertean	1	0.005		
	Unknown	.	0.129		
	Total		0.185		
180.1	Amphipod	10	0.053		
	Decapod	192	1.250		
	Isopod	4	0.028		
	Polychaete	1	0.003		
	Total		1.334		

Table 4.9-4. Continued.

Area*	Fish Species	Fish Length (mm)	Major Group	Total Number	Wet Weight (g)
SW	<i>U. Regia</i>	185.0	Amphipod	15	0.061
			Decapod	194	0.847
			Isopod	5	0.106
			Mysid	2	0.002
			Total		1.016
		200.0	Amphipod	6	0.029
			Decapod	111	0.913
			Isopod	4	0.070
			Mysid	5	0.012
			Polychaete	1	0.026
		Total		1.050	
		205.0	Bivalve	1	0.005
			Decapod	10	0.398
			Isopod	4	0.209
		Total		0.612	
		210.0	Amphipod	12	0.088
			Bivalve	1	0.020
			Decapod	4	0.032
		Total		0.140	
		215.0	Decapod	1	0.150
			Isopod	1	0.065
			Unknown	.	0.197
		Total		0.412	
65.1	Empty				
73.0	Empty				
88.4	Empty				

Table 4.9-5

## Annual P/B ratios of macroinfauna from the MD/DE study area

Station	Nemertean		Oligochaeta		Gastropods		Isopods		Crustaceans		Sipunculids	
	Anemonies		Polychaete		Bivalves		Amphipods		Phoronids		Cephalochordates	
BB02	7.8	6.2	8.9	4.6		4.0	7.4	7.3	8.5			
BB04	9.1		9.1	4.1		5.4		3.5	8.5			
FS01G	4.2		7.4	3.4	0.6	9.0	3.9	4.9	8.5	8.5		
FS02.5D	7.4			4.8		6.4	5.2	3.3	7.4			
FS02C	2.3	8.4	13.3	3.4	5.4	1.2	5.7	3.3	7.8			2.2
FS03E						2.1	5.7	4.1	8.0			2.7
FS04C	3.6		9.6	2.4	3.4	2.1	7.9	6.1				
FS04E	6.2		7.4		4.0	3.6		3.8				3.5
FS06C	5.6	8.2	8.2	3.6	2.9	3.2	6.5	6.5	7.4			2.9
FS06D	12.2		8.8	5.1	5.4	2.7	5.9	2.8				
FS07B	6.4	4.0	8.4	2.7	2.6	3.3	4.7	3.7	5.7	8.7	7.4	
FS07F	7.2		8.5	4.6		2.0	7.4	4.3				
FS08B	6.6			2.1		7.4	7.1	6.6	4.8	8.5		
FS08C	6.2		11.1	2.6	2.1	2.5		7.2			5.5	
FS08D	6.3	6.6	8.2	3.9	4.1	2.2	6.8	6.2				3.8
FS08E	6.2	7.4	8.3	4.7	4.2	5.6	5.3	3.4		8.5		
FS09A			10.3	4.1		5.7		4.1	6.2			1.9
FS09B	5.7		7.9	4.3	4.1	3.9	4.1	4.4	7.5			
FS09C			8.5	5.3		5.4	3.9	2.9				
FS09D	5.2		9.7	3.0				6.6				
FS10.5D				4.4			4.4	4.1				
FS10A	8.0		11.1	3.9				4.5	9.9			
FS10B	5.4	7.4	8.7	3.6		3.3		3.8	5.2			
FS11C	5.5		7.9	4.1	4.1	3.4	2.0	3.2				
FS12B	5.4		8.4	3.4		6.4		7.8	9.3			3.4
FS12C	7.8	6.2	8.6	5.5		3.7		4.8	8.2			3.8
FS12E	7.4			5.3	4.1	2.2	3.8	4.0				3.6
FS12F	6.5		7.7	3.6	4.7	2.5	7.4	2.7				3.5
FS13A	5.9		7.4	4.1					5.5	6.9		
FS13C	7.0	6.0	11.1	3.1	3.8	3.5		4.1	8.6			3.2
FS13E						2.8	2.1	4.3				
FS13F	7.4	8.5	8.4	4.2	4.8	6.1	4.2	4.8	10.1			2.5
FS14A	7.3		7.6	4.0		2.9	4.1	3.7	5.5			
FS14D				5.0		2.7		4.2	7.4			
FS14E	7.4		7.4	5.8			2.0	3.9				
FS14F	4.3		8.9	4.1		7.5		6.5	7.1			
FS14G	7.4					2.3	4.4	3.9	7.2			
HCS31	2.8		9.3	2.5		2.1	6.1	4.1	5.9	4.0		
IR02B	6.7		9.7	3.1	6.4	6.5		7.4	7.4			3.0
IR02C	6.8		8.6	4.2		3.5	9.9	8.5				
IR02D	6.7		8.1	3.4		1.6		6.2	6.2			
IR04B	6.2		8.5	2.0		2.7		3.8	7.2			
IR04D			7.4	2.1	7.4	8.0	4.7	5.1	5.2			
IR04E	7.4		9.5	2.4	3.1	6.3	4.6	4.2			7.2	
IR05.5C	3.1		9.5	2.9		0.4	2.4	3.4				
IR05D			10.4	2.8	6.4	0.4	4.6	8.2	7.4	8.5	7.4	
IR07C	8.7		7.4	1.7		4.1		5.0	7.2			
IR07E			10.4	3.5				7.8	7.4	7.4	3.6	
IR08B			10.4	4.0		2.3	2.5	3.4	8.5			
IR08C	9.9			3.0	1.1	6.4		5.6				
IR09A	5.2	2.7	9.9	3.3		5.5	8.5	6.2				
IR09C	6.7		8.7	4.3		0.9			3.3			
Average	6.5	6.5	8.9	3.7	4.0	3.9	5.2	4.9	7.2	7.6	6.2	3.1
SD	1.8	1.8	1.3	1.0	1.7	2.1	2.0	1.6	1.5	1.6	1.6	0.6
Min	2.3	2.7	7.4	1.7	0.6	0.4	2.0	2.7	3.3	4.0	3.6	1.9
Max	12.2	8.5	13.3	5.8	7.4	9.0	9.9	8.5	10.1	8.7	7.4	3.8
Median	6.5	6.6	8.6	3.7	4.1	3.3	4.7	4.3	7.4	8.5	7.2	3.2

Table 4.9-6

Relationship between P/B ratio and sediment type for the May 1998 grab data. Based on discriminant analysis of sediment grain-size categories and major taxa P/B ratios. A total of 48 stations were classified, four stations did not have grain-size data. CS = coarse sand, FS = fine sand, GR = gravel, MU = mud.

---

Original Sediment Group		Predicted Sediment Group Membership							Total
		CS	FS	GRCS	GRFS	GRMUCS	MUCS	MUFS	
CS	Stations	14	1	1	0	0	0	0	16
	%	87.5	6.2	6.2	0	0	0	0	100
FS	Stations	1	10	0	0	0	0	0	11
	%	9.1	90.9	0	0	0	0	0	100
GRCS	Stations	1	0	12	0	0	0	0	13
	%	7.7	0	92.3	0	0	0	0	100
GRFS	Stations	0	0	0	2	0	0	0	2
	%	0	0	0	100	0	0	0	100
GRMUCS	Stations	0	0	0	0	1	0	0	1
	%	0	0	0	0	100	0	0	100
MUCS	Stations	0	0	0	0	0	2	0	2
	%	0	0	0	0	0	100	0	100
MUFS	Stations	0	0	0	0	0	0	3	3
	%	0	0	0	0	0	0	100	100
Total	Stations	16	11	13	2	1	2	3	48
	%	33.3	22.9	27.1	4.2	2.1	4.2	6.3	100

Table 4.10-1

Average abundance (individuals/m<sup>2</sup>) of selected taxa (occurring at five or more stations) by cluster subgrouping for the MD/DE study area.

	Cluster Analysis Subgroups										
	A	A'	A''	B	B'	C	D	D'	D''	E	E'
CNIDARIA											
Anthozoa	13	43	0	130	0	0	0	0	25	4	0
NEMERTINEA											
Nemertinea	286	254	75	155	242	8	43	31	30	129	5
ANNELIDA											
Oligochaeta	960	632	38	950	650	0	111	128	15	1054	395
<i>Spiophanes bombyx</i>	172	61	25	15	8	33	14	108	5	19918	650
<i>Aricidea (Acmira) cerrutii</i>	299	146	75	10	858	0	7	56	0	57	35
<i>Aricidea (Acmira) catherinae</i>	108	246	13	0	42	0	0	22	0	261	45
<i>Parapionosyllis longicirrata</i>	94	71	25	20	33	0	0	6	0	4	40
<i>Aphelochaeta</i> sp.	188	25	13	0	33	0	4	8	0	46	5
<i>Brania wellfleetensis</i>	260	71	125	0	8	0	0	3	0	0	5
<i>Hesionura elongata</i>	24	21	13	80	600	0	0	6	5	0	0
<i>Hemipodus roseus</i>	31	68	38	5	67	0	0	3	0	0	0
<i>Nephtys</i> spp.	6	11	50	0	0	0	4	50	0	75	10
<i>Asabellides oculata</i>	3	7	38	0	0	0	150	56	0	832	200
<i>Spio setosa</i>	8	79	13	0	0	0	0	0	0	2589	170
<i>Caulleriella</i> sp. B	24	4	0	0	8	0	4	94	0	64	60
<i>Streptosyllis pettiboneae</i>	43	21	50	5	75	0	0	8	0	0	0
<i>Glycera americana</i>	13	21	0	20	0	0	0	6	0	32	0
<i>Protodorvillea kefersteini</i>	29	282	13	30	0	0	0	0	0	0	0
<i>Parougia caeca</i>	14	82	0	0	8	0	0	0	0	0	0
<i>Mediomastus ambiseta</i>	0	4	0	5	0	0	14	0	0	1093	70
<i>Tharyx acutus</i>	25	57	0	0	0	0	0	0	0	121	35
<i>Ampharete finmarchica</i>	13	7	0	10	0	0	0	8	5	11	15
<i>Pisione remota</i>	14	125	0	85	75	0	0	0	0	0	0
<i>Paradoneis</i> sp. B	175	4	0	5	8	0	0	0	0	0	0
<i>Paradoneis</i> sp. A	24	25	0	20	0	0	0	6	0	0	0
<i>Lumbrinerides dayi</i>	14	0	0	0	17	0	0	3	0	4	0
<i>Polycirrus eximius</i>	0	11	0	15	0	0	0	0	0	0	330
<i>Sigalion arenicola</i>	4	0	0	0	0	0	0	3	10	4	0
<i>Glycera dibranchiata</i>	0	4	0	0	0	0	4	3	0	7	25
<i>Amastigos caperatus</i>	0	4	0	0	0	0	0	14	0	111	0
<i>Macroclymene zonalis</i>	0	0	0	5	0	0	7	0	0	993	0
<i>Sthenelais limicola</i>	3	0	0	0	0	0	18	0	0	11	0
<i>Lumbrineris fragilis</i>	0	4	0	0	0	0	0	17	0	0	10
<i>Monticellina baptistaeae</i>	39	0	0	0	217	0	0	0	0	0	5
<i>Travisia parva</i>	3	7	0	100	0	0	0	3	0	0	5
<i>Sabaco elongatus</i>	0	0	0	0	0	0	0	0	0	32	35
<i>Clymenella torquata</i>	0	4	0	0	0	0	4	0	0	364	0
<i>Ancistrosyllis hartmanae</i>	0	25	0	0	0	0	0	0	0	4	0
<i>Paraonis fulgens</i>	10	0	25	5	0	8	0	6	0	0	0
<i>Polydora cornuta</i>	0	0	0	0	0	0	0	3	0	282	0
<i>Apoprionospio pygmaea</i>	0	0	0	0	0	0	7	0	5	1696	0
<i>Notomastus</i> spp.	0	7	0	0	0	0	0	3	0	7	0
GASTROPODA											
<i>Natica pusilla</i>	10	14	0	30	8	0	0	0	90	11	0
<i>Nassarius trivittatus</i>	0	4	0	0	0	0	7	3	0	18	5
<i>Turbonilla interrupta</i>	0	0	0	0	0	0	4	0	0	46	35

Table 4.10-1. Continued.

	Cluster Analysis Subgroups										
	A	A'	A''	B	B'	C	D	D'	D''	E	E'
<b>BIVALVIA</b>											
<i>Tellina</i> spp.	43	14	38	20	25	42	896	97	120	1311	25
<i>Crenella glandula</i>	14	29	0	410	67	0	4	0	20	50	5
<i>Astarte</i> spp.	29	46	13	425	0	0	0	3	185	25	0
<i>Mytilus edulis</i>	6	50	0	250	8	0	4	111	5	57	15
<i>Spisula solidissima</i>	13	0	0	45	8	0	4	14	0	0	5
<i>Lyonsia hyalina</i>	19	4	0	5	0	0	0	3	0	29	0
<i>Nucula</i> spp.	3	0	0	0	0	0	1682	53	0	471	0
<i>Ensis directus</i>	0	0	38	0	0	0	0	3	0	296	5
<i>Pleuromeris tridentata</i>	1	0	0	215	25	0	0	6	0	4	0
<i>Pitar morrhuanus</i>	0	7	0	0	0	0	0	0	0	143	5
<i>Crassinella martinicensis</i>	1	0	0	25	0	0	0	3	0	0	5
<i>Bushia elegans</i>	1	7	0	45	0	0	0	0	0	0	0
<b>CRUSTACEA</b>											
<i>Unciola irrorata</i>	15	46	63	10	0	8	39	8	15	718	145
<i>Protohaustorius wigleyi</i>	21	7	0	5	33	0	11	175	85	7	15
<i>Tanaissus psammophilus</i>	115	7	100	15	0	8	7	0	0	0	10
<i>Chiridotea coeca</i>	7	4	0	35	17	208	4	3	70	0	0
<i>Byblis serrata</i>	57	4	2488	5	0	0	0	11	15	0	0
<i>Pseudunciola obliqua</i>	117	18	700	0	0	0	0	19	0	282	0
<i>Pseudoleptocuma minor</i>	14	0	0	5	17	0	0	14	0	18	10
<i>Oxyurostylis smithi</i>	4	4	0	0	8	8	0	19	0	18	5
<i>Politolana concharum</i>	3	0	0	35	8	25	32	6	5	0	5
<i>Rhepoxynius hudsoni</i>	15	4	13	0	0	0	0	28	0	4	0
<i>Ampelisca</i> spp.	0	0	0	0	0	0	0	3	5	346	10
<i>Americhelidium americanum</i>	11	4	0	0	0	0	0	3	5	0	0
<i>Edotea triloba</i>	1	18	0	0	0	8	150	0	0	104	10
<i>Parahaustorius holmesi</i>	0	0	0	20	17	0	7	3	10	0	0
<i>Parahaustorius longimerus</i>	17	0	0	0	0	158	0	0	0	0	0
<i>Bathyporeia parkeri</i>	13	0	0	0	0	17	0	3	0	4	5
<b>PHORONIDA</b>											
<i>Phoronis</i> sp.	0	0	0	0	0	0	7	22	0	157	15
<b>SIPUNCULA</b>											
Sipuncula	0	0	0	0	0	0	0	6	0	4	25
<b>ECHINODERMATA</b>											
<i>Leptosynapta tenuis</i>	4	11	0	70	0	0	0	0	5	0	0
<b>CEPHALOCHORDATA</b>											
<i>Branchiostoma caribaeum</i>	8	11	25	40	0	8	4	3	15	0	0

Table 5.3-1.

Scenarios depicting the effect of season and climatology on infaunal recolonization trajectory. Faunal characteristics favored by the combinations season and climate are listed in each cell of the table.

<b>Climate immediately after mining</b>	<b>Season When Sandmining is Conducted</b>	
	<b>Spring/Summer</b>	<b>Fall/Winter</b>
<b>Stormy/Energetic</b>	<ul style="list-style-type: none"> <li>• Transport of small to large individuals into and out of mined area</li> <li>• Dispersal of organic matter and fine sediments</li> <li>• Dispersal of individuals form mass recruitment events</li> <li>• Lower potential for shift in community structure</li> <li>• Recolonization rate intermeidate</li> <li>• Production lowered</li> </ul>	<ul style="list-style-type: none"> <li>• Transport of small to large individuals into and out of mined area</li> <li>• Dispersal of organic matter and fine sediments</li> <li>• Physical and physiological stress highest, sensitive life history stages eliminated</li> <li>• Recolonization slowed to lowest rate</li> <li>• High potential for delay of community structure recovery</li> <li>• Production at lowest point</li> </ul>
<b>Calm/Quiescent</b>	<ul style="list-style-type: none"> <li>• Deposition of water column primary production</li> <li>• Fine sediments accumulate in mined area</li> <li>• Recruitment of warm water larval forms favored</li> <li>• Surface and subsurface deposit feeders favored</li> <li>• Species that queue on fine sediments favored</li> <li>• Recolonization proceeds at highest rate</li> <li>• Highest potential for shift in community structure</li> <li>• Extended quiescence may lead to hypoxia, regionally or within mined pit</li> <li>• Highest production</li> </ul>	<ul style="list-style-type: none"> <li>• Fines accumulate in mined area</li> <li>• Recruitment of cold water larval forms favored</li> <li>• Recolonization rate intermeidate</li> <li>• High potential for shift in community structure</li> <li>• Pulse of high production</li> </ul>

---

# Environmental Survey of Potential Sand Resource Sites Offshore Delaware and Maryland

## Part 2: Transitory Species (Vertebrate Nekton)

---

Final Report

OCS Study 2000-055

January 1999

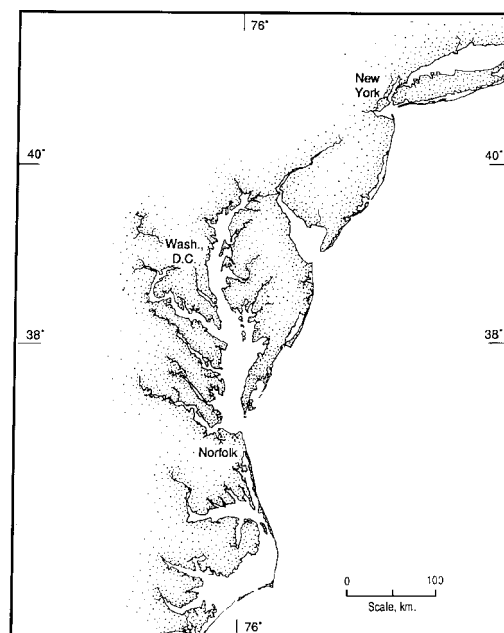
Author:

John A. Musick  
Virginia Institute of Marine Science

Project Manager:

Carl H. Hobbs, III  
Virginia Institute of Marine Science

Prepared under MMS contract 1435-01-97-CT-30853 to  
the  
Virginia Institute of Marine Science  
College of William & Mary



**MMS** U.S. Department of the Interior  
Minerals Management Service

International Activities and Marine Minerals Division

College of William and Mary  
**VIAS**  
Virginia Institute of Marine Science  
School of Marine Science

## DISCLAIMER

This report has been reviewed by the Minerals Management Service and approved for publication. Approval does not signify that the contents necessarily reflect the views and policies of the Service, nor does mention of trade names or commercial products constitute endorsement or recommendation for use.

Final Report  
Environmental Survey of Potential Sand Resource Sites  
Offshore Delaware and Maryland  
Part 2  
Transitory Species (Vertebrate Nekton)

John A. Musick, Principal Investigator  
Virginia Institute of Marine Science

Carl H. Hobbs, III, Project Manger  
Virginia Institute of Marine Science

for

U. S. Department of the Interior  
Minerals Management Service  
International Activities and Marine Minerals Division  
Contract 1435-01-97-CT-30853  
OCS Study 2000-055

December 1998

## INTRODUCTION AND DISCUSSION

### Transitory Species (Vertebrate Nekton)

Three major groups of transitory vertebrate nekton species are to be expected in the proposed mining area: fishes, sea turtles, and marine mammals. The coastal area off Delaware has one of the most extreme seasonal ranges of sea temperature in the world. Consequently, most of the fishes and all of the sea turtles and marine mammals migrate seasonally, with boreal species present in winter and warm-temperate/sub-tropical species present in summer (Musick *et al.*, 1986).

### Fishes

The coastal region wherein the mining site resides provides habitat for a wide variety of demersal and pelagic fishes with highest diversity in September and lowest diversity in late winter (February/March) (Colvocoresses and Musick, 1984; Phoel, 1985; Musick *et al.*, 1986). Only a small percentage of species are resident year-round. Rather most establish seasonal residency. Thus, the area is an important foraging and spawning ground for a wide variety of fishes. In winter, the fauna is dominated by broad species such as sea herring (*Clupea harengus*), Atlantic mackerel (*Scomber scombrus*), hakes (*Urophycis*, *Merluccius*), monkfish (*Lophius americanus*), and spiny dogfish (*Squalus acanthias*), (Musick, 1974; Armstrong *et al.*, 1992; Phoel, 1985; Nammack *et al.*, 1985). In summer the fauna is dominated by warm temperate and sub-tropical species such as summer flounder (*Paralichthys dentatus*), croakers, drums, and sea trouts (Sciaenids), menhaden (*Brevoortia tyrannus*), and large coastal sharks (*Carcharhinidae*) (Desfosse *et al.*, 1990; Musick *et al.*, 1993). In spring and fall the area is an important migration corridor for striped bass (*Morone saxatilis*) and bluefish (*Pomatomus saltatrix*). Many of the dominant species noted above are extremely valuable and important to recreational or commercial fisheries or both.

Much of the information needed to provide a detailed assessment of the fish communities at the proposed mining site can be gleaned from the existing literature and data

base at the Virginia Institute of Marine Science and at the National Marine Fisheries Service laboratory in Woods Hole, Massachusetts.

## **Sea Turtles**

Sea turtles are sub-tropical animals that occur in the mid-Atlantic Bight seasonally (Musick and Limpus, 1996). The loggerhead sea turtle (*Caretta caretta*) is by far the most abundant species nesting regularly as far north as southern Virginia and occasionally on Assateague Island (Lutcavage and Musick, 1985; Musick, 1988). Loggerheads spend the winter south of Cape Hatteras and migrate north in spring entering Virginia waters as early as mid-April in some years but usually in mid-May. As many as 10,000 mostly juvenile loggerheads enter Chesapeake Bay in the summer and the coastal waters from about Cape May, New Jersey south represent an important seasonal developmental area for the species (Keinath *et al.*, 1988). The species occurs regularly each summer as far north as Cape Cod (Keinath and Musick, 1981a and Shoop and Kenny, 1992).

The second most abundant sea turtle in the mid-Atlantic Bight in summer is the Kemp's ridley (*Lepidochys kempi*), the most endangered sea turtle on earth (Keinath and Musick, 1991b). Kemp's ridley is represented mostly by juvenile individuals in the mid-Atlantic and occurs regularly as far north as southern New England (Musick, 1988). This species forages for decapod crustaceans usually over shallow estuarine flats in summer and reaches its maximum abundance along the coast in autumn when it leaves the estuaries and migrates south to overwinter south of Cape Hatteras (Musick and Limpus, 1996). Although seasonal distribution and abundance for the species are well known for Chesapeake Bay, southern Virginia, and North Carolina, little specific information is available for the area between Cape Charles, Virginia and Long Island, New York but it probably reaches peak abundance during the autumn migration in September and October.

The leatherback sea turtle (*Dermochelys coriacea*) is the third most abundant sea turtle in the mid-Atlantic Bight (Keinath and Musick, 1991c). This species exhibits gigantothermy (it is warm-blooded) and migrates into the Bight earlier than the other species, usually in April (Barnard *et al.*, 1989; Musick, unpublished data). It appears that most of the population migrates north into the Gulf of Maine for the summer (Shoop and Kenny, 1992), but some individuals remain as far south as Virginia (Musick, 1988). The green sea turtle (*Chelonia mydas*) occurs occasionally in summer in estuarine waters of the mid-Atlantic Bight (Keinath and Musick, 1991d), but occurs too infrequently there to be of any consideration for this project. The hawksbill (*Eretmochelys imbricata*) occurs even less frequently (Keinath and Musick, 1991e). All of the sea turtles are classified as threatened or endangered under the U.S. Endangered Species Act, and they are completely protected by the U. S. Fish and Wildlife Service, and National Marine Fisheries Service ( Federal Register, 1978; Terwilliger and Musick, 1995; Anonymous, 1998).

Of the species which occur regularly in the mid-Atlantic Bight, the loggerhead and Kemp's ridley are highly vulnerable to entrainment and mortality by hopper dredging (Moein *et al.*, 1994). Thus, dredging operations (under the control of the U.S. Army Corps of Engineers) have come under close scrutiny and stringent regulation by the NMFS. Incidental take limits of sea turtles during dredging operations are defined by the NMFS through consultations authorized under Section 7 of the Endangered Species Act. The most recent consultation in the mid-Atlantic was for emergency work done to stabilize the beaches on Assateague Island in April, 1998. For the project NMFS allowed a take of one Kemp's ridley, one green turtle, and two loggerheads (Conant, personal communication).

### **Marine Mammals**

Marine mammals are highly migratory and seasonal in the mid-Atlantic Bight (Shoop and Kenny, 1992; Terwilliger and Musick, 1995). The marine mammal fauna off Delmarva is dominated by the boreal harbor porpoise (*Phocoena phocoena*) in winter and by the bottlenose dolphin (*Tursiops truncatus*) in summer (Kenney, 1990; Keinath *et al.*, 1994;

Wang *et al.*, 1994. Several other cetacean species are transient seasonally through the area. Of note are juvenile humpback whales (*Megaptera novaeangliae*) that have recently begun to overwinter between Cape Hatteras, North Carolina and Virginia (Swingle *et al.*, 1993; Wiley *et al.*, 1993) and right whales (*Eubalaena glacialis*) which briefly pass through the area in fall (peak in December) on the way to their calving grounds off southern Georgia and northern Florida. The right whales must return north with their calves in the spring (peak in April) on the way to their summer foraging area off northern New England and Nova Scotia (Winn *et al.*, 1986). There have been no recent sightings of right whales in Delaware Bay where the species was historically hunted. The endangered right whale is vulnerable to collision with moving ships, but their tenure in the dredging area is brief.

## RECOMMENDATIONS

**Fishes:** Future sand mining (dredging) may result in local displacement of mobile fish assemblages and limited mortality of some of the benthic species during the dredging operation. However the limited geographic size of likely dredging areas relative to the very large geographic ranges and estimated population sizes of the fishes involved would suggest that sand mining would have very little effect on fish populations.

**Sea Turtles:** Endangered and threatened sea turtles are particularly vulnerable to entrapment by dredges. However, sea turtles are tropical to subtropical animals and may be avoided by restricting dredging operations to the colder portion of the year, November 15 - April 15.

**Marine Mammals:** All marine mammals in the study area are migratory and highly mobile and easily can avoid dredges. Sand mining poses no foreseeable threat to the marine mammal population.

## Literature Cited

- Anonymous, 1988. Endangered Species Act of 1973, as amended through the 100th Congress. U. S. Fish and Wildlife Service, U. S. Department of Interior, Washington, D. C.: 45 pp.
- Armstrong, M. P., J.A. Musick and J. A. Colvocoresses. 1996. Food and ontogenetic shifts in feeding of the goosefish, *Lophius americanus*. *J. Northw. Atl. Fish. Sci.*, (18):99-103.
- Colvocoresses, J. A. and J. A. Musick. 1984. Species association and community structure of middle Atlantic Bight continental shelf demersal fishes. *Fish. Bull.*, 82 (2):295-313.
- Conant, T. 1998, personal communication. NMFS, Office of Protected Resources, Silver Spring, MD
- Desfosse, J. C., J. A. Musick, A. D. Estes, and P. Lyons. 1990. Stock identification of summer flounder (*Paralichthys dentatus*) in the southern mid-Atlantic Bight. Final Report to Virginia Marine Resources Commission, WB-86-01-02.
- Federal Register, July 28, 1978. Listing and Protecting Loggerhead Sea Turtles as "Threatened Species" and Populations of Green and Olive Ridley Sea Turtles as "Threatened Species" or "Endangered Species." *Federal Register* 43:144:32800-32811.
- Keinath, J. A. and J. A. Musick. 1991a. Atlantic loggerhead turtle. pp. 445-448. *In*: K. Terwilliger (coordinator), Endangered and Threatened Species in Virginia. McDonald Woodward Pub. Co., Blacksburg, VA.
- Keinath, J. A. and J. A. Musick. 1991b. Kemp's ridley turtle. p. 451-453. *In*: K. Terwilliger (coordinator), Endangered and Threatened Species in Virginia. McDonald Woodward Pub. Co., Blacksburg, VA.
- Keinath, J. A. and J. A. Musick. 1991c. Atlantic hawksbill turtle. p. 450-451. *In*: K. Terwilliger (coordinator), Endangered and Threatened Species in Virginia. McDonald Woodward Pub. Co., Blacksburg, VA.
- Keinath, J. A. and J. A. Musick. 1991d. Atlantic green turtle. pp. 448-450. *In*: K. Terwilliger (coordinator), Endangered and Threatened Species in Virginia. McDonald Woodward Pub. Co., Blacksburg, VA.
- Keinath, J. A. and J. A. Musick. 1991f. Atlantic leatherback turtle. pp. 453-455. *In*: K. Terwilliger (coordinator), Endangered and Threatened Species in Virginia. McDonald Woodward Pub. Co., Blacksburg, VA.
- Keinath, J. A., J. A. Musick, and D. E. Barnard. 1995. Abundance and distribution of sea turtles off North Carolina. U.S. Dept. of Interior, Minerals Management Service, Gulf of Mexico OCS Region. Contract Report 19-35-0001-30590: 158pp.
- Keinath, J. A., J. A. Musick and R. A. Byles. 1988. Aspects of the biology of Virginia's sea turtles: 1979-1986. *VA J. Sci.*, 38:329-336.
- Lutcavage, M. and J. A. Musick. 1985. Aspects of the biology of sea turtles in Chesapeake Bay and nearby coastal waters. *Copeia*, 2:449-456.
- Moein, S. E., J. A. Musick, J. A. Keinath, D. E. Barnard, and M. Lenhardt. 1994. Evaluation of seismic sources for repelling sea turtles from hopper dredges. Final Report submitted to the U. S. Army Corps of Engineers Waterways Experiment Station,

- Vicksburg, MS: 33 pp.
- Musick, J. A. 1974. Seasonal distribution of the sibling hakes, *Urophycis chuss* and *U. tenuis* (Pisces, Gadidae) in New England. *Nat. Mar. Fish. Ser. Fish. Bull.*, 72:481-495.
- Musick, J. A. 1988. The Sea Turtles of Virginia with Notes on Identification and Natural History. VA Inst. Mar. Sci., Educational Series 24, 22 pp, Gloucester Pt., VA.
- Musick, J. A., J. A. Colvocoresses, E. J. Foell. 1986. Seasonality and distribution, availability and composition of fish assemblages in Chesapeake Bight. Chapter 21, *In*: A. Yanez y. Arancibia (ed.), *Fish Community Ecology in Estuaries and Coastal Lagoons: Towards an Ecosystem Integration*. Univ. Mexico Press., Mexico City.
- Musick, J. A. and C. J. Limpus. 1996. Habitat utilization and migration in juvenile sea turtles. Chapter 6, pp. 139-165. *In*: *Biology of Sea Turtles*. P. Lutz and J. A. Musick (eds.), CRC Press: 412 pp.
- Nammack, M. F., J. A. Musick, and J. A. Colvocoresses. 1985. Life history of spiny dogfish off the northeastern United States. *Trans. Amer. Fish. Soc.*, 114:367-376.
- Phoel, W. C. 1985. Community structure of demersal fishes on the inshore U.S. Atlantic continental shelf: Cape Anna, Massachusetts to Cape Fear, North Carolina. Ph.D. dissertation presented to the School of Marine Science, Virginia Institute of Marine Science, College of William & Mary, 95 pp.
- Shoop, C. R. and R. D. Kenny. 1992. Seasonal distribution and abundance of loggerhead and leatherback sea turtles in waters of the northeastern United States. *Herp. Monographs*, 6: 43-67 pp.



#### The Department of the Interior

As the Nation's principal conservation agency, the Department of the Interior has responsibility for most of our nationally owned public lands and natural resources. This includes fostering sound use of our land and water resources, protecting our fish, wildlife, and biological diversity, preserving the environmental and cultural values of our national parks and historic places; and providing for the enjoyment of life through outdoor recreation. The Department assesses our energy and mineral resources and works to ensure that their development is in the best interests of all our people by encouraging stewardship and citizen participation in their care. The Department also has a major responsibility for American Indian reservation communities and for people who live in island territories under U.S. Administration.



#### The Minerals Management Service Mission

As a bureau of the Department of the Interior, the Minerals Management Service's (MMS) primary responsibilities are to manage the mineral resources located on the Nation's Outer Continental Shelf (OCS), collect revenue from the Federal OCS and onshore federal and Indian lands, and distribute those revenues.

Moreover, in working to meet its responsibilities, the Offshore Minerals Management Program administers the OCS competitive leasing program and oversees the safe and environmentally sound exploration and production of our Nation's offshore natural gas, oil and other mineral resources. The MMS Royalty Management Program meets its responsibilities by entrusting the efficient, timely and accurate collection and distribution of revenue from mineral leasing and production due to Indian tribes and allottees, States and the U. S. Treasury

The MMS strives to fulfill its responsibilities through the general guiding principles of: (1) being responsive to the public's concerns and interests by maintaining a dialog with all potentially affected parties and (2) carrying out its programs with an emphasis on working to enhance the quality of life for all Americans by lending MMS assistance and expertise to economic development and environmental protection.

---

# Environmental Survey of Potential Sand Resource Sites Offshore Delaware and Maryland

## Part 3: Literature Survey of Reproductive Finfish and Ichthyoplankton Present in Proposed Sand Mining Locations

---

Final Report

OCS Study 2000-055

November 1998

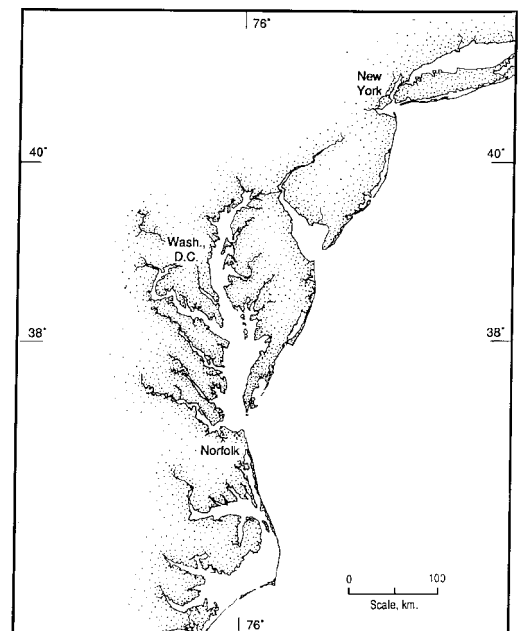
Authors:

John Olney, Sr. and Donna Marie Bilkovic  
Virginia Institute of Marine Science

Project Manager:

Carl H. Hobbs, III  
Virginia Institute of Marine Science

Prepared under MMS contract 1435-01-97-CT-30853 to  
the  
Virginia Institute of Marine Science  
College of William & Mary



**MMS** U.S. Department of the Interior  
Minerals Management Service

College of William and Mary  
**VIMS**  
Virginia Institute of Marine Science  
School of Marine Science

International Activities and Marine Minerals Division

## DISCLAIMER

This report has been reviewed by the Minerals Management Service and approved for publication. Approval does not signify that the contents necessarily reflect the views and policies of the Service, nor does mention of trade names or commercial products constitute endorsement or recommendation for use.

Final Report  
Environmental Survey of Potential Sand Resource Sites  
Offshore Delaware and Maryland  
Part 3

Literature Survey of Reproductive Finfish and Ichthyoplankton Present in  
Proposed Sand Mining Locations within the Middle Atlantic Bight

John Olney, Sr., Principal Investigator and  
Donna Marie Bilkovic  
Virginia Institute of Marine Science

Carl H. Hobbs, III, Project Manager  
Virginia Institute of Marine Science

for

U. S. Department of the Interior  
Mineral Management Service  
International Activities and Marine Minerals Division  
Contract 1435-01-97-CT-30853  
OCS Study 2000-055

November 1998

## Introduction

Ichthyofauna of the Middle Atlantic Bight (the region between Cape Cod and Cape Hatteras) is dynamic and highly variable due to seasonal and climatic changes, varying life history strategies, hydrographic phenomena, fishing pressure, and natural cycles of abundance. While there are distinct faunal assemblages in the boreal waters north of Cape Cod and in the warm waters south of Cape Hatteras, there are few endemic fish species in the variable Middle Atlantic Bight (MAB) waters. However, the fauna is diverse since numerous species, including commercially and recreationally important species, migrate seasonally through this region to spawn. This fauna is composed of both northern and southern fish populations that undergo extensive migrations as they follow temperature isotherms. Thus the MAB is a valuable migratory path as well as spawning area for numerous species.

Grosslein and Azarovitz (1982) noted that all year "significant quantities of fish larvae" can be found throughout the MAB. This may be due to the large number of spawning species, extensive dispersal of eggs and larvae, and spawning periods of long duration, as well as to the continuous influx/outflux of northern and southern species. Warm water species such as, bluefish (*Pomatomus saltatrix*), and weakfish (*Cynoscion regalis*) enter the region as temperatures rise in the spring and summer while cold water species such as, Atlantic cod (*Gadus morhua*), Atlantic herring (*Clupea harengus harengus*), and American shad (*Alosa sapidissima*) migrate north. Similarly, as fall approaches, warm water species such as summer flounder (*Paralichthys dentatus*), butterfish (*Peprilus triacanthus*), and black sea bass (*Centropristis striata*) may migrate offshore toward deeper waters and then move southward, while cold water species move south into the MAB (Grosslein and Azarovitz, 1982). It is also possible for a pelagic species such as *Scomber scombrus* to have both a southern and a northern contingent which spawn within the Bight during different periods, or in the case of *Brevoortia tyrannus*, spawning episodes during migrations into and out of the Bight.

In the following report, available data on reproductive finfish species located within the

MAB are summarized with emphasis placed on economically important species previously observed within or near proposed mining sites. As coastal finfish often have ichthyofauna that utilize estuarine environments, estuarine residents may have ichthyofauna transported by estuarine plumes into coastal assemblages. Thus, the report includes some estuarine resident species, that may have ichthyoplankton interspersed with coastal fauna near the mining sites.

### **Distribution Data**

Information was compiled on 36 fish species that utilize the potential mining locations or immediate surrounding areas for spawning or nursery grounds (Tables 1 and 2). Table 1 depicts reported periods of spawning and egg and larval presence of fish species that utilize portions of the MAB within the vicinity of the proposed mining areas. Species are categorized by spawning mode, either pelagic or benthic, and by general spawning location, including offshore (areas greater than 27 m in depth), inshore (areas less than 27 m in depth), tributaries, estuaries, and bays. Table 2 summarizes the data by spawning season. Relative abundance within the MAB also is depicted based on literature cited; “frequent” implies regular spawning judged by the presence of eggs and larvae in the study area, and “infrequent” implies infrequent use based on lack of observations of eggs/larvae or spawning adults in the region. Important data sources include trawl and plankton surveys from the National Marine Fisheries Service summarized by Grosslein and Azarovitz (1982), ichthyoplankton surveys in nearshore and bay regions summarized by Wang and Kernehan (1979), ichthyoplankton surveys made in the 1950s and 1960s from the National Marine Fisheries Service summarized by Colton *et al.*, (1979), neuston and bongo sampling of both inshore and offshore stations off the coast of Virginia and New Jersey (Comyns and Grant, 1993); as well as additional studies cited within the tables. Often spawning periods and locations were determined based on the presence of eggs and/or prolarval stages. Commercial and recreational landings data were obtained from The National Marine Fisheries Service (NMFS) and are reported for the Mid-Atlantic region which consists of the following states: Delaware, Maryland, New York, New Jersey, and Virginia.

## Results

In general, fish that spawn in the MAB broadcast pelagic eggs (31 species in this study). Thus, eggs and larvae have the potential to be dispersed throughout the region and into habitats different than the spawning grounds. Often, offshore spawners have larvae that are transported with currents to inshore or estuarine nursery grounds. Five benthic spawners were included in this study: *Clupea harengus harengus*, *Fundulus heteroclitus*, *Ammodytes* spp., *Menidia menidia*, and *Pseudopleuronectes americanus*. Although these species have benthic eggs, often larvae exhibit a dispersive pelagic stage.

Spawning and egg/larval populations vary seasonally within the Bight (Table 2). The majority of the species present have a spawning period that includes spring and/or summer (29 species). Approximately ten species have a spawning period in the study area during the winter: *Urophysis regia*, *Leiostomus xanthurus*, *Micropogon undulatus*, *Paralichthys dentatus*, *Physis chesteri*, *P. americanus*, *Urophysis floridiana*, *Urophysis cirrata*, *Gadus morhua* and *Ammodytes* spp. Of these species only *U. floridiana* and *cirrata* spawn primarily in the winter. The other eight species have overlap with other seasons. Some species are present and may spawn throughout at least three seasons, including *Physis chesteri*, and *Pseudopleuronectes americanus*.

## Commercial and Recreational Species within the Mid-Atlantic Bight

Commercially and recreationally important species that utilize the MAB and the proposed mining areas during spawning or in early life stages include, but are not limited to bluefish, summer flounder, Atlantic mackerel, Atlantic Butterfish, scup, and black sea bass. These species are all managed under Fishery Management Plans (FMPs).

### Bluefish (*Pomatomus saltatrix*)

Within the bight, bluefish is one of the most important recreational species. Its commercial value has increased since the 1960s and 1970s. Among sport fish, bluefish ranked first in the MAB from 1979-1989 with catches occurring inshore and offshore (Pottern, 1989). Recreational landings historically exceed commercial landings in the mid-Atlantic region (Figure

1). However, combined landings, which peaked in 1980, have declined steadily since that time, and the stock has been considered overharvested (O'Reilly and Austin, 1996).

Along the eastern U.S. coast, bluefish have two major spawning aggregations: a southern Atlantic stock which spawns in the spring and a mid-Atlantic stock which spawns in the summer. Both of these stocks utilize the MAB at differing life stages and times. The summer spawning contingent arrives and most spawn offshore between Cape Cod and Cape Hatteras from June through August. Subsequently, eggs and larvae remain offshore, and, typically, juveniles remain offshore as well until the onset of cooling water induces southern migrations. Some juveniles from the summer spawn will migrate into coastal and bay regions for the early portion of fall. Additionally, there is the potential for inshore and lower estuary spawning to occur, as ripe females, eggs, and larvae were observed in lower Chesapeake Bay, off Indian River Inlet and Ocean City, Maryland, respectively (Wang and Kernehan, 1979). The spring spawning contingent spawns south of Cape Hatteras and juveniles eventually will migrate into mid-Atlantic bays and estuaries which are used as nursery areas until fall (June through September) (Pottern *et al.*, 1989; Grosslein and Azarovitz, 1982; Wang and Kernehan, 1979).

Essential Fish Habitat (EFH) as described in the draft fishery Management Plan (FMP) for egg and larval bluefish includes pelagic waters found over the Continental Shelf (from the coast out to the limits of the EEZ), from Montauk Point, New York to Cape Hatteras, North Carolina that encompass the highest 90% of the area where eggs or larvae were collected in the National Marine Fisheries Service (NMFS) Marine Resources Monitoring, Assessment, and Prediction (MARMAP) ichthyoplankton survey (MAFMC, July 1998). Eggs typically are found at mid-shelf depths, whereas larvae most commonly are observed above 49 ft (15 m). EFH of juveniles includes pelagic waters found over the Continental Shelf (from the coast out to the limits of the EEZ), from Nantucket Island, Massachusetts to Cape Hatteras, North Carolina that encompass the highest 90% of the area where juveniles were collected in MARMAP ichthyoplankton survey. Additionally, juvenile bluefish are in "Mid-Atlantic estuaries

from May through October within the ‘mixing’ and ‘seawater zones’ (MAFMC, July 1998). Adult EFH is over the Continental shelf (from the coast out to the limits of EEZ) in waters greater than 66 ft (20 m), from Cape Cod Bay, Massachusetts south to Cape Hatteras, in the highest 90% of the area where adult bluefish were collected in the NEFSC trawl survey. From April through October, adult bluefish are located within Mid-Atlantic estuaries (MAFMC, July 1998). Eggs, larvae, juveniles, and adults have EFH that may overlap the borrow sites. Designated estuaries that are EFH for juveniles and adults include Delaware Bay, Delaware Inland Bay, and Chincoteague Bay based on NOAA’s Estuarine Living Marine Resources (ELMR) data.

### **Summer flounder (*Paralichthys dentatus*)**

Summer flounder are important both commercially and recreationally in the MAB. There is a significant offshore commercial fishery that occurs during the spring inshore migration and fall offshore migration and continues during the winter. During the summer, commercial and recreational fisheries are concentrated in coastal and estuarine waters. Recreational landings typically exceed the commercial landings in the mid-Atlantic region. Steep declines in both recreational and commercial landings in 1989 were followed by slight increases in recreational landings, while commercial landings remained constant (Figure 2). O'Reilly and Austin (1996) attributed the declines to overfishing and year-class failure. Currently, summer flounder are managed under Amendment 10 of the Summer Flounder, Scup, and Black Sea Bass Fishery Management Plan, and the stocks are considered over exploited (NEFSC, 1997).

In the MAB, summer flounder spawning occurs during the fall and winter months (September through February) offshore and the larvae and young become demersal and migrate inshore to estuaries. In the winter and spring, adult summer flounder move into inshore and estuary waters (Pottern *et al.*, 1989; Grosslein and Azarovitz, 1982; Wang and Kernehan, 1979).

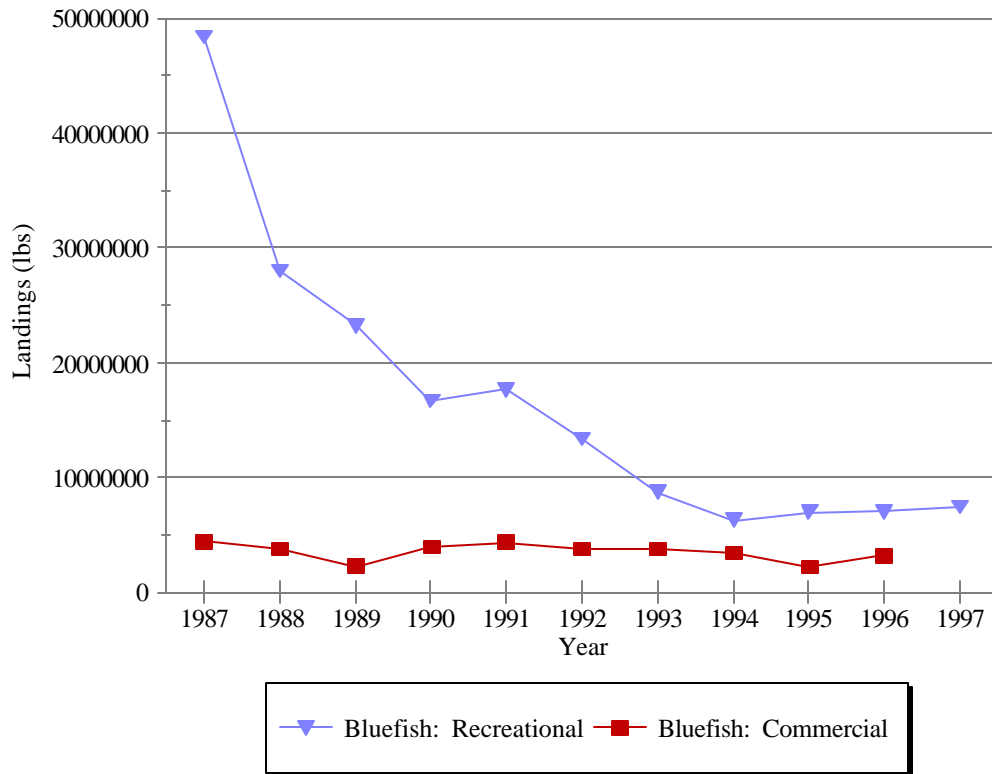


Figure 1: Commercial and recreational landings of bluefish in the Mid-Atlantic Bight

Essential Fish Habitat (EFH) as described in the draft Fishery Management Plan (FMP) for summer flounder includes pelagic waters found over the Continental Shelf (from the coast out to the limits of the EEZ), from the Gulf of Maine to Cape Hatteras, North Carolina that encompass the highest 90% of the area where summer flounder (eggs and larvae) were collected in the (MARMAP) ichthyoplankton survey (MAFMC, August 1998). For juveniles and adults, the EFH is the demersal waters (near bottom-waters utilized by demersal fish) over the Continental Shelf (from the coast out to the limits of the EEZ), from the Gulf of Maine to Cape Hatteras, North Carolina that encompass the highest 90% of the area where summer flounder were collected in the MARMAP ichthyoplankton survey. Using this definition and the MARMAP surveys, the borrow sites are within the designated EFH for this species for all life stages. Additionally, estuaries designated as EFH for summer flounder include Delaware Inland Bays, Delaware Bay, and Chincoteague Bay based on ELMR data.

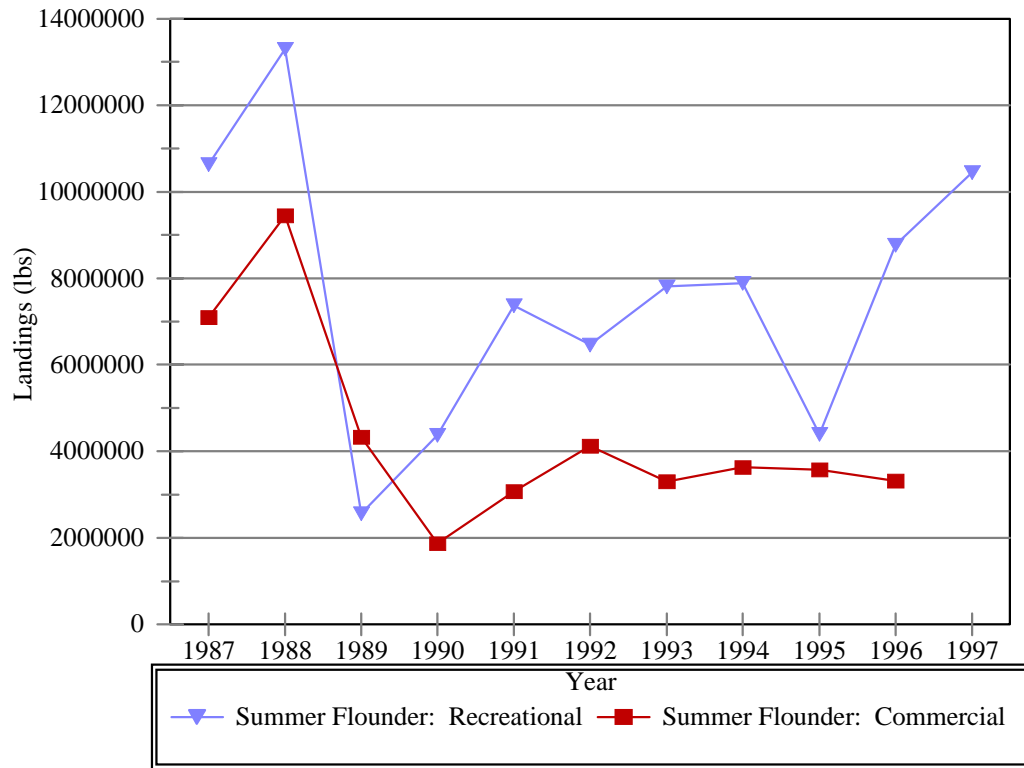


Figure 2: Commercial and recreational landings of summer flounder in the Mid-Atlantic Bight

### **Atlantic Mackerel (*Scomber scombrus*)**

The Atlantic mackerel fishery has strong recreational and commercial components. Historically, the recreational component has exceeded commercial catch and foreign commercial catches had dominated landings. Controls on foreign catch in the 1970s reduced that proportion of the landings. Since 1987, recreational landings have remained lower than commercial landings in the mid-Atlantic region (Figure 3). Landings closely follow abundance fluctuations; peaks in abundance in the late 1960s led to peaks in landings as well. Fluctuations in year-class are postulated to be related to larval survival which may be influenced by several factors including water temperature, zooplankton abundance, and currents (Grosslein and Azarovitz, 1982).

Southern populations of Atlantic mackerel from between Long Island and Chesapeake Bay migrate inshore and/or north beginning in March and April and spawn progressively in a northward direction during the spring and summer. In the mid-

Atlantic, spawning occurs from mid-April to June and the adult population begins to migrate and temporarily intermingles with the northern population which subsequently migrates north to spawn in June and July. During the fall, the southern population migrates south once again (Grosslein and Azarovitz, 1982). EFH as described in the FMP for Atlantic mackerel includes pelagic waters found over the Continental Shelf (from the coast out to the limits of the EEZ), from Maine to Cape Hatteras, North Carolina that encompass the highest 75% of the area where Atlantic mackerel eggs, larvae or juveniles were collected in the MARMAP ichthyoplankton survey (MAFMC, August 1998). Using this definition, the borrow sites would not be considered EFH for eggs or larvae of this species. However, juvenile and adult mackerel designated EFH overlap with the borrow sites. Estuaries that are designated EFH for mackerel include Delaware Bay and Delaware Inland Bays based on ELMR data.

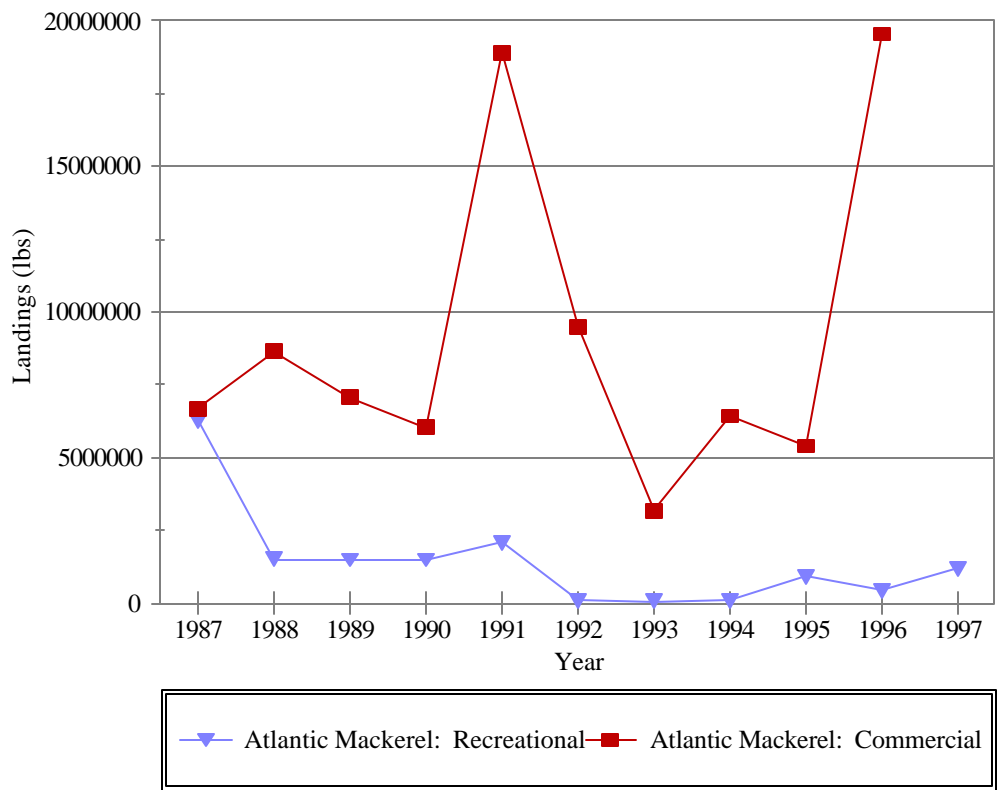


Figure 3: Commercial and recreational landings of Atlantic Mackerel in the Mid-Atlantic Bight.

### **Butterfish (*Peprilus triacanthus*)**

The only fishery for butterfish in the mid-Atlantic Bight is the domestic commercial fishery, since the foreign fishery was phased out in 1986 and there is no reported recreational fishery (NEFSC, 1997). Commercial landings in the Bight have fluctuated between one and two million pounds since 1987 (Figure 4).

The butterfish currently is managed under Amendment 8 of the Atlantic Mackerel, Squid and Butterfish Fishery Management Plan and is defined as an under-exploited fishery.

Adult butterfish migrate inshore following seasonal changes in temperature during the spring and summer and remain inshore until colder temperatures occur in October and November (Wang and Kernehan, 1979). Wang and Kernehan (1979) also reported spawning to occur typically inshore from June to August. Larvae and young may remain a few miles offshore or move further inshore. Grosslein and Azarovitz (1982) reported spawning from April through December inshore and in estuaries. Essential Fish Habitat (EFH) as described in the draft Fishery Management Plan (FMP) for Butterfish includes pelagic waters found over the Continental Shelf (from the coast out to the limits of the EEZ), from the Gulf of Maine through Cape Hatteras, North Carolina that encompass the highest 75% of the area where butterfish eggs, larvae or juveniles were collected in the MARMAP ichthyoplankton survey. EFH is also the 'mixing' and/or 'seawater' portions of all estuaries where butterfish are 'common,' abundant,' or 'highly abundant' on the Atlantic coast, from Passamaquaddy Bay, Maine to James River, Virginia" (MAFMC, August 1998). Based on MARMAP surveys, larvae, juveniles, and adults are found within the Delaware Bay and Chincoteague Bay, and juveniles and adults also appear to be found in the Delaware Inland Bays. Likewise, eggs, larvae, juveniles, and adults are noted to have 75% of their catch within the Maryland-Delaware study area indicating an overlap with designated EFH for this species.

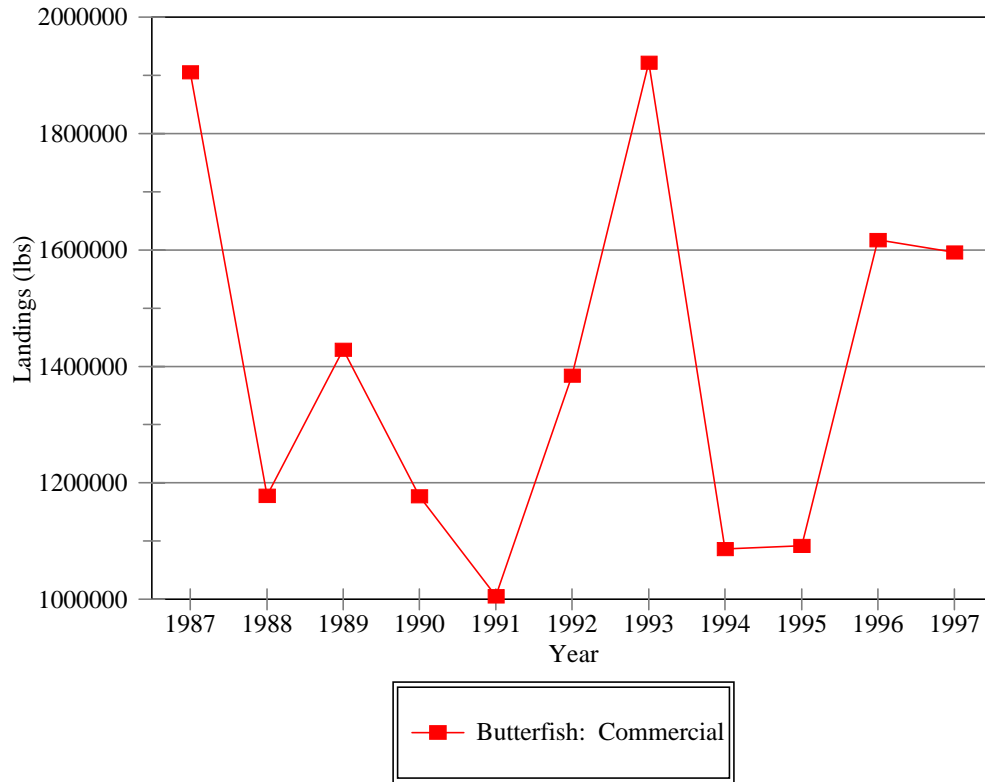


Figure 4: Commercial landings of butterfish in the Mid-Atlantic Bight

### Scup (*Stenotomus chrysops*)

Commercial landings historically have exceeded or outweighed recreationally landings in the mid-Atlantic region. Since 1986 there have been declines in both commercial and recreational landings with marked declines in 1995 through 1997 (Figure 5). The fishery currently is managed under Amendment 8 of the Summer Flounder, Scup, and Black Sea Bass Fishery Management Plan, and the Middle Atlantic bight stock is considered overexploited (NEFSC, 1997).

In the winter, this species is located primarily offshore in deep waters from Hudson Canyon to Cape Hatteras. Migrations occur during the spring inshore and during the autumn offshore. Spawning occurs in the summer (May through August) rarely south of New Jersey. Scup eggs and larvae or spawning adults have rarely been observed south of New Jersey (Eklund and Targett, 1990; Grosslein and Azarovitz, 1982). Juveniles, which are bottom dwelling, have been reported offshore, inshore, and in bays and estuaries from May through November from New England to Chesapeake Bay

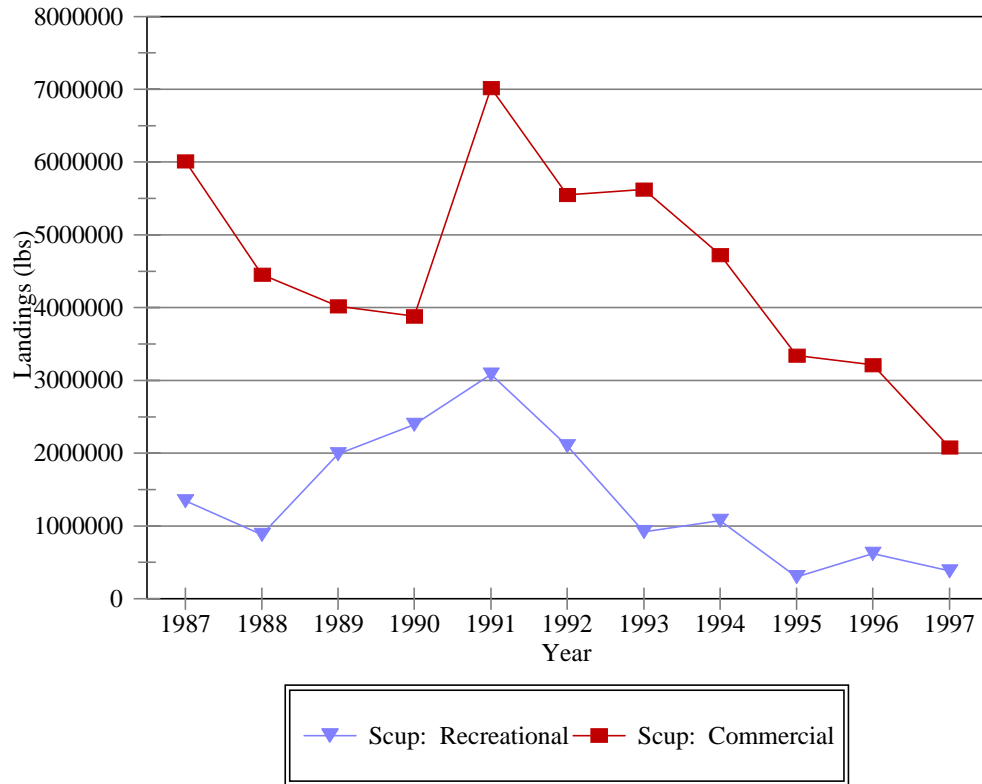


Figure 5: Commercial and recreational landings of scup in the Mid-Atlantic Bight

(Grosslein and Azarovitz, 1982). Estuaries designated as EFH for scup are areas where scup eggs and larvae were identified as common, abundant, or highly abundant in the ELMR data base for the ‘mixing’ and ‘seawater’ salinity zones. EFH for juveniles and adults is the demersal waters over the Continental Shelf (from the coast out to the limits of the EEZ), from the Gulf of Maine to Cape Hatteras, North Carolina that encompass the highest 90% of the area where scup were collected in the MARMAP ichthyoplankton survey (MAFMC, August 1998). Using this definition and MARMAP surveys, EFH for juvenile and adults overlaps borrow sites during the Spring and Fall. Juveniles and adults also commonly appear to be found in Delaware Bay, and Delaware Inland Bays, and, rarely, in the Chincoteague Bay according to ELMR data.

### **Black Sea Bass (*Centropristis striata*)**

Within the middle Atlantic states, recreational landings are comparable to or greater than those from the commercial fishery. Within the past 10 years commercial landings have remained level, while there has been some fluctuation in the recreational

fishery (Figure 6). Currently, black sea bass are managed under Amendment 9 of the Summer Flounder, Scup, and Black Sea Bass Fishery Management Plan, and the stocks are considered overexploited (NEFSC, 1997).

Two stocks of black sea bass are recognized: northern and southern. The northern stock (north of Cape Hatteras) is found offshore in deep waters during the winter and then migrates inshore to spawn, typically from April through November in the Mid-Atlantic Bight waters. Peaks in larval abundance occur from July through November in the Bight (Able *et al.*, 1995). Although the larvae are planktonic, the young black sea bass quickly become demersal and use estuaries and the inner continental shelf as nursery grounds (Able *et al.*, 1995; Grosslein and Azarovitz, 1982). When juveniles settle, they typically become associated with bottom structure, such as peat and shell accumulations. Migrations offshore begin as water temperature cools in the fall (Able *et al.*, 1995).

For black sea bass eggs, “EFH is the estuaries where eggs were identified as ‘common,’ abundant,’ or ‘highly abundant’ in the ELMR database for the ‘mixing’ and/or ‘seawater’ salinity zones” (MAFMC, August 1998). EFH for larval black sea bass is the pelagic waters found over the Continental Shelf (from the coast out to the limits of the EEZ), from the Gulf of Maine to Cape Hatteras, North Carolina that encompass the highest 90% of the catch where larvae were collected in the MARMAP ichthyoplankton survey. EFH for juveniles and adults is the demersal waters over the Continental Shelf (from the coast out to the limits of the EEZ), from the Gulf of Maine to Cape Hatteras, North Carolina that encompass the highest 90% of the area where black sea bass were collected in the MARMAP ichthyoplankton survey (MAFMC, August 1998). Juveniles and adults appear to be present in Chincoteague Bay, Delaware Bay, and Delaware Inland Bays based on ELMR data. Based on MARMAP surveys, the designated EFH pelagic and demersal waters for larvae, juveniles and adults overlap with the borrow sites.

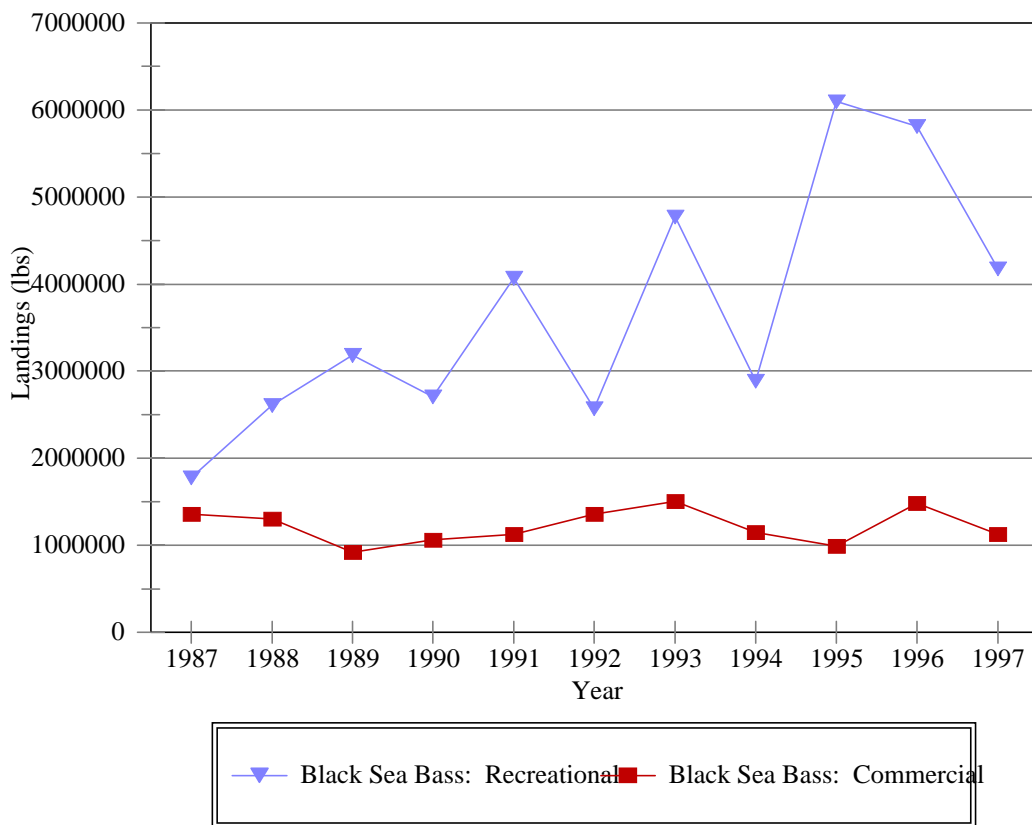


Figure 6: Commercial and recreational landings of Black Sea Bass in the Mid-Atlantic Bight

**Summary**

Of the 36 species listed in this survey, approximately 22 species have the potential to be influenced by inshore sand-mining activity depending on the time of the disturbance. These species either directly utilize inshore areas for spawning and nursery habitats or transverse these areas during spawning migrations, on a frequent basis. Three additional species have the potential to use the study region, but are infrequently observed within the targeted reach of the MAB (*Clupea harengus harengus*, *Stenotomus chrysops*, *Engraulis eurystole*). *Menidia menidia* is believed to spawn only in the bays/estuaries of the Bight, but nearshore areas can be influenced by estuarine outflows (Olney and Wagner, in prep.). Seven species of hakes (*Urophycis*, *Phycis* and *Merluccius* spp.) have larval stages present in the MAB year-round. However, temporal patterns of occurrence and distributions are not well understood due to difficulties in distinguishing

larvae of those species. Typically, it is believed that spawning and larval growth occurs offshore, however, there is some evidence of inshore spawning (Comyns and Grant, 1993). Species that are believed to be located primarily offshore include *Hippoglossina oblonga*, *Gadus morhua*, and *Limanda feruginea*.

Potential use of the proposed mining area by finfish varies. Some species may use the area in more than one capacity, (*i.e.*, a primary nursery area for larvae or young, a spawning and nursery area, or as a fall migration path for young and adults). Species that historically have been observed using the targeted inshore areas as nursery grounds include *Lopholatilus chamaeleonticeps*, *Pomatomus saltatrix*, *Leiostomus xanthurus*, *Micropogon undulatus*, *Menticirrhus saxatilis*, *Paralichthys dentatus*, *Brevoortia tyrannus*, *Lophius americanus*, *Prionotus carolinus*, and *Scomber scombrus*. Species that also may use the area as spawning grounds include *Anchoa mitchilli*, *Anchoa hepsetus*, *Centropristis striata*, *Cynoscion regalis*, *Tautoga onitis*, *Peprilus triacanthus*, *Scophthalmus aquosus*, *Fundulus heteroclitus*, *Ammodytes*, and *Pseudopleuronectes americanus*. Many of the above species as well as *Alosa sapidissima* and *Morone saxatilis*, which are freshwater spawners, subsequently traverse the inshore areas during fall migrations offshore.

This survey is not an exhaustive survey of all species that may be present at some time in the MAB. Instead, it relies on published literature which may have introduced some bias due to sampling location or time. Extensive ichthyoplankton surveys in the area occurred in the 1960s and 1970s; thus natural cycles of abundance may have altered species composition or occurrence since that time. In order to completely assess potential impacts of sand mining on finfish reproduction, ichthyoplankton sampling is recommended. Sampling is necessary to determine changes in species composition and use, that could not be elucidated from published literature. In addition, a more accurate description of relative abundance of species in the area, including economically important ones, will result from a more current ichthyoplankton survey.

## Literature Cited

- Able, K.W., M.P. Fahay and G.R. Shepherd. 1995. Early life history of black sea bass, *Centropristis striata*, in the mid-Atlantic Bight and a New Jersey estuary. *Fish. Bull.* 93: 429-445.
- Able, K. W. , R. E. Matheson, W. W. Morse, M. P. Fahay and G. Shepard. 1990. Patterns of summer flounder (*Paralichthys dentatus*) early life history of the Mid-Atlantic Bight and New Jersey Estuaries. *Fish. Bull. U.S.* 88:1-12.
- Abram, B. J. 1985. Species profiles: life histories and environmental requirements of coastal fishes and invertebrates (Mid-Atlantic) - mummichog and striped killifish. U.S. Fish Wildl. Serv. Biol. Rep. 82 (11.40).
- Chittenden, M. E. Jr. 1976. Present and historical spawning grounds and nurseries of American shad, *Alosa sapidissima*, in the Delaware River. *Fish. Bull. U.S.* 74:343-352.
- Colton, J. B. Jr., W. G. Smith, A. W. Kendall Jr., P. L. Berrien and M. P. Fahay. 1979. Principal spawning areas and times of marine fishes, Cape Sable to Cape Hatteras. *Fish. Bull.* 76(4): 911-915.
- Comyns, B. H. and G. C. Grant. 1993. Identification and distribution of *Urophycis* and *Phycis* (Pisces, Gadidae) larvae and pelagic juveniles in the U.S. middle Atlantic Bight. *Fish. Bull. U.S.* 91:210-223.
- Eklund, A. M and Targett, T. E., 1990. Reproductive seasonality of fishes inhabiting hard bottom areas in the Middle Atlantic Bight. *Copeia.* 1990(4): 1180-1184.
- Fahay, M. P., 1974. Occurrence of silver hake, *Merluccius bilinearis* eggs and larvae along the middle Atlantic Continental Shelf during 1966. NOAA *Fish. Bull.* 72(3): 813-834.
- Fay, C. W., R. J. Neves, and G. B. Pardue. 1983. Species profiles: life histories and environmental requirements of coastal fishes and invertebrates (Mid-Atlantic) - striped bass. *U.S. Fish Wildl. Serv. Biol. Rep.* 82 (11.8)
- Fay, C. W., R. J. Neves, and G. B. Pardue. 1983. Species profiles: life histories and environmental requirements of coastal fishes and invertebrates (Mid-Atlantic) - alewife / blueback herring. *U.S. Fish Wildl. Serv. Biol. Rep.* 82 (11.9)
- Fay, C. W., R. J. Neves, and G. B. Pardue. 1983. Species profiles: life histories and environmental requirements of coastal fishes and invertebrates (Mid-Atlantic) - Atlantic silverside. *U.S. Fish Wildl. Serv. Biol. Rep.* 82 (11.10)
- Grimes, B. H., M. T. Huish, J. H. Kerby, D. Moran. 1898. Species profiles: life histories and environmental requirements of coastal fishes and invertebrates (Mid-Atlantic) - summer and winter flounder. *U.S. Fish Wildl. Serv. Biol. Rep.* 82 (11.112).
- Grosslein, M. D., and T. Azarovitz (eds.), 1982. Ecology of the middle Atlantic Bight fish and shellfish Monograph 15. Fish Distribution. *MESA New York Bight Atlas.* New York Sea Grant Inst., Albany, N.Y.
- Hare, J. A. and R. K. Cowen. 1993. Ecological and evolutionary implications of the larval transport and reproductive strategy of bluefish *Pomatomus saltatrix*. *Mar. Ecol. Prog. Ser.* 98(1-2): 1-16.
- Kendall, A. W. Jr. 1976. Patterns of larval fish distributions in the Middle Atlantic bight. Pages 126-145 In: B. Manowitz (ed.) Proceedings of Conference 'Effects of Energy-Related Activities on the Atlantic Continental Shelf'. Brookhaven National Laboratory, Upton N.Y.

- Kendall, A. W. Jr. and L.A. Walford. 1979. Sources and distribution of bluefish *Pomatomus saltatrix*, larvae and juveniles off the east coast of the United States. *Fish. Bull.* 77(1): 213-227.
- Lewis, R. M. 1966. Effects of salinity and temperature on survival and development of Atlantic menhaden, *Brevoortia tyrannus*. *Trans. Am. Fish. Soc.* 95:423-426.
- MAFMC. August 1998. Amendment 8 to the Atlantic Mackerel, Squid, and Butterfish Fishery Management Plan (Includes draft environmental assessment and draft regulatory impact review).
- MAFMC. August 1998. Amendment 12 to the Summer Flounder, Scup, and Black Sea Bass Fishery Management Plan (Includes draft environmental assessment and draft regulatory impact review).
- MAFMC. July 1998. Amendment 1 to the Bluefish Fishery Management Plan (Includes draft environmental assessment and draft regulatory impact review).
- MacKenzie, C., L. S. Weiss-Glanz, and J. R. Moering. 1985. Species profiles: life histories and environmental requirements of coastal fishes and invertebrates (Mid-Atlantic) - American shad. *U.S. Fish Wildl. Serv. Biol. Rep.* 82 (11.37).
- Mercer, L. P. 1989. Species profiles: life histories and environmental requirements of coastal fishes and invertebrates (Mid-Atlantic) - weakfish. *U.S. Fish Wildl. Serv. Biol. Rep.* 82 (11.109).
- Morse, W. W. 1980. Spawning and fecundity of Atlantic mackerel, *Scomber scombrus*, in the Middle Atlantic Bight. *Fish. Bull.* 78(1): 103-108.
- Morse, W. W. 1981. Reproduction in summer flounder, *Paralichthys dentatus* (L.) *J.Fish. Biol.* 19(2): 189-203.
- Morton, T. 1989. Species profiles: life histories and environmental requirements of coastal fishes and invertebrates (Mid-Atlantic) - bay anchovy. *U.S. Fish Wildl. Serv. Biol. Rep.* 82 (11.97).
- NEFSC [Northeast Fisheries Science Center]. 1997. Report of the 19<sup>th</sup> Northeast Regional Stock Assessment Workshop, Woods Hole, MA: NOAA/NMFS/MEFSC. NEFSC Ref. Doc. 97-14.
- O'Reilly, R. and Austin, H. 1996. Status of stock assessment knowledge used to manage important Virginia finfish species. *Special report in Applied Marine Science and Ocean Engineering* No. 332.
- Phillips, J. M., M. T. Huish and J. H. Kerby. 1989. Species profiles: life histories and environmental requirements of coastal fishes and invertebrates (Mid-Atlantic) - spot. *U.S. Fish Wildl. Serv. Biol. Rep.* 82 (11.98).
- Pottern, G. B., M. T. Huish and J. H. Kerby. 1989. Species profiles: life histories and environmental requirements of coastal fishes and invertebrates (Mid-Atlantic) - bluefish. *U.S. Fish Wildl. Serv. Biol. Rep.* 82 (11.94).
- Rogers, S. G. and M. J. Van Den Avyle. 1989. Species profiles: Life histories and environmental requirements of coastal fishes and invertebrates (Mid-Atlantic) - Atlantic menhaden. *U.S. Fish Wildl. Serv. Biol. Rep.* 82 (11.108).
- Smith, W. G. 1973. The distribution of summer flounder *Paralichthys dentatus*, eggs and larvae on the continental shelf between Cape Cod and Cape Lookout, 1965-66. *Fish. Bull. Fish Wildl. Serv. U.S.* 71:527-548.

- Wang, Johnson C .S., and Kernehan, R. J. 1979. Fishes of the Delaware Estuaries: a Guide to the Early Life Histories. Ecological Analysts, Inc., Towson, MD.
- Wenner, C. A. 1983. Biology of the Longfin Hake (*Physis chesteri*) in the Western North Atlantic. *Biol. Oceano.*, Vol. 3, No. 1: 41-75.

Table 1. Reported periods of spawning and egg and larval presence of fish species located within the Middle-Atlantic Bight categorized by spawning mode (Pelagic or Benthic) and location of spawning.							
O = offshore (areas greater than 27 m in depth); I = inshore (areas less than 27 m in depth);							
T = Tributaries; E = Estuaries; B = Bays. Bays/Estuaries include Delaware Bay and Indian River Bay.							
<i>Fish Species</i>	<i>Spawning</i>	<i>Egg</i>	<i>Larvae</i>	<i>Reference</i>	<i>FMP</i>	<i>Presence</i>	<i>Comments</i>
<b>PELAGIC SPAWNERS</b>							
<b>OFFSHORE</b>							
<i>Physis chesteri</i>			Feb-Nov, O	Comyns and Grant, 1993		Frequent	
	late Sept-April	late Sept -April		Wenner, 1983			peak spawning in Dec and Jan off Virginia
<i>Urophycis tenuis</i>			May-June, O	Comyns and Grant, 1993		Frequent	
<i>Urophycis chuss</i>			Aug-Nov, O	Comyns and Grant, 1993		Frequent	
	May-Nov	May-Nov	May-Nov	Wang and Kernehan, 1979			infrequent in offshore Delaware waters (more northern species)
<i>Urophycis regia</i>			Oct-May, O	Comyns and Grant, 1993		Frequent	
	fall/winter	fall/winter	March/April, E/I	Wang and Kernehan, 1979			peak spawning in Sept-Nov
<i>Urophycis floridiana</i>			Feb-Mar, O	Comyns and Grant, 1993		Infrequent	
<i>Urophycis cirrata</i>			Feb-Mar, O	Comyns and Grant, 1993		Infrequent	
<i>Merluccius bilinearis</i>	May-Nov	May-Nov	Aug-Oct, O	Grosslein and Azarovitz, eds. 1982			peak spawning in June-July
	May-Nov	May-Nov	late summer/fall, O	Wang and Kernehan, 1979; Fahay, 1974		Infrequent	infrequent south of Hudson Canyon
	June-Dec	June-Dec		Colton et al., 1979		Frequent	
<i>Gadus morhua</i>	Dec-May	Dec-May	O	Grosslein and Azarovitz, eds. 1982		?	peak spawning in Dec and Jan
<i>Lopholatilus chamaeleonticeps</i>	March-Sept	March-Sept	June-Oct, O	Grosslein and Azarovitz, eds. 1982		Frequent	
<i>Pomatomus saltatrix</i>	June-Aug	June-Aug	July-Aug; O	Hare and Cowen, 1993	Yes	Frequent	Larvae restricted to MAB in July-Aug
	June-Aug	June-Aug	June-Sept; O/E	Pottern et al., 1989			juveniles from the southern bight spring spawn episode migrate north
	June-Aug	June-Aug	June-Sept, O	Grosslein and Azarovitz, eds. 1982			into the MAB bays and estuaries by early summer and fall
			Aug, O	Kendall and Walford, 1979			
	June-Aug,O/I/E	June-Aug,O/I/E	June-Sept, O/I/E	Wang and Kernehan, 1979			Most spawning offshore, some in nearshore and some lower estuaries
<i>Leiostomus xanthurus</i>	Oct-March	Oct-March	Dec-April, O/I/E	Phillips et al., 1989		Frequent	some reports of spot spawning inshore
	Dec-March	Dec-March	Dec-May, I/E	Wang and Kernehan, 1979			young emigrate to estuaries during spring and migrate out in late fall
<i>Micropogon undulatus</i>	Aug-Dec	Aug-Dec		Grosslein and Azarovitz, eds. 1982			peak spawning in Oct
	Oct-Feb	Oct-Feb	Oct-July, E	Wang and Kernehan, 1979			larvae and young move into low salinity nursery areas
<i>Menticirrhus saxatilis</i>	May-Aug	May-Aug		Grosslein and Azarovitz, eds. 1982		Frequent	
	May-Aug	May-Aug	May-Oct, O/E	Wang and Kernehan, 1979			young emigrate into estuaries throughout the summer
	May-Sept	May-Sept		Fahay, 1974			
<i>Hippoglossina oblonga</i>	May-Oct	May-Oct		Colton et al., 1979		Frequent	
	May-Oct	May-Oct	May-Oct, O	Grosslein and Azarovitz, eds., 1982			peak spawning in June-July; larvae become demersal ca. 8mm
<i>Paralichthys dentatus</i>	Sept-Jan	Sept-Jan	Oct-May, I/E/O	Able et al., 1990	Yes	Frequent	young and late larvae move inshore to estuaries
	Sept-Feb	Sept-Feb	migrate I/E	Grimes et al., 1989			
	Sept-Dec	Sept-Dec	Sept-Feb, O	Grosslein and Azarovitz, eds. 1982			
	Sept-Feb	Sept-Feb		Morse, 1981			
	Sept-April	Sept-April		Colton et al., 1979			
	Aug-Feb	Aug-Feb	Oct-June, I/E	Wang and Kernehan, 1979			
	Nov-Dec	Nov-Dec	Nov-Dec, I/O	Kendall, 1976			
	Sept-Nov	Sept-Nov	Sept-Feb, O	Smith, 1973			
	March-July	March-July	O	Grosslein and Azarovitz, eds. 1982			
<i>Limanda ferruginea</i>	April-Aug	April-Aug		Colton et al., 1979		Frequent	peak spawning spawning in May-June
<b>OFFSHORE AND INSHORE</b>							
<i>Brevoortia tyrannus</i>	Spring/Fall, I	Spring/Fall, I	Oct-June, E	Rogers and Van Den Avyle, 1989		Frequent	possibility of estuarine spawning exists
	April-Oct	April-Oct	April-Oct/E	Grosslein and Azarovitz, eds. 1982			
	Spring/late Fall	Spring/late Fall	Dec-May/E; April-Oct/E	Wang and Kernehan, 1979			Larvae emigrate to estuaries from offshore; young emigrate to offshore areas in autumn
			June - Dec, I/E	Kendall, 1976			
			E	Lewis, 1966			Spawning occurs during spring and fall migrations
<i>Lophius americanus</i>	May-Nov	May-Nov	O/I	Grosslein and Azarovitz, eds. 1982		Frequent	eggs and larvae found both inshore and offshore
<i>Prionotus carolinus</i>	May-Nov	May-Nov		Colton et al., 1979		Frequent	
	May-Oct	May-Oct	May-Oct, O/I/E	Wang and Kernehan, 1979			larvae collected offshore (Atlantic City), and in lower estuaries
	May-Nov	May-Nov	June - Nov, O	Kendall, 1976			larvae further offshore in late fall/winter
<i>Scomber scombrus</i>	April-May, I	April-June		Grosslein and Azarovitz, eds. 1982	Yes	Frequent	
	April-June	April-June		Colton et al., 1979; Morse, 1980			peak spawning in May



Table 2. Reported periods of spawning and egg and larval presence categorized by the peak spawning season for fish species that utilize the Middle-Atlantic Bight and surrounding areas. Spring = March through May; Summer = June through August; Fall = September through November; Winter = December through February.

<i>Fish Species</i>	<i>Spawning</i>	<i>Egg</i>	<i>Larvae</i>	<i>Reference</i>	<i>FMP</i>	<i>Presence</i>	<i>Comments</i>
<b>Spring-Summer</b>							
<i>Alosa sapidissima</i>			Sept-Nov, O	MacKenzie et al., 1985		Frequent	spawning occurs in freshwater tributaries; young migrate into offshore regions in the fall
	April-July	April-July		Fay et al, 1983			
	April-June	April-June	April-Aug, T	Wang and Kernehan, 1979			
	April-July	April-July	April-Aug, T	Chittenden, 1976			In Fall, young begin seaward migration
<i>Anchoa hepsetus</i>	April-July	April-July		Grosslein and Azarovitz, eds. 1982		Frequent	
	May-Aug	May-Aug	fall/winter, E	Wang and Kernehan, 1979			young migrate to deeper waters in fall/winter
<i>Urophycis tenuis</i>			May-June, O	Comyns and Grant, 1993		Frequent	
<i>Menidia menidia</i>	March-June	March-June		Fay et al., 1983		Frequent	eggs attach to submerged objects; larvae are pelagic
	April-Aug	April-Aug	April-Aug, E	Wang and Kernehan, 1979			
<i>Morone saxatilis</i>	April-June	April-June		Fay et al., 1983		Frequent	
	March/April-June	March/April-June	fall, E	Grosslein and Azarovitz, eds. 1982			
	April-July	April-July	summer-fall, E	Wang and Kernehan, 1979			
<i>Stenotomus chrysops</i>	<b>May-Aug</b>	<b>May-Aug</b>		<b>Grosslein and Azarovitz, eds. 1982</b>	<b>Yes</b>	<b>Infrequent</b>	<b>peak spawning in June; nearshore only; Scup eggs and larvae not reported South of N. Jersey</b>
<i>Menticirrhus saxatilis</i>	May-Aug	May-Aug		Grosslein and Azarovitz, eds. 1982		Frequent	
	May-Aug	May-Aug	May-Oct, O/E	Wang and Kernehan, 1979			young emigrate into estuaries throughout the summer
	May-Sept	May-Sept		Fahay, 1974			
<i>Cynoscion regalis</i>	May-July	May-July	O/I	Mercer, 1989		Frequent	
	May-Oct	May-Oct		Grosslein and Azarovitz, eds. 1982			peak spawning May and June
	May-Aug	May-Aug	May-Aug, E	Wang and Kernehan, 1979			young emigrate from estuaries by mid-November
<i>Scomber scombrus</i>	<b>April-May, I</b>	<b>April-June</b>		<b>Grosslein and Azarovitz, eds. 1982</b>	<b>Yes</b>	<b>Frequent</b>	
	<b>April-June</b>	<b>April-June</b>		<b>Colton et al., 1979; Morse, 1980</b>			<b>peak spawning in May</b>
<i>Limanda ferruginea</i>	April-Aug	April-Aug		Colton et al., 1979		Frequent	peak spawning spawning in May-June
<b>Spring-Summer-Fall</b>							
<i>Anchoa mitchilli</i>			May-Oct, E	Morton, 1989		Frequent	
	late April-Sept	late April-Sept		Grosslein and Azarovitz, eds. 1982			spawn throughout salinity gradient
	May-Sept	May-Sept	June-Oct, E	Wang and Kernehan, 1979			
<i>Lophius americanus</i>	May-Nov	May-Nov	O/I	Grosslein and Azarovitz, eds. 1982		Frequent	eggs and larvae found both inshore and offshore
<i>Fundulus heteroclitus</i>	April-Sept	April-Sept		Abraham, 1985		Frequent	eggs demersal on shells, leaves, Spartina, algal mats, pits in substrate
	April-Sept	April-Sept	I/E/B	Wang and Kernehan, 1979			
<i>Lopholatilus chamaeleonticeps</i>	March-Sept	March-Sept	June-Oct, O	Grosslein and Azarovitz, eds. 1982		Frequent	
<i>Peprilus triacanthus</i>	<b>April-Dec, I/E</b>	<b>April-Dec, I/E</b>		<b>Grosslein and Azarovitz, eds. 1982</b>	<b>Yes</b>	<b>Frequent</b>	
	<b>May-Oct</b>	<b>May-Oct</b>		<b>Colton et al., 1979</b>			<b>peak spawning in July-Aug</b>
	<b>June-Aug, O</b>	<b>June-Aug, O</b>	<b>June-Sept, I/E</b>	<b>Wang and Kernehan, 1979</b>			
<i>Prionotus carolinus</i>	May-Nov	May-Nov		Colton et al., 1979		Frequent	
	May-Oct	May-Oct	May-Oct, O/I/E	Wang and Kernehan, 1979			larvae collected offshore (Atlantic City), and in lower estuaries
	May-Nov	May-Nov	June - Nov, O	Kendall, 1976			larvae further offshore in late fall/winter
<i>Hippoglossina oblonga</i>	May-Oct	May-Oct		Colton et al., 1979		Frequent	
	May-Oct	May-Oct	May-Oct, O	Grosslein and Azarovitz, eds., 1982			peak spawning in June-July; larvae become demersal ca. 8mm
<i>Scophthalmus aquosus</i>	April-Dec	April-Dec		Grosslein and Azarovitz, eds. 1982		Frequent	young move offshore in winter
	April-Dec	April-Dec		Colton et al, 1979			
	April-Dec	April-Dec	May-Dec, I/E	Wang and Kernehan, 1979			
<b>Summer</b>							
<i>Tautoga onitis</i>	May-July	May-July	I	Eklund and Targett, 1990		Frequent	
<i>Pomatomus saltatrix</i>	<b>June-Aug</b>	<b>June-Aug</b>	<b>July-Aug; O</b>	<b>Hare and Cowen, 1993</b>	<b>Yes</b>	<b>Frequent</b>	<b>Larvae restricted to MAB in July-Aug</b>
	<b>June-Aug</b>	<b>Jun-Aug</b>	<b>June-Sept; O/E</b>	<b>Pottern et al., 1989</b>			<b>juveniles from the southern bight spring spawn episode migrate north</b>
	<b>June-Aug</b>	<b>June-Aug</b>	<b>June-Sept, O</b>	<b>Grosslein and Azarovitz, eds. 1982</b>			<b>into the MAB bays and estuaries by early summer and fall</b>
			<b>Aug, O</b>	<b>Kendall and Walford, 1979</b>			
	<b>June-Aug,O/I/E</b>	<b>June-Aug,O/I/E</b>	<b>June-Sept, O/I/E</b>	<b>Wang and Kernehan, 1979</b>			<b>Most spawning offshore, some in nearshore and some lower estuaries</b>
<b>Summer-Fall</b>							
<i>Engraulis eurystole</i>	July-Nov	July-Nov	May-Dec	Grosslein and Azarovitz, eds. 1982		Infrequent	spawn in polyhaline waters (offshore or lower estuary)
<i>Urophycis chuss</i>			Aug-Nov, O	Comyns and Grant, 1993		Frequent	

	May-Nov	May-Nov	May-Nov	Wang and Kernehan, 1979			infrequent in offshore Delaware waters (more northern species)
<i>Merluccius bilinearis</i>	May-Nov	May-Nov	Aug-Oct, O	Grosslein and Azarovitz, eds. 1982			peak spawning in June-July
	June-Dec	June-Dec		Colton et al., 1979		Frequent	
	May-Nov	May-Nov	late summer/fall, O	Wang and Kernehan, 1979; Fahay, 1974		Infrequent	infrequent south of Hudson Canyon
<i>Centropristis striata</i>	April-Nov	April-Nov	June-Nov, I/E	Able et al., 1995	Yes	Frequent	peak larval abundance in July-Sept or Oct
	June-Nov	June-Nov	I/E	Grosslein and Azarovitz, eds. 1982			peak spawning in June and July
	May-Oct	May-Oct	June-Nov, I/E	Wang and Kernehan, 1979			
<b>Fall</b>							
<i>Clupea harengus harengus</i>	August-Oct	August-Oct	O	Grosslein and Azarovitz, eds. 1982		Infrequent	larvae pelagic; juveniles migrate inshore
	Nov-Dec	Nov-Dec		Colton et al., 1979			Typically spawns north of Delaware
	Fall	Fall		Wang and Kernehan, 1979			
<b>Fall-Winter</b>							
<i>Urophysis regia</i>			Oct-May, O	Comyns and Grant, 1993		Frequent	
	fall/winter	fall/winter	March/April, E/I	Wang and Kernehan, 1979			peak spawning in Sept-Nov
<i>Leiostomus xanthurus</i>	Oct-March	Oct-March	Dec-April, O/I/E	Philips et al., 1989		Frequent	some reports of spot spawning inshore
	Dec-March	Dec-March	Dec-May, I/E	Wang and Kernehan, 1979			young emigrate to estuaries during spring and migrate out in late fall
<i>Micropogon undulatus</i>	Aug-Dec	Aug-Dec		Grosslein and Azarovitz, eds. 1982			peak spawning in Oct
	Oct-Feb	Oct-Feb	Oct-July, E	Wang and Kernehan, 1979			larvae and young move into low salinity nursery areas
<i>Paralichthys dentatus</i>	Sept-Jan	Sept-Jan	Oct-May, I/E/O	Able et al., 1990	Yes	Frequent	young and late larvae move inshore to estuaries
	Sept-Feb	Sept-Feb	migrate I/E	Grimes et al., 1989			
	Sept-Dec	Sept-Dec	Sept-Feb, O	Grosslein and Azarovitz, eds. 1982			
	Sept-Feb	Sept-Feb		Morse, 1981			
	Sept-April	Sept-April		Colton et al., 1979			
	Aug-Feb	Aug-Feb	Oct-June, I/E	Wang and Kernehan, 1979			
	Nov-Dec	Nov-Dec	Nov-Dec, I/O	Kendall, 1976			
	Sept-Nov	Sept-Nov	Sept-Feb, O	Smith, 1973			
	March-July	March-July	O	Grosslein and Azarovitz, eds. 1982			
<b>Fall-Winter-Spring</b>							
<i>Physis chesteri</i>			Feb-Nov, O	Comyns and Grant, 1993		Frequent	
	late Sept-April	late Sept -April		Wenner, 1983			peak spawning in Dec and Jan off Virginia
<i>Pseudopleuronectes americanus</i>	Nov-June	Nov-June		Grimes et al, 1989		Frequent	
	Nov-April	Nov-April	Nov-June, E	Wang and Kernehan, 1979			eggs demersal; larvae pelagic; late-larvae and young benthic-oriented
<b>Winter</b>							
<i>Urophysis floridiana</i>			Feb-Mar, O	Comyns and Grant, 1993		Infrequent	
<i>Urophysis cirrata</i>			Feb-Mar, O	Comyns and Grant, 1993		Infrequent	
<b>Winter-Spring</b>							
<i>Gadus morhua</i>	Dec-May	Dec-May	O	Grosslein and Azarovitz, eds. 1982		?	peak spawning in Dec and Jan
<i>Ammodytes spp.</i>	Dec-Feb	Dec-Feb		Colton et al., 1979		Frequent	
	Dec-April	Dec-April	Dec-May, E/B/I	Wang and Kernehan, 1979			pelagic larvae for approximately 2-3 months; migrate to offshore areas
<b>Spring and Fall</b>							
<i>Brevoortia tyrannus</i>	Spring/Fall, I	Spring/Fall, I	Oct-June, E	Rogers and Van Den Avyle, 1989		Frequent	possibility of estuarine spawning exists
	April-Oct	April-Oct	April-Oct/E	Grosslein and Azarovitz, eds. 1982			
	Spring/late Fall	Spring/late Fall	Dec-May/E; April-O	Wang and Kernehan, 1979			Larvae emigrate to estuaries from offshore; young emigrate to offshore areas in autumn
			June - Dec, I/E	Kendall, 1976			
			E	Lewis, 1966			Spawning occurs during spring and fall migrations

Table 3. Species List of Mid-Atlantic Bight species examined in this study.

Scientific Name	Common Name
<i>Alosa sapidissima</i>	American Shad
<i>Ammodytes spp.</i>	Sand Lances
<i>Anchoa mitchilli</i>	Bay Anchovy
<i>Anchoa hepsetus</i>	Striped Anchovy
<i>Brevoortia tyrannus</i>	Atlantic Menhaden
<i>Centropristis striata</i>	Black Sea Bass
<i>Clupea harengus harengus</i>	Atlantic herring
<i>Cynoscion regalis</i>	Weakfish
<i>Engraulis eurystole</i>	Silver Anchovy
<i>Fundulus heteroclitus</i>	Mummichog
<i>Gadus morhua</i>	Atlantic Cod
<i>Hippoglossina oblonga</i>	Fourspot Flounder
<i>Leiostomus xanthurus</i>	Spot
<i>Limanda ferruginea</i>	Yellowtail Flounder
<i>Lophius americanus</i>	Goosefish
<i>Lopholatilus chamaeleonticeps</i>	Tilefish
<i>Menidia menidia</i>	Atlantic Silverside
<i>Menticirrhus saxatilis</i>	Northern Kingfish
<i>Merluccius bilinearis</i>	Silver Hake
<i>Micropogon undulatus</i>	Atlantic Croaker
<i>Morone saxatilis</i>	Striped Bass
<i>Paralichthys dentatus</i>	Summer Flounder
<i>Peprilus triacanthus</i>	Butterfish
<i>Physis chesteri</i>	Longfin Hake
<i>Pomatomus saltatrix</i>	Bluefish
<i>Prionotus carolinus</i>	Northern Seabrobin
<i>Pseudopleuronectes americanus</i>	Winter Flounder
<i>Scomber scombrus</i>	Atlantic Mackerel
<i>Scophthalmus aquosus</i>	Windowpane
<i>Stenotomus chrysops</i>	Scup
<i>Tautoga onitis</i>	Tautog
<i>Urophycis cirrata</i>	
<i>Urophycis regia</i>	Spotted Hake
<i>Urophycis chuss</i>	Red Hake
<i>Urophycis tenuis</i>	White Hake
<i>Urophycis floridiana</i>	Southern Hake



#### The Department of the Interior

As the Nation's principal conservation agency, the Department of the Interior has responsibility for most of our nationally owned public lands and natural resources. This includes fostering sound use of our land and water resources, protecting our fish, wildlife, and biological diversity, preserving the environmental and cultural values of our national parks and historic places; and providing for the enjoyment of life through outdoor recreation. The Department assesses our energy and mineral resources and works to ensure that their development is in the best interests of all our people by encouraging stewardship and citizen participation in their care. The Department also has a major responsibility for American Indian reservation communities and for people who live in island territories under U.S. Administration.



#### The Minerals Management Service Mission

As a bureau of the Department of the Interior, the Minerals Management Service's (MMS) primary responsibilities are to manage the mineral resources located on the Nation's Outer Continental Shelf (OCS), collect revenue from the Federal OCS and onshore federal and Indian lands, and distribute those revenues.

Moreover, in working to meet its responsibilities, the Offshore Minerals Management Program administers the OCS competitive leasing program and oversees the safe and environmentally sound exploration and production of our Nation's offshore natural gas, oil and other mineral resources. The MMS Royalty Management Program meets its responsibilities by entrusting the efficient, timely and accurate collection and distribution of revenue from mineral leasing and production due to Indian tribes and allottees, States and the U. S. Treasury

The MMS strives to fulfill its responsibilities through the general guiding principles of: (1) being responsive to the public's concerns and interests by maintaining a dialog with all potentially affected parties and (2) carrying out its programs with an emphasis on working to enhance the quality of life for all Americans by lending MMS assistance and expertise to economic development and environmental protection.

---

# Environmental Survey of Potential Sand Resource Sites Offshore Delaware and Maryland

## Part 4: Potential Modifications to Waves Due to Dredging and Other Oceanographic Considerations

---

Final Report

OCS Study 2000-055

August 2000

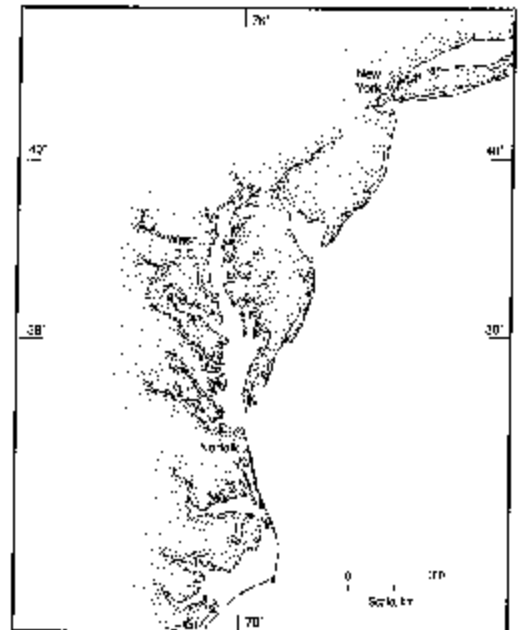
Authors:

Jerome P.-Y. Maa and Sung. C. Kim  
Virginia Institute of Marine Science

Project Manager:

Carl H. Hobbs, III  
Virginia Institute of Marine Science

Prepared under MMS contract 1435-01-97-CT-30853 to  
the  
Virginia Institute of Marine Science  
College of William & Mary



**MMS** U.S. Department of the Interior  
Minerals Management Service

College of William and Mary  
**WIMS**  
Virginia Institute of Marine Science  
School of Marine Science

International Activities and Marine Minerals Division

## DISCLAIMER

This report has been reviewed by the Minerals Management Service and approved for publication. Approval does not signify that the contents necessarily reflect the views and policies of the Service, nor does mention of trade names or commercial products constitute endorsement or recommendation for use.

Final Report

Environmental Survey of Potential Sand Resource Sites

Offshore Delaware and Maryland

Part 4

Potential Modifications to Waves Due to Dredging and Other  
Oceanographic Considerations

Jerome P.-Y. Maa and Sung. C. Kim  
Principal Investigators  
Virginia Institute of Marine Science

Carl H. Hobbs, III, Project Manger

Virginia Institute of Marine Science

for

U. S. Department of the Interior

Minerals Management Service

International Activities and Marine Minerals Division

Contract 1435-01-97-CT-30853

OCS Study 2000-055

August 2000

## TABLE OF CONTENTS

1. INTRODUCTION .....	1
1.1. Objective .....	1
1.2. Scope of Study .....	3
1.3. Methods and Approach .....	3
2. BATHYMETRY AND WAVE DATA .....	5
2.1. Introduction .....	5
2.2. Bathymetric Data .....	5
2.3. Wave Data .....	14
2.4. Statistical Analysis .....	15
2.5. Model Waves .....	17
2.6. Wave Direction .....	17
3. SELECTION OF POSSIBLE WAVE TRANSFORMATION MODELS .....	25
3.1. Introduction .....	25
3.2. SWAN Model .....	25
3.3. HISWA (Cycle 2). .....	27
3.4. STWAVE .....	28
3.5. RDE .....	30
3.6. REF/DIF-S .....	31
3.7. REF/DIF-1 .....	31
3.8. Calibration of REF/DIF-1 .....	33
4. WAVE TRANSFORMATION FOR ORIGINAL BATHYMETRY .....	39
4.1. Introduction .....	39
4.2. Calculated Wave Conditions .....	39
4.3. Results .....	40
4.4. Criterion to Judge the Influence of Dredging .....	43
5. CHANGES OF WAVE ENVIRONMENTS AFTER ONE-TIME DREDGING .....	61
5.1. Introduction .....	61
5.2. Wave Height Difference in Spatial Domain .....	61
5.3. Changes in Breaking Wave Heights .....	78
5.4. Conclusions .....	79
6. CHANGES OF WAVE ENVIRONMENTS AFTER THE ACCUMULATIVE DREDGING .....	95
6.1. Introduction .....	95
6.2. Wave Height Difference in Spatial Domain .....	95

6.3. Changes in Breaking Wave Heights .....	112
6.4. Conclusions .....	114
7. POSSIBLE INFLUENCE ON STORM SURGES .....	131
7.1 Introduction .....	131
7.2 SLOSH Model .....	131
7.3 Model Grid .....	134
7.4 Results and Discussion .....	136
8. POSSIBLE IMPACT ON TIDAL CURRENT .....	141
8.1. Introduction .....	141
8.2. The POM Hydrodynamic Model .....	141
8.3. Model Grid .....	142
8.4. Lateral and Open Boundary Condition .....	142
8.5. Model Verification .....	143
8.6. Results .....	144
8.7. Conclusions .....	145
9. BENTHIC STRESS ANALYSES .....	149
9.1. Introduction .....	150
9.2. GMG Model .....	151
9.3. GMG Model Simulation .....	152
9.4. Results .....	152
10. SUMMARY AND CONCLUSIONS .....	163
11. REFERENCES CITED .....	167

## LIST OF FIGURES

Fig. 1-1. Location Map of the Study Area .....	2
Fig. 2-1. A Plot Depicts the High Density of Digital Bathymetric Data Points (red) and the Relationship between the Model Grid Coordinates (XG, YG) and the Maryland State Plane Coordinates (MD-E, MD-N) .....	6
Fig. 2-2. Bathymetric Image of the Entire Computation Domain. The computing results will be displayed for a much smaller display domain marked by the white dashed lines .....	7
Fig. 2-3. Bathymetric Contours (in meters) for the display Domain. The modeled extensive ( $24 \times 10^6 \text{ m}^3$ ) dredging sites are marked by red dashed polygons .....	10
Fig. 2-4. Bathymetric Images after the One-time Dredging of $2 \times 10^6 \text{ m}^3$ Sand at each site. (a) Fenwick Shoal, and (b) Isle of Wight Shoal .....	11
Fig. 2-5. Bathymetric Images at the Fenwick Shoal (a) Original; (b) after Dredging for $16 \times 10^6 \text{ m}^3$ .....	12
Fig. 2-6. Bathymetric Images at the Isle of Wight Shoal (a) Original; (b) after Dredging for $8.4 \times 10^6 \text{ m}^3$ .....	13
Fig. 2-7. Comparison of Measured Waves at Offshore ( 44009), and Near Shore (MD001 & MD002) from Nov. 1 to 30, 1997. (a) $H_s$ ; (b) Peak Energy Wave Period .....	16
Fig. 2-8. Significant Wave Height and Peak Energy Wave Period Joint Distribution at Station 44009 .....	22
Fig. 2-9. Significant Wave Height Rose at Station 44009. The scale of 3.4% occurrence is plotted in the legend .....	23
Fig. 2-10. Peak Energy Wave Period Rose at Station 44009. The scale of 7.3% occurrence is plotted in the legend .....	24
Fig. 3-1. Comparison of REF/DIF-1 Calculated and Measured $H_s$ at MD001 Using Idealized Wave Conditions at Offshore Boundary and Wave Friction Factor = 0.02 .....	37
Fig. 4-1. Bathymetric Image for the Display Domain .....	41

Fig. 4-2. Normalized Wave Height Distribution for the Original Bathymetry with $H_0 = 8$ m, $T = 16$ s. (a) ENE, (b) E, (c) ESE, and (d) SE .....	44
Fig. 4-3. Normalized Wave Height Distribution for the Original Bathymetry with $H_0 = 8$ m, $T = 20$ s. (a) ENE, (b) E, (c) ESE, and (d) SE .....	45
Fig. 4-4. Normalized Wave Height Distribution for the Original Bathymetry with $H_0 = 6$ m, $T = 14$ s. (a) ENE, (b) E, (c) ESE, and (d) SE .....	46
Fig. 4-5. Normalized Wave Height Distribution for the Original Bathymetry with $H_0 = 6$ m, $T = 16$ s. (a) ENE, (b) E, (c) ESE, and (d) SE .....	47
Fig. 4-6. Normalized Wave Height Distribution for the Original Bathymetry with $H_0 = 6$ m, $T = 20$ s. (a) ENE, (b) E, (c) ESE, and (d) SE .....	48
Fig. 4-7. Normalized Wave Height Distribution for the Original Bathymetry with $H_0 = 4$ m, $T = 10$ s. (a) ENE, (b) E, (c) ESE, and (d) SE .....	49
Fig. 4-8. Normalized Wave Height Distribution for the Original Bathymetry with $H_0 = 4$ m, $T = 12$ s. (a) ENE, (b) E, (c) ESE, and (d) SE .....	50
Fig. 4-9. Normalized Wave Height Distribution for the Original Bathymetry with $H_0 = 4$ m, $T = 14$ s. (a) ENE, (b) E, (c) ESE, and (d) SE .....	51
Fig. 4-10. Normalized Wave Height Distribution for the Original Bathymetry with $H_0 = 4$ m, $T = 16$ s. (a) ENE, (b) E, (c) ESE, and (d) SE .....	52
Fig. 4-11. Normalized Wave Height Distribution for the Original Bathymetry with $H_0 = 4$ m, $T = 20$ s. (a) ENE, (b) E, (c) ESE, and (d) SE .....	53
Fig. 4-12. Normalized Wave Height Distribution for the Original Bathymetry with $H_0 = 2$ m, $T = 10$ s. (a) ENE, (b) E, (c) ESE, and (d) SE .....	54
Fig. 4-13. Normalized Wave Height Distribution for the Original Bathymetry with $H_0 = 2$ m, $T = 12$ s. (a) ENE, (b) E, (c) ESE, and (d) SE .....	55
Fig. 4-14. Normalized Wave Height Distribution for the Original Bathymetry with $H_0 = 2$ m, $T = 14$ s. (a) ENE, (b) E, (c) ESE, and (d) SE .....	56
Fig. 4-15. Normalized Wave Height Distribution for the Original Bathymetry with $H_0 = 2$ m, $T = 16$ s. (a) ENE, (b) E, (c) ESE, and (d) SE .....	57
Fig. 4-16. Normalized Wave Height Distribution for the Original Bathymetry	

with $H_0 = 2$ m, $T = 20$ s. (a) ENE, (b) E, (c) ESE, and (d) SE . . . . .	58
Fig. 4-17. A Conceptual Diagram Showing the Criterion for Determining the Effect of Bathymetric Change . . . . .	59
Fig. 5-1. Calculated Changes of Wave Height (Normalized) for the One-time Dredging with $H_0 = 8$ m, $T = 16$ s coming from (a) ENE, (b) E, (c) ESE, and (d) SE . . . . .	63
Fig. 5-2. Calculated Changes of Wave Height (Normalized) for the One-time Dredging with $H_0 = 8$ m, $T = 20$ s coming from (a) ENE, (b) E, (c) ESE, and (d) SE . . . . .	64
Fig. 5-3. Calculated Changes of Wave Height (Normalized) for the One-time Dredging with $H_0 = 6$ m, $T = 14$ s coming from (a) ENE, (b) E, (c) ESE, and (d) SE . . . . .	65
Fig. 5-4. Calculated Changes of Wave Height (Normalized) for the One-time Dredging with $H_0 = 6$ m, $T = 16$ s coming from (a) ENE, (b) E, (c) ESE, and (d) SE . . . . .	66
Fig. 5-5. Calculated Changes of Wave Height (Normalized) for the One-time Dredging with $H_0 = 6$ m, $T = 20$ s coming from (a) ENE, (b) E, (c) ESE, and (d) SE . . . . .	67
Fig. 5-6. Calculated Changes of Wave Height (Normalized) for the One-time Dredging with $H_0 = 4$ m, $T = 10$ s coming from (a) ENE, (b) E, (c) ESE, and (d) SE . . . . .	68
Fig. 5-7. Calculated Changes of Wave Height (Normalized) for the One-time Dredging with $H_0 = 4$ m, $T = 12$ s coming from (a) ENE, (b) E, (c) ESE, and (d) SE . . . . .	69
Fig. 5-8. Calculated Changes of Wave Height (Normalized) for the One-time Dredging with $H_0 = 4$ m, $T = 14$ s coming from (a) ENE, (b) E, (c) ESE, and (d) SE . . . . .	70
Fig. 5-9. Calculated Changes of Wave Height (Normalized) for the One-time Dredging with $H_0 = 4$ m, $T = 16$ s coming from (a) ENE, (b) E, (c) ESE, and (d) SE . . . . .	71
Fig. 5-10. Calculated Changes of Wave Height (Normalized) for the One-time Dredging with $H_0 = 4$ m, $T = 20$ s coming from (a) ENE, (b) E, (c) ESE, and (d) SE . . . . .	72
Fig. 5-11. Calculated Changes of Wave Height (Normalized) for the One-time Dredging with $H_0 = 2$ m, $T = 10$ s coming from (a) ENE, (b) E, (c) ESE, and (d) SE . . . . .	73
Fig. 5-12. Calculated Changes of Wave Height (Normalized) for the One-time Dredging with $H_0 = 2$ m, $T = 12$ s coming from (a) ENE, (b) E, (c) ESE, and (d) SE . . . . .	74
Fig. 5-13. Calculated Changes of Wave Height (Normalized) for the One-time Dredging with $H_0 = 2$ m, $T = 14$ s coming from (a) ENE, (b) E, (c) ESE, and (d) SE . . . . .	75

Fig. 5-14. Calculated Changes of Wave Height (Normalized) for the One-time Dredging with $H_0 = 2$ m, $T = 16$ s coming from (a) ENE, (b) E, (c) ESE, and (d) SE . . . . .	76
Fig. 5-15. Calculated Changes of Wave Height (Normalized) for the One-time Dredging with $H_0 = 2$ m, $T = 20$ s coming from (a) ENE, (b) E, (c) ESE, and (d) SE . . . . .	77
Fig. 5-16. Comparison of Breaking Wave Heights for Original Bathymetry and after One-time Dredging with $H_0 = 8$ m, $T = 20$ s coming from (a) ENE, (b) E, (c) ESE, and (d) SE. Solid black line is for the original bathymetry, and Dashed red line is after the modeled dredging . . . . .	80
Fig. 5-17. Comparison of Breaking Wave Heights for Original Bathymetry and after One-time Dredging with $H_0 = 8$ m, $T = 16$ s coming from (a) ENE, (b) E, (c) ESE, and (d) SE . . . . .	81
Fig. 5-18. Comparison of Breaking Wave Heights for Original Bathymetry and after One-time Dredging with $H_0 = 6$ m, $T = 20$ s coming from (a) ENE, (b) E, (c) ESE, and (d) SE . . . . .	82
Fig. 5-19. Comparison of Breaking Wave Heights for Original Bathymetry and after One-time Dredging with $H_0 = 6$ m, $T = 16$ s coming from (a) ENE, (b) E, (c) ESE, and (d) SE . . . . .	83
Fig. 5-20. Comparison of Breaking Wave Heights for Original bathymetry and after One-time Dredging with $H_0 = 6$ m, $T = 14$ s coming from (a) ENE, (b) E, (c) ESE, and (d) SE . . . . .	84
Fig. 5-21. Comparison of Breaking Wave Heights for Original Bathymetry and after One-time Dredging with $H_0 = 4$ m, $T = 20$ s coming from (a) ENE, (b) E, (c) ESE, and (d) SE . . . . .	85
Fig. 5-22. Comparison of Breaking Wave Heights for Original Bathymetry and after One-time Dredging with $H_0 = 4$ m, $T = 16$ s coming from (a) ENE, (b) E, (c) ESE, and (d) SE . . . . .	86
Fig. 5-23. Comparison of Breaking Wave Heights for Original bathymetry and after One-time Dredging with $H_0 = 4$ m, $T = 14$ s coming from (a) ENE, (b) E, (c) ESE, and (d) SE . . . . .	87
Fig. 5-24. Comparison of Breaking Wave Heights for Original Bathymetry and after One-time Dredging with $H_0 = 4$ m, $T = 12$ s coming from (a) ENE, (b) E, (c) ESE, and (d) SE . . . . .	88

Fig. 5-25. Comparison of Breaking Wave Heights for Original Bathymetry and after One-time Dredging with $H_0 = 4$ m, $T = 10$ s coming from (a) ENE, (b) E, (c) ESE, and (d) SE . . . . .	89
Fig. 5-26. Comparison of Breaking Wave Heights for Original Bathymetry and after One-time Dredging with $H_0 = 2$ m, $T = 20$ s coming from (a) ENE, (b) E, (c) ESE, and (d) SE . . . . .	90
Fig. 5-27. Comparison of Breaking Wave Heights for Original Bathymetry and after One-time Dredging with $H_0 = 2$ m, $T = 16$ s coming from (a) ENE, (b) E, (c) ESE, and (d) SE . . . . .	91
Fig. 5-28. Comparison of Breaking Wave Heights for Original Bathymetry and after One-time Dredging with $H_0 = 2$ m, $T = 14$ s coming from (a) ENE, (b) E, (c) ESE, and (d) SE . . . . .	92
Fig. 5-29. Comparison of Breaking Wave Heights for Original Bathymetry and after One-time Dredging with $H_0 = 2$ m, $T = 12$ s coming from (a) ENE, (b) E, (c) ESE, and (d) SE . . . . .	93
Fig. 5-30. Comparison of Breaking Wave Heights for Original Bathymetry and after One-time Dredging with $H_0 = 2$ m, $T = 10$ s coming from (a) ENE, (b) E, (c) ESE, and (d) SE . . . . .	94
Fig. 6-1. Calculated Changes of Wave Height (Normalized) for the Accumulative Dredging with $H_0 = 8$ m, $T = 16$ s coming from (a) ENE, (b) E, (c) ESE, and (d) SE . . . . .	97
Fig. 6-2. Calculated Changes of Wave Height (Normalized) for the Accumulative Dredging with $H_0 = 8$ m, $T = 20$ s coming from (a) ENE, (b) E, (c) ESE, and (d) SE . . . . .	98
Fig. 6-3. Calculated Changes of Wave Height (Normalized) for the Accumulative Dredging with $H_0 = 6$ m, $T = 14$ s coming from (a) ENE, (b) E, (c) ESE, and (d) SE . . . . .	99
Fig. 6-4. Calculated Changes of Wave Height (Normalized) for the Accumulative Dredging with $H_0 = 6$ m, $T = 16$ s coming from (a) ENE, (b) E, (c) ESE, and (d) SE . . . . .	100
Fig. 6-5. Calculated Changes of Wave Height (Normalized) for the Accumulative Dredging with $H_0 = 6$ m, $T = 20$ s coming from (a) ENE, (b) E, (c) ESE, and (d) SE . . . . .	101

Fig. 6-6. Calculated Changes of Wave Height (Normalized) for the Accumulative Dredging with $H_0 = 4$ m, $T = 10$ s coming from (a) ENE, (b) E, (c) ESE, and (d) SE .....	102
Fig. 6-7. Calculated Changes of Wave Height (Normalized) for the Accumulative Dredging with $H_0 = 4$ m, $T = 12$ s coming from (a) ENE, (b) E, (c) ESE, and (d) SE .....	103
Fig. 6-8. Calculated Changes of Wave Height (Normalized) for the Accumulative Dredging with $H_0 = 4$ m, $T = 14$ s coming from (a) ENE, (b) E, (c) ESE, and (d) SE .....	104
Fig. 6-9. Calculated Changes of Wave Height (Normalized) for the Accumulative Dredging with $H_0 = 4$ m, $T = 16$ s coming from (a) ENE, (b) E, (c) ESE, and (d) SE .....	105
Fig. 6-10. Calculated Changes of Wave Height (Normalized) for the Accumulative Dredging with $H_0 = 4$ m, $T = 20$ s coming from (a) ENE, (b) E, (c) ESE, and (d) SE .....	106
Fig. 6-11. Calculated Changes of Wave Height (Normalized) for the Accumulative Dredging with $H_0 = 2$ m, $T = 10$ s coming from (a) ENE, (b) E, (c) ESE, and (d) SE .....	107
Fig. 6-12. Calculated Changes of Wave Height (Normalized) for the Accumulative Dredging with $H_0 = 2$ m, $T = 12$ s coming from (a) ENE, (b) E, (c) ESE, and (d) SE .....	108
Fig. 6-13. Calculated Changes of Wave Height (Normalized) for the Accumulative Dredging with $H_0 = 2$ m, $T = 14$ s coming from (a) ENE, (b) E, (c) ESE, and (d) SE .....	109
Fig. 6-14. Calculated Changes of Wave Height (Normalized) for the Accumulative Dredging with $H_0 = 2$ m, $T = 16$ s coming from (a) ENE, (b) E, (c) ESE, and (d) SE .....	110
Fig. 6-15. Calculated Changes of Wave Height (Normalized) for the Accumulative Dredging with $H_0 = 2$ m, $T = 20$ s coming from (a) ENE, (b) E, (c) ESE, and (d) SE .....	111
Fig. 6-16. Comparison of Breaking Wave Heights for Original Bathymetry and after Accumulative Dredging with $H_0 = 8$ m, $T = 20$ s .....	115

Fig. 6-17. Comparison of Breaking Wave Heights for Original Bathymetry and after Accumulative Dredging with $H_0 = 8$ m, $T = 16$ s . . . . .	116
Fig. 6-18. Comparison of Breaking Wave Heights for Original Bathymetry and after Accumulative Dredging with $H_0 = 6$ m, $T = 20$ s . . . . .	117
Fig. 6-19. Comparison of Breaking Wave Heights for Original Bathymetry and after Accumulative Dredging with $H_0 = 6$ m, $T = 16$ s . . . . .	118
Fig. 6-20. Comparison of Breaking Wave Heights for Original Bathymetry and after Accumulative Dredging with $H_0 = 6$ m, $T = 14$ s . . . . .	119
Fig. 6-21. Comparison of Breaking Wave Heights for Original Bathymetry and after Accumulative Dredging with $H_0 = 4$ m, $T = 20$ s . . . . .	120
Fig. 6-22. Comparison of Breaking Wave Heights for Original Bathymetry and after Accumulative Dredging with $H_0 = 4$ m, $T = 16$ s . . . . .	121
Fig. 6-23. Comparison of Breaking Wave Heights for Original Bathymetry and after Accumulative Dredging with $H_0 = 4$ m, $T = 14$ s . . . . .	122
Fig. 6-24. Comparison of Breaking Wave Heights for Original Bathymetry and after Accumulative Dredging with $H_0 = 4$ m, $T = 20$ s . . . . .	123
Fig. 6-25. Comparison of Breaking Wave Heights for Original Bathymetry and after Accumulative Dredging with $H_0 = 4$ m, $T = 16$ s . . . . .	124
Fig. 6-26. Comparison of Breaking Wave Heights for Original Bathymetry and after Accumulative Dredging with $H_0 = 2$ m, $T = 20$ s . . . . .	125
Fig. 6-27. Comparison of Breaking Wave Heights for Original Bathymetry and after Accumulative Dredging with $H_0 = 2$ m, $T = 16$ s . . . . .	126
Fig. 6-28. Comparison of Breaking Wave Heights for Original Bathymetry and after Accumulative Dredging with $H_0 = 2$ m, $T = 14$ s . . . . .	127
Fig. 6-29. Comparison of Breaking Wave Heights for Original Bathymetry and after Accumulative Dredging with $H_0 = 2$ m, $T = 20$ s . . . . .	128
Fig. 6-30. Comparison of Breaking Wave Heights for Original Bathymetry and after Accumulative Dredging with $H_0 = 2$ m, $T = 16$ s . . . . .	129

Fig. 7-1. Bathymetry in the SLOSH Model Computation Domain . . . . .	135
Fig. 7-2. Bathymetry and 10 Coastal Monitoring Stations in the SLOSH Model. Also shown are the modeled dredging sites at two offshore shoals . . . . .	135
Fig. 7-3. Surge Envelop from Cross-shore Track . . . . .	136
Fig. 7-4. Time Series of Coastal Surges at 10 Monitoring Stations, Cross-shore Track . .	136
Fig. 7-5. Time Series of Coastal Surge Changes by Dredging at 10 Monitoring Stations, Cross-shore Track . . . . .	137
Fig. 7-6. Surge Envelop from Shore-parallel Track . . . . .	138
Fig. 7-7. Time Series of Coastal Surges at 10 Monitoring Stations, Shore-parallel Track .	138
Fig. 7-8. Time Series of Coastal Surge Changes by Dredging At 10 Monitoring Stations, Shore-parallel Track . . . . .	139
Fig. 8-1. Comparison of Calculated and Analyzed Tidal Elevation at Ocean City Inlet from May 5-15, 1985. Solid line is the Calculated, Dashed line is the Analyzed .	143
Fig. 8-2. Contours of Near-bed Tidal Current Velocity (in cm/s), Zero Contour line is also the Shoreline. (a) Maximum Flood; (b) maximum Ebb . . . . .	146
Fig. 8-3. Near-bed Tidal Current Velocity Vectors at the maximum Flood (left) and Maximum Ebb (right). The Shoals are also Plotted . . . . .	147
Fig. 8-4. Difference (in %) in Tidal Current Caused by Dredging at the Modeled Sites (a) for Maximum Flood, and (b) for Maximum Ebb . . . . .	148
Fig. 9-1. Definition Sketch of Two-layer Wave-current Bottom Boundary Layer . . . . .	149
Fig. 9-2. Solution Procedure for the GMG Model . . . . .	151
Fig. 9-3. Effect of Wave Direction on Friction Velocity. Offshore wave condition is $T = 14$ s and $H = 6$ m . . . . .	153
Fig. 9-4. Effect of Wave Direction on the Change in Bottom Friction Velocity. waves condition is $T = 14$ s and $H = 6$ m . . . . .	154
Fig. 9-5. (1). Possible Maximum Change in Bottom Friction Velocity. Offshore wave condition is $T = 10$ s and $H = 2$ m . . . . .	155

Fig. 9-5. (2). Possible Maximum Change in Bottom Friction Velocity. Offshore wave condition is $T = 10$ s and $H = 4$ m . . . . .	155
Fig. 9-5. (3). Possible Maximum Change in Bottom Friction Velocity. Offshore wave condition is $T = 12$ s and $H = 2$ m . . . . .	156
Fig. 9-5. (4). Possible Maximum Change in Bottom Friction Velocity. Offshore wave condition is $T = 12$ s and $H = 4$ m . . . . .	156
Fig. 9-5.(5). Possible Maximum Change in Bottom Friction Velocity. Offshore wave condition is $T = 14$ s and $H = 2$ m . . . . .	157
Fig. 9-5. (6). Possible Maximum Change in Bottom Friction Velocity. Offshore wave condition is $T = 14$ s and $H = 4$ m . . . . .	157
Fig. 9-5. (7). Possible Maximum Change in Bottom Friction Velocity. Offshore wave condition is $T = 14$ s and $H = 6$ m . . . . .	158
Fig. 9-5. (8). Possible Maximum Change in Bottom Friction Velocity. Offshore wave condition is $T = 16$ s and $H = 2$ m . . . . .	158
Fig. 9-5. (9). Possible Maximum Change in Bottom Friction Velocity. Offshore wave condition is $T = 16$ s and $H = 4$ m . . . . .	159
Fig. 9-5. (10). Possible Maximum Change in Bottom Friction Velocity. Offshore wave condition is $T = 16$ s and $H = 6$ m . . . . .	159
Fig. 9-5. (11). Possible Maximum Change in Bottom Friction Velocity. Offshore wave condition is $T = 16$ s and $H = 8$ m . . . . .	160
Fig. 9-5. (12). Possible Maximum Change in Bottom Friction Velocity. Offshore wave condition is $T = 20$ s and $H = 2$ m . . . . .	160
Fig. 9-5. (13). Possible Maximum Change in Bottom Friction Velocity. Offshore wave condition is $T = 20$ s and $H = 4$ m . . . . .	161
Fig. 9-5. (14).18. Possible Maximum Change in Bottom Friction Velocity. Offshore wave condition is $T = 20$ s and $H = 6$ m . . . . .	161
Fig. 9-5. (15). Possible Maximum Change in Bottom Friction Velocity. Offshore wave condition is $T = 20$ s and $H = 8$ m . . . . .	162

## LIST OF TABLES

Table 2-1. Corner Coordinates for the Modeled One-time Dredging (in Maryland State Plane Coordinates, NAD83, Meters) . . . . .	9
Table 2-2. Corner Coordinates for the Modeled Accumulative Dredging (in Maryland State Plane Coordinates, NAD83, Meters) . . . . .	9
Table 2-3. The Height and Period Distribution for Waves Coming from ENE (8.600%) . . . . .	19
Table 2-4. The Height and Period Distribution for Waves Coming from E (13.086%) . . . . .	19
Table 2-5. The Height and Period Distribution for Waves Coming from ESE (13.709%) . . . . .	20
Table 2-6. The Height and Period Distribution for Waves Coming from SE (14.653%) . . . . .	20
Table 2-7. Observed Annual Maximum Significant Waves . . . . .	21
Table 2-8. Selected Model Waves . . . . .	21
Table 3-1. Comparison of Spectrum Wave Prediction Models . . . . .	29
Table 3-2. Comparison of Wave Transformation Models . . . . .	33
Table 3-3. Wave Conditions Used for Calibrating REF/DIF-1 . . . . .	36
Table 4-1. Selected Wave Heights and Periods for Checking Wave Transformation . . . . .	39
Table 4-2. Non-linear Dissipation of Wave Energy . . . . .	42
Table 5-1. Summary of the Changes on Breaking Wave Heigh Modulation for the One-time Dredging . . . . .	79
Table 6-1. Summary of the Changes on Breaking Wave Heigh Modulation for the Cumulative Dredging . . . . .	113
Table 8-1. Amplitude and Epoch of Major Constituents Specified at Offshore Boundary . . . . .	144

## CHAPTER I. INTRODUCTION

### 1.1. Objective

A well maintained beach can serve several purposes, *e.g.*, (1) providing a public recreational area, (2) protecting valuable properties that are located near the coastline, and (3) reducing the rate of land loss. Thus, a great deal of effort has been devoted to understanding the processes that change the shoreline. Among the several erosion processes, waves are the most important because their great energy can produce severe erosion and significantly alter the shoreline.

One can use several approaches, either separately or in combination, to maintain a beach. In the coastal sector near the Maryland - Delaware border, especially around Ocean City, Maryland, the beach has been nourished with sand from inland borrow pits throughout the past two decades. It has become increasingly difficult to find terrestrial sources of good, beach-quality sand. The shore's continual loss of sand to shore normal and alongshore transport processes requires a reliable source of good quality sand for future nourishment.

Two offshore shoals, Fenwick Shoal and Isle of Wight Shoal, have been identified as potential sources for beach-quality sand (Figure 1-1). Fenwick Shoal is approximately 10 km west of the Maryland - Delaware border. Isle of Wight Shoal is about 8 km south of Fenwick. There is concern that utilization of sand from these shoals may cause unwanted alterations to the shoreline, which may be near its equilibrium state. Dredging on the shoals definitely will alter the wave transformation processes which, depending upon the dredging plan, may induce unfavorable consequences.

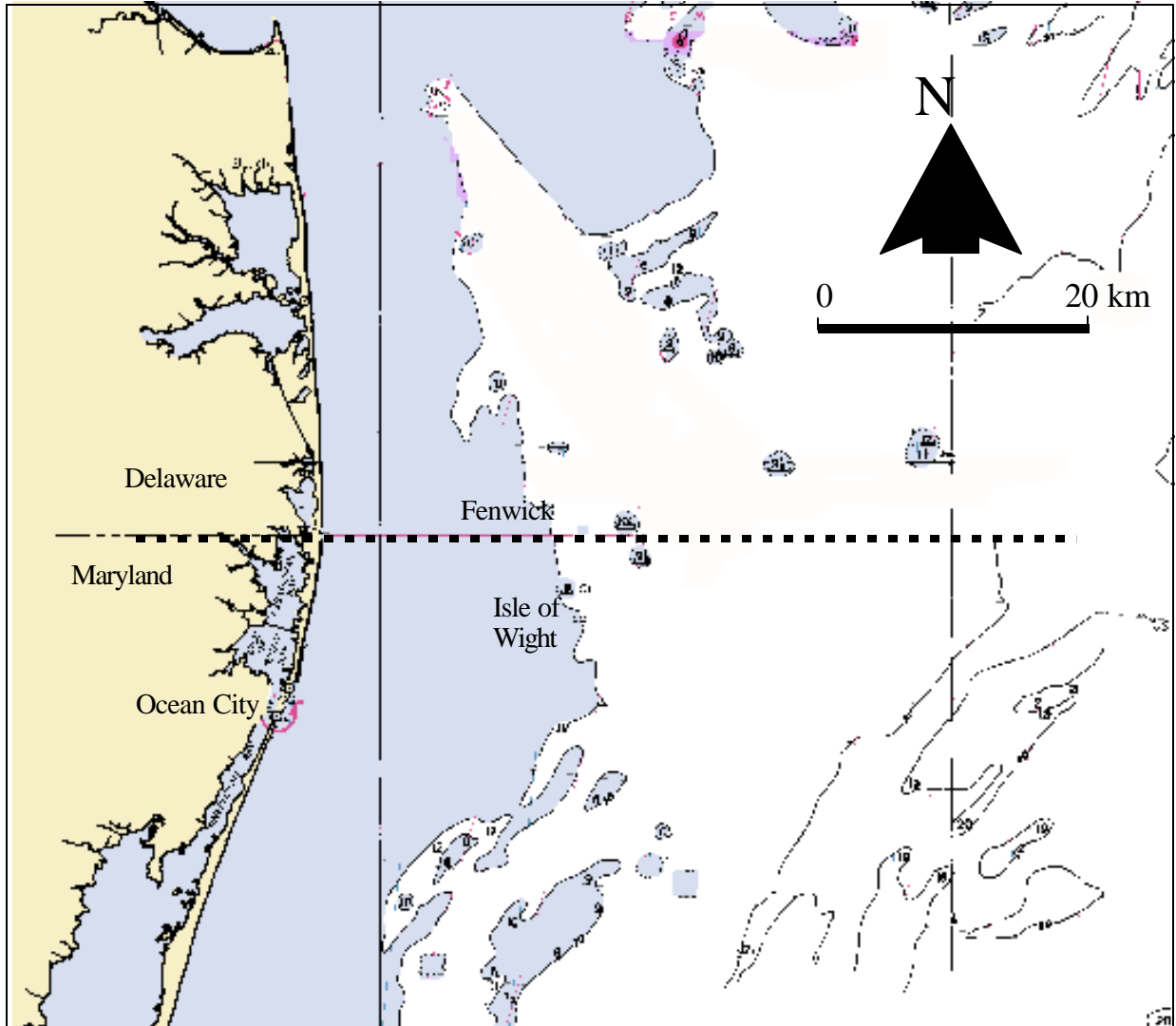


Fig. 1-1. Location Map of the Study Area

## 1.2. Scope of Study

In order to understand the possible changes in the shoreline resulting from dredging requires a comprehensive understanding of the wave climate, the wave transformation processes, the possible changes of wave transformation caused by changing the bathymetry, and the associated shoreline responses.

In a study of a similar problem, Maa and Hobbs (1998) concluded that if the sand taken from the shoal they studied were limited to the order of  $10^6 \text{ m}^3$ , the impact on wave transformation would be less than 5% for the maximum, severe sea that occurs once every 10 to 20 years. They concluded that the 5% change is not significant because (1) the maximum 5% change was determined using the wave transformation model (RCPWAVE) that is known to overestimate wave height near shore (Maa *et al*, in press) and (2) the direction of wave approach is critical, the calculated maximum change statistically has a very low likelihood of occurrence. The foci of the present study are (1) check if the possible impact caused by an one-time dredging on the order of  $2 \times 10^6 \text{ m}^3$  of sand at each of the two shoals acceptable or not, and (2) Is the impact on wave alterations resulting from removal of significantly more sand, on the order of  $10^7 \text{ m}^3$ , acceptable?

## 1.3. Methods and Approach

In order to estimate the possible impact, a computational bathymetric grid system must be established. This is described in Chapter 2. What kind of waves have occurred in the area is the next subject. We analyzed wave data measured at offshore station 44009 (from 1986 -1998) and two near shore wave stations (MD001 and MD002) in the area. The results are summarized in Chapter 2.

A brief description of available wave models is given in Chapter 3. After selecting REF/DIF-1 as a feasible and practical model with which to explore the possible impact, we calibrated the model by comparing 103 cases of calculated and measured wave heights at a near shore wave station, MD001, using the given offshore wave conditions and the bathymetric grid described in Chapter 2.

Wave transformations for 60 selected offshore wave conditions with the original bathymetry were calculated first. The results, in terms of wave height distributions, are presented in Chapter 4 as background information.

In order to check if a small amount of dredging ( $2 \times 10^6 \text{ m}^3$ ) at each of the two shoals is acceptable, the same 60 offshore wave conditions are re-run with an appropriately modified bathymetric grid. The differences for each wave condition are given in Chapter 5.

To find the possible impact of accumulated dredging at the two sites, the same 60 offshore wave conditions were re-run with bathymetry altered to provide a total of  $24.4 \times 10^7 \text{ m}^3$  sand. The differences of wave height distribution caused by dredging for each wave condition are given in Chapter 6.

The possible influence on storm surge is considered and a study using a NOAA model has been carried out. The results are presented in Chapter 7.

In this study, we further addressed the possible change of bed shear stress between the targeted shoals and the coast. The objective is to examine the possible influence on benthic organisms. For this reason, we studied the possible change of tidal currents (Chapter 8) because of the accumulative dredging. After combining with the possible change of wave height (Chapter 6), the possible change of bed shear stress distribution is given in Chapter 9.

The conclusions of possible physical impacts caused by dredging at the two offshore shoals are summarized in Chapter 10.

## CHAPTER 2, BATHYMETRIC AND WAVE DATA

### 2.1. Introduction

This chapter discusses the collection and processing of bathymetric and wave data. The main objective is to put these data in a useful format for further access and use.

### 2.2. Bathymetric Data

The bathymetric data were obtained from the NOAA Data Center. The data were sorted in one degree latitude-longitude domains and distributed in CD-ROM. The software to retrieve bathymetric data for selected areas was also in the CD-ROM. A previously developed FORTRAN program was used to remove the bathymetric data for lakes and inland waterways. Then the remaining bathymetric data were merged with shoreline data (also from NOAA) to form a completed data file (Fig. 2-1). The original coordinates of the data were latitude and longitude, which were transferred to Maryland State Plane Coordinate System using the CORPSCON software from the Waterways Experiment Station, U.S. Army Corps of Engineers. The relative locations of wave station 44009, MD001, and MD002 are also indicated in Fig. 2-1.

In order to obtain a computation grid with evenly spaced grid size for wave and tidal current calculation, a new grid system (marked by the white box with 44.970 km x 67.560 km in XG and YG directions, respectively) was created (Fig. 2-1). The origin of this new grid is also shown in Fig. 2-1. A FORTRAN computer program previously developed for other MMS projects was used again to generate a computation grid for wave transformation computations. Figure 2-2 shows the bathymetry for this computing domain. Notice that the coordinates of this grid are specified as XG and YG. The coordinates of the origin of this computation domain are E561.000 km and N61.000 km in NAD83 Maryland State Plane Coordinate System, and YG is rotated 4.2 degrees from the Maryland State Plane Coordinates' North coordinate (Fig. 2-1).

This computation domain has a grid size of 30 m in the XG direction and 60 m in the YG direction, respectively, *i.e.*, 1500 and 1127 grid points in these two directions, respectively. The small grid size is needed for having a better simulation of wave transformation, especially for

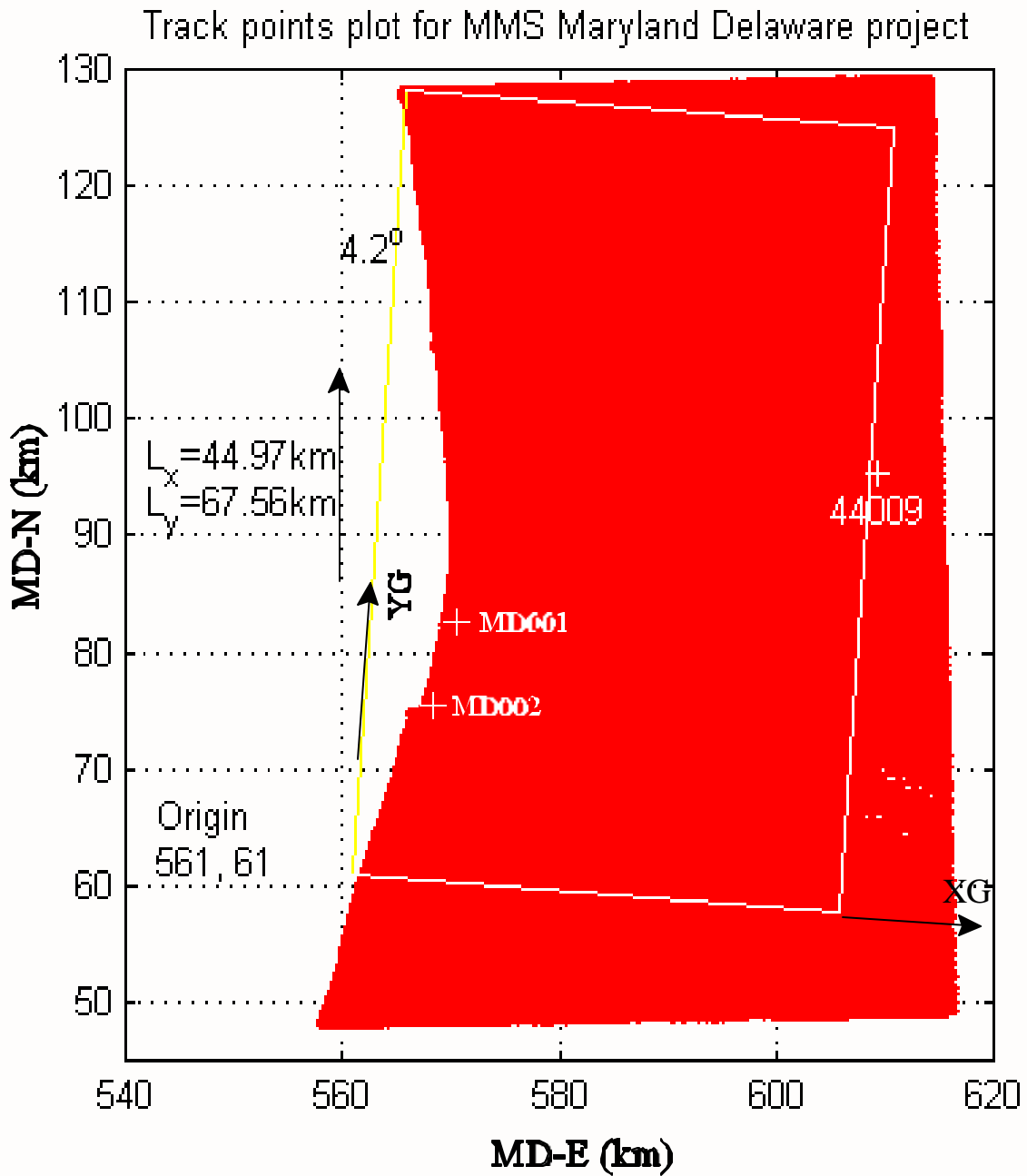


Fig. 2-1. A plot depicts the high density of Digital Bathymetric Data Points (red) and the Relationship between the Grid Coordinates (XG, YG) and the Maryland State Plane Coordinates(MD\_E, MD\_N)

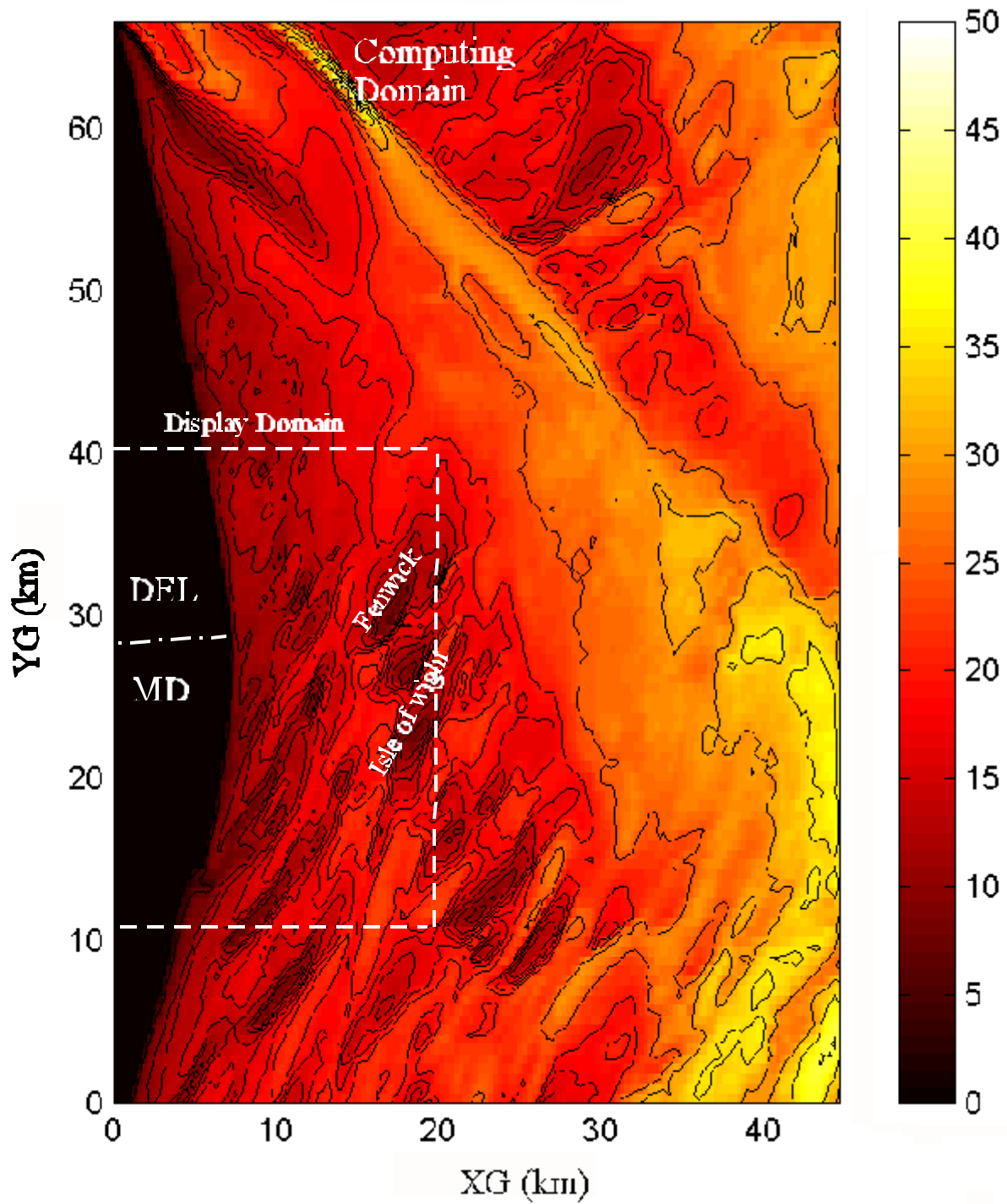


Fig. 2-2. Bathymetric Image of the Entire Computing Domain. The Computing Results will be displayed in a much smaller Display Domain marked by the white Dashed lines.

wave diffraction. The large computation domain is necessary to minimize the possible inaccurate boundary effects specified at the lateral boundaries for wave transformation simulation. For displaying the computation results, however, a much smaller domain is sufficient, hereafter called the display domain (Fig. 2-3), and marked as the dashed lines in Fig. 2-2. Detailed water depth contours at the vicinity of Fenwick Shoal and Isle of Wight Shoal are given in the display domain.

Two possible scenarios for dredging were considered. The first plan is targeted for a total removal of  $4 \times 10^6 \text{ m}^3$  of sand from the two shoals, *i.e.*,  $2 \times 10^6 \text{ m}^3$  of sand from each shoal. The purpose is to determine if a single harvest of the quantity of sand would result in an unacceptable impact. In this scenario, the dredging would be the same on both Fenwick and Isle of Wight Shoals. The NAD83 Maryland State Plane Coordinates for the four corners of the two modeled dredging sites are given in Table 2-1. The resulted bathymetry is depicted in Fig. 2-4.

The second scenario is to dredge at the two shoals with a possible maximum sand removal (*i.e.*, on the order of  $20 \times 10^6 \text{ m}^3$ ). This scenario is for the possible accumulative sand removal from the two shoals for about 10 years. The two possible dredging sites are drawn in Fig. 2-3. Site A is on Fenwick Shoal and site B is on Isle of Wight Shoal. The NAD83 Maryland State Plane Coordinates for the four corners of the two possible dredging sites are given in Table 2-2. The selection of these two dredging areas was rather arbitrary and was based on the geometry. It is suggested that it is better to flatten a shoal rather than to create a big hole on an otherwise flat area. The two modeled dredging areas will give a total of  $24.4 \times 10^6 \text{ m}^3$  sand if the dredging depth is selected as a uniform 3 meters within the domain. The comparison of bathymetry before and after dredging for the second plan is shown in Fig. 2-5 and 2-6.

Table 2-1. Corner Coordinates for the Modeled One-time Dredging.  
(Maryland State Plane Coordinates, NAD83, meters)

Item	Site A	Site B
Area	0.675 x 10 <sup>6</sup> m <sup>2</sup>	0.675 x 10 <sup>6</sup> m <sup>2</sup>
Volume	2 x 10 <sup>6</sup> m <sup>3</sup>	2 x 10 <sup>6</sup> m <sup>3</sup>
E (m)	579,600.250	580,301.938
N (m)	89,213.5391	81,892.4922
E (m)	580,469.813	581,458.563
N (m)	90,322.8359	82,760.1094
E (m)	580,899.563	581,739.938
N (m)	90,030.5781	82,358.4297
E (m)	580,013.063	580,630.188
N (m)	88,882.4141	81,447.2500

Table 2-2. Corner Coordinates for the Modeled Accumulative Dredging  
(Maryland State Plane Coordinates, NAD83, meters).

Item	Site A	Site B
Area	5.36 x 10 <sup>6</sup> m <sup>2</sup>	2.82 x 10 <sup>6</sup> m <sup>2</sup>
Volume	16 x 10 <sup>6</sup> m <sup>3</sup>	8.4 x 10 <sup>6</sup> m <sup>3</sup>
E (m)	578,406.0000	580071.0630
N (m)	88,298.5469	81889.3906
E (m)	581,607.3750	582308.5630
N (m)	92,705.9219	83820.7109
E (m)	582,123.0000	582634.3130
N (m)	91,535.0156	83205.1953
E (m)	579,939.2500	580428.6250
N (m)	88,286.2266	80750.1406

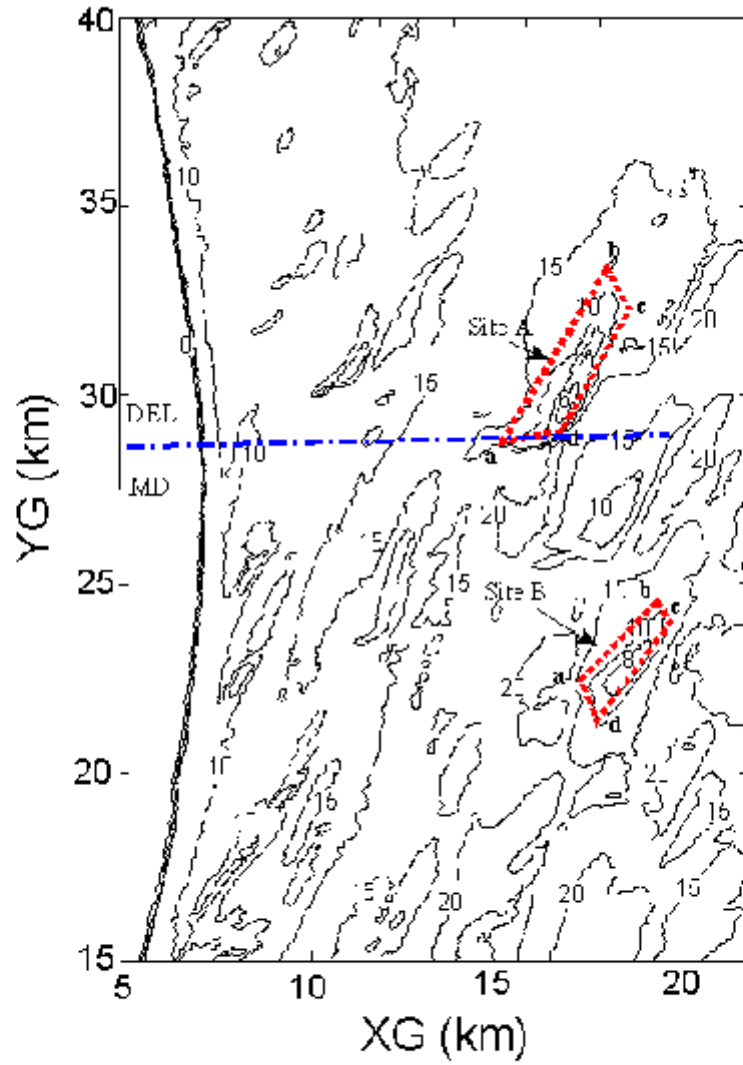


Fig. 2-3. Bathymetry Contours (in meter) for the Display Domain. The Modeled Extensive ( $24.4 \times 10^6 \text{ m}^3$ ) Dredging Sites are Marked by Red Dash Polygons.

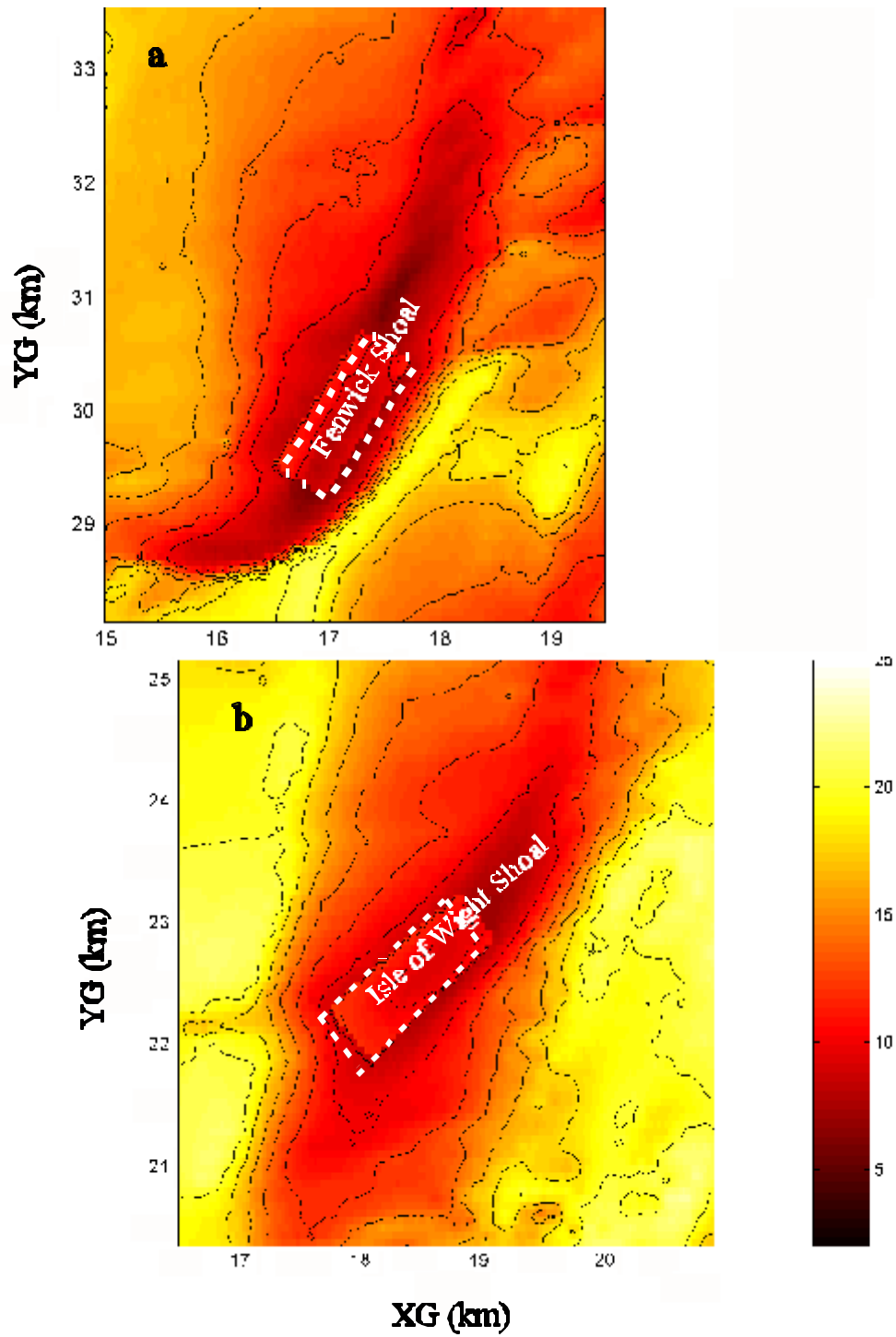


Fig. 2.4. Bathymetric Images after the One-time Dredging for  $2x$  and (b) Isle of Wight Shoal.

$10^6 \text{ m}^3$  (a) Fenwick Shoal,

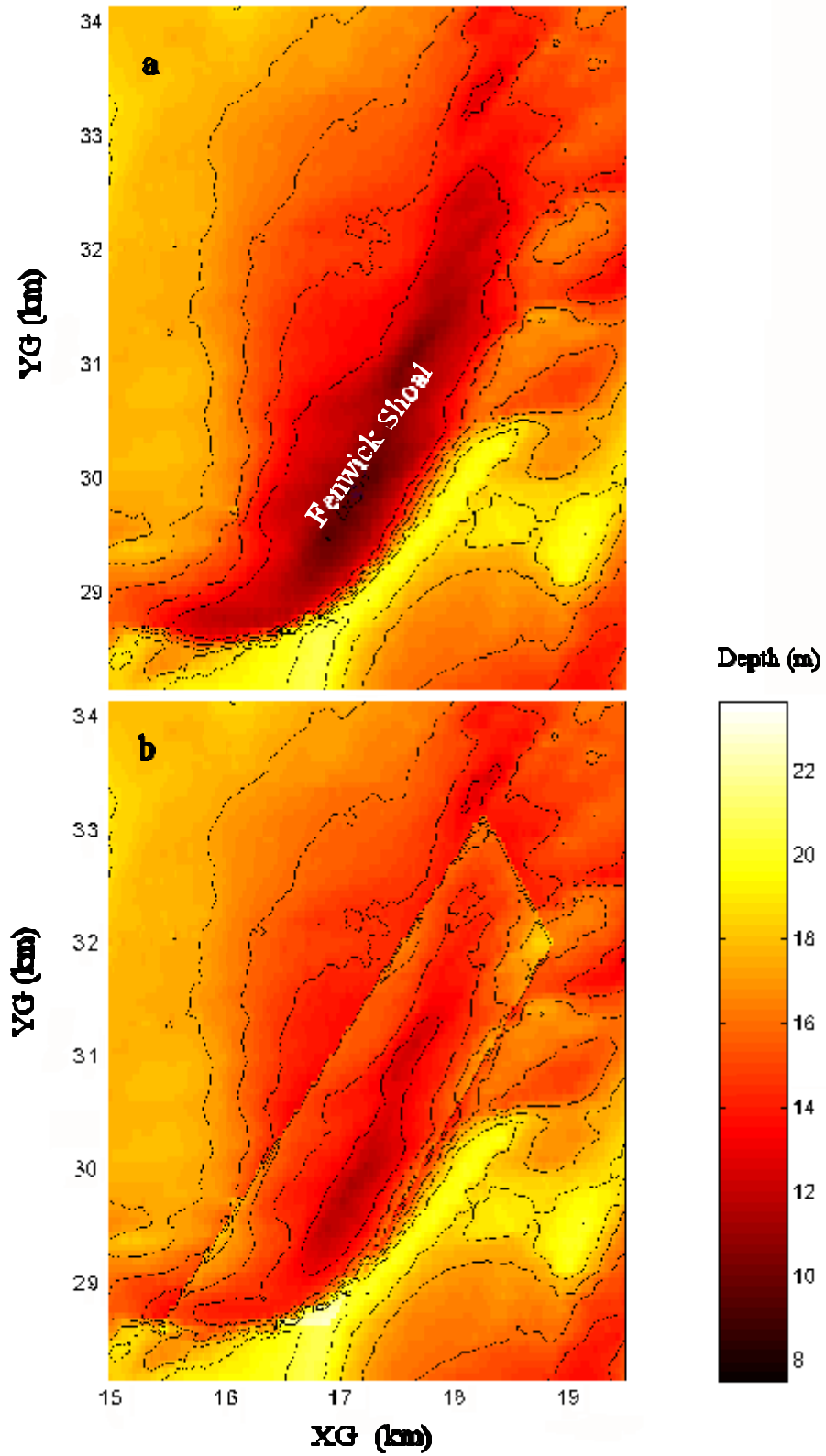


Fig. 2.5. Bathymetric Images at Fenwick Shoal. (a) original, (b) after the accumulative Dredging for  $16 \times 10^6 \text{ m}^3$ .

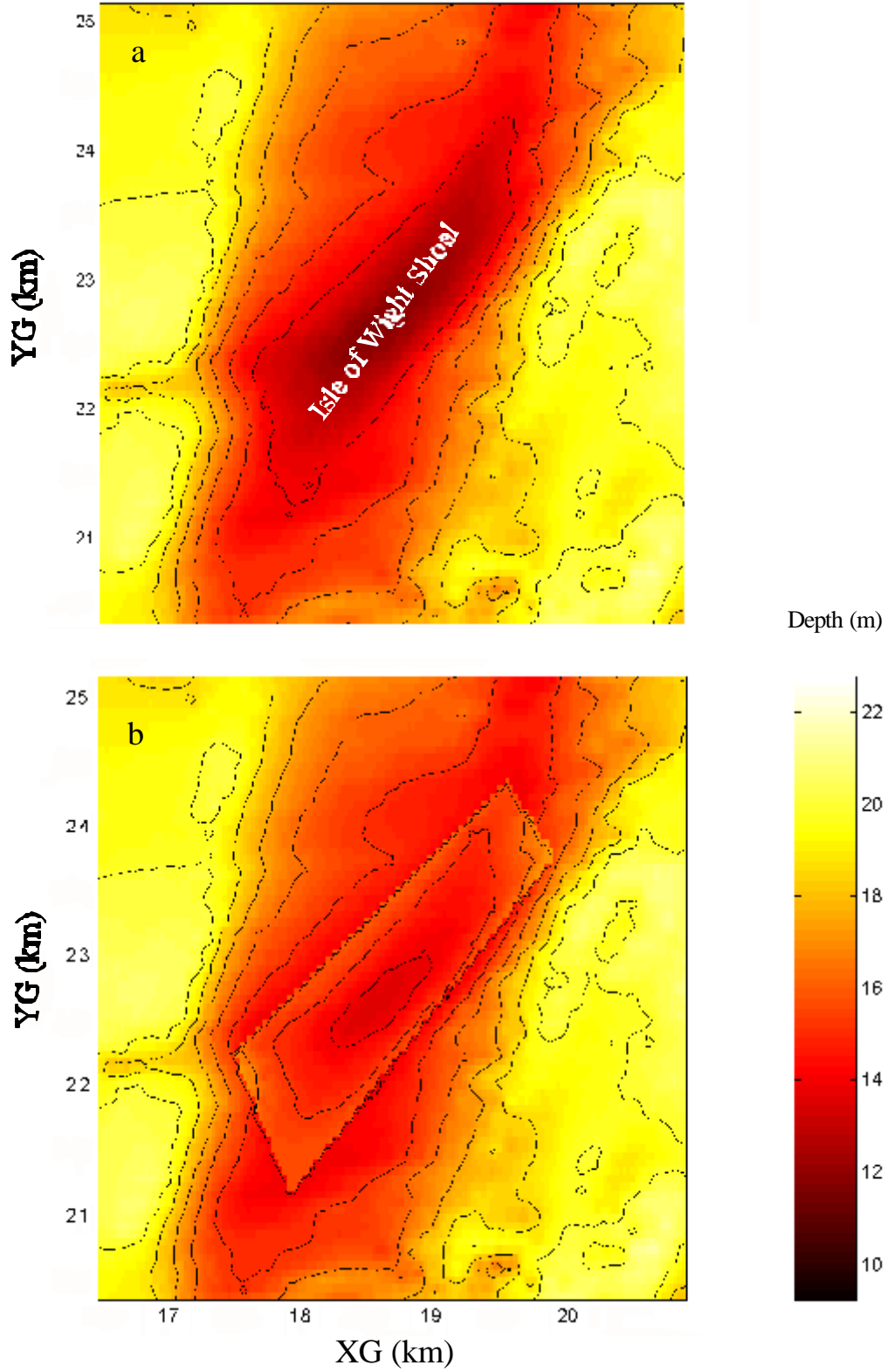


Fig. 2-6. Bathymetric Images at the Isle of Wight Shoal. (a) Original, (b) after Dredging for  $8.4 \times 10^6 \text{ m}^3$ .

### 2.3. Wave Data

The National Data Buoy Center (NDBC) has a moored buoy station, 44009 (Latitude 38°27'49"N and Longitude 74°42'07"W), located about 40 km offshore at the Ocean City with a water depth of 28 m. This station has collected wave height information since May 1986 and wave directional wave spectrum information since 1993. Because of the sites proximity (Fig. 2-1), these wave measurements are the most important wave information used in this study.

At a near shore site, the U.S. Army Corps of Engineers had one wave station, MD001, north of Ocean City, Maryland (Lat. 38°24'00"N, Long. 75°30'00"W) from Oct. 1993 to Jan. 1998. The Corps also has another station, MD002 (Lat. 38°20'24"N and Long. 75°04'12"W), south of Ocean City. The water depth at both stations is 9 m. Their locations also are given in Fig. 2-1.

The recent wave measurement system at station 44009 used an accelerometer to record the buoy's heave, pitch, and roll motions. A NDBC onboard Wave Data Analyzer computed the wave spectral information from the time series of buoy motion and transmitted the results to the Stennis Space Center in Mississippi for further analysis and quality assurance. The approach proposed by Longuet-Higgins *et al.* (1963) was used to obtain the wave spectral data. The overall accuracy of all systems for significant wave height, wave period, and wave direction is 0.2 m (or 5%), 1.0 s., and  $\pm 5^\circ$ , respectively (Meindl and Hamilton 1992). All processed data were achieved in National Oceanic Data Center (NODC) in Washington, D.C. using a special ASCII format. These data were stored in CD-ROM and are easily retrieved.

Wave measurements at the two near shore stations MD001 and MD002 were carried out with a pressure gauge to measure the surface displacements and a current meter to measure the two horizontal velocity components. Based on the linear wave theory, the directional wave spectrum can be calculated.

In this study, wave data at the two near shore stations are mainly used for checking the accuracy of calculated wave heights using the wave information (significant wave height, peak

wave period, and peak wave direction) specified at the offshore boundary where station 44009 is located. For example, wave records from Nov. 1 to Nov. 30, 1997 at both stations 44009, MD001, and MD002 are plotted in Fig. 2-7 to show the differences in wave conditions among the three stations. The comparison reveals that the significant wave heights (blue line and green line) at both the near shore stations are very close, at least for the November 1997. Only a minor difference (about 10 cm) observed in late November. The peak wave periods at the two near shore stations are also very close, except a short period of time in late November, 1997. Notice that in this selected period (November, 1997) the offshore wave height varies from less than 0.5 m to 5 m, which is sufficient for the purpose of calibrating the wave transformation model selected.

#### **2.4. Statistical Analysis**

The joint distribution of significant wave height and peak energy wave period for station 44009 (Fig. 2-8) reveals that the most frequently occurring wave has a period of 9 seconds and significant wave height of 0.6 meters. Wave height greater than 6 m is rare, only occurring few times during the entire 13 years of observation (1986-1998) with a total duration of 46 hours which is about 0.04 percent. The total duration of significant wave height greater than 5 meters increases to 94 hours (about 0.08 percent).

The available directional wave data (1993-1997) indicates that waves mainly come from the following 7 directions: SSE, SE, ESE, E, ENE, NE, and NNE (Figs. 2-9 and 2-10). A few large waves came from NNW and NW, which are ignored in this study because these are offshore-going waves.

Assuming the available wave directional information represents the true wave condition distribution, we can regroup the waves into selected bins for future analyses. For the practical and feasible computational purposes, wave height distribution is sorted from 0.25 to 8 m with an interval of 0.5 m, wave period distribution is sorted from 3 to 20 s with an interval of 2 s, and wave direction distribution is sorted for the 16 major directions. Using the above specified condition to sort the waves, a table of wave occurrence for the major 4 directions is given in

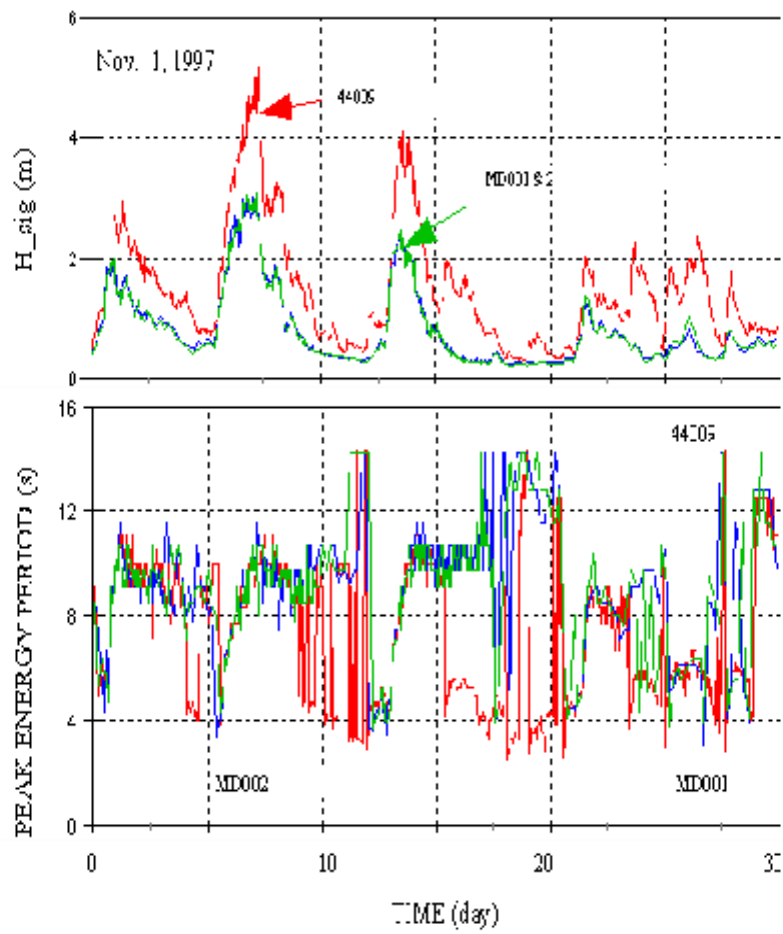


Fig. 2-7. Comparison of Measured Waves at Offshore (44009) and Nearshore (MD001 and MD002) from Nov. 1 to 30, 1997. (a)  $H_s$ ; (b) peak energy wave period.

Table 2-3 to Table 2-6. Notice that wave conditions in these four directions counted for more than 50 percent of all the wave conditions.

Table 2-7 shows the maximum significant wave heights that were observed at station 44009 from 1986 to 1998. The recorded maximum significant wave height (7.6 m with a peak wave period of 16.7 seconds, occurred on 1/04/92) during the 13 observation years suggests that the possible most severe sea probably can have a significant wave height of 8 m and wave period of 20 s. Notice that among the observed maximum  $H_s$ , only one is possibly induced by a hurricane (August 16, 1995). The famous “Halloween Storm,” also known as the “Perfect Storm,” in late October 1991 did not produce the largest significant wave height in 1991. This may be because of the different wind field location in the Atlantic Ocean. Along Virginia’s coast, the “Halloween Storm” did produce the largest wave at station CHLV2 in 1991.

## **2.5. Model Waves**

Based on the measurements at station 44009 and Table 2-1, we have identified the following four wave heights (2m, 4m, 6m, and 8m) and five wave periods (10s, 12s, 14s, 16s and 20s) that require analysis for possible changes in wave transformation due to dredging at the Fenwich Shoal and Isle of Wight Shoal. Short wave periods (less than 10 s) are excluded because they were not affected by the shoals. This selection covers the majority of the wave conditions that can be happened at the project site. We did not run a particular measured wave condition (for example, the most frequently occurring waves,  $T = 9$  s,  $H = 0.5$  m) because (1) the period is too short to be affected by the modeled dredging, and (2) we believe through checking the selected 60 wave conditions, all possible waves that might be affected by dredging were considered. Because of the stochastic nature of waves, we should examine all possible wave conditions, and that is why we selected 60 waves to represent the whole figure.

## **2.6. Wave Direction**

The available directional wave data indicate that large waves can come from the following seven directions: NNE, NE, ENE, E, ESE, SE, and SSE (Fig. 2-9). The orientation of the coast line at the Maryland and Delaware border is also given in the figure. Large waves coming from

NNE to ENE are mainly caused by northeasters. Long period waves coming from these two directions, however, are relatively rare (Fig. 2-10). Most of the waves in NNE and NE are less than 8 sec. Long period waves mainly come from ENE, E, ESE, and SE because of the long fetch. Thus, waves coming from ENE, E, ESE, and SE are selected as the important wave directions because of the possible large wave height and long period. Large and long waves coming from SSE direction must be induced by hurricane and the chance of this is relatively small, and thus, is not selected for study.

Table 2-3. The Height and Period Distribution for Waves Coming from ENE (8.600%)

H(m)	4s	6s	8s	10s	12s	14s	16s	>17s
0.5	0.1638	0.3545	0.3009	0.3515	0.3277	0.0596	0.0060	0.0
1.0	0.3128	0.9294	0.4737	0.5898	0.4975	0.0089	0.0	0.0
1.5	0.0834	0.5898	0.4290	0.5362	0.3634	0.0119	0.0	0.0
2.0	0.0	0.3426	0.3098	0.2800	0.1728	0.0149	0.0089	0.0
2.5	0.0	0.0715	0.1430	0.0983	0.0626	0.0119	0.0	0.0
3.0	0.0	0.0060	0.1370	0.1341	0.0626	0.0	0.0	0.0
3.5	0.0	0.0030	0.0715	0.0745	0.0387	0.0	0.0	0.0
4.0	0.0	0.0	0.0298	0.0298	0.0060	0.0	0.0	0.0
4.5	0.0	0.0	0.0030	0.0268	0.0030	0.0	0.0	0.0
5.0	0.0	0.0	0.0030	0.0060	0.0030	0.0	0.0	0.0
5.5	0.0	0.0	0.0	0.0030	0.0030	0.0	0.0	0.0
6.0	0.0	0.0	0.0	0.0119	0.0	0.0	0.0	0.0
6.5	0.0	0.0	0.0	0.0	0.0089	0.0	0.0	0.0
7.0	0.0	0.0	0.0	0.0	0.0030	0.0	0.0	0.0
E				2.1419	1.5522	0.1072	0.0149	0.0

Table 2-4. The Height and Period Distribution for Waves Coming from E (13.086%)

H(m)	4s	6s	8s	10s	12s	14s	16s	>17s
0.5	0.1013	0.4051	1.0962	0.9413	0.8073	0.2324	0.0447	0.0
1.0	0.2145	0.7328	1.1439	1.2333	0.9682	0.0923	0.0149	0.0
1.5	0.0238	0.3664	0.4647	0.6792	0.6643	0.1043	0.0	0.0
2.0	0.0030	0.1430	0.2353	0.4022	0.3485	0.2204	0.0119	0.0
2.5	0.0	0.0268	0.1698	0.2324	0.1549	0.0655	0.0209	0.0
3.0	0.0	0.0030	0.0923	0.1102	0.1341	0.0060	0.0	0.0
3.5	0.0	0.0	0.0238	0.1192	0.0715	0.0	0.0	0.0
4.0	0.0	0.0	0.0119	0.0298	0.0298	0.0	0.0	0.0
4.5	0.0	0.0	0.0	0.0149	0.0060	0.0030	0.0	0.0
5.0	0.0	0.0	0.0	0.0	0.0000	0.0060	0.0	0.0
5.5	0.0	0.0	0.0	0.0	0.0030	0.0	0.0	0.0
6.0	0.0	0.0	0.0	0.0	0.0030	0.0	0.0	0.0
6.5	0.0	0.0	0.0	0.0	0.0030	0.0	0.0	0.0
7.0	0.0	0.0	0.0	0.0	0.0	0.0	0.0	0.0
E				3.7625	3.1936	0.7299	0.0924	0.0

Table 2-5. The Height and Period Distribution for Waves Coming from ESE (13.709%)

H(m)	4s	6s	8s	10s	12s	14s	16s	>17s
0.5	0.0894	0.6792	2.3236	1.8499	0.9145	0.3575	0.0745	0.0
1.0	0.2234	0.6286	1.3554	1.1797	0.8996	0.1370	0.0298	0.0
1.5	0.0179	0.1966	0.3366	0.4468	0.4468	0.0923	0.0089	0.0
2.0	0.0	0.1072	0.2026	0.1817	0.1311	0.0566	0.003	0.0
2.5	0.0	0.0357	0.1102	0.0834	0.1013	0.0268	0.0	0.0
3.0	0.0	0.0030	0.0298	0.0477	0.0566	0.0030	0.0	0.0
3.5	0.0	0.0030	0.0030	0.0209	0.0417	0.0089	0.003	0.0
4.0	0.0	0.0	0.0	0.0149	0.0357	0.0060	0.0	0.0
4.5	0.0	0.0	0.0	0.0089	0.0387	0.0089	0.0	0.0
5.0	0.0	0.0	0.0	0.0030	0.0030	0.0089	0.0	0.0
5.5	0.0	0.0	0.0	0.0	0.0060	0.0	0.0	0.0
6.0	0.0	0.0	0.0	0.0	0.0030	0.0	0.0	0.0
6.5	0.0	0.0	0.0	0.0	0.0	0.0	0.0	0.0
7.0	0.0	0.0	0.0	0.0	0.0	0.0	0.0	0.0
E				3.8369	2.678	0.7059	0.1192	0

Table 2-6. The Height and Period Distribution for Waves Coming from SE (14.653%)

H(m)	4s	6s	8s	10s	12s	14s	16s	>17s
0.5	0.1221	1.2154	2.5172	1.6563	0.5392	0.2085	0.0328	0.0
1.0	0.2383	0.7596	1.8142	1.0456	0.7239	0.0685	0.0209	0.0
1.5	0.0179	0.2413	0.6703	0.4141	0.4319	0.1430	0.0209	0.0
2.0	0.0030	0.0923	0.3098	0.2949	0.1400	0.0626	0.0238	0.0
2.5	0.0	0.0209	0.0953	0.1400	0.0804	0.0328	0.0209	0.0030
3.0	0.0	0.0030	0.0179	0.0417	0.0655	0.0149	0.0030	0.0030
3.5	0.0	0.0030	0.0060	0.0268	0.0864	0.0149	0.0030	0.0
4.0	0.0	0.0	0.0030	0.0030	0.0417	0.0328	0.0	0.0
4.5	0.0	0.0	0.0060	0.0030	0.0179	0.0060	0.0	0.0
5.0	0.0	0.0	0.0	0.0	0.0	0.0	0.0	0.0
5.5	0.0	0.0	0.0	0.0	0.0	0.0	0.0	0.0
6.0	0.0	0.0	0.0	0.0	0.0	0.0	0.0	0.0
E				3.6254	2.1269	0.584	0.1253	0.0060

Table 2-7. Observed Annual Maximum Significant Waves

Date	Time	H_significant (m)	T_Peak (sec)
12/03/86	08:00	4.7	12.5
01/02/87	08:00	5.9	11.1
4/08/88	04:00	4.3	9.1
2/24/89	17:00	5.4	11.1
10/26/90	18:00	4.6	10.0
11/10/91	03:00	4.9	9.1
01/04/92	11:00	7.6	16.7
10/27/93	12:50	4.6	11.1
12/23/94	19:50	5.4	12.5
8/16/95	10:50	4.2	14.3
01/08/96	04:00	7.0	11.1
11/08/97	06:00	5.2	11.1
2/05/98	16:00	7.4	12.5

Table 2-8. Selected Model Waves

Wave Height (m)	Wave Period (sec)	Remark
8.0	20	The most severe sea
6.0	16	Severe sea
4.0	14	Rough sea
2.0	12	Northeaster
	10	



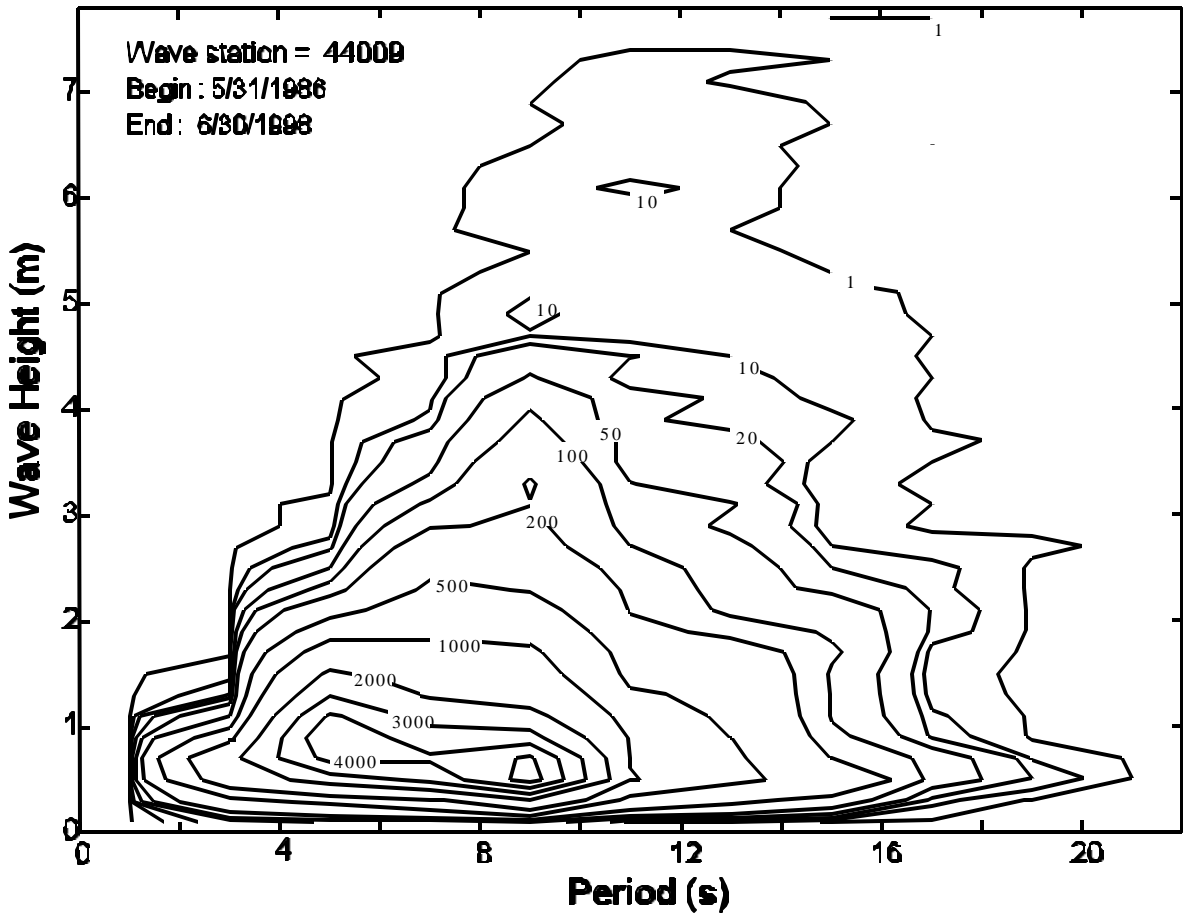
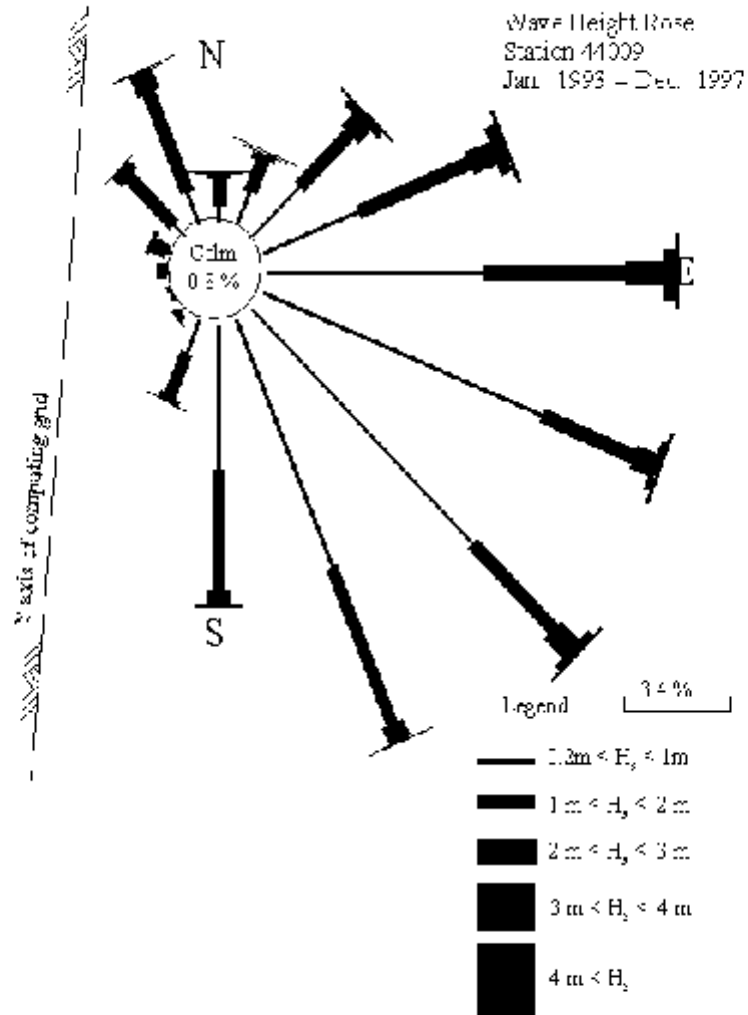


Fig. 2-8. Significant Wave Height and Peak Energy Wave Period Joint Distribution at Sation 44009.



3

Fig. 2-9. Significant Wave Height Rose at Station 44009. The scale of 3.4% occurrence is plotted in the legend.

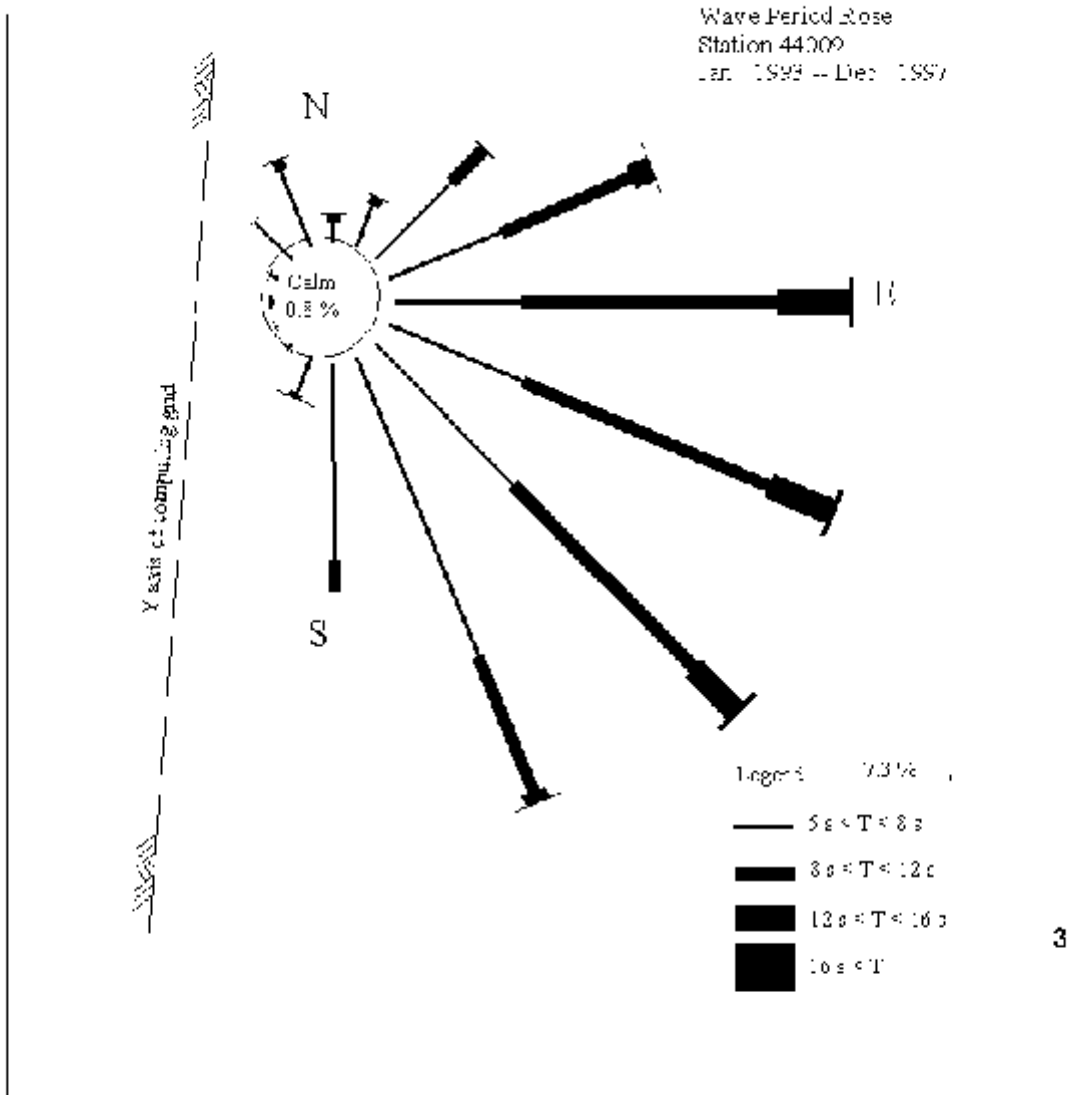


Fig. 2-10. Peak Energy Wave Period Rose at Station 44009. The scale of 7.3% occurrence is plotted in the legend.

## CHAPTER 3, SELECTION OF WAVE MODELS

### 3.1. Introduction

There are many numerical models for simulating water waves. In general, they can be divided into two categories: (1) Wave hindcast/prediction models (*e.g.*, SWAN, HISWAP, NSW in Mike 21, and STWAVE) and (2) Wave transformation models (*e.g.*, RCPWAVE, REF/DIF-1, REF/DIF-S, RDES, and EMS module in Mike 21). Models in the first category are designed for wave predictions. Although they are intended to provide accurate predictions at near shore areas by including some of the wave transformation processes (*e.g.*, shoaling, refraction, bottom friction), they cannot include all (*e.g.*, diffraction, reflection, resonance), and thus, the accuracy of these models is limited in the near shore. Models in the second category are designed to simulate wave transformation processes, and thus, they don't have the capability to simulate wave growth, white capping, and wave-wave interactions. Thus, the use of models in the second category is limited to the conditions in which wave growth is not important, *i.e.*, the wind is not strong or the study domain is not large enough to produce significant wave growth.

Even in the second category, not all the models have the same capability. For example, REF/DIF-1 and RCPWAVE deal with a much simple conditions (monochromatic waves, no wave reflection, and weak diffraction) but with an excellent computing efficiency. Others deal with all the five major wave transformation processes but at the cost of high computing time. A preprint of comparison of six selected wave transformation models (Maa *et al.*, in press) is given in Appendix I. The following are brief descriptions of each available model. The key features are summarized in Tables 3-1 and 3-2.

### 3.2. SWAN

The SWAN (Simulating WAVes Nearshore) model computes random, short-crested, wind-generated waves in coastal regions and inland waters (Booij *et al.* 1996; Holthuijsen *et al.* 1997). This model solves the following equation:

$$\frac{M/V}{M_T} \% \frac{M/C_x}{M_V} \% \frac{M/C_y}{M_V} \% \frac{M/C_{\hat{u}}}{M_{\hat{u}}} \% \frac{M/C_{\hat{e}}}{M_{\hat{e}}} \quad , \quad S/\zeta \quad (3-1)$$

with

$$N(t, x, y, \theta, \omega) = E(t, x, y, \theta, \omega) / (\omega \cdot k \cdot V) \quad (3-2)$$

where  $N$  is the spectral action density (energy density,  $E$ , divided by absolute frequency,  $\omega$ ),  $t$  is time,  $x$  and  $y$  are two horizontal directions,  $\theta$  is spectral wave direction,  $c_x$  and  $c_y$  are energy propagation speed in  $x$  and  $y$  directions, respectively,  $c_\theta$  and  $c_\omega$  are energy propagation speed in  $\theta$  and  $\omega$  domain, respectively,  $\sigma = [gk \tanh(kd)]^{1/2}$  is the intrinsic frequency,  $g$  is the gravitational acceleration,  $k$  is wave number,  $d$  is water depth, and  $S$  is the summation of energy source and sink terms representing the effects of wind energy input,  $S_i$ , bottom friction,  $S_f$ , white capping,  $S_c$ , breaking dissipation,  $S_b$ , as well as wave-wave interactions,  $S_w$ . Details of each source and sink terms are not presented here, but it would be an important item that affect the performance of SWAN model. Although this equation is a first order partial differential equation, there are five variables ( $t, x, y, \theta, \omega$ ) to deal with, and thus, it is very time consuming.

The current SWAN model is Cycle 2 with version 30.62. It accounts for the following physic processes: (1) Wave propagation in time and space, (2) Shoaling, (3) Refraction due to current and depth, (4) frequency shifting due to currents and non-stationary depth, (5) Wave generation by wind, (6) Three- and four-wave interactions, (7) White capping, bottom friction, and depth-induced breaking. SWAN computations can be made on an evenly spaced Cartesian grid system or a curvilinear grid system. Because it is an energy redistribution approach, the grid size can be large, on the order of half wave length ( $L/2$ ). Even with this relatively large grid size, however, the computing time is still formidably long because of the complexity of Eq. 1. For this reason, we can not afford to use it at this time.

A major drawback of this model is the lack of capability to resolve wave diffraction process (Kaihatu *et al.*, 1998). Under the first category of wave model, however, SWAN is the most advanced and up-to-date model mainly because of the inclusion of wave evolution, and most accurate source/sink terms. The question of “How significant is the limitation caused by not having the capability to include wave diffraction,” needs more study. Also the relevance and significance of each source and sink term should be examined and compared with other similar models (*e.g.*, HISWA, STWAVE).

### 3.3. HISWA (Cycle 2)

Unlike the SWAN model, HISWA uses a parametrization process on the frequency domain to reduce the huge computing time required for SWAN model (Holthuijsen *et al.*, 1997). The parametrization is formulated in the zero and first order of moment of spectrum in each spectral direction. Let the n-th order of moment of spectrum defined as

$$m_n(\hat{e}) = \int_0^{2\pi} \int_0^{2\pi} \int_0^{2\pi} \int_0^{2\pi} \hat{u}^n N(\hat{u}, \hat{e}) d\hat{u} \quad (3-3)$$

Integrate Eq. 1 in frequency domain, one will get the evolution equation for the zero-order moment of the action density spectrum.

$$\frac{Mm_o}{Mt} \% \frac{Mc_x^* m_o}{Mx} \% \frac{Mc_y^* m_o}{My} \% \frac{Mc_{\hat{e}}^* m_o}{M\hat{e}} = S_o \quad (3-4)$$

where  $c_x^*$  and  $c_y^*$  are the propagation speed of zero-order moment in x and y directions, respectively,  $c_{\hat{e}}^*$  is the propagation speed of zero-order moment in the direction domain,  $S_o$  is the sum of generation and dissipation of  $m_o$ . Notice that  $c_x^*$ ,  $c_y^*$ , and  $c_{\hat{e}}^*$  can only be estimated at the mean frequency.

Multiple  $\hat{u}$  and Eq. 1, then integrate in the frequency domain and one will get the evolution equation for the first-order moment of the action density spectrum.

$$\frac{Mm_1}{Mt} \% \frac{Mc_x^+ m_1}{Mx} \% \frac{Mc_y^+ m_1}{My} \% \frac{Mc_{\hat{e}}^+ m_1}{M\hat{e}} = c_{\hat{u}}^*(m_o) \% S_1 \quad (3-5)$$

where  $c_x^+$  and  $c_y^+$  are the propagation speeds of first-order moment in x and y directions, respectively,  $c_{\hat{e}}^+$  is the propagation speed of first-order moment in the direction domain;  $c_{\hat{u}}^* m_o$  represents the effect of time variations in currents and depth on the mean frequency; and  $S_1$  is the sum of generation and dissipation of  $m_1$ . Similarly,  $c_x^+$ ,  $c_y^+$ , and  $c_{\hat{e}}^+$  can only be estimated at the mean frequency.

Solving Eqs. 4 and 5 is the main body of the HISWA (Cycle 2) model: Inasmuch as the equation use the central frequency propagation speed to represent all frequency bands, errors can result if there is more than one energy peak in the wave spectrum. The positive side of this approach is that the computer time is significantly reduced, compared with that of the SWAN model. The HISWA model also suffers the same drawback that it cannot address wave diffraction accurately.

### 3.4. STWAVE

The STWAVE model was developed on a series of studies carried out by Resio (1987, 1988) and Resio and Perrie (1989). The first two characters, “ST,” stand for the steady state, and thus, there is no local time derivative term in Eq. 6. For this reason, this model does not provide information on wave evolution. It only provides wave condition under the fully developed condition. Two important features of this model are (1) a depth independent equilibrium range of a wind wave spectrum in shallow water and (2) a limitation on the growth of spectral peak frequency. In a coordinate system moving with the group velocity of the spectral peak, the governing equation for the redistribution of the spectrum energy is approximated as

$$c_{gx} \frac{ME(\hat{u}, \hat{e})}{M_x} \% c_{gy} \frac{ME(\hat{u}, \hat{e})}{M_y} \cdot S \quad (3-6)$$

where  $E(\hat{u}, \hat{e})$  is the energy spectrum in frequency and direction space. Here,  $S$  is the sum of source and sink terms including shoaling, refraction, wind energy input, wave-wave interactions, bottom friction loss, and wave breaking.

As the waves propagate toward the coast with all the effects from source and sink terms, Eq. 6 gives energy spectra at each grid point. Because of the assumption of steady state as well as the moving with the spectral center, the computational speed of STWAVE is fast. The accuracy, compared with other similar models, is not clearly documented at this time yet.

Table 3-1. Comparison of Wave Prediction Models

Model	SWAN	HISWA (cycle2)	STWAVE
Wave direction spreading	+180°--180°	+180°--180°	+60°--60°
Multiple peak frequency	Yes	No	No
Wave growth	Yes	Yes	No
Shoaling	Yes	Yes	Yes
Diffraction not having an accurate approximation yet			
Reflection	No	No	No
Resonance	No	No	No
Grid size	# L/2	# L/2	# L/2
Bottom friction	Yes	Yes	yes
White Cap	Yes	Yes	Yes
Current Effect	Yes	No	No

Notice that the directional spread is limited in the STWAVE model, wave energy only can transferred within  $\pm 60$  degrees from the main direction. A full spectrum model, however, should allow energy transfer for  $\pm 180$  degrees.

Although all the aforementioned models have the source/sink terms specified in the energy distribution equation, they do not necessarily use the same function for each possible source (*e.g.*, wind energy input) or sink (*e.g.*, white capping). The different selection may affect their accuracy.

We foresee that the differences among the three above models should not be significant for a narrow band, fully developed wave spectrum. For a spectrum with multiple peaks and developing sea, the SWAN model should be a better model. The critical issue is that a comprehensive comparison

should be carried out first to understand the accuracy of the models, so that each model will be used in its best application

### 3.5. RDE

With the previous support from MMS, we developed a wave transformation model by solving the Elliptic governing equation directly (RDE, Maa and Hwung, 1997). This model provides accurate information on wave height and direction distribution, but with a cost of long computing time (when compared with REF/DIF-1 or RCPWAVE). The computing speed actually is better than most of the models that solves the elliptic equation (Maa *et al.*, in press).

This model solves the extended mild slope equation given by Massel (1995):

$$\frac{M^2 \ddot{\phi}}{M_x^2} + \frac{M^2 \ddot{\phi}}{M_y^2} + \frac{e_0}{h} \left( \frac{Mh}{M_x} \frac{M \ddot{\phi}}{M_x} + \frac{Mh}{M_y} \frac{M \ddot{\phi}}{M_y} \right) + k^2 \left( 1 + \phi + \frac{i f_d}{n \sigma} \right) \ddot{\phi} = 0 \quad (3-7)$$

where  $\phi$  is the velocity potential function for a simple harmonic wave flow,  $e_0$  is a function affected by wave number ( $k = 2\delta/L$ ) and local water depth,  $h$ ,  $L$  is local wave length,  $\phi$  is a correction term for steep bed slope and bed curvature,  $i = (-1)^{1/2}$ ,  $f_d$  is a friction coefficient,  $\sigma = 2\delta/T$  is wave frequency,  $n = 0.5[1 + 2kh/\sinh(2kh)]$ ,  $Mh/M_x$  and  $Mh/M_y$  are bottom slopes in the  $x$  and  $y$  directions, respectively, and  $x$  and  $y$  are the two horizontal coordinates.

As mentioned before, in addition to simulate wave shoaling, refraction, and bottom energy loss, the RDE is capable of simulating strong wave diffraction and wave reflection. The last two features may not be needed for studies along an open coast, but the accurate wave direction information is a baseline for comparison with other models.

Inasmuch as the model lacks a method for incorporating wave-wave interaction in Eq. 6, wind energy input and white capping energy loss cannot be included in this kind of model even though the calculation of each frequency band can be performed separately and then combined together to study spectrum transformation. This is because wind energy input and white capping energy loss mainly occur in the high frequency domain, and only through wave-wave interactions, the energy can be transferred across each frequency band.

### 3.6. REF/DIF-S

Using a parabolic approximation (Radder, 1979) to simplify Eq. 6, Kirby and Dalrymple (1991, 1994) presented the REF/DIF-1 model for monochromatic waves. This model, however, is capable of simulating only wave shoaling, refraction, and weak diffraction. Based on the same principle as monochromatic waves, this model cuts the wave spectrum into many frequency bands and determines a representative wave height for each band. Kirby and Ozkan (1994) then computed wave refraction and diffraction for each component band and re-constructed the wave spectrum after all frequency bands were calculated. For this reason, wave-wave interactions and wind energy input cannot be incorporated in REF/DIF-S. Nevertheless, a model to simulate part of the spectrum wave transformation was introduced as REF/DIF-S.

The above information clearly indicates that REF/DIF-S, and RDE are mainly wave transformation models with no capability to simulate wave growth. On the other hand, SWAN, HISWA (cycle 2), and STWAVE are mainly wave prediction models with limited capability to simulate wave transformation. They all are capable of giving wave spectra in coastal seas.

Since there are other simple wave transformation models available (*i.e.*, REF/DIF-1 and RCPWAVE), it would be worthwhile to investigate whether or not these simple models can do the job reasonably well. In our previous study (Maa *et al.*, in press), we found that overall performance of RCPWAVE model is not accurate, and thus, discarded from this study. Although REF/DIF-1 is not good in modeling wave direction, its accuracy in wave height calculation is excellent. Because a simple model (*i.e.*, REF/DIF-1) does not require tremendous computing time, it allows us to model many wave conditions. For this reason, we carried out an experiment to check the applicability of REF/DIF-1. Before the experiment, however, a briefing of REF/DIF-1 is given first.

### 3.7. REF/DIF-1

Radder (1979) developed a parabolic approximation of Eq. 3 which had several advantages over the original elliptic equation. First, the down-wave end boundary conditions is not needed for a parabolic equation. This implies the REF/DIF-1 model cannot simulate a process that has reflected

waves. Second, the computing efficiency is high for a parabolic equation, and the required grid size can be relatively large (less than one-fifth-wave length). For these reasons, the parabolic approximation of Eq. 3 has prevailed for simulating wave transformation on open coasts, where wave reflection is negligibly small and only weak diffraction exists.

A drawback of parabolic approximation is that the wave propagation direction can not deviate too much from the assumed direction (usually the x-axis of the grid system). When they developed the model REF/DIF-1, Dalrymple and Kirby (1991) had a special technique to insure that the model is stable if the calculated wave angle is less than 60 degrees off from the x-axis.

Three important advantages of this model that deserve mention are (1) the fast computing speed because of the full implicit scheme, (2) the high stability for waves propagating less than 60 degrees off the x-axis, (3) the inclusion of various type of energy loss (*e.g.*, bottom friction) as well as tidal current effects on wave transformation, and (4) a choice of weak non-linear wave models.

Two important disadvantages of using this model are (1) the calculated wave direction is not correct, and therefore, not usable, (2) it only deals with regular monochromatic waves.

In summary, we selected using the REF/DIF-1 model over others because of the following reasons:

1. The spectrum models used for wave prediction do not have the capability to simulate combined wave diffraction and refraction, which are the major effects that should be considered for our study: dredging at shoals.
2. The spectrum model that can simulate combined wave diffraction and refraction, *i.e.*, REF/DIF-S, actually runs REF/DIF-1 many times by considering the major contribution from the major direction, period, and wave heights with minor contributions from other frequencies, directions, and heights. Instead of doing that for few selected wave conditions, we broke it down by doing 60 wave conditions, so we can see the differences between pre- and post dredging and between different wave conditions more clearly.

3. When dealing with each component wave, the REF/DIF-1 is a very accurate wave transformation model for wave energy distribution.
4. The concern of over/under prediction by using REF/DIF-1 is not necessary because we are dealing with each component of a wave spectrum. The random sea is surely better represented using a wave spectrum, but each component's behavior still can be modeled accurately using a monochromatic wave model.

Table 3-2. Comparison of Wave Transformation Models

Model	REF/DIF-1	REF/DIF-S	RDE
Refraction	Yes	Yes	Yes
Diffraction	weak	Weak	Yes
Shoaling	Yes	Yes	Yes
Reflection	No	No	Yes
Resonance	No	No	Yes
Grid size	# L/5	# L/5	# L/10
Bottom friction	Yes	yes	Yes
Current effect	Yes	Yes	No
Computing speed	Excellent	Fair	Fair
Accuracy	Good*	Good*	Excellent

\*Excellent in wave height, not good in wave direction

### 3.8. Calibration of REF/DIF-1

In this model, there are choices on using (1)linear wave, Hedged weak non-linear, or stoke non-linear wave model; (2) selecting bottom friction type of laminar, percolation, and turbulent wave boundary; (3) selecting a pass-through or reflection lateral boundary conditions.

To address the first possible choice, we tried the three possible options on two wave conditions. The results from the second possible choice, *i.e.*, Hedged weak non-linear wave model, provide the closest match with observations at station MD001. Thus, for all other computations, we used this option.

To allow oblique incident waves, or normal incident waves which changed their direction while propagating toward the coast line, to pass-through the lateral boundary without causing reflection, the passing-through boundary condition was selected for all the tests. The lateral dimension on the computing grid was also selected to be large enough (67.56 km) to avoid any possible influence by the imperfect boundary conditions implemented in the numerical scheme. These two processes take care of the third option.

It is well documented that bottom friction caused by turbulent wave boundary is the major source of energy loss among the three possible selections (*e.g.*, Maa and Kim, 1992). It is also documented that one should test the model by using different wave friction factors in order to match the predictions and observations (Maa and Wang, 1995). In summary, the reasons to conduct the calibration of a wave transformation are summarized as follows.

1. We want to make sure that the selected wave model can simulate the wave transformation processes that are critical for the objective. Only through calibration, will we be able to know if the selected model has been set up properly. Any bug in the application of the selected computer model can be removed, assuring correct results.
2. After we know the model results are accurate, then we can interpret the shoreline responses based on wave energy distribution. For example, the severe beach erosion on the south of Ocean City has been noticed 100 years ago. This severe erosion correlates very well with the model's calculated relatively large waves in that area.
3. Application of any model requires acceptance of many assumptions, including select a proper value for bottom friction. The calibration process provides the ability to apply rational selected as opposed to arbitrary values.
4. Calibration is a form of quality control. Verification of model's results against measurements contributes to the confidence with which we view the work and to the credibility with which others can attach to the results.

In this study, we arbitrarily selected a month (Nov. 1 - 30, 1997, Fig. 2-10) to calibrate the bottom friction coefficient.

To calibrate a wave transformation model's performance, we need input wave conditions specified at the offshore boundary of the computing domain as well as wave measurements at near shore stations. Wave measurements at Station 44009 and MD001 were selected to serve this purpose. The coordinates of MD001 were translated to grid locations and wave heights calculated at all the nine neighboring grid points were averaged to compare with the measurements.

Even within one month, there are too many wave conditions to calculate if all the measured data were used directly. For this reason, we have to idealize the wave conditions according to the regroup process given in Chapter 2 to find a time series of representative wave conditions for model calibration. After regrouping the wave conditions that actually were observed at Station 44009, we have 113 wave conditions (Table 3-3) based on different significant wave height (with 0.5 m interval), wave period at the peak frequency of wave spectrum (with 2 s interval), and the wave direction at the peak frequency of wave spectrum (with 22.5 degrees interval). Using these 113 wave conditions, a time series of idealized wave conditions at the offshore boundary can be obtained (Fig. 3-1). Because waves that travel away from shore are excluded in this comparison, some data are excluded, and thus, the time series is not a continuous line. The calculated and observed wave height time series at Station MD001 also are plotted in Fig. 3-1. As a result of trial and error, we found that when the wave friction factor is selected as 0.02, the calculated and measured wave heights matched the best

Considering that the significant wave height is a widely accepted parameter to represent wave severity, a comparison given in Fig. 3-1 demonstrates that even the simple model (REF/DIF-1) performs well in wave height. Since the sediment transport modeling is based only on the breaking wave heights, not the breaking wave spectra, to estimate alongshore sediment transport, this study demonstrates that the REF/DIF-1 is sufficient to do the job.

In the selected calibration period (Nov. 1-30, 1997), the maximum significant wave height at the offshore boundary was five meters. This is not large enough to include the possible most severe sea ( $H_s = 8$  m), but is close to the severe sea condition ( $H_s = 6$  m), thus, the calibration is considered sufficient.

Table 3-3. Wave Conditions Used for Calibrating REF/DIF-1

Hs (m)	T (s)	Dir. (Deg)	Surge (m)	Hs (m)	T (s)	Dir. (Deg)	Surge (m)	Hs (m)	T (s)	Dir. (Deg)	Surge (m)
2.00	10.00	45.00	1.0	1.00	10.00	157.50	1.0	1.00	10.00	157.50	1.0
2.00	6.00	67.50	1.0	1.00	8.00	157.50	1.0	1.00	8.00	157.50	1.0
2.00	10.00	135.00	1.0	1.00	4.00	157.50	1.0	1.00	4.00	157.50	1.0
5.00	10.00	45.00	2.0	2.00	8.00	135.00	1.0	0.50	10.00	112.50	1.0
5.00	12.00	67.50	2.0	2.00	10.00	157.50	1.0	0.50	12.00	112.50	1.0
5.00	10.00	67.50	2.0	2.00	8.00	157.50	1.0	0.50	12.00	112.50	1.0
4.50	10.00	67.50	2.0	2.00	10.00	22.50	1.0	0.50	14.00	112.50	1.0
4.50	10.00	45.00	2.0					0.50	10.00	45.00	1.0
4.00	10.00	45.00	2.0					0.50	10.00	67.50	1.0
4.00	8.00	45.00	2.0					0.50	14.00	67.50	1.0
4.00	10.00	67.50	2.0					0.50	12.00	67.50	1.0
4.00	8.00	67.50	2.0					0.50	10.00	67.50	1.0
3.50	10.00	45.00	1.5	1.50	10.00	45.00	1.0	0.50	14.00	90.00	1.0
3.50	8.00	45.00	1.5	1.50	8.00	45.00	1.0	0.50	12.00	90.00	1.0
3.50	12.00	67.50	1.5	1.50	4.00	45.00	1.0				
3.50	10.00	67.50	1.5	1.50	12.00	67.50	1.0				
3.50	8.00	67.50	1.5	1.50	10.00	67.50	1.0				
3.50	10.00	90.00	1.5	1.50	8.00	67.50	1.0				
3.50	8.00	90.00	1.5	1.50	6.00	67.50	1.0				
3.00	10.00	45.00	1.5	1.50	4.00	67.50	1.0				
3.00	8.00	45.00	1.5	1.50	10.00	112.50	1.0				
3.00	12.00	67.50	1.5	1.50	10.00	135.00	1.0	0.50	10.00	90.00	1.0
3.00	10.00	67.50	1.5	1.50	8.00	135.00	1.0	0.50	12.00	135.00	1.0
3.00	8.00	67.50	1.5	1.50	12.00	157.50	1.0	0.50	10.00	135.00	1.0
3.00	12.00	90.00	1.5	1.50	10.00	157.50	1.0	0.50	12.00	157.50	1.0
3.00	10.00	90.00	1.5	1.50	8.00	157.50	1.0	0.50	10.00	157.50	1.0
3.00	12.00	157.50	1.5	1.50	10.00	22.50	1.0	0.50	10.00	22.50	1.0
3.00	10.00	22.50	1.5	1.00	8.00	22.50	1.0	0.50	8.00	112.50	1.0
2.50	12.00	112.50	1.5	1.00	6.00	22.50	1.0	0.50	8.00	135.00	1.0
2.50	10.00	112.50	1.5	1.00	4.00	22.50	1.0	0.50	6.00	22.50	1.0
2.50	10.00	45.00	1.5	1.00	4.00	22.50	1.0	0.50	4.00	22.50	1.0
2.50	6.00	45.00	1.5	1.00	12.00	45.00	1.0	0.50	6.00	45.00	1.0
2.50	12.00	67.50	1.5	1.00	10.00	45.00	1.0	0.50	6.00	45.00	1.0
2.50	10.00	67.50	1.5	1.00	10.00	45.00	1.0	0.50	4.00	45.00	1.0
2.50	8.00	67.50	1.5	1.00	8.00	45.00	1.0	0.50	4.00	135.00	1.0
2.50	6.00	67.50	1.5	1.00	6.00	45.00	1.0	0.50	4.00	157.50	1.0
2.50	12.00	90.00	1.5	1.00	4.00	45.00	1.0				
2.50	10.00	90.00	1.5	1.00	12.00	112.50	1.0				
2.50	12.00	135.00	1.5	1.00	10.00	112.50	1.0				
2.50	10.00	135.00	1.5	1.00	8.00	112.50	1.0				
2.50	12.00	157.50	1.5	1.00	6.00	112.50	1.0				
2.50	10.00	157.50	1.5	1.00	4.00	112.50	1.0				
2.50	10.00	22.50	1.5	1.00	10.00	135.00	1.0				
2.00	6.00	45.00	1.0	1.00	8.00	135.00	1.0				
2.00	12.00	45.00	1.0	1.00	12.00	157.50	1.0				

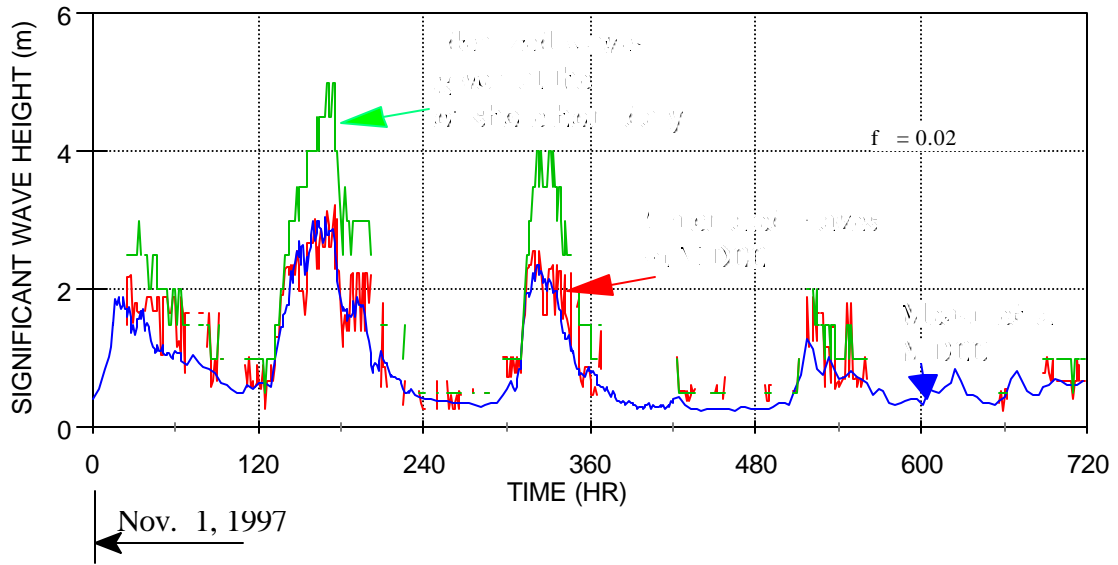


Fig. 3-1. Comparison of REF/DIF-1 Calculated and Measurements Hs at MD001 Using Idealized Wave Conditions at Offshore Boundary and Wave Friction Factor  $f = 0.02$ .



## CHAPTER 4. WAVE TRANSFORMATION FOR THE ORIGINAL BATHYMETRY

### 4.1. Introduction

In order to obtain a baseline for estimating the possible impact of dredging for sand resources at the two offshore shoals, We calculated wave transformation for the original bathymetry first. The details of calculated conditions and results are given in this chapter. A proposed criterion for deciding the impact would be positive or negative is presented at the end of this chapter.

### 4.2. Calculated Wave Conditions

Based on available wave data, four model wave heights (2 m, 4 m, 6 m, and 8 m) were selected to represent different sea severities: northeaster wave, rough sea, severe sea, and the most severe sea. Although the REF/DIF-1 model is a linear wave transformation model with a weak-nonlinear feature in wave transformation, each wave height has to be computed independently to include the energy dissipation caused by bottom friction.

Based on the recorded wave periods, a set of possible wave period also was selected for each wave height. This combination of wave heights and periods (Table 4-1) was applied to all the four major wave directions (ENE, E, ESE, and SE). Thus a total of 60 wave conditions, which cover the majority of all possible waves that can be affected by dredging at the modeled sites, were calculated.

Table 4-1. A Selection of Wave Heights and Periods for Modeling

Wave Height (m)	Wave Period (s)
8	16, 20
6	14, 16, 20
4	10, 12, 14, 16, 20
2	10, 12, 14, 16, 20

### 4.3. Results

The calculated wave height distributions in the display domain (Fig. 4-1) are shown in Fig. 4-2 to 4-16. The relationship between the grid coordinates and Maryland State Plane Coordinates are given in Figs. 2-1 and 2.2. Fenwick Shoal is located between  $XG = 16 - 18$  km and  $YG = 29 - 35$  km, and the Isle of Wight Shoal is located between  $XG = 17 - 20$  km and  $YG = 23 - 27$  km (Fig. 4-1). The figures use a natural and intuitive color to show the variation of normalized wave height,  $H/H_0$  (local wave height/incident wave height). In the figures, green indicates that the normalized wave height is small than 1 (the smaller the number, the deeper the green), and red indicates that the normalized wave height is large than 1 (the large the number, the deep the red). White means the normalized wave height is one.

In general, large waves attenuated significantly (Figs. 4-2 to 4-6) because of the great energy dissipation caused by large near-bed velocity. Large waves also may break because of the shoals, see the dark green areas in Figs. 4-2 and 4-6 for the waves coming from E and ENE. Notice, however, at the area between  $XG = 8$  to  $20$  km and  $YG = 10$  to  $13$  km, waves could be quite large if coming from East.

For the Northeaster and rough sea conditions ( $H_s = 2$  and  $4$  m,  $T = 10 - 20$  s), wave height distributions (Fig. 4-7 to 4-16) show a mixed results toward the coast. Near the location mentioned in the past paragraph (*i.e.*,  $XG = 4 - 15$  km and  $YG = 10 - 13$  km) which is on the south of Ocean City, however, waves coming from East have a tendency to converge. The high wave energy (for all wave that coming from east) may be responsible for causing the shore line retreat at this area.

The relatively severe beach erosion at the south side of Ocean City has been noticed at least 100 years ago. After the construction of jetties at the Ocean City Inlet (in 1930s), the severity increases because the jetties block out the southward alongshore sediment transport, at least for many years before the by-pass system was implemented (Smith, 1988).

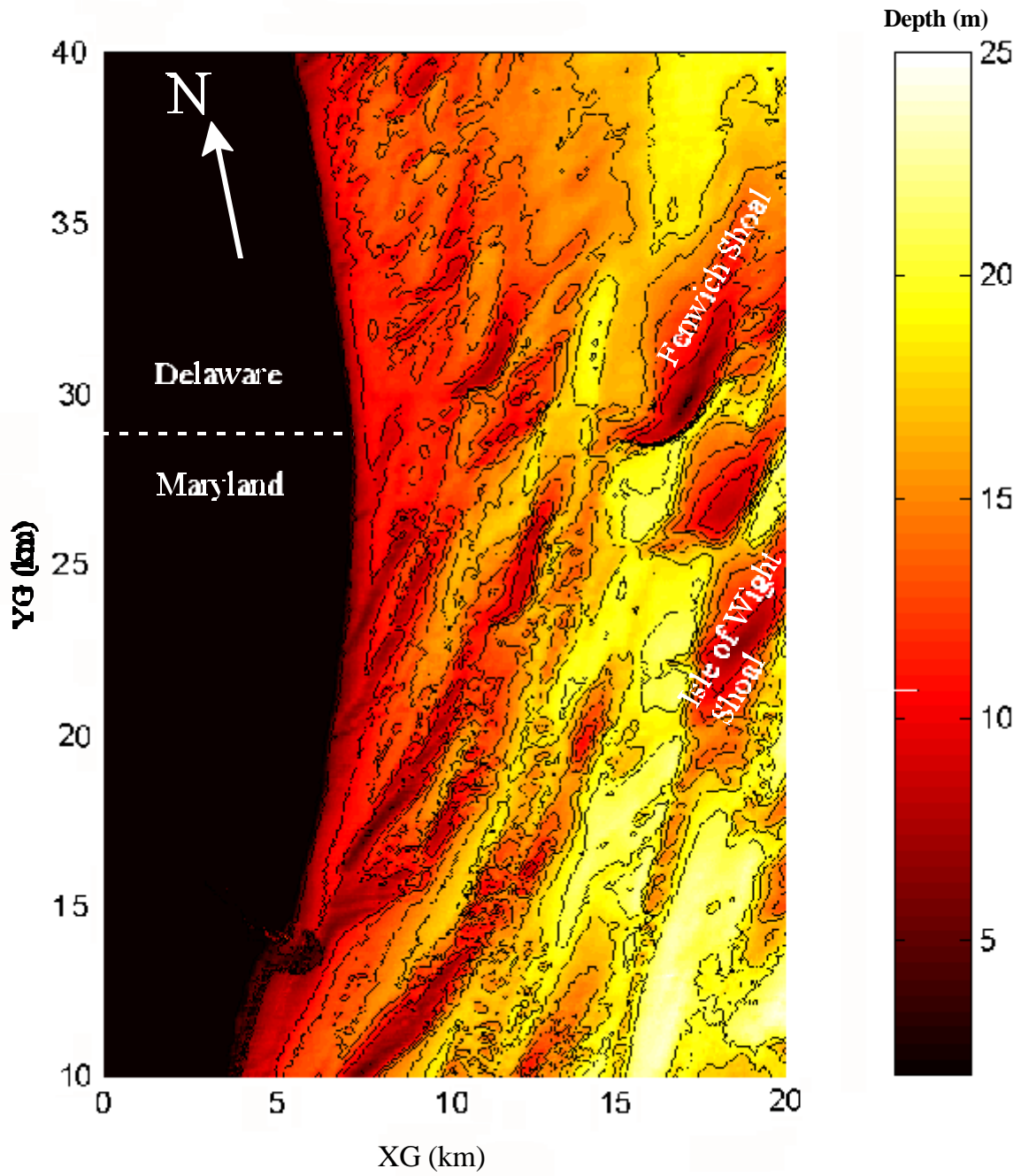


Fig. 4-1. Bathymetric Image for the Display Domain

Notice that near the Maryland-Delaware border (*i.e.*, XG = 7-10 km, and YG = 24-28 km), the extensive wave height attenuation is obvious (the dark green in Fig. 4-7 to 4-16). This may be caused by wave shoaling and breaking, after wave passed the Fenwick Shoal which is approximately 10 km from the coast.

For a random sea that does not have the pure single wave frequency for the wave conditions used as input for the REF/DIF-1 model, we may expect the wave height contours showing in Figs. 4-2 to 4-16 would be a little smoother. The general trend, however, should remain the same.

It is worthwhile to point out that energy loss caused by bottom friction is not a linear process. This is because the energy loss is proportional to  $u_b^3$ , where  $u_b$  is the near bed velocity induced by wave. An example (Table 4-2) clearly shows the difference of local wave height within the area between XG = 10-15 km and YG = 10-12 km for four wave heights with period = 16 s and coming from E.

Table 4-2. Wave Height within XG = 10-15 km and YG = 10-12 km to Show the Non-linear Dissipation of Wave Energy

Wave condition	$H_0$ (m)	H (m)	Fig. #
The most severe sea	8	~8	4-2
Severe Sea	6	7-8	4-5
Rough Sea	4	4-6	4-10
Northeastern	2	3-4	4-15

If bottom friction is not considered, one may use an unit deepwater wave height,  $H_0 = 1$ , to estimate local wave heights for all levels of sea severity. The above table, however, shows that this idea cannot be used because of the non-linear bottom friction energy dissipation. The ratio between H (the 3<sup>rd</sup> column) and  $H_0$  (the 2<sup>nd</sup> column) in table 4-2 is not a constant. The ratio increases as the  $H_0$  decreases. This is the reason why all four wave heights have to be included in the calculations. It also

can be interpreted that when simulating beach responses using all the reorganized wave heights and wave periods given in Chapter 2, one has to calculate hundreds of wave conditions. It is not an impossible but rather a time consuming and tedious job.

#### **4.4. Criterion for Estimating the Influence of Dredging**

When waves approach a coast, their trajectories may change because of wave transformation. Finally waves will break at a critical water depth,  $d_b$ , with a breaking wave height,  $H_b$  and a breaking angle  $A_b$ . For a perfectly straight shoreline with parallel bathymetric contours and a uniform offshore wave boundary condition, the line of  $H_b$  and  $A_b$  will be parallel to the shoreline (see the ideal condition in Fig. 4-17). Under this condition, the alongshore sediment transport rate is the same anywhere along the coast. Whether or not the beach will erode depends purely on the on-off shore sediment transport which is a rather slow process when compared with the along shore sediment transport. In reality, however, the breaking wave conditions will never be the same along a coast line, and a certain degrees of modulation exists (see the dashed line in Fig. 4-17). If the bathymetric change from dredging amplify the modulation, see the dotted-dashed lined in Fig. 4-17, the impact is not favorable. This is simply because there is more severe erosion where the breaking wave height is large. On the other hands, it would be a favorable change of bathymetry if the modulation decreased, see the dotted line in Fig. 4-17.

In the evaluation of computing results given in the next section, we use the original breaking wave height modulation as the basis (thus, a number of 1). For a favorable change of bathymetry, the modulation should be reduced, *i.e.*, less than 1.0 (*e.g.*, 0.5 in Fig. 4-17). Any change of bathymetry that increases the modulation (*e.g.*, 1.35 in Fig. 4-17) can be classified as unfavorable.

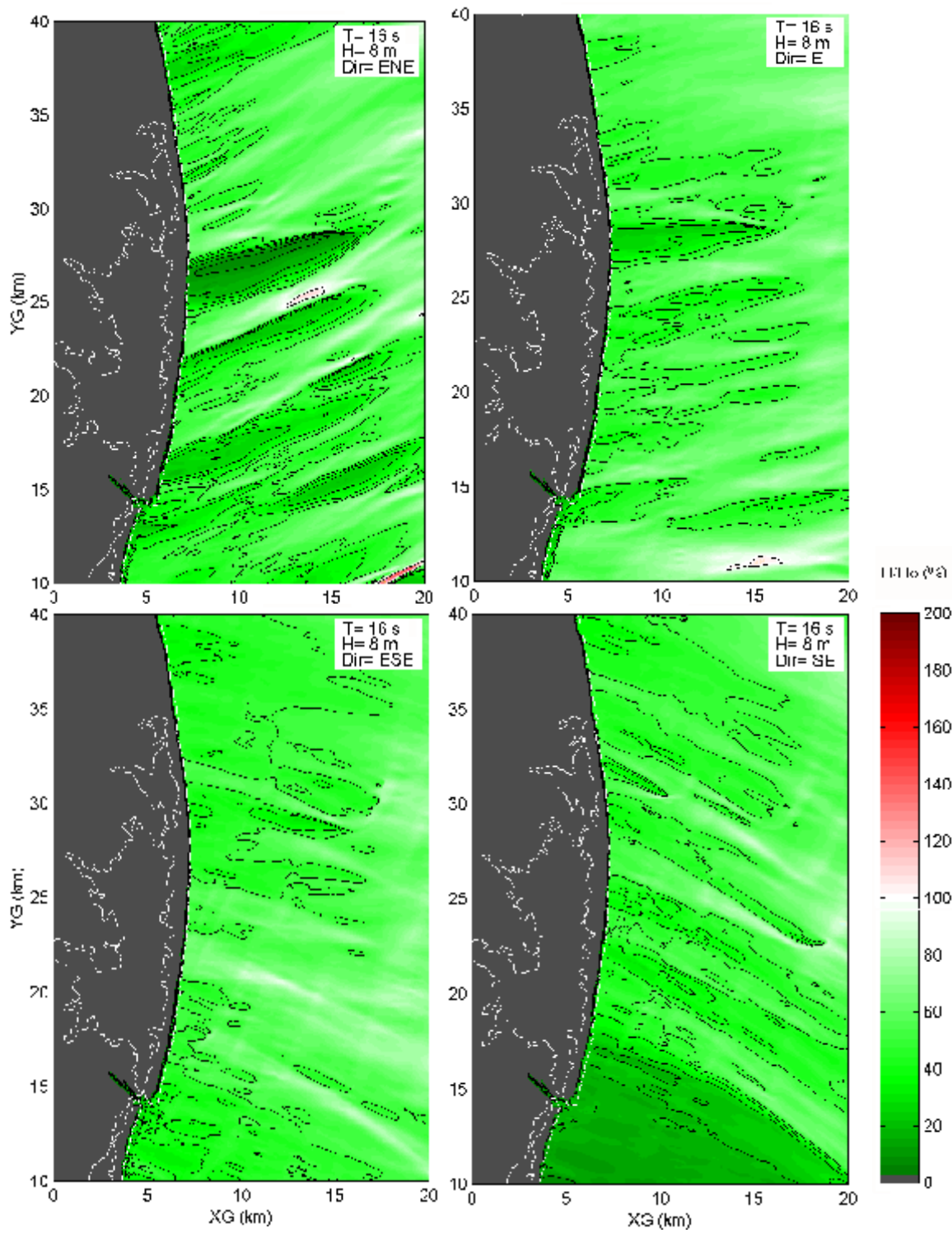


Fig. 4-2. Normalized Wave Height Distribution for the Original Bathymetry with  $H_0 = 8$  m,  $T = 16$  s.

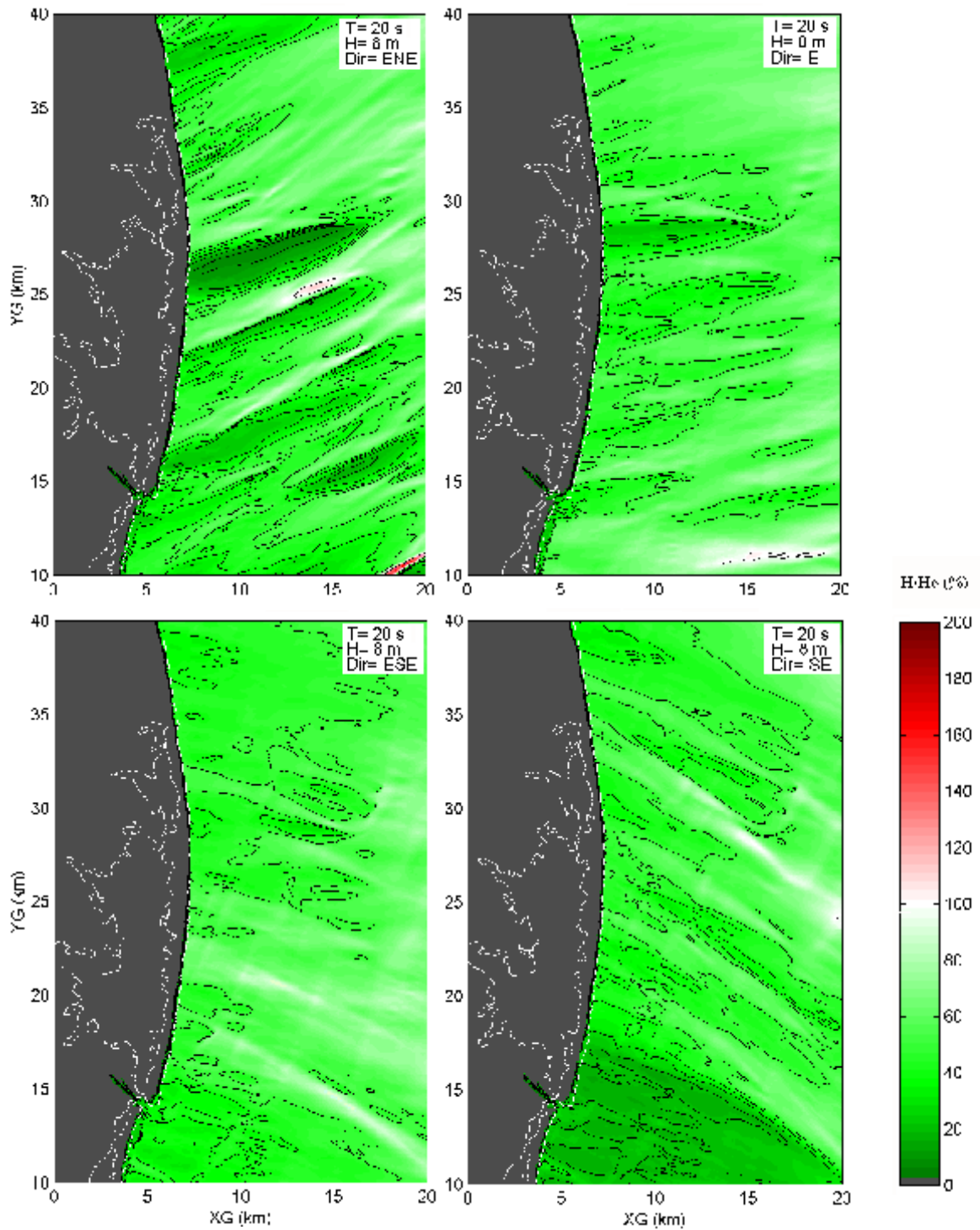


Fig. 4-3. Normalized Wave Height Distribution for the Original Bathymetry with  $H_0 = 8$  m,  $T = 20$  s.

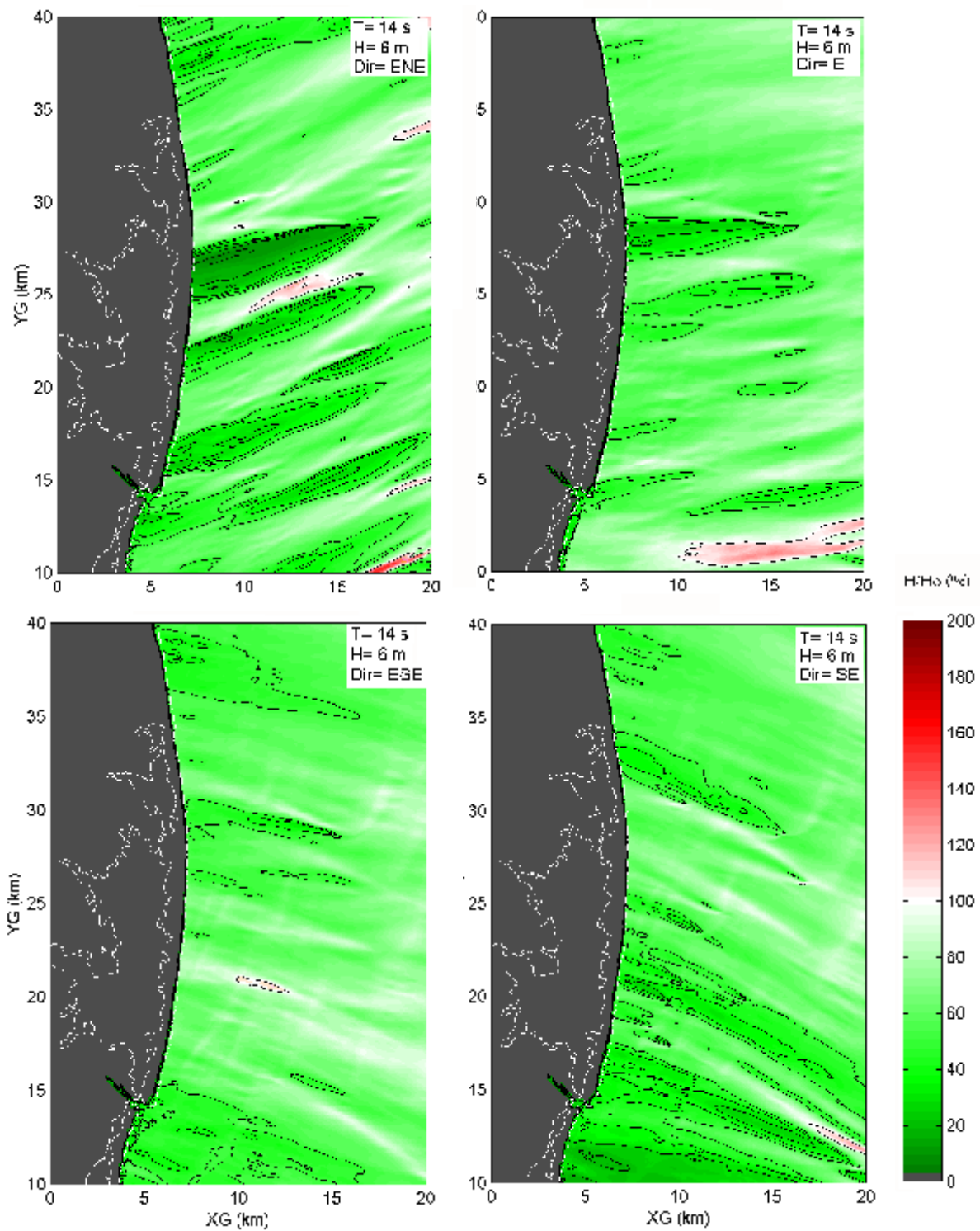


Fig. 4-4. Normalized Wave Height Distribution for the Original Bathymetry with  $H_0 = 6$  m,  $T = 14$  s.

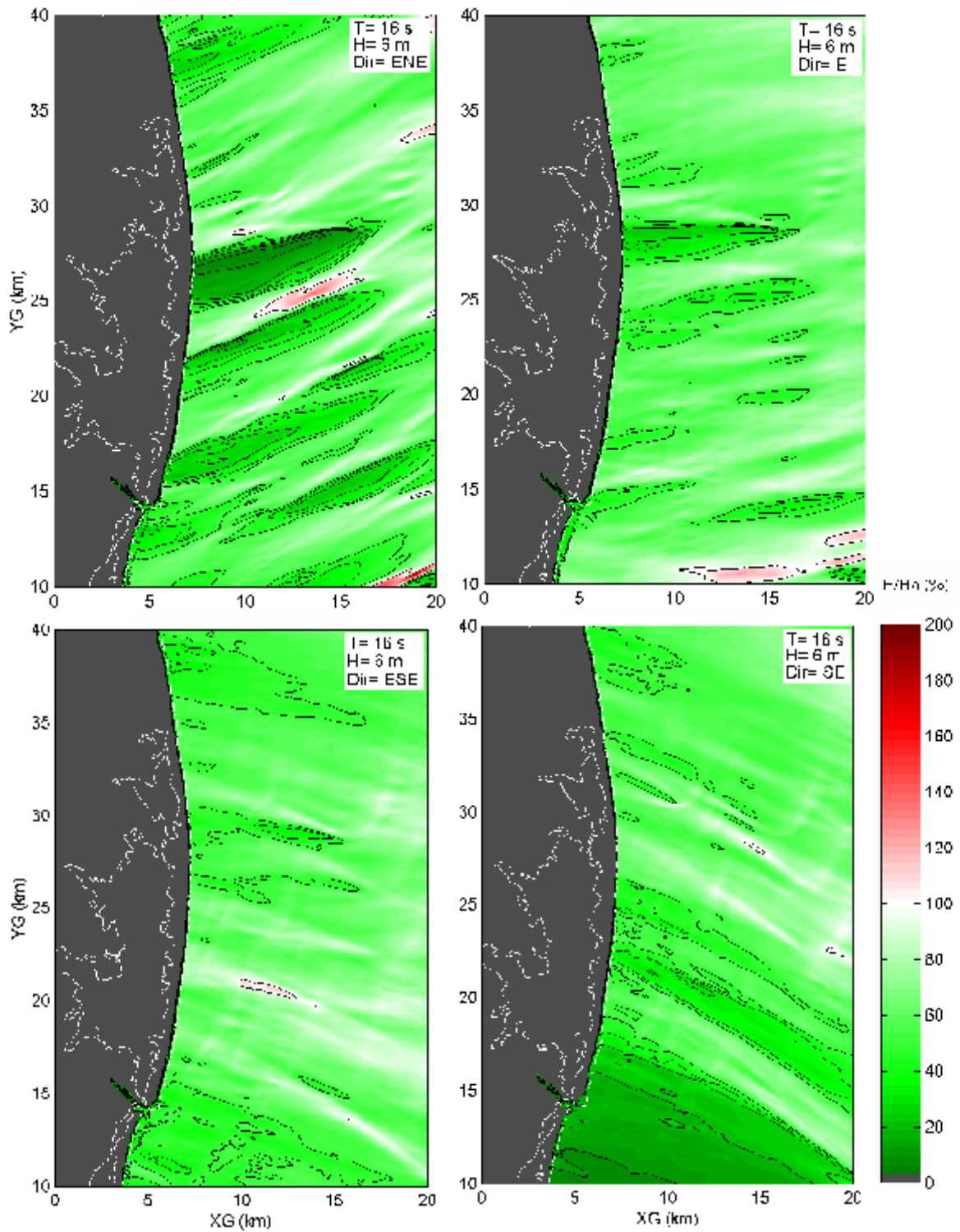


Fig. 4-5. Normalized Wave Height Distribution for the Original Bathymetry with  $H_0 = 6$  m,  $T = 16$  s.

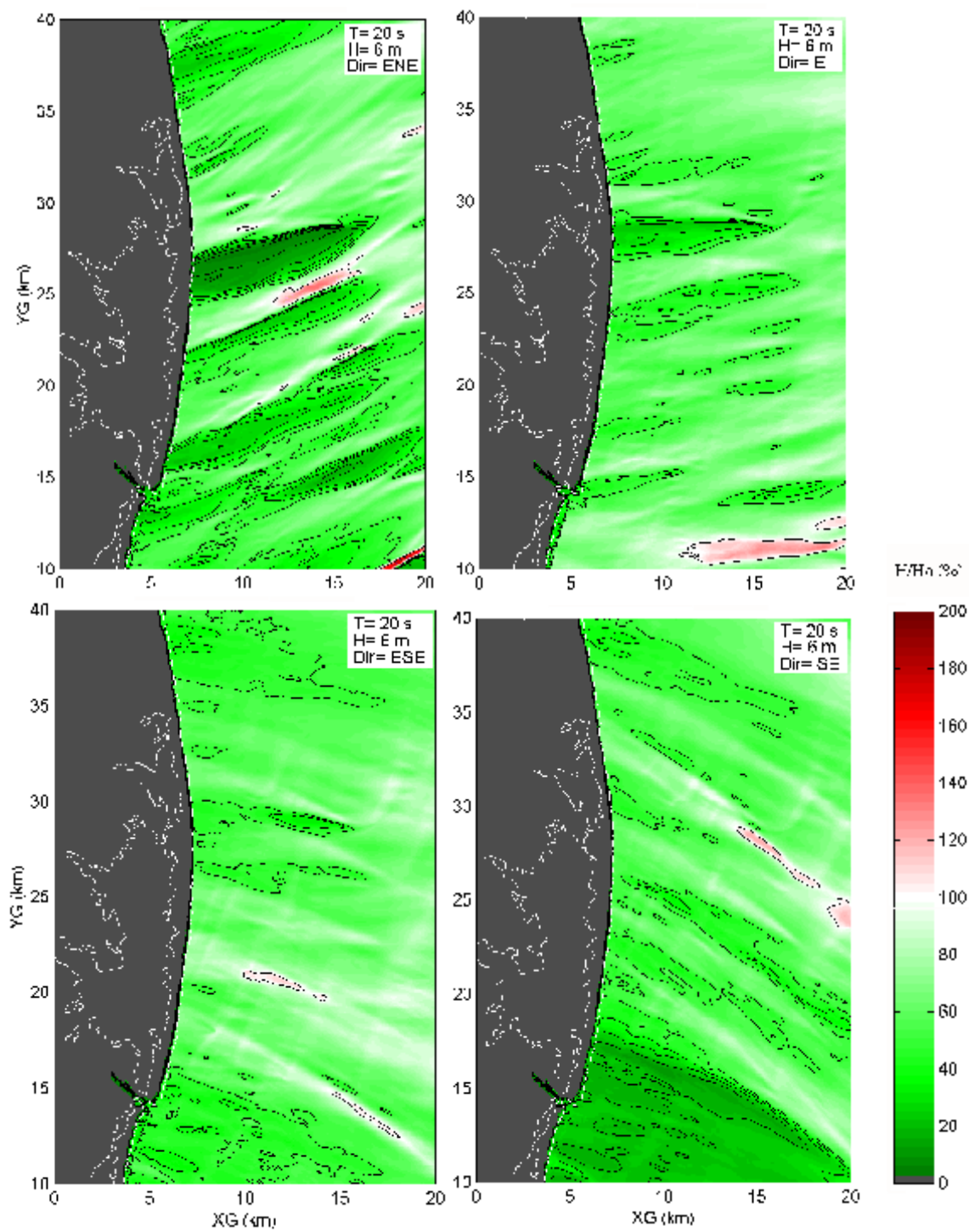


Fig. 4-6. Normalized Wave Height Distribution for the Original Bathymetry with  $H_0 = 6$  m,  $T = 20$  s.

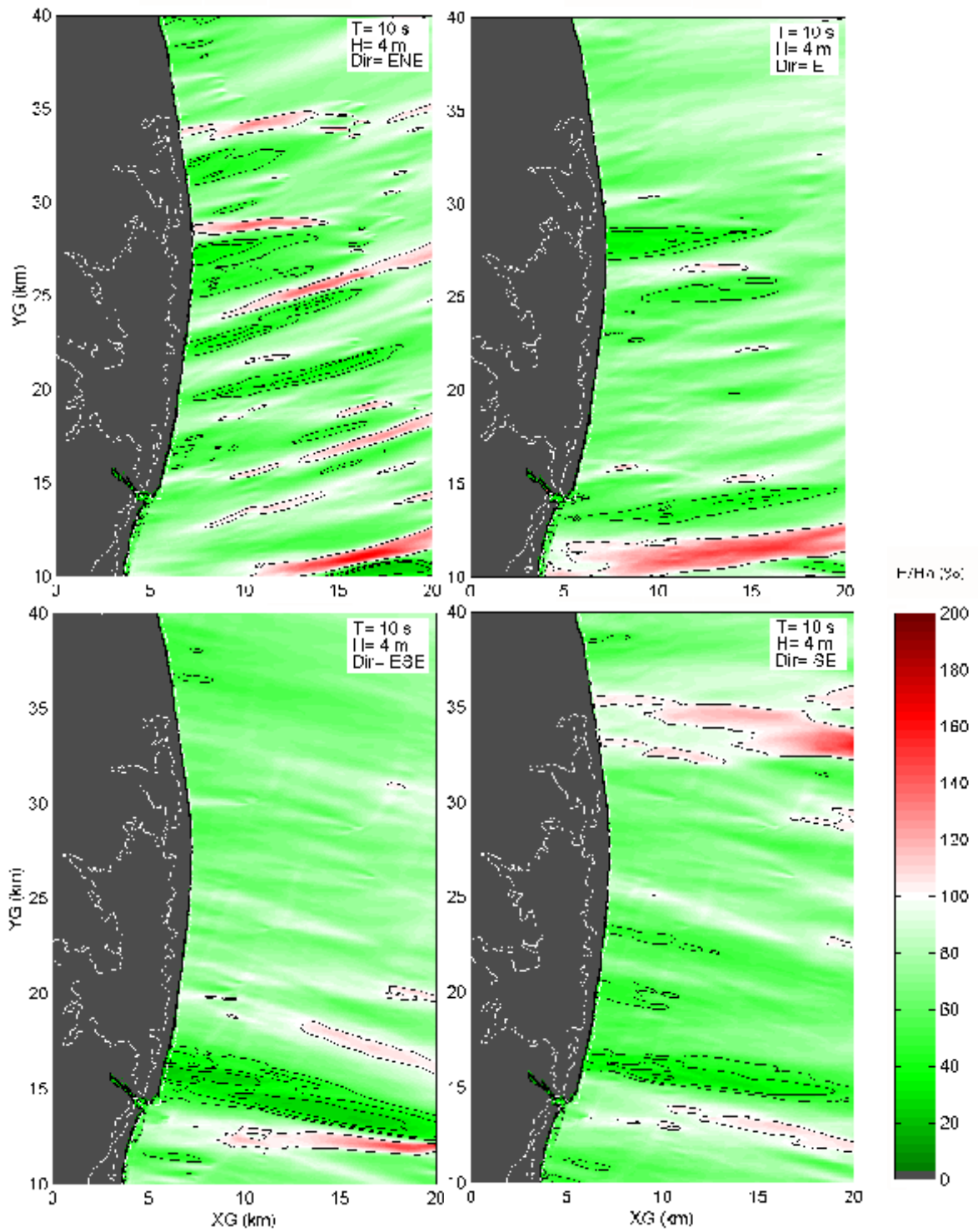


Fig. 4-7. Normalized Wave Height Distribution for the Original Bathymetry with  $H_0 = 4$  m,  $T = 10$  s.

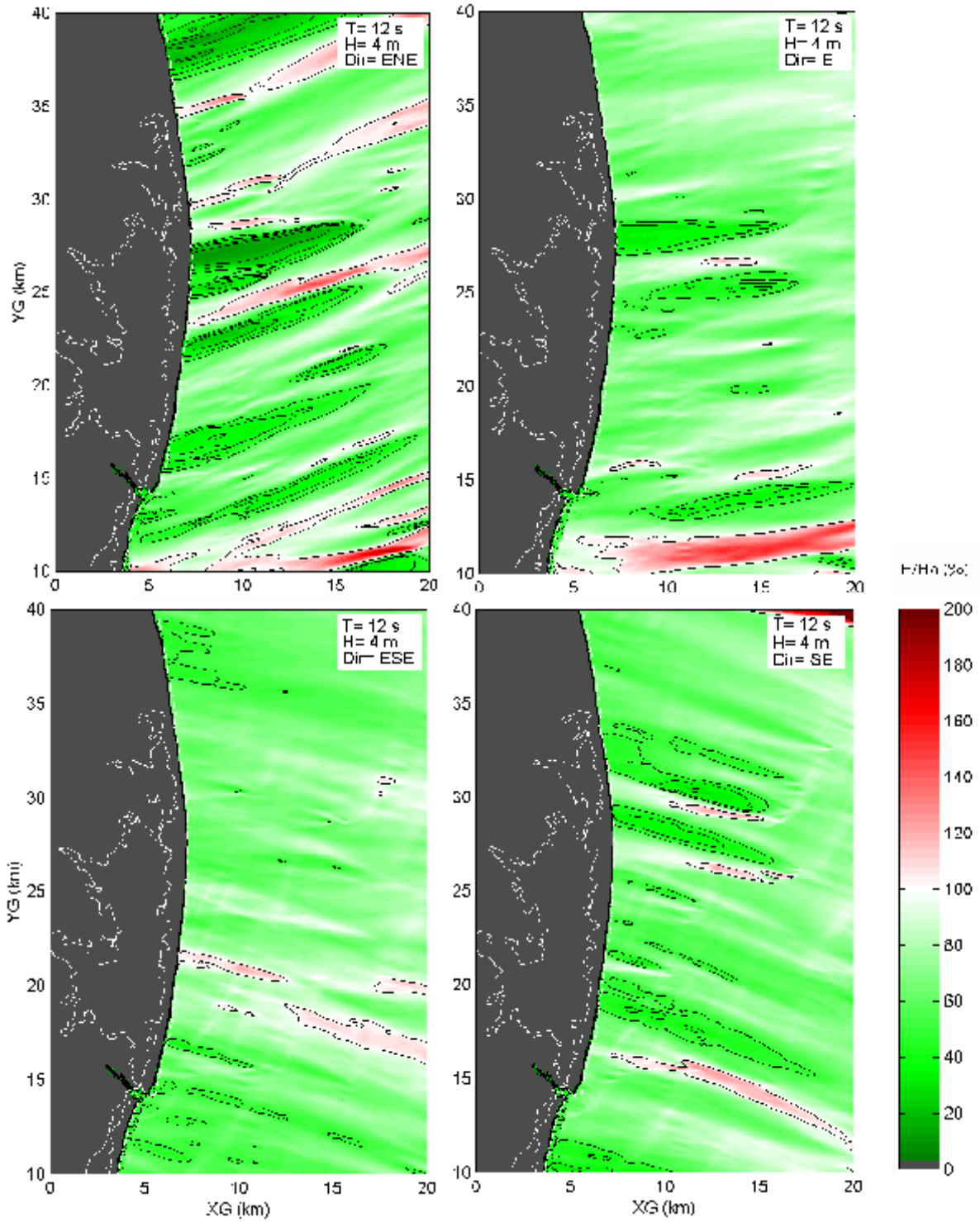


Fig. 4-8. Normalized Wave Height Distribution for the Original Bathymetry with  $H_0 = 4$  m,  $T = 12$  s.

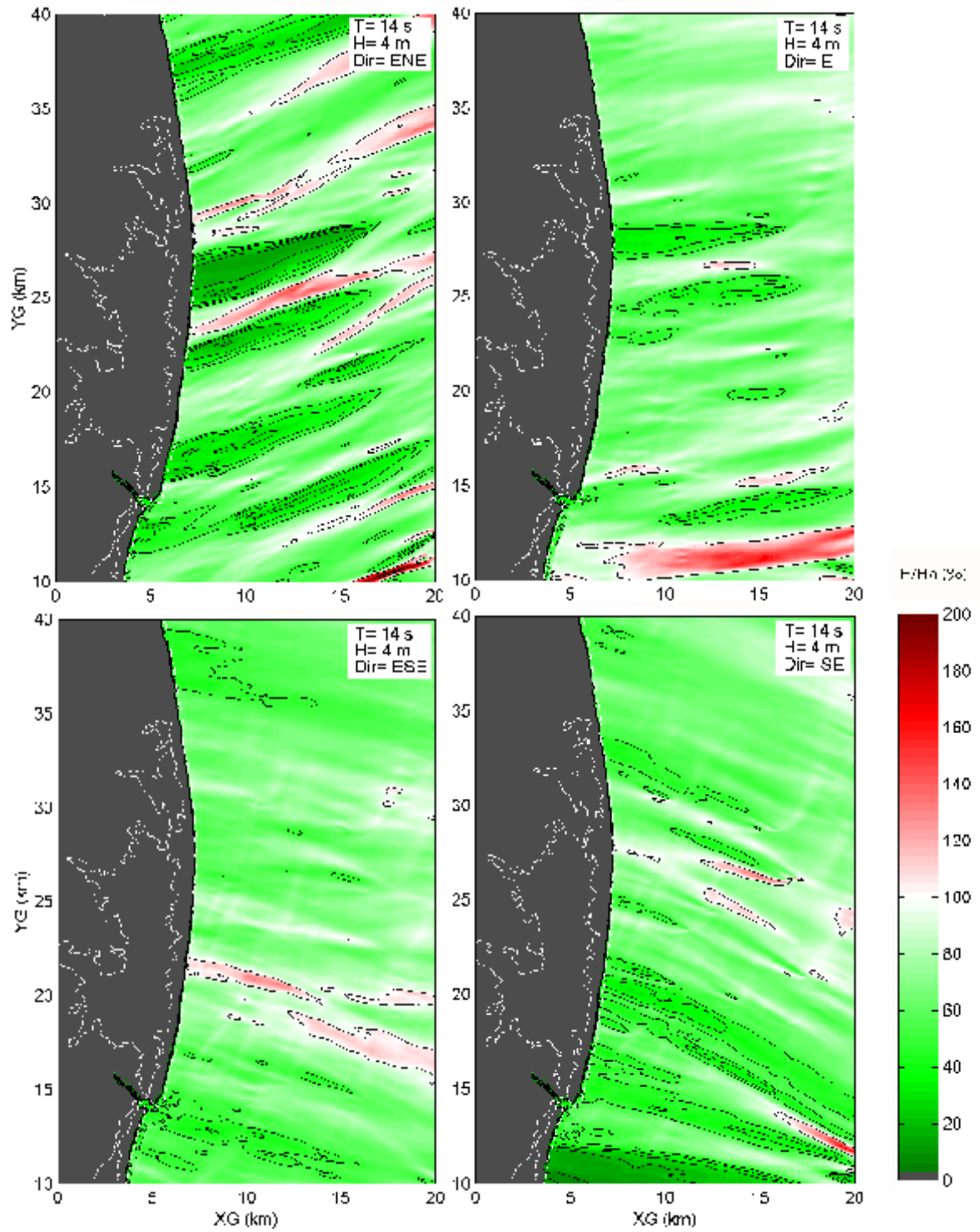


Fig. 4-9. Normalized Wave Height Distribution for the Original Bathymetry with  $H_0 = 4$  m,  $T = 14$  s.

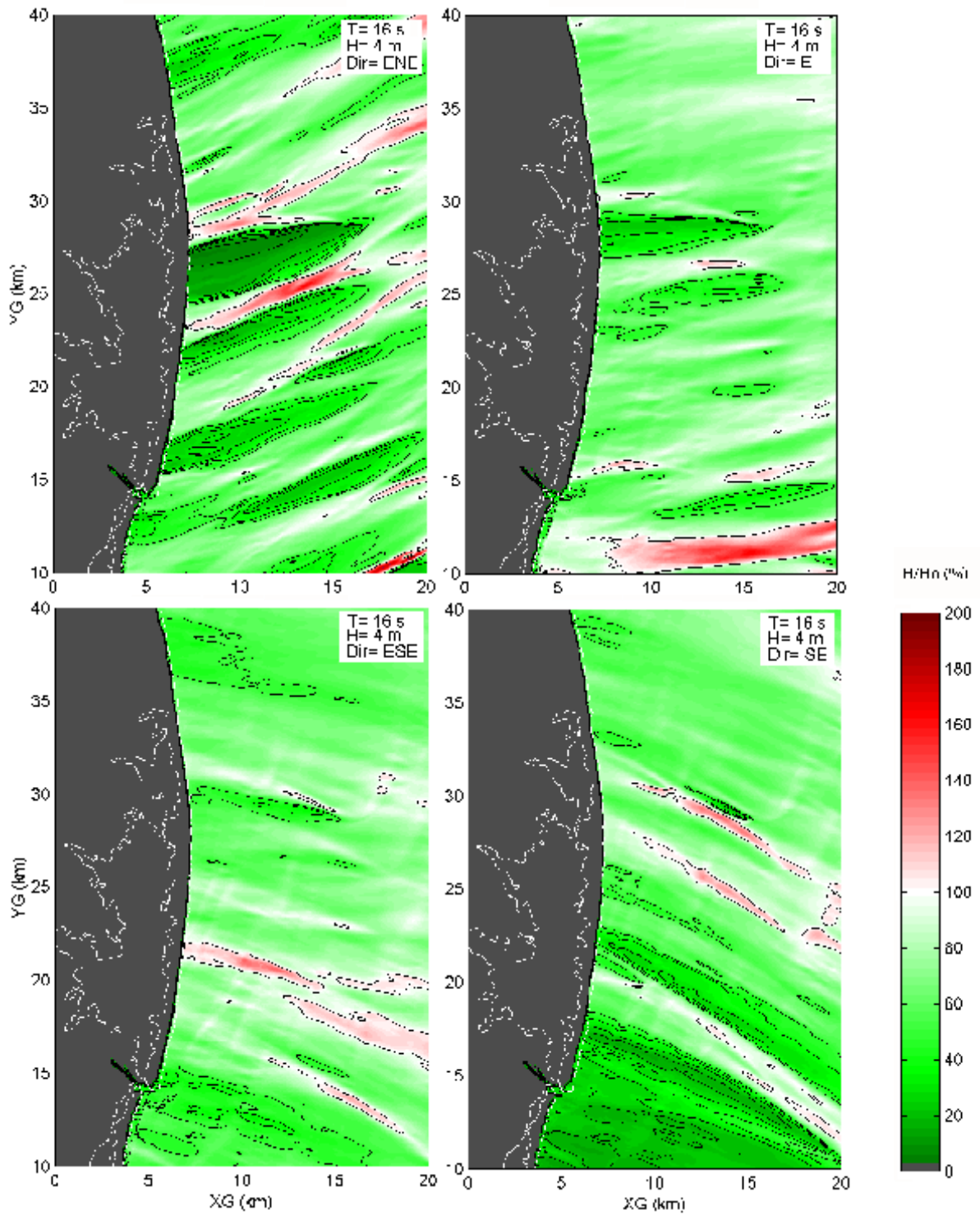


Fig. 4-10. Normalized Wave Height Distribution for the Original Bathymetry with  $H_0 = 4$  m,  $T = 16$  s.

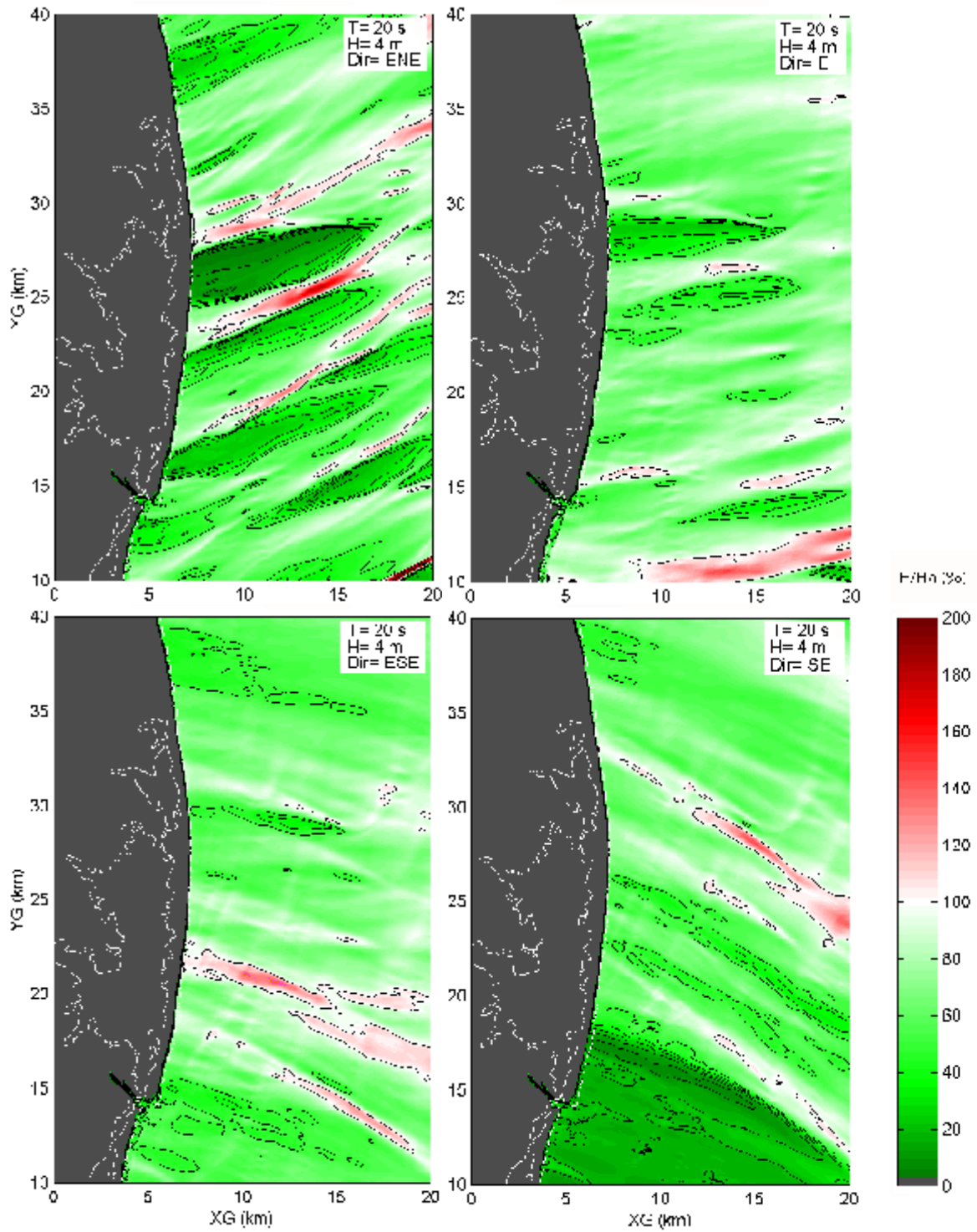


Fig. 4-11. Normalized Wave Height Distribution for the Original Bathymetry with  $H_0 = 4$  m,  $T = 20$  s.

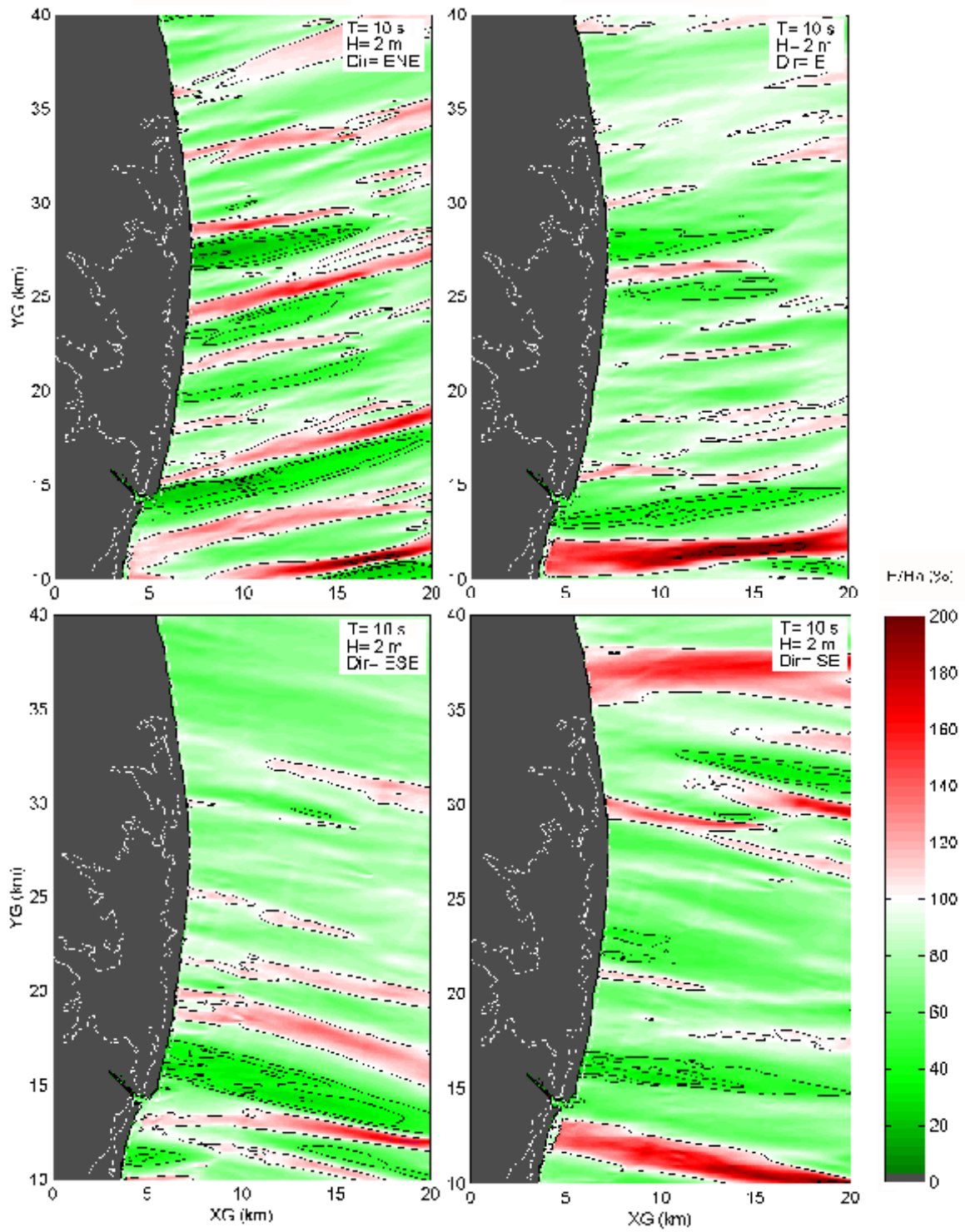


Fig. 4-12. Normalized Wave Height Distribution for the Original Bathymetry with  $H_0 = 2$  m,  $T = 10$  s.

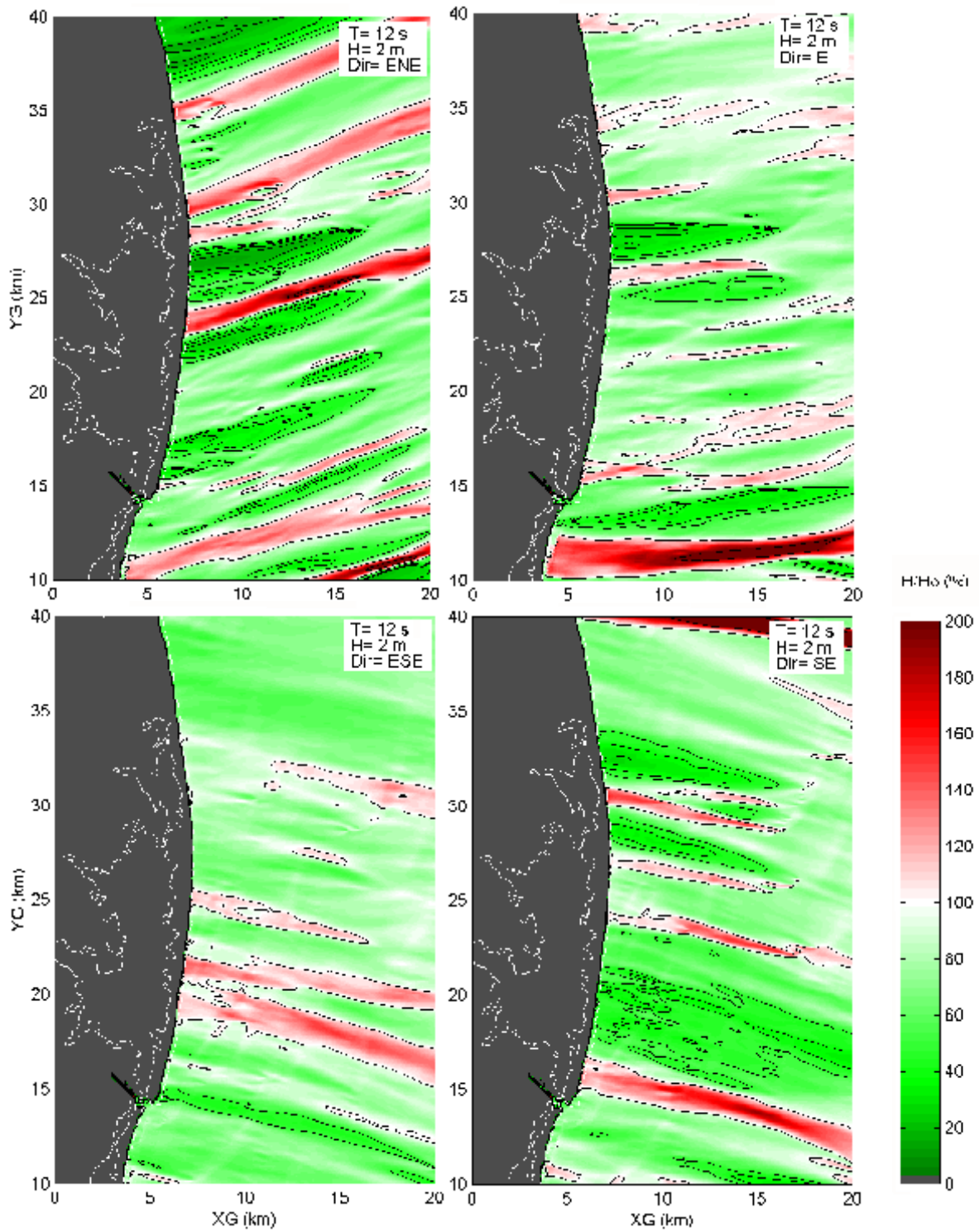


Fig. 4-13. Normalized Wave Height Distribution for the Original Bathymetry with  $H_0 = 2$  m,  $T = 12$  s.

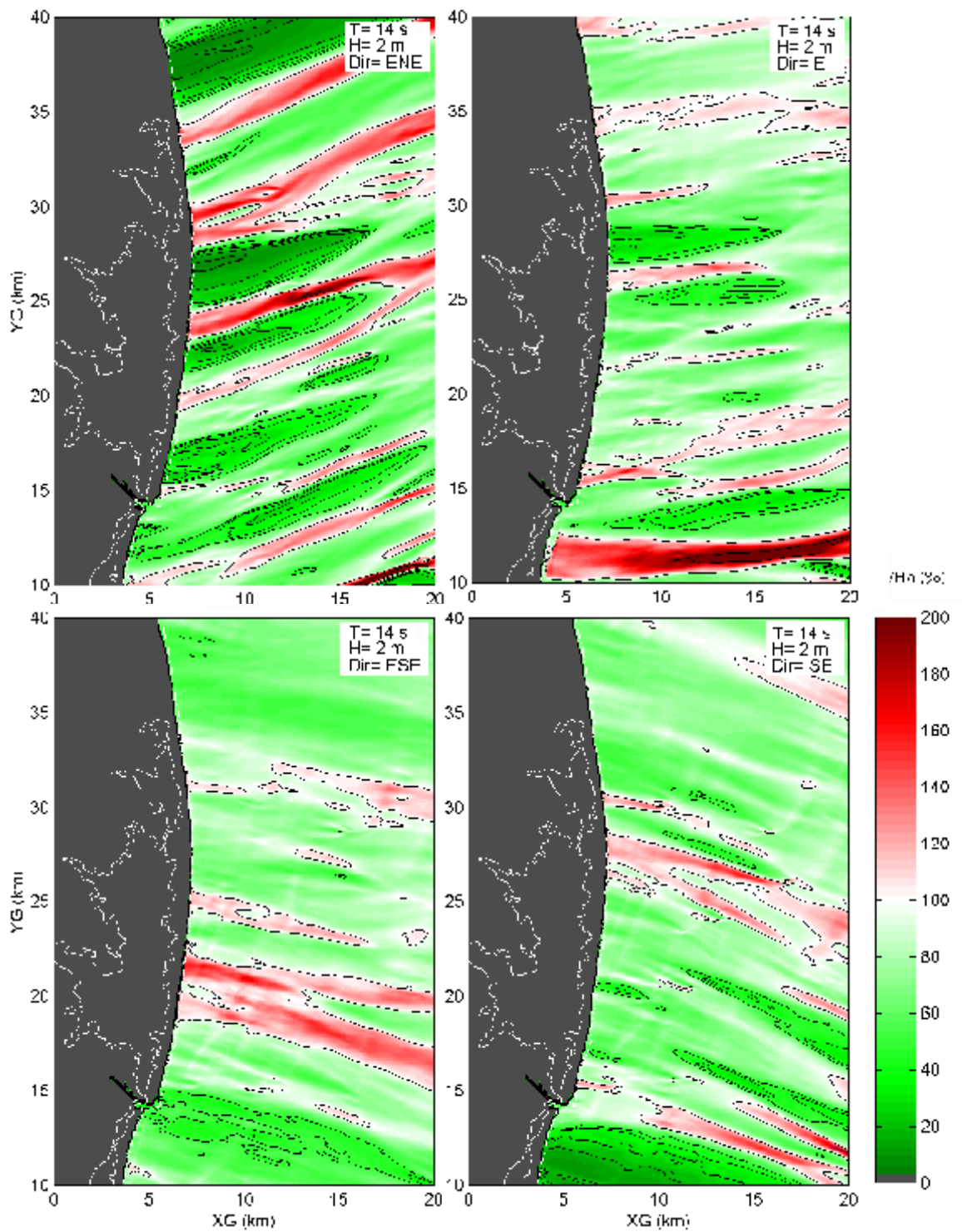


Fig. 4-14. Normalized Wave Height Distribution for the Original Bathymetry with  $H_0 = 2$  m,  $T = 14$  s.

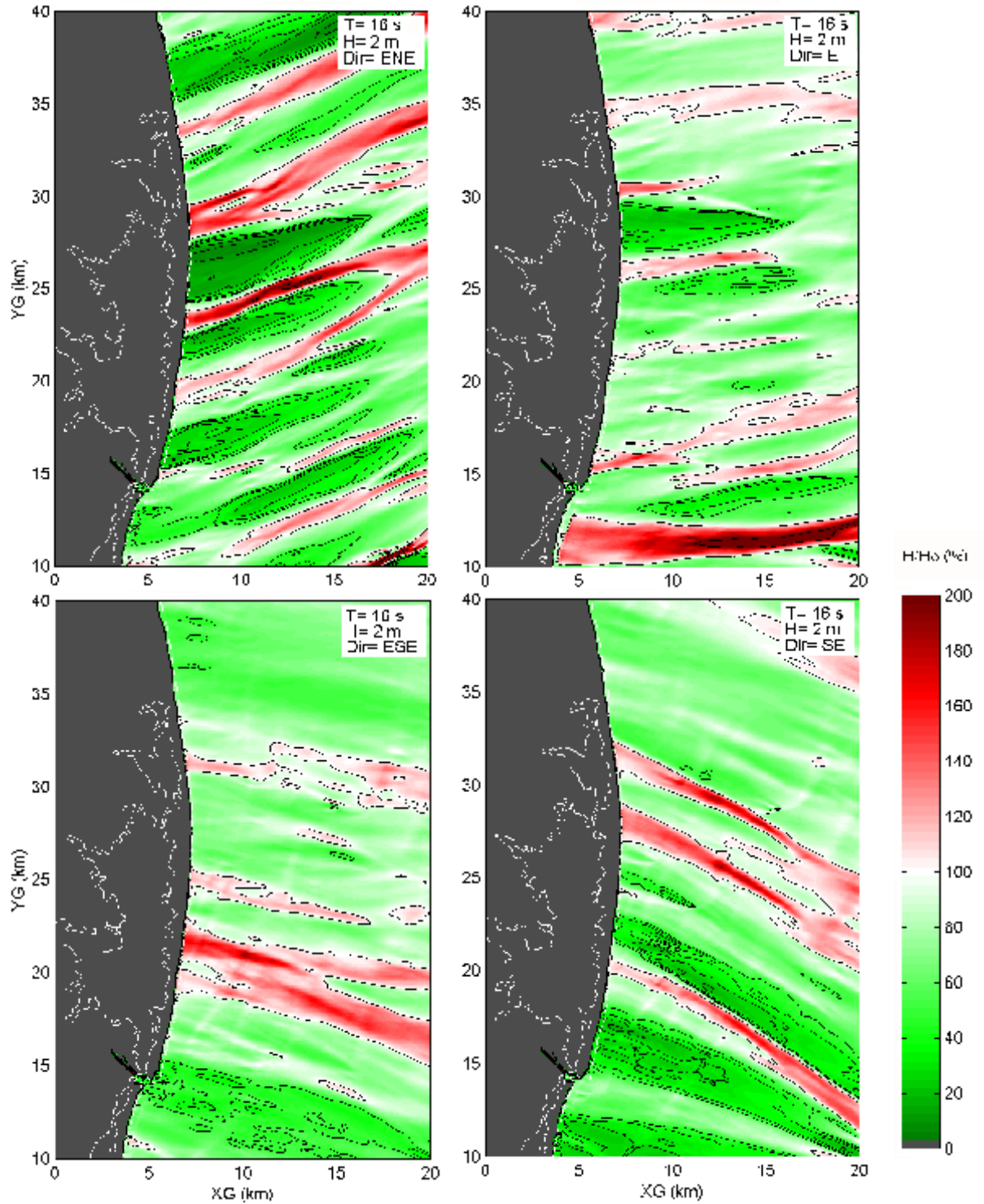


Fig. 4-15. Normalized Wave Height Distribution for the Original Bathymetry with  $H_0 = 2$  m,  $T = 16$  s.

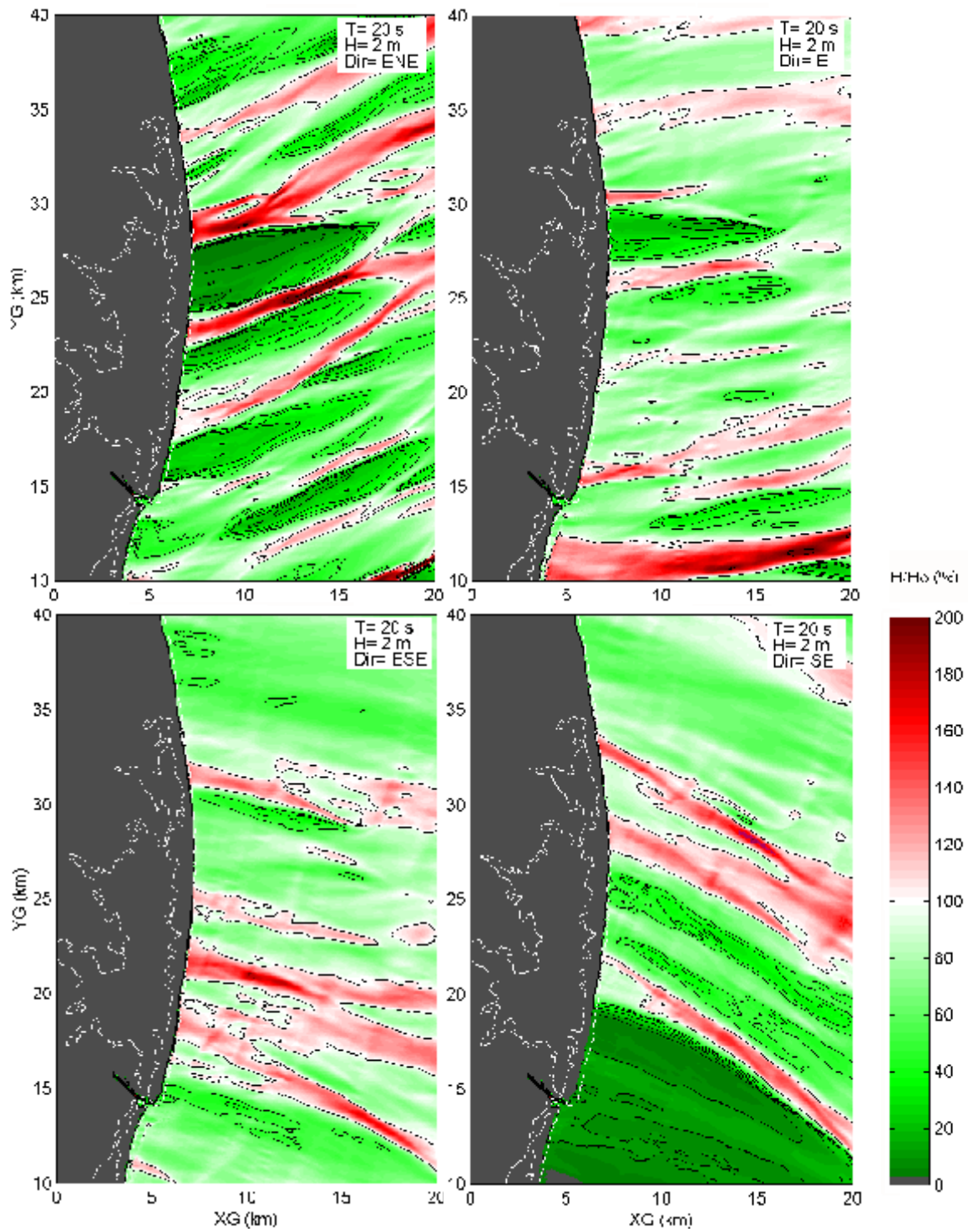


Fig. 4-16. Normalized Wave Height Distribution for the Original Bathymetry with  $H_0 = 2$  m,  $T = 20$  s.

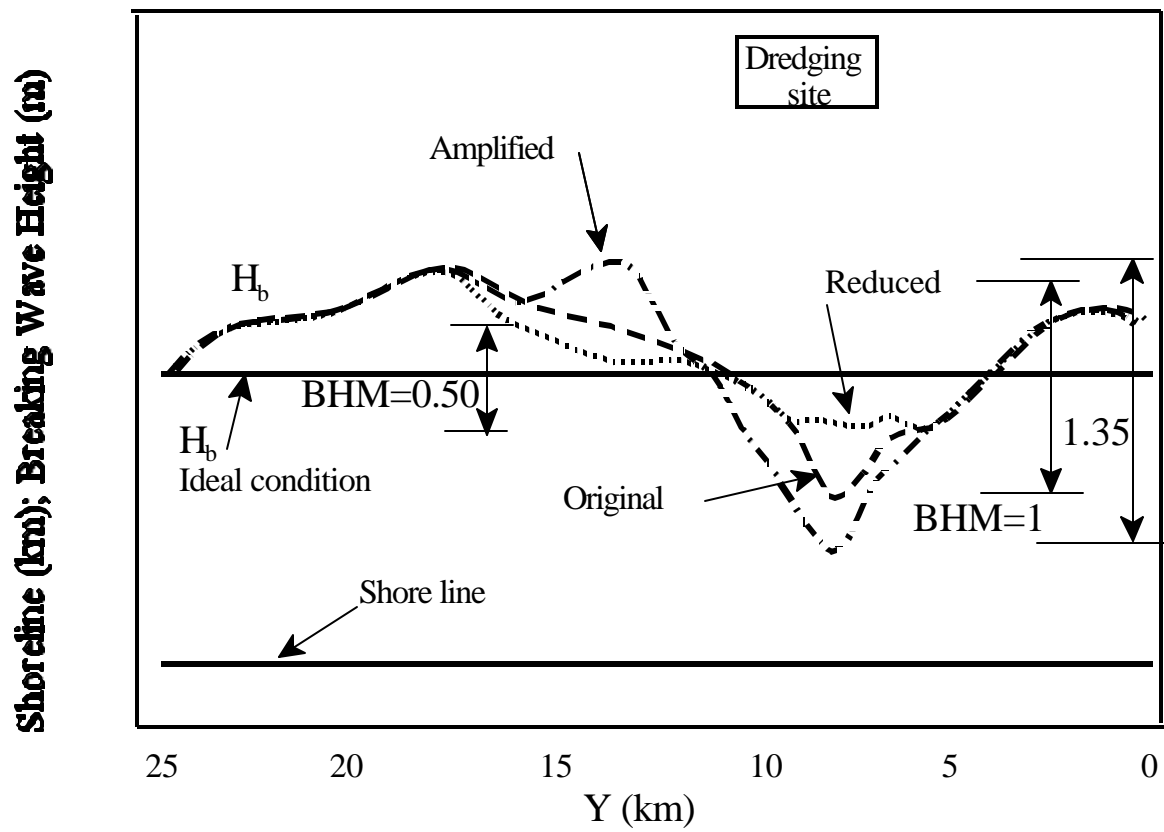


Figure 4.17: A line graph of Dredging Site height and wave height. Dredging will increase the breaking wave height of the dredging site.



## CHAPTER 5. CHANGES OF WAVE ENVIRONMENTS AFTER A ONE-TIME DREDGING

### 5.1. Introduction

The dredging scenario considered in this chapter is for providing a one-time sand resource on the order of  $2 \times 10^6 \text{ m}^3$  for Maryland-Delaware coast. The objective of study for this scenario is to determine if the impact of even a small amount of dredging at the selected shoals is acceptable. The differences in computed wave heights between the offshore dredging sites and the shoreline for the pre- and post-dredging are presented first to obtain a general idea of the spatial differences. Then the differences in breaking wave heights along the coast are presented. Conclusions on the possible impact are presented at the end.

### 5.2. Wave Height Difference in Spatial Domain

The 60 wave conditions described in Chapter 4 were run with the bathymetry altered as shown in Fig. 2-4. In order to clearly show the change in wave height distribution, only the normalized difference (*i.e.*,  $\Delta H/H$ , in units of %, where  $H$  is the local wave height calculated using the original bathymetry, and  $\Delta H$  is the change of local wave height) in the display domain are plotted in an intuitive manner (Figs. 5-1 to 5-15). Red represents increase (*i.e.*,  $\Delta H/H > 0\%$ ), green represents decrease (*i.e.*,  $\Delta H/H < 0\%$ ), and white represents no change (*i.e.*,  $\Delta H/H = 0\%$ ). The modeled dredging areas also are depicted as the dashed boxes in these figures.

Dredging always alters the wave transformation. Wave height is reduced at some places but increased at others (Figs. 5-1 to 5-15). In general, the modeled dredging at Fenwick shoal has a relatively severe influence on wave height (*i.e.*,  $\Delta H/H \gg 0\%$ ) for waves that come from ENE and E. The area affected by dredging, however, is not as large as those waves come from SE and ESE. Only occasionally, waves come from SE produce severe difference (Figs. 5-7 and 5-12).

Notice that the red-colored area is larger than the green-colored area. This indicates that the difference is mainly in increasing wave height (red color). These figures also reveal that at some places, the increase of wave height is quite large (the dark red areas in Figs. 5-1 to 5-15). The large increase

of wave height is a negative consequence of dredging and may have influence on sea-floor mobility. Because of the stochastic nature of waves, a quantitative conclusion on the sea floor mobility would require more study.

Also notice that the changes of wave height at the dredging sites are not significant. Actually, the major change of wave height occurs between the dredging sites and the shoreline.

The figures indicate that the change of local wave height can be as much as 100%. This is a significant alteration on wave height itself. But when dealing with alongshore sediment transport, the only parameter considered is breaking wave height. That is why we have to check the change of breaking wave height profiles. For a nonlinear wave breaking process, a 100% increase of local wave height at some place not right before the breaking point, the breaking wave height does not necessary also increase 100%. Actually the increase of breaking wave height can be quite limited.

It is a quite challenge question: “How much is the influence on the change of local wave height, which is not necessarily close to the breaking line, to the shore line change?” It is understood that the increase of local wave height on the shelf face might alter the on-off shore sediment transport rate. However, a predictive formulation and numerical model is still far from available.

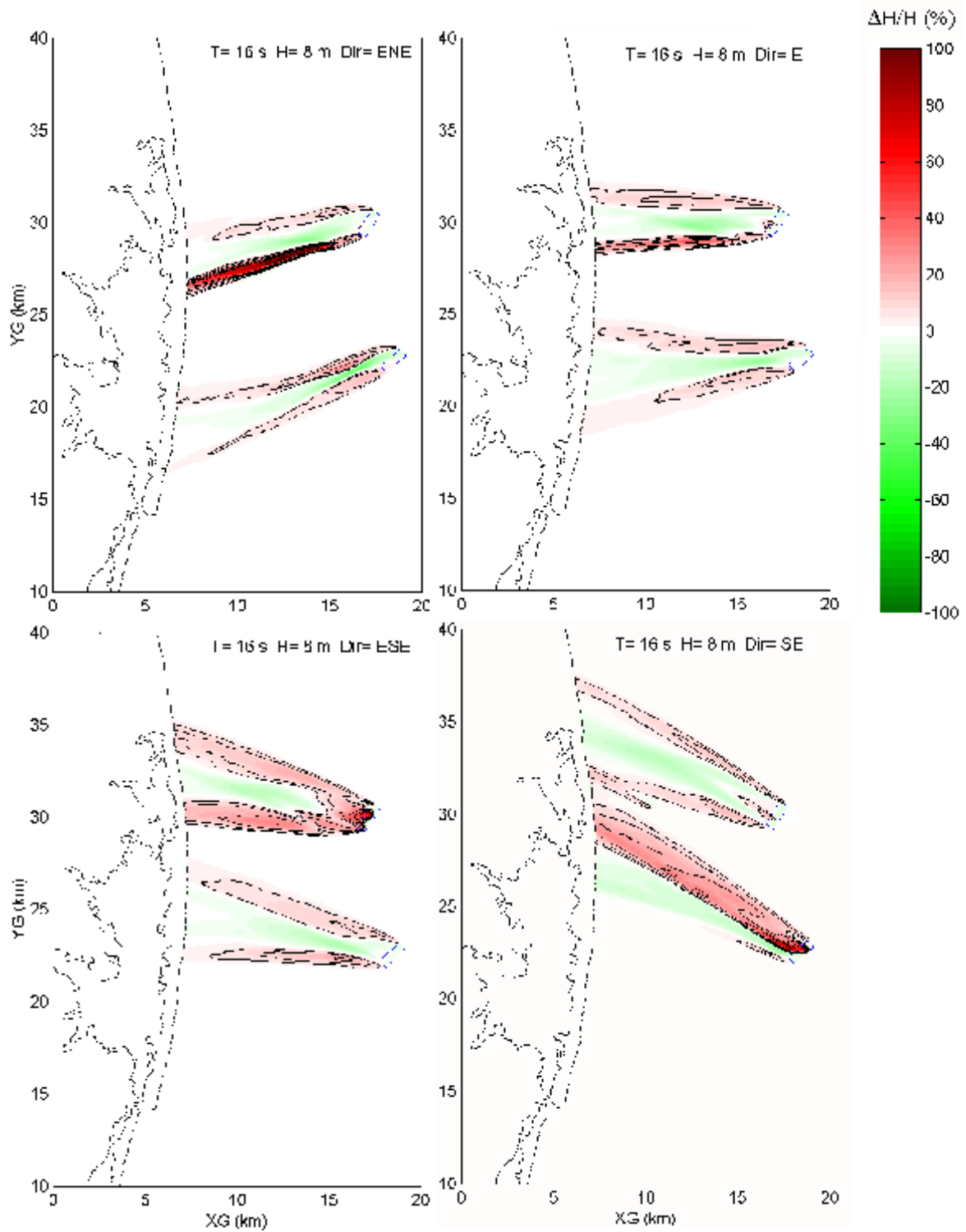


Fig. 10. Contour plots of wave height change ( $\Delta H/H$ ) for the 1000-Daguerre-1000-Run.

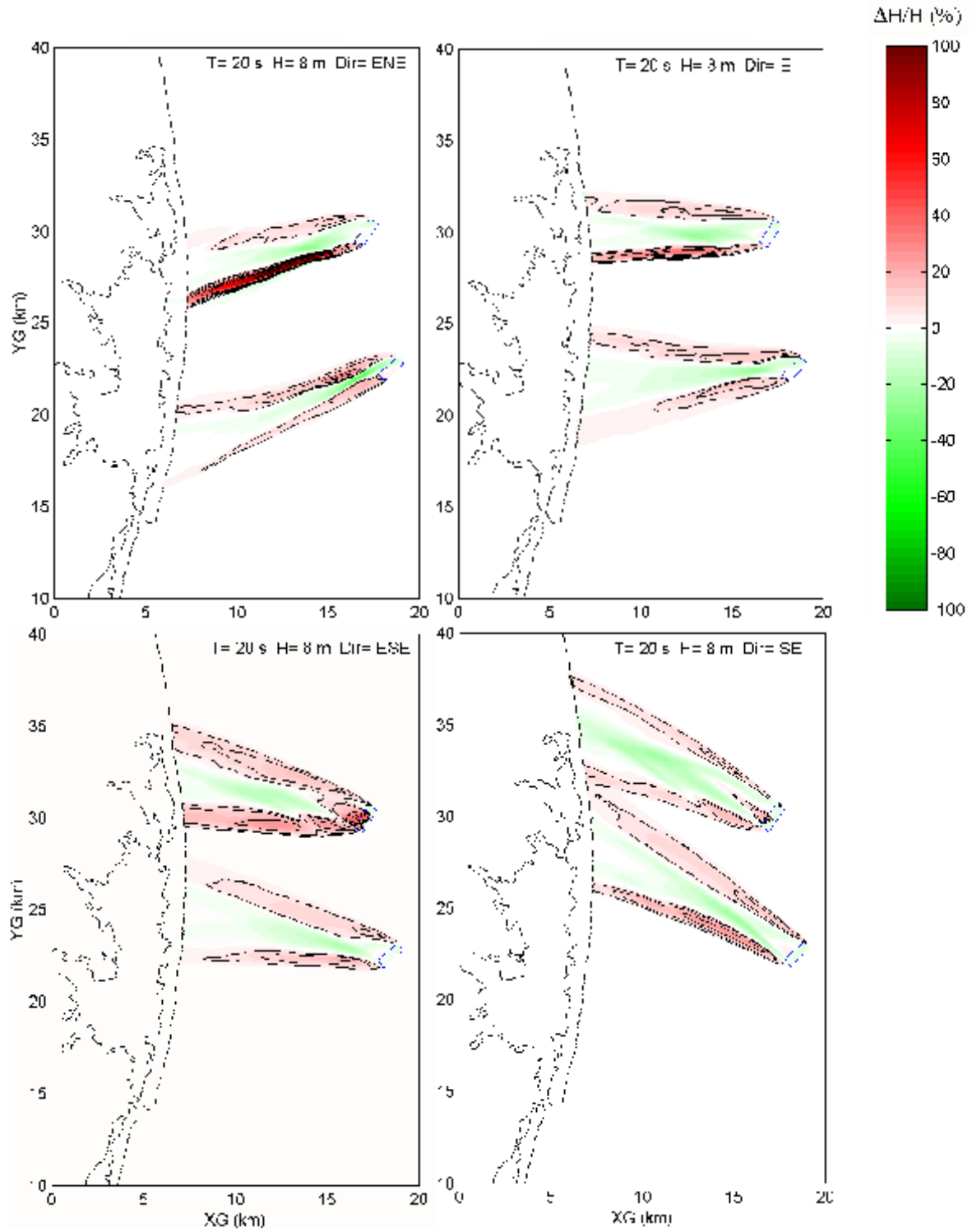


Fig. 10. Relative height change  $\Delta H/H$  (%) for  $T=20$  s,  $H=8$  m,  $\text{Dir}=\text{ENE}$ ,  $\Xi$ ,  $\text{ESE}$ ,  $\text{SE}$ .

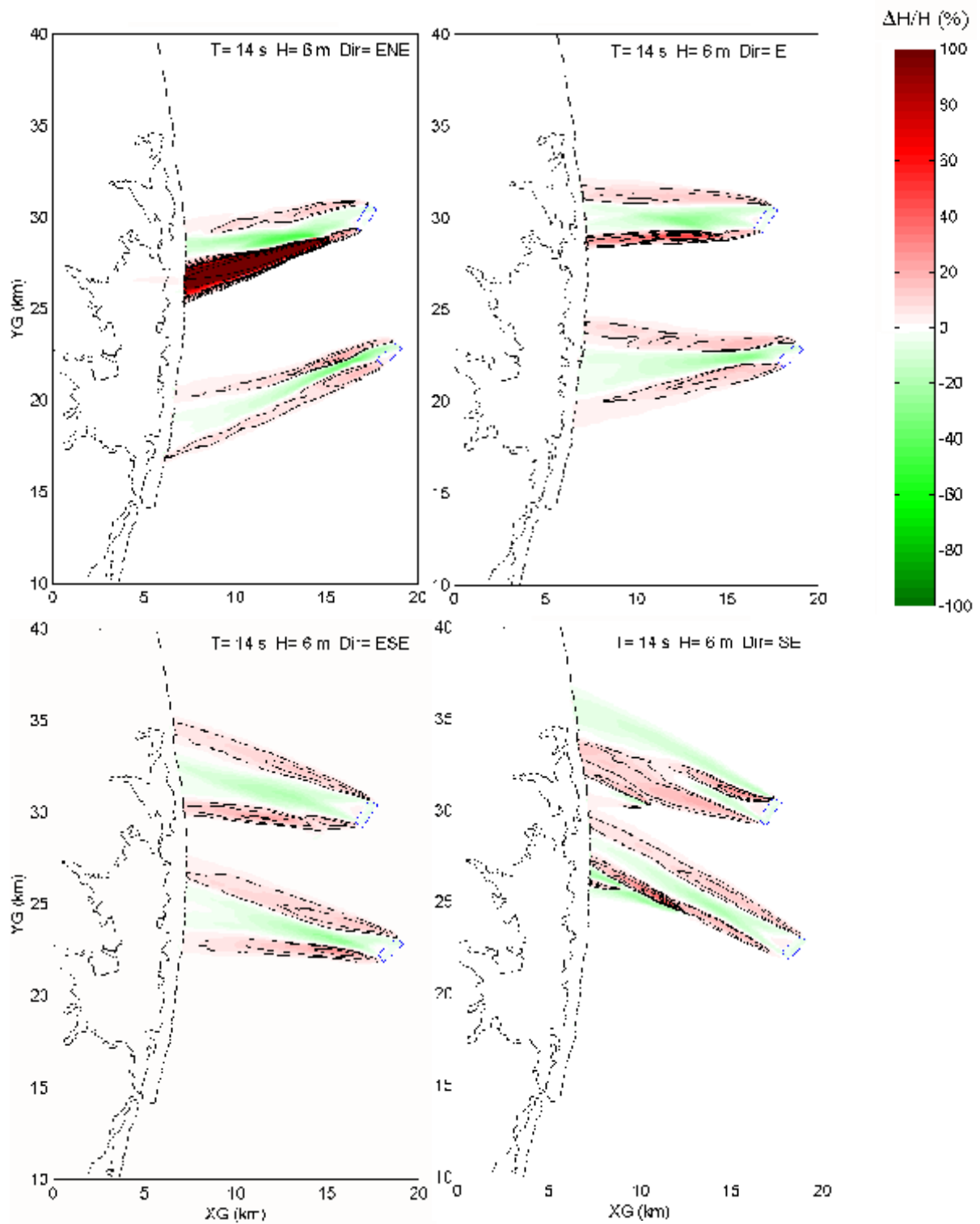


Fig. 5-3. Calculated Changes of Wave Height (Normalized) for the One-time Dredging with  $H_0=6$  m,  $T=14$  s.

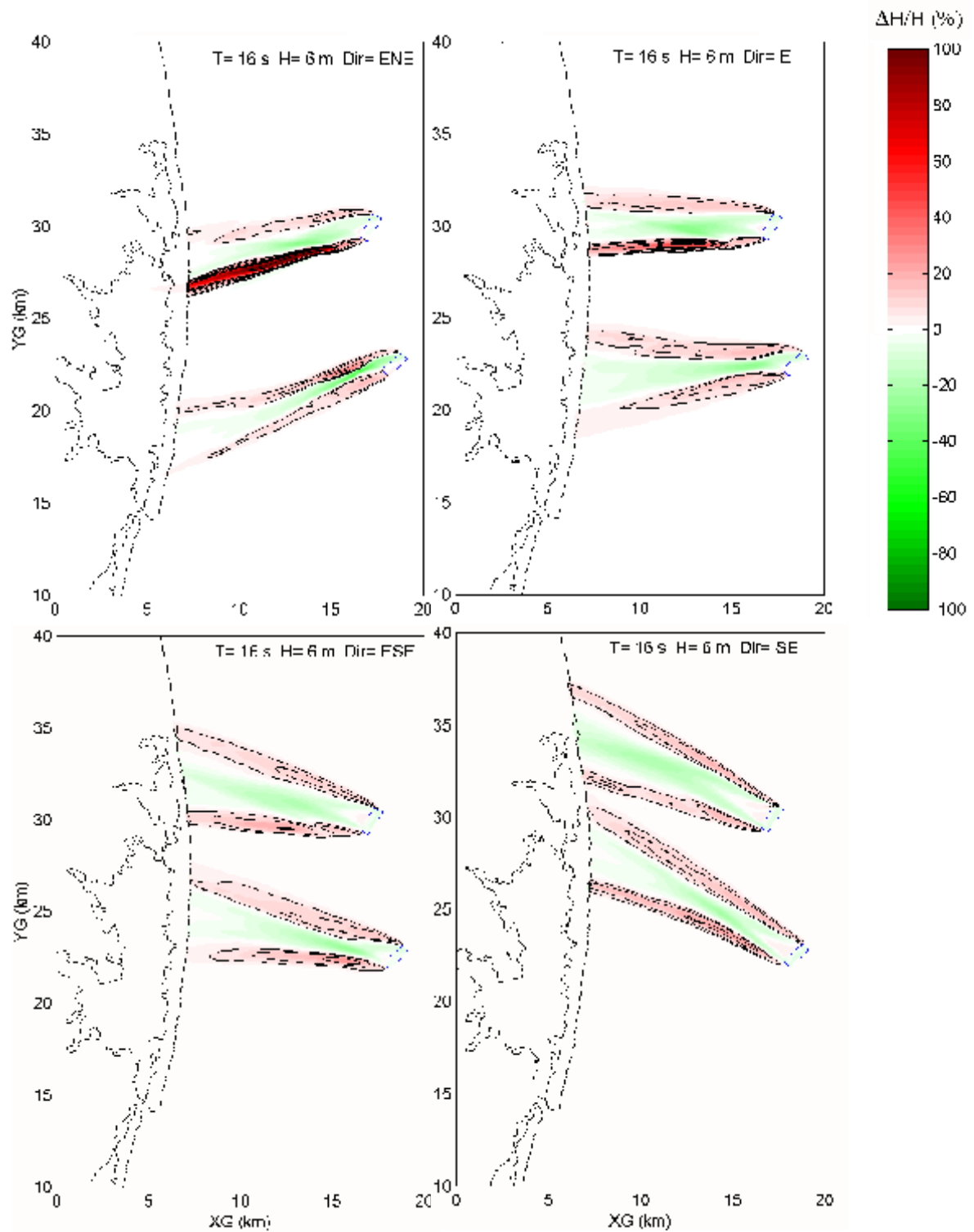


Fig. 5-4. Calculated Changes of Wave Height (Normalized) for the One-time Dredging with  $H_0 = 6$  m,  $T = 16$  s.

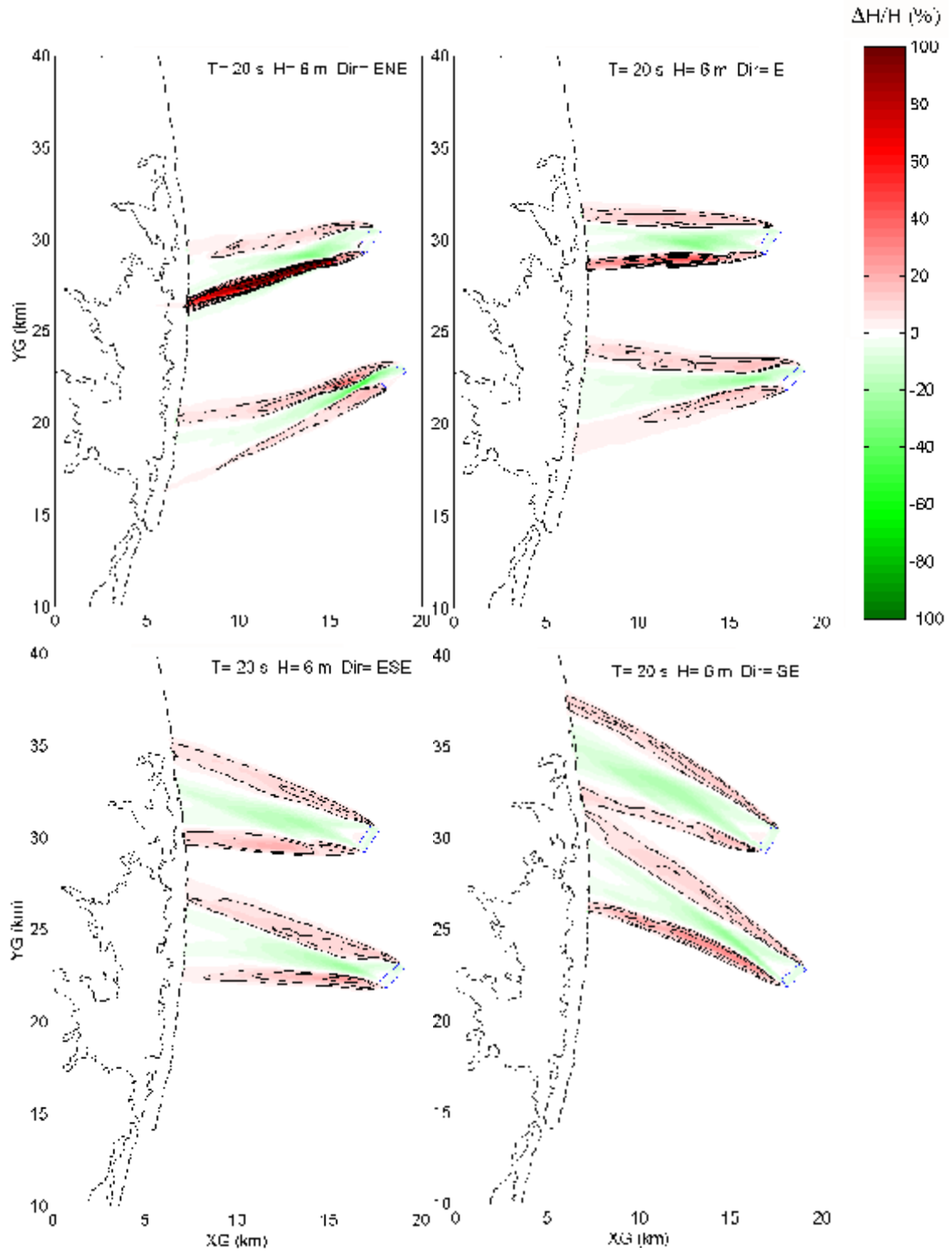


Fig. 5-5. Calculated Changes of Wave Height (Normalized) for the One-time Dredging with  $H_0=6$  m,  $T=20$  s.

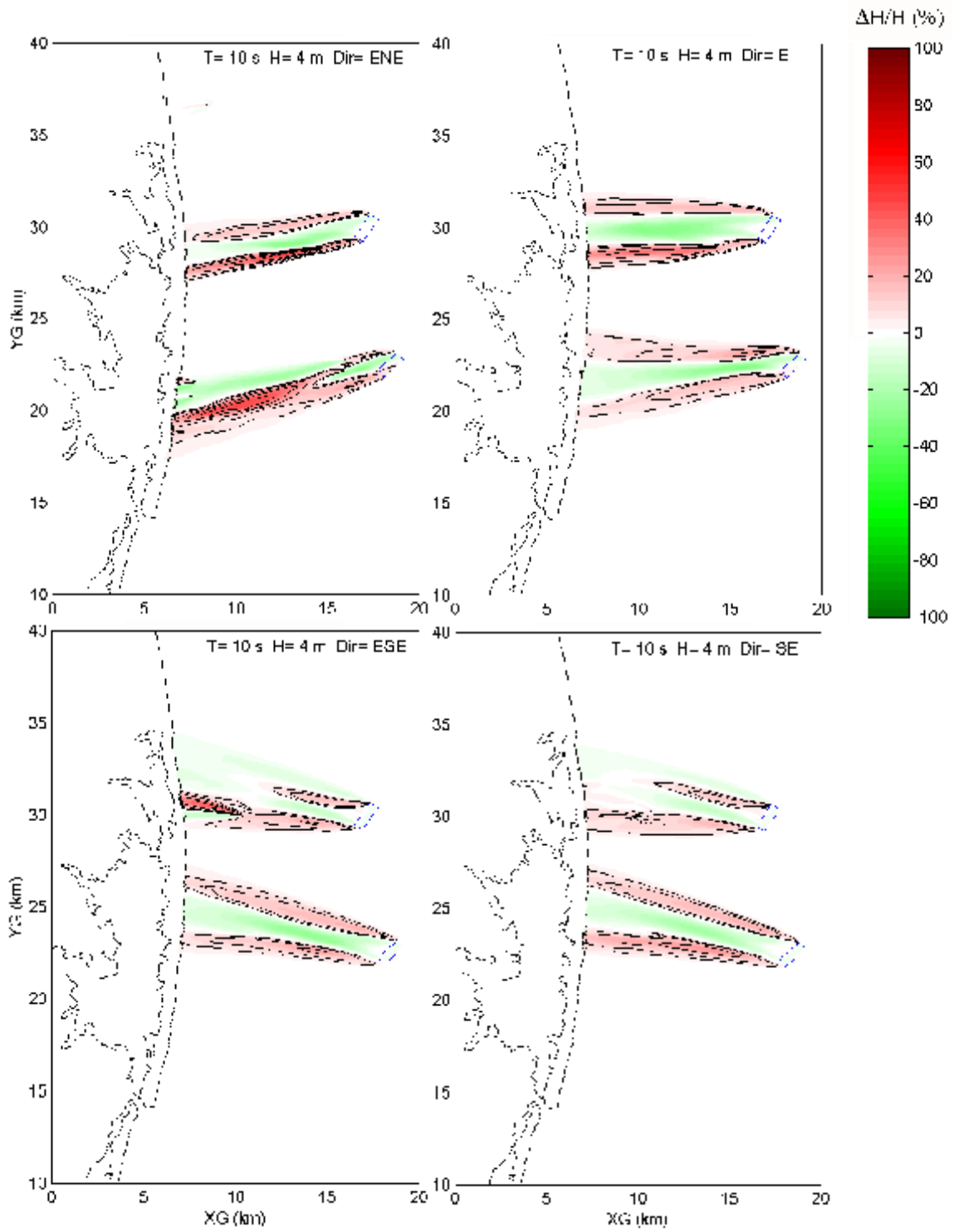


Fig. 5-6. Calculated Changes of Wave Height (Normalized) for the One-time Dredging with  $H_0=4$  m,  $T=10$  s.

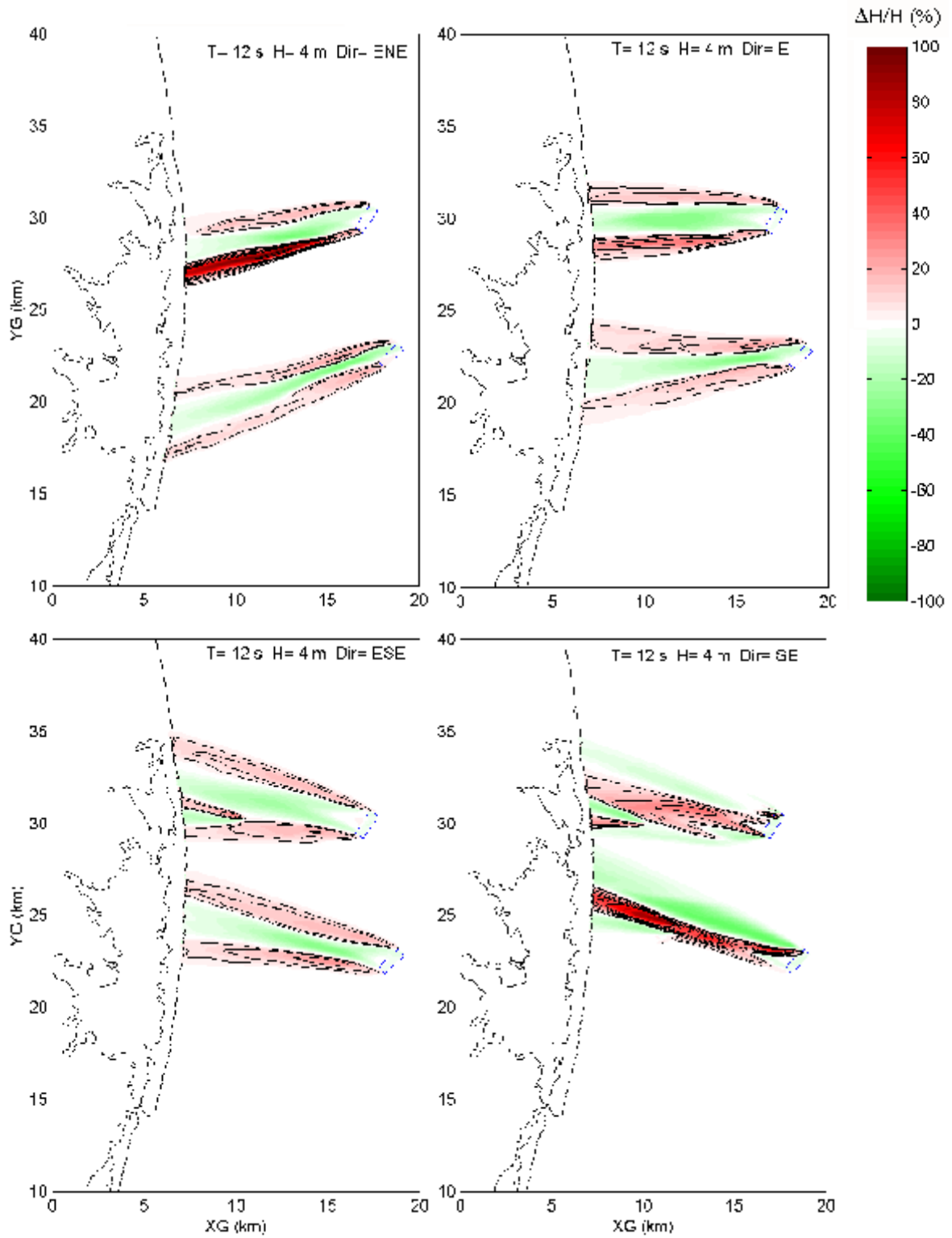


Fig. 5-7. Calculated Changes of Wave Height (Normalized) for the One-time Dredging with  $H_0 = 4$  m,  $T = 12$  s.

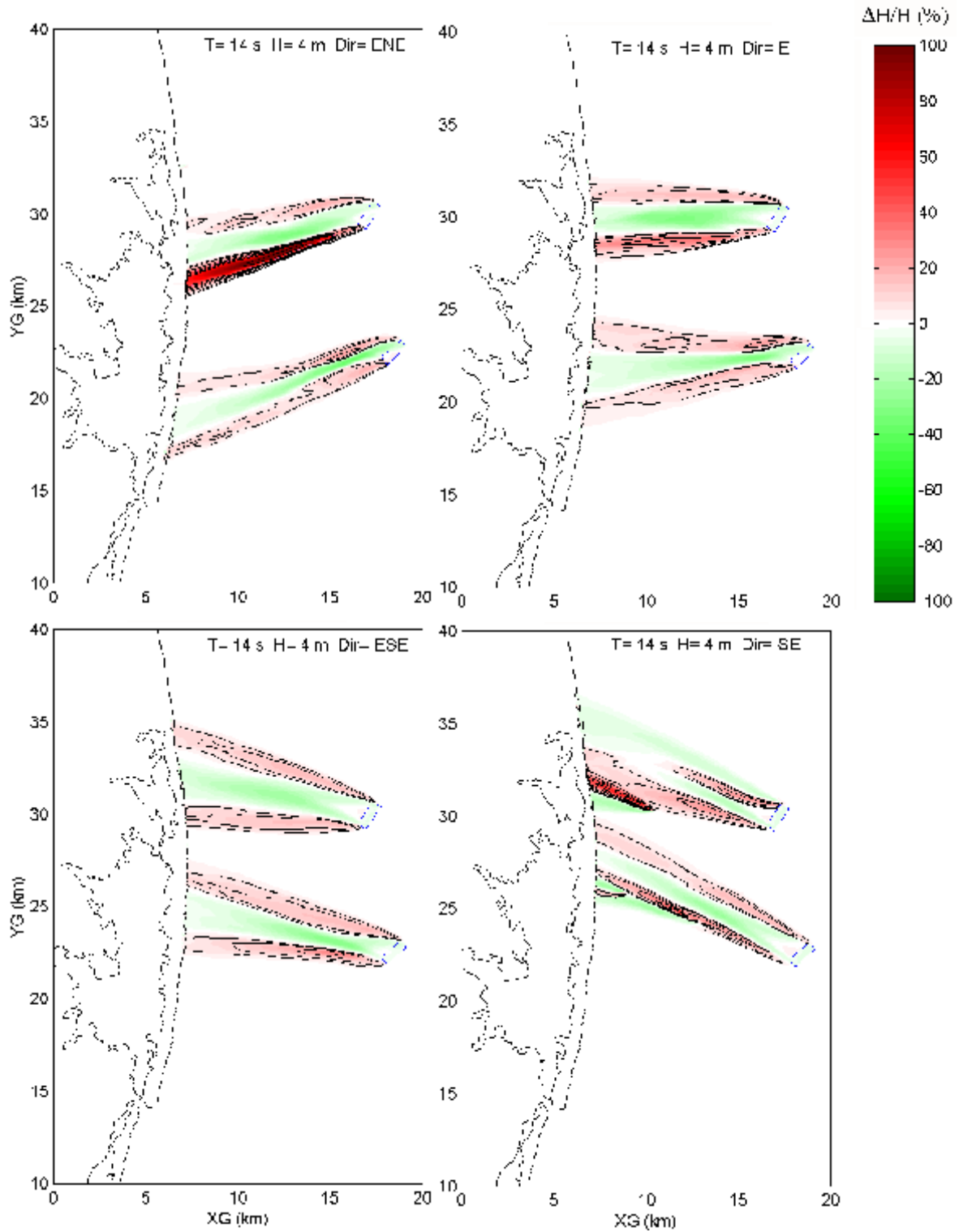


Fig. 5-8. Calculated Changes of Wave Height (Normalized) for the One-time Dredging with  $H_o=4$  m,  $T=14$  s.

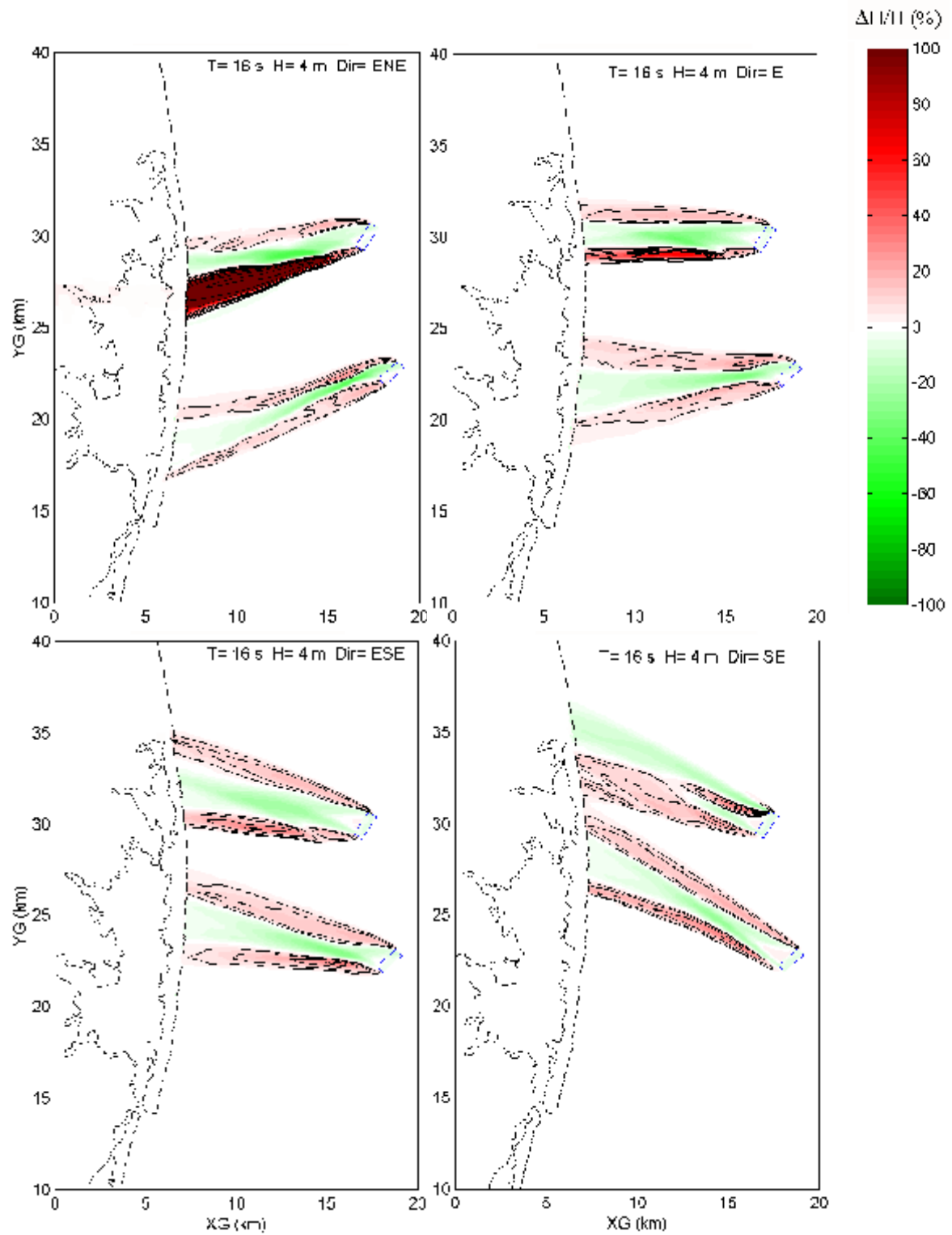


Fig. 5-9. Calculated Changes of Wave Height (Normalized) for the One-time Dredging with  $H_o=4 \text{ m}$ ,  $T=16 \text{ s}$ .

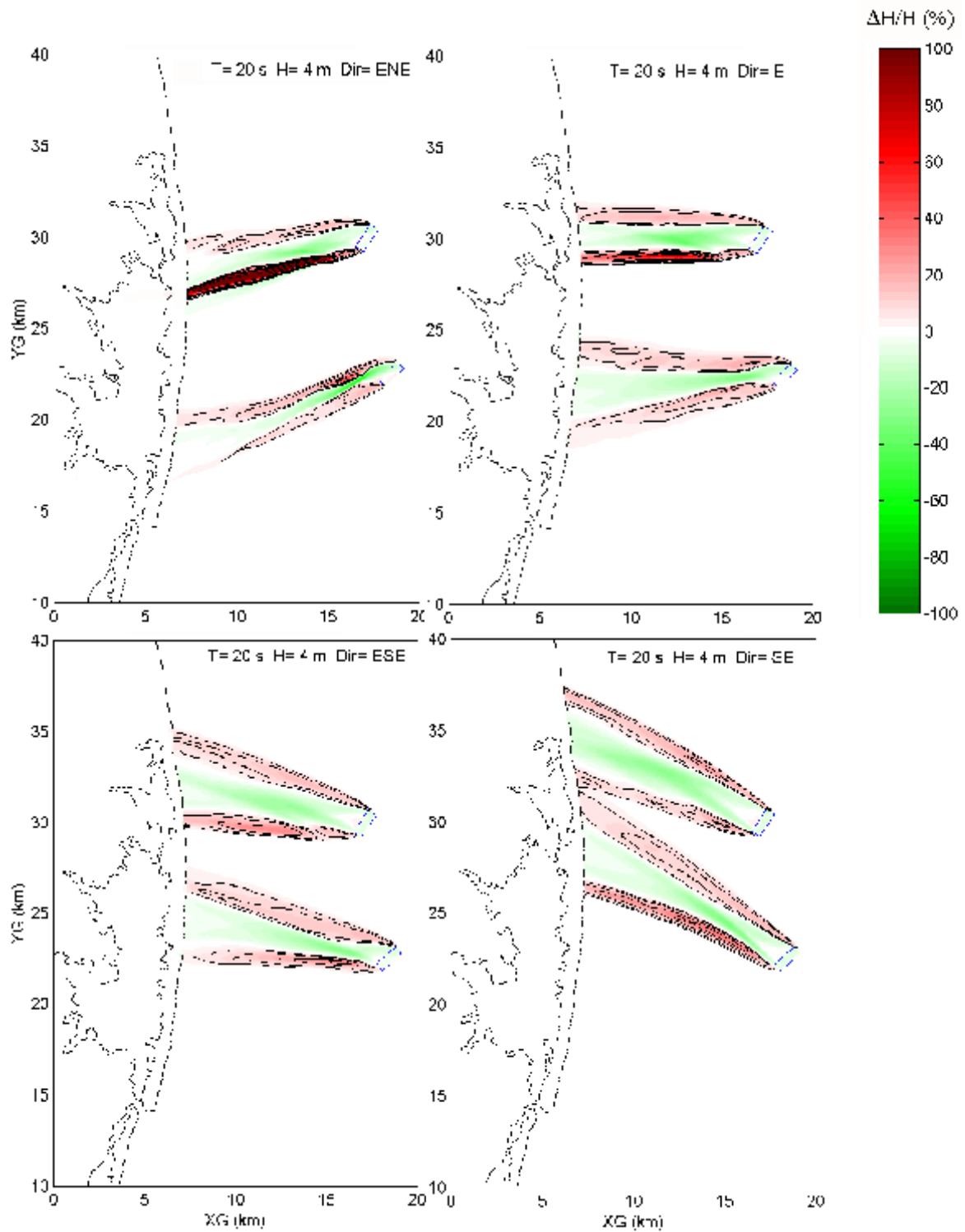


Fig. 5-10. Calculated Changes of Wave Height (Normalized) for the One-time Dredging with  $H_0 = 4$  m,  $T = 20$  s.

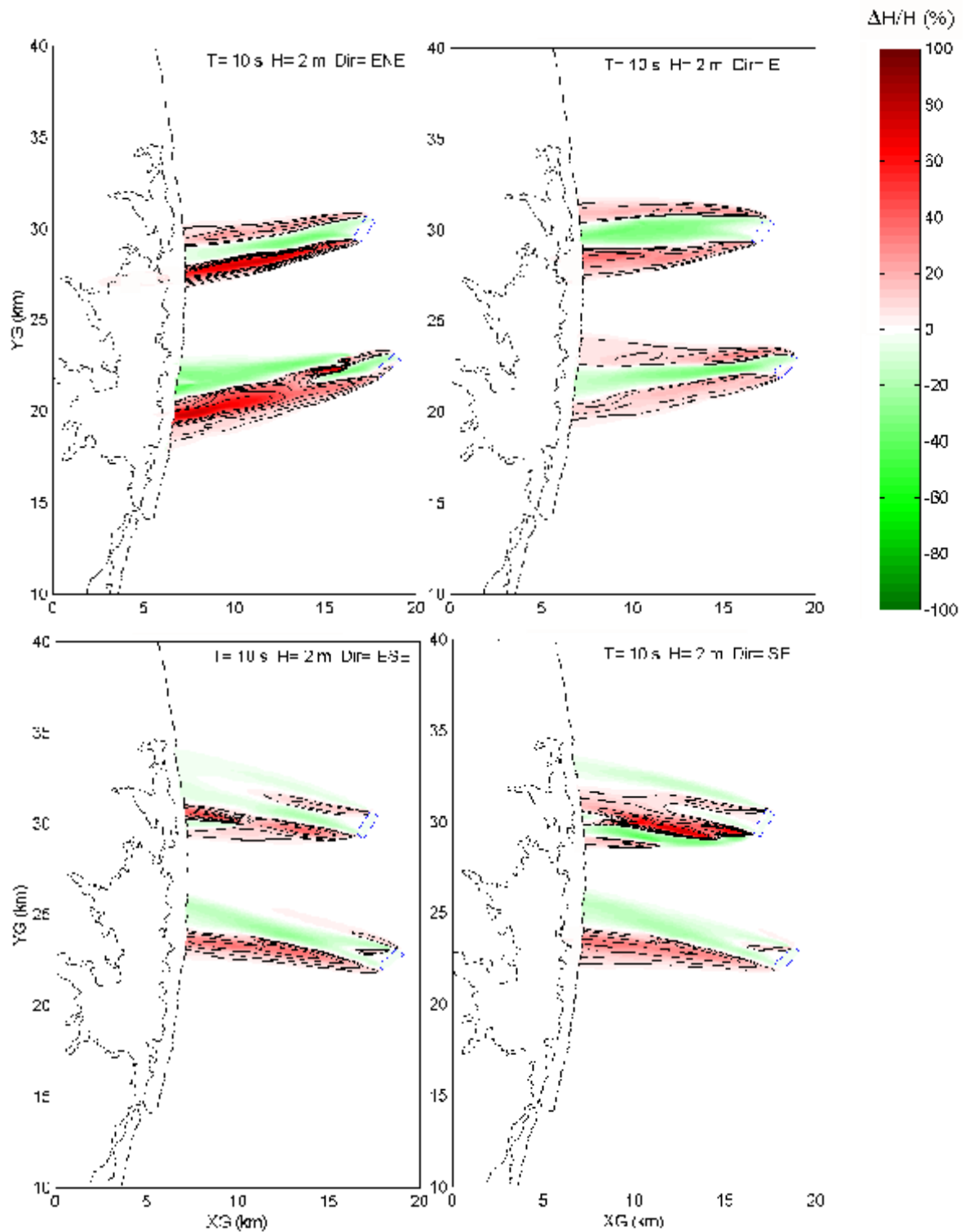


Fig. 5-11. Calculated Changes of Wave Height (Normalized) for the One-time Dredging with  $H_0 = 2$  m,  $T = 10$  s.

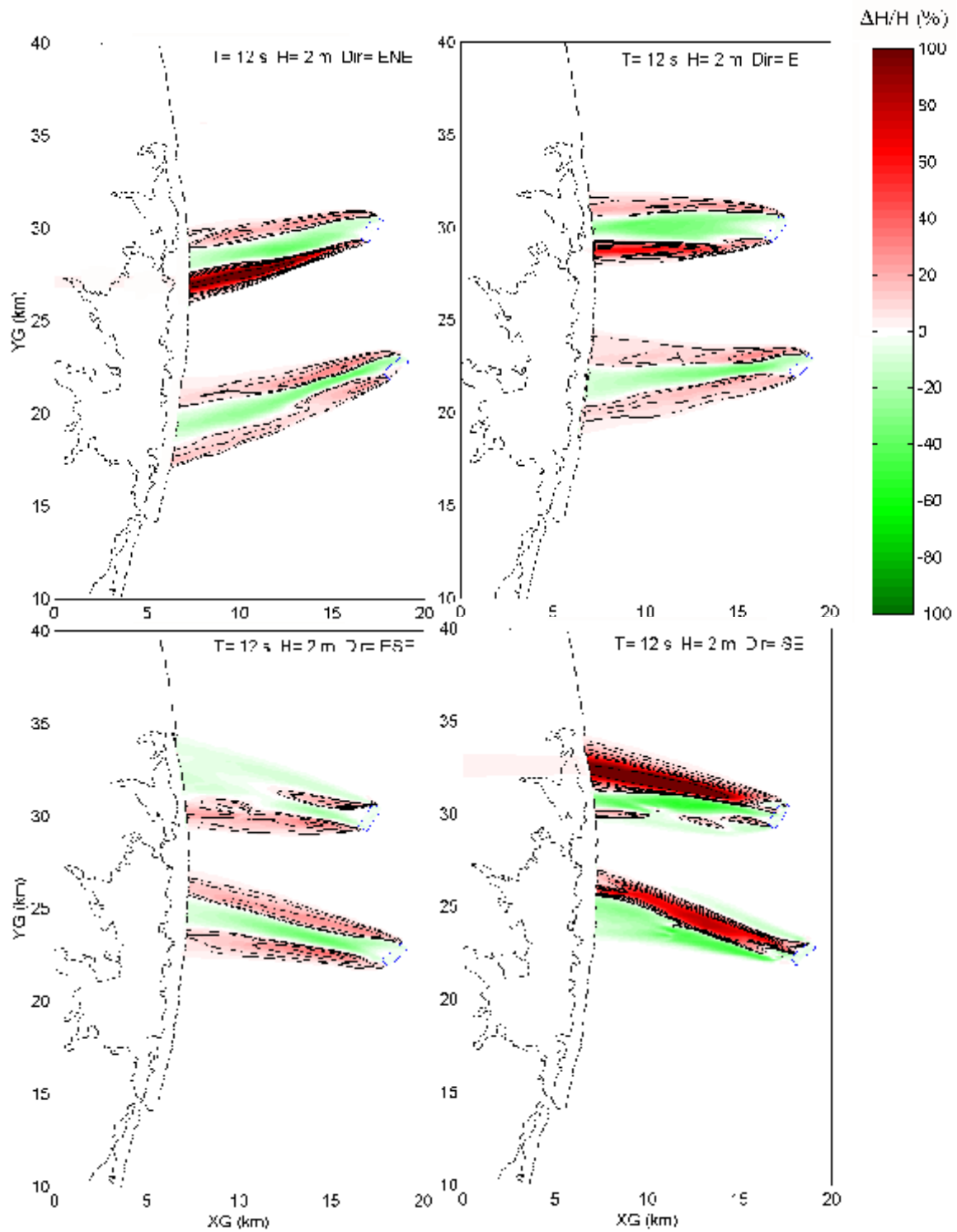


Fig. 5-12. Calculated Changes of Wave Height (Normalized) for the One-time Dredging with  $H_0 = 2$  m,  $T = 12$  s.

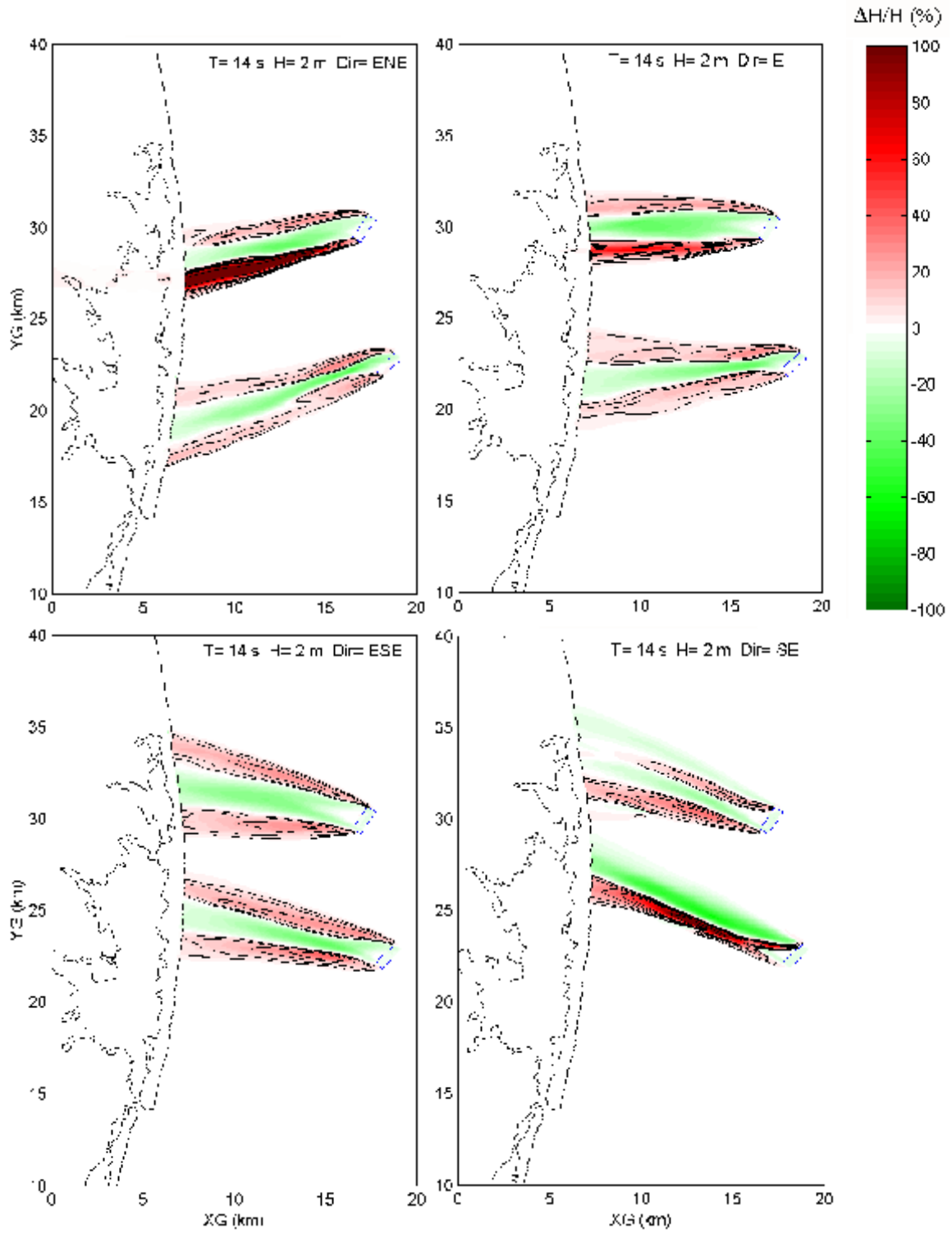


Fig. 5-13. Calculated Changes of Wave Height (Normalized) for the One-time Dredging with  $H_0=2$  m,  $T=14$  s.

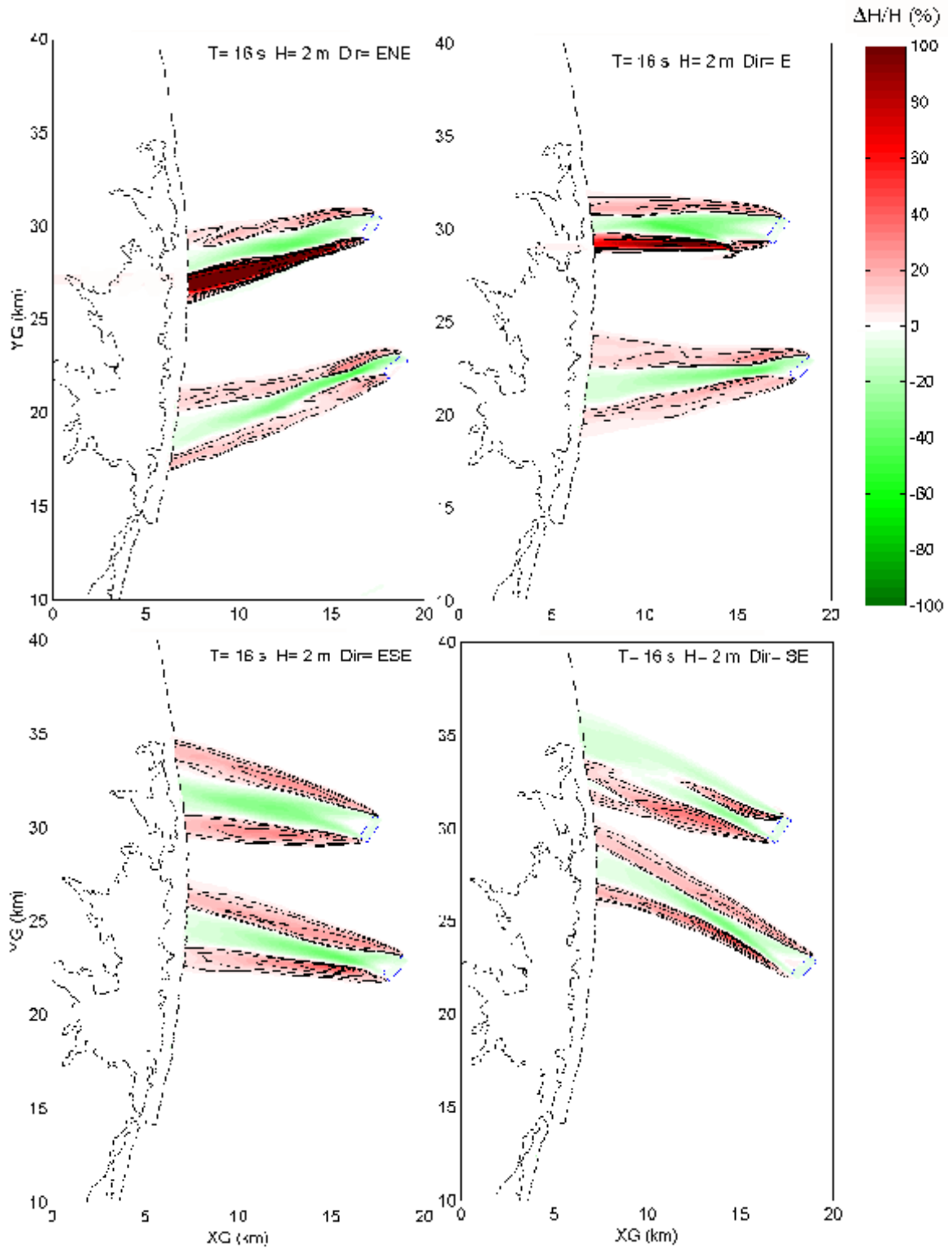


Fig. 5-14. Calculated Changes of Wave Height (Normalized) for the One-time Dredging with  $H_0=2$  m,  $T=16$  s.

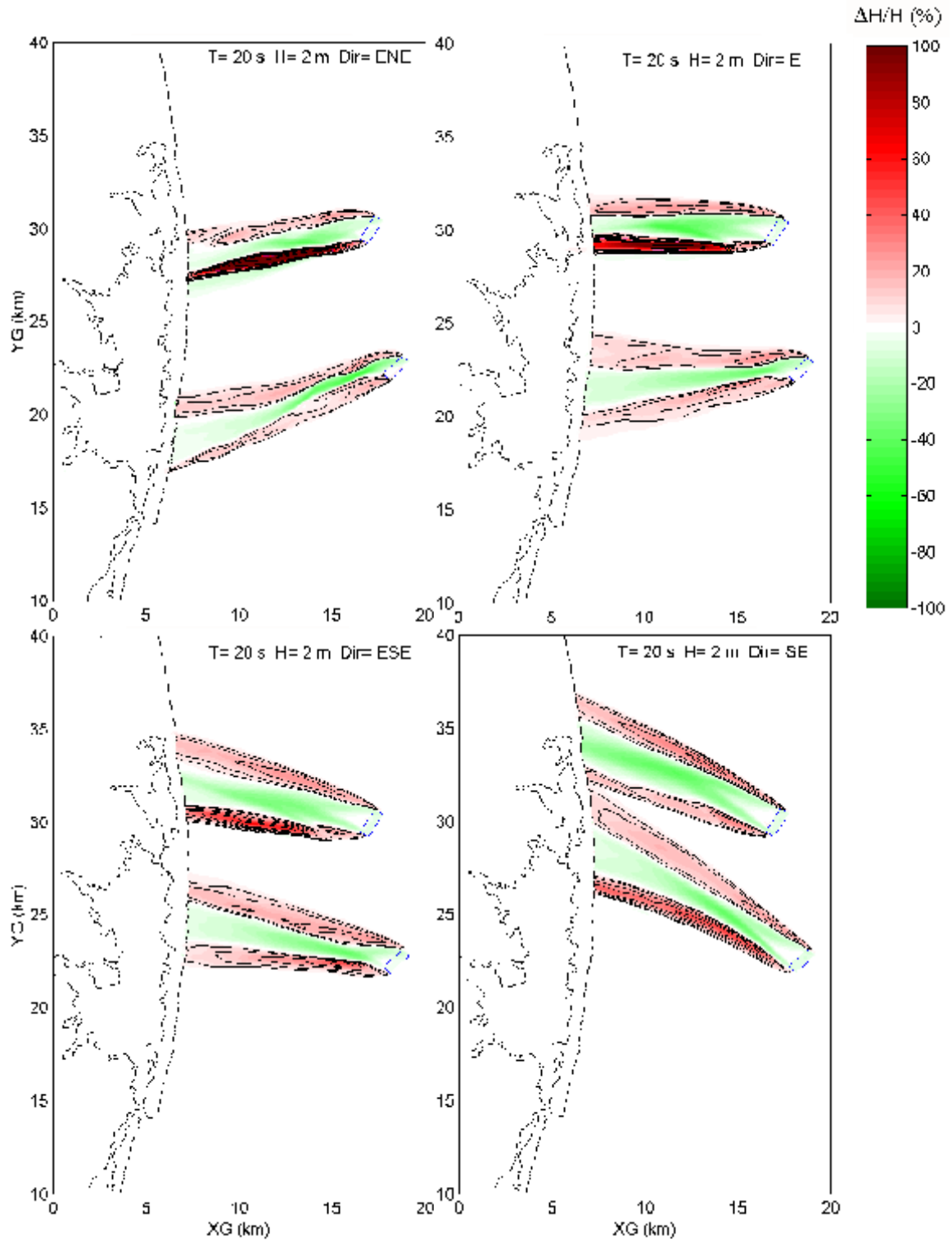


Fig. 5-15. Calculated Changes of Wave Height (Normalized) for the One-time Dredging with  $H_0 = 2$  m,  $T = 20$  s.

### 5.3. Changes in Breaking Wave Heights

As to possible shoreline variation, it is necessary to study the possible change of breaking wave height along the coast (see the criterion in Chapter 4). For this reason, the changes of breaking wave heights along the coast in the display domain are plotted in Figs. 5-16 to 5-30. The modeled dredge areas are located between  $YG = 22$  to  $24$  km and  $YG = 29$  and  $31$  km. The black lines in these figures represent the profiles of breaking wave height for the original bathymetry. The red dashed lines in these figures are the breaking wave height profile after the modeled one-time dredging. Shore line was also given in these plots for a better indication of location.

The possible changes for the most severe sea ( $H_o = 8$  m,  $T = 20$  s) that comes from ENE (Fig. 5-16) indicates that the Breaking wave Height Modulation (BHM, Chapter 4) increased a little (BHM = 1.3) at  $YG = 18.5$  km, but decreased a little at  $YG = 26$  km (BHM = 0.85). For the most severe sea coming from E, the possible impact is slightly unfavorable; At  $YG = 22.5$ , BHM = 1.09, and between  $YG = 17 - 18$  km, BHM . 1. If the waves come from ESE, the results are all negative (BHM = 1.6 at  $YG = 31$  km; BHM = 1.8 at  $YG = 22.5$  km). If the waves come from SE, the only possible impact can be seen is at  $YG = 31$  km with a BHM . 1. The modulation has the same amplitudes but shifted laterally along the shore. Thus, for the most severe waves come from SE, we can considered that there is no significant change (marked as NG thereafter).

As an aid to assessing the overall effect, the breaking wave height modulation is summarized in Table 5-1. It is clearly indicated in Table 5-1 that for a total of 60 wave conditions, only 10 wave conditions show that the change of breaking wave height is noticeable, or measurable from Fig. 5-16 to 5-30. Among these 10 wave conditions, only for the most severe sea that comes from ESE may have a significant impact on the breaking wave height modulation. All others either have a mixed impact (some areas positive, some negative) or the impact is positive, *i.e.*, the BHM decreases.

Table 5-1, Summary of Changes on Breaking Wave Height Modulation for the One-time Dredging

Wave Dir.	T = 10s	12s	14s	16s	20s	
ENE	: M <sup>1</sup>	— <sup>5</sup>	--	--	0.9/1.2	1.26/0.84
	: S <sup>2</sup>	--	--	0.66	NG	NG
	: R <sup>3</sup>	NG <sup>6</sup>	0.9	0.9/1.25	0.83	NG
	: N <sup>4</sup>	NG	NG	NG	NG	NG
E	: M	--	--	--	NG	1.09/1
	: S	--	--	NG	NG	NG
	: R	NG	NG	NG	NG	NG
	: N	NG	NG	NG	NG	NG
ESE	: M	--	--	--	NG	1.6/1.8
	: S	--	--	NG	NG	NG
	: R	NG	NG	NG	NG	NG
	: N	NG	NG	NG	NG	NG
SE	: M	--	--	--	NG	NG
	: S	--	--	NG	NG	NG
	: R	NG	NG	1.16	NG	NG
	: N	NG	0.55/1.75	NG	NG	NG

<sup>1</sup>: represents Northeastern wave condition.

<sup>2</sup>: represents Rough Sea wave condition.

<sup>3</sup>: represents Severe Sea wave condition.

<sup>4</sup>: represents the Most Severe Sea wave condition.

<sup>5</sup>: NG is a shorthand for negligible small.

<sup>6</sup>: — is a shorthand for not included in computation.

## 5.4. Conclusions

This study indicates that for the one-time dredging at Fenwick Shoal and Isle of Wight Shoal for a total of  $4 \times 10^6$  m<sup>3</sup> of sand is acceptable in terms of potential modification to wave transformation. The major change to waves occurred not at the modeled dredging sites nor at the coast, but between these two.

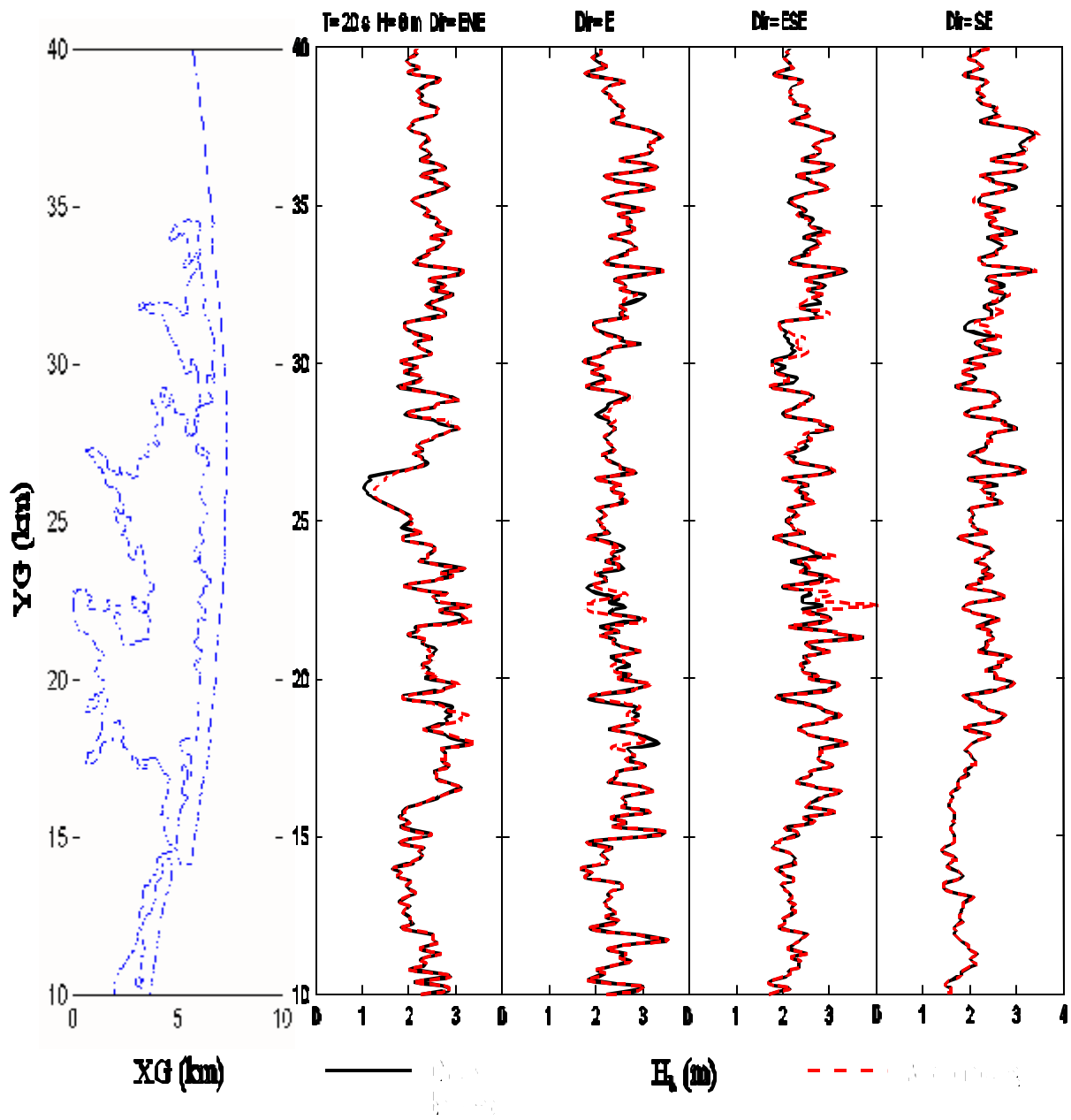


Fig. 5-16. Comparison of Breaking Wave Heights for Original Bathymetry and after One-time Dredging with  $H_s = 8$  m,  $T = 20$  s.

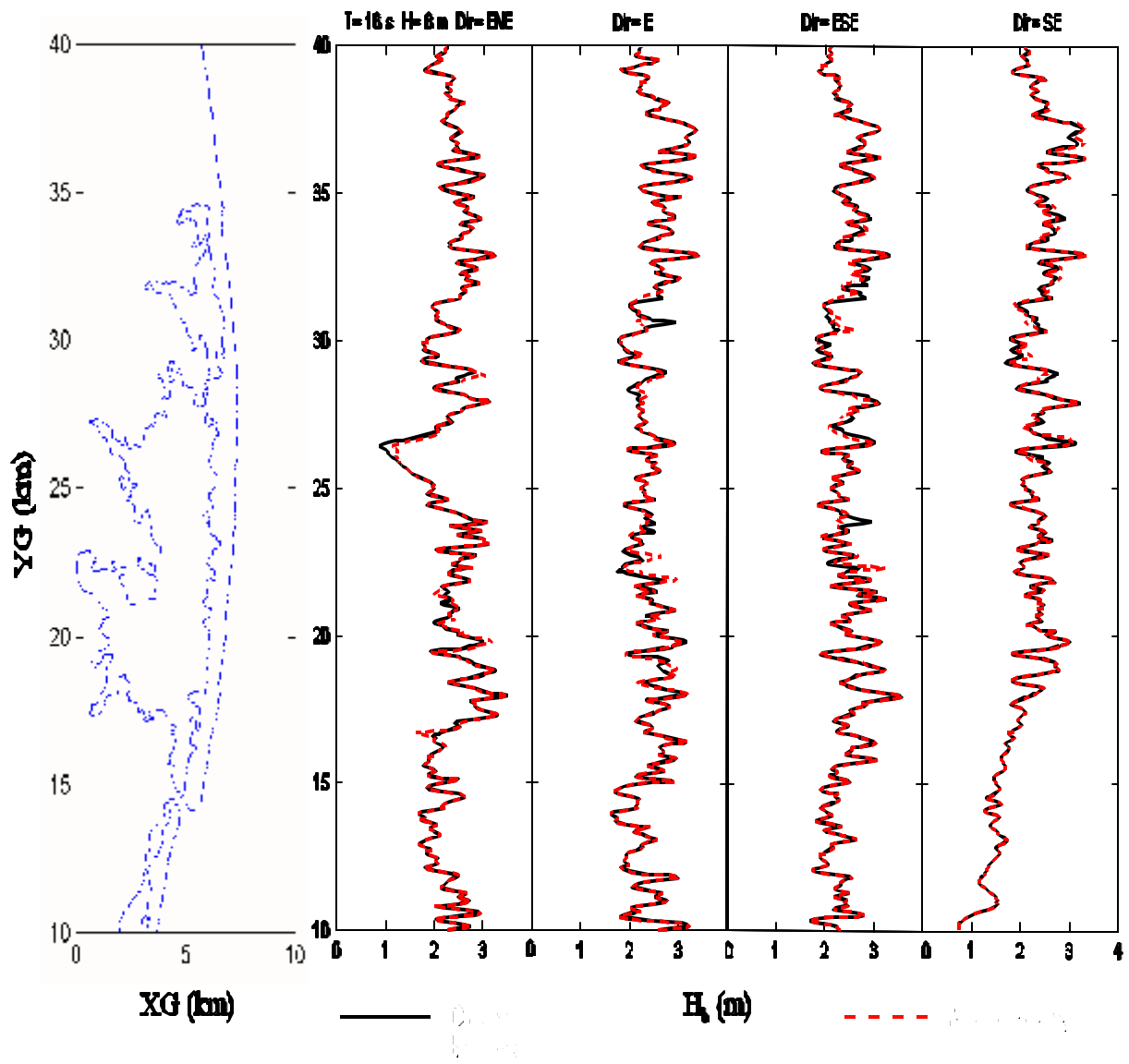
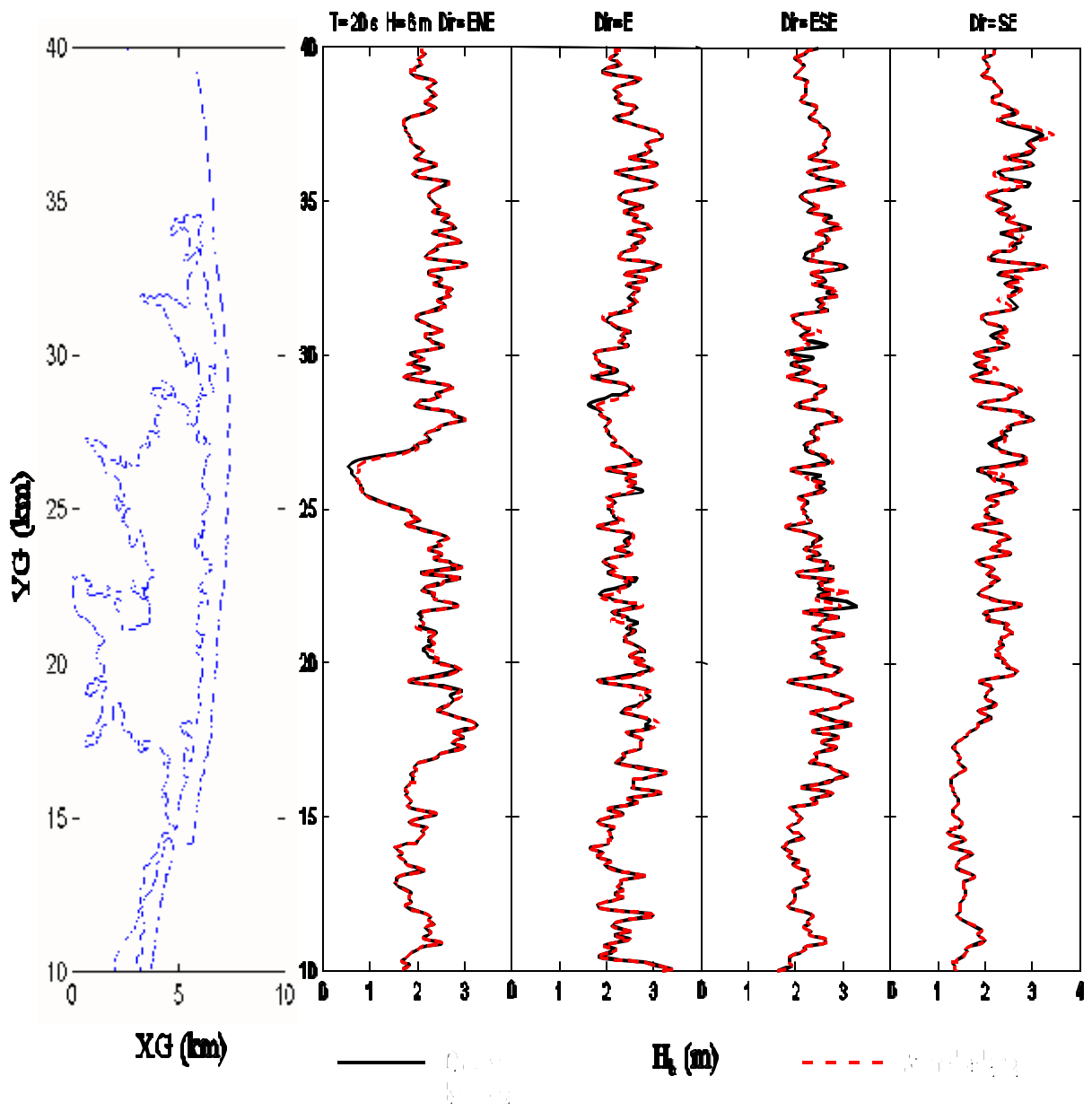


Fig. 5-17. Comparison of Breaking Wave Heights for Original Bathymetry and after One-time Dredging with  $H_b = 8$  m,  $T = 16$  s.



**Fig. 5-18. Comparison of Breaking Wave Heights for Original Bathymetry and after One-time Dredging with  $H_b = 6$  m,  $T = 20$  s.**

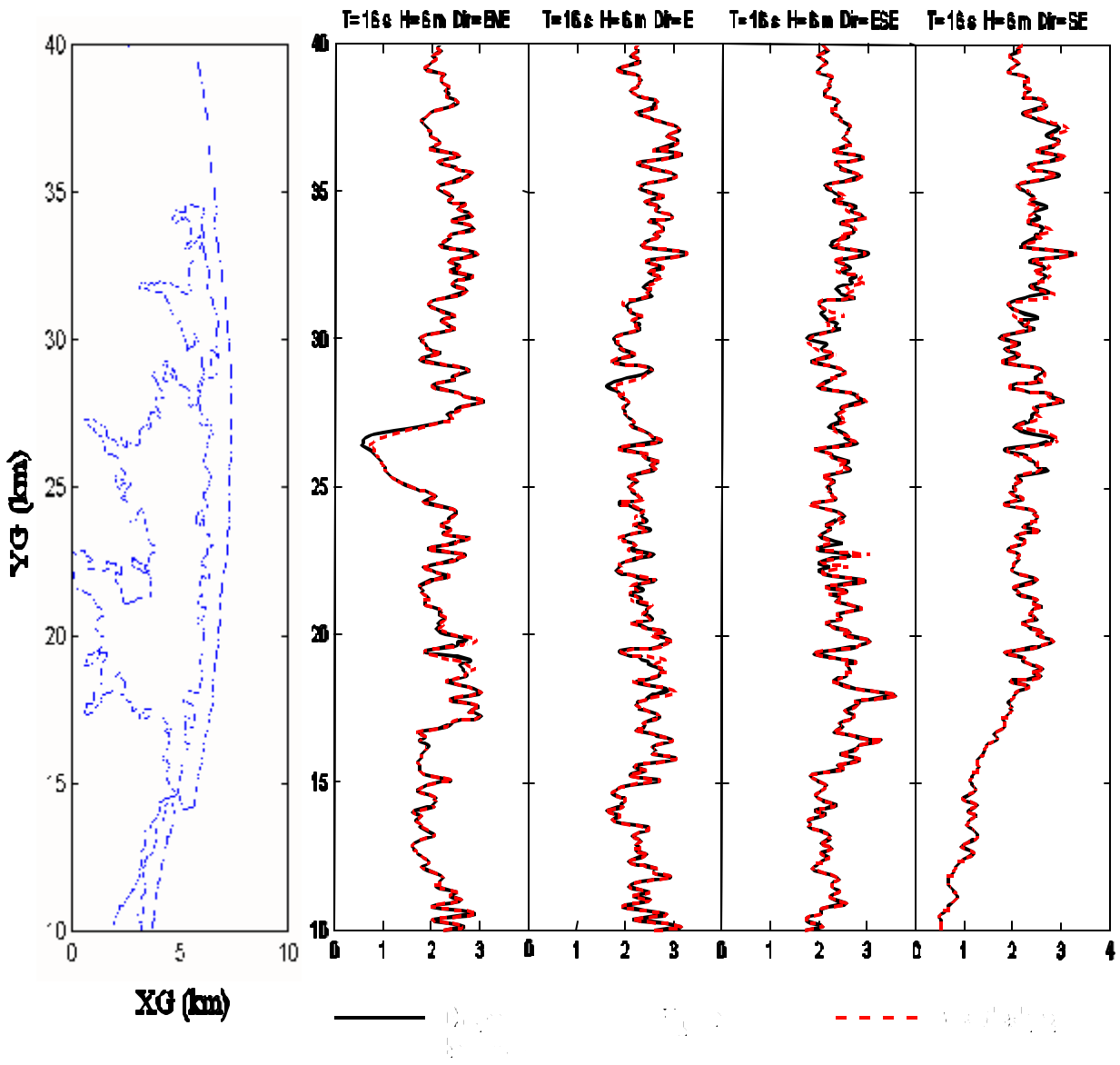


Fig. 5-19. Comparison of Breaking Wave Heights for Original Bathymetry and after One-time Dredging with  $H_b = 6$  m,  $T = 16$  s.

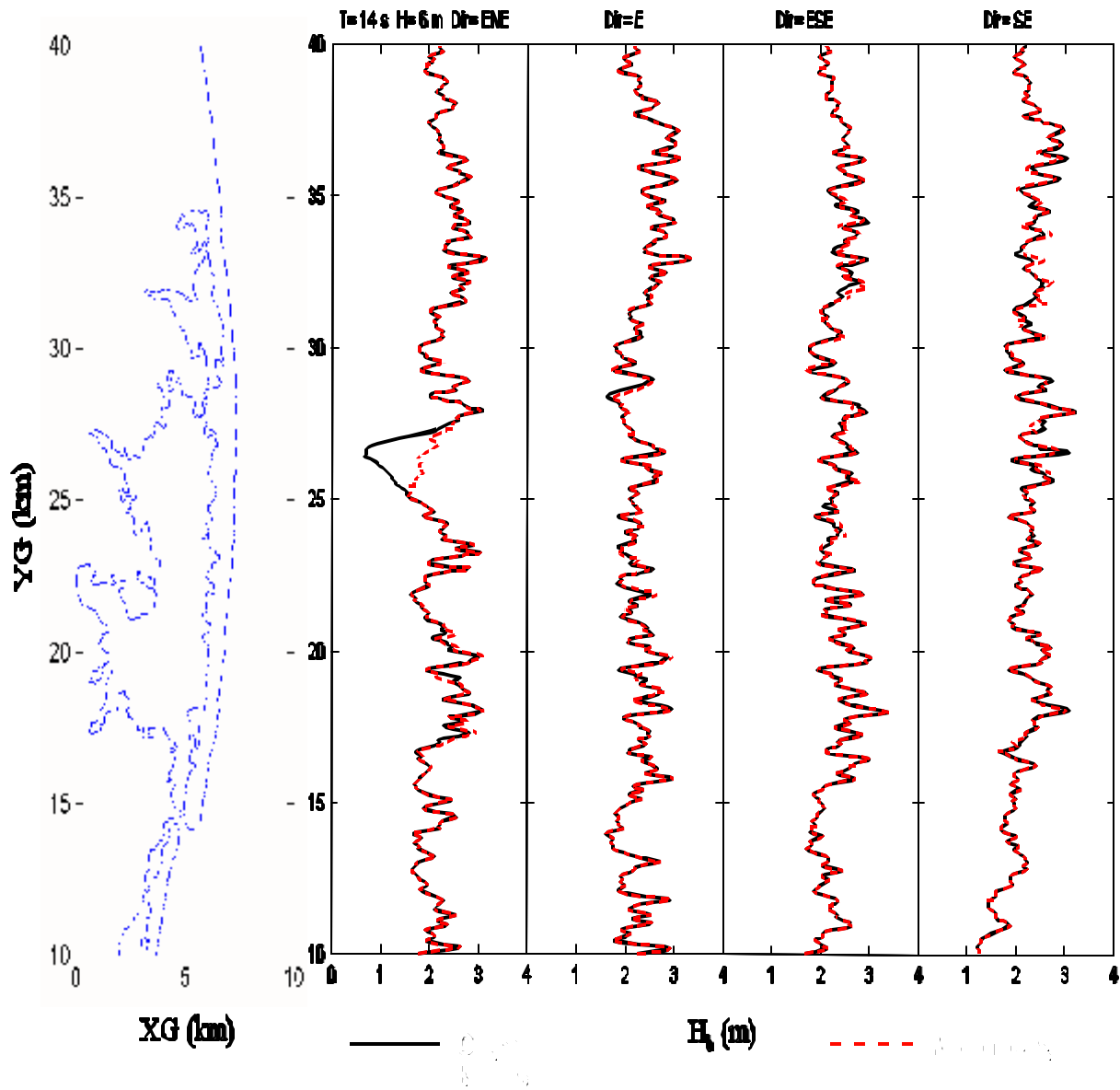


Fig. 5-20. Comparison of Breaking Wave Heights for Original Bathymetry and after One-time Dredging with  $H_b = 6$  m,  $T = 14$  s.

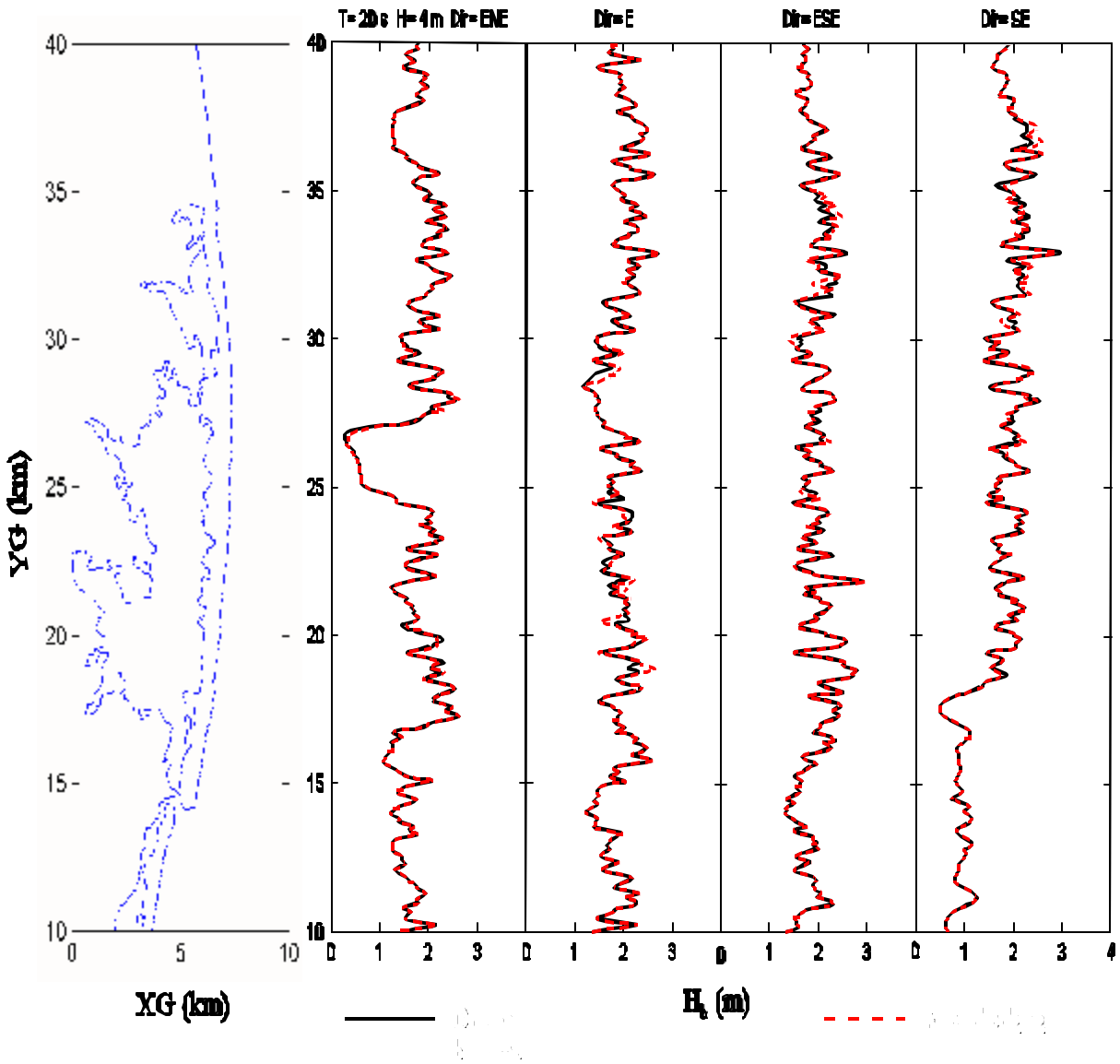


Fig. 5-21. Comparison of Breaking Wave Heights for Original Bathymetry and after One-time Dredging with  $H_b = 4$  m,  $T = 20$  s.

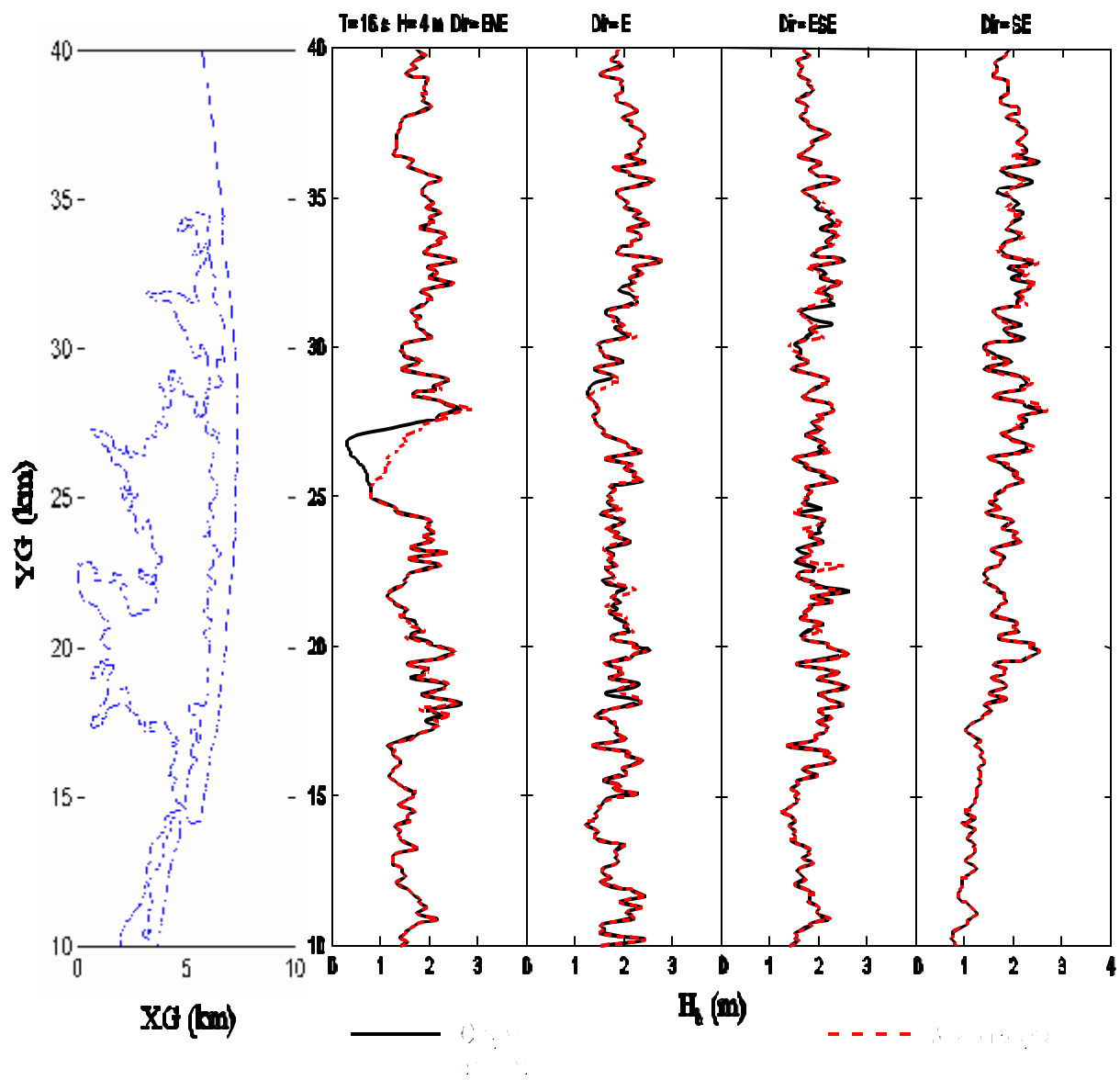


Fig. 5-22. Comparison of Breaking Wave Heights for Original Bathymetry and after One-time Dredging with  $H_s = 4$  m,  $T = 16$  s.

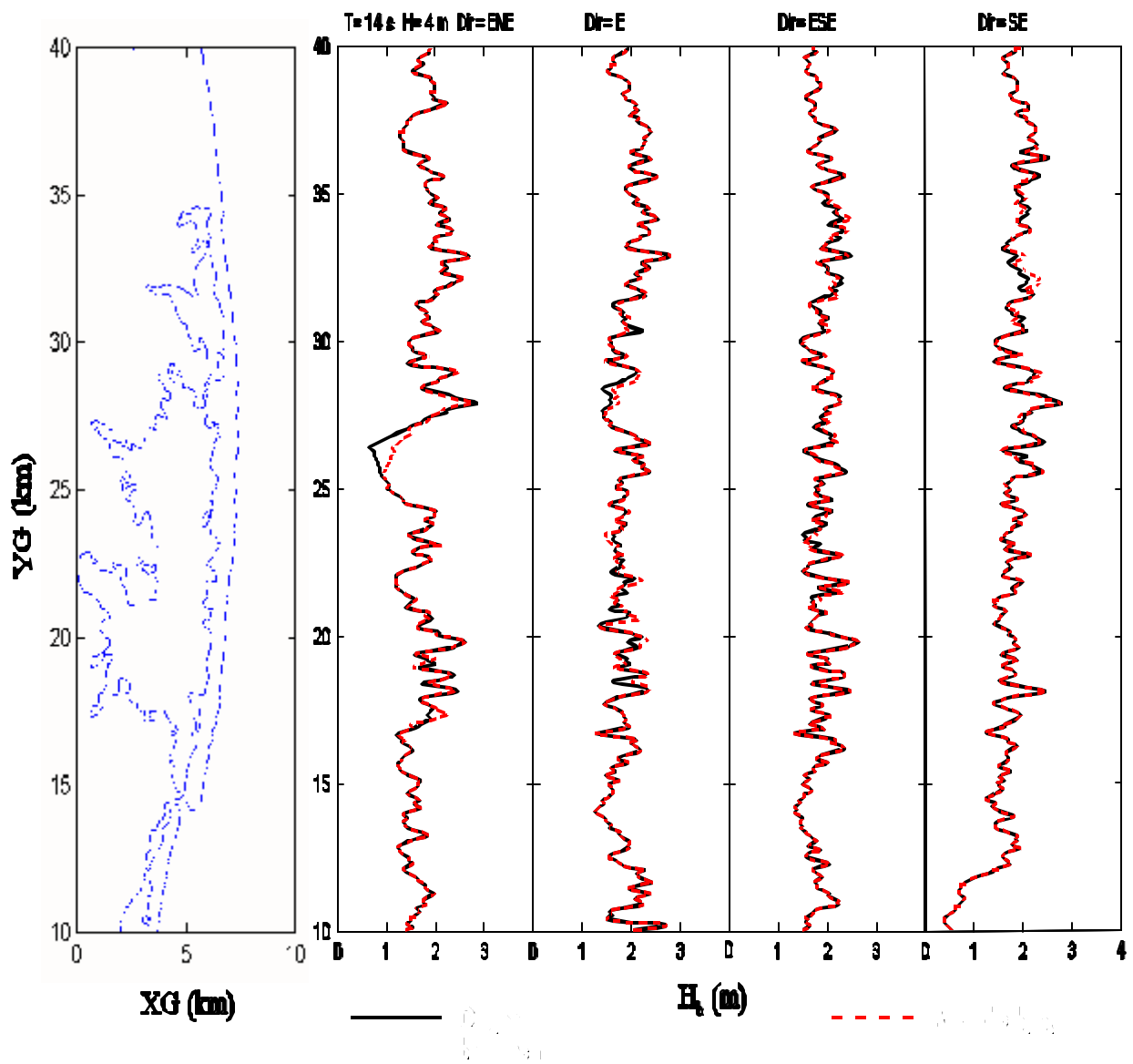


Fig. 5-23. Comparison of Breaking Wave Heights for Original Bathymetry and after One-time Dredging with  $H_b = 4$  m,  $T = 14$  s.

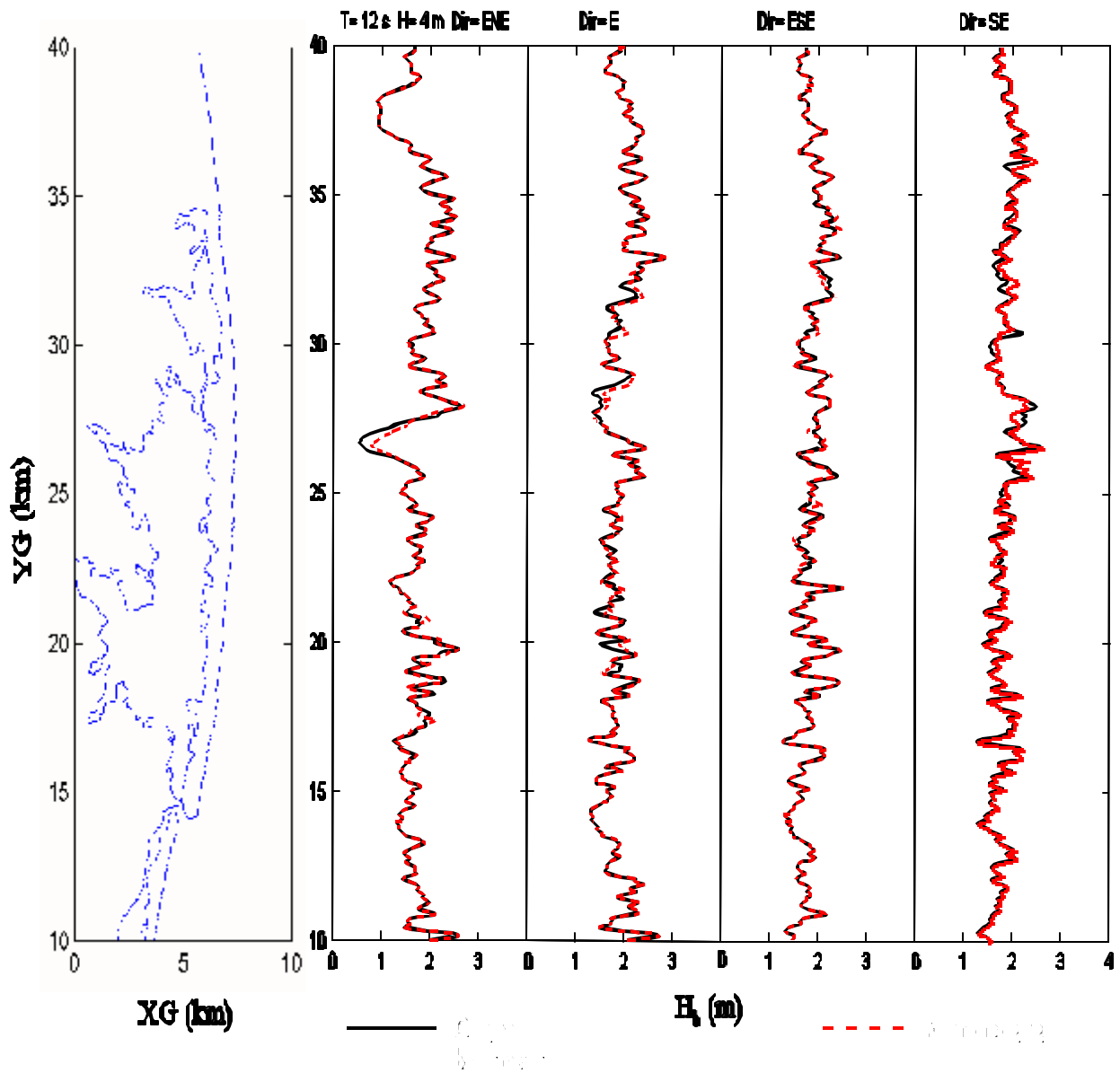


Fig. 5-24. Comparison of Breaking Wave Heights for Original Bathymetry and after One-time Dredging with  $H_b = 4\text{ m}$ ,  $T = 12\text{ s}$ .

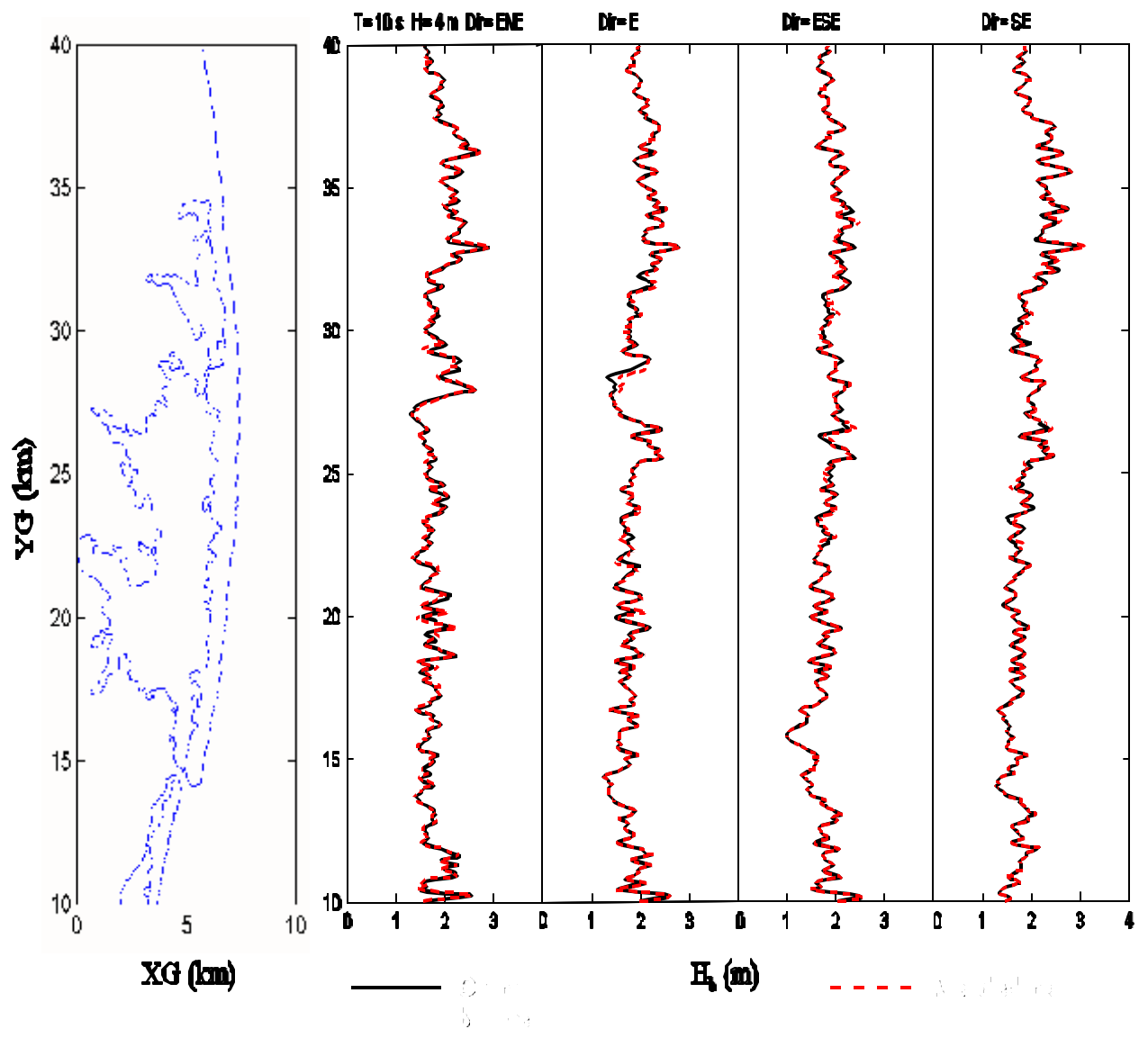


Fig. 5-25. Comparison of Breaking Wave Heights for Original Bathymetry and after One-time Dredging with  $H_o = 4$  m,  $T = 10$  s.

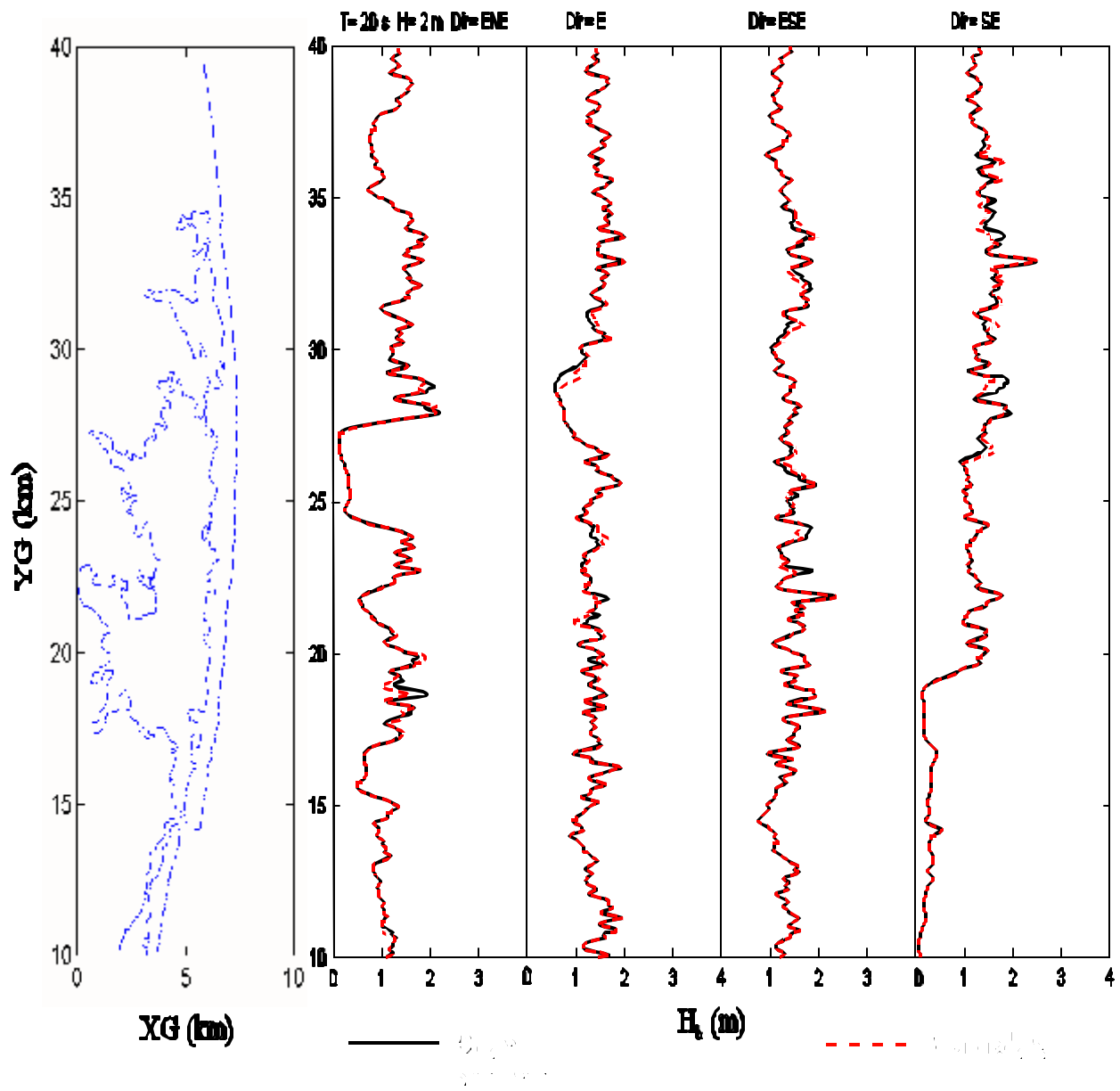


Fig. 5-26. Comparison of Breaking Wave Heights for Original Bathymetry and after One-time Dredging with  $H_s = 2\text{ m}$ ,  $T = 20\text{ s}$ .

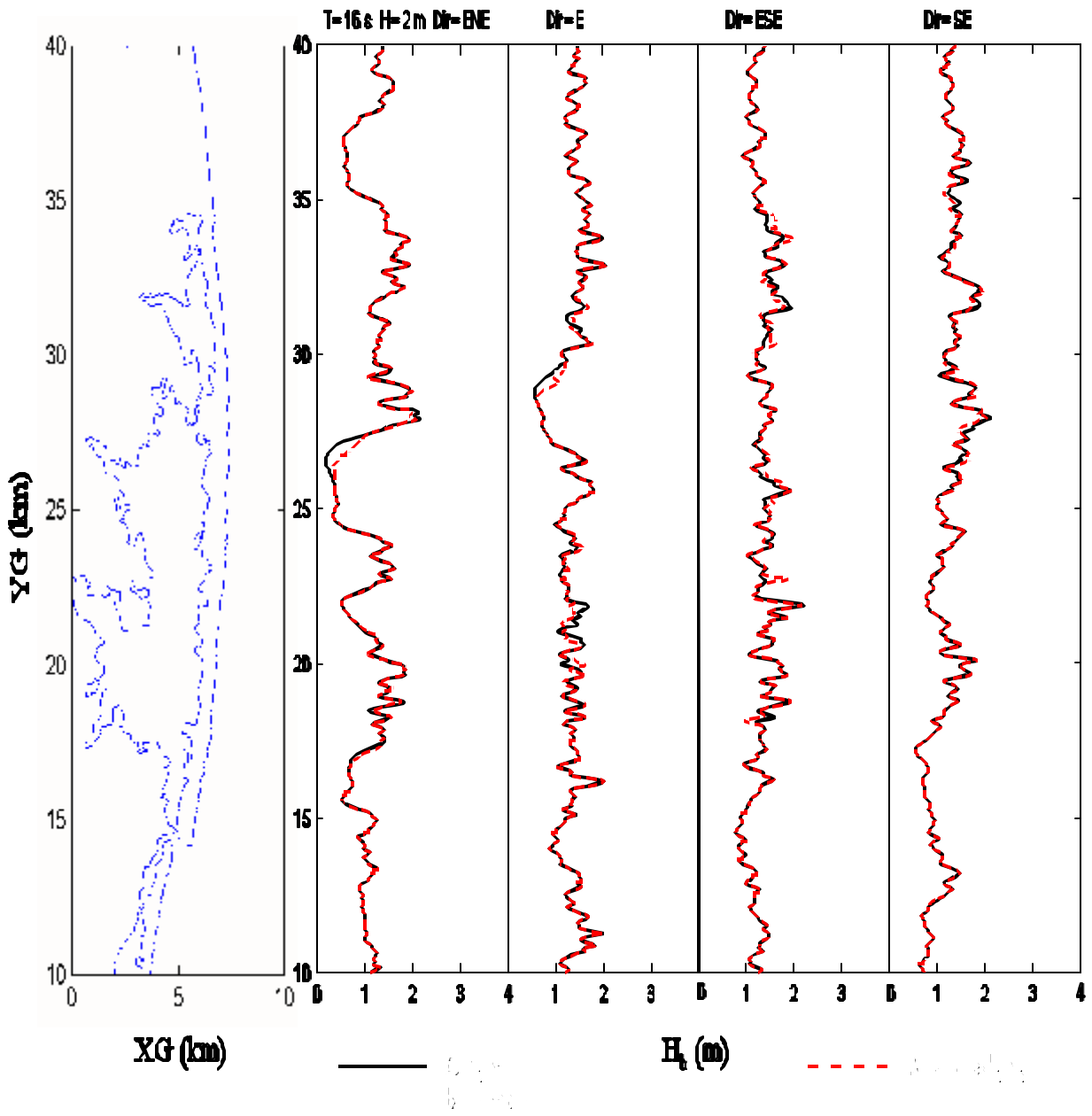


Fig. 5-27. Comparison of Breaking Wave Heights for Original Bathymetry and after One-time Dredging with  $H_s = 2m$ ,  $T = 16s$ .

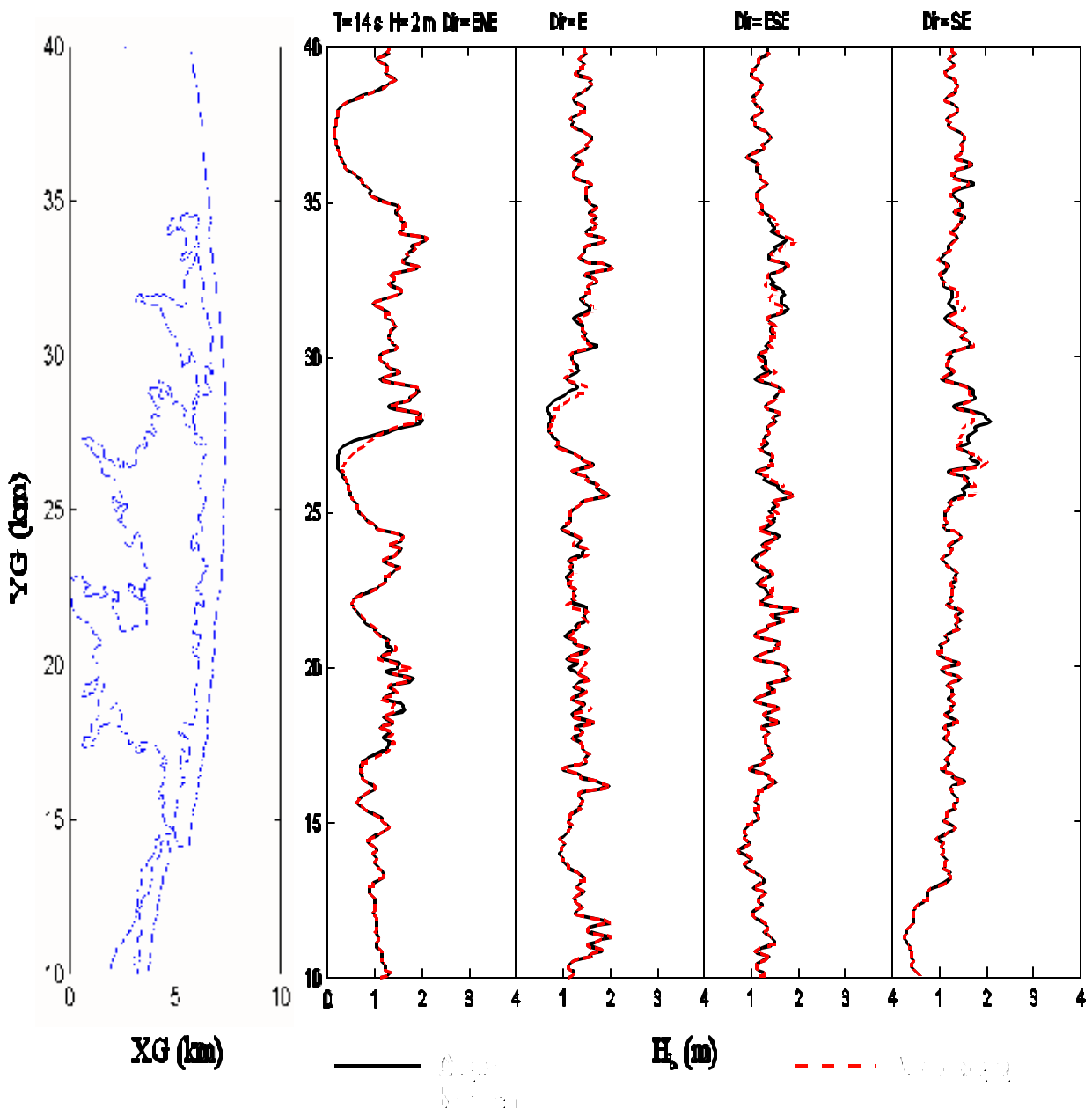


Fig. 5-28. Comparison of Breaking Wave Heights for Original Bathymetry and after One-time Dredging with  $H_b = 2$  m,  $T = 14$  s.

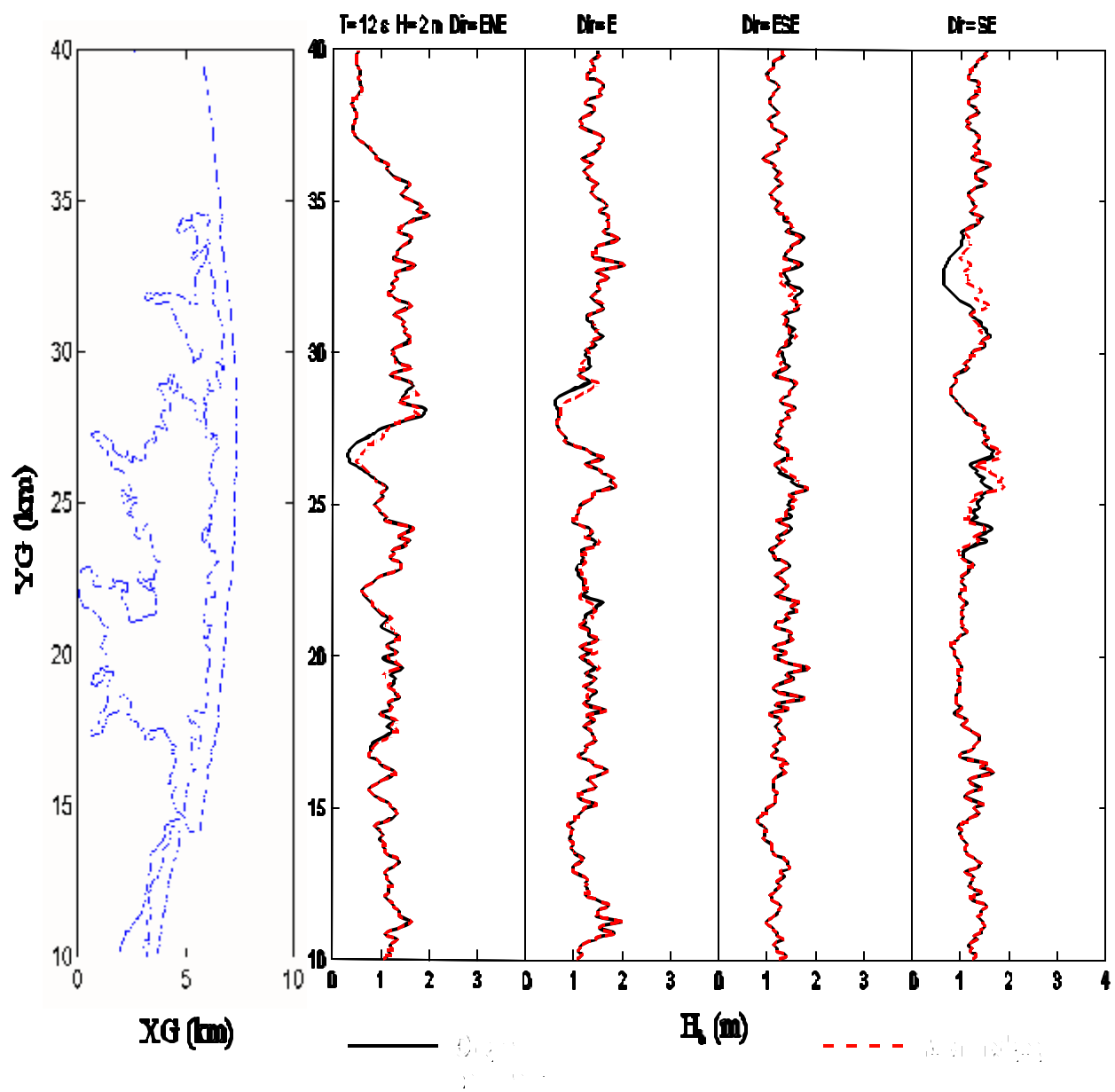


Fig. 5-29. Comparison of Breaking Wave Heights for Original Bathymetry and after One-time Dredging with  $H_b = 2$  m,  $T = 12$  s.

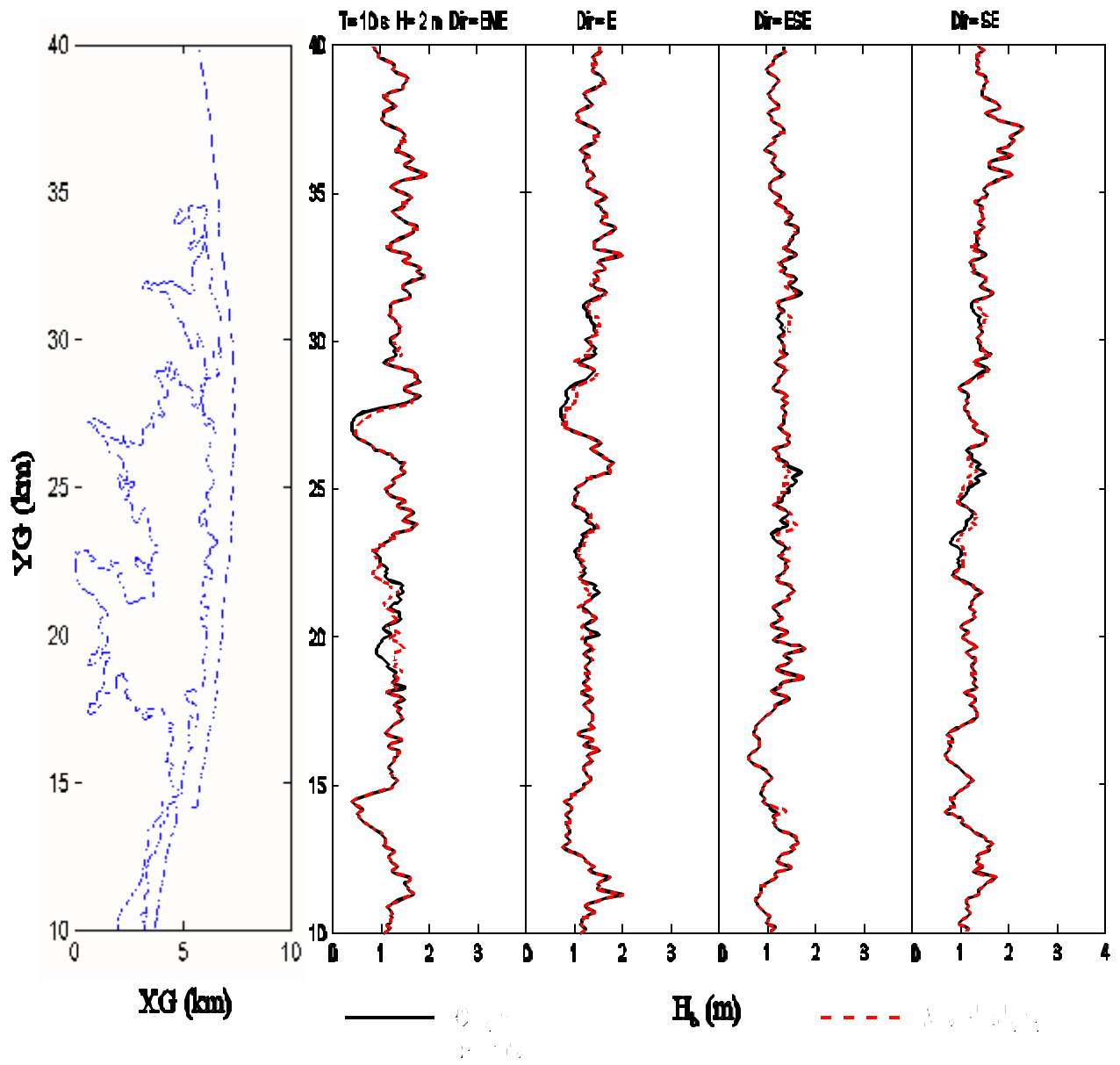


Fig. 5-30. Comparison of Breaking Wave Heights for Original Bathymetry and after One-time Dredging with  $H_s = 2$  m,  $T = 10$  s.

## CHAPTER 6. CHANGES OF WAVE ENVIRONMENTS AFTER THE ACCUMULATIVE DREDGING

### 6.1. Introduction

The scenario of dredging considered in this chapter is for providing a long term (10 to 20 years) sand resource on the order of  $24 \times 10^6 \text{ m}^3$  for Maryland and Delaware coast. The objective is to determine if the impact of this accumulated dredging at the two selected shoals is acceptable or not. The same wave conditions given in Chapter 5 are used here again. The difference in computed wave height between the offshore dredging sites and the coast line are presented first to obtain a general idea of spatial difference. Then the differences in breaking wave heights along the coast are studied.

### 6.2. Results in Spatial Variation

The afore selected 60 wave conditions were run with the bathymetry altered as shown in Figs. 2-5 and 2-6. Similar to Chapter 5, the normalized difference in wave height (*i.e.*,  $\Delta H/H$ , in unit of %) are given in Figs. 6-1 to 6-15. Again, red represents increase (*i.e.*,  $\Delta H/H > 0\%$ ), green represents decrease (*i.e.*,  $\Delta H/H < 0\%$ ), and white represents no change (*i.e.*,  $\Delta H/H = 0\%$ ). The modeled dredging areas are shown as the dashed boxes in these figures.

Since the dredging areas are much larger than those given in Chapter 5, the affected areas also are larger. It is important, however, to point out that because the distance between these two dredging sites (Fenwick Shoal and Isle of Wight Shoal) is large, there is no interaction between the alterations to wave transformation (Figs. 6-1 to 6-15). In other words, the possible impact caused by dredging at the modeled sites can be treated independently. Notice that the severely affected ( $\Delta H/H \gg 1$ ) areas are limited on the north and south sides of the entire affected area, see the dark red areas on the south and north for each affected area. In the middle of these severely affected area, wave heights are actually reduced ( $\Delta H/H < 1$ ), see the light green area in Figs. 6-1 to 6-15. As pointed out in the previous chapter, the most affected areas are between the coast line and the dredging sites. At the dredging sites, there are only small differences in terms of wave height alteration.

Notice that large differences are mainly in increasing wave height (dark red color in Figs 6-1 to 6-15). Only occasionally in the affected area that wave height would be significantly reduced (see the green area in Figs. 6-1 to 6-15). The large increase of wave height is negative and may have an influence on sea-floor mobility. Again, because of the stochastic nature of waves, a quantitative conclusion on sea floor mobility is not addressed at this time.

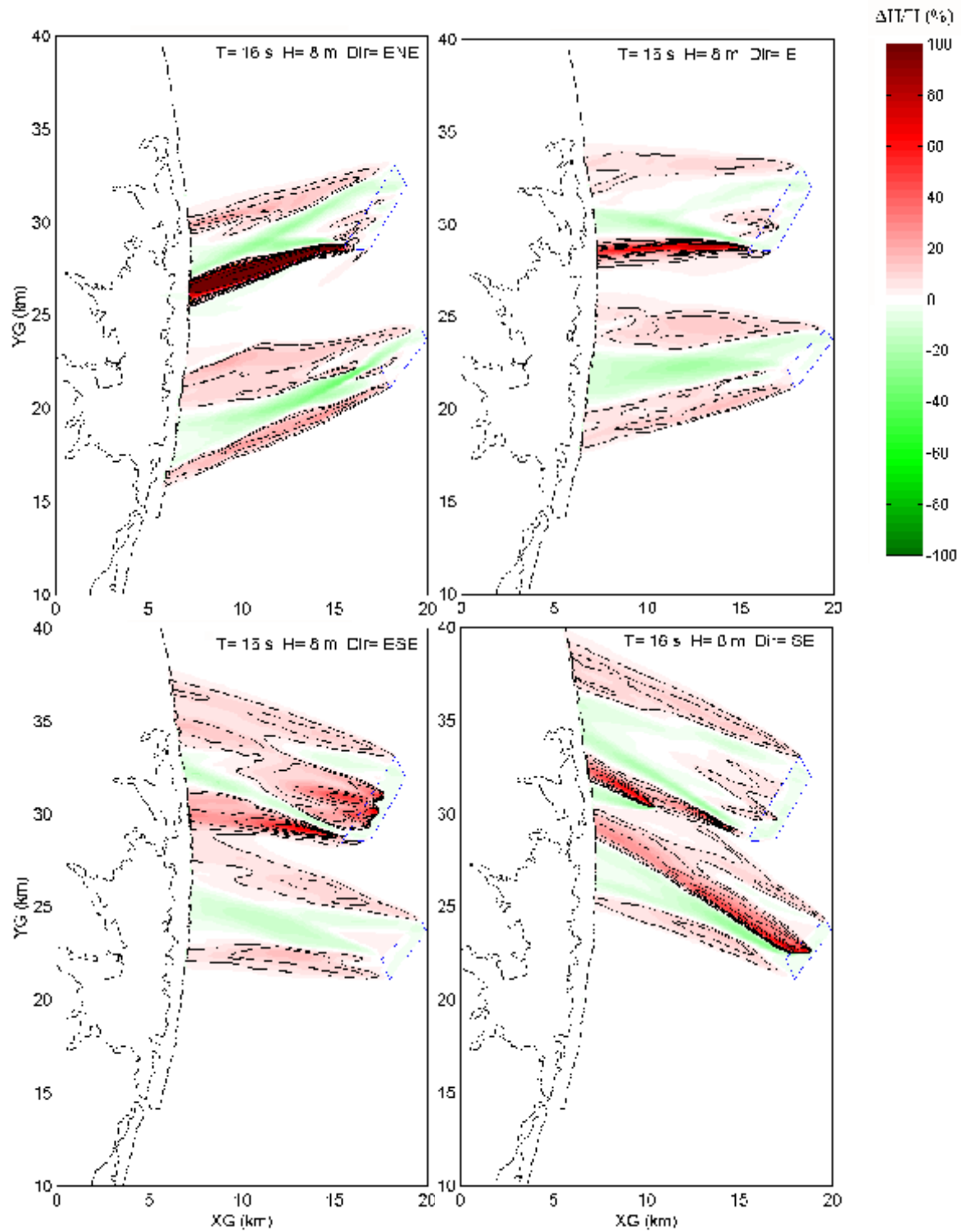


Fig. 8. Spatial distribution of the change in temperature  $\Delta T/T$  (%) due to a Dir of 15 s and 16 s. The Dir is ENE, E, ESE, and SE.

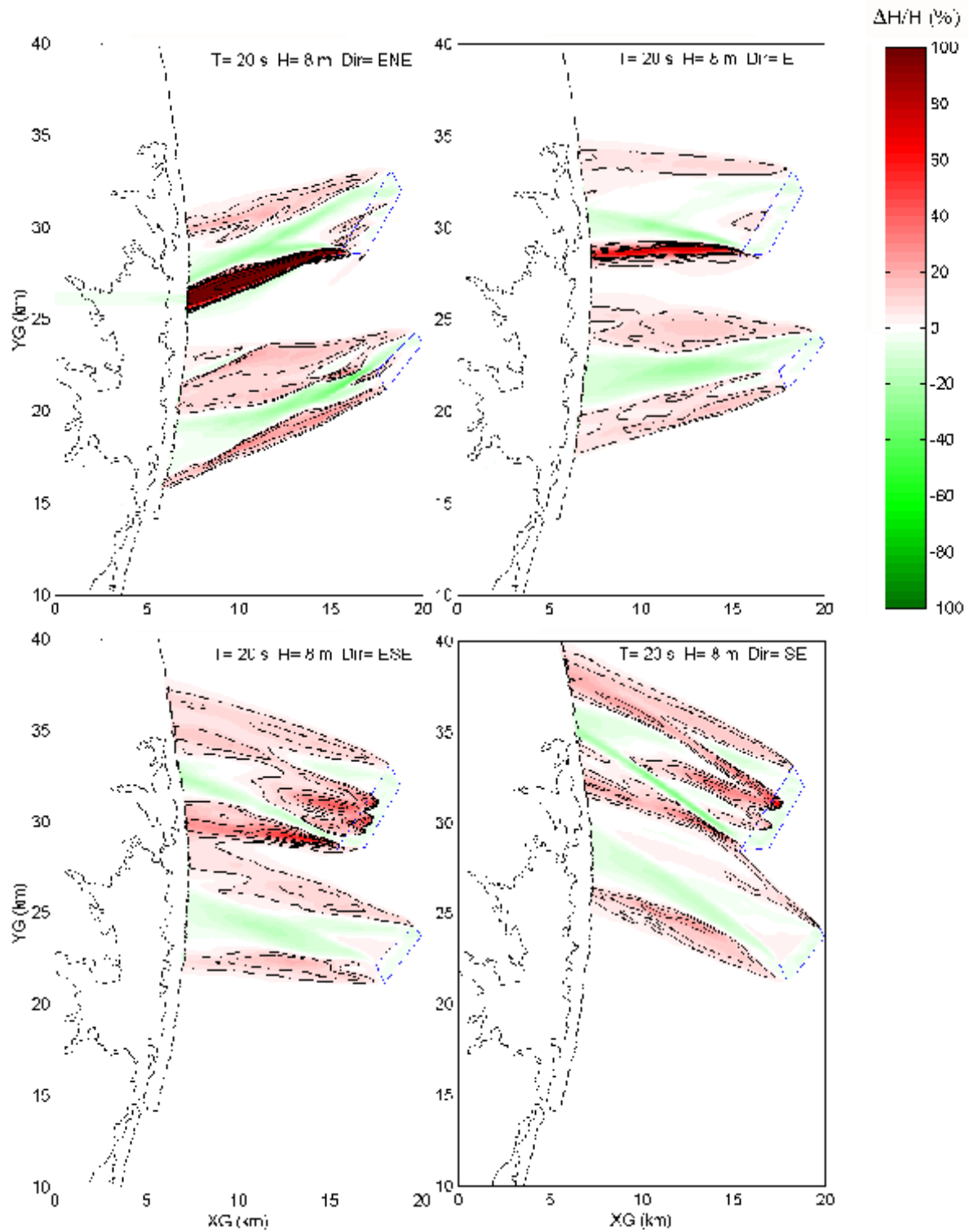


Figure 10: Relative sea level change for waves with  $T = 20$  s,  $H = 8$  m and  $Dir = ENE, E, ESE, SE$ .

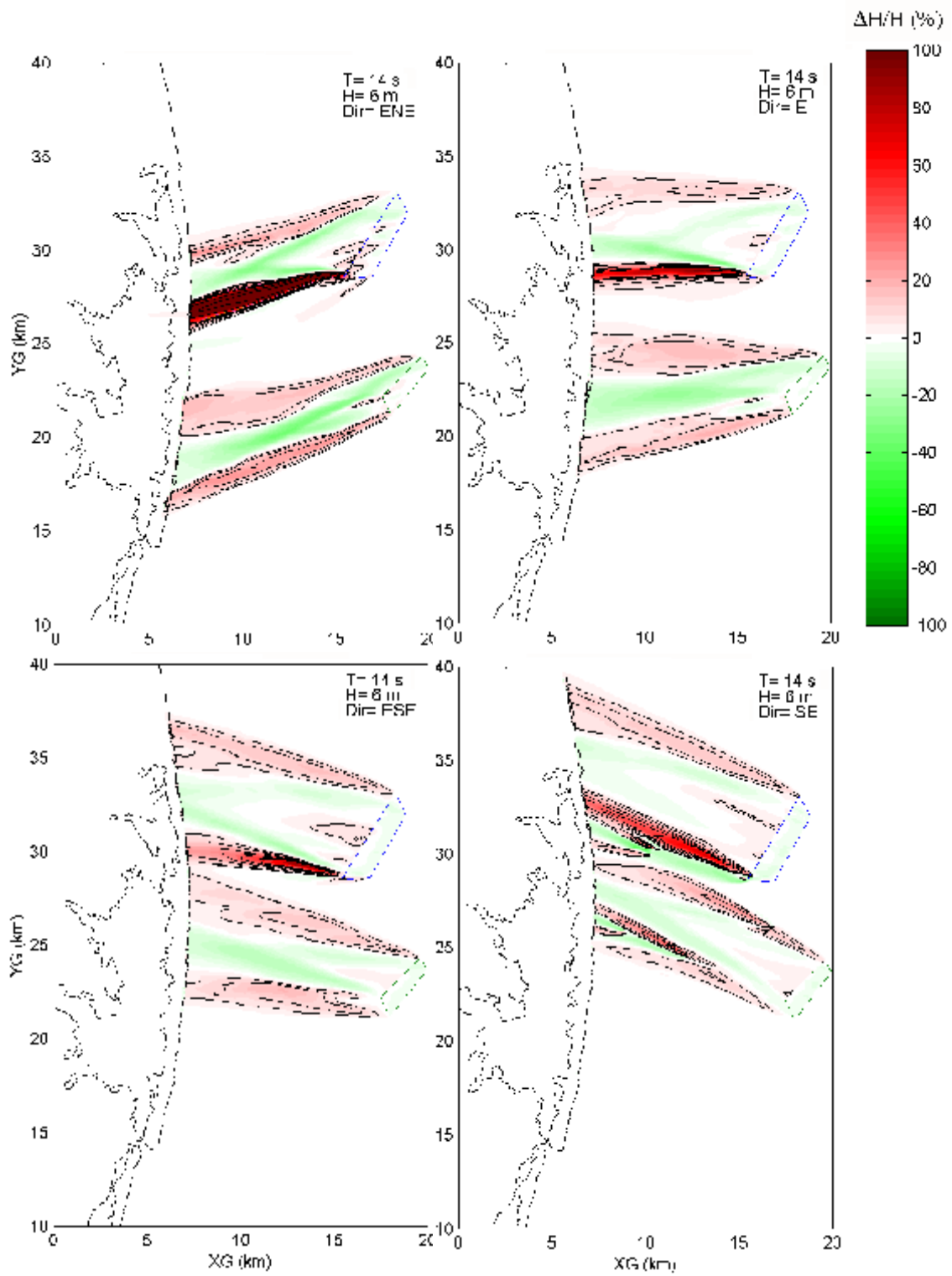


Figure 10. Relative height change of the wave height in the bay area for different wave conditions.

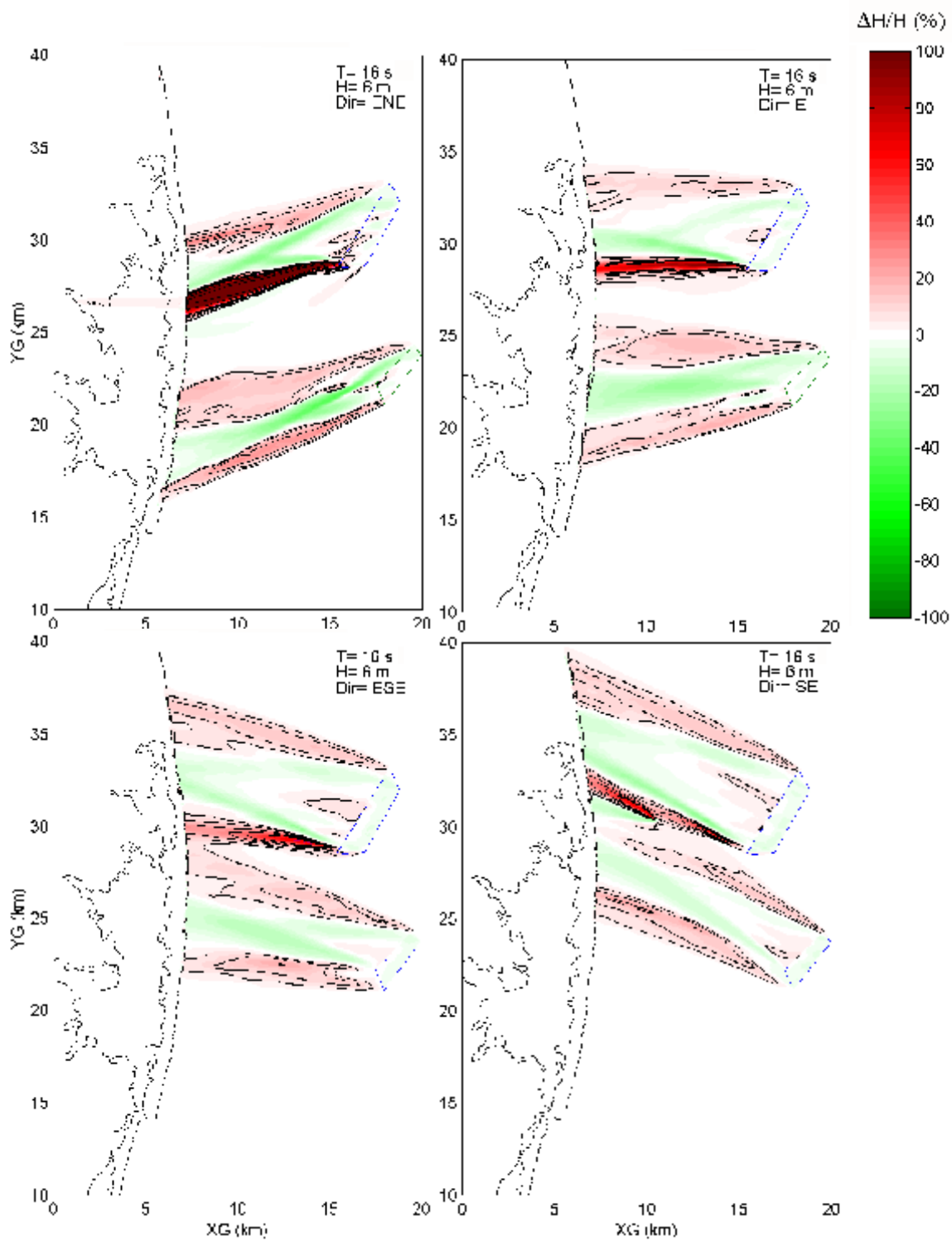


Figure 10: Relative change in height  $\Delta H/H$  (%) for  $T=16$  s and  $H=6$  m (top row) and  $T=10$  s and  $H=10$  m (bottom row).

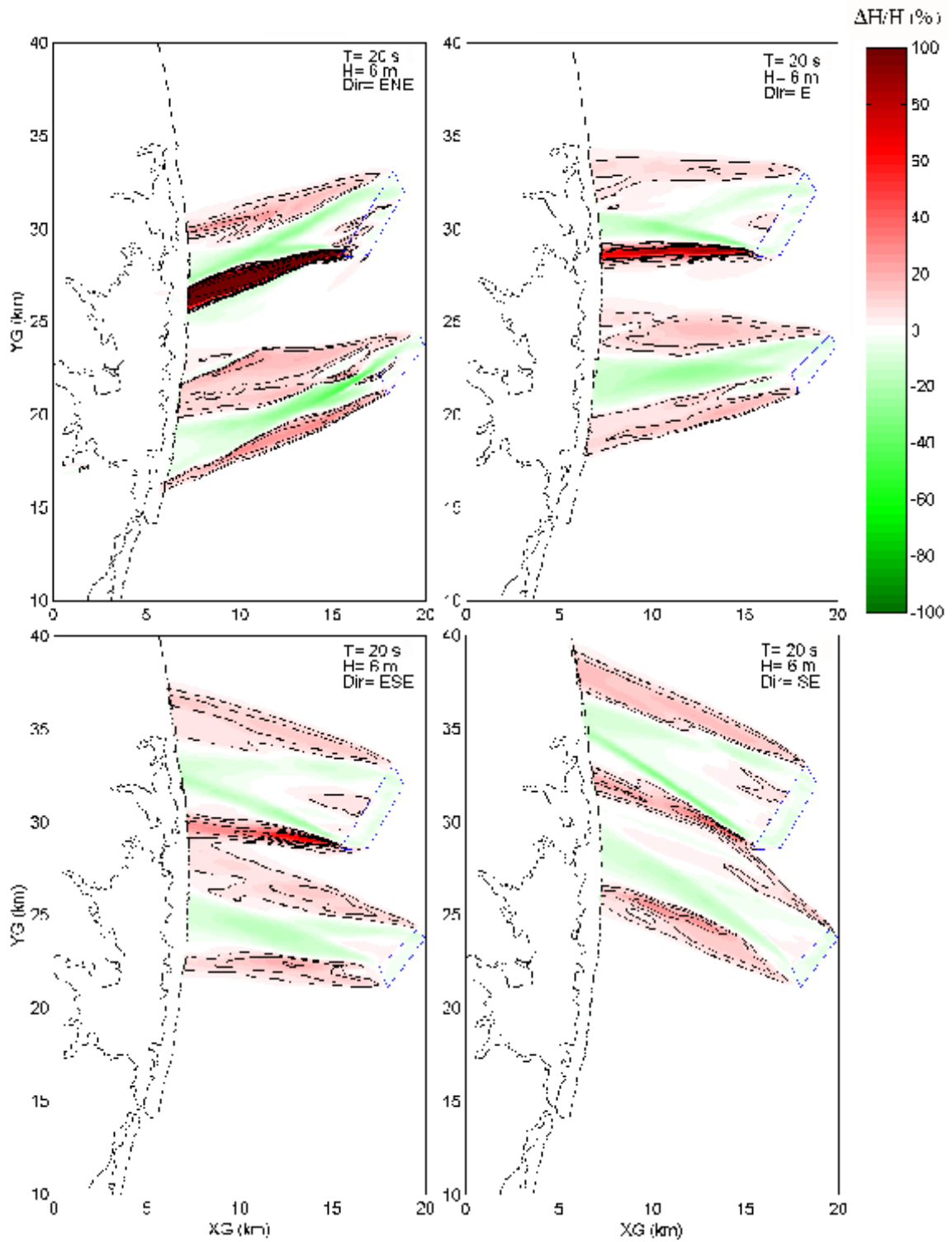


Figure 10: Relative height change (contour) for waves from different directions at  $T=20$  s and  $H=6$  m.

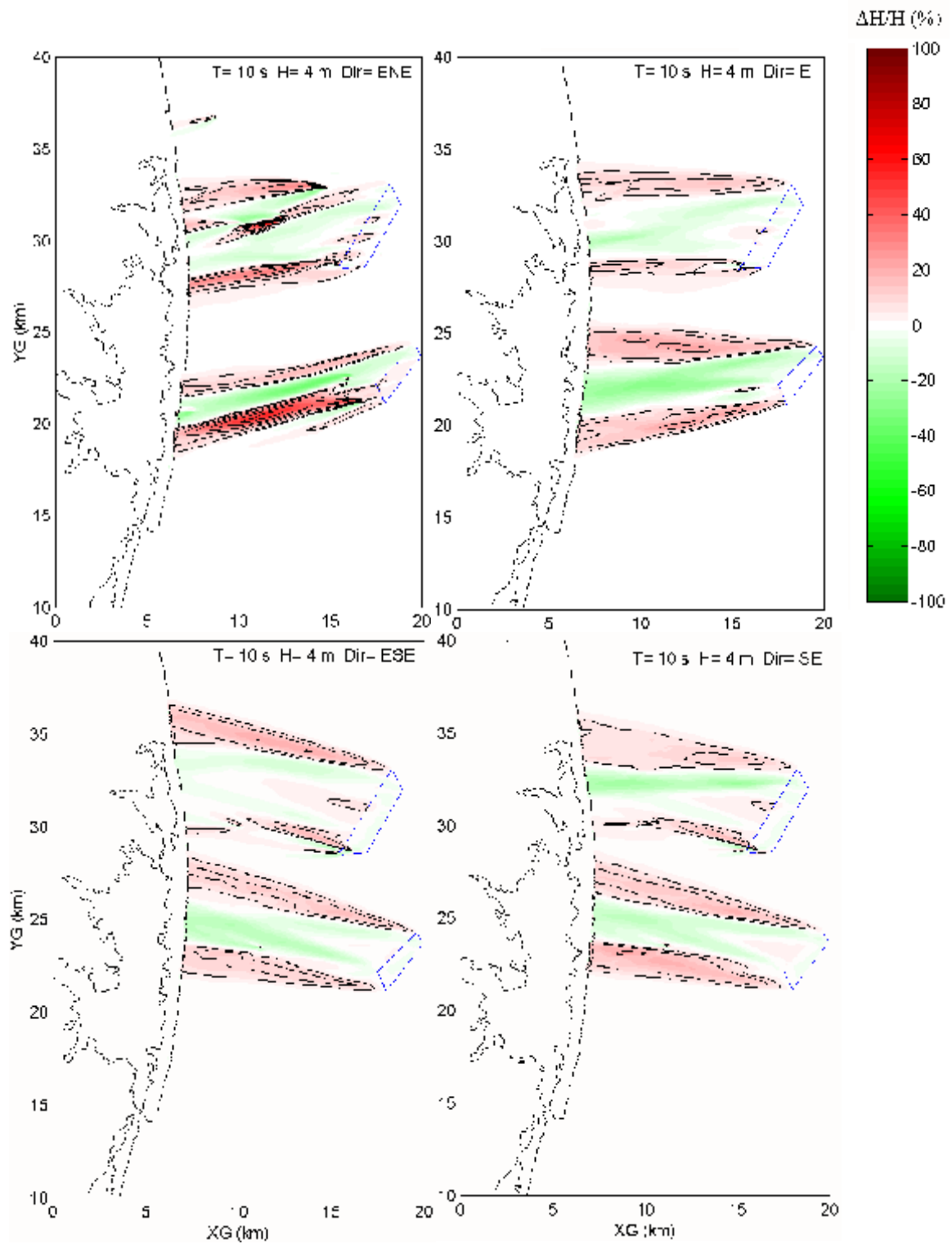


Figure 6: The effect of wave direction on the magnitude of wave height change. The blue dashed box indicates the region of interest.

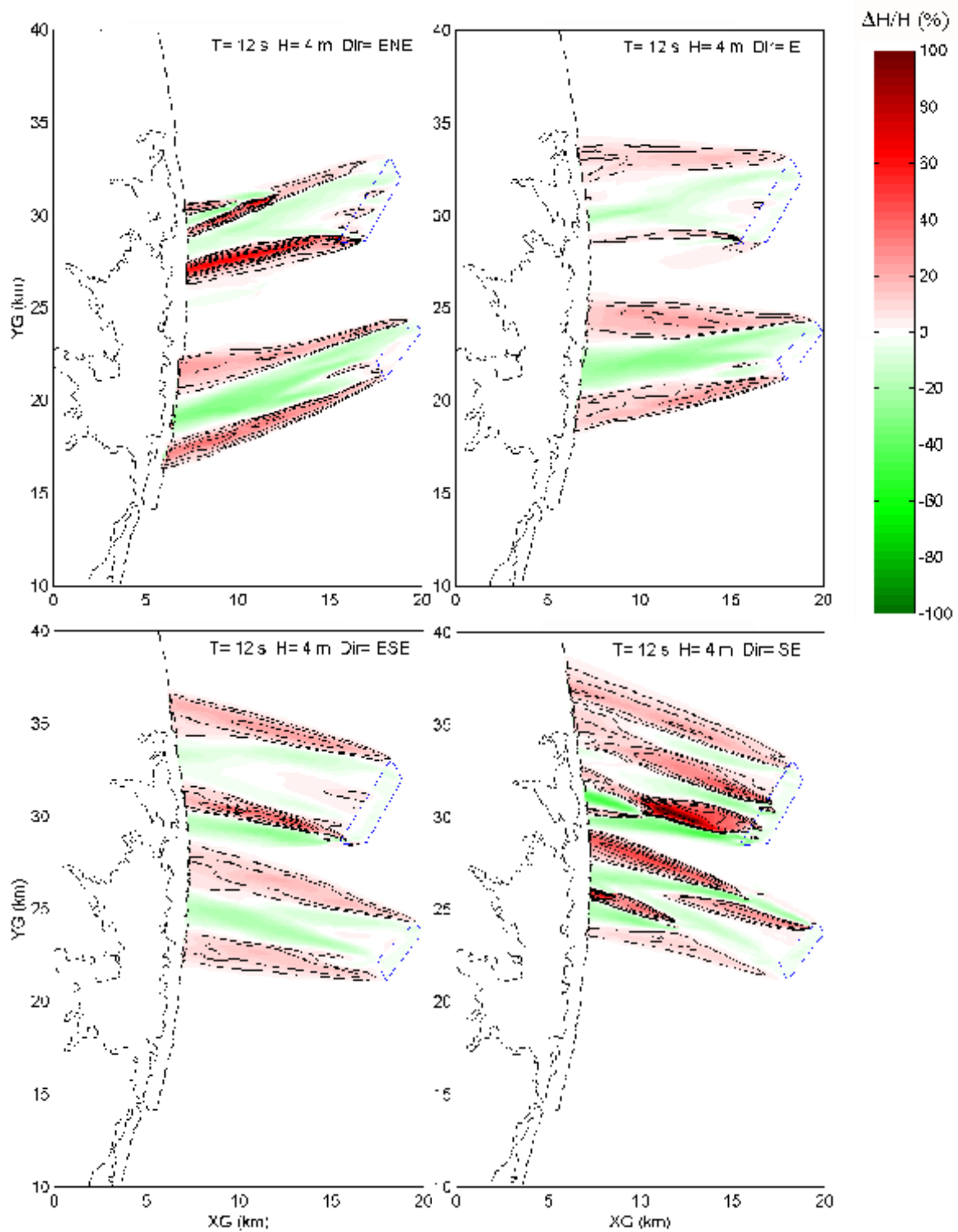


Fig. 4. Relative height change for waves with wave period 12 s and wave height 4 m for the four directions.

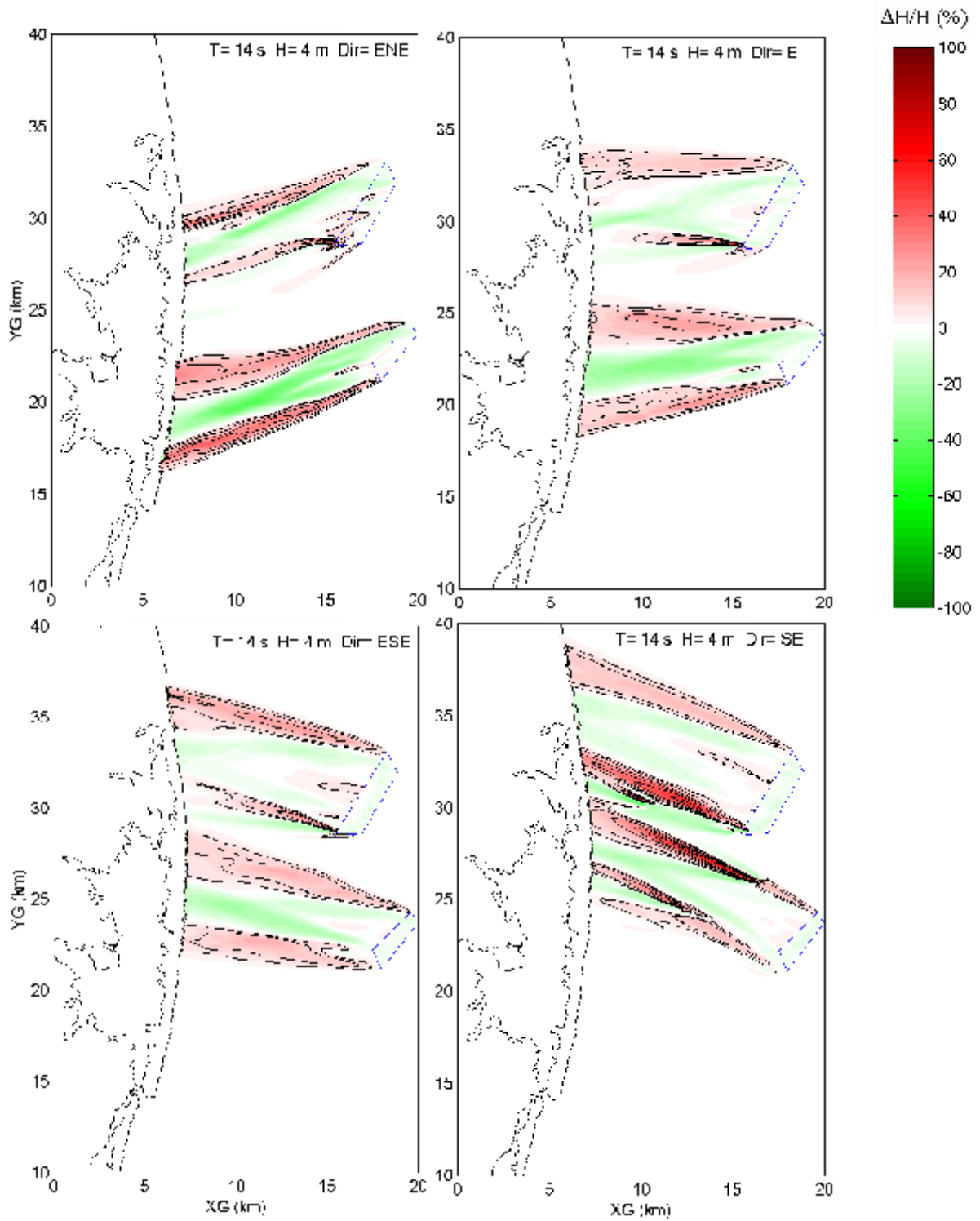


Figure 10: Relative height change  $\Delta H/H$  for waves with  $T=14$  s and  $H=4$  m for different wave directions. The color scale is in %.

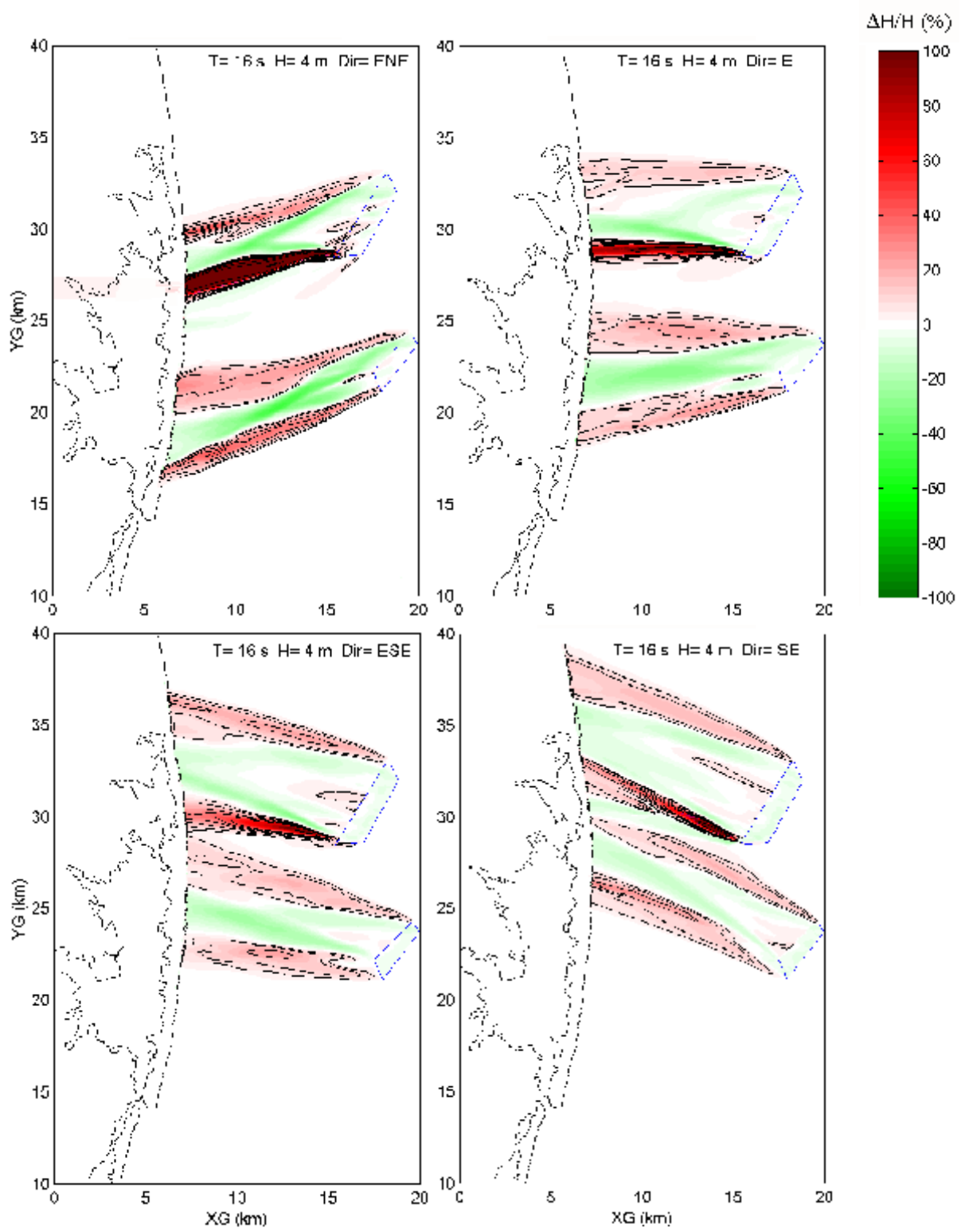


Figure 4: Relative change in height with varying wave direction for a wave period of 6 s and 16 s.

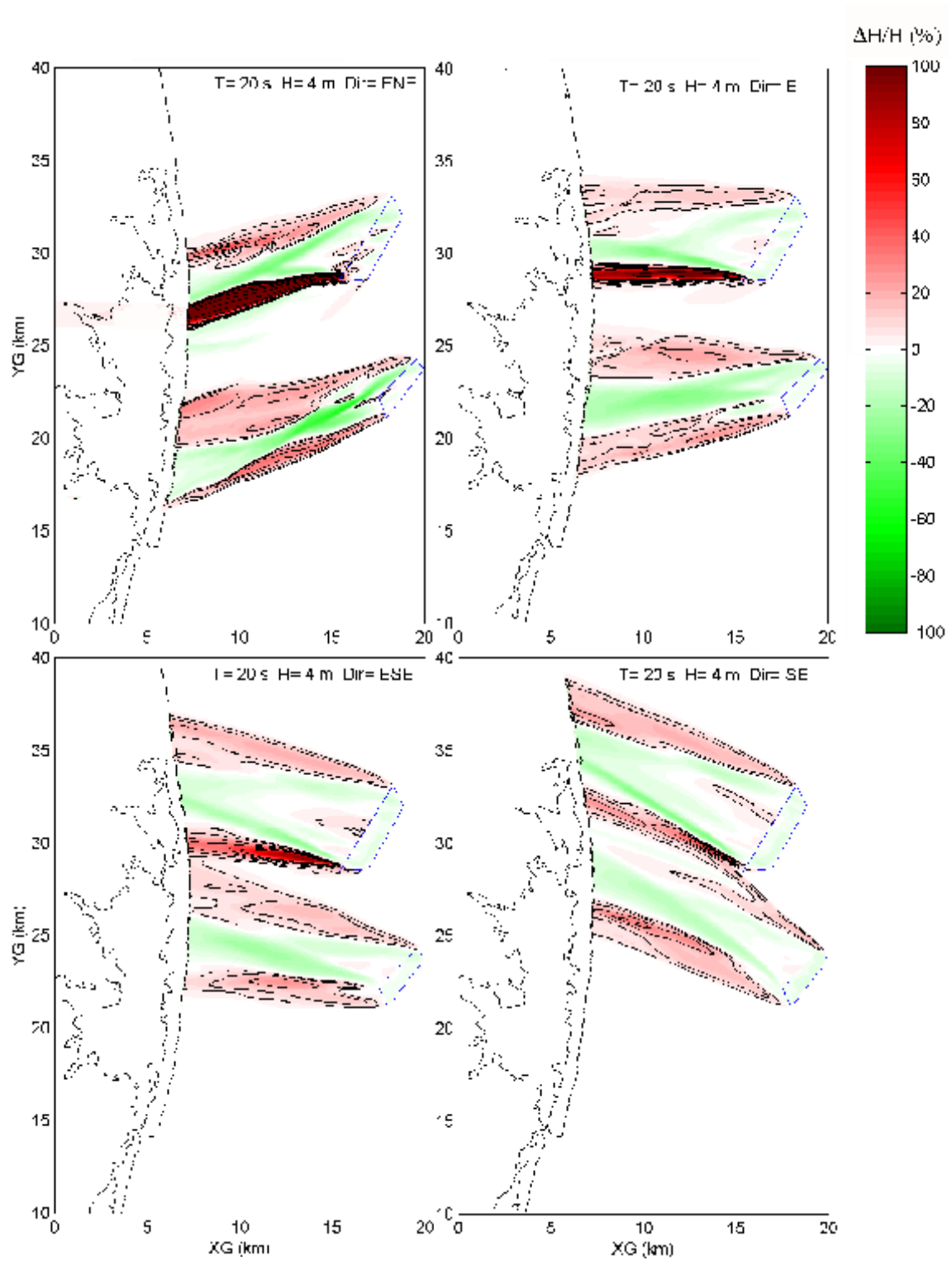


Figure 10: Relative height change of the wave height in the Bay of Amundsen-Davis for different wave directions.

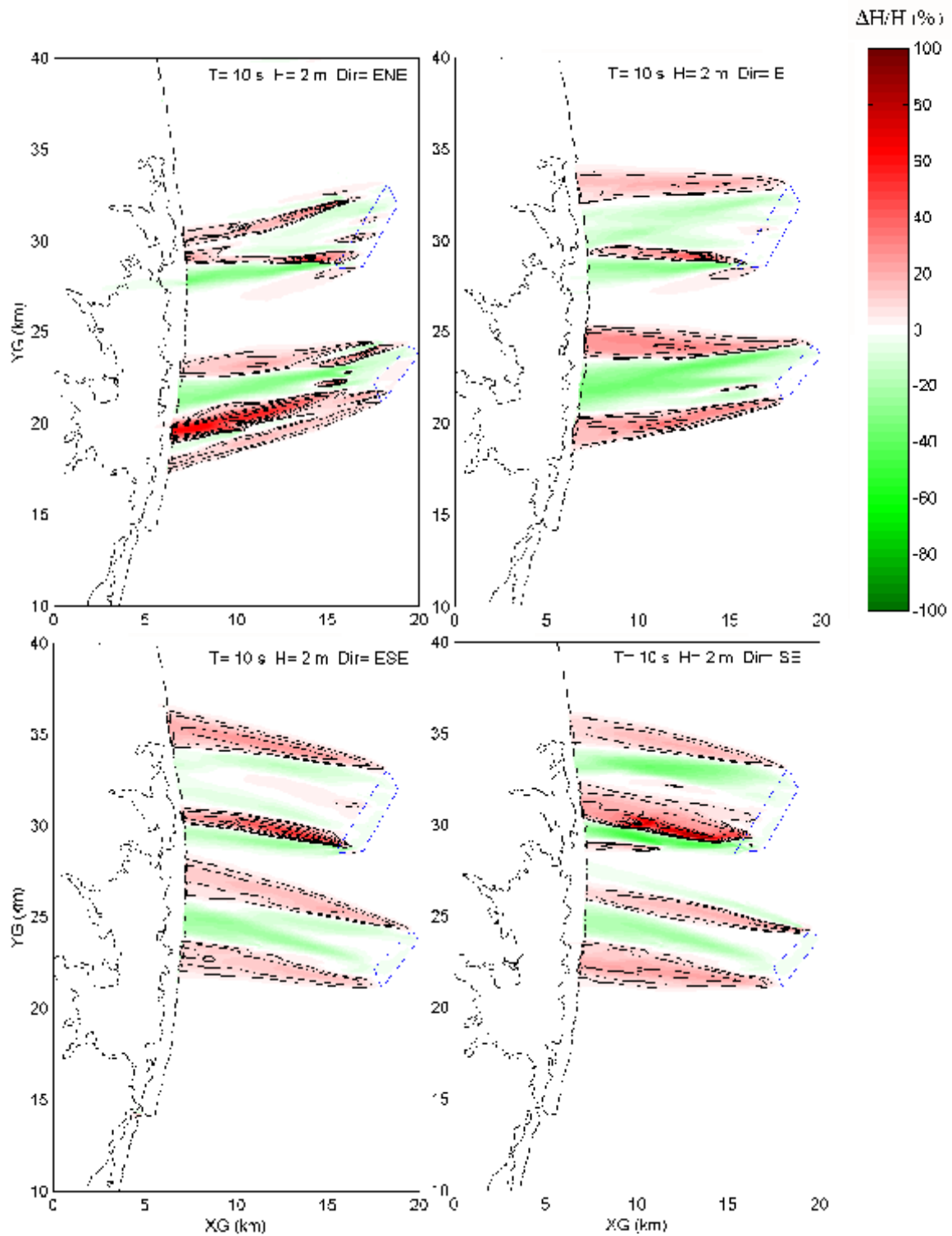


Figure 10: Relative sea level change (ΔH/H (%)) for different wave parameters (T, H, Dir) along the coast.

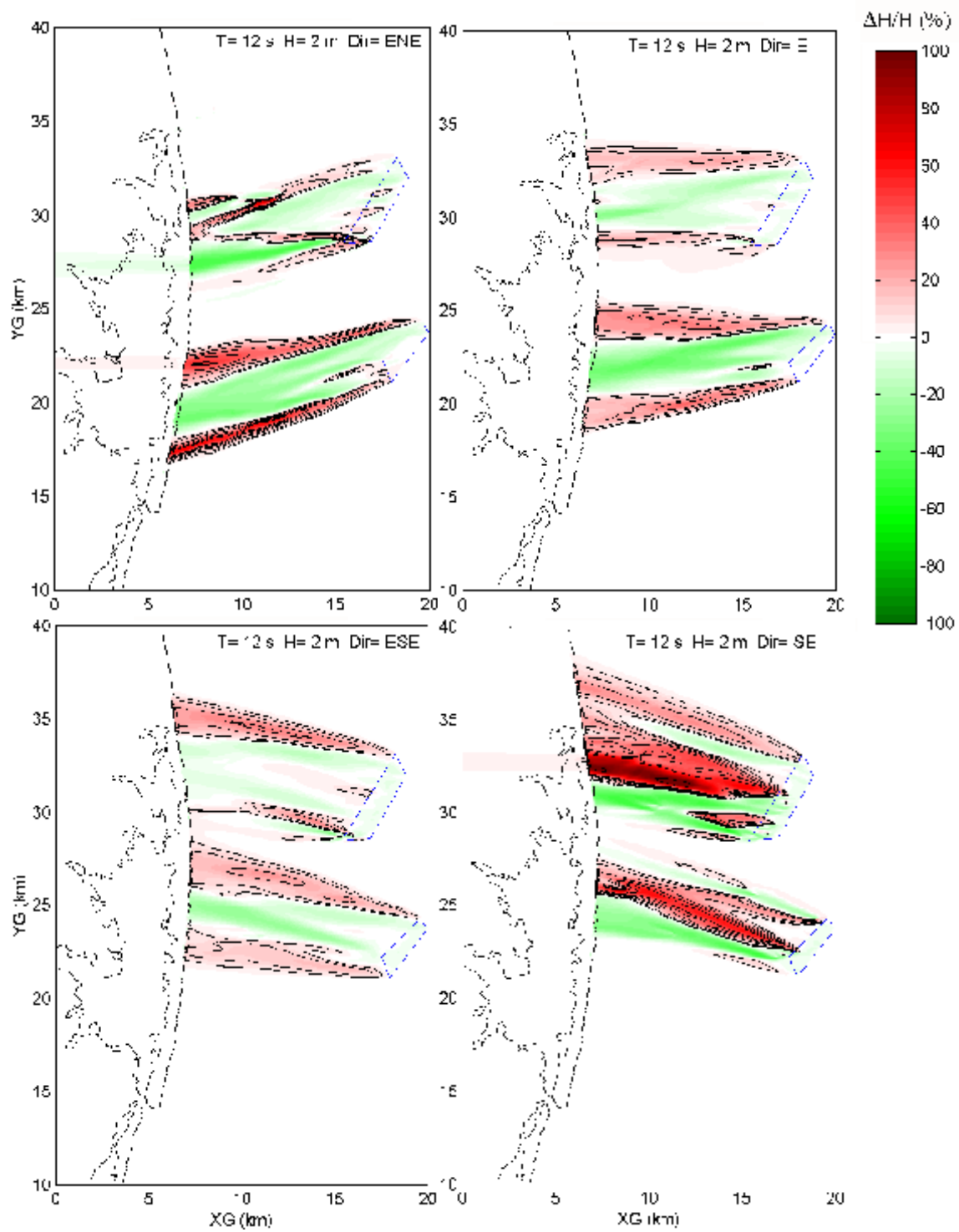


Figure 8: Relative change in height for waves with a period of 12 s and a height of 2 m. The wave direction is indicated in the panel titles.

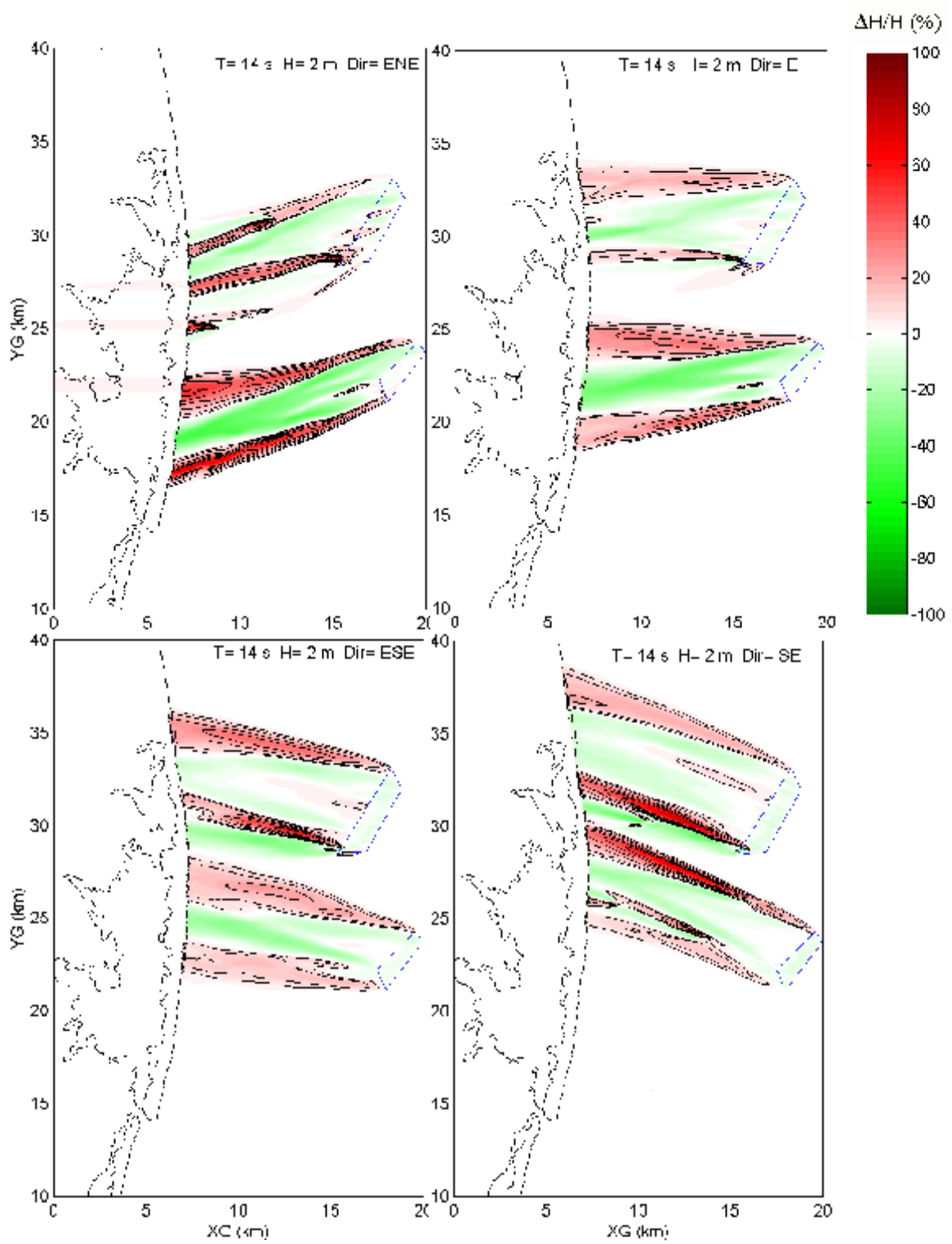


Fig. A1. Relative sea level change for waves with a period of 14 s and a height of 2 m. Direction of wave propagation is indicated by the panel label.

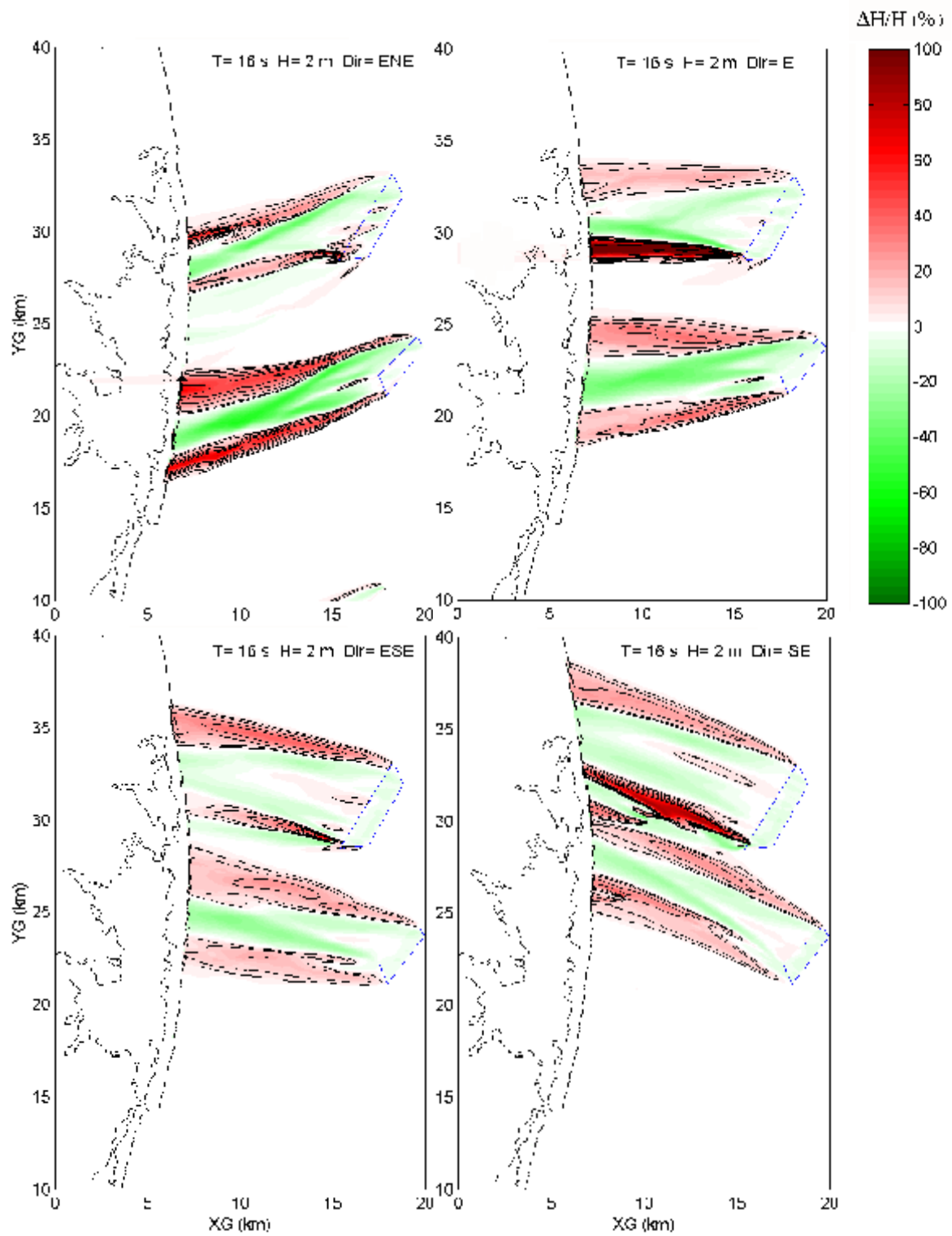


Fig. 6.11. Relative change in sea level for North Atlantic storm surge (Dir=Dir, T=16 s, H=2 m).

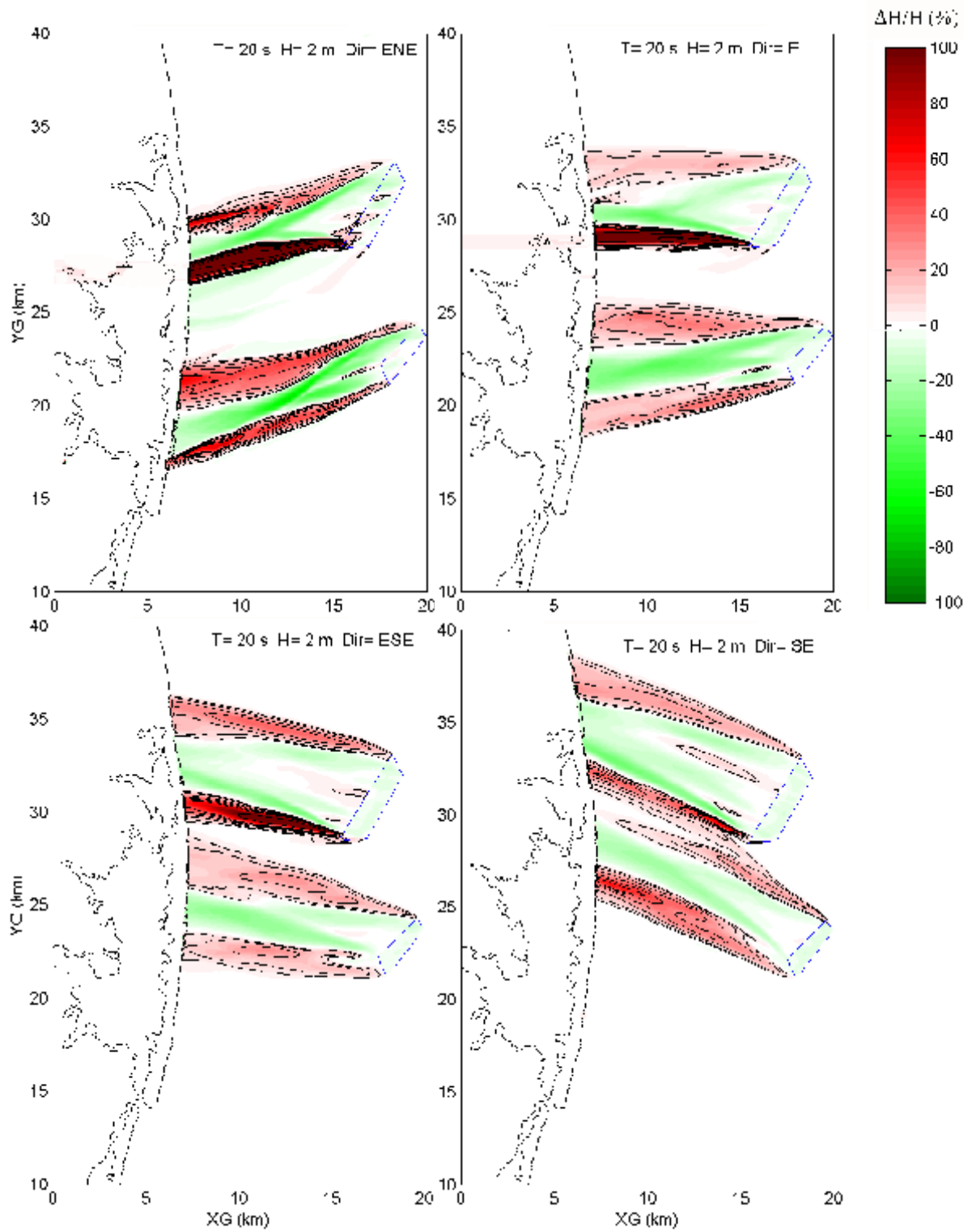


Figure 10: Relative water level change ( $\Delta H/H$  (%)) around the island for different wave directions.  $T=20$  s,  $H=2$  m.

### 6.3. Results in Changing Breaking Wave Height

As far as the possible shoreline variations are concerned, we need to consider the change of breaking wave height along the shore (see the criterion in Chapter 4). For this reason, the changes of breaking wave heights in the display domain are plotted in Figs. 6-16 to 6-30. The modeled dredge areas are located between  $YG = 21$  to  $28$  km and  $YG = 28$  and  $33$  km. The black lines in these figures represent the profiles of breaking wave height for the original bathymetry. The red dashed lines in these figures are the breaking wave height profile after the proposed long-term dredging.

Again, we will use one specific case to explain the possible changes in details, and summarize the results in Table 6-1. For the most severe sea ( $H_o = 8$  m,  $T = 20$  s) that comes from ENE, Fig. 6-16 indicates that the breaking wave height modulation increases a little ( $BHM = 1.33$ ) between  $YG = 20$  and  $22$  km, but the BHM has a significant decrease ( $BHM = 0.38$ ) between  $YG = 25$  to  $27$  km. If the waves come from E, the possible impact is on positive side (*i.e.*,  $BHM = 0.61$  at  $YG = 30.5$  km and  $0.75$  at  $YG = 19$  km). If the waves come from ESE, the results are all negative ( $BHM = 1.75$  at  $YG = 30.5$  km and  $BHM = 2.67$  at  $YG = 23$  km). If the waves come from SE, then there is almost no change.

Table 6-1 clearly shows that the results on breaking wave height modulation is a mix of positive and negative impacts. Within the 60 studied wave conditions, 18 wave conditions do not show a measurable/significant change. Although for some waves that come from the ESE there is a relatively large negative impact (e.g.,  $BHM > 2$ ), it is not a really big negative impact because of the original small BHM. It is necessary to point out that the numbers displayed in Table 6-1 are indices to show the relative significance, Figs. 6-16 to 6-30 are still the important information with which to make a judgement.

Table 6-1, Summary of Changes on Breaking Wave Height Modulation for the Cumulative Dredging

Wave Dir.	T = 10s	12s	14s	16s	20s	
ENE	: M <sup>1</sup>	-- <sup>5</sup>	--	--	0.5	0.38/1.33
	: S <sup>2</sup>	--	--	0.6	0.64/1.22	0.69
	: R <sup>3</sup>	NG <sup>6</sup>	0.9	1.38	0.83	0.86/1.33
	: N <sup>4</sup>	0.5	NG	NG	0.83	NG
E	: M	--	--	--	0.5/1.54	0.61/0.75
	: S	--	--	0.88	0.7/1.14	0.94/1.72
	: R	NG	NG	NG	1.2	1.27/1.2
	: N	0.9	0.33	0.87	0.5	0.71
ESE	: M	--	--	--	3.0	1.75/2.67
	: S	--	--	NG	NG	1.22
	: R	2.0	NG	NG	2.25	1.6/0.75
	: N	NG	NG	2.25	2.0	NG
SE	: M	--	--	--	1.12	NG
	: S	--	--	1.33	1.28/1.16	1.55
	: R	NG	1.83	1.5	1.5	2.0
	: N	NG	0.46	2.0	1.55	NG

<sup>1</sup>: represents Northeaster wave condition.

<sup>2</sup>: represents Rough Sea wave condition.

<sup>3</sup>: represents Severe Sea wave condition.

<sup>4</sup>: represents the Most Severe Sea wave condition.

<sup>5</sup>: NG is a shorthand for negligible small.

<sup>6</sup>: — is a shorthand for not included in computation.

The most important feature in Figs. 6-16 to 6-30 is the obvious reduction of BHM around YG = 26 km, the border between Maryland and Delaware. The original low breaking wave height means the sediment transport activities at this border location is minimal. The obvious reduction of BHM (mainly for long period waves) actually increases the breaking wave height, and thus, indicates that the along shore sediment transport will move more sediment away from this location. Shoreline recession would be expected as a consequence. This is a negative impact at this particular location, however, the

increased amount of sediment transport, moving either north or south, will benefit the downstream beaches. If sand resources have to be taken from the two modeled shoals, some sort of beach protect project should be considered, or at least a monitoring project that closely checks the shoreline change at the Maryland and Delaware border should be established. If it is necessary to maintain the original shoreline, then part of the sand resources obtained from the offshore dredging should be placed at this location.

#### **6.4. Conclusions**

The results suggest that the major change of wave height is between the dredging site and the shore line. The local increase of wave height can be as much as two times. The change of breaking wave height, on the other hand, is not so obvious except the clear reduction of BHM at the Maryland and Delaware border. The reduction of BHM at this location, however, is not necessarily a positive impact because it increases the breaking wave height at that location. As a consequence, more erosion and shoreline recession at that location may be resulted. Otherwise, the possible impact is not significant.

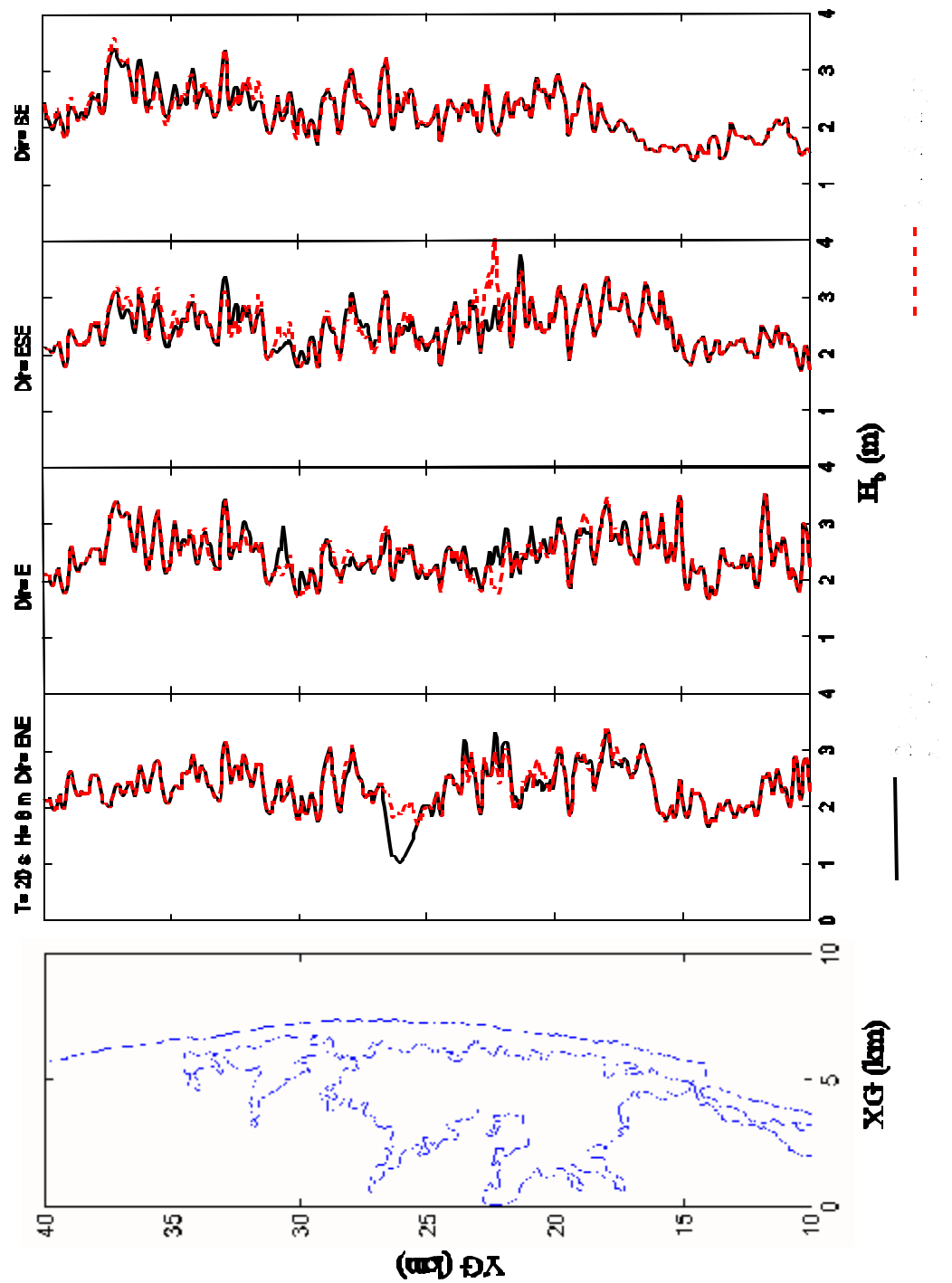


Fig. 6-16. Comparison of Breaking Wave Heights for Original Bathymetry and after Accumulative Dredging with  $H_b = 8$  m,  $T = 20$  s.

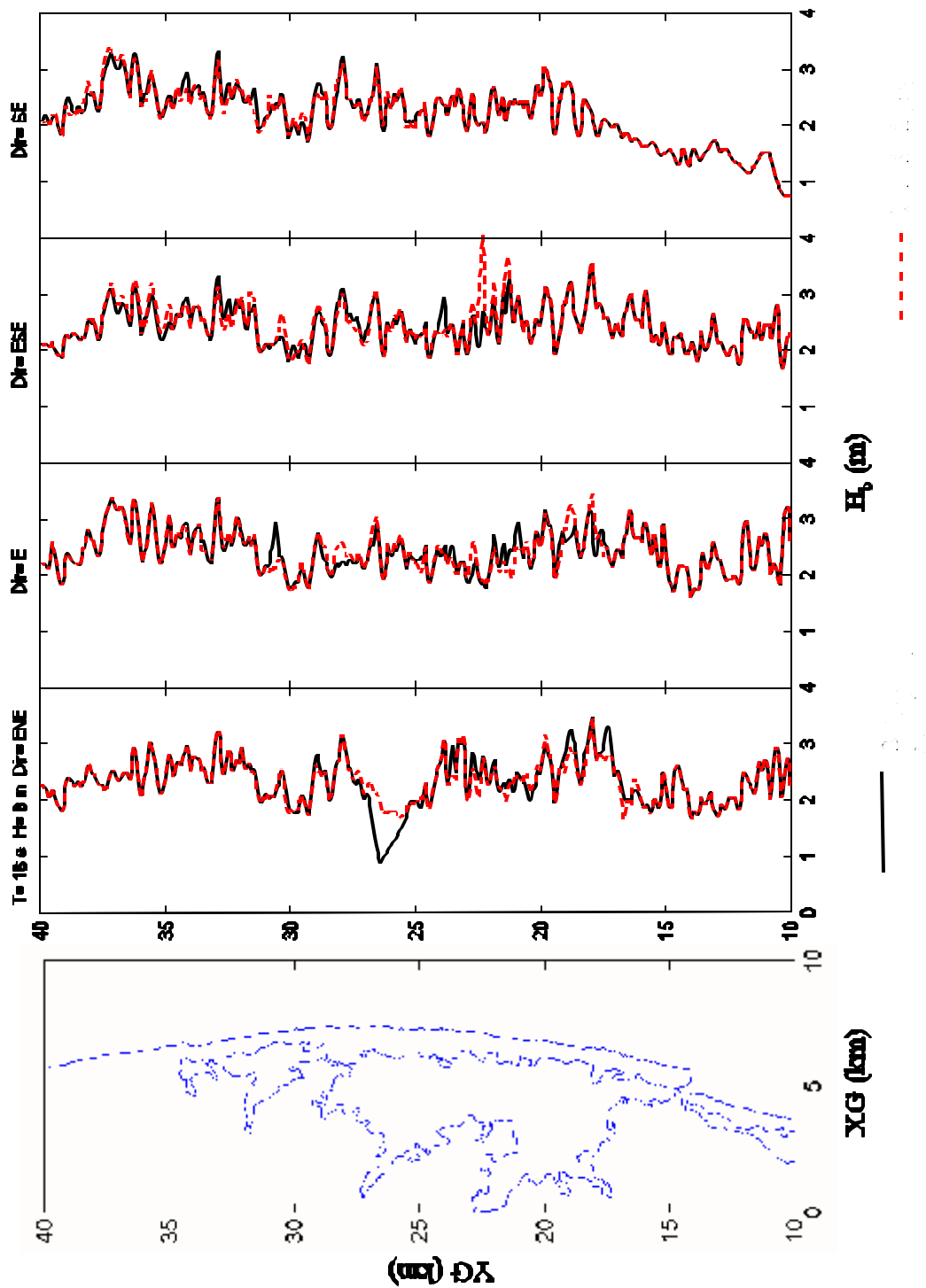


Fig. 6-17. Comparison of Breaking Wave Heights for Original Bathymetry and after Accumulative Dredging with  $H_b = 8$  m,  $T = 16$  s.

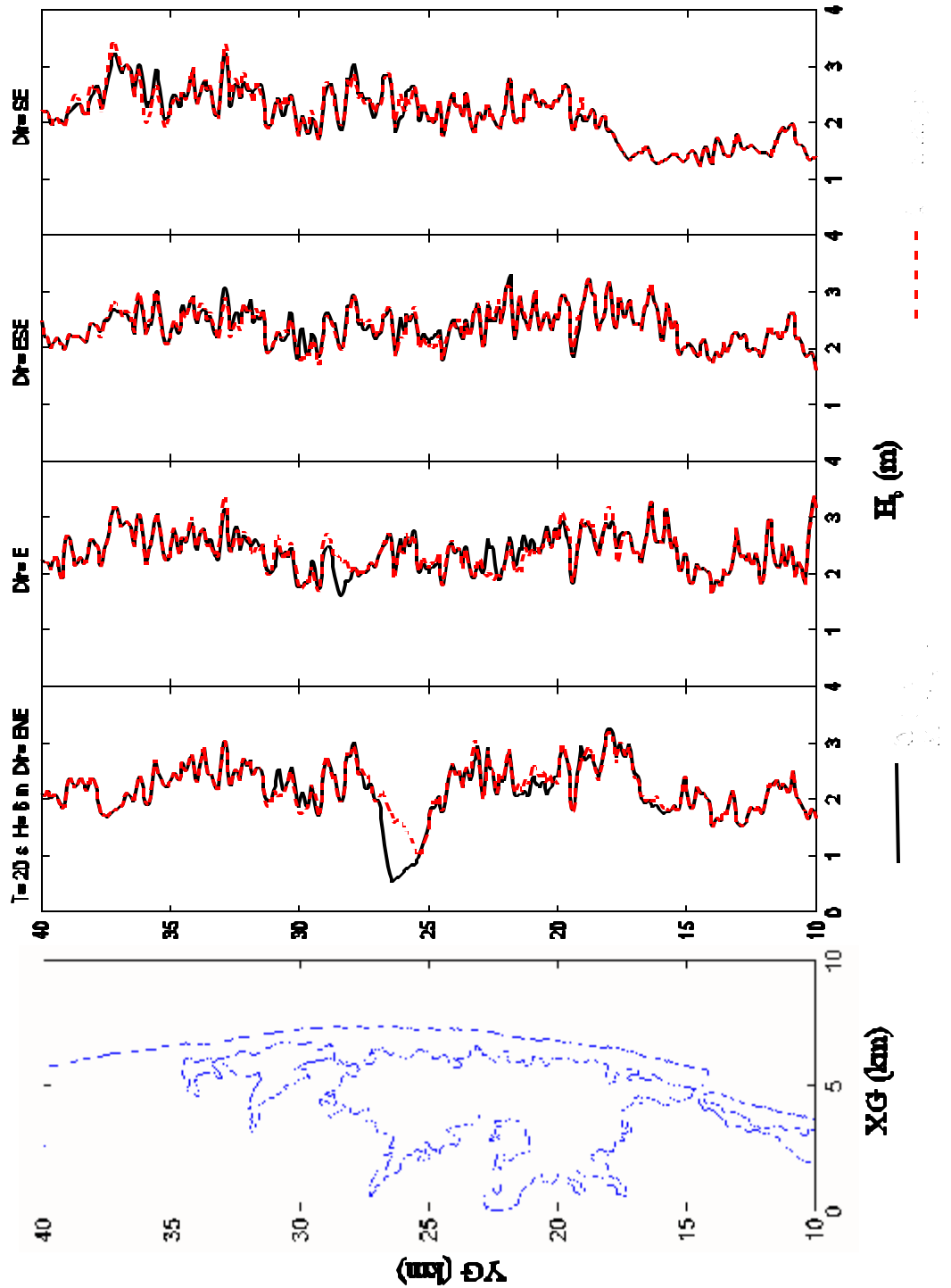


Fig. 6-18. Comparison of Breaking Wave Heights for Original Bathymetry and after Accumulative Dredging with  $H_b = 6\text{ m}$ ,  $T = 20\text{ s}$ .

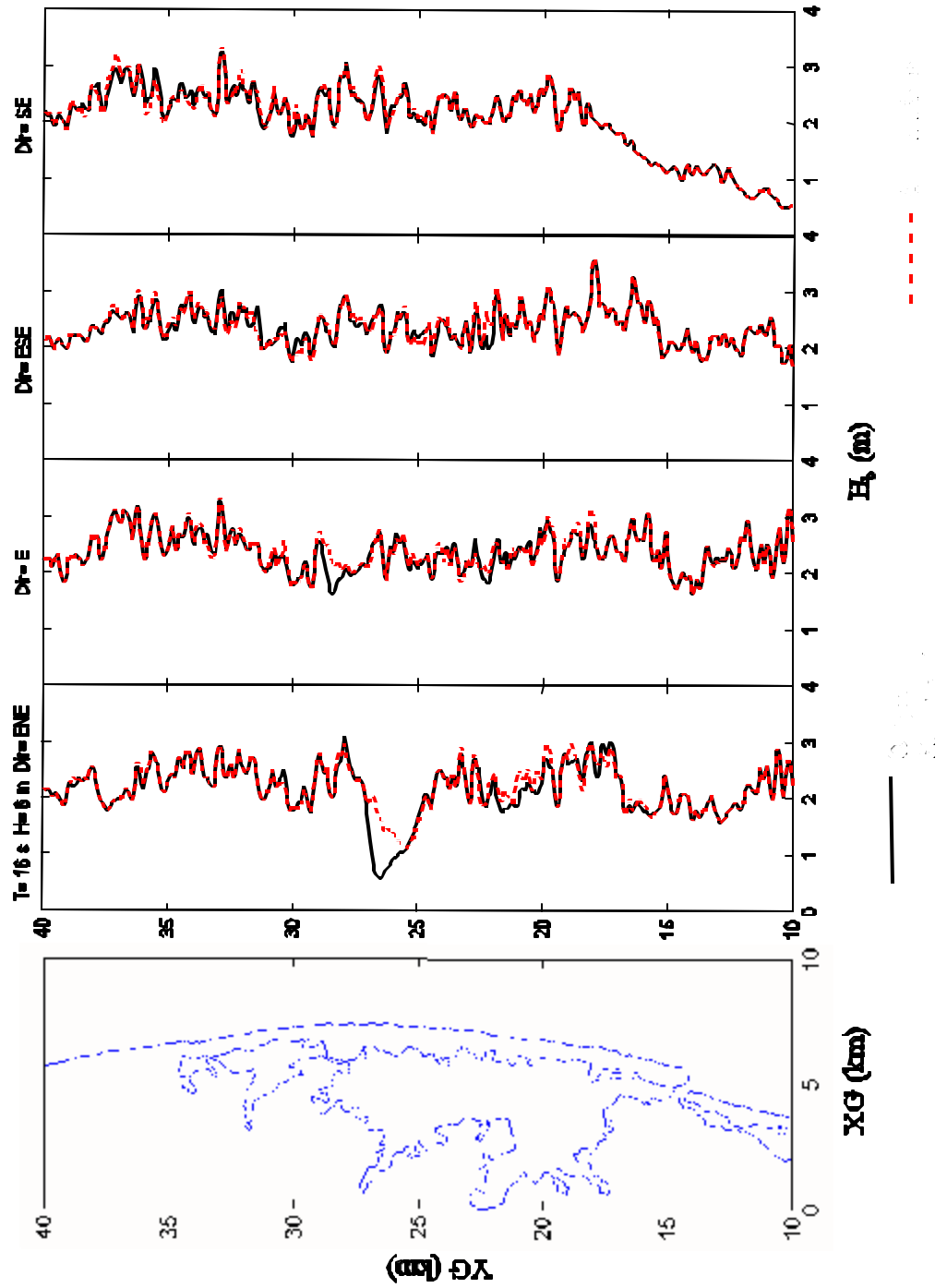


Fig. 6-19. Comparison of Breaking Wave Heights for Original Bathymetry and after Accumulative Dredging with  $H_b = 6$  m,  $T = 16$  s.

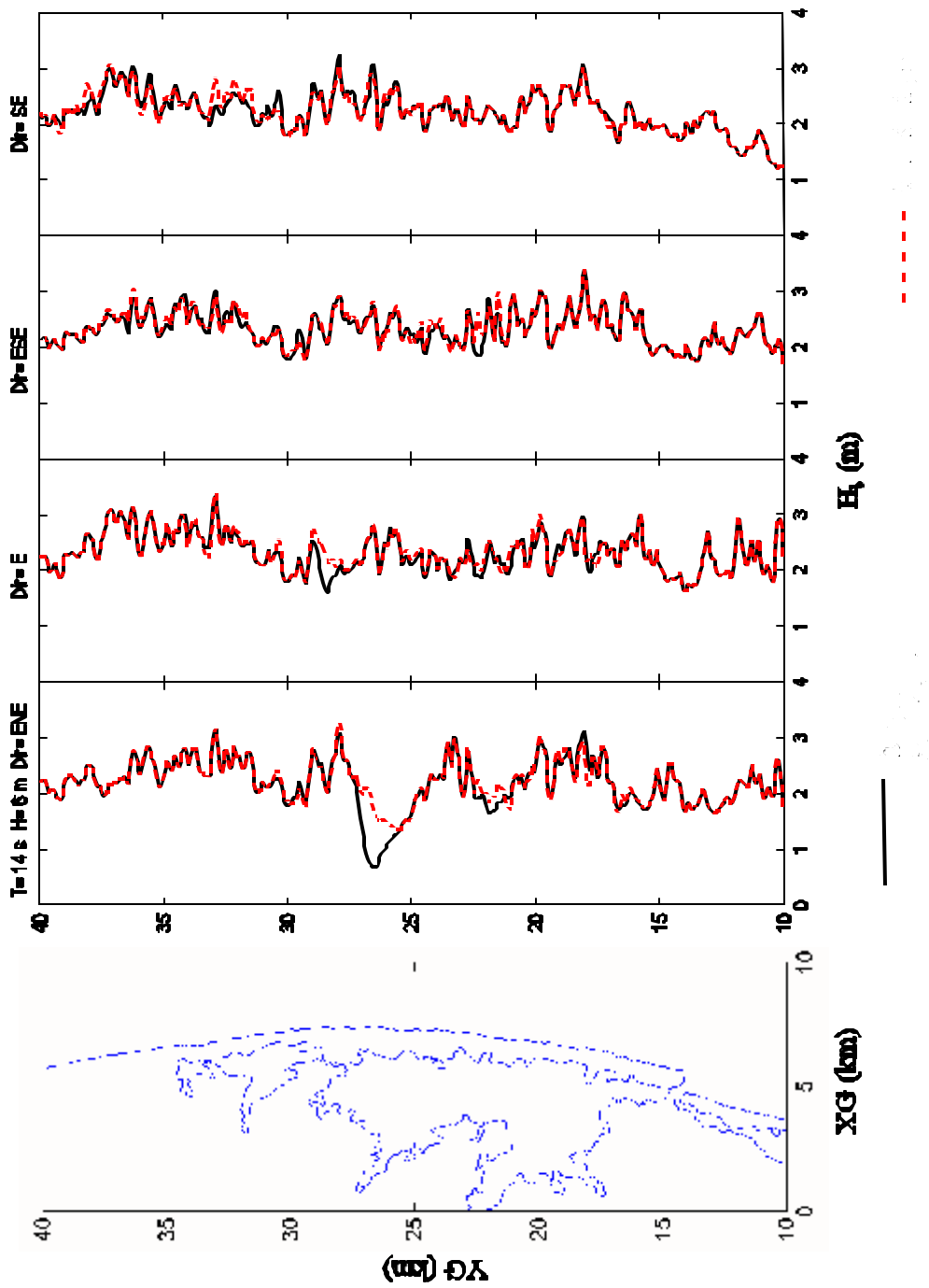


Fig. 6-20. Comparison of Breaking Wave Heights for Original Bathymetry and after Accumulative Dredging with  $H_b = 6$  m,  $T = 14$  s.

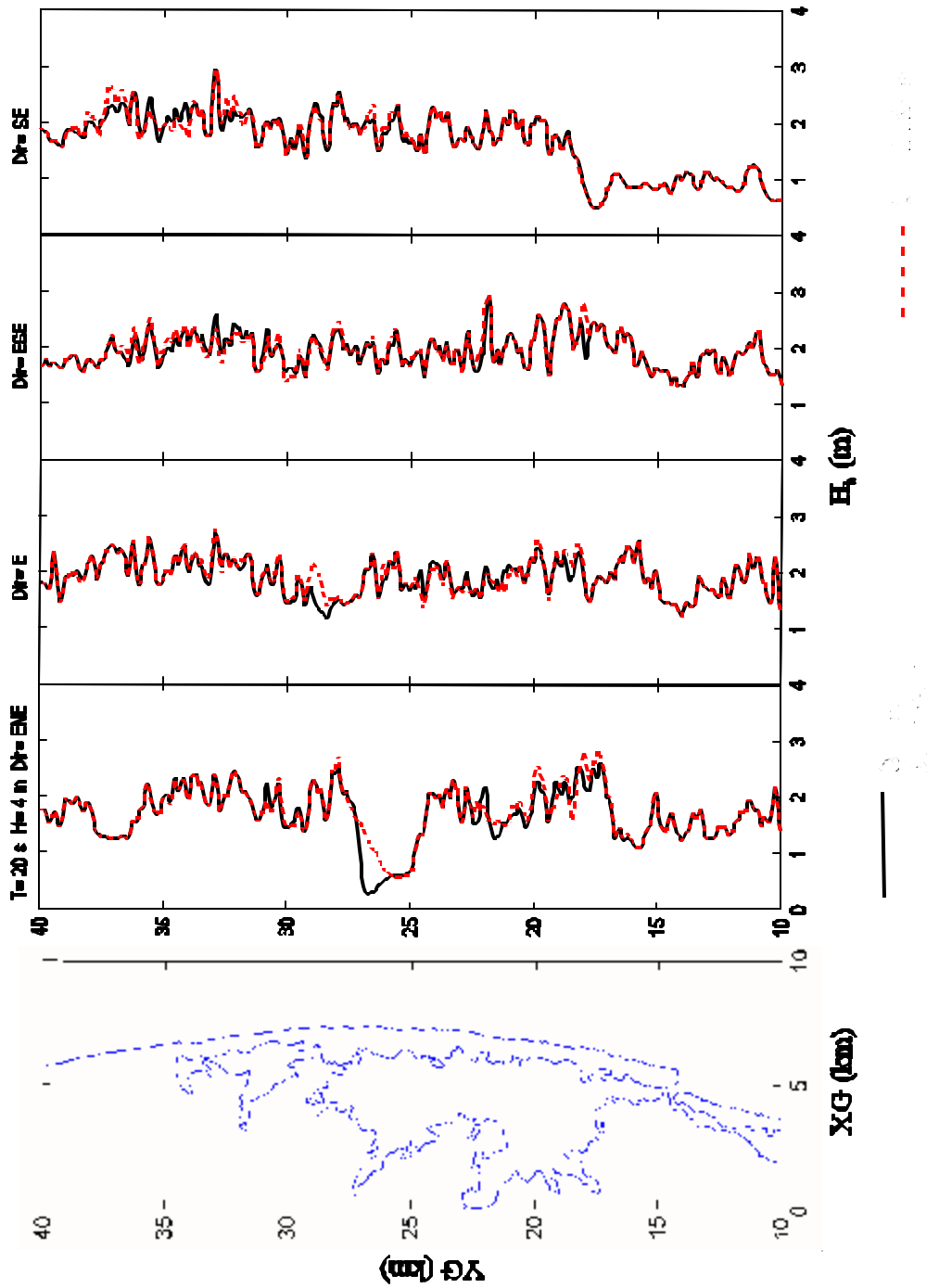


Fig. 6-21. Comparison of Breaking Wave Heights for Original Bathymetry and after Accumulative Dredging with  $H_0 = 4$  m,  $T = 20$  s.

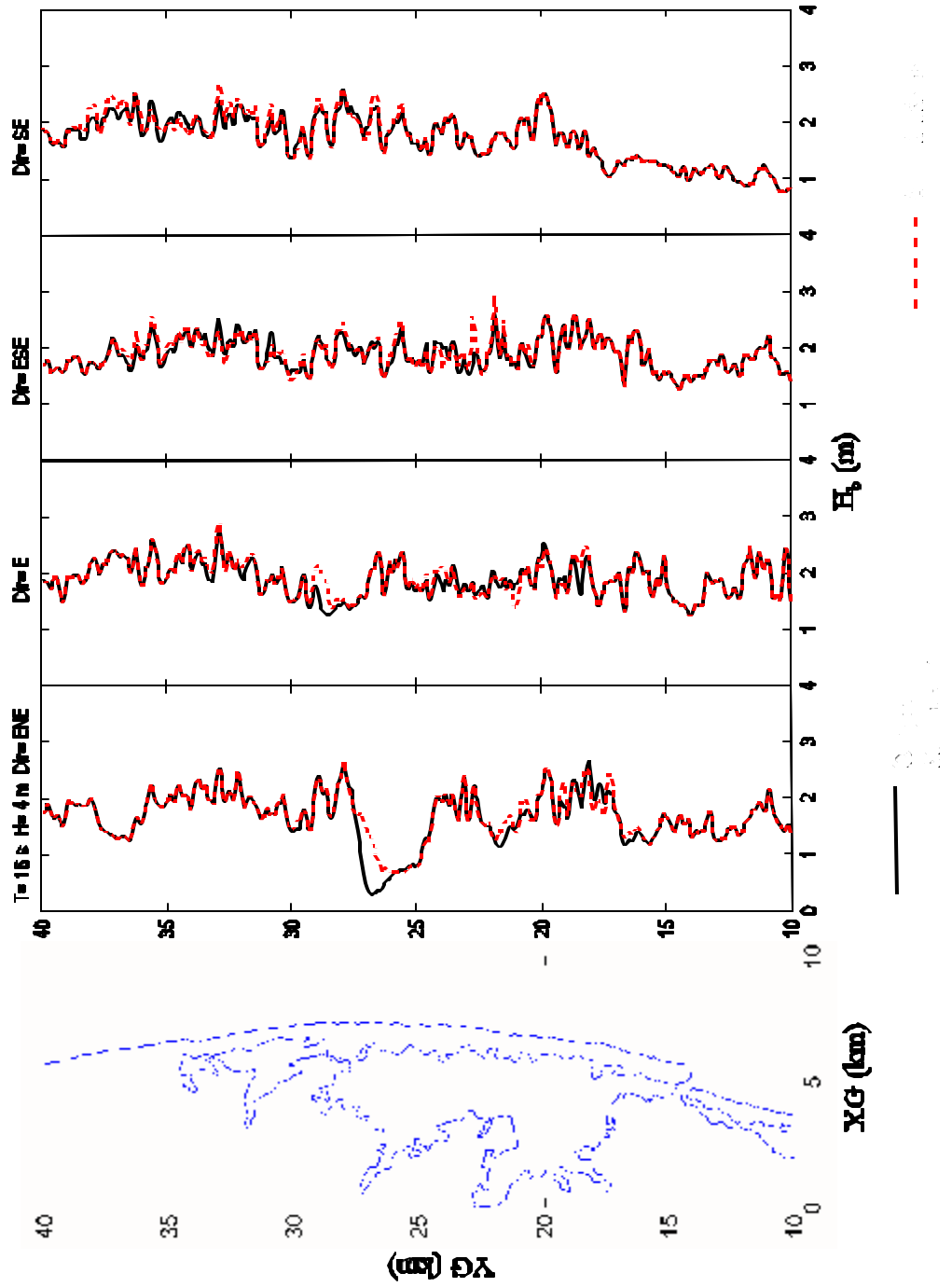


Fig. 6-22. Comparison of Breaking Wave Heights for Original Bathymetry and after Accumulative Dredging with  $H_b = 4$  m,  $T = 16$  s.

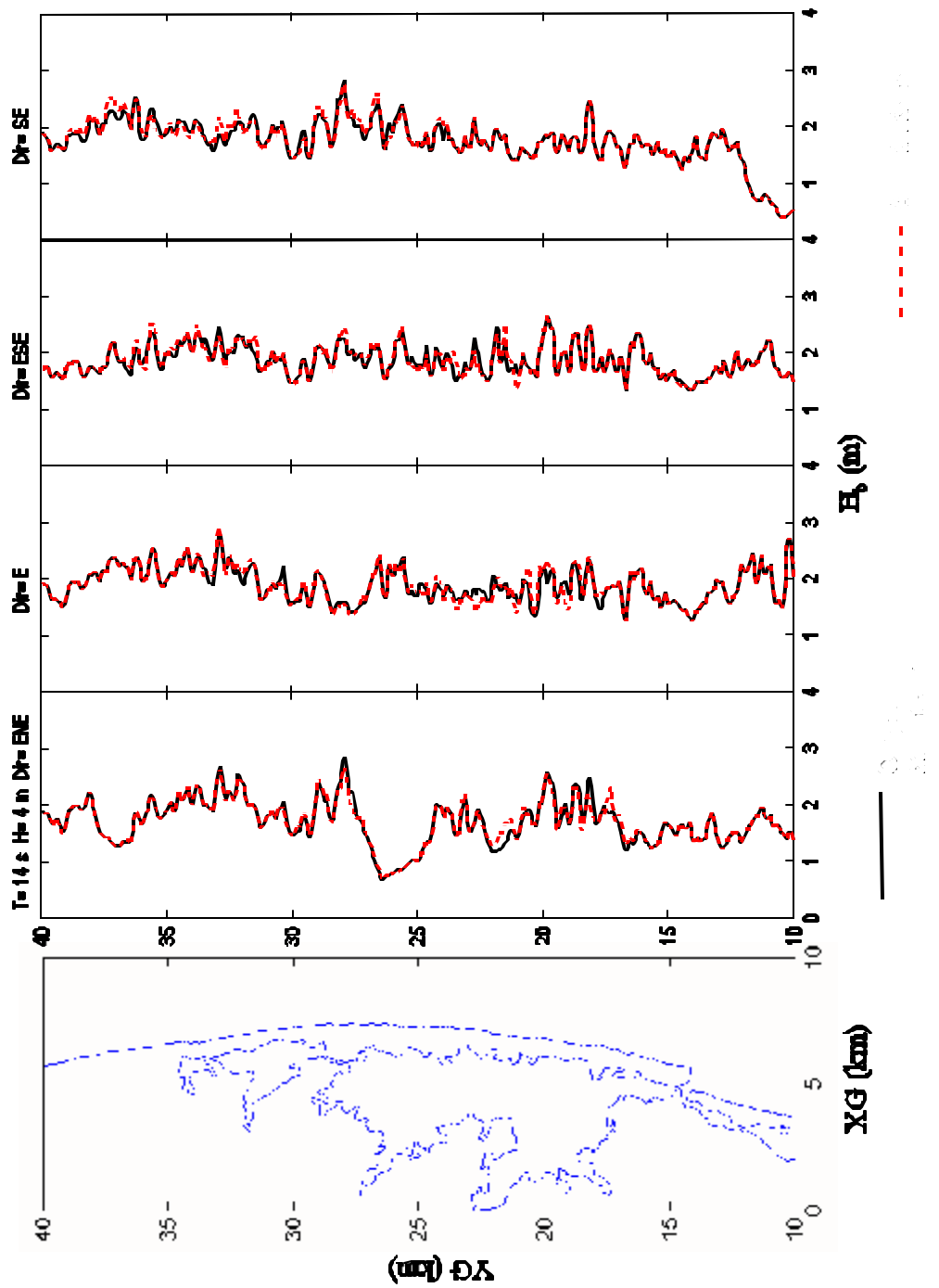


Fig. 6-23. Comparison of Breaking Wave Heights for Original Bathymetry and after Accumulative Dredging with  $H_0 = 4$  m,  $T = 14$  s.

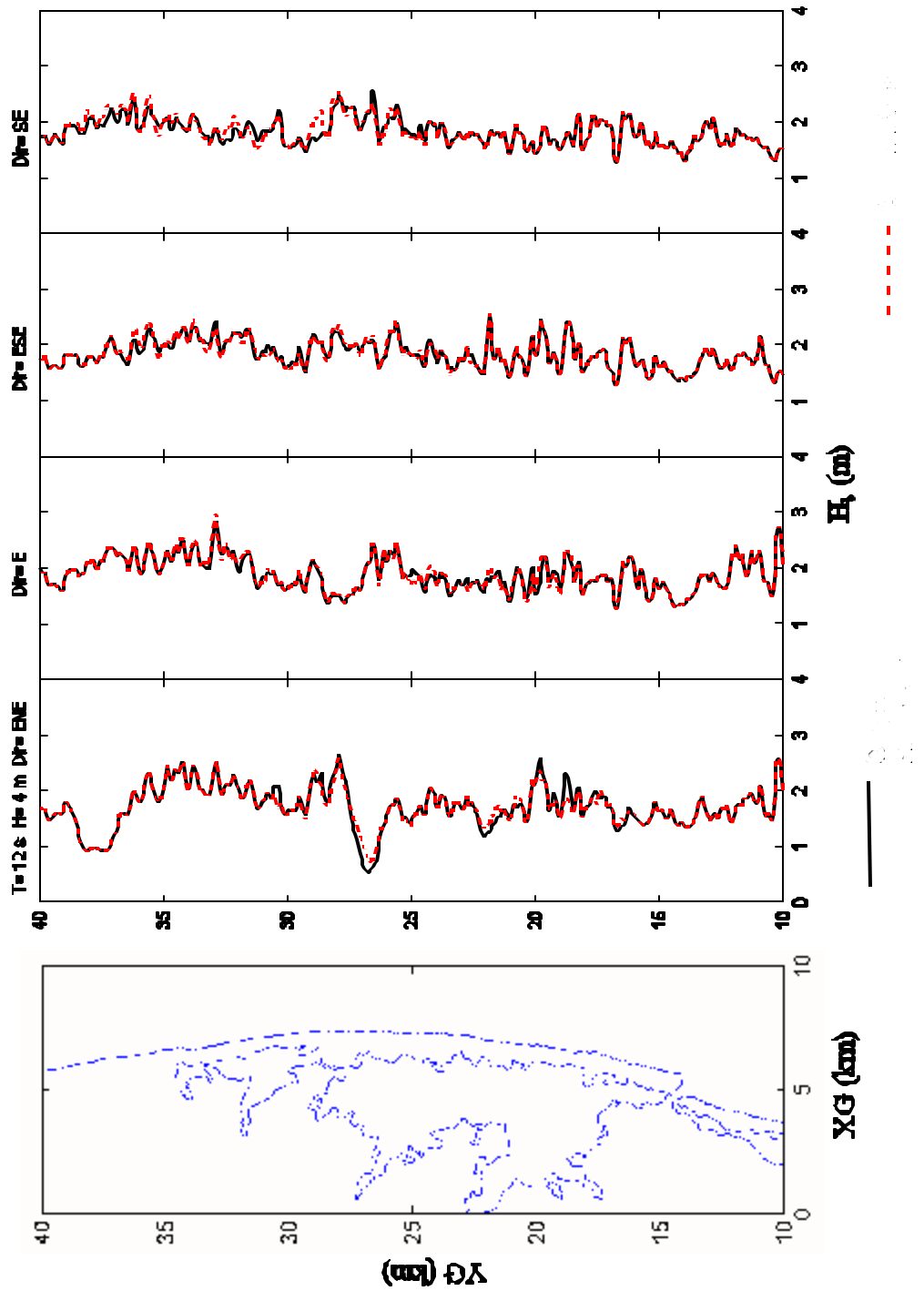


Fig. 6-24. Comparison of Breaking Wave Heights for Original Bathymetry and after Accumulative Dredging with  $H_b = 4$  m,  $T = 12$  s.

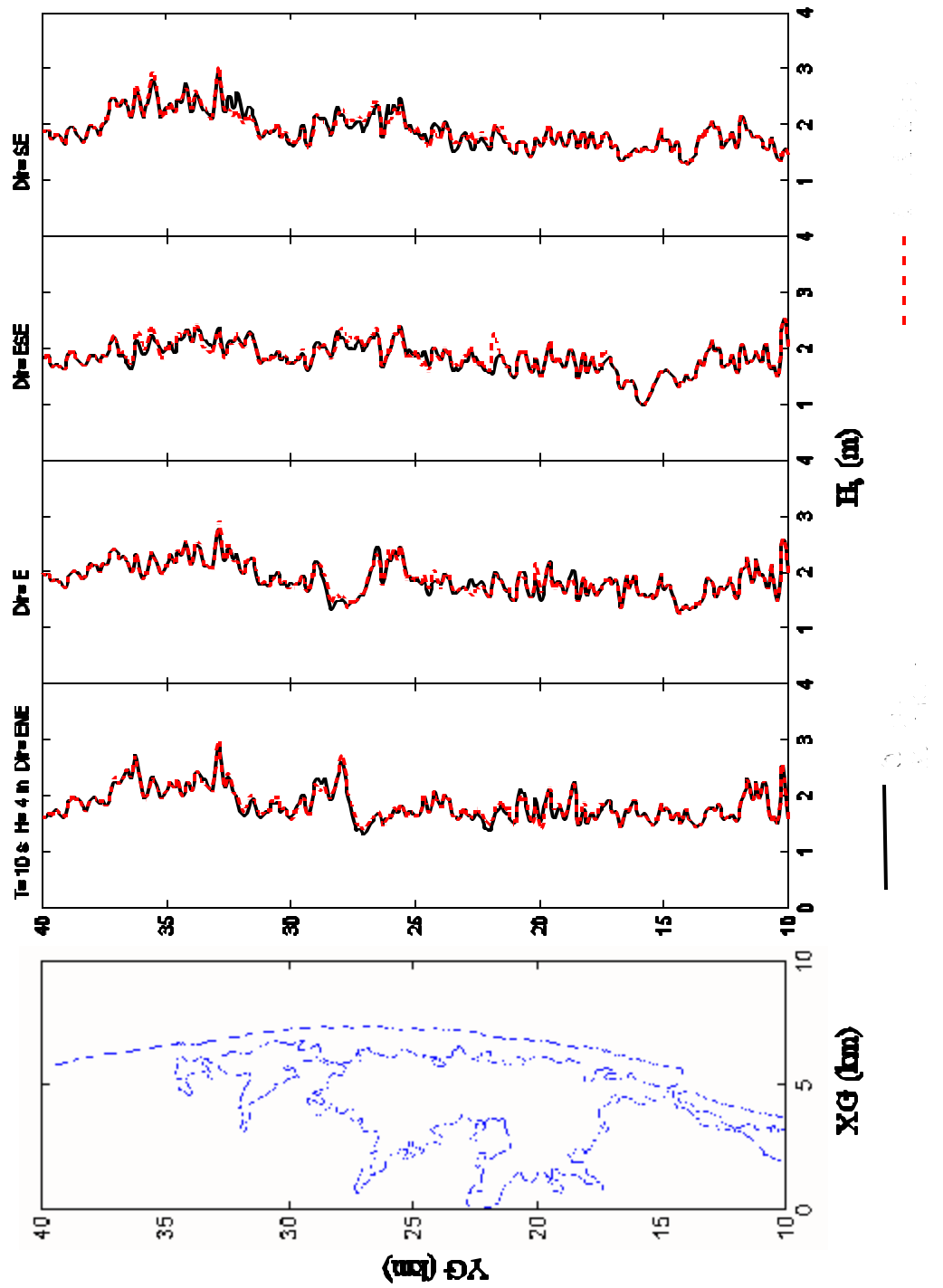


Fig. 6-25. Comparison of Breaking Wave Heights for Original Bathymetry and after Accumulative Dredging with  $H_b = 4$  m,  $T = 10$  s.

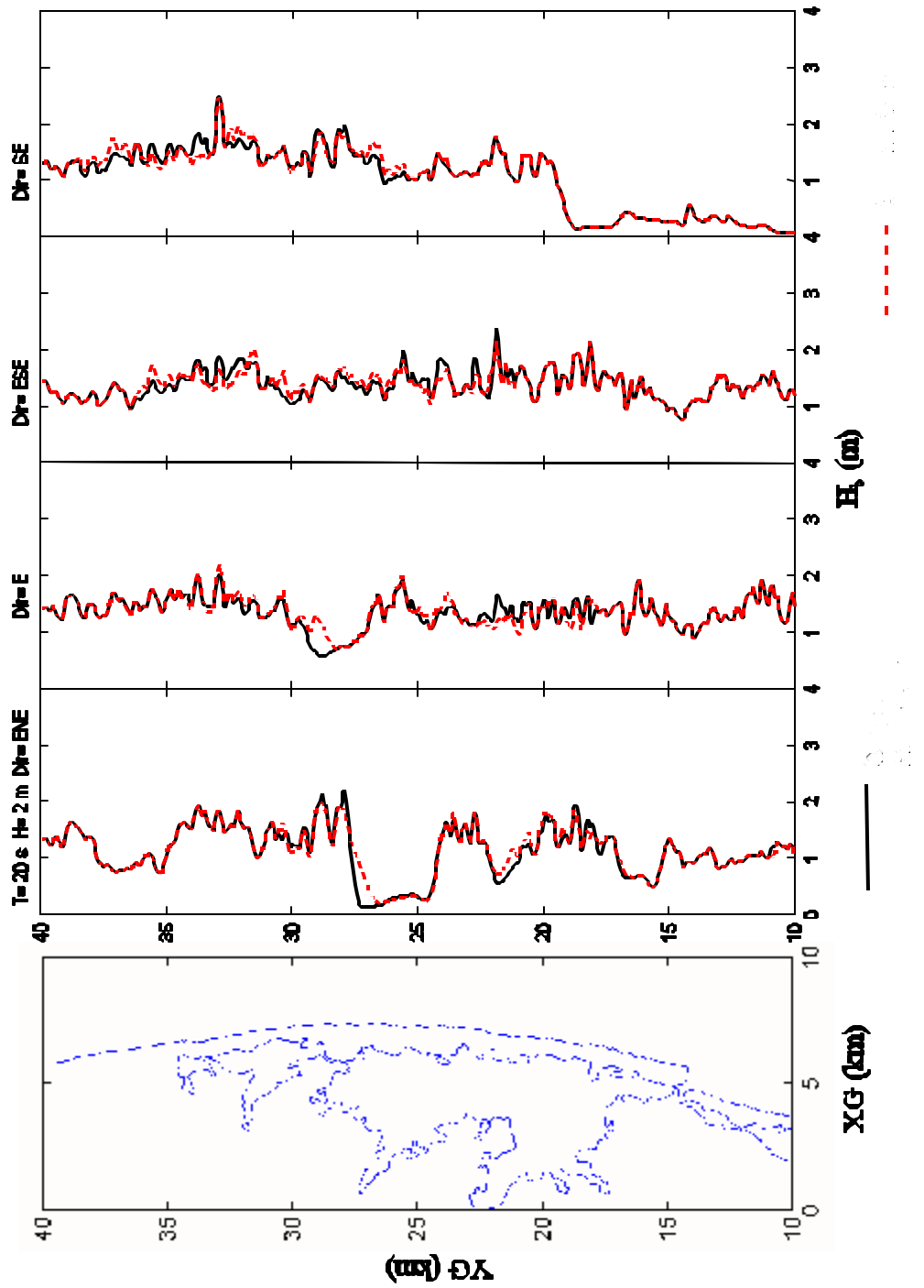


Fig. 6-26. Comparison of Breaking Wave Heights for Original Bathymetry and after Accumulative Dredging with  $H_b = 2$  m,  $T = 20$  s.

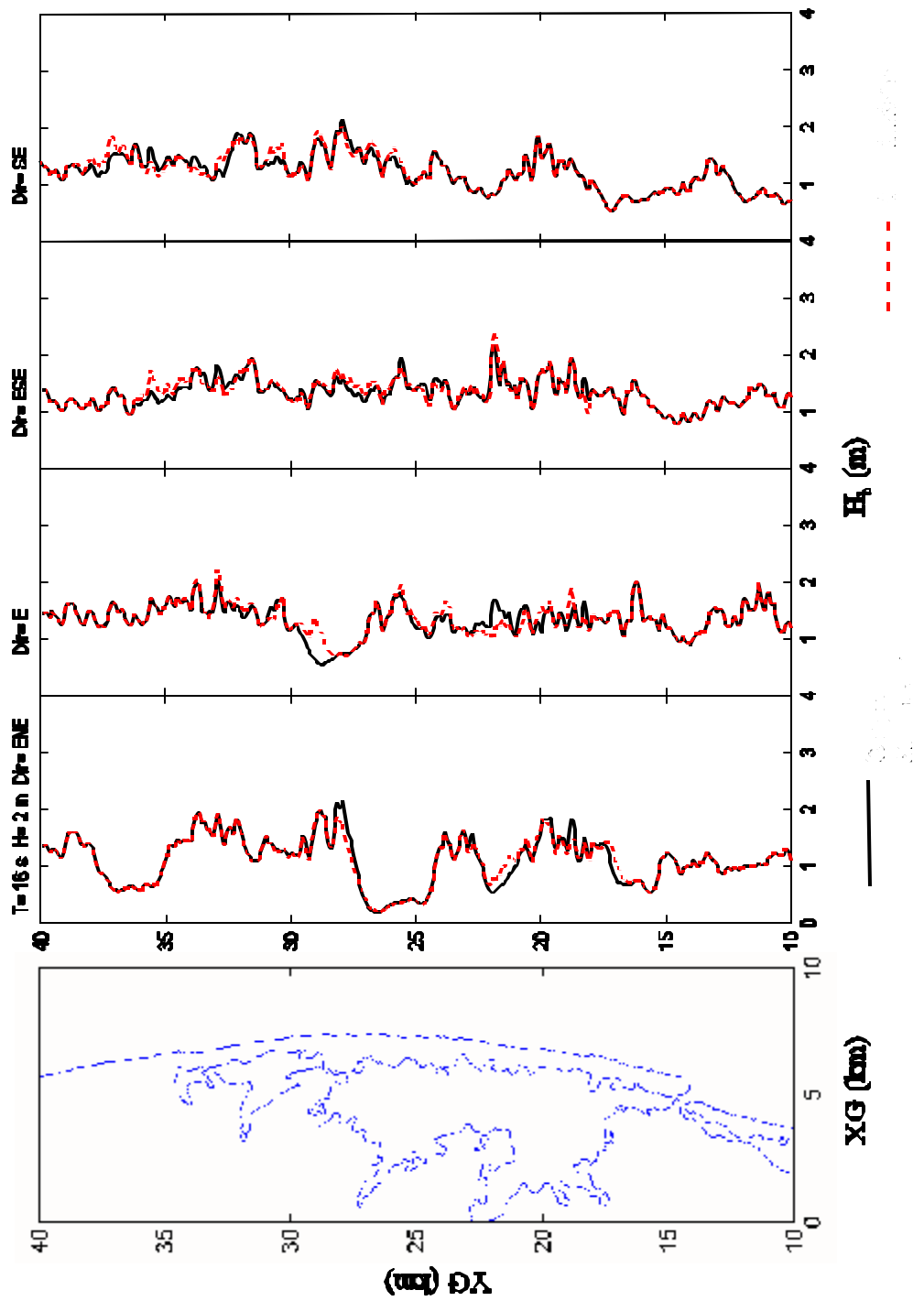


Fig. 6-27. Comparison of Breaking Wave Heights for Original Bathymetry and after Accumulative Dredging with  $H_b = 2$  m,  $T = 16$  s.

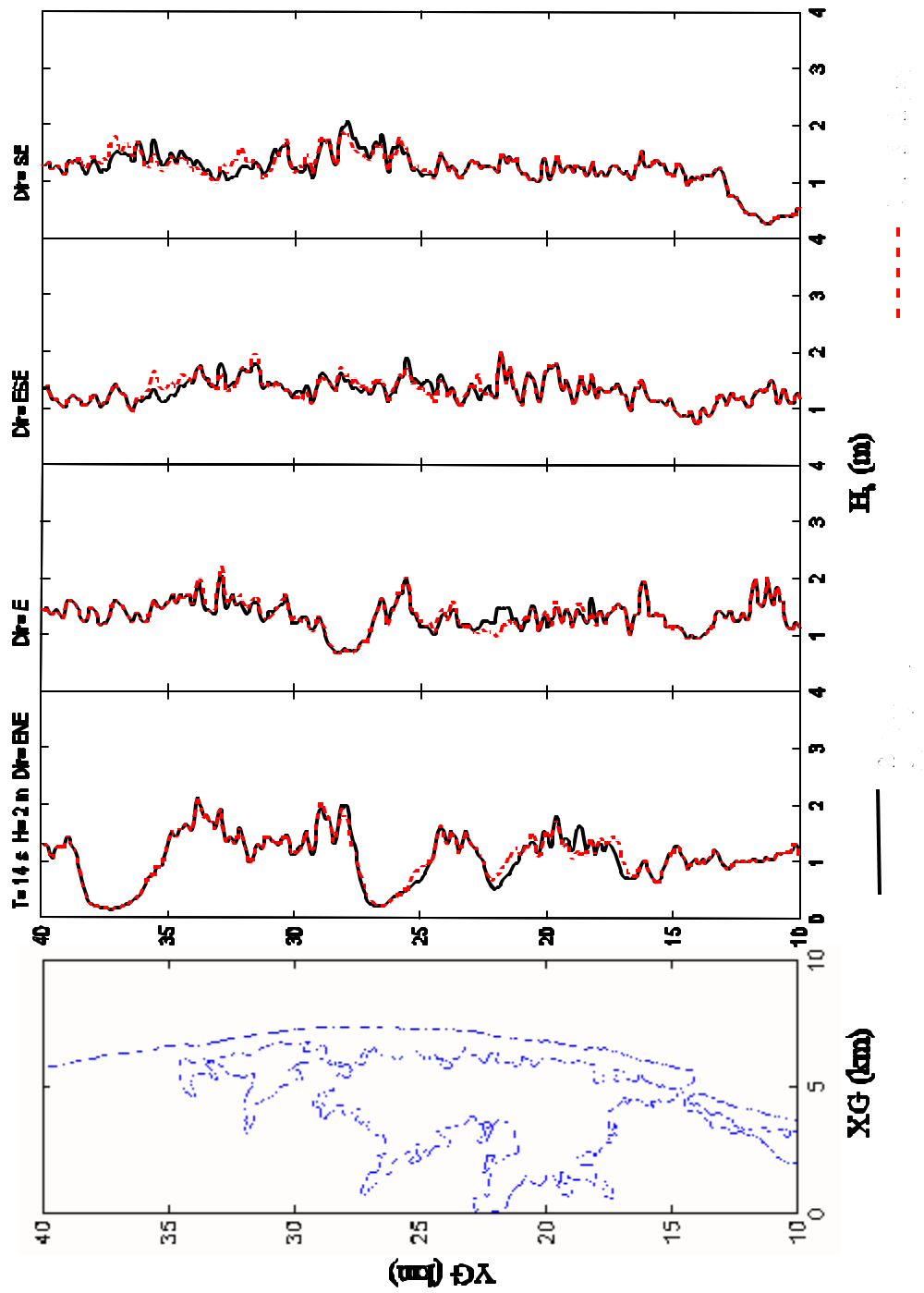


Fig. 6-28. Comparison of Breaking Wave Heights for Original Bathymetry and after Accumulative Dredging with  $H_b = 2$  m,  $T = 14$  s.

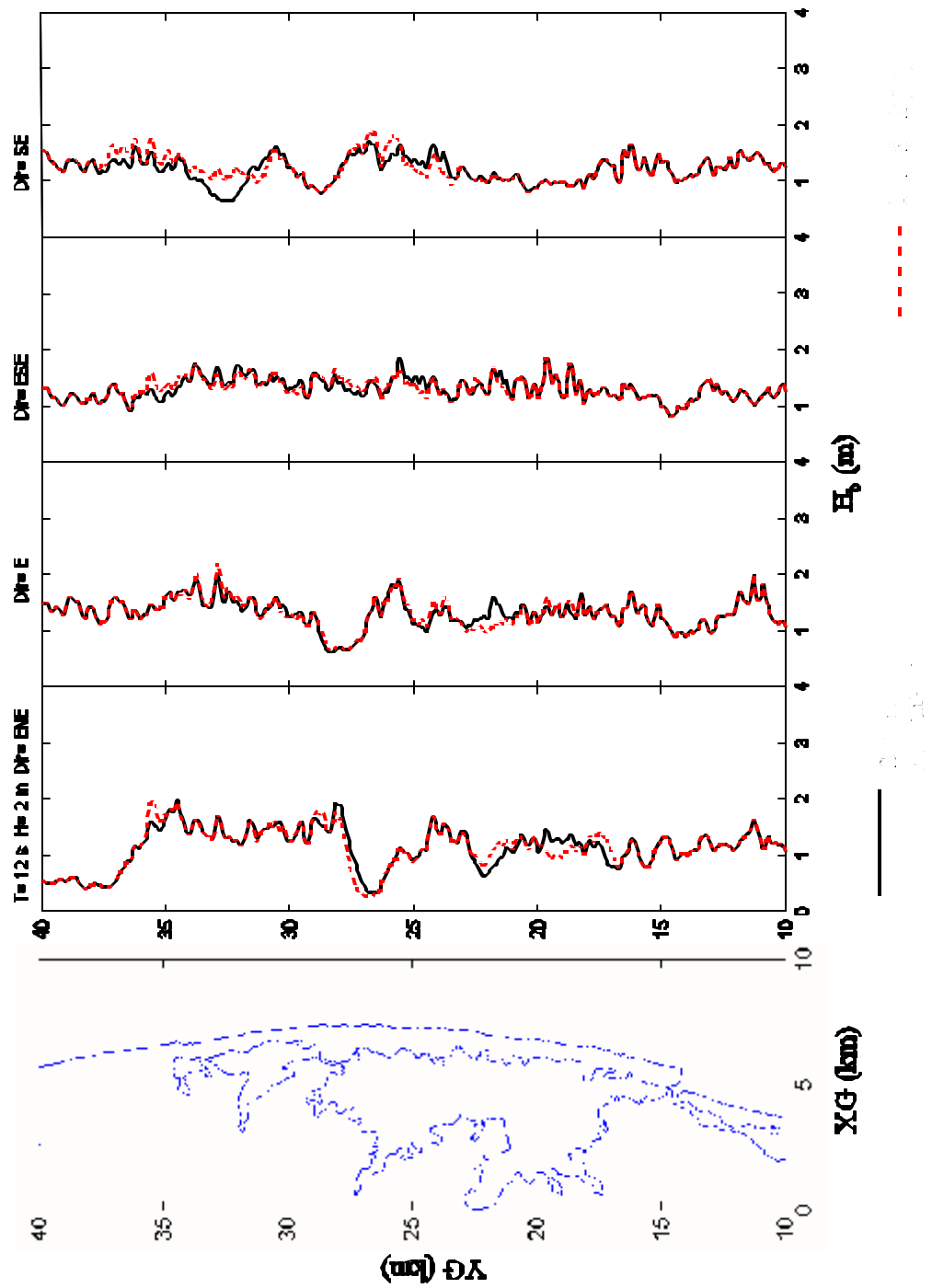


Fig. 6-29. Comparison of Breaking Wave Heights for Original Bathymetry and after Accumulative Dredging with  $H_0 = 2$  m,  $T = 12$  s.

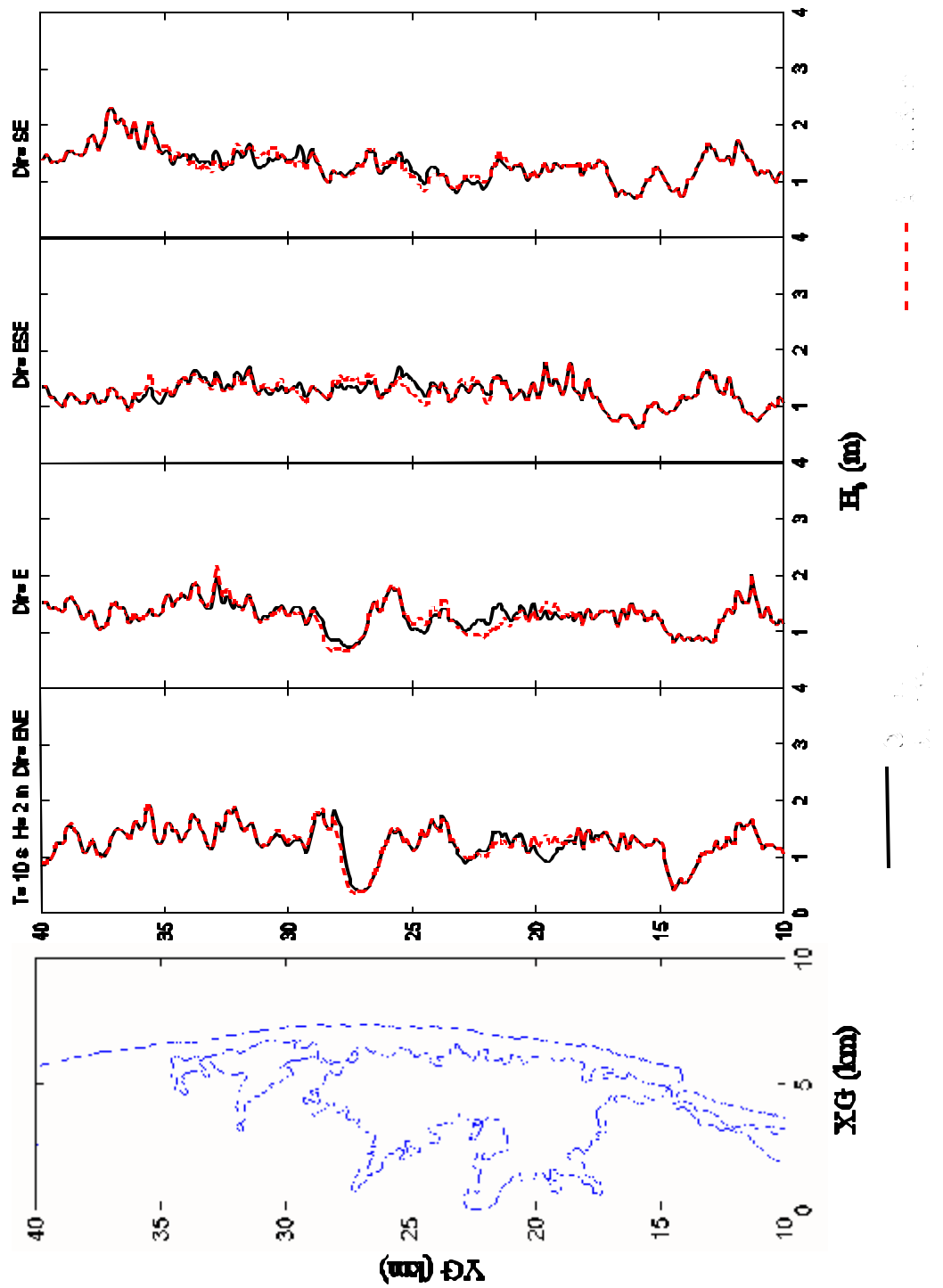


Fig. 6-30. Comparison of Breaking Wave Heights for Original Bathymetry and after Accumulative Dredging with  $H_b = 2$  m,  $T = 10$  s.



## CHAPTER 7. POSSIBLE INFLUENCE OF STORM SURGES

### 7.1. Introduction

Coastal storm surge, defined as the anomaly of water level from astronomical tide, threatens coastal communities. The storm surge is also known as wind tide because it stems from storms of tropical or extratropical origins. The storm surge has been expressed as barotropic response of coastal water body to meteorological forcing and the controlling parameters are geometry of coastlines and bathymetry (e.g. Murty, 1984). A concern would arise from the changing offshore bathymetry by dredging operation.

SLOSH (Sea, Lake, and Overland Surges from Hurricanes) model was developed in NOAA (Jelesnianski et al., 1992). This model is known as 2-1/2 dimensional model because it assumes a vertical structure of velocity profile. The SLOSH model has been utilized to generate evacuation maps for FEMA. It was also extended to incorporate extratropical storms (Kim et al., 1996). In this study, the SLOSH model was used to study the impact of offshore shoal removal by dredging. Two typical storm tracks—shore normal and shore parallel—were used. Only category 4 storms were modeled because the objective is to see the possible maximum impact.

### 7.2. SLOSH model

We use horizontal coordinate,  $Z=x+iy$  where  $i$  denotes the complex number. When  $u$  and  $v$  are velocities in the  $x$ - and  $y$ -directions of Cartesian coordinate, respectively, the complex horizontal velocity,  $w$ , is expressed analogously

$$w = u + iv \tag{7-1}$$

The horizontal pressure gradient,  $q$ , is defined with the water level,  $h$  and the gravitational acceleration,  $g$ ,

$$q = -g \left( \frac{\partial \mathbf{h}}{\partial x} + i \frac{\partial \mathbf{h}}{\partial y} \right) \quad (7-2)$$

We define transport,  $W$ , as depth integrated horizontal velocity

$$W = h \int_0^1 w \, dz \quad (7-3)$$

Here, the vertical coordinate,  $z$ , is normalized by water depth,  $h$ , and thus varies between 0 at the bottom and 1 at the surface. The surface stress term,  $R$ , is defined as

$$R = \frac{\mathbf{t}_s}{\mathbf{r}} = u_{*s}^2 \quad (7-4)$$

The bottom stress term,  $T$ , is defined as

$$T = \frac{\mathbf{t}_b}{\mathbf{r}} = u_{*b}^2 \quad (7-5)$$

The gradient term,  $Q$ , is

$$Q = qh \quad (7-6)$$

Here,  $\mathbf{t}_s$  is surface stress,  $\mathbf{t}_b$  is bottom stress, and  $\mathbf{r}$  is water density.

Linearized transport equation then becomes

$$\frac{\partial W}{\partial t} + ifW = Q + R - T \quad (7-7)$$

where  $f$  is Coriolis parameter. Solution of equation (7-7) depends on the bottom stress term  $T$  which is not easy to obtain from depth integrated transport,  $W$ , because it is a function of flow structure especially in the bottom boundary layer.

Assuming constant eddy viscosity ( $\nu = 0.0225 \text{ m}^2/\text{sec}$ ) and introducing a slip boundary condition at the bed ( $\mathbf{t}_b = s \mathbf{w}|_{z=0}$ ) with slip coefficient ( $s = 0.0009 \text{ m/sec}$ ), Jelesnianski et al. (1992) derived

$$\frac{\partial W}{\partial t} + ifAW = BQ + CR \quad (7-8)$$

Here, complex coefficients,  $A$ ,  $B$ , and  $C$ , become functions of water depth,  $h$ , eddy viscosity,  $\nu$ , Coriolis parameter,  $f$ , and slip coefficient,  $s$ . Equation (7-8) can be expressed as

$$\frac{\partial W}{\partial t} + ifAW = -gh2B \frac{\partial \mathbf{h}}{\partial Z^*} + CR \quad (7-9)$$

where the asterisk represents the complex conjugate. Now we consider conformal transformation,  $\mathbf{z} = \mathbf{c} + i\mathbf{y}$ . Then, we have

$$\frac{\partial W}{\partial t} + ifAW = -gh2B \left( \frac{d\mathbf{z}}{dZ} \right)^* \frac{\partial \mathbf{h}}{\partial \mathbf{z}^*} + CR \quad (7-10)$$

A normalized transport term is introduced

$$\mathbf{v} = \left( \frac{dZ}{d\mathbf{z}} \right)^* W \quad (7-11)$$

Then, equation (7-10) becomes

$$\frac{\partial \mathbf{v}}{\partial t} + ifA \mathbf{v} = -ghB \left( \frac{\partial}{\partial \mathbf{c}} + i \frac{\partial}{\partial \mathbf{y}} \right) \mathbf{h} + \left( \frac{dZ}{d\mathbf{z}} \right)^* CR \quad (7-12)$$

This gives a similar form as the original equation except that the complex magnification factor is in the stress term. The continuity also gives

$$\frac{\partial \mathbf{h}}{\partial t} = - \left| \frac{d\mathbf{z}}{dZ} \right|^2 \left[ \frac{\partial \mathbf{v}}{\partial \mathbf{z}} + \left( \frac{\partial \mathbf{v}}{\partial \mathbf{z}} \right)^* \right] \quad (14)$$

This becomes dependent on the Jacobian,  $|d\mathbf{z}/dZ|^2$ . The SLOSH model is a finite difference model and utilizes Arakawa and Mesinger's B-scheme which makes solution of the Coriolis term easier compared to the C-scheme.

### 7.3 Model grid

A polar grid with 130 by 280 grid cells were constructed. The coastal grid cells are approximately 150 m by 150 m in dimension. Figure 7-1 shows the bathymetry represented on the computational grid. In order to investigate the impact from dredging of offshore sand shoals, we selected 10 coastal stations to monitor surge behaviors. Figure 7-2 shows the location of monitoring stations and two shoals to be removed by dredging.

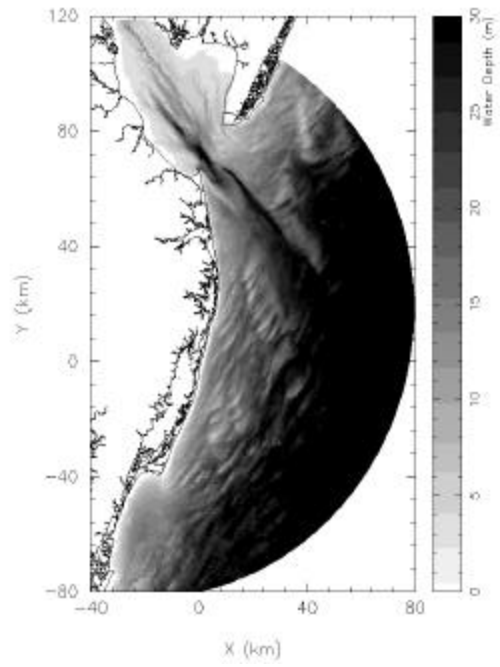


Fig 7-1. Bathymetry in the SLOSH model computation domain

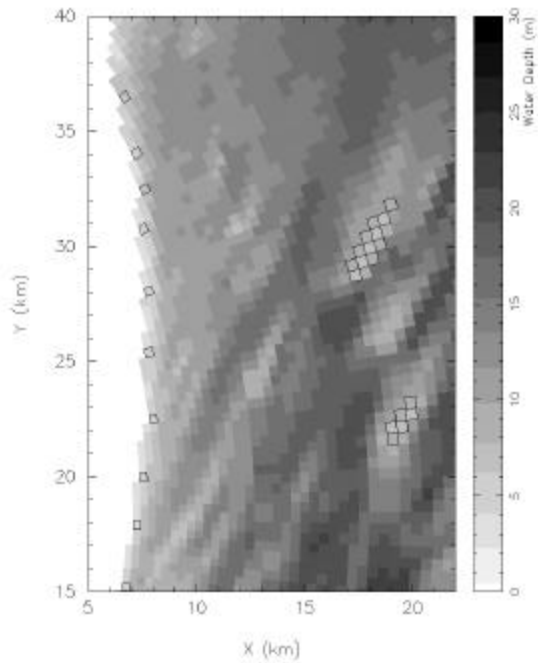


Fig 7-2. Bathymetry and 10 coastal monitoring stations in the SLOSH model. Also shown are the intended dredging sites at two offshore shoals.

## 7.4 Results and discussion

Tropical storms with 86 mbar central pressure drop and 15-mile maximum wind radius (comparable to category 4 storm) were used to simulated the coastal storm surges. Two orthogonal tracks of across- and along-shore directions were simulated. Figure 7-3 shows the ensemble of maximum surges from the cross-shore track simulation. It clearly shows the higher coastal surges in the right hand side of the storm landfall points .

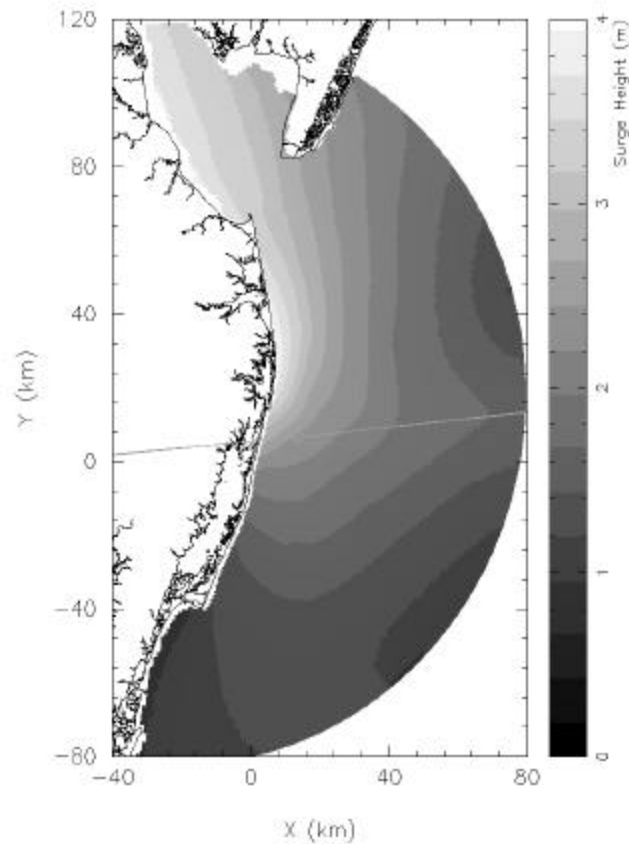


Fig 7-3. Surge envelop from cross-shore track

Figure 7-4 shows the time history of the coastal surges. Increased coastal surges from south (St. 1) to north (St. 10) was apparent. Figure 7-5 shows the change by dredging operation. The changes are about 0.1 cm which is negligible compared to the maximum surges of 3.5 m. Figure 7-6 shows the surge envelop from the along-shore track. In general the coastal surges were lower compared to the cross-shore track. South-north propagation of surges was evident (Fig 7-7). The

changes were also around 0.1 cm which is again negligible compared to the maximum surge of 2.5 m.

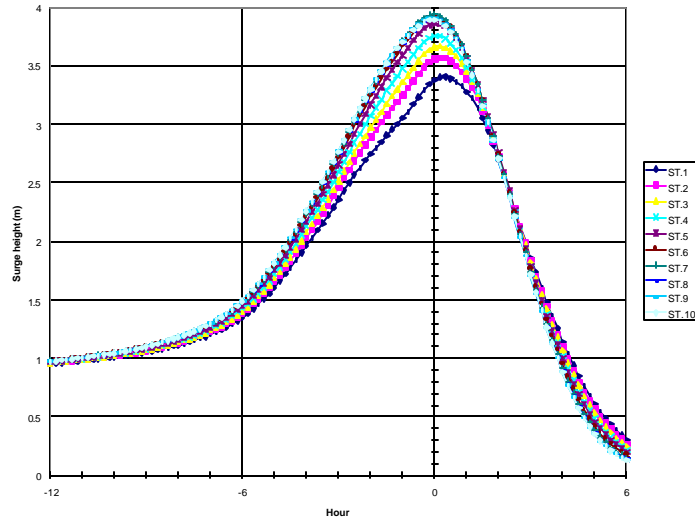


Fig 7-4. Time series of coastal surges at 10 monitoring stations. Cross-shore track

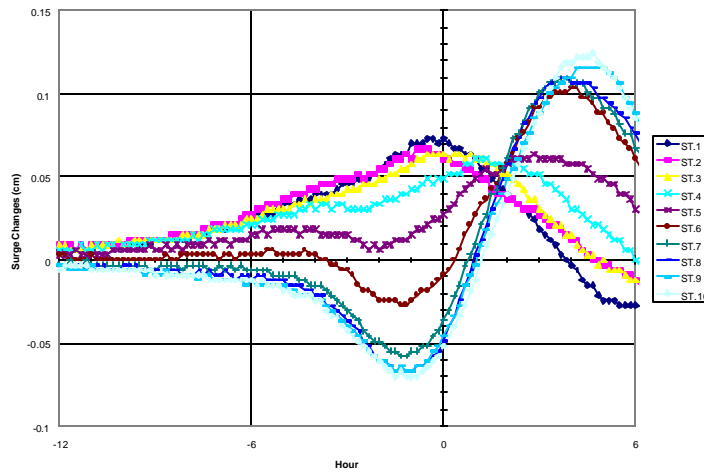


Fig 7-5. Time series of the coastal surge changes by dredging at 10 monitoring stations. Cross-shore track

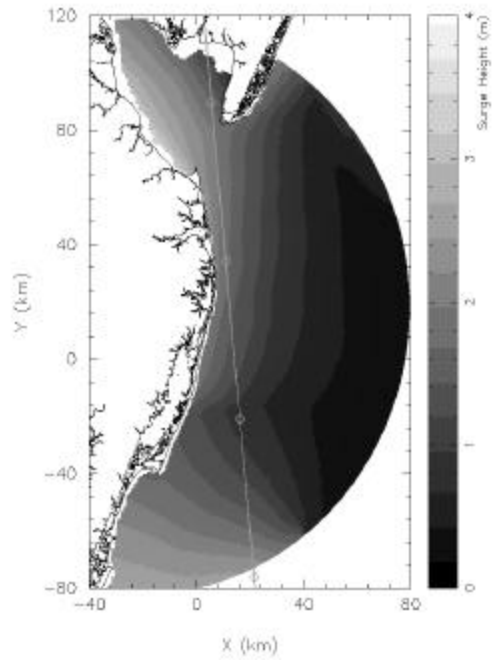


Fig 7-6. Surge envelop from shore-parallel track

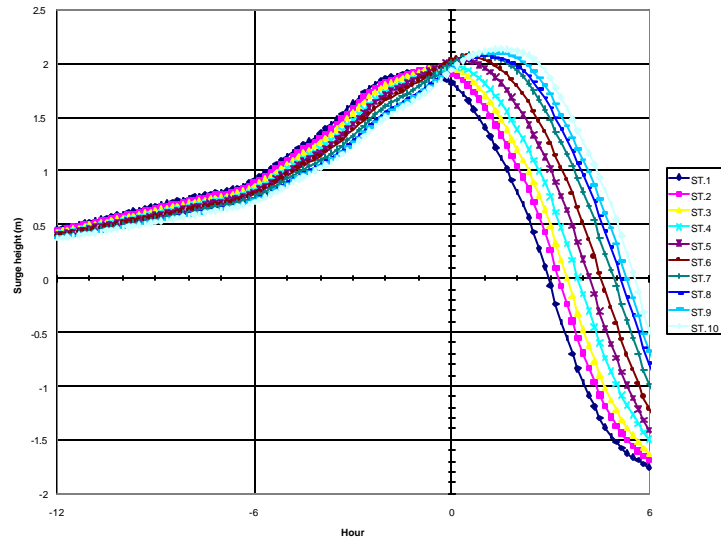


Fig 7-7. Time series of coastal surges at 10 monitoring stations. Shore-parallel track.

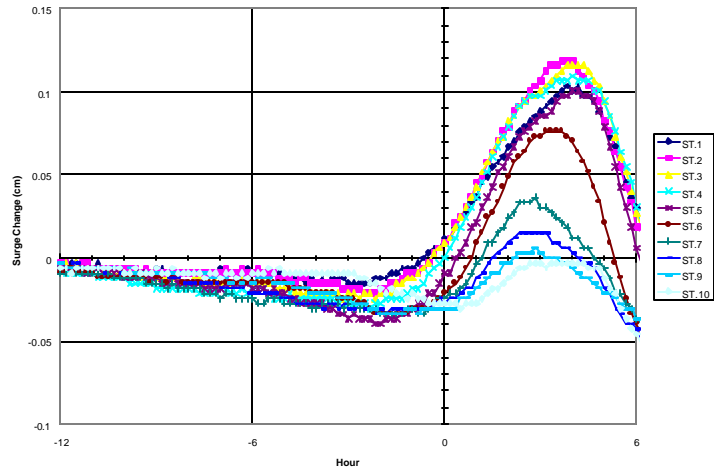


Fig 7-8. Time series of the coastal surge changes by dredging at 10 monitoring stations. Shore-parallel track



## CHAPTER 8. POSSIBLE IMPACT ON TIDAL CURRENT

### 8.1. Introduction

This chapter describes the effort on the study of possible impact on tidal currents, especially the near bottom current, potentially caused by dredging at the offshore shoals. A three-dimensional (3-D) hydrodynamic model: the Princeton Ocean Model (POM) was used to simulate the possible influence on the tidal current caused by dredging. The basics of the POM model are introduced first, followed by a description of the open boundary conditions and model verification. The original tidal current distributions at the modeled dredging sites are presented and followed by the differences in tidal current after dredging.

### 8.2. The POM Hydrodynamic Model

The 3-D barotropic version of the POM (Blumberg and Mellor, 1987) was employed to study the tidal currents in the Maryland-Delaware coastal waters. The POM model is a well established 3-D numerical model for tidal simulation. For this reason, only the basics are presented as follows. The governing equations of this bottom following sigma coordinate system are:

$$\frac{\eta h}{\eta t} + \frac{\eta UD}{\eta x} + \frac{\eta VD}{\eta y} + \frac{\eta w}{\eta s} = 0 \quad (8-1)$$

$$\begin{aligned} \frac{\eta UD}{\eta t} + \frac{\eta U^2 D}{\eta x} + \frac{\eta UVD}{\eta y} + \frac{\eta Uw}{\eta s} - F_x - fVD + gD \frac{\eta h}{\eta x} = \\ \frac{1}{r} (\mathbf{t}_{sx} - \mathbf{t}_{bx}) + \frac{\eta}{\eta s} \left[ \frac{K_M}{D} \frac{\eta U}{\eta s} \right] \end{aligned} \quad (8-2)$$

$$\begin{aligned} \frac{\eta VD}{\eta t} + \frac{\eta UVD}{\eta x} + \frac{\eta V^2 D}{\eta y} + \frac{\eta Vw}{\eta s} - F_y + fVD + gD \frac{\eta h}{\eta y} = \\ \frac{1}{r} (\mathbf{t}_{sy} - \mathbf{t}_{by}) + \frac{\eta}{\eta s} \left[ \frac{K_M}{D} \frac{\eta V}{\eta s} \right] \end{aligned} \quad (8-3)$$

where  $H$ ,  $\hat{\tau}_s$  and  $\hat{\tau}_b$  are water depth, wind stress and bottom friction,  $K_M$  is the vertical kinematic viscosity calculated from the turbulence closure model (Mellor and Yamada, 1982) and

$$F_x = \frac{\tau_x}{K} \left[ H 2 A_M \frac{\tau_x}{K} \right] + \frac{\tau_x}{K} \left[ H A_M \left( \frac{\tau_x}{K} + \frac{\tau_y}{K} \right) \right], \quad (8-4)$$

$$, F_y = \frac{\tau_y}{K} \left[ H 2 A_M \frac{\tau_y}{K} \right] + \frac{\tau_y}{K} \left[ H A_M \left( \frac{\tau_x}{K} + \frac{\tau_y}{K} \right) \right] \quad (8-5)$$

$$A_M = C \Delta x \Delta y \frac{1}{2} \left| \nabla V + \nabla V^T \right|, \quad (8-6)$$

$$D = H + \mathbf{h}.$$

### 8.3. Model Grid

The orthogonal curvilinear model grid is the same as displayed in Fig. 2-2, except that the cell size is increased to 300 m x 600 m in the east-west and north-south directions, respectively. The total dimension is also the same: 44.97 km x 67.56 km. There are 6 sigma layers in the vertical direction, *i.e.*, the total water depth was divided into 6 layers with equal thickness, and the thickness of these layers varies because of the different total water depth. The model computation internal and external time steps were 90 and 6 seconds, respectively. The horizontal diffusion coefficient was set as a constant of 50 m<sup>2</sup>/s.

### 8.4. Lateral and Open Boundary Conditions

Since the east open ocean boundary of the model domain is located only about 45 km offshore from the Maryland and Delaware shorelines, the tidal level gradient is expected to be insignificant within this short distance. Therefore, the east open ocean boundary can be specified using the tidal levels measured from a tidal station on the west side of the study domain: Ocean City, Maryland. Hourly water level records at Ocean City Inlet (NOS Station ID 8570283), Maryland for the entire year of 1985 were processed by using the least square harmonic analysis to obtain amplitudes and epoches of 29 tidal constituents (Table 8-1).

Using the 29 constituents, a tidal time series can be reconstructed to remove the wind effects: wind set-up or set-down. The reconstructed tide levels were specified as the east open ocean boundary condition while a velocity radiation condition was specified at the north and south boundaries. As mentioned before, the gradient of water surface elevation is negligible small in this small domain, the reconstructed tidal elevations really serve two purposes: (1) to provide the boundary condition at the offshore border, and (2) to serve as a verification of the model performance by comparing the calculated and the reconstructed tidal elevation at the Ocean City Inlet.

### 8.5. Model Verification

Using the original bathymetry, the POM model was run with a cold start (assuming the tidal elevation and tidal current are all zero in the computation domain) for 30 days. The model calculated tide levels at Ocean City, Maryland are compared with the re-constructed tide levels and the results are showing in Fig. 8-1. It reveals a very good agreement, less than 1 cm RMS (root-mean-square) errors. This calibration indicates that the model is capable of reproducing the water levels accurately for the existing bathymetry in the study area. Although there is no tidal current data available to verify the simulated velocity, the model produces a reasonable (20 cm/s) maximum surface current speed at proposed dredging sites. Therefore, the model will be used to evaluate the tidal current changes before and after the proposed dredging.

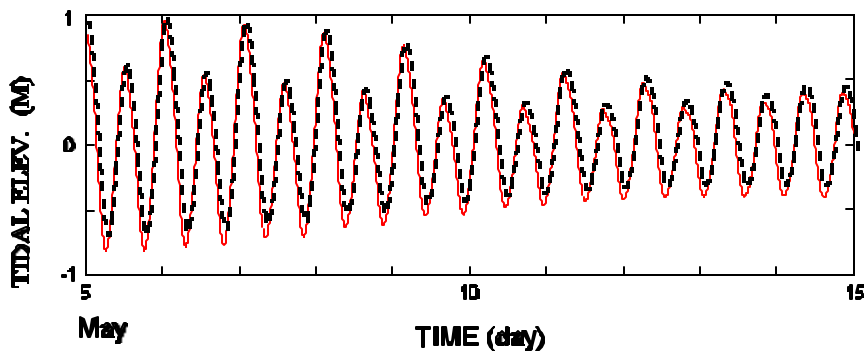


Fig. 8-1. Comparison of Calculated and Analyzed Tidal Elevation at Ocean City Inlet from May 5 -15, 1985. Solid line is the Calculated and Dashed line is the Analyzed Tidal Elevation.

Table 8-1. Amplitude and Epoch of Major Constituents Specified at offshore Boundary

Constituents	Amplitude (M)	Epoch (Degrees)
M(2)	0.4873	191.73
N(2)	0.1185	164.85
O(1)	0.0843	234.62
K(1)	0.0848	114.43
K(2)	0.0243	235.72
MU(2)	0.0197	150.68
NU(2)	0.0212	158.97
Q(1)	0.0147	67.97
2N(2)	0.0152	142.26
L(2)	0.0148	174.59
M(6)	0.0124	159.93
M(1)	0.0054	129.06
J(1)	0.0068	131.36
LAMBDA(2)	0.0075	231.29
M(4)	0.0073	243.31
MN(4)	0.0056	192.86
OO(1)	0.0030	160.99
S(4)	0.0042	271.35
RHO(1)	0.0033	48.96
2Q(1)	0.0026	62.87
2SM(2)	0.0022	216.68
M(3)	0.0022	150.38
MS(4)	0.0017	32.22
2MK(3)	0.0015	94.34
M(8)	0.0014	357.20
MK(3)	0.0010	187.03

## 8.6. Results

The contours of near-bed (bottom layer) tidal flow fields at the maximum flood and the maximum ebb, within the display domain (Fig. 2-2), are given in Fig. 8-2. In general, these two figures reveal that the near-bed tidal current is weak, less than 5 cm/s for the near coastal area (water depth < 10 m), except at the shoals, where the near-bed maximum flood velocity is on the order of 8 cm/s. For the maximum ebb, the same conclusions also hold. Fig. 8-3 shows the details of velocity vectors within a small domain that includes Fenwick Shoal and Isle of Wight Shoal for the maximum flood and ebb. It

reveals clearly the effect of bathymetry on tidal currents. When tidal current was forced to flow over the shoal, the current velocity increased because of the decreasing water depth. If the tidal current can find a way to avoid climb the shoal, it will take the easy route.

Since the influence of an one-time dredging on waves is limited, and also because tidal waves have a much longer wave length, the small change in bathymetry may not be seen by the tidal waves, we only investigated the scenario for long-term dredging. Using the same offshore boundary condition, the same lateral boundary condition and the bathymetry with the long-term dredging, the POM model was re-run to calculate the possible difference. For better visual presentation of the differences in such a small tidal current environment, we normalized the differences by presenting the difference in percentage (Fig. 8-4) for the maximum flood and ebb. It clearly shows that a maximum difference on the order of 10% can result. In general, at the place that the water depth increases because of dredging, the tidal current velocity decreases. Immediately after the dredging site, and on the leeward side or tidal flow, tidal current velocity increases. The affected area is rather large, see Fig. 8-4, but the amount of velocity increasing is rather small, even in percentage. If considering that the maximum tidal current velocity is only around 8 cm/s at the shoal, and around 5 cm/s away from the shoal, the change in tidal current caused by the proposed dredging is negligibly small to affect biological living conditions.

## **8.7. Conclusions**

Tidal current is rather weak in this area. The maximum tidal current is only around 20 cm/s at the surface layer. Near the bottom, the tidal current is even weaker, on the order of 5 cm/s except at the shoals, where current velocity increases to around 8 - 10 cm/s. The postulated dredging at the shoals will reduce the maximum near-bed tidal current velocity (around 10%) because of the increase of water depth. This is a positive point for biological recovery in this area. Immediately on the leeward side of tidal flow, the dredging increases the tidal velocity, up to 10%. Because of the weak currents in this area, the 10% increase only contributes less than 1 cm/s increase of tidal current, from 5-8 cm/s to 6-9 cm/s. For this reason, the possible impact of tidal current is negligibly small.

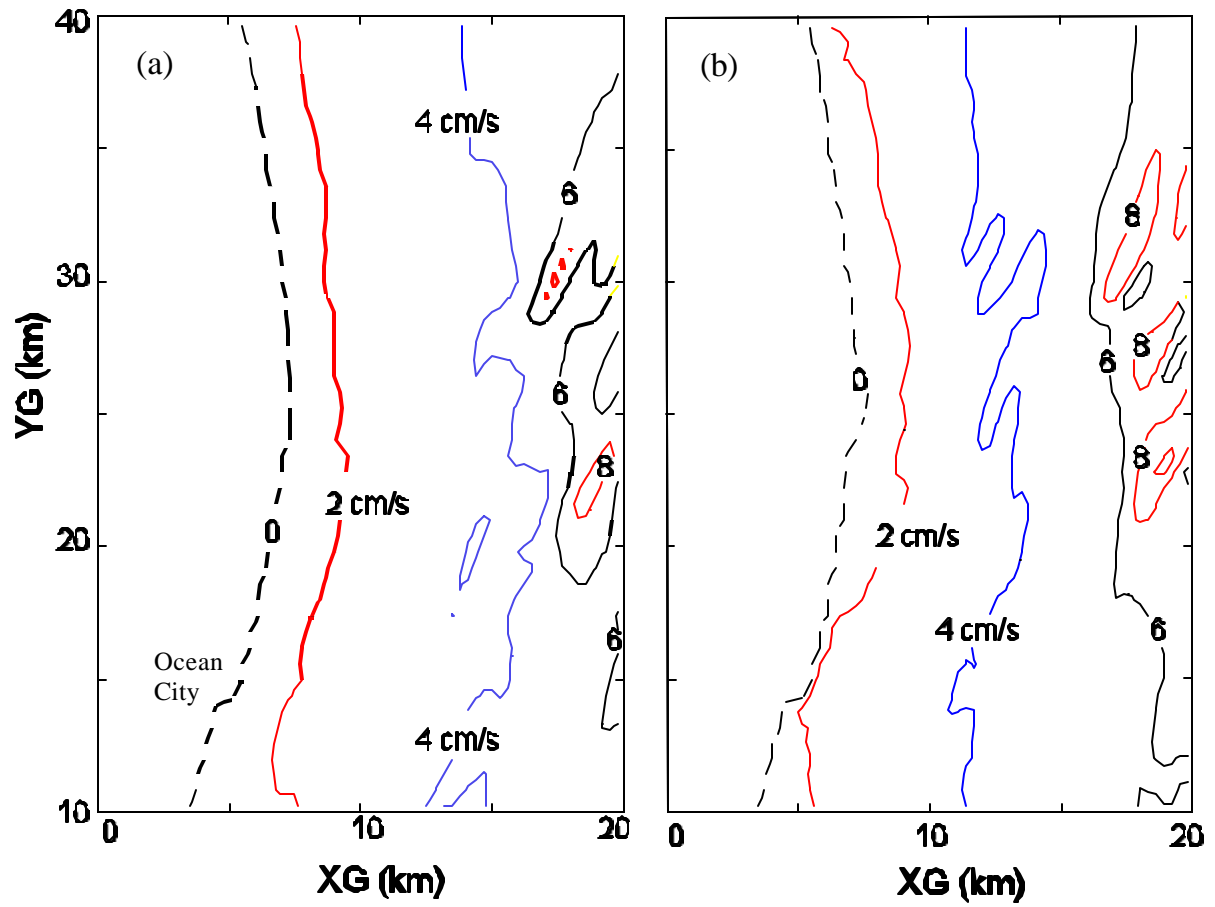
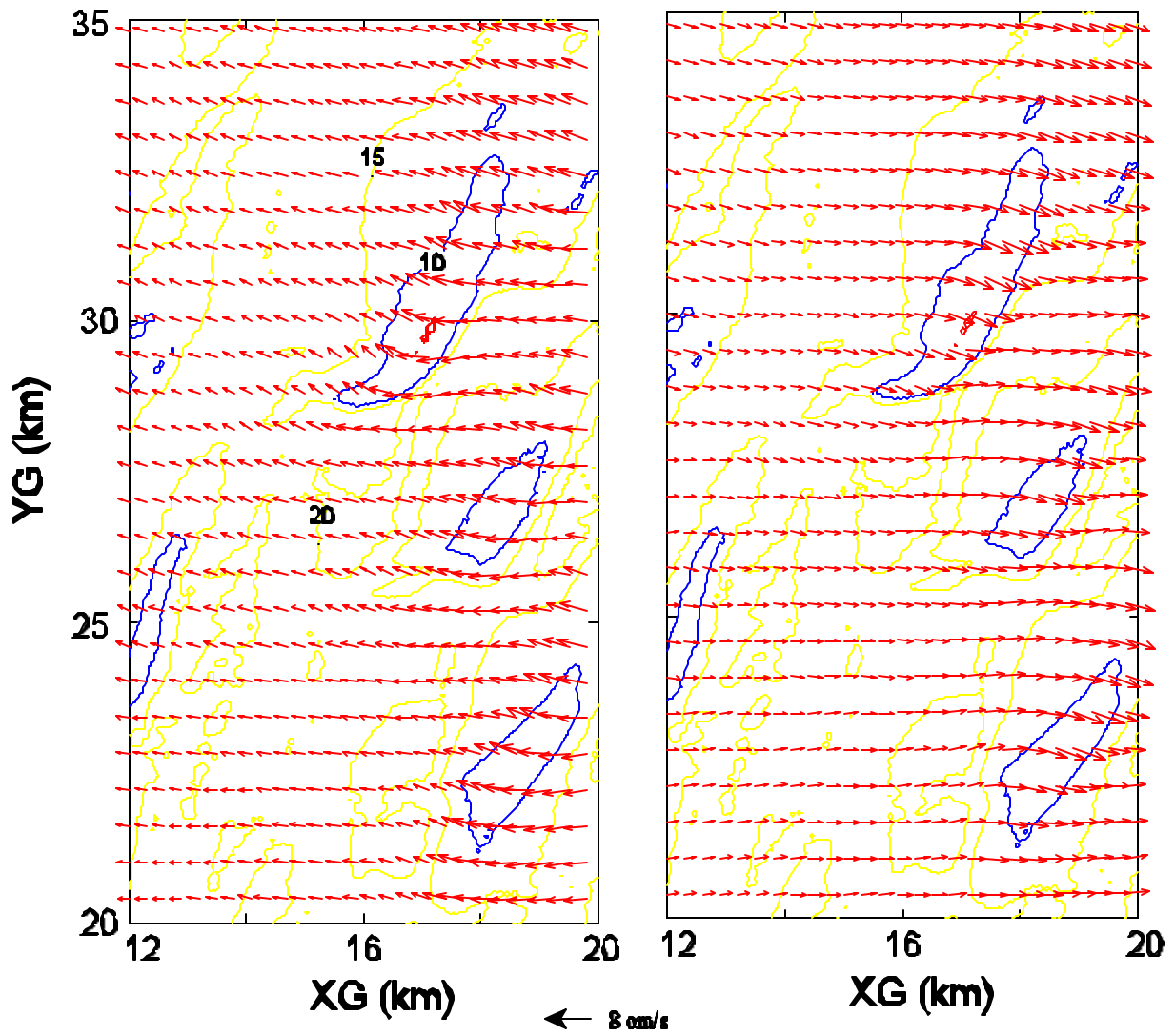


Fig. 8-2. Contours of Near-bed Tidal Current Velocity. Zero Contour Line is also the Shoreline. (a) Maximum Flood; (b) Maximum Ebb.



**Fig. B-3. Near-bed Tidal Current Velocity Vectors at the Maximum Flood (Left) and maximum Ebb (right). The Shoals are also Plotted.**

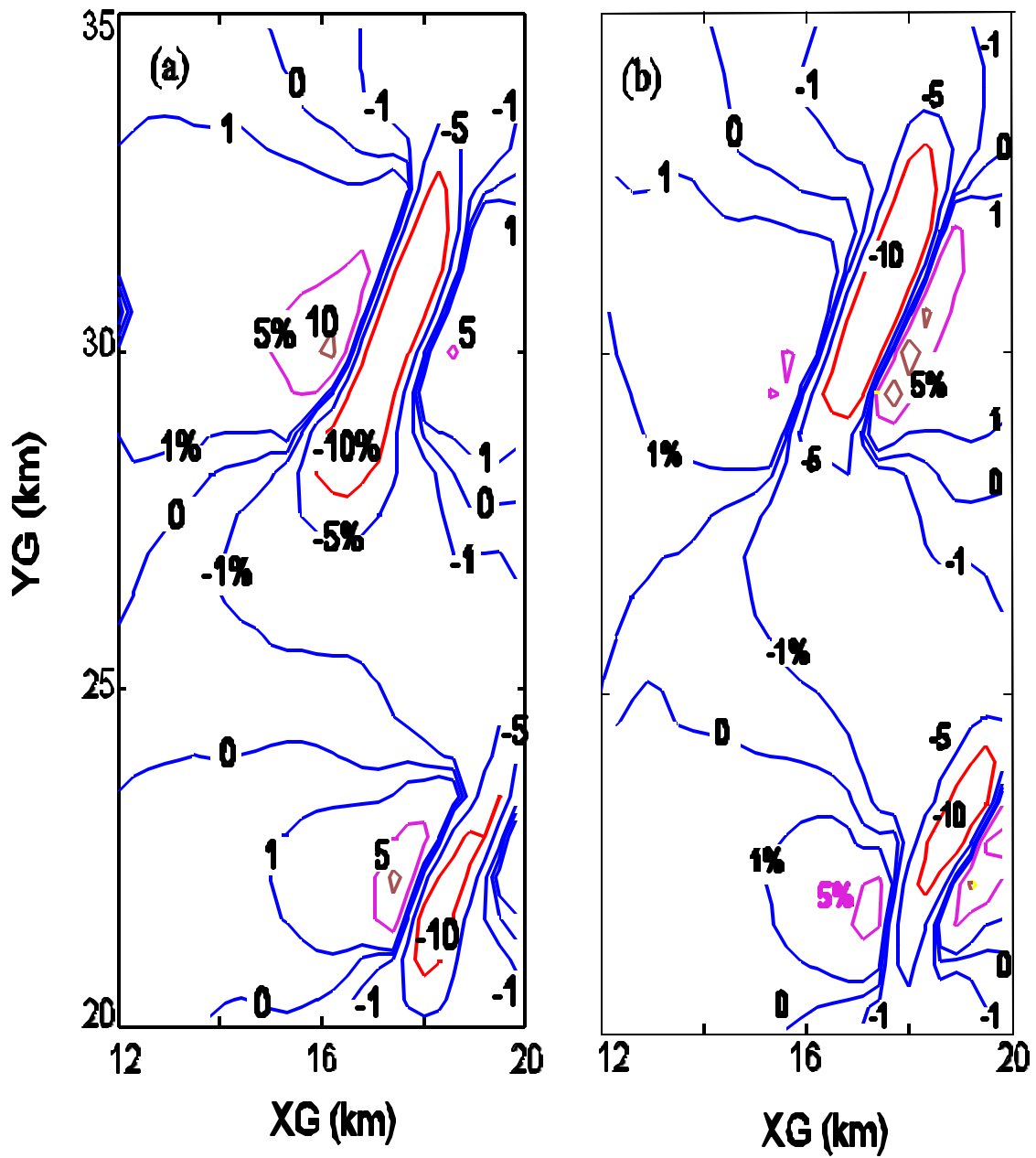


Fig. 8-4. Difference (in %) in Tidal Current Caused by Dredging at the Modeled Sites. (a) Maximum Flood; (b) Maximum Ebb

## CHAPTER 9. BENTHIC STRESS ANALYSES

### 9.1. Introduction

Natural flow consists of steady and unsteady parts in velocity distribution. The combined wave-current bottom boundary layer has been known to exert enhanced bottom stress on the bed. In general, a thin wave boundary layer can be viewed as nested beneath current boundary layer with the thickness of water depth in coastal zone. In this study, we adopted the Grant-Madsen-Glenn (GMG) model which is considered to be simple to solve but dynamically thorough. The enhanced bottom stress is calculated by combining wave-model generated wave field with an assumed steady current.

### 9.2. GMG model

The GMG model is based on the two-layer eddy viscosity model of Grant and Madsen (1979; 1986) and the modification by Glenn and Grant (1987) to account for suspended-sediment stratification above the wave boundary layer of thickness,  $d_{cw}$ . The eddy viscosities are characterized by different friction velocities,  $u_{*cw}$  and  $u_*$  inside and above the wave boundary layer, respectively (Fig 9-1):

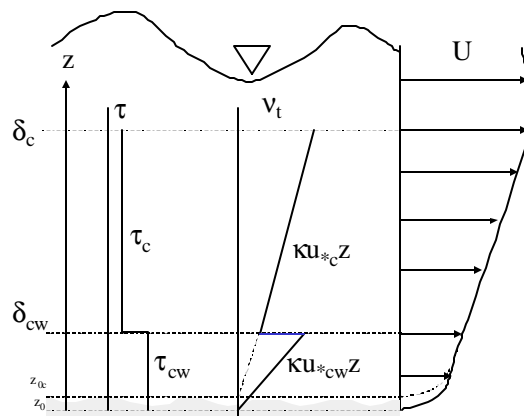


Fig 9-1. Definition sketch of two-layer wave-current bottom boundary layer.

$$\mathbf{n}_t = \begin{cases} \mathbf{k}u_{*cw}z & \text{for } z < \mathbf{d}_{cw} \\ \mathbf{k}u_{*c}z & \text{for } z > \mathbf{d}_{cw} \end{cases} \quad (9-1)$$

The bottom stress is represented by the wave-current stress,  $\mathbf{t}_{cw} = \mathbf{n}u_{*cw}^2$  where  $\mathbf{n}$  is water density. This operates within the thin wave-current boundary layer just above the bed. The wave-current boundary layer thickness,  $\mathbf{d}_{cw}$ , is

$$\mathbf{d}_{cw} = 2\mathbf{k}u_{*cw} / \mathbf{w} \quad (9-2)$$

Taking account of the effects of sediment-induced stratification via the Monin-Obukov length scale,  $L_c (= \mathbf{n}u_{*c}^3 / 6g\langle \mathbf{r}'w' \rangle)$ , where  $\mathbf{r}'$  and  $w'$  are turbulent fluctuations in fluid density and vertical velocity, respectively, and  $\langle \rangle$  is time average), the current structure becomes

$$u_c = \begin{cases} \frac{u_{*c}}{u_{*cw}} \frac{u_{*c}}{\mathbf{k}} \ln\left(\frac{z}{z_0}\right) & \text{for } z < \mathbf{d}_{cw} \\ \frac{u_{*c}}{\mathbf{k}} \left( \ln\left(\frac{z}{z_{0c}}\right) + \mathbf{b} \int_{\mathbf{d}_{cw}}^z \frac{dz}{L_c} \right) & \text{for } z > \mathbf{d}_{cw} \end{cases} \quad (9-3)$$

Here,  $\mathbf{k}$  is von Karman's constant ( $\sim 0.4$ ), roughness height  $z_0$  is related to the height,  $k_r$ , of the effective roughness elements by  $z_0 = k_r/30$ , and  $z_{0c}$  is the intercept expressing apparent roughness. By matching velocity at  $z = \mathbf{d}_{cw}$ , apparent roughness,  $z_{0c}$ , is related to "true" (i.e. without wave effects) bottom roughness,  $z_0$ , by

$$\frac{z_{0c}}{z_0} = \left( \frac{\mathbf{d}_{cw}}{z_0} \right)^{\left( 1 - \frac{u_{*c}}{u_{*cw}} \right)} \quad (9-4)$$

The roughness height,  $k_r$ , is considered to be related to grain size, ripple geometry, and bed load transport:

$$k_r = D_s + 8\mathbf{h} \frac{\mathbf{h}}{\mathbf{l}} + k_{bm} \quad (9-5)$$

Here,  $D_s$  is sediment grain diameter and  $h$  and  $l$  are ripple height and length, respectively. Ripple geometry was calculated according to Wiberg and Harris (1994). The moveable bed roughness,  $k_{bm}$ , is given by

$$k_{bm} = 5D_s (\mathbf{y}'_m - \mathbf{y}_{cr}) \quad (9-6)$$

where  $\mathbf{y}'_m$  is the maximum Shields parameter and  $\mathbf{y}_{cr}$  is the critical Shields parameter. Solution scheme is shown in Fig 9-2.

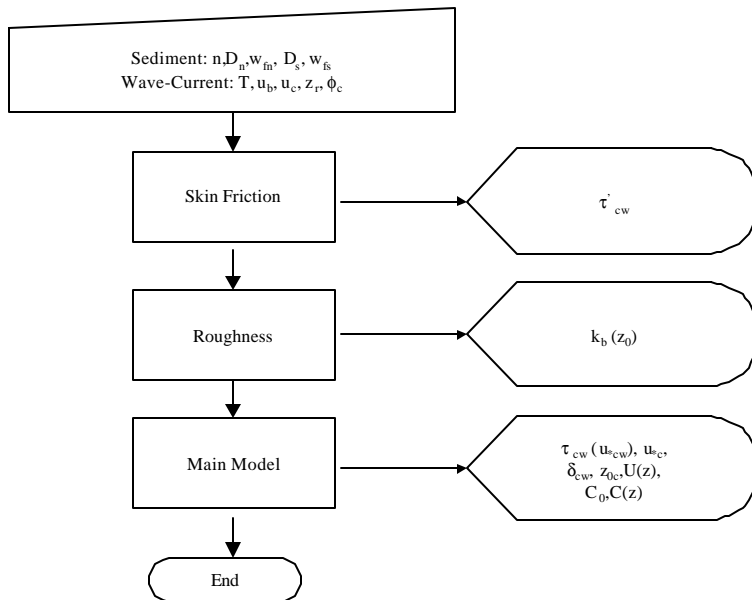


Fig 9-2. Schematics of the GMG model solution procedure

### 9.3. GMG Model Simulation

The same grid as was used in the wave model (1500 by 1127,  $\Delta x = 30$  m,  $\Delta y = 60$  m) was used. Current was assumed to be constant with 10 cm/s at 50 cm above bed. Also assumed was that the wave propagation aligned with the current direction. Grain size was assumed to be 0.1 mm (very fine sand). Only the cumulative dredging ( $2.4 \times 10^7$  m<sup>3</sup>) was considered for checking the possible impact caused by sand removal. The offshore wave conditions tested were given in Table 4-1. For each of the wave conditions tested, four different directions of wave propagation were calculated as described in Chapter 2 (i.e., ENE, E, ESE, and SE), respectively.

### 9.4. Results

Fig 9-3 shows the effect of propagation angle. For a given offshore wave height-period condition (6 m and 14 s in this case), ENE waves result in the most variability; higher bottom friction over shoals and lower bottom friction near the coastline along the trough between two shoals. Figure 9-4 shows the changes in bottom friction by removal of shoal materials according to different directions of wave propagation. The most visible changes were induced by ENE wave setting near the coastline along the trough between two shoals. Because the lower bottom stresses were seen in the troughs compared with the shoal crests, the visible changes in the trough were translated into the slight change. In Fig 9-5, the distribution of the estimated bottom frictions and their change induced by the dredging were compiled for the ENE offshore waves with varying period and significant wave conditions which are supposed to have the most impact if there are any. Consistently, the most visible changes were observed in the troughs where the bottom frictions are small. This indicates that the impact from the dredging is not substantial.

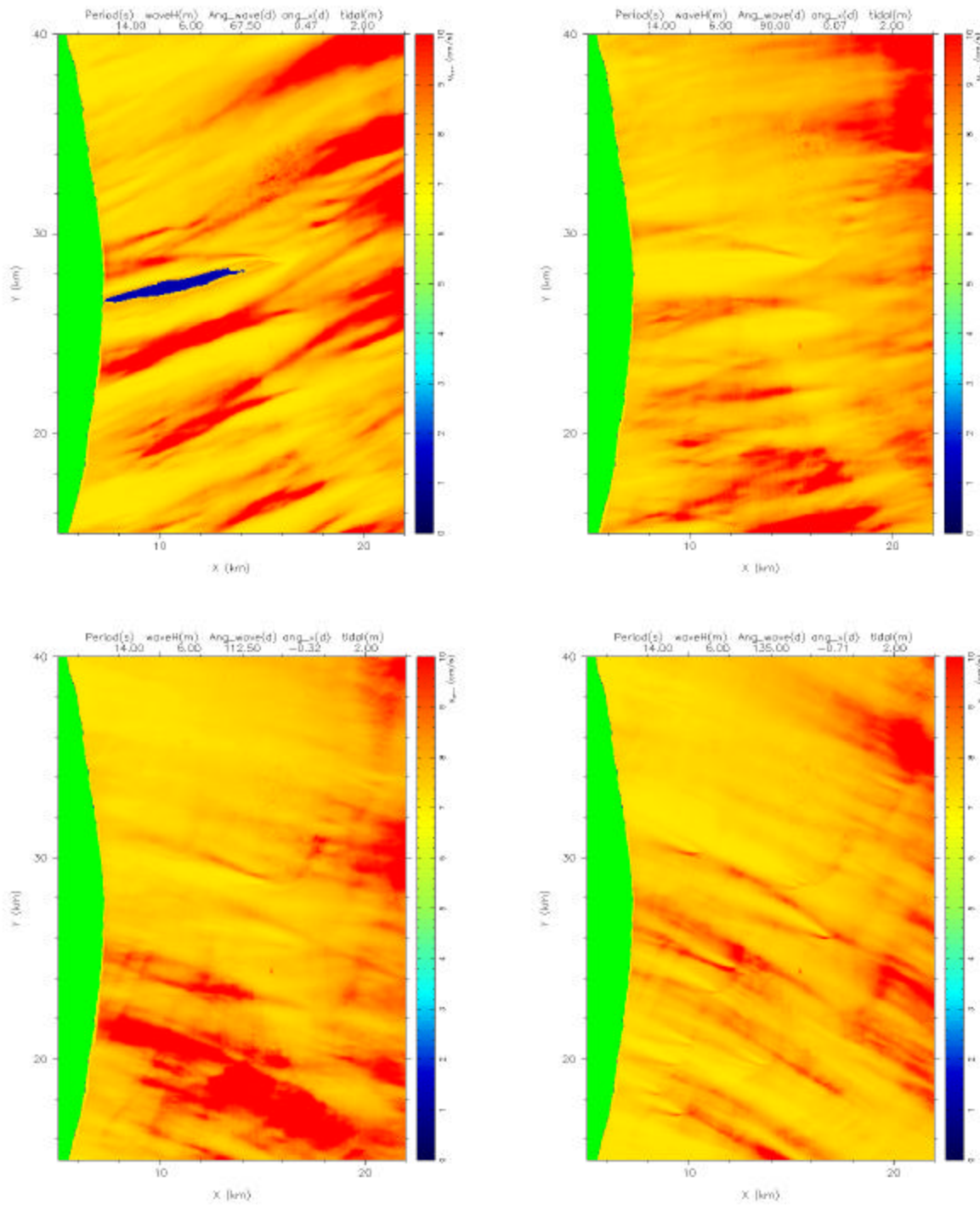


Fig 9-3. Bottom friction velocity from different directions of wave propagation for offshore waves of  $T = 14$  s and  $h_{mo} = 6$  m.

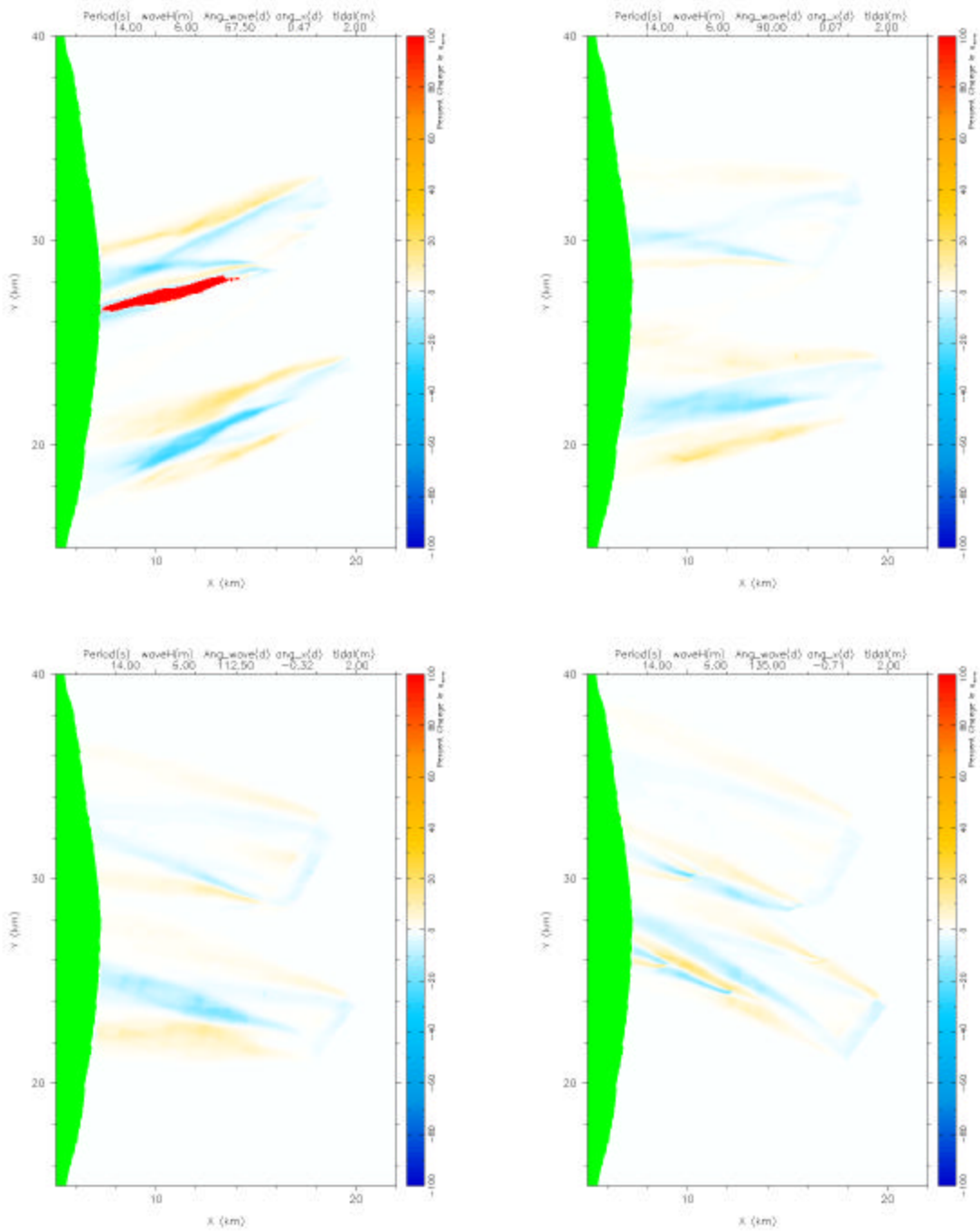
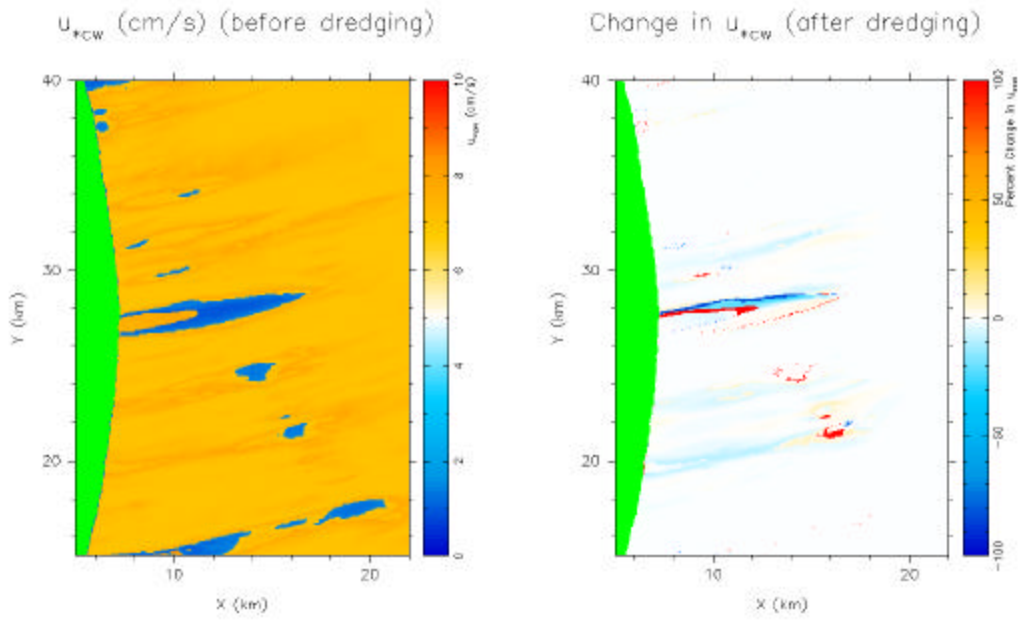
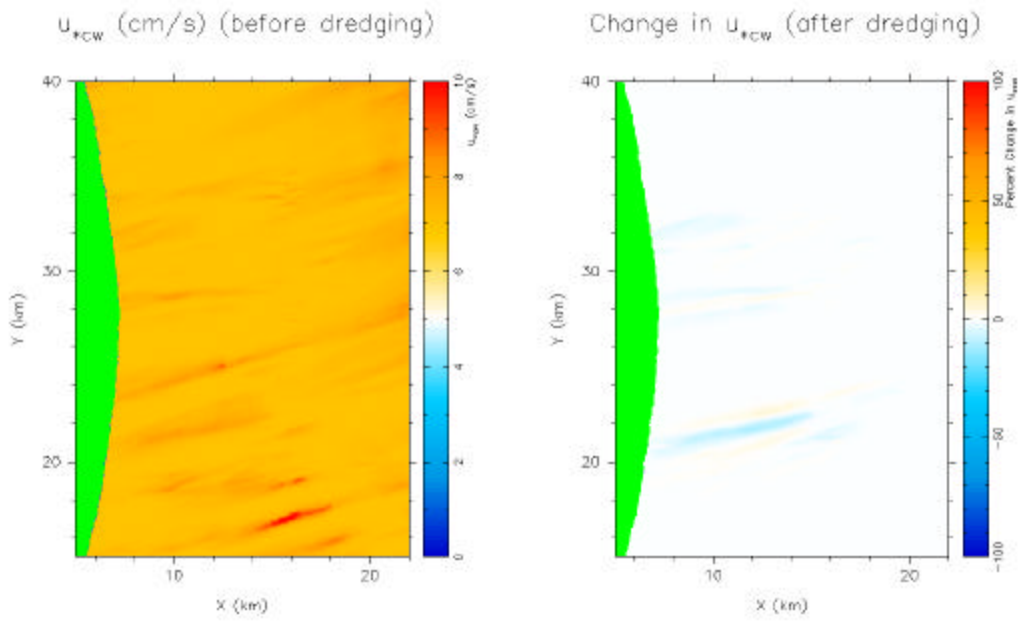


Fig 9-4. Change resulting from removal of sands from the shoals in bottom friction velocity from different directions of wave propagation for offshore waves of  $T = 14$  s and  $h_{m0} = 6$  m.



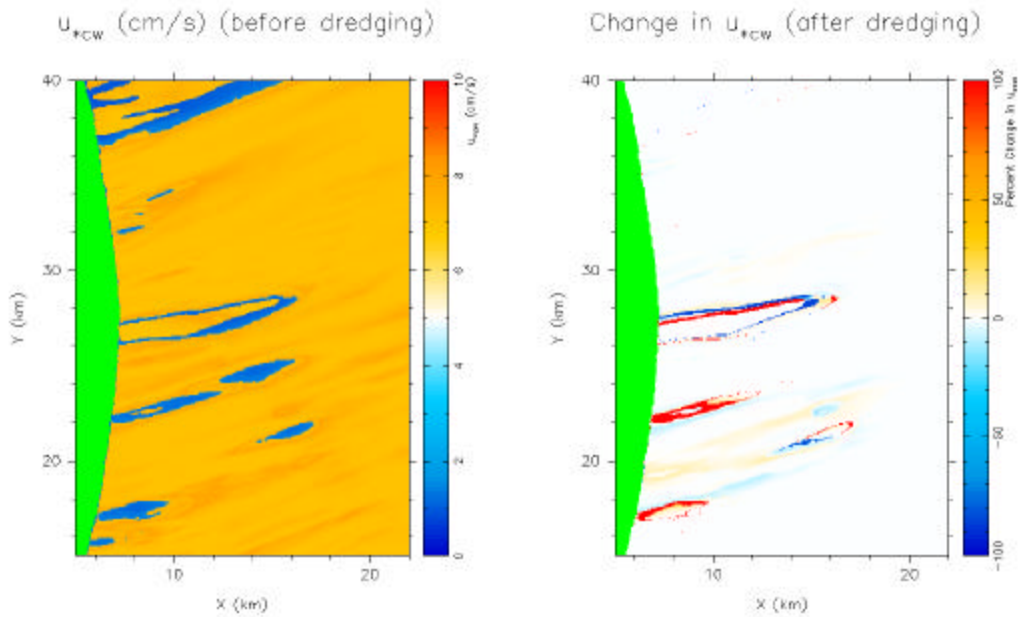
$$T = 10.0 \text{ s}, \quad H = 2.0 \text{ m}, \quad \theta = 67.5^\circ$$

Fig 9-5. (1) NE simulation result for T=10 s and Hmo=2 m



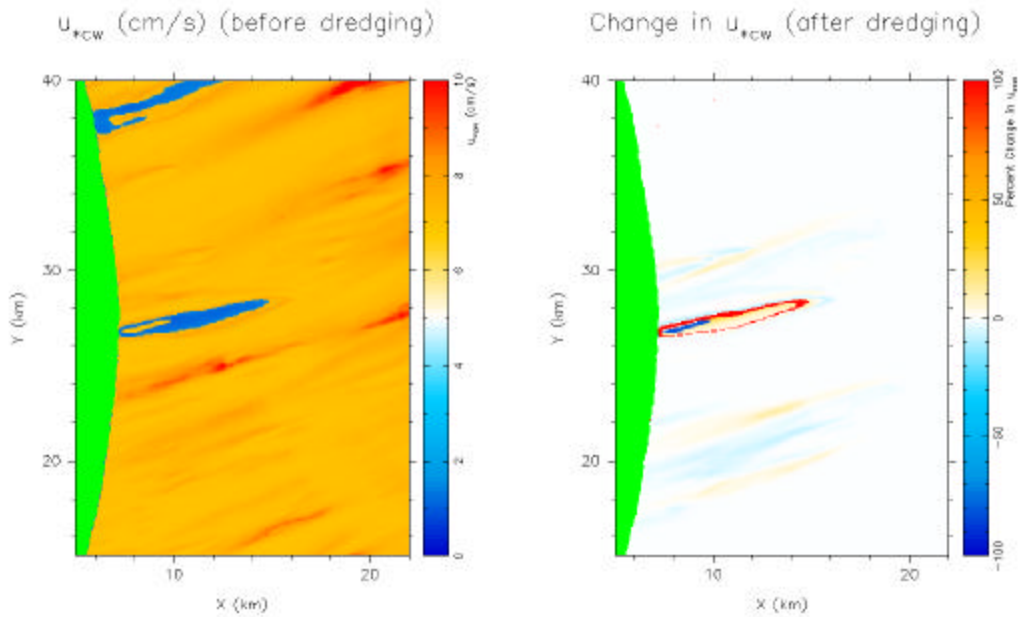
$$T = 10.0 \text{ s}, \quad H = 4.0 \text{ m}, \quad \theta = 67.5^\circ$$

Fig 9-5. (2) NE simulation result for T=10 s and Hmo=4 m



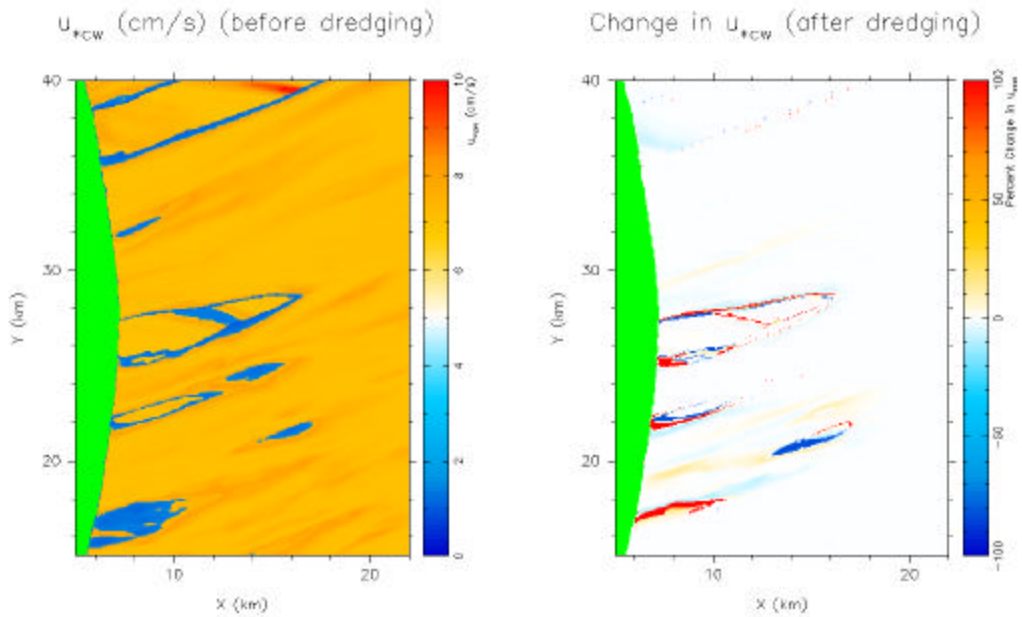
$T = 12.0 \text{ s}, H = 2.0 \text{ m}, \theta = 67.5^\circ$

Fig 9-5. (3) NE simulation result for  $T=12 \text{ s}$  and  $H_{mo}=2 \text{ m}$



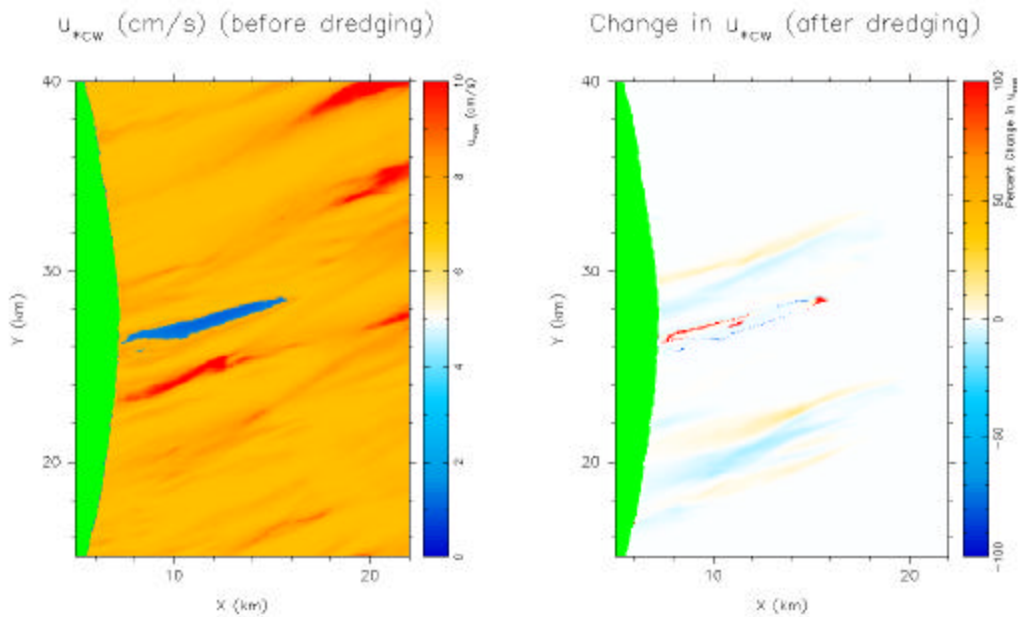
$T = 12.0 \text{ s}, H = 4.0 \text{ m}, \theta = 67.5^\circ$

Fig 9-5. (4) NE simulation result for  $T=12 \text{ s}$  and  $H_{mo}=4 \text{ m}$



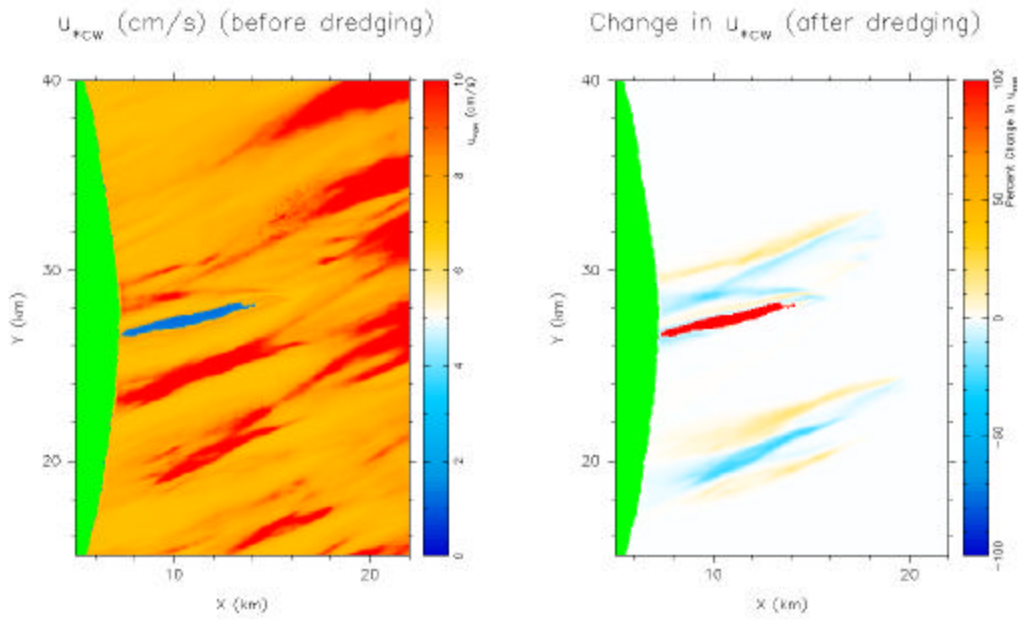
$T = 14.0 \text{ s}, H = 2.0 \text{ m}, \theta = 67.5^\circ$

Fig 9-5. (5) NE simulation result for  $T=14 \text{ s}$  and  $H_{mo}=2 \text{ m}$



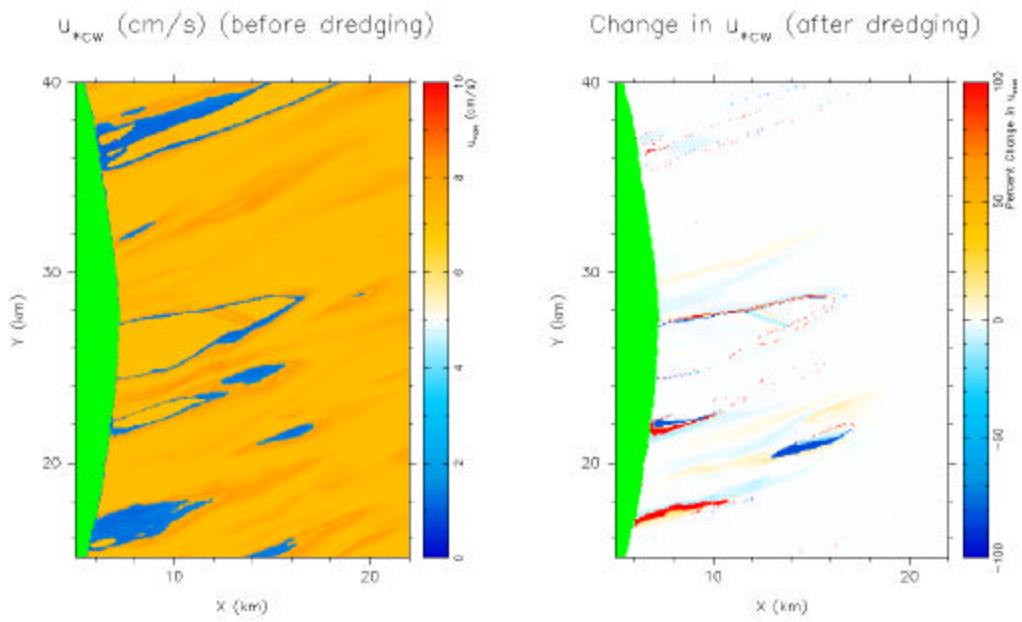
$T = 14.0 \text{ s}, H = 4.0 \text{ m}, \theta = 67.5^\circ$

Fig 9-5. (6) NE simulation result for  $T=14 \text{ s}$  and  $H_{mo}=4 \text{ m}$



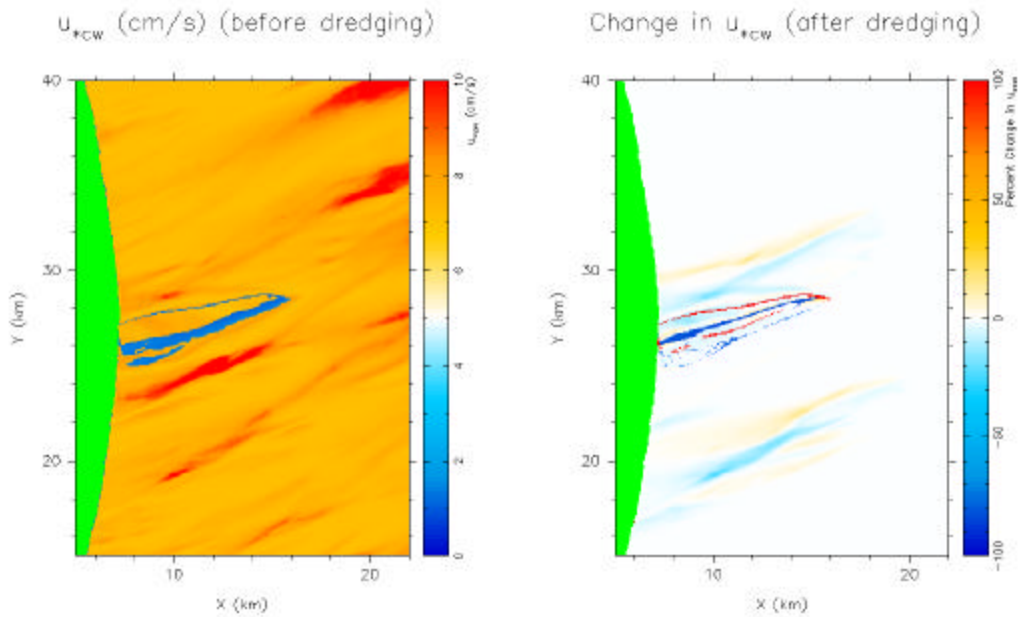
$T = 14.0 \text{ s}, H = 6.0 \text{ m}, \theta = 67.5^\circ$

Fig 9-5. (7) NE simulation result for  $T=14 \text{ s}$  and  $H_{mo}=6 \text{ m}$



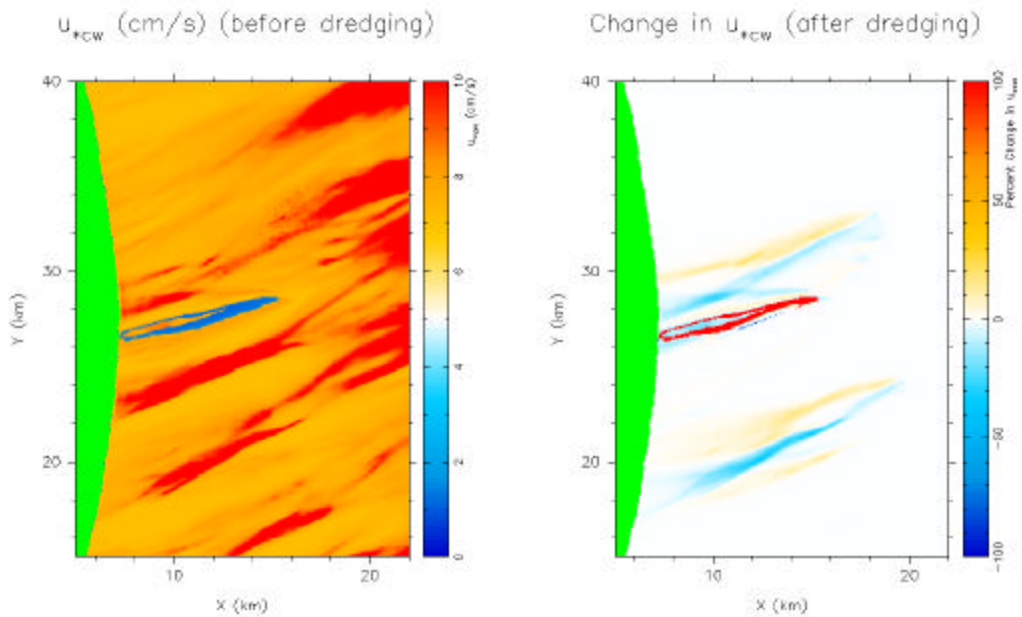
$T = 16.0 \text{ s}, H = 2.0 \text{ m}, \theta = 67.5^\circ$

Fig 9-5. (8) NE simulation result for  $T=16 \text{ s}$  and  $H_{mo}=2 \text{ m}$



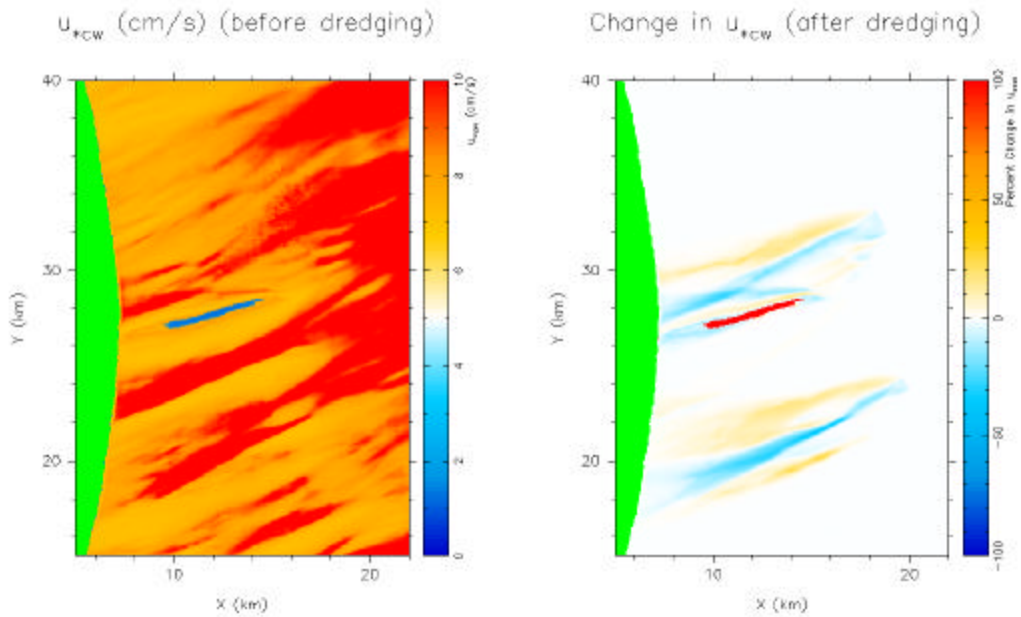
$T = 16.0 \text{ s}, H = 4.0 \text{ m}, \theta = 67.5^\circ$

Fig 9-5. (9) NE simulation result for T=16 s and Hmo=4 m



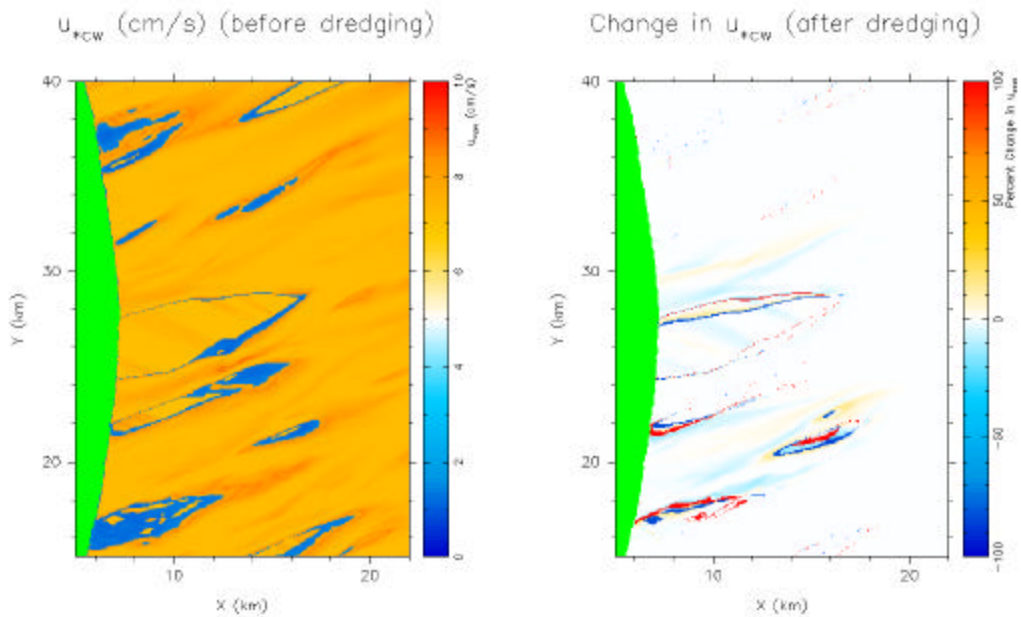
$T = 16.0 \text{ s}, H = 6.0 \text{ m}, \theta = 67.5^\circ$

Fig 9-5. (10) NE simulation result for T=16 s and Hmo=6 m



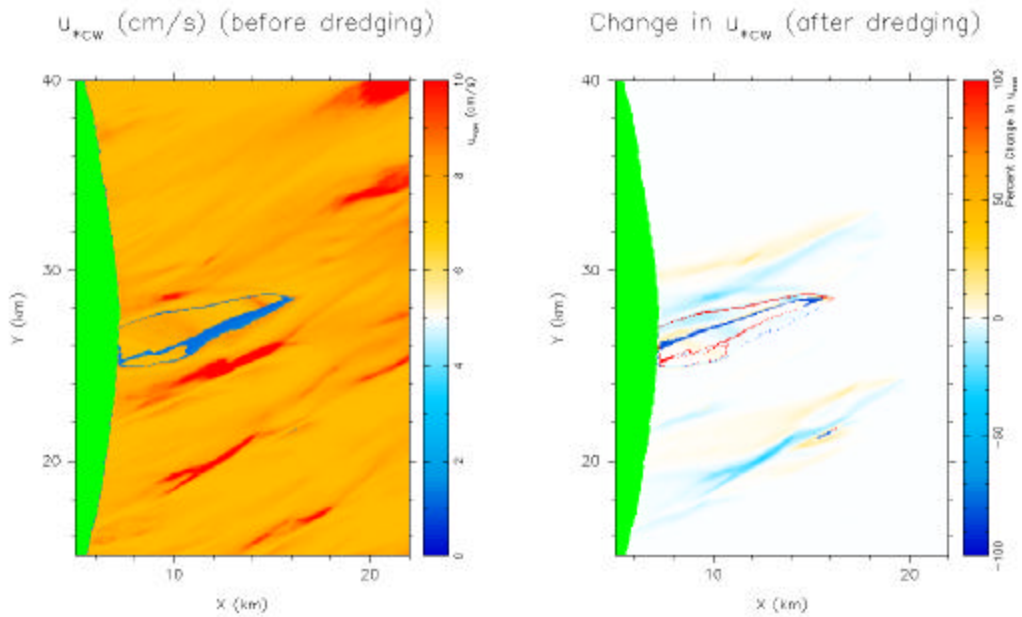
$$T = 16.0 \text{ s}, \quad H = 8.0 \text{ m}, \quad \theta = 67.5^\circ$$

Fig 9-5. (11) NE simulation result for T=16 s and Hmo=8 m



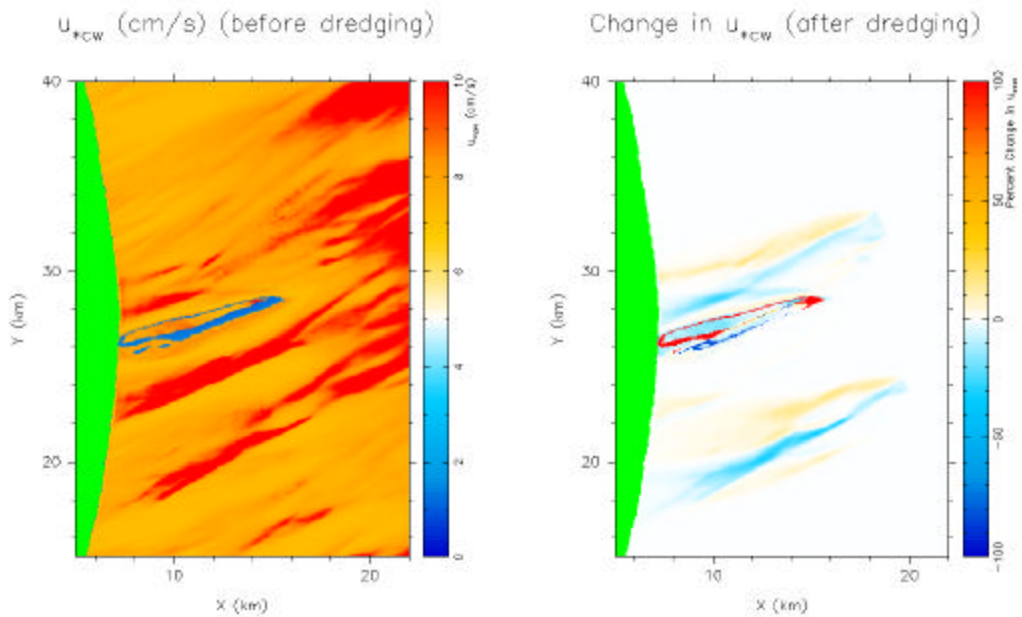
$$T = 20.0 \text{ s}, \quad H = 2.0 \text{ m}, \quad \theta = 67.5^\circ$$

Fig 9-5. (12) NE simulation result for T=20 s and Hmo=2 m



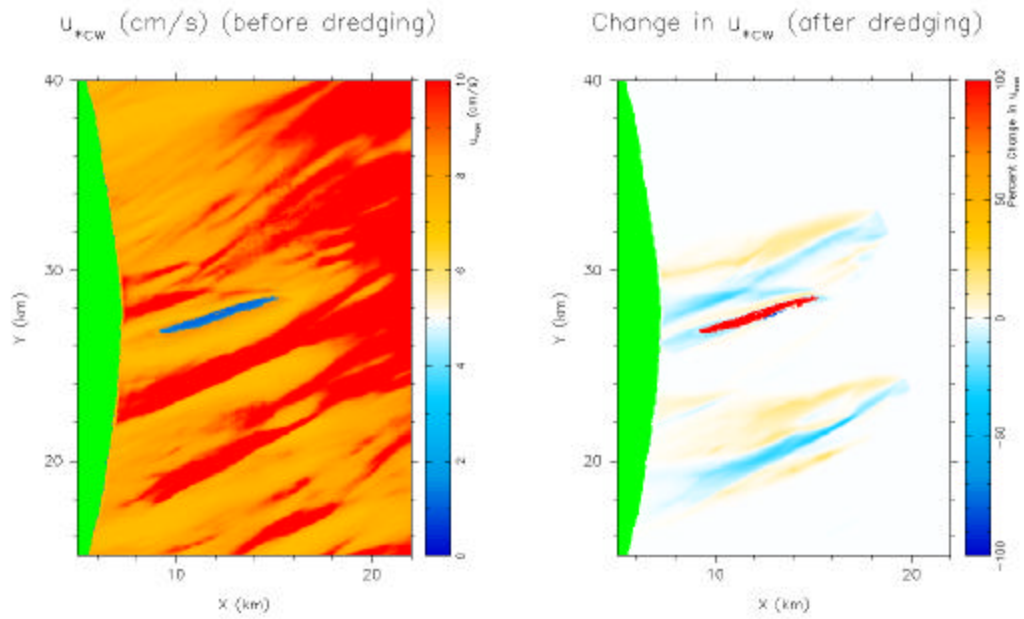
$$T = 20.0 \text{ s}, \quad H = 4.0 \text{ m}, \quad \theta = 67.5^\circ$$

Fig 9-5. (13) NE simulation result for T=20 s and Hmo=4 m



$$T = 20.0 \text{ s}, \quad H = 6.0 \text{ m}, \quad \theta = 67.5^\circ$$

Fig 9-5. (14) NE simulation result for T=20 s and Hmo=6 m



$$T = 20.0 \text{ s}, \quad H = 8.0 \text{ m}, \quad \theta = 67.5^\circ$$

Fig 9-5. (15) NE simulation result for T=20 s and Hmo=8 m

## CHAPTER 10. SUMMARY AND CONCLUSIONS

The following conclusions provide a review of the impacts to waves and other oceanographic processes that might be caused by the modeled dredging at Fenwick Shoal and Isle of Wight shoal.

1. Using high quality raw bathymetric data, a grid of 44.970 km x 67.560 km was created for studying the possible changes on wave transformation and tidal currents. This grid is large enough to directly use wave data measured at an NOAA offshore wave station, 44009, and to exclude the possible inaccuracy caused by side boundaries. The grid cell size, however, is small enough (30 m x 60 m) to show the effect of wave diffraction.
2. Fenwick Shoal and Isle of Wight Shoal are identified as the potential sources of beach quality sand. It is recommended to borrow sand from a shoal as opposed to a flat.
3. Two possible scenarios for dredging were considered. The first scenario is  $2 \times 10^6$  m<sup>3</sup> of sand from each shoal. The purpose is to determine if a single harvest of sand would result in an unacceptable impact. The second scenario is a total of  $2.4 \times 10^7$  m<sup>3</sup> of sand from the two shoals. The objective is to determine if a cumulative sand borrow is acceptable or not.
4. A total of 13 years wave measurements from NDBC station 44009, about 45 km offshore at the Ocean City, were used to analyze the possible choices of wave heights, periods, and directions that should be analyze for alteration because of the modeled dredging at the two shoals.
5. Two near shore wave stations, MD001 and MD002, provide about 4 years measurements. The measured waves at these two near shore stations are almost identical. Data from both the offshore and near shore stations provide a complete set for checking the selected wave transformation model.
6. Sixty wave conditions are selected as model wave conditions. These wave conditions include four possible wave heights (2 m, 4 m, 6 m, and 8 m), five wave periods (10 s, 12 s, 14 s, 16 s, and 20 s),

and four wave directions (ENE, E, ESE, SE). Wave energy loss caused by bottom friction is not a linear process, and thus, all four wave heights have to be included in the calculations.

7. Among the available numerical models for simulating water waves, wave hindcast/prediction models (*e.g.*, SWAN, HISWAP, NSW in Mike 21, and STWAVE) are not recommended because the objective is not to look for wave growth nor to predict what kind of waves may be developed for a given wind field. Among the wave transformation models (*e.g.*, RCPWAVE, REF/DIF-1, REF/DIF-S, RDE, and EMS module in Mike 21), REF/DIF-1 was selected because of the excellent accuracy in wave height and computing efficiency.

8. REF/DIF-1 was calibrated using one-month wave measurements (Nov. 1 to 30, 1997) from station 44009 and MD001. A total of 113 wave conditions were calculated and compared.

9. The calculated wave height distributions for the original bathymetry indicate that large waves attenuated significantly because of the great energy dissipation caused by large near-bed velocity. Large waves also may break because of the shoals.

10. Near a location on the south of Ocean City, waves coming from the East have a tendency to converge. The high wave energy (for all waves that come from the east) may be responsible for causing the shore line retreat at the south of Ocean City.

11. Near the Maryland-Delaware border, there is an area of extensive wave height attenuation because of wave shoaling and breaking, after waves pass Fenwick Shoal which is approximately 10 km from the coast. The relatively small breaking wave heights at this area may explain the relatively stable shoreline near the border.

12. This study indicates that the one-time dredging at Fenwick Shoal and Isle of Wight Shoal for a total of  $4 \times 10^6 \text{ m}^3$  of sand is acceptable in terms of potential modification to wave transformation. The major change to waves occurred not at the modeled dredging sites nor at the coast but between these

two.

13. For the cumulative dredging at Fenwick Shoal and Isle of Wight Shoal for a total of  $2.4 \times 10^7$  m<sup>3</sup> of sand, this study suggests that the major change of wave height is also between the dredging site and the shore line. The increase of local wave height can be as much as two times. The change of breaking wave height, on the other hand, is not so obvious except the clear reduction of BHM at the Maryland and Delaware border.

14. The reduction of BHM at this location, however, is not necessarily a positive impact because it increases the breaking wave height at that location. As a consequence, more erosion and shoreline recession at that location might occur. Otherwise, the possible impact is not significant.

15. The SLOSH model developed in NOAA (the standard model used by FEMA) was used to check the possible change of storm surge caused by the modeled dredging. A polar grid with 130 by 280 grid cells was constructed for this project.

16. Tropical storms with an 86 mbar central pressure drop and 15-mile maximum wind radius (comparable to a category 4 storm) were used to simulate the coastal storm surges. Two orthogonal tracks, one across- and one along-shore were simulated. The maximum change on storm surges are about 0.1 cm which is negligible compared to the maximum surge (around 3 m).

17. The maximum near-bed tidal current is weak, on the order of 5 cm/s except at the shoals, where current velocity increases to around 8 cm/s. The postulated dredging at the shoals will reduce the maximum near-bed tidal current velocity (around 10%). Immediately on the leeward side of tidal flow, the dredging increases the tidal velocity, up to 10%. Because of the weak currents in this area, the 10% change only contributes less than 1 cm/s increase/decrease of tidal current. For this reason, the possible impact on tidal currents is negligible.

18. The results from Chapters 7 and 8 provide evidence that dredging at the two selected offshore

shoals has little influence on tidal currents and storm surges. For future studies, these two processes can be excluded.

19. The Grant-Madsen-Glenn (GMG) model was used to study the possible change of bed shear stress caused by dredging. The results indicate that the change of bottom stress distribution is not substantial.

20. After dredging and beach nourishment sites have been decided, further studies on the shoreline responses would be necessary. For studying the possible shoreline change, however, deterministic wave forces are needed. An idealized time series (up to many years) should be established first to change the original stochastic nature of wave occurrence to a deterministic process. In Chapter 2, a method to idealize the wave time series has been suggested. All wave conditions (even small waves) in the idealized time series should be calculated with a properly selected wave transformation model to provide accurate breaking wave height and direction information for studying beach responses. How to incorporate the extreme wave condition (e.g., the most severe sea reported in Chapter 2) in the idealized time series for checking the possible beach responses may require more studies.

## CHAPTER 11. BIBLIOGRAPHY

- Blumberg, A.F. and Mellor, G.F., 1987. A Description of a Three-dimensional Coastal Ocean Circulation Model, *In: Three-dimensional Coastal Ocean Models, Coast and Estuarine Science, Vol. 4* (Heaps, N.S. ed.), American Geophysical Union, Washington, D.C., 1-16.
- Booij, N., Holthuijsen, L.H. and R.C. Ris, 1996. The SWAN Wave Model for Shallow Water, *Proc. 25th Int. Conf. Coastal Engng.*, Orlando, Fla., USA, 1: 668-676.
- CERC Shore Protection Manual, 1984. 4th Ed., U.S. Army Engineer Waterways Experiment Station, Coastal Engineering Research Center, Vicksburg, Miss.
- Ebersole, B. A., 1985. Refraction-Diffraction Model for Linear Water Waves, *J. of Waterway, Port, Coastal, and Ocean Engrg.*, ASCE, 111(6): 939-953.
- Glenn S. M. and W. D. Grant, 1987. A Suspended Sediment Stratification Correction for Combined Wave and Current Flows, *Journal of Geophysical Research*, 92: 8244-8264.
- Grant W. D. and O. S. Madsen, 1979. Combined Wave and Current Interaction with a Rough Bottom, *Journal of Geophysical Research*, 84: 1797-1808.
- Grant W. D. and O. S. Madsen, 1986. The Continental Shelf Bottom Boundary Layer, *Annual Review of Fluid Mechanics*, 18: 265-305.
- Holthuijsen, L.H., N. Booij, R. Padilla-Hernandez, 1997. A Non-stational, Parametric Coastal Wave Model, *Ocean Wave Measurement and Analysis*, ASCE, Ed.: B.L.Edge and J.M. Hemsley, 1: 630-638.
- Jelesnianski, C.P., J. Chen, and W.A. Shaffer, 1992. SLOSH: Sea Lake, and Overland Surges from Hurricanes, NOAA Technical Report NWS 48, Department of Commerce, USA, 71.
- Kaihatu, J.M., W.E. Rogers, Y.L. Hsu, and C.O'Reilly. 1998. Use of phase-resolving numerical wave models in coastal areas, *Proceedings, 5<sup>th</sup> International Workshop on Wave Hindcasting and Forecasting*, January 26-30, Melbourne, Fla.
- Kim, S.-C., J. Chen and W.A. Shaffer, 1996. An Operational Forecast Model for Extratropical Storm Surges along the US East Coast, *Proceedings, Conference on Oceanic and Atmospheric Prediction*, American Meteorological Society, 281-286.
- Kirby, J.T., and Dalrymple, R.A., 1991. User's Manual, Combined Refraction/Diffraction Model, REF/DIR 1, Version 2.3, Center for applied Coastal Research, Dept. of Civil Engineering, Univ. of Delaware, Newark, DE 19716.
- Kirby, J. T and R.A. Dalrymple. 1994. Combined refraction/ diffraction model REF/DIF-1, version 2.5, documentation and user's manual. CACR report 94-22, Center for Applied Coastal Research, University of Delaware, Newark, Delaware, 171 p.
- Kirby, J. T. and H. T. Ozkan, 1994. User Manual of REF-DIF S, Version 1.1, CACR-94-04, Center for applied Coastal Research, Dept. of Civil Engineering, Univ. of Delaware, Newark, DE 19716.
- Longuet-Higgins, M.S., Cartwright, D.E., and Smith, N.D., 1963. Observations of the Directional Spectrum of Sea Waves Using the Motions of a Floating Buoy, in *Ocean Wave Spectra*, Prentice-Hall, 111-136.
- Maa, J. P.-Y., C. H. Hobbs, III, and C. S. Hardaway Jr., in press. A Criterion for Determining the Impact on Shorelines Caused by Altering Wave Transformation, *J. Coastal Research*.

- Maa, J.P.-Y., T.-W. Hsu, C.-H. Tsai and W.J. Juang, in press. Comparison of wave refraction and diffraction models, *Journal of Coastal Research*.
- Maa, J. P.-Y. and C.H. Hobbs, III, 1998. Physical Impact of Waves on Adjacent Coasts Resulting from Dredging at Sandbridge Shoal, Virginia, *J. Coastal Research*, 14(2):525-536.
- Maa, J. P.-Y., and H.-H. Hwung, 1997. A Wave Transformation Model for Harbor Planning, in B.L.Edge and J.M. Hemsley (eds.), *Ocean Wave Measurement and Analysis*, ASCE, 1:256-270.
- Maa, J. P.-Y. and D. W.-C. Wang, 1995. Wave Transformation near Virginia Coast: The 1991 Halloween Northeaster, *J. Coastal Research*, 11(4), 1258-1271.
- Maa, J. P.-Y. and C.-S. Kim, 1992. The Effect of Bottom Friction on Breaking Waves using RCPWAVE Model, *J. Waterway, Port, Coastal and Ocean Engrg.*, 118(4), 387-400.
- Massel, S. R., 1995. Ocean Surface Waves: Their Physics and Prediction, World Scientific Publ., Singapore.
- Meindl. E.A., and Hamilton, G.D., 1992. Programs of the National Data Buoy Center. *Bulletin of the American Meteorological Society*, 73(7), 985 - 993.
- Mellor, G.L. and Yamada, T., 1982. Development of a Turbulence Closure Model for Geophysical Fluid Problems, *Rev. Geophys. Space Phys.*, 20(4): 851-875.
- Murty, T.S., 1984, Storm surges-meteorological ocean tides, *Canadian Bulletin of Fisheries and Aquatic Sciences*, 212: 897.
- Radder, A.C., 1979. On the Parabolic Equation Method for Water Wave Propagation, *J. Fluid Mechanics*, 95: 159-176.
- Resio, D.T., 1987. Shallow water waves. I: Theory, *J. of Waterway, Port, Coastal, and Ocean Engineering*, 113: 264-281.
- Resio, D.T., 1988. Shallow water waves. II: Data comparison, *J. of Waterway, Port, Coastal, and Ocean Engineering*, 114: 50-65.
- Resio, D.T. and Perrie, W., 1989. Implication of  $f^4$  Equilibrium Range for Wind-generated Waves, *J. of Physical Oceanography*, 19: 193-204.
- Smith, E.R., 1988. Case Histories of Corps Breakwater and Jetty Structures, Technical Report REMR-CO-3. Coastal Engineering Research Center, Dept. of the Army, Waterways Experiment Station, Corps of Engineers, Vicksburg, Mississippi, 133 pp.
- Watts, G.M., 1953. A Study of Sand Movement at South Lake Worth Inlet, Florida, Tech. Memo. No. 42, Beach Erosion Board.

## The Department of the Interior



As the Nation's principal conservation agency, the Department of the Interior has responsibility for most of our nationally owned public lands and natural resources. This includes fostering sound use of our land and water resources, protecting our fish, wildlife, and biological diversity, preserving the environmental and cultural values of our national parks and historic places; and providing for the enjoyment of life through outdoor recreation. The Department assesses our energy and mineral resources and works to ensure that their development is in the best interests of all our people by encouraging stewardship and citizen participation in their care. The Department also has a major responsibility for American Indian reservation communities and for people who live in island territories under U.S. Administration.

## The Minerals Management Service Mission



As a bureau of the Department of the Interior, the Minerals Management Service's (MMS) primary responsibilities are to manage the mineral resources located on the Nation's Outer Continental Shelf (OCS), collect revenue from the Federal OCS and onshore federal and Indian lands, and distribute those revenues.

Moreover, in working to meet its responsibilities, the Offshore Minerals Management Program administers the OCS competitive leasing program and oversees the safe and environmentally sound exploration and production of our Nation's offshore natural gas, oil and other mineral resources. The MMS Royalty Management Program meets its responsibilities by entrusting the efficient, timely and accurate collection and distribution of revenue from mineral leasing and production due to Indian tribes and allottees, States and the U. S. Treasury

The MMS strives to fulfill its responsibilities through the general guiding principles of: (1) being responsive to the public's concerns and interests by maintaining a dialog with all potentially affected parties and (2) carrying out its programs with an emphasis on working to enhance the quality of life for all Americans by lending MMS assistance and expertise to economic development and environmental protection.

## Environmental Survey of Potential Sand Resource Sites Offshore Delaware and Maryland

### Part 5: Maryland/Delaware Shoreline: Long-Term Trends and Short-Term Variability

This Adobe Acrobat file includes bookmarks and hot links. It has been set up to print two-sided. This means that blank sheets may be inserted into the report to keep the page numbers correct. Also, Figures 14 and 15 were created on tabloid size (11"x17" ) paper.

---

# Environmental Survey of Potential Sand Resource Sites Offshore Delaware and Maryland

## Part 5: Maryland/Delaware Shoreline: Long-Term Trends and Short-Term Variability

---

### Final Report

July 2000

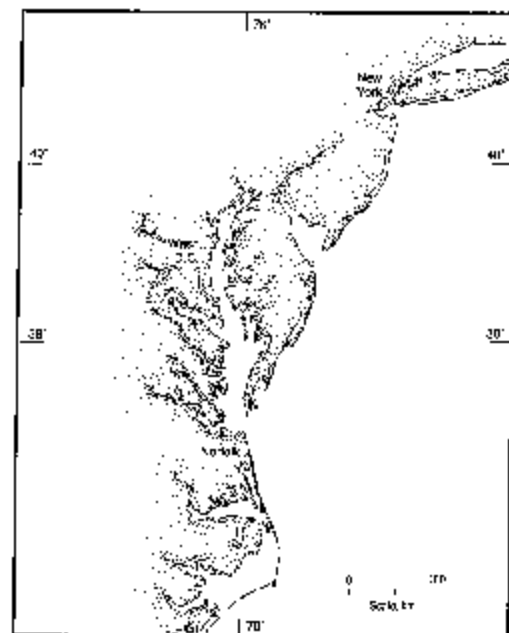
#### Authors:

C. S. Hardaway, Jr., D. A. Milligan, R.C.H. Brindley,  
and C. H. Hobbs, III  
Virginia Institute of Marine Science

#### Project Manager:

Carl H. Hobbs, III  
Virginia Institute of Marine Science

Prepared under MMS contract 1435-01-97-CT-30853 to the  
Virginia Institute of Marine Science  
College of William & Mary



**MMS** U.S. Department of the Interior  
Minerals Management Service

International Affairs and Marine Minerals Division

College of William and Mary  
**VIIMS**  
Virginia Institute of Marine Science  
School of Marine Science

#### DISCLAIMER

This report has been reviewed by the Minerals Management Service and approved for publication. Approval does not signify that the contents necessarily reflect the views and policies of the Service, nor does mention of trade names or commercial products constitute endorsement or recommendation for use.

Final Report

Environmental Survey of Potential Sand Resource Sites

Offshore Delaware and Maryland

Part 5

Maryland/Delaware Shoreline: Long-Term Trends and Short-Term Variability

C. S. Hardaway, Jr., D. A. Milligan, R.C.H. Brindley, and C. H. Hobbs, III

Virginia Institute of Marine Science

Carl H. Hobbs, III, Project Manager

Virginia Institute of Marine Science

for

U. S. Department of the Interior  
Mineral Management Service  
Contract 1435-01-97-CT-30853

July 2000



## TABLE OF CONTENTS

TABLE OF CONTENTS .....	<a href="#">iii</a>
LIST OF FIGURES .....	<a href="#">iv</a>
LIST OF TABLES .....	<a href="#">v</a>
1. INTRODUCTION .....	<a href="#">1</a>
1.1. Study Scope and Purpose .....	<a href="#">1</a>
1.2. Environmental Impacts of Sand Mining and Emplacement .....	<a href="#">3</a>
2. COASTAL SETTING .....	<a href="#">7</a>
2.1. Geomorphic Setting .....	<a href="#">7</a>
2.1.1. Geologic History and Sea-Level Change .....	<a href="#">8</a>
2.1.2. Coastal Barrier Migration .....	<a href="#">9</a>
2.1.3. Linear Shoals .....	<a href="#">14</a>
2.1.4. Tidal Inlets .....	<a href="#">16</a>
2.2. Hydrodynamic Processes .....	<a href="#">18</a>
2.2.1. Wave Climate .....	<a href="#">20</a>
2.2.2. Tide Levels .....	<a href="#">21</a>
2.2.3. Storms .....	<a href="#">21</a>
2.2.4. Sediment Characteristics and Transport .....	<a href="#">24</a>
2.3. Cultural History and Shore Management Strategies .....	<a href="#">26</a>
2.3.1. Rehoboth Beach .....	<a href="#">26</a>
2.3.2. Dewey Beach .....	<a href="#">27</a>
2.3.3. Bethany and South Bethany Beaches .....	<a href="#">28</a>
2.3.4. Fenwick Island .....	<a href="#">31</a>
2.3.5. Ocean City .....	<a href="#">31</a>
2.4. Offshore Sand Resources .....	<a href="#">32</a>
3. METHODS .....	<a href="#">33</a>
3.1. Background: Shore Change Analysis .....	<a href="#">33</a>
3.2. Data Analysis .....	<a href="#">36</a>
3.2.1. Rates of Change .....	<a href="#">36</a>
3.2.2. Regression Analysis .....	<a href="#">36</a>
4. RESULTS AND DISCUSSION .....	<a href="#">39</a>
4.1. Delaware .....	<a href="#">39</a>
4.1.1. Historic Shore Change .....	<a href="#">39</a>
4.1.2. Recent Shore Change .....	<a href="#">45</a>
4.1.3. Shoreface Retreat .....	<a href="#">49</a>
4.2. Maryland .....	<a href="#">54</a>
4.2.1. Historic Shoreline Change .....	<a href="#">54</a>
4.2.2. Recent Shore Change .....	<a href="#">54</a>
4.2.3. Shoreface Retreat .....	<a href="#">65</a>
4.3. Wave Analysis .....	<a href="#">67</a>
5. CONCLUSION .....	<a href="#">69</a>
6. REFERENCES .....	<a href="#">71</a>
<a href="#">Appendix 1. Dewey Beach regression analysis results</a>	

## LIST OF FIGURES

Figure 1.	Delaware and Maryland study site location. . . . .	<a href="#">2</a>
Figure 2.	Coastal geomorphic compartment of the East Coast (after Kraft, 1985). . . . .	<a href="#">7</a>
Figure 3.	Paleochannels and the position of the Delaware coast approximately 7,000 years ago (Kraft, 1971). . . . .	<a href="#">8</a>
Figure 4.	Present day coastal geomorphology of the Delaware coast from the Rehoboth headland south (Belknap and Kraft, 1985). . . . .	<a href="#">10</a>
Figure 5.	Present day coastal geomorphology of the Delaware coast from the Bethany headland north (Belknap and Kraft, 1985). . . . .	<a href="#">11</a>
Figure 6.	Evolution of transgressive coastal systems during net shoreface erosion and sea-level rise at Rehoboth Bay and Rehoboth Beach. . . . .	<a href="#">13</a>
Figure 7.	Location of linear ridges on the Mid-Atlantic shelf. . . . .	<a href="#">15</a>
Figure 8.	The genesis of linear ridges based on a model developed by McBride and Moslow (1991). . . . .	<a href="#">16</a>
Figure 9.	Location of historical tidal inlets along the Delaware and Maryland coasts (McBride 1999). . . . .	<a href="#">17</a>
Figure 10.	Aerial photos of A.) Indian River Inlet and B.) Ocean City Inlet. . . . .	<a href="#">19</a>
Figure 11.	Aerial photos of A.) Bethany Beach and B.) South Bethany Beach. . . . .	<a href="#">30</a>
Figure 12.	Location of Delaware and Maryland ocean coast beach profiles as well as Delaware coastal segments from U.S. Army Corps of Engineers (1996) analysis. . . . .	<a href="#">35</a>
Figure 13.	Historic shorelines at A.) Cape Henlopen and B.) Indian River Inlet. . . . .	<a href="#">41</a>
Figure 14.	Historic shore positions and historic and recent rates of change along the Delaware and Maryland shoreline. . . . .	<a href="#">43</a>
Figure 15.	Erosion of the shoreface represented by beach profiles taken in 1964, 1982, and 1999. . . . .	<a href="#">51</a>
Figure 16.	Alongshore variability in seaward distance of active profile envelope relative to the two shoreface-attached shoals (Stauble <i>et al.</i> , 1993). . . . .	<a href="#">58</a>
Figure 17.	Three-dimensional plot of pre- and post- state fill beach profiles . . . . .	<a href="#">59</a>
Figure 18.	Three-dimensional plot of state fill pre- and post- storm beach profiles (Stauble <i>et al.</i> , 1993). . . . .	<a href="#">60</a>
Figure 19.	Three-dimensional plot of pre- and post- federal fill beach profiles (Stauble <i>et al.</i> , 1993). . . . .	<a href="#">61</a>
Figure 20.	Three-dimensional plot of federal fill pre- and post- storm beach profiles (Stauble <i>et al.</i> , 1993). . . . .	<a href="#">62</a>
Figure 21.	Percent of fill remaining above NGVD, below NGVD, and over the total profile length after the 28 month state and federal fill monitoring as measured from September 1988 to January 1992 (Stauble <i>et al.</i> , 1993). . . . .	<a href="#">63</a>
Figure 22.	Normalized wave height distribution offshore of Delaware and Maryland in the vicinity of the proposed dredging sites (Maa and Kim, 2000). . . . .	<a href="#">68</a>

## LIST OF TABLES

Table 1.	Ocean tide ranges in centimeters for the study area (NOAA, 1989). . . . .	<a href="#">21</a>
Table 2.	Vertical Datums for Breakwater Harbor, Lewes, and Indian River Inlet, Delaware and Ocean City, Maryland. . . . .	<a href="#">22</a>
Table 3.	High tides of record for Breakwater Harbor, Lewes, Delaware. Elevations referenced to MLLW (modified from Ramsey <i>et al.</i> , 1998). . . . .	<a href="#">23</a>
Table 4.	The adopted stage frequency data at Rehoboth and Dewey Beaches (modified from House Document No. 105-144, 1997). . . . .	<a href="#">24</a>
Table 5.	Information on beach nourishment projects that have taken place along the Delaware Coast (Valverde <i>et al.</i> , 1999). . . . .	<a href="#">29</a>
Table 6.	Information on beach nourishment projects that have taken place along the Maryland Coast (Valverde <i>et al.</i> , 1999). . . . .	<a href="#">32</a>
Table 7.	Rates of change along the northernmost section of Delaware between 1845 and 1943 . . . . .	<a href="#">39</a>
Table 8.	Delaware historic regression analysis results by profile. . . . .	<a href="#">47</a>
Table 9.	Recent regression of Delaware’s ocean coast profile data. . . . .	<a href="#">48</a>
Table 10.	Comparison of rates of change obtained by various methods. . . . .	<a href="#">49</a>
Table 11.	Regression analysis of profile data taken at Dewey Beach. . . . .	<a href="#">50</a>
Table 12.	Shoreface rate of change by offshore contour. . . . .	<a href="#">53</a>
Table 13.	Maryland historic regression analysis results. . . . .	<a href="#">55</a>
Table 14.	Ocean City Beach condition on October 1995. . . . .	<a href="#">57</a>
Table 15.	Ocean City Beach Condition Assessment Table for May 1996. . . . .	<a href="#">64</a>
Table 16.	Ocean City Beach Condition Assessment in June 1997. . . . .	<a href="#">65</a>
Table 17.	Ocean City Beach Condition Assessment Table for October 1997. . . . .	<a href="#">66</a>
Table 18.	Maryland recent regression analysis results. . . . .	<a href="#">66</a>



# 1. INTRODUCTION

## 1.1. Study Scope and Purpose

The Maryland-Delaware ocean coast is a continuous shoreline with varying geomorphology, shoreline erosion rate, and degree of human development. The Delaware coast stretches from Cape Henlopen in the north to the border with Maryland at Fenwick Island (Figure 1). The shoreline has an approximate north-south orientation and consists of six distinct locales, Henlopen Acres, Rehoboth Beach, Dewey Beach, Bethany Beach, South Bethany, and Fenwick Island, that together have 39 km of sandy shoreline. Several unincorporated private developments exist in the study area as do three state parks. Cape Henlopen State Park is located at the northern end of the study area extending from Cape Henlopen to the private community of North Shores. Delaware State Park occupies the central portion of the state's coast both north and south of Indian River Inlet. Fenwick Island State Park is located in the southern section of Delaware between South Bethany and Fenwick Island. Most of the residential communities are characterized by a barrier beach system, except for Rehoboth Beach and Bethany Beach, which are formed against headlands. The coast of Delaware is broken midway by Indian River Inlet.

The Maryland coast stretches from the Maryland-Delaware border on Fenwick Island to about three-fourths the way down Assateague Island (Figure 1). The Ocean City portion of Fenwick Island, which extends from the Maryland-Delaware state line to Ocean City Inlet, is 14 km long. The shoreline from Ocean City Inlet to Fishing Point, Virginia (Assateague Island) is about 60 km long. Only the Ocean City portion of the Maryland shore will be discussed in this report.

The Maryland-Delaware Atlantic coast lies in the Atlantic Coastal Plain province which is comprised fundamentally of unconsolidated sediments with emerged (coastal plain) and submerged (continental shelf) sections divided by the Atlantic shoreline. This coast is characterized by the Atlantic barrier system which consists of coastal marshes, beach-dune complexes, and tidal lagoons; all of which are constantly changing. Historically an erosive shoreline, the Maryland/Delaware coast erodes across the entire shoreface in response to sea-level rise and storm events. Shoreline erosion and shoreface retreat provide sediments to the littoral system.

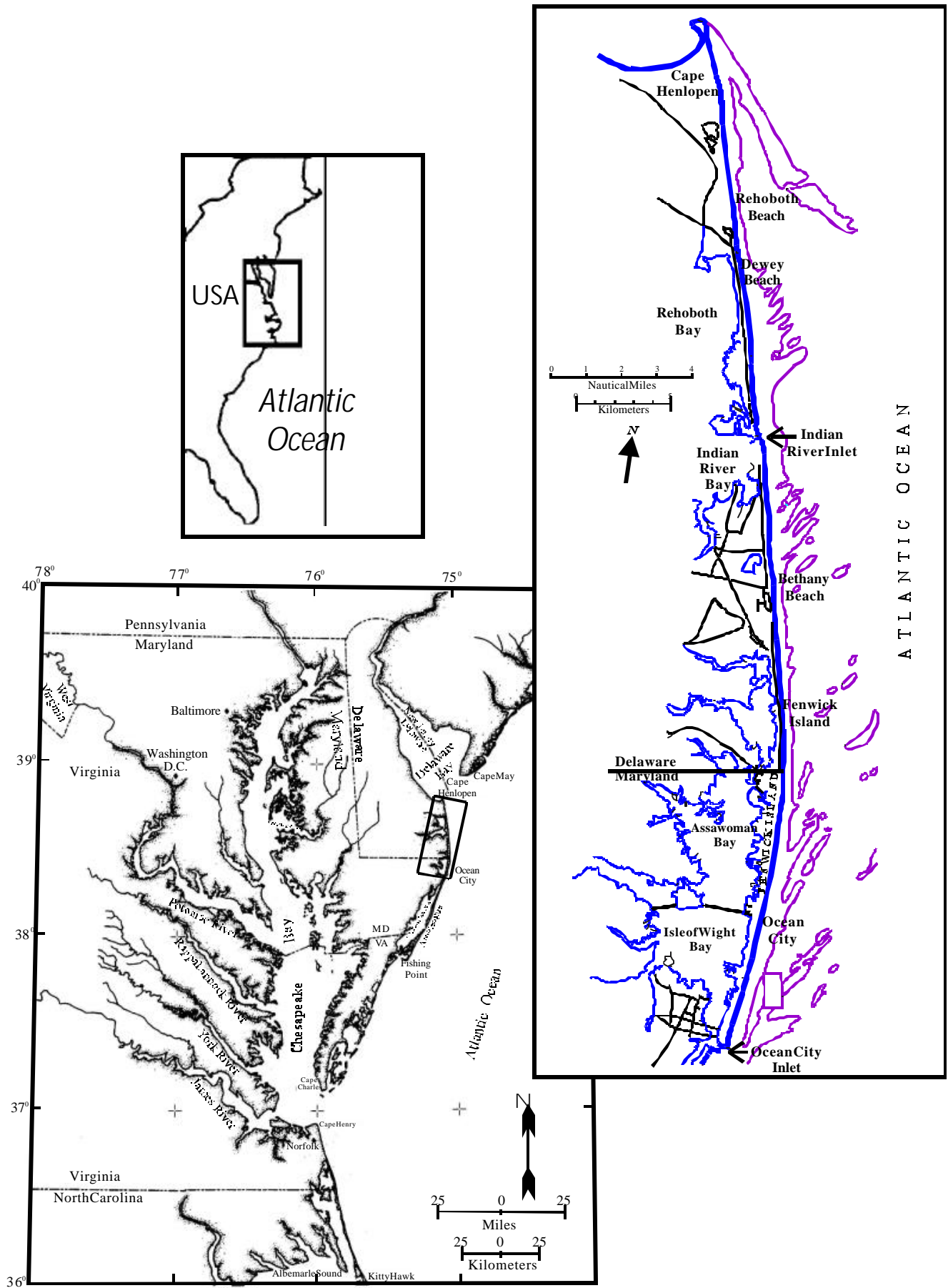


Figure 1. Delaware and Maryland study site location.

Beaches are constantly in transition. Their shape is related to both short-term and long-term factors including relative sea level, beach migration, and wave climates. Relative sea level is a long-term factor associated with beach transition since geological processes such as emergence or subsidence of the land and level of the sea effect changes. Relative sea level change causes the coast to re-adjust to the new sea level which causes beach migration by either accretion or erosion of the shoreline and shoreface (Bosma and Dalrymple, 1997).

The Maryland-Delaware coast is one of the most intensely studied coasts in the world. Professor John Kraft of the University of Delaware and his students have performed the bulk of the geological research within the Delaware coastal system. The Maryland Geological Survey and the U.S. Army Corps of Engineers have performed several studies of the Ocean City area.

Over the past 20 years, several beach nourishment projects have injected a significant volume of sand into the region's littoral system. These beach nourishment projects have used sand from both submarine sand bodies and upland borrow areas. Sand mining beyond the 3-mile limit in Federal waters is under the jurisdictional authority of the U. S. Department of the Interior Minerals Management Service (MMS).

The purpose of this study is to evaluate the impacts of beach nourishment on shoreline change along the Maryland-Delaware coast. Modifying the offshore topography through mining and the shore through nourishment potentially can cause significant change to the littoral transport system and can alter the patterns of shoreline change along the entire coast.

## **1.2. Environmental Impacts of Sand Mining and Emplacement**

Both Maryland and Delaware have beach nourishment needs. Delaware has coastal resort communities at Rehoboth, their largest resort, Dewey Beach, just south of Rehoboth, and Bethany Beach. Maryland has one the largest resorts on the east coast at Ocean City. Most of the Delaware Atlantic coastline is in a state of erosion (Bosma and Dalrymple, 1997). The state's Department of Natural Resources and Environmental Control (DNREC) has been responsible for preservation and

enhancement of the beaches since 1972. DNREC has used several methods including sand bypassing, beach nourishments, groins, and dune stabilization to stabilize the shoreline. Delaware projects a sand need for 18 million m<sup>3</sup> of sand over the next 50 years. Ocean City, Maryland will require 9.2 million m<sup>3</sup> within the next 50 years (Maryland Geological Survey Website, 2000). The only cost effective means of supplying sand for these projects is the use of offshore sources of beach quality sand. Sand resources dot the offshore region of Maryland and Delaware, but known borrow sites within the 5 km (3 nautical miles) limit may not be sufficient to meet demands.

Existing geologic conditions place constraints on offshore sand mining since geomorphic features and geologic features with obtainable and suitable sand reserves determine the mining site. However, dredging may impact present geologic, physical, and biological processes and conditions. Indeed, the act of mining offshore sand reserves has potential environmental impacts to the mining area as well as the adjacent coast.

The sedimentary condition at the offshore borrow site also is impacted by offshore dredging. Dredging increases water depth by changing the bathymetry at the borrow site by removing topographic features (*i.e.* a shoal) or creating a depression or pit. If large alterations in the bathymetry occur, they can impact local wave and current patterns which, in turn, can alter depositional and erosional trends. These changes may affect both local biological resources and water chemistry.

After completion of a beach nourishment project, the longshore transport system may be affected by an increase in sediment transport away from the nourished beach. At fill sites without sand retention structures, there may be a temporary positive impact on beaches downdrift of the nourished beach as the newly placed material spreads. Changes in nearshore bathymetry may occur as finer material winnows from the newly-placed sand and deposits offshore. Several months of tidal and wave action may be needed to redistribute this material so that the substrate elevations and slopes can return to pre-placement conditions (Louis Berger Group, 1999). Other possible impacts onshore from dredging include nourishment impact from sands that are too fine or too coarse and altered offshore current patterns from the dredging site which can affect onshore sediment transport and wave energy.

Burial due to sand placement and subsequent transport can have long-term biological and cultural impacts. Even though grain size distribution is of concern when choosing a beach fill material, shell content, sediment type, and color may be as important for recreational beaches since aesthetic appearances of the beach are important in affecting the user's perception of the beach.



## 2. COASTAL SETTING

### 2.1. Geomorphic Setting

The Maryland-Delaware coast comprises the northern half of the major geomorphic coastal compartment that extends from Cape Henlopen, Delaware on the northern boundary, southward to Cape Charles, Virginia (Figure 2). Maryland and Delaware occupy the northern three-fourths of the subreach from Cape Henlopen to Fishing Point, Virginia. The compartment is subdivided into four geomorphic regions: a spit complex on the north, a series of eroding headlands and baymouth barriers, linear barriers, and, finally, a long reach of island barriers.

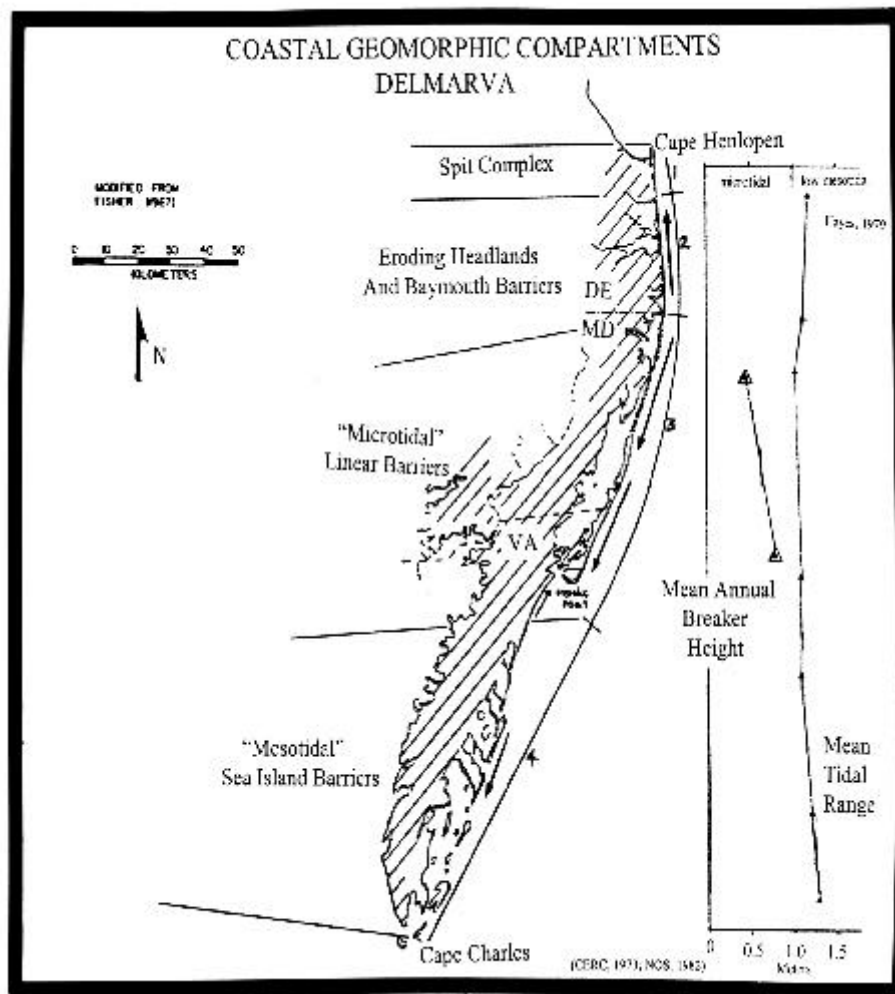


Figure 2. Coastal geomorphic compartment of the East Coast (after Kraft, 1985).

### 2.1.1. Geologic History and Sea-Level Change

About 14,000 years ago, the ocean coast of Maryland-Delaware was about 100 km to the east, and sea level was about 90 m lower. The lower coastal plain was dissected with a complex dendritic drainage pattern that, in large part, was controlled by previous low sea levels as channels were incised into older Pliocene strata to set the drainage “template” for subsequent transgressive/regressive sedimentary sequences. Figure 3 schematically portrays the Delaware coast 7,000 years B.P.

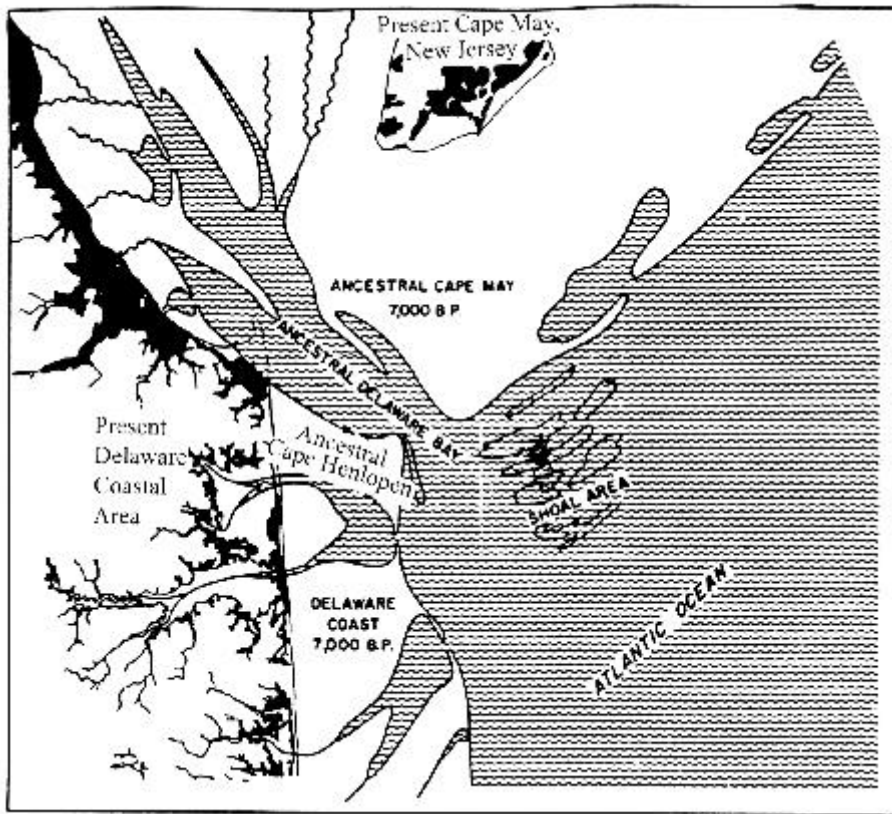


Figure 3. Paleochannels and the position of the Delaware coast approximately 7,000 years ago (Kraft, 1971).

Since that time, sea level has been rising across the low gradient coastal plain (Kraft and John, 1976). Eroded sands are transported alongshore and cross-shore (on-offshore) by the impinging waves and currents. However, the background driving force behind shore change is the slow, continuous rise in sea level. As a result, the shoreline and shoreface region has

transgressed across the upland system eroding interflaves and flooding and filling the adjacent stream and river beds.

Today, these eroding interflaves are headlands, and the cross drainage sedimentary sequences are bay-mouth barriers. Tidal records at Baltimore, Maryland from 1903 to 1986, indicate that relative sea level continues to rise at about 0.3 m per century (Lyles, Hickman, & Debaugh, 1988) which

would force continued shoreline regression. Erosion of the underlying material along the shoreface provides the sediment, particularly the sands and gravels, necessary to create and maintain the sandy barrier beaches and dunes. The degree of down-cutting and the type underlying strata dictate the type and quantity of sediment that is available.

Belknap and Kraft (1985) show the three dimensional nature of the present marine transgression. [Figure 4](#) and [Figure 5](#) indicate the current coastal morphology from the Rehoboth Beach headland to the Bethany Beach headland and describe the stratigraphic relationships of the Pleistocene substrate, ancestral creeks and rivers, and Holocene barrier, backbarrier, and nearshore sedimentary environments. Shoreface erosion supplies material to the littoral system, and these materials may be predominantly sand, silts, or clays depending on the nature of the eroding strata. Historical shoreline recession rates are a measure of shoreface retreat and averaged about 1 m/yr from 1843 to 1961 (Belknap and Kraft, 1985). Cape Henlopen was the only area of significant deposition.

The Maryland coast has a similar but distinctive transgressive history. Although, the study area is confined to Fenwick Island, a transgressive barrier, from Ocean City Inlet to the MD-DE state line, it is noteworthy that Assateague Island is a major, transgressive barrier that is morphologically part of the MD-DE coastal compartment. Fishing Point at the distal end of Assateague Island has been is a major sediment sink. Nearshore linear sand ridges are common to this coastal compartment and have a significant impact on the impinging wave climate and, therefore, the nature and patterns of shoreline recession and shoreface retreat.

### **2.1.2. Coastal Barrier Migration**

A coastal barrier beach must retreat and adjust to a new equilibrium as sea level rises. Erosion occurs from the beach face as sea level rises. The eroded sediment generally is deposited landward across the barrier. The U.S. Army Corps of Engineers (1996) reports that this principal edge of marine transgression has advanced across nearly two-thirds of the Coastal Plain province of Maryland and Delaware in the past 15,000 years.

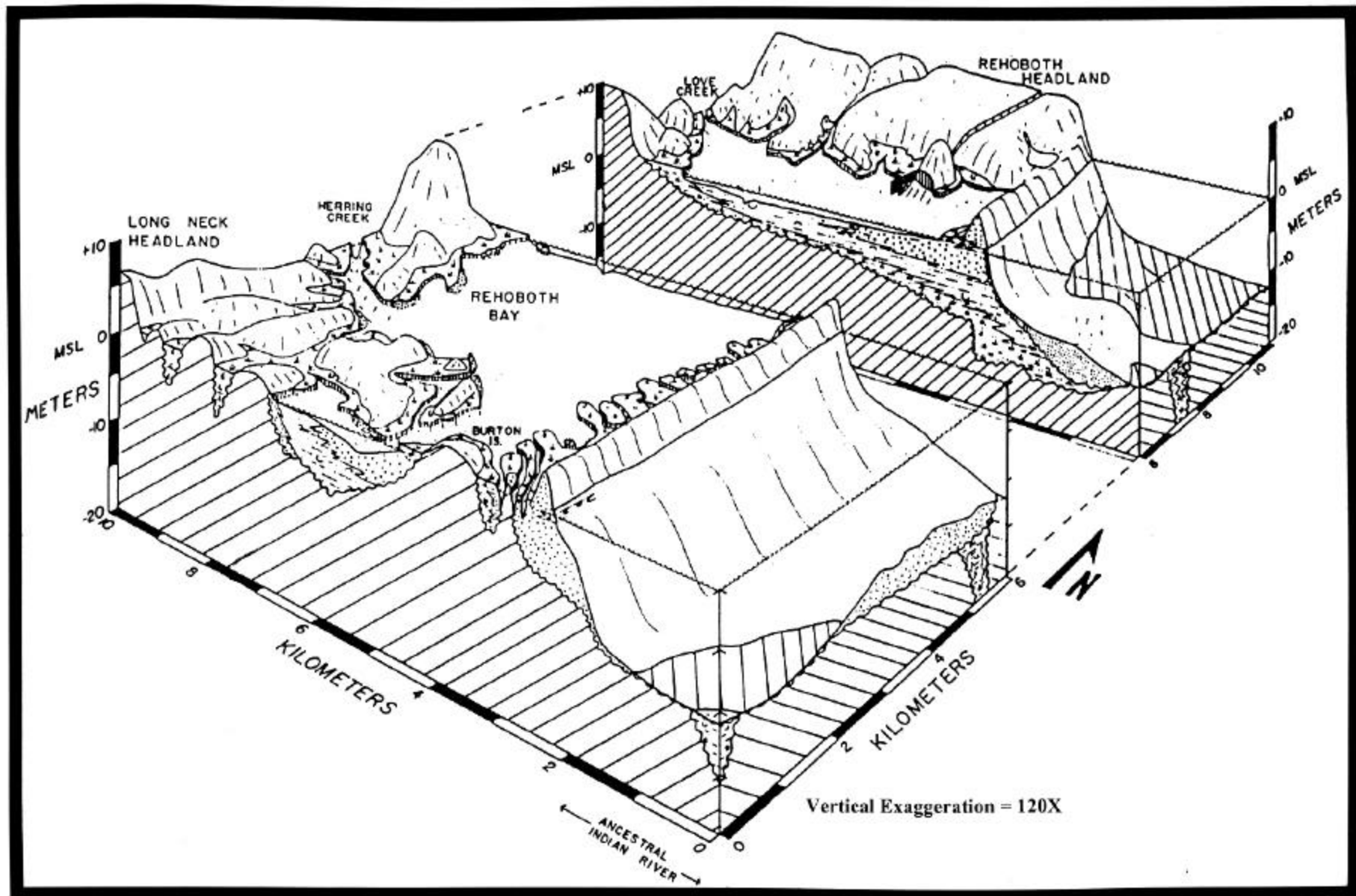


Figure 4. Present day coastal geomorphology of the Delaware coast from the Rehoboth headlands south (Belknap and Kraft, 1985).

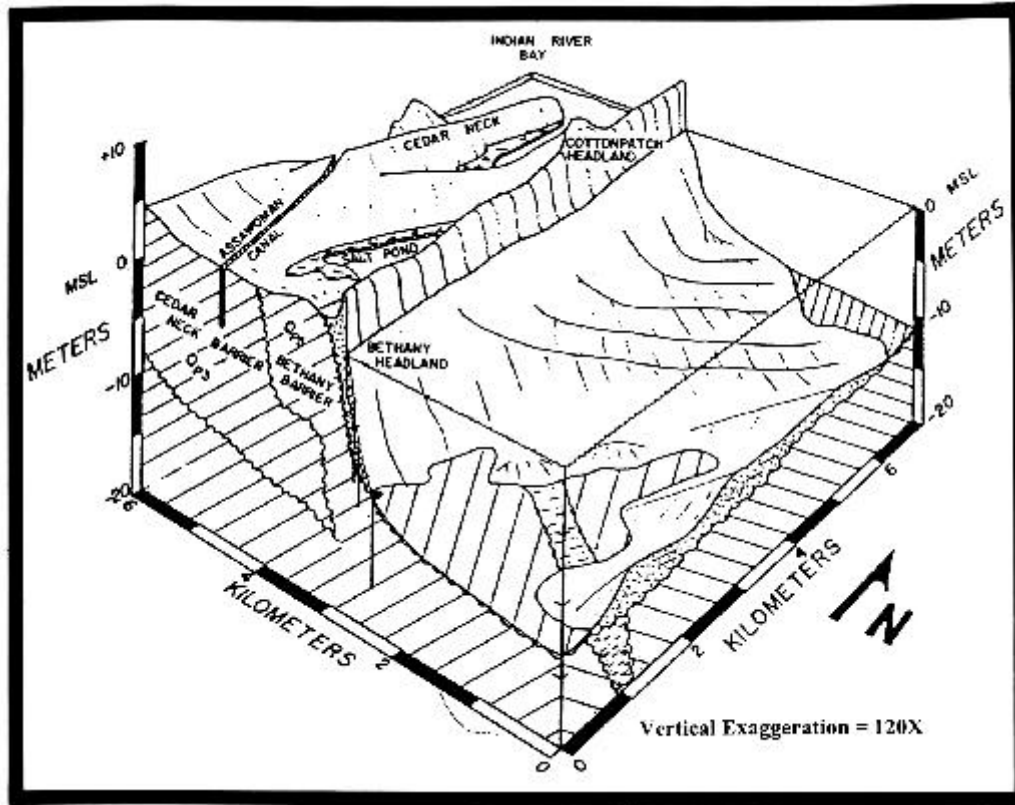


Figure 5. Present day coastal geomorphology of the Delaware coast from the Bethany headland north (Belknap and Kraft, 1985).

Beach erosion and reconstruction are phases that occur cyclically. Some studies suggest that the phases are controlled by the seasons. Winter storms erode beaches and summer swells rebuild beaches (Dubois, 1988). Other studies suggest that beach erosion and reconstruction does not coincide with the seasons. They suggest that because storms occur throughout the year, the erosional phase is not strictly in the winter (Hayes and Boothroyd, 1969; Owens, 1977; Carr *et al.*, 1982). They state that a typical summer or winter profile can occur in any season. However, one variable that may control the extent of progradation is the amount of transportable sediments in the nearshore. The processes responsible for aggradation were more important in the total construction of the beach than those responsible for progradation (Dubois, 1988).

Barrier beaches normally migrate landward with overwash of storm waves which transports sand from the ocean side of the barrier to the bay side. Inlets also contribute to beach migration as the ebb and flood tidal deltas serve as traps and reservoirs of sediment.

Fenwick Island is a sandy barrier spit that extends between Indian River Inlet, Delaware to the north and Ocean City Inlet, Maryland to the south. The distance between these two points is approximately 32 km. Isle of Wight and Assawoman Bays back Fenwick Island in Maryland (excluding back-bay wetlands and marinas). The average widths of the island between the two bays and ocean are about 610 m and 460 m, respectively. Assateague Island, which lies south of Ocean City Inlet, is a 60 km long sandy barrier island backed by Sinepuxent Bay to the north and by Chincoteague Bay to the south. It terminates at Chincoteague Inlet, Virginia.

Assateague and Fenwick Islands once were joined. A powerful hurricane separated the islands on 23 August 1933 by opening what is now called Ocean City Inlet. The inlet was made permanent by the construction of jetties in 1934 by the U.S. Army Corps of Engineers which maintains the inlet for navigation. The jetties have allowed the development of large ebb and flood tidal shoals which have diminished the supply of sediment which normally would have reached Assateague Island through littoral drift which is from the north (Stauble *et al.*, 1993).

Fenwick Island is interrupted by the Bethany Beach headland and Cottonpatch Hill headland before reaching Indian River Inlet. This part of the barrier is backed by Little Assawoman Bay south of Bethany Beach and Indian River Bay north of Bethany and landward of Cottonpatch Hill. North of the inlet, the barrier continues toward Dewey Beach and the Rehoboth Beach headland. This unnamed barrier is backed by Rehoboth Bay.

Rehoboth and Bethany Beach are found against headlands and are characterized by a lack of lagoons and higher elevations. Headland erosion occurs by sediment transport along and offshore, not by overwash (Bosma and Dalrymple, 1997). The difference between lagoon-baymouth barrier transgression and headland beach transgression is illustrated in [Figure 6](#) for past, present, and future projections of the present sea level rise for Rehoboth Bay and Rehoboth Beach, respectively. Barrier beach transgression is characterized by shoreface erosion of Pleistocene and Holocene substrates. Shoreface erosion of headland beaches works primarily on the underlying pre-Holocene material.

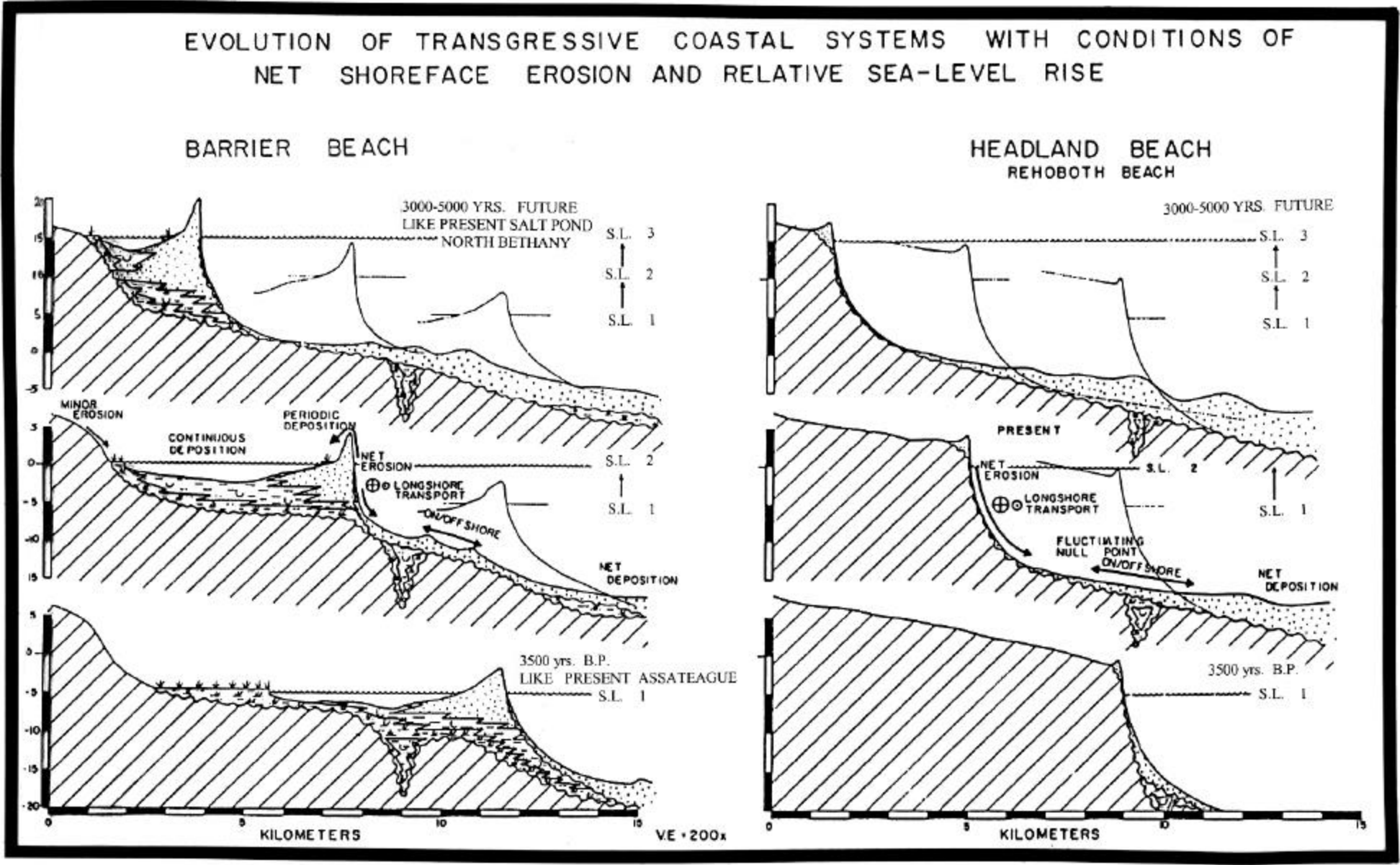


Figure6. Evolutionoftransgressivecoastalsystemsduringnetshoreface erosion and se-level riseatRehobothBay andRehobothBeach.

### 2.1.3. Linear Shoals

Besides Cape Henlopen, other Holocene accretionary features along the MD-DE coastal compartment include various linear ridge shoal systems. Linear ridges are a dominant topographic feature of the Mid-Atlantic shelf, and they are particularly well-defined on the Maryland shelf (Figure 7). Here sand ridges can be seen in all stages of formation. A systematic morphologic change occurs from *shoreface ridges*, through *nearshore ridges* to *offshore ridges*, reflecting changes in the hydraulic regime (Swift and Field, 1981). As one examines more seaward ridges, maximum side slopes decrease, the ratio of maximum seaward slope to maximum landward slope decreases, and the cross-sectional area increases. These changes in ridge morphology with depth and distance from shore appear to be equivalent to the morphologic changes experienced by a single ridge during the course of the Holocene transgression (Swift and Field, 1981).

The genesis of the shoal ridges is depicted with a model that couples inlet migration with shore retreat (Figure 8). A genetic relationship exists between the ebb-tidal delta sand body and the location and orientation of shoreface-attached sand ridges (McBride and Moslow, 1991). The changes in bottom characteristics that accompany large-scale morphologic features include megaripples, sand waves, and mud lenses in the troughs between nearshore and offshore ridges. These changes indicate that storm flows, which maintain ridges, are less frequently experienced in the deeper ridge field sectors and that the role of high-frequency wave surge becomes less important relative to the role of the mean flow component shaping the sea-floor.

Sand ridges are considered a consequence of constructive feedback between initial topography and the resulting distribution of bottom shear stress. The relationship between grain size and topography supports this model but does not account directly for the oblique angle of the ridge with respect to the coastline. A more rapid alongshore migration of the inshore edge of the ridge than the offshore edge as well as the relationship between this migration and the rate of shoreface retreat may create the angle (Swift and Field, 1981).

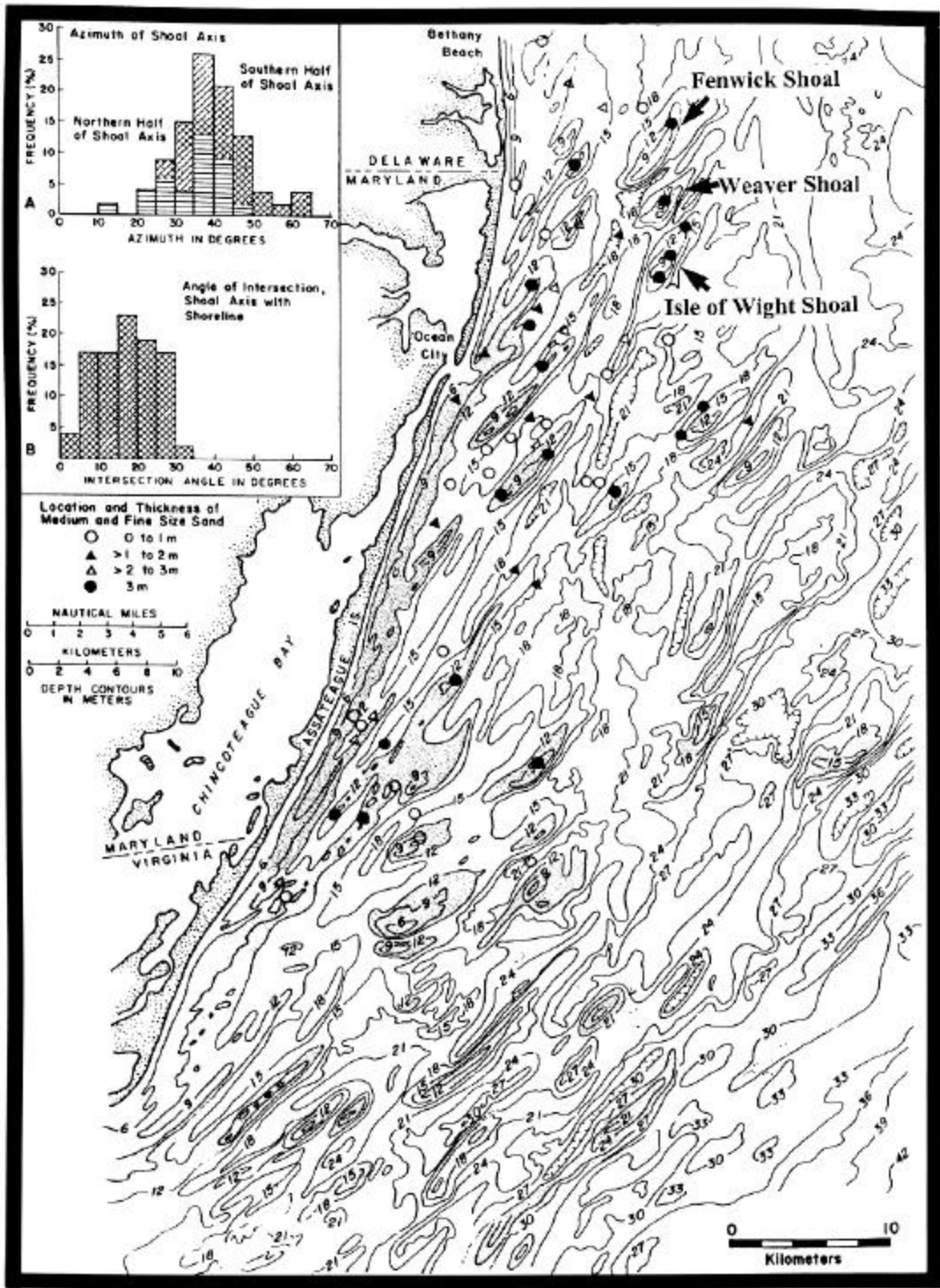


Figure 7. Location of linear ridges on the Mid-Atlantic shelf.

Shore-attached and nearshore sand ridges have the most economically feasible sources of beach-quality sand. Those shoals have been exploited for beach nourishment in the past and will be looked to in the future. Removal of a small volume of sand has a relatively insignificant impact on the impinging waves. Removal of very large volumes, however, can have the effect of focusing or de-focusing storm waves which, in turn, may impact the littoral processes on adjacent shorelines.

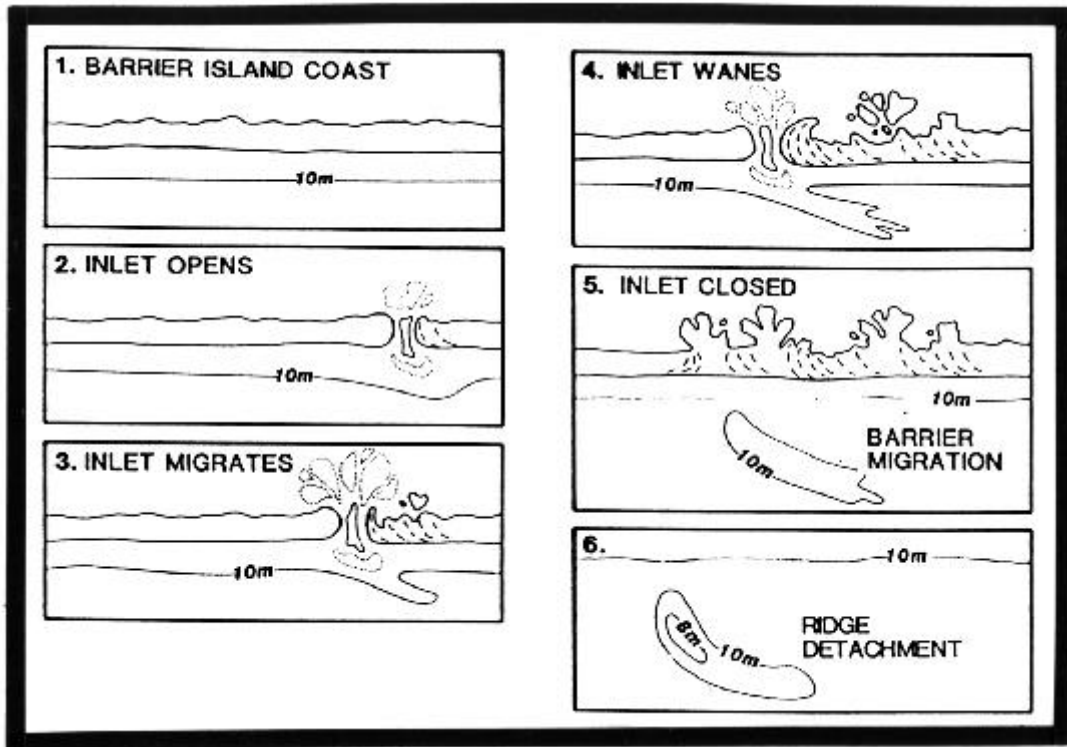


Figure 8. The genesis of linear ridges based on a model developed by McBride and Moslow (1991).

#### 2.1.4. Tidal Inlets

The historical existence of tidal inlets has controlled, in part, sand movement through sedimentation processes associated with ebb and flood shoals. The inlets have, through time, partially determined the rate and patterns of shoreline change. As discussed in the previous section, inlets have been an influential parameter in the development and morphology of shelf sand ridges. McBride (1999) identified 22 historical inlets from as early as 1649 along the MD-DE coast (Figure 9). As the number of inlets increase from north to south so too does the density of offshore sand ridges.

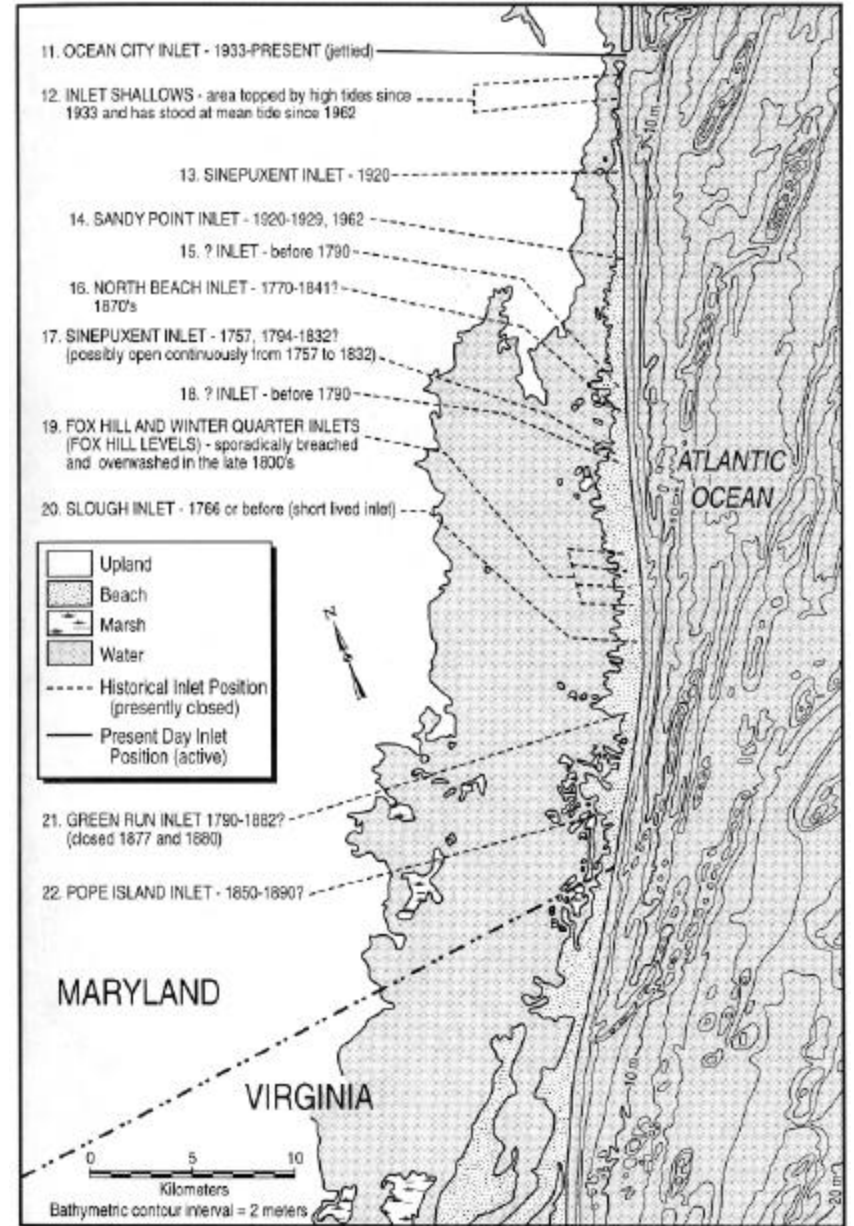
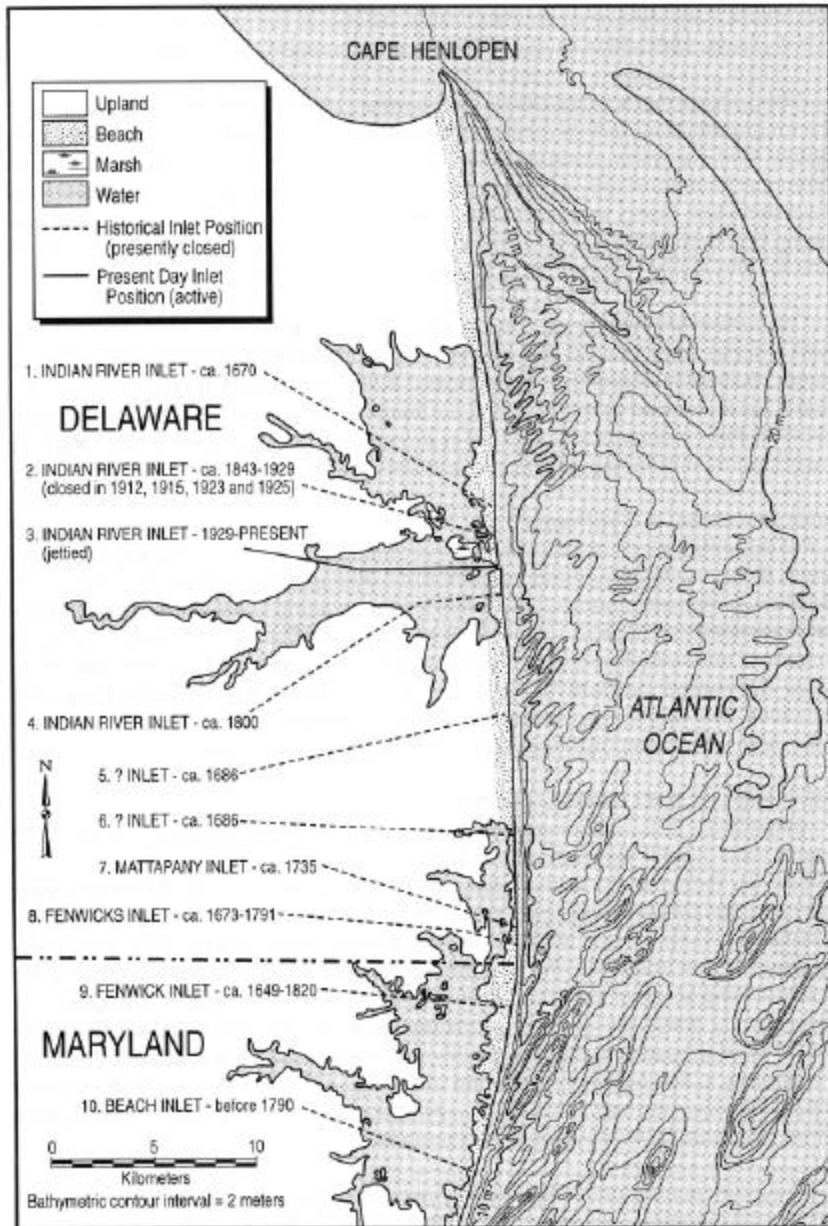


Figure 9. Location of historical tidal inlets along the Delaware and Maryland coasts (McBride 1999).

Two major tidal inlets interrupt the MD-DE coastal reach between Indian River and Ocean City (Figure 10). They have been “hardened” with jetties and dramatically indicate the net alongshore movement of beach sands in their respective shore subreaches. In 1937, Congress authorized a 5 m deep channel from the ocean to 2130 m into Indian River Bay and two jetties to stabilize the channel (House Document No. 105-144, 1997). Before its construction in 1939 (Smith, 1988), Indian River Inlet was an intermittent tidal channel that breached during storms. It was an area of extensive sand washover and accretion. Since installation in 1937, the jetties have had to be extended landward and the channel bulkheaded in order to maintain steady tidal flow. In 1990, a sand bypassing system was installed to reduce downdrift erosion and provide for more continuous alongshore sediment transport. The plant pumps sand from the south side of the inlet to various points along a 460 m section of the shore north of the inlet. The plant was designed to pump on the average 76,000 m<sup>3</sup> of sand per year (House Document No. 105-144, 1997).

In 1934, Ocean City inlet was hardened with jetties and dredged (Smith, 1988). This provided for a permanent separation between Fenwick and Assateague Islands. Since the net alongshore sediment drift along this reach is southward, the inlet and jetties accumulate sand to the north. Several major beach nourishment projects at Ocean City have supplied a relatively large amount of sand to the littoral system. Some of this material is directed offshore by the north side inlet jetty where it becomes part of the ebb-shoal. This ebb shoal currently is reported to be bypassing sand effectively to the north end of Assateague Island (D. Stauble, personal communication).

## **2.2. Hydrodynamic Processes**

The shoreline along the MD-DE coastal reach generally is recessive in response to present day hydrodynamic forces. The coast is eroding along most of its length with alongshore transport patterns showing a dominant southerly drift from about the state line southward and a dominant northerly drift from about Bethany Beach north. There is a sediment transport node in between. The resultant sedimentary features include accretionary spits at the distal end of the MD-DE coastal reach -- Cape Henlopen and Fishing Point.



A



B

Figure 10. Aerial photos of A.) Indian River Inlet and B.) Ocean City Inlet (Beach-Net Website, 2000).

### **2.2.1. Wave Climate**

With the exception of gravity, waves are the dominant factor affecting the form of a beach profile. “The energy they carry to the shoreline and the variety of currents and turbulence they generate play the leading role in the orientation of the beach” (Bosma and Dalrymple, 1997).

Bosma and Dalrymple (1997) used the 20-year hindcast of general wave climatology, presented in the Corps of Engineers’ WIS Report 30, to develop wave data for shoreline research along the Delaware coast. Waves approach the shore from the northeast to the southeast directions, with the greatest incident levels coming from the east and southeast. A March 1962 northeaster (from the hindcast data) generated the largest wave height at 7.7 m. The highest wave height off Dewey Beach between 1992 and 1993 recorded by a wave gauge was 4.1 m during a December 1992 northeaster.

As of 1980, there were no recorded wave data for the Ocean City, Maryland area. Data from the Atlantic City wave gage, located 70 miles north, was taken as representative of the wave climate at Ocean City. Average waves had a height of 0.8 m and a period of 8.2 seconds. Average storm conditions had a wave height of 2.7 m and a period of 11 seconds (Louis Berger Group, 1999).

The annual average wind speed along the Delaware Coast is 6.5 m/s. In the 5-degree quadrangle nearest the Delaware Coast, the winds over the offshore areas are distributed with respect to direction as follows: onshore (northeast, east, and southeast) 27%; (south) 11%, offshore (southwest, west and northwest) 44 %; and (north) 15%. Winds from the northeast have the greatest average velocity of approximately 9m/s. The wind data also show that winds in excess of 13 m/s occur from the northeast more than twice as frequently as from any other direction (House Document No. 105-144, 1997).

Maa and Kim (2000) investigated the impacts of linear shoals on waves along the MD-DE coast with goal of evaluating the effect of shoal removal from mining for beach nourishment. They also report on the statistical distribution of wave characteristics in the present study area.

### 2.2.2. Tide Levels

The tide at Ocean City is semidiurnal (*i.e.*, there are two low and two high waters each day). The mean and spring tide ranges for the study are shown in [Table 1](#). Generally, the tide range is greatest at Cape Henlopen and decreases toward the south. The National Ocean Service records for tidal datums at the Ocean City Fishing Pier for the tidal epoch 1960-1978 show mean high water (MHW) at 55 centimeters (cm) above the National Geodetic Vertical Datum (NGVD), mean low water (MLW) is 49 cm below NGVD, and mean sea level is 4 cm above NGVD. At Rehoboth and Dewey Beaches, MHW is 70 cm above NGVD. The location of MHW at Bethany, South Bethany, and Fenwick Island is 64 cm NGVD (A. Kansak, personal communication). [Table 2](#) indicates the relationships amongst the various vertical datums for Lewes and Indian River Inlet, Delaware and Ocean City, Maryland.

Table 1. Ocean tide ranges in centimeters for the study area (NOAA, 1989).

Location	Mean (cm)	Spring (cm)
Cape Henlopen	125	149
Rehoboth Beach	119	143
Fenwick Island Light	113	137
Ocean City, Maryland	107	128

### 2.2.3. Storms

Northeasters are the most frequent significant major storm systems that strike the Atlantic coasts of Maryland and Delaware (Grosskopf and Resio, 1988). Northeasters are extratropical cyclones that mainly occur from late fall through late spring. They usually form along the mid-Atlantic shore, often off the capes of North and South Carolina. They tend to be relatively large in size and can work on any specific section of shore for more than one tidal cycle.

Hurricanes are tropical cyclones that form in lower latitudes and often travel northward along the U. S. Atlantic coast. Although hurricanes are more intense storms with higher winds and larger waves than northeasters, usually they move more rapidly and may not even last through a full tidal cycle

at any particular location. The hurricane season extends from the first of June through the end of November, but September and October are the most active months. During the late fall, the area is susceptible to both hurricanes and northeasters. As hurricanes move up the mid-Atlantic coast, their tracks tend to swing clockwise through north toward northeast rarely crossing the Maryland-Delaware shore. No hurricane center has made landfall along the Delaware coast since 1871 when formal records began being kept (House Document No. 105-144, 1997).

Table 2. Vertical Datums for Breakwater Harbor, Lewes, and Indian River Inlet, Delaware and Ocean City, Maryland.

Datum	Breakwater Harbor, Lewes, DE Elevation (m)	Indian River Inlet, DE Elevation (m)	Ocean City, MD Elevation (m)
Highest observed water level	2.89 6 Mar 1962	2.06 5 Feb 1998	1.95 5 Feb 1998
Mean Higher High Water (MHHW)	1.44	0.92	0.79
Mean High Water (MHW)	1.31	0.83	0.72
NAVD 88	0.89		
Mean Sea Level (MSL)			0.4
Mean Tide Level (MTL)	0.68	0.45	0.38
NGVD 29	0.52		
NGVD 29 (1972 Adjustment)		0.41	
NGVD 29 (1967 Adjustment)		0.27	
Mean Low Water (MLW)	0.05	0.08	0.04
Mean Lower Low Water (MLLW)	0	0	0
Lowest Observed Water level	-1.2	-1.19	-0.59

In addition to producing high waves, storms also affect water level. Elevated water-levels cause coastal flooding. Storm tides, or storm surges as they also are known, raise the level of wave attack. The high water levels and high waves frequently cause overwash of low barriers. [Table 3](#) lists the high tides of record for Breakwater Harbor, Delaware.

Table 3. High tides of record for Breakwater Harbor, Lewes, Delaware. Elevations referenced to MLLW (modified from Ramsey *et al.*, 1998).

Rank	Date	Tide Height (m)	Storm Type	Name
1	6 March 1962	2.89	Northeaster	
2	4 January 1992	2.75	Northeaster	
3	28 January 1998	2.73	Northeaster	
4	5 February 1998	2.67	Northeaster	
5	27 September 1985	2.53	Hurricane	Gloria
6	3 March 1994	2.52	Northeaster	
7	25 October 1980	2.50	Northeaster	
8	29 March 1984	2.49	Northeaster	
9	8 March 1996	2.47	Northeaster	
10	12 December 1992	2.44	Northeaster	
11	22 October 1961	2.43	Hurricane	Esther
12	14 October 1977	2.41	Hurricane	Evelyn
13	31 October 1991	2.38	Northeaster	“Perfect”
14	18 September 1936	2.35	Hurricane	No. 13
	22 October 1972	2.35	Northeaster	
	14 November 1997	2.35	Northeaster	
17	2 January 1987	2.32	Northeaster	
18	8 October 1996	2.32	Northeaster	
19	14 October 1953	2.31	Northeaster	
	9 December 1973	2.31	Northeaster	

The most extreme storm on record in regards to the highest offshore waves, greatest surge, and longest duration, was the northeaster of March 6-8, 1962. The storm is referred to as the “Ash Wednesday” or the “Five High” storm. The storm moved directly offshore from the Ocean City area, intensified, and became stationary. This created persistent onshore winds in excess of 27 m/s (60 mph, 52 kn) for five high tides (*i.e.*, “Five High”). These conditions continued for over 60 hours and produced the area’s record high storm surge (Table 3). The storm caused \$16.7 million (1962 dollars) in damage.

As well as the water levels reported in [Table 3](#), it should be noted that the third and fourth highest tides occurred within eight days of one another, January 28 and February 5, 1998. Also only one of the top ten storms was a hurricane, Gloria in September 1985. The 13<sup>th</sup> highest tide level reported for Breakwater Harbor, DE, October 31, 1991, is the so called “Perfect Storm” which had its greatest impacts north of Delaware Bay.

[Table 4](#) presents a tide-stage frequency analysis for Delaware’s ocean coast. Although storms commonly are referred to as “the ten year storm” or the “hundred year storm,” it is better to consider the probability that a particular storm strength, or water level, will occur in any one year as the sense of frequency can give a false sense of security – “We had the 50 year storm last year so we don’t have anything to worry about for decades.”

Table 4. The adopted stage frequency data at Rehoboth and Dewey Beaches (modified from House Document No. 105-144, 1997).

Probability of Exceedance (%) in Any Year	Return Interval (years)	Elevation (m NGVD)
99	1	1.7
50	2	2
10	10	2.2
5	20	2.4
2	50	2.7
1	100	3
0.5	200	3.2
0.2	500	3.5

#### 2.2.4. Sediment Characteristics and Transport

The U.S. Army Corps of Engineers Automated Coastal Engineering System (ACES) was used to develop composite beach grain size curves for Dewey Beach, Rehoboth Beach, Bethany Beach, and South Bethany. Predicated on winter and summer beach composites, Dewey and Rehoboth beaches had a mean grain size of 0.28 mm with a standard deviation of 0.23 mm, and Bethany Beach and South Bethany had a mean grain size of 0.29 mm with a standard deviation of 0.48 mm. This relates to a

poorly graded, or well sorted, fine to medium sands for all four beaches. Ocean City sediments have a mean grain size of 0.25 mm with a standard deviation of 0.51 mm. Assateague Island has a mean grain size of 0.23 mm and a standard deviation of 0.69 mm (Louis Berger Group, 1999).

Typically, waves strike beaches at an oblique angle which creates both longshore and cross-shore sediment transport. Cross-shore sediment transport is the movement of sand on and offshore while longshore sediment transport is the movement of sand along the beach (*i.e.* littoral drift). Cross-shore sediment transport is normally temporary or seasonal. Dick and Dalrymple (1983) found that cross-shore sediment movement (on- and offshore movement of sand) was directed seaward during winter seasons and landward in the summer and fall. Longshore transport has the most central influence on the amount of sediment leaving or entering a given location. Longshore transport direction changes with the course of wave approach.

The change in orientation of the coast which occurs along Fenwick Island may have consequences for longshore sand transport direction. Evidence of impoundment at the south jetty and erosion at the north jetty at Indian River Inlet indicates net longshore sand transport on the order of 76,000 m<sup>3</sup>/yr to the north (Clausner *et al.*, 1991). Impoundment at the north jetty of Ocean City Inlet and shoreline recession on Assateague Island adjacent to the south jetty, indicate transport toward the south end of Fenwick Island. A divergent nodal point in transport along Fenwick Island has been placed in the vicinity of Bethany Beach. However, long-term trends in the wave climate imply great spatial and temporal variability in the location of the nodal point (Dean and Perlin, 1977).

Cape Henlopen, at the northern end of the study area, has an historic northward growth spit which is evidence of a predominant northward longshore transport whose rate ranges between 115,000 m<sup>3</sup>/yr to 191,000 m<sup>3</sup>/yr. At Indian River Inlet, 21 km south of Cape Henlopen, sediment transport also is toward the north as evidenced by long-term erosion and deposition patterns on either side of the inlet. Indian River Inlet had a northward net transport ranging between 57,000 m<sup>3</sup>/yr to 115,000 m<sup>3</sup>/yr. A southward net transport ranging between 96,000 m<sup>3</sup>/yr to 153,000 m<sup>3</sup>/yr was calculated along the southern border of Delaware with Maryland (Louis Berger Group, 1999).

Average net longshore transport rates for Ocean City were computed over a twenty year period from 1956 through 1975. Ocean City Inlet's littoral drift is to the south, deposition on the up-drift inlet jetty, and erosion on the down-drift beach (Assateague Island) is evidence of this southward predominance. Ocean City had a net longshore transport to the south ranging between 115,000 m<sup>3</sup>/yr to 230,000 m<sup>3</sup>/yr. Assateague Island also indicated a net southerly transport of 122,000 m<sup>3</sup>/yr with the exception of Fishermans Point which had a net sediment transport rate of 18,000 m<sup>3</sup>/yr to the north (Louis Berger Group, 1999).

Due to the northward littoral drift, sand is bypassed across Indian River Inlet from the south side of the inlet to the north side of the inlet. Between 1990 and 1995, approximately 350,000 m<sup>3</sup> of sand was pumped across the inlet. Bypassing helps stabilize areas just north of the inlet. While south of the inlet, bypassing created short-term mining effects on the shoreline that quickly dissipated. During the summer season the inlet effect is more pronounced, while during the winter months maximum changes occur further from the inlet due to partial reversal of littoral drift.

### **2.3. Cultural History and Shore Management Strategies**

Development of the beaches began by settling on the headlands then moving onto the barriers as population increased. Since shoreline recession has been the rule along the MD-DE coast, early developments had to retreat with the shoreline. Historically, beach erosion has been recorded in Delaware since 1843; it was not considered a significant problem until the 1950s when tourism, and hence development, increased and the economic impact of beach erosion became apparent. Local interests constructed nine groins in Rehoboth Beach between 1922 and 1964 indicating that beach erosion was a problem prior to 1950 (House Document No. 105-144, 1997).

#### **2.3.1. Rehoboth Beach**

Rehoboth Beach is highly developed, has generally suburban characteristics, and is a heavily populated resort area on the Delaware ocean coast. The beach is lined with high rise hotel and condominium complexes as well as typical summer cottages. A boardwalk runs for 1,600 m along the beach. The northernmost 1,070 m of the boardwalk has commercial development whereas the

remaining part of the boardwalk is fronted by residences. There are a total of 3,105 housing units within the town, of which only 21% are occupied year round. While there are only 1,234 year-round residents, Rehoboth Beach attracts thousands of summer residents with its beaches and boardwalk. The tourist population can increase to over 100,000 on a typical holiday weekend (House Document No. 105-144, 1997).

Rehoboth Beach is located on a headland and extends for about 1,500 m along the shore. The general condition at Rehoboth is a beach with substantial width, little or no dune, bulkheads, and high backshore elevations. The elevation of the beach generally is +2 m NGVD, and the elevation of the upland area generally ranges between +7 m NGVD at the north part of town to +5 m NGVD on the southern edge of town. The shoreline has groin fields which have acted to stabilize the shoreline in recent history. All nine groins are in poor condition, but they are functioning and are not in imminent danger of failing. The three northernmost groins continue to function; however, they are exposed to the predominant wave action from the northeast and have been damaged in recent storm events (House Document No. 105-144, 1997).

In 1958, congress authorized the Corps of Engineers to participate in the cost of restoration and subsequent periodic renourishment for up to ten years in a beach erosion control project that extended from Rehoboth Beach to Indian River Inlet. About 795,000 m<sup>3</sup> of sand was placed on the beach in 1957, 1961, and 1963. Much of the material was lost during the Five-High Storm in March of 1962 (House Document No. 105-144, 1997). Other beach fill projects are listed in [Table 5](#).

### **2.3.2. Dewey Beach**

Dewey Beach lies just south of Rehoboth Beach and is about 1.6 km long. The northern portion is a headland whereas the southernmost 900 m is a barrier with the Atlantic Ocean to the east and Rehoboth Bay to the west. The barrier is about 460 m wide. The elevation of the beach is about +2 m NGVD whereas the elevation of the upland is about +5 m NGVD in the north decreasing to +3 m NGVD in the southern part of the town. The town of Dewey Beach is highly developed with generally suburban characteristics (House Document No. 105-144, 1997).

Dewey Beach has become a developed overflow area for Rehoboth Beach, but it is a changing community where older residences still exist. Over 41% of the population is retired, and although more than half of the current residents have lived in their present homes for the past 15 years, the situation is starting to change. Many of the older properties are being sold, the cottages then razed, and new modern townhouses built in their place. The population at Dewey can rise to 35,000 on a summer holiday weekend (House Document No. 105-144, 1997).

According to Bosma and Dalrymple (1997), the area has experienced major flooding, erosion, and wave attack causing damage to many shoreline structures. A system of bulkheads and groins has been installed to stabilize the northern shore. The southern shore which is a barrier between the Atlantic Ocean and Rehoboth Bay, is highly vulnerable to storm damage. Along the entire beach, there are seven timber bulkheads totaling 530 m in length and five bulkheads totaling 350 m in length (House Document No. 105-144, 1997).

Several times between 1992 and 1996, the President of the United States declared the region a National Disaster Area because of storm damage (U.S. Army Corps of Engineers, 1996). In the summer of 1994, 453,300 m<sup>3</sup> of a beach-fill was placed on Dewey Beach. The majority of the beach-fill was taken from the Hen and Chickens Shoal which is approximately 3 to 5 km offshore of the Rehoboth Beach area. The fill extended roughly 2,000 m alongshore from Collins Street in the south to the south end of Silver Lake in the north (Bosma and Dalrymple, 1997). Several other beach fills that have taken place at Dewey are shown in [Table 5](#).

### **2.3.3. Bethany and South Bethany Beaches**

Bethany Beach is the second largest beach municipality in Delaware ([Figure 11A](#)). It is less developed than Rehoboth Beach but more developed than Dewey Beach and accommodates many thousands of summer visitors in its hotels, motels, condos, and beach cottages. The town also maintains a boardwalk along its approximately 800 m long oceanfront. The general conditions at Bethany are beaches with substantial width, little or no dune, bulkheads, and high backshore elevations. Bethany has groin fields which have acted to stabilize the shoreline. South Bethany is different ([Figure 11B](#)). Beach front cottages and houses dominate the landscape along with a much smaller business area (House Document No. 105-144, 1997).

Table 5. Information on beach nourishment projects that have taken place along the Delaware Coast (Valverde *et al.*, 1999).

Beach Location	Date	Funding Type	Volume (m <sup>3</sup> )	Length (m)	Documented Cost \$
Fort Miles	1962	Federal: Emergency	72,943	2560.32	\$46,300
North Shores	1962	Federal: Emergency	53,063	1493.52	\$36,100
Rehoboth Beach	1962	Federal: Emergency	165,307	1524	\$318,900
Dewey Beach	1962	Federal: Emergency	62,697	1082.04	\$132,500
Dewey Beach	1993	State/Local	4,400	579.12	\$30,210
Dewey Beach	1994	State/Local	442,607	1828.8	\$2,342,230
Dewey Beach	1994	Federal: Storm and Erosion	10,707	422.148	\$60,000
North Indian Beach	1994	Private	16,057	122.834	\$61,400
Indian Beach	1962	Federal: Emergency	113,696	5638.8	\$94,700
Indian Beach		Private	3,670	46.9392	\$20,435
N. Indian River Inlet	1957	Federal: Storm and Erosion	391,781		\$316,500
N. Indian River Inlet	1961	Federal: Navigation	36,701		
N. Indian River Inlet	1962	Federal: Emergency	221,734	2560.32	\$182,600
N. Indian River Inlet	1963	Federal: Storm and Erosion	451,343		\$374,900
N. Indian River Inlet	1965	Federal: Navigation	68,814		
N. Indian River Inlet	1972	Federal: Storm and Erosion	592,030	1524	\$637,200
N. Indian River Inlet	1974	Federal: Emergency			
N. Indian River Inlet	1975	Federal: Storm and Erosion	108,956	2560.32	\$276,600
N. Indian River Inlet	1978	Federal: Emergency	409,367	1524	\$714,600
N. Indian River Inlet	1982	State	171,194		
N. Indian River Inlet	1984	Federal: Emergency	412,884		
N. Indian River Inlet	1990	State	133,805		
N. Indian River Inlet	1991	State	52,681		
N. Indian River Inlet	1992	State	30,584		
Beach Cove to Bethany Beach	1962	Federal: Emergency	28,367	2897	\$32,900
Bethany Beach	1961	Federal: Storm and Erosion	76,460		
Bethany Beach	1962	Federal: Emergency	53,293		\$138,400
Bethany Beach	1989	State	217,529	1566.06	\$1,630,241
Bethany Beach	1992	State	168,009	1566.06	\$1,037,303
Bethany Beach	1994	State/Local	141,032	1264.92	\$838,953
South Bethany to York Beach	1962	Federal: Emergency	49,699	7563.92	\$119,000
South Bethany	1989	State	177,081	1267.36	\$1,307,849
South Bethany	1992	State	147,376	1478.28	\$905,786
South Bethany	1994	State/Local	75,251	777.24	\$452,165
York Beach to Fenwick Island	1962	Federal: Emergency	227,621	4632.96	\$454,900
Fenwick Island	1962	Federal: Emergency	51,687		\$121,900
Fenwick Island	1988	State	254,994	1828.8	\$1,572,993
Fenwick Island	1991	Federal: Storm and Erosion	96,951	487.68	\$443,603
Fenwick Island	1992	Federal: Storm and Erosion	28,290	515.112	\$269,234
Fenwick Island	1992	State	110,791	1264.92	\$716,916
Fenwick Island	1994	Federal: Emergency	52,173	701	\$369,809



A



B

Figure 11. Aerial photos of A.) Bethany Beach and B.) South Bethany Beach (Beach-Net Website, 2000).

Between 1937 and 1943, Delaware constructed nine groins which have been effective at accumulating sand during normal wave conditions (Bosma and Dalrymple, 1997). From 1938 to 1977, the overall rate of accretion was 0.1 to 0.2 m/yr (Dick and Dalrymple, 1983). More groins were constructed in the 1970s. In 1989, 545,000 m<sup>3</sup> of beach fill was placed at Bethany and South Bethany (Table 5). In 1992, 168,000 m<sup>3</sup> of material was placed at Bethany and 147,000 m<sup>3</sup> was placed at South Bethany. In 1994, 141,000 m<sup>3</sup> of material was placed at Bethany and 75,000 m<sup>3</sup> was placed at South Bethany.

#### **2.3.4. Fenwick Island**

Fenwick Island is somewhat different in character from Rehoboth, Dewey, and Bethany Beaches. Beach front cottages and houses dominate the landscape along with much smaller associated business communities (House Document No. 105-144, 1997).

#### **2.3.5. Ocean City**

Maryland's Atlantic coast is a popular year-round recreational destination. Ocean City is Maryland's only coastal resort. It hosted over eight million visitors in 1996. In 1988, the U.S. Army Corps of Engineers started the Ocean City Beach replenishment project which was designed to restore the recreational beach to a uniform 67 m width by pumping approximately 1.7 million m<sup>3</sup> of sand from a shoal in state waters along 13.4 km of beach over a 5 month period. In 1990, a 13.8 km long "hurricane protection dune" was constructed with 2.7 million m<sup>3</sup> of dredged sand (Maryland Geological Survey website, 2000).

The original plan called for the maintenance of the beach with between 535,000 and 764,000 m<sup>3</sup> to be placed on the beach every four years for the next 50 years. Since 1988, 7.3 million m<sup>3</sup> of offshore sand have been placed on Ocean City beaches (Maryland Geological Survey website, 2000). Table 6 shows the beach nourishment projects that have taken place at Ocean City.

Table 6. Information on beach nourishment projects that have taken place along the Maryland Coast (Valverde *et al.*, 1999).

Beach Location	Date	Funding Type	Volume (m <sup>3</sup> )	Length (m)	Documented Cost \$
Ocean City	1963	Federal: Emergency	802,830	12,875	\$1,517,600
Ocean City	1988	State/Local	2,064,420	11,265	\$14,200,000
Ocean City	1991	Federal: Storm&Erosion	2,905,480	11,265	\$15,003,269
Ocean City	1992	Federal: Emergency	933,873		\$10,800,000
Ocean City	1993	Federal: Emergency	170,900		\$960,000
Ocean City	1994	Federal: Emergency	993,980		\$8,800,000

#### 2.4. Offshore Sand Resources

The Delaware Geological Survey (DGS) is examining its database of core samples taken from state and federal waters to identify borrow sites for beach nourishment. Two areas beyond the 5 km (3-mile) limit have been identified. One area lies off the Indian River Inlet; the other is the Fenwick Shoal Field which borders Delaware and Maryland. The southern portion of the Fenwick Shoal Field lies in Maryland. The Indian River Inlet site is associated with ebb/flood tidal delta shoals and is a relatively flat area. The Fenwick Shoal Field is near the Maryland border in a ridge and swale field.

The DGS (1988) recommended that sand used to nourish the beaches have a median grain size of 0.35 to 0.71 mm; a sorting of 0.71 mm or less, and negative skewness. Both sites contain sand that meet the criteria for Delaware beach renourishment.

The Indian River Inlet offshore borrow area is larger than 5 km by 6 km. The upper 3 m is estimated to have approximately 69 million m<sup>3</sup> of suitable and available sand. The Fenwick Shoal borrow site extends over a 5 km by 4 km area. The upper 3 m is estimated to have approximately 46 million m<sup>3</sup> of suitable and available sand (Louis Berger Group, 1999).

### 3. METHODS

#### 3.1. Background: Shore Change Analysis

The coastal geology and management literature is rife with studies describing the pros and cons of many methods of interpreting the temporal and spatial variations in shoreline change (McBeth 1956, Shalowitz 1964, Stafford 1971, Ellis 1978, Dolan *et al.* 1978, Morton 1978, Dolan *et al.* 1980, Leatherman 1983, Elliot and Clarke 1989, Foster and Savage 1989, Smith and Zarillo 1990, Crowell *et al.* 1991, Dolan *et al.* 1991, Anders and Byrnes 1991, Larson and Kraus 1994 Crowell *et al.* 1997, Lacey and Peck 1998, Morton and Speed 1998). In general, calculation of long-term rates of shoreline change have relied on positioning a tidal datum, usually mean high water (MHW), on a map utilizing cartographic data or aerial photos (Everts *et al.* 1983). According to Shalowitz (1964), prior to 1927 the topographic supplement to hydrographic charts was made with plane-table surveys which since have been replaced by (aerial) photogrammetric methods. Both methods embody error in the determination of the horizontal location of the “shoreline,” the lateral position of mean high water on the date of the survey. Foster and Savage (1989) determined that the error associated with analysis of shoreline change is dependent upon the method of study. They calculated that the error can be +/- 9.1 m for map data, +/- 6.1 m for aerial photographs, and +/- 3.1 m for surveyed points. In all cases, more closely spaced data points yielded tighter error limits.

Fenster *et al.* (1993) described a simple method to determine rates of shoreline change from profile data. The End Point Rate (EPR) method utilizes the distance from the profile benchmark to the intersection of the profile with Mean High Water (MHW) on the earliest and latest surveys at each profile; dividing this differential distance by the number of years between the profiles gives a rate of shoreline change comparable to rates obtained from aerial photos or maps.

Since the 1980s, and in some cases even earlier, many localities have monitored their beaches through surveying. How the short-term changes reflected in profile data relate to the long-term historical trends has been the subject of debate. Eliot and Clarke (1989) indicated that approximately 10 years of monthly profiles are necessary to minimize the effects of seasonal and other short-term changes. Lacey and

Peck (1998), utilizing 33 years of profile data, attributed annual variations in beach morphology and volume to the onshore-offshore transport of sediment associated with seasonal variations in storm frequency and intensity. Shorelines can exhibit trends toward erosion, accretion, or relative stability depending on the individual profile. These trends relate to average wave height, sediment transport, depth to 10 m contour or closure, and regional management issues such as how a beach nourishment project will perform.

Delaware has intensely monitored its entire ocean coast for the last 18 years. One survey was performed in 1964, but it was not until after 1982 that most of the thirty six profiles (Figure 12) were surveyed regularly. These profiles are spaced an average of 1,200 m apart along the Delaware ocean coast. In addition, the state has established more closely-spaced profile lines at Rehoboth, Dewey, Bethany, South Bethany and along Fenwick Island. Most of those profiles were established in the late 1980s or early 1990s to monitor the beach nourishment projects that have taken place along the shoreline. At Dewey Beach, 16 profiles were established 150 m apart. Data were collected from May 1991 to January 1996. Nine to eleven surveys were performed at each profile over the five year period. Four surveys were performed after the beach was nourished; the others were pre-nourishment. All the Delaware profile data were made available in digital format. These data have been analyzed in great detail by Dick and Dalrymple (1983), Dubois (1988), Clausner *et al.* (1991), U.S. Army Corps of Engineers (1996), and Bosma and Dalrymple (1997).

Maryland has a long-term beach monitoring program that began in earnest in 1988 just before the large beach fill project (Figure 12). These data have been analyzed by Grosskopf and Resio (1988), Anders and Hanson (1990), and Stauble *et al.* (1993). The Maryland profile data were not available in digital format at the writing of this report which greatly reduced the amount of analysis that could be performed. As a result of availability, we used data from published (Stauble *et al.*, 1993) and unpublished reports (provided by Jordan Loran, Maryland Department of Natural Resources (MD-DNR)).

We have not attempted to duplicate the efforts of earlier researchers. Instead our focus is tying together the many studies that have been performed on this section of coast in order to assess the impact of beach nourishment on shoreline/shoreface change.

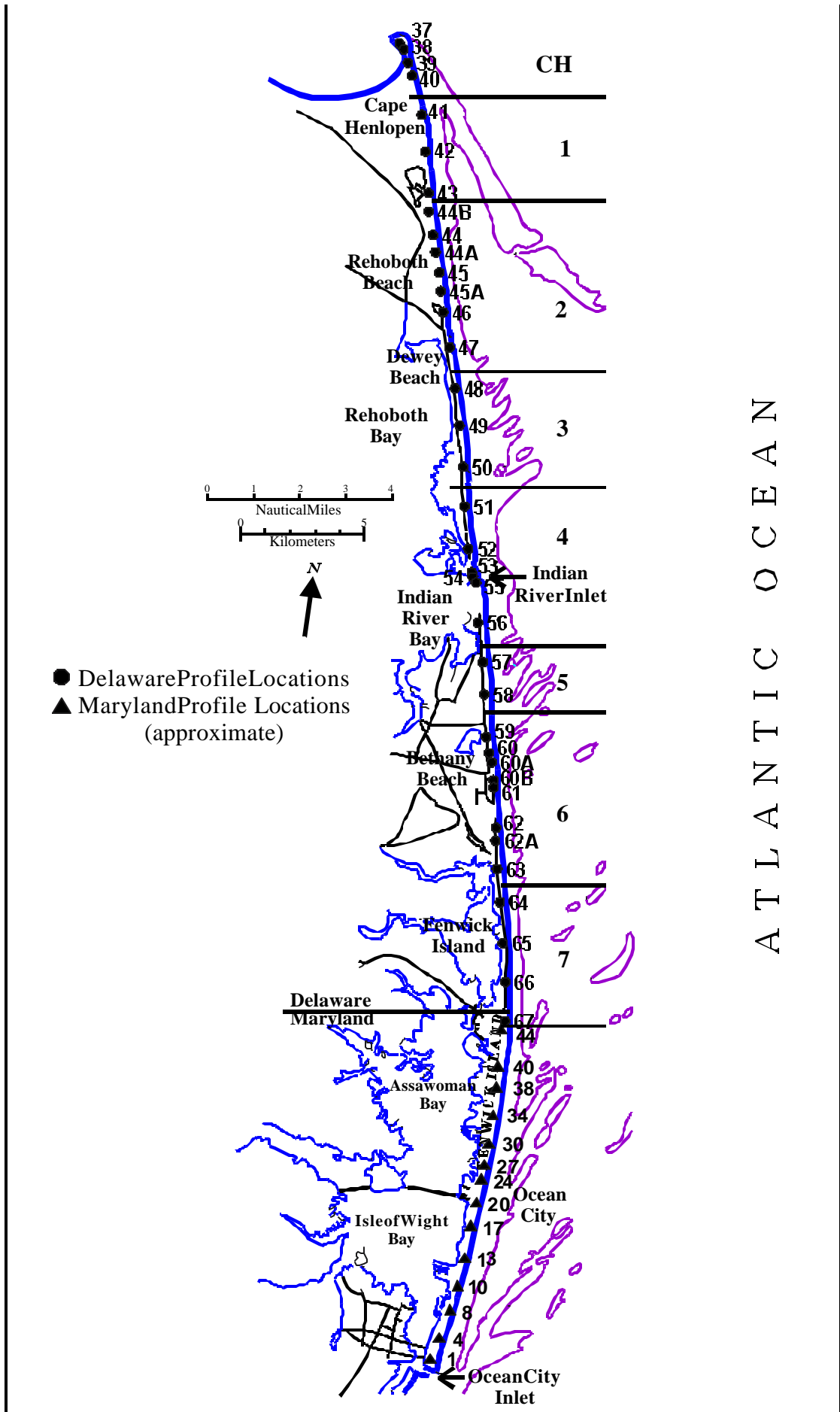


Figure 12. Location of Delaware and Maryland ocean coast beach profiles as well as Delaware coastal segments from U.S. Army Corps of Engineers (1996) analysis.

## **3.2. Data Analysis**

### **3.2.1. Rates of Change**

In order to determine the historical rates of change along the shoreline, the location of the profiles was plotted on topographic scale NOAA/NOS-CERC Cooperative maps prepared for the Shoreline Movement Study in the 1980s. The position of the shoreline was determined for all available shoreline survey dates between 1849 and 1980 at the profile locations. Once the shoreline locations were determined from the position of the profile benchmark, rates of shoreline change were calculated. This analysis was performed for both the Delaware and Maryland coasts. For recent rates of change (1982-1999), the Delaware survey benchmark and profile data were used to determine the horizontal position of NAVD.

For Maryland, profile data had to be manually extracted from published sources (Stauble *et al.*, 1993). The position of zero elevation (NGVD) either was taken from the profile data published in ISRP format or determined from profile plots provided by Jordan Loran (MD-DNR). The analysis is limited to 13 profiles selected along the Ocean City shore. Shoreline position dates used in the analysis are June 1998, June 1990, February 1994, May 1997, and October 1997. These generally correspond with pre-fill conditions of the beach and the last date of profile-data availability.

### **3.2.2. Regression Analysis**

Linear regression analysis was performed on both historical (1845-1980) and recent (1982/1988-present) shoreline position data. In order to determine a long-term rate of change, regression analysis was performed on the positions of the historic shorelines. The analysis was customized to the particular geographic subreach. For instance, some of the Maryland historical data show a much higher regression coefficient for the period 1929 and 1980 than for 1880 to 1980. This likely is due to construction of the inlet jetty in the 1930s. The geologically-sudden, anthropogenic change in coastal processes caused by the jetties was significant enough to displace the long-term trend since analyses of the time periods before and after construction of the jetties show consistent trends.

The Corps of Engineers has divided Delaware's shoreline into eight segments, based on shore morphology, for a linear regression analysis of beach profile data (Figure 12). These recent data tend to have low regression coefficients since the adjustment of beach fill is non-linear. However, analysis of shoreline movement between beach nourishment projects yields similar rates of change for individual projects.



## 4. RESULTS AND DISCUSSION

### 4.1. Delaware

#### 4.1.1. Historic Shore Change

The net change between the first date shown on the shoreline change maps (1845/50/82) and 1929 probably represents the long-term historical rate of change relatively unaffected by anthropogenic activities along the coast. Average rates of change show that between 1845 and 1929, the Delaware shoreline was retreating at a rate of about -1.7 m/yr.

Two events occurred between 1929 and 1943 that impacted shoreline change rate. First, the 1933 hurricane greatly impacted the region. Between 1929 and 1933 from Cape Henlopen to Dewey Beach or profiles 39 to 51 (the only location shore change data were available), the rate of shoreline change was -12 m/yr (Table 7). This is significantly greater than the rates of change on either side of these dates. This can be attributed partially to the short time span; but the shoreline retreated an average of about 46 m in this four-year period. The second event was the installation of the jetties at Indian River Inlet in the late 1930s. At the time of construction, these jetties extended 183 m from the shoreline. Gebert *et al.* (1992) found that the jetties created significant problems including accelerated scour along the jetties and massive downdrift erosion due to the predominant northward littoral transport system.

Table 7. Rates of change along the northernmost section of Delaware between 1845 and 1943.

Profile	Rate of Change (m/yr)			Shore Change (m)
	1845-1929	1929-1933	1933-1943	1929-1933
39	-3	-15	0	-61
40	-4	-10	-2	-41
41	-4	-13	2	-52
42	-3	-13	2	-50
43	-3	-10	-0	-61
44B	-3	-10	0	-24
44	-2	-12	2	-61
44A	-2	-13	2	-40
45	-2	-4	3	-38
45A	-2	-8	5	-49
46	-2	-11	4	-52
47	-2	-10	4	-15
48	-1	-19	5	-32
49	-1	-15	6	-44
50	-2	-6	5	-41
51	-2	-15	10	-76
<b>Average</b>	<b>-2</b>	<b>-12</b>	<b>3</b>	<b>-46</b>

Cape Henlopen has been eroding along its ocean coast. The northerly drift of sand has elongated the Cape through time (Figure 13A). Further south at the present Indian River Inlet, significant change has occurred (Figure 13B). The Inlet was an ephemeral coastal feature until it was stabilized with jetties in 1939.

Between 1929 to 1943, shoreline modifications began along the Rehoboth and Bethany Beaches. Bulkheads and groins were built. These likely affected the local rates of shoreline change but probably had little effect either up or down drift. Overall, the rate of shoreline change along the Delaware coast decreased during this period to only -0.5 m/yr.

Between 1943 and 1962, the average rate of change for the Delaware coast was -1.9 m/yr (Figure 14). This is in-line with the long-term rate of change. The impact of Indian River Inlet is evident with continued erosion on the north side of the inlet. In an attempt to mitigate downdrift impacts, approximately 38,000 m<sup>3</sup> was dredged from the Inlet every five years between 1957 to 1990 and placed on the north side of the inlet. Also, a total of about 428,000 m<sup>3</sup> of sand was placed on the beach north of Indian River Inlet in 1957 and 1961 (Valverde *et al.*, 1999). However, much of the material was lost during the Ash Wednesday/Five High storm in March 1962. The month and day of the 1962 shoreline used in the historical analysis is unavailable. Most likely the field survey was performed after the storm but before the emergency placement of fill.

Shore positions were plotted in 1961 and 1962 for the stretch of shore between just north of Indian River Inlet and South Bethany Beach. While the shore positions varied, in general, there was severe erosion in South Bethany and Bethany. These two localities lost about 8 m of beach width in that one year, likely as a result of the Five-High Storm. The beach north of Bethany, however, gained an average of about 6 m in beach width during that same year. Severe scour occurred on either side of the Indian River Inlet jetties, particularly on the northern side which lost 52 m. Sand appeared to be transported to the north as the section of beach just north of the Inlet showed an increased beach width between those two dates.

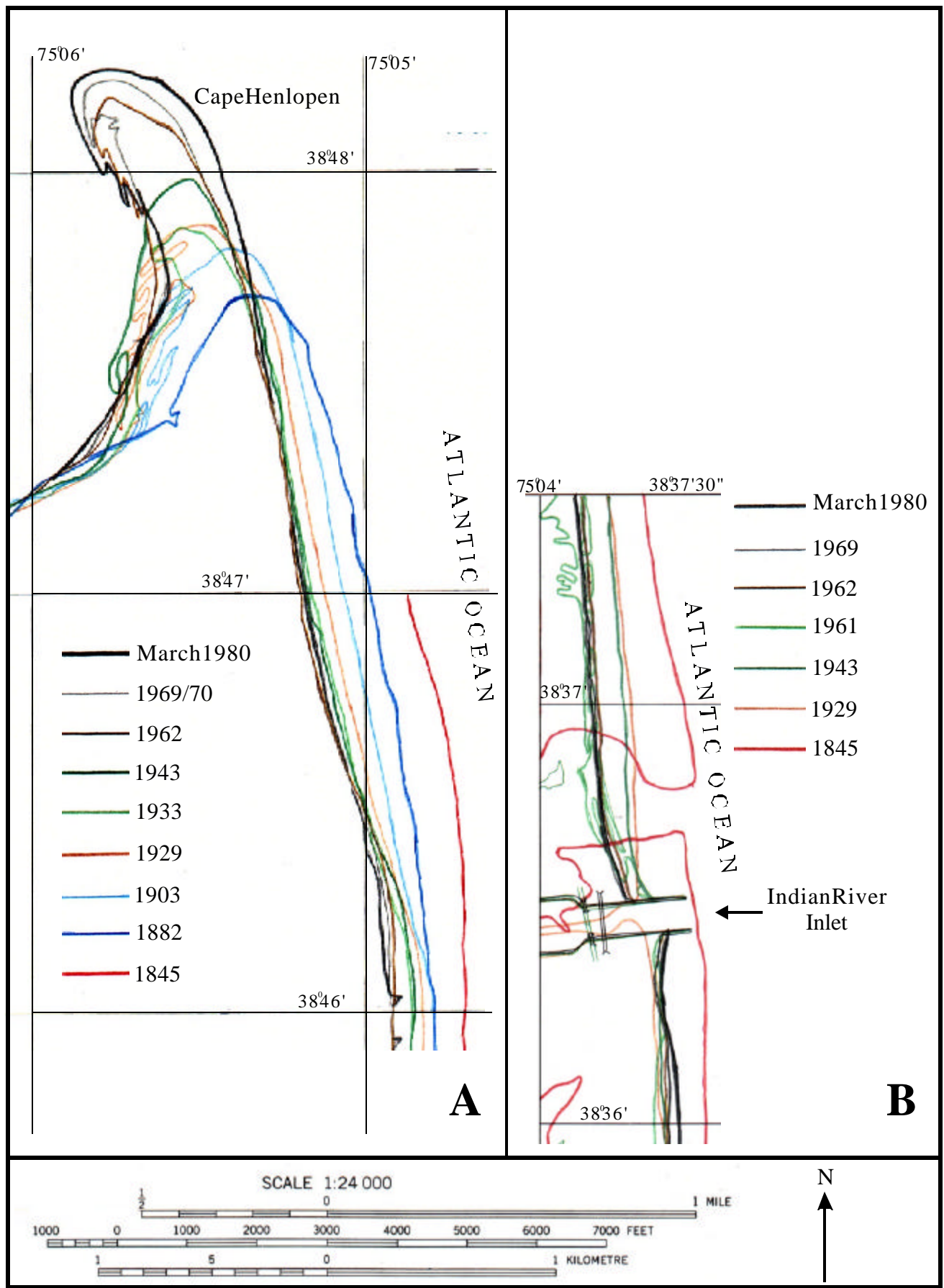


Figure 13. Historic shorelines at A.) Cape Henlopen and B.) Indian River Inlet.



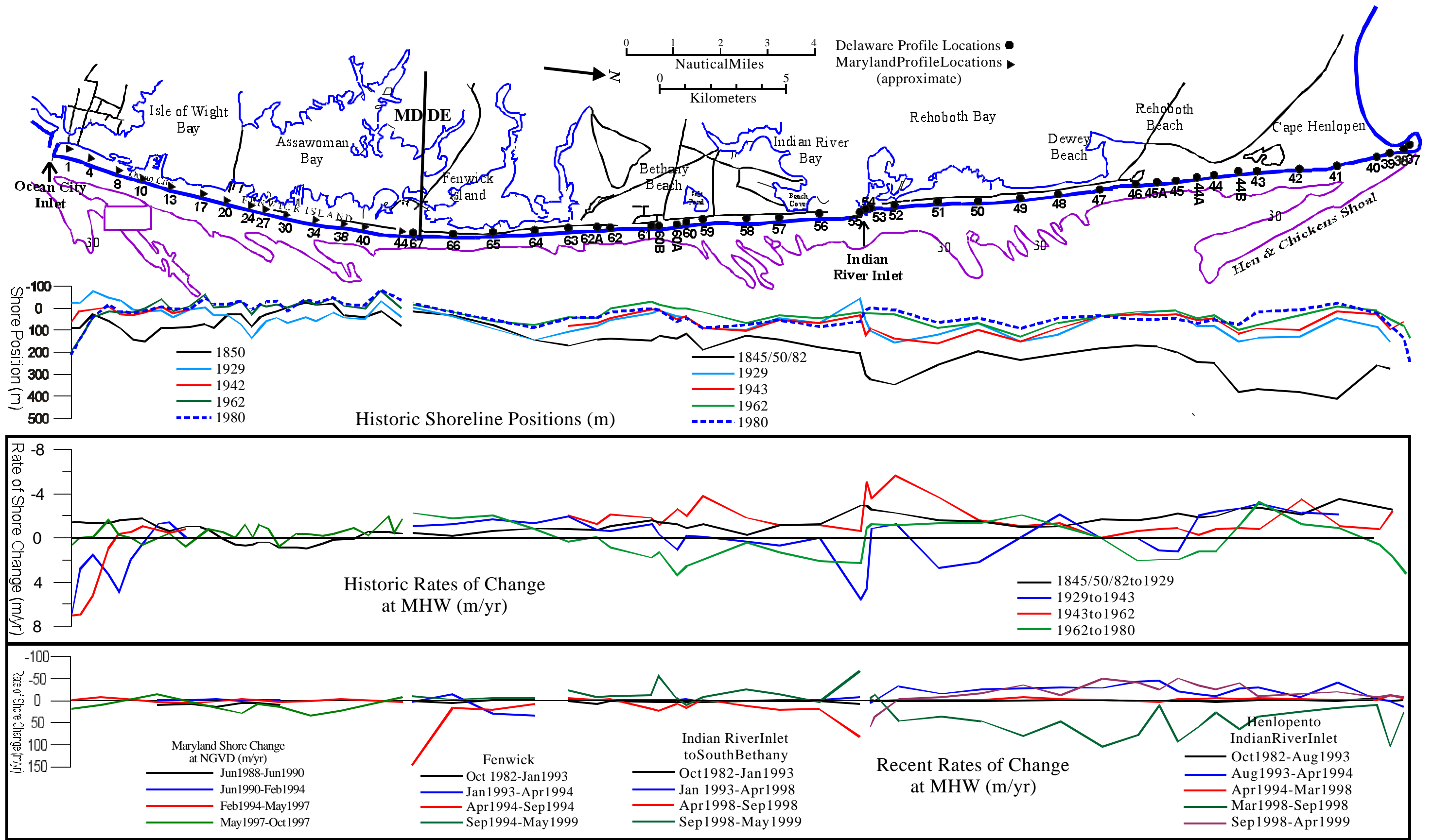


Figure 14. Historic shore positions and historic and recent rates of change along the Delaware and Maryland shoreline.



The alteration of shoreline change rates due to the influence of post-storm beach fill is shown in the 1962 to 1980 data. Following the 1962 storm, 689,000 m<sup>3</sup> of material was placed along 15,000 m of shore north of Indian River Inlet. 411,000 m<sup>3</sup> of sand was placed along the shore from Indian River Inlet to Fenwick Island (Valverde *et al.*, 1999). Both Rehoboth and Bethany Beaches show positive rates of change which likely is the result of the addition of the emergency beach fill sand following the 1962 Ash Wednesday/Five High storm since no other fill projects took place at those beaches during that period (Figure 14). Between 1963 and 1980, approximately 1.6 million m<sup>3</sup> of sand was placed north of Indian River Inlet (Valverde *et al.*, 1999). That is a lot of sand to be placed along the shore, yet it is not seen in the rate of change along most of the shoreline. There is accretion at the southern jetty and on the northernmost section of the reach at Cape Henlopen. The positive rates do influence the overall shoreline rate of change to +0.4 m/yr. The overall net rate of change between the mid 1800s and 1980 was -1.5 m/yr.

#### **4.1.2. Recent Shore Change**

In order to determine the more recent trends along the shoreline, the beach profile data were used to calculate the horizontal position of MHW. In an attempt to show the influence of beach fill along the shore, the data graphed on Figure 14 are from profile dates that most closely correspond to beach nourishment projects along each section of the Delaware coast. In 1994, 453,000 m<sup>3</sup> of sand was placed at Dewey Beach.

The most obvious difference between the long-term and short-term change rates is their order of magnitude. Short-term rates can be an order of magnitude greater than the long-term rates. The high rates generally are associated with beach fill and its subsequent dispersal at a higher rate than the usual background. Also, shorter time frames tend to exaggerate trends. Such is the case for Rehoboth and Dewey Beaches. A large beach nourishment project in the summer of 1998 resulted in an average rate of change of +35.7 m/yr. The dispersal of this material between September 1998 and April 1999 resulted in a rate of -13.4 m/yr. However, the net change between 1982 and 1999 was -0.5 m/yr.

Bosma and Dalrymple (1997) analyzed profile data from Dewey Beach. They measured the cumulative shoreline change relative to the position of the shoreline in May 1991. The shoreline retreated

approximately 23 m (75 ft) after July of 1993. During the winter of 1994, the beach fill spread quickly while high waves acted on the shoreline. The next survey showed that the coast had recovered substantially, but was roughly 15 m (50 ft) short of the original post-nourishment stance. However, the stations further north retreated only 9 m (25 ft) over the first two surveys.

Analysis of the long-term data for Delaware yielded rates of change ranging from -3 m/yr to +6 m/yr with an average rate of -1 m/yr (Table 8). The areas near Indian River Inlet and just south of Cape Henlopen had relatively high rates of erosion. The only area of accretion was Cape Henlopen. In general, the negative rates of change decrease south of Indian River Inlet, with the exception of a slight increase in erosion rates at Bethany Beach. The minimum occurs near the Maryland-Delaware line which has been reported as the nodal zone of sediment transport. These trends in the historic data are not shown in the analysis of recent profile data which showed that the average rate of change had decreased to -0.3 m/yr (Table 9). Many areas showed accretion due to the influence of beach fill. However, a small region just south of Bethany Beach (Profiles 63, 64, and 65) showed erosion while accretion in recent years occurred on either side. Likely this indicates that the nodal zone of sediment transport is not fixed but it can move alongshore in response to changes in wave climate, nearshore bathymetric features, and possibly the influx of sand from beach fill projects.

The U.S. Army Corps of Engineers performed a regression analysis on the Delaware profile data. They determined the rates of change for the short-term profile data (Table 10). Table 10 compares their data with calculated rates of change with an analysis done by the authors of this report and Belknap and Kraft (1985). General agreement and orderliness occurs among the rates of change.

A more detailed analysis of shore change using linear regression was performed on the profile data taken at Dewey Beach after renourishment took place in 1991 (Appendix 1). Table 11 displays the results of this effort. Regressions were performed on profile data taken between projects in order to determine the rates of change after beach fills. While regression coefficients are low for this analysis, the beach displayed similar rates and patterns in response to the fill during the four years between the first two projects. An initial large adjustment period takes place immediately after the project as demonstrated by the data regressed

between 1998 and 1999. The regression coefficients are high for this analysis indicating a linear loss of fill material. However, after this initial adjustment, the rate of change tapers off creating a non-linear fill adjustment period.

Table 8. Delaware historic regression analysis results by profile.

Profile	Rate of Change (m/yr)	R <sup>2</sup>	No. points	Dates Spanned		Comment
37	6.2	91%	3	1962	1980	Cape Henlopen
38	0.5	47%	3	1943	1980	
39	-3.2	94%	4	1882	1980	
40	-2.4	84%	8	1882	1980	
41	-3.1	89%	9	1845	1980	
42	-2.7	97%	8	1845	1980	
43	-2.3	93%	8	1845	1980	
44	-1.4	78%	8	1845	1980	
44A	-1.1	59%	8	1845	1980	
44B	-2.1	90%	8	1845	1980	
45	-1.0	48%	8	1845	1980	
45A	-0.8	42%	8	1845	1980	
46	-0.8	41%	8	1845	1980	
47	-1.2	72%	7	1845	1980	
48	-1.3	86%	7	1845	1980	
49	-1.0	79%	7	1845	1980	
50	-1.1	82%	7	1845	1980	
51	-1.4	78%	7	1845	1980	
52	-2.7	94%	7	1845	1980	
53	-2.5	98%	7	1845	1980	
54	-2.2	90%	7	1845	1980	North of Indian River Inlet
55	-1.2	50%	7	1845	1980	South of Indian River Inlet
56	-0.9	77%	7	1845	1980	
57	-0.8	81%	6	1845	1980	
58	-0.4	73%	6	1845	1980	
59	-1.1	68%	6	1845	1980	
60	-0.8	72%	6	1850	1980	
60A	-0.9	65%	6	1850	1980	
60B	-1.1	88%	6	1850	1980	
61	-1.3	90%	6	1850	1980	
62	-1.0	95%	6	1850	1980	
62A	-0.8	97%	6	1850	1980	
63	-1.0	95%	6	1850	1980	
64	-0.5	63%	4	1850	1980	
65	-0.2	33%	4	1850	1980	
66	-0.1	45%	4	1850	1980	
67	-0.3	97%	4	1850	1980	North Ocean City, MD
<b>Average</b>	<b>-1.1</b>					

Table 9. Recent regression of Delaware's ocean coast profile data.

Profile	1964-1999		1982-1999		Comment
	Rate of Change (m/yr)	R <sup>2</sup>	Rate of Change (m/yr)	R <sup>2</sup>	
38	-0.8	19%	-0.8	19%	Cape Henlopen
39	0.4	6%	0.9	79%	
40	-0.3	3%	-0.3	3%	
41	-1.2	45%	-1.2	45%	
42	-1.2	55%	-1.2	55%	
43	-3.0	84%	-3.0	84%	
44	-0.3	4%	-0.3	4%	
44A	0.2	3%	0.2	3%	
44B	-1.6	35%	-1.6	35%	
45	-0.3	4%	-0.3	4%	
45A	-0.5	8%	-0.5	8%	
46	0.3	2%	0.3	2%	
47	-1.2	23%	-1.2	23%	
48	-1.4	48%	-1.4	48%	
49	-0.9	31%	-0.9	31%	
50	-1.9	58%	-1.9	58%	
51	-0.8	28%	-0.8	28%	
52	-1.1	27%	-1.1	27%	
53	-1.3	37%	-1.3	37%	
54	-1.3	48%	-1.3	48%	North of Indian River Inlet
55	0.3	1%	0.9	3%	South of Indian River Inlet
56	0.9	74%	0.9	74%	
57	0.0	0%	0.0	0%	
58	-0.1	4%	-0.1	4%	
59	1.2	54%	1.2	54%	
60	1.5	24%	1.5	24%	
60A	0.8	15%	0.8	15%	
60B	0.7	26%	0.7	26%	
61	0.1	0%	0.1	0%	
62	-0.3	4%	-0.3	4%	
62A	2.4	35%	2.4	35%	
63	-0.5	12%	-0.4	8%	
64	-0.4	6%	-0.4	6%	
65	-0.3	3%	-0.3	3%	
66	0.5	8%	0.7	12%	
67	1.3	22%	1.3	22%	North Ocean City, MD
<b>Average</b>	<b>-0.3</b>		<b>-0.2</b>		

Table 10. Comparison of rates of change obtained by various methods.

Shore Section	Method	Historical			Recent		
		EPR*	EPR	Linear Regression	Linear Regression	Linear Regression	Linear Regression
	Dates Spanned	1843-1961	1850-1980	1850-1980	1962-1994	1982-1994	1964-1999
	Units	(m/yr)	(m/yr)	(m/yr)	(m/yr)	(m/yr)	(m/yr)
	Reference	Belknap and Kraft (1985)	VIMS (2000)	VIMS (2000)	Corps (1996)	Corps (1996)	VIMS (2000)
CH			-2.2	+0.3	+0.9	+0.3	-0.3
1			-2.9	-2.7	-2.0	-1.6	-1.8
2		-1	-1.3	-1.2	-0.5	-0.6	-0.5
3		-1.2	-1.2	-1.2	-2.0	-1.1	-1.2
4		-0.9	-2.0	-1.9	-1.7	-0.8	-0.5
5		-1.1	-1.0	-0.6	-0.4	-0.8	-0.1
6		-0.9	-1.1	-1.0	+0.1	-1.1	+0.7
7			-0.9	-0.3	-0.4	-2.1	+0.3

\*EPR=End Point Rate Method

### 4.1.3. Shoreface Retreat

Profile data collected between 1964 and 1982 show a net retreat of the shoreface along Delaware’s coast from the intertidal zone to approximately -9 meters (Figure 15). However, between 1982 and 1999, the data show that, in general, the shoreface has experienced a net accretion, particularly in the nearshore. The beach nourishment placed along the shore in the last 28 years has eroded from the shoreline, but it has been deposited farther offshore. After the 1962 storm, eight beach nourishment projects were done with the largest (1.1 million m<sup>3</sup>) just north of Indian River Inlet bringing the total to about 2.0 million m<sup>3</sup> (Valverde *et al.*, 1999). Between 1963 and 1982, about 1.2 million m<sup>3</sup> was placed north of Indian River Inlet. It was not until after 1982 that further beach nourishment projects were performed particularly at Dewey Beach, Bethany Beach and Fenwick Island. Between 1982 and 1994, another 630,800 m<sup>3</sup> was placed north of Indian River Inlet for a total sand placement of about 2.5 million m<sup>3</sup> along the Delaware Coast between 1963 and 1994.

Table 11. Regression analysis of profile data taken at Dewey Beach.

Profile	1991-1994		1994-1998		1998-1999	
	Rate of Change (m/yr)	R <sup>2</sup>	Rate of Change (m/yr)	R <sup>2</sup>	Rate of Change (m/yr)	R <sup>2</sup>
145	-0.3	0.1%	-4.3	20.4%	-2.2	1.7%
140	-8.2	25.1%	-6.2	35.2%	-81.8	100.0%
135	-4.2	12.0%	-6.7	43.7%	-29.1	86.2%
130	-11.2	38.6%	-7.1	41.2%	-37.8	93.7%
125	-8.3	24.1%	-8.3	51.5%	-59.0	95.1%
120	-3.9	26.4%	-8.6	51.8%	-35.5	78.3%
115	-7.4	25.4%	-9.6	53.2%	-52.4	94.2%
110	-4.7	18.0%	-10.9	64.3%	-38.0	81.4%
105	-6.8	37.4%	-8.4	36.7%	-31.4	89.5%
100	-4.3	9.7%	-9.5	54.8%	-43.9	91.6%
225	-3.6	10.7%	-4.5	22.3%	-17.2	63.5%
230	-5.9	15.0%	-4.1	22.1%	-3.5	6.8%
<b>Average</b>	<b>-5.7</b>		<b>-7.4</b>		<b>-36.0</b>	

The profiles depicted in Figure 15 are representative of portions of the Delaware coast (*i.e.* headlands and barriers). Analysis of data from the three dates shows that the entire shoreface profile had a net recession between 1964 and 1982 eroding the sand placed in the large beach nourishment project of 1962. Not only did the shoreline recede but the shoreface at the -3, -4.6, -6.1, and -7.6 m (-10, -15, -20, and -25 ft) contours eroded as well (Table 12). In contrast, between 1982 and 1999, 5 of the 10 profiles receded at the beach, particularly those on the north end, but all profiles showed a net advance at the subaqueous contours. It would appear that the nourishment, although lost from the shoreline, has moved offshore and remained, abating the shoreface retreat for now. The consequence is that shoreface processes are being influenced by beach nourishment projects and that shoreface erosion/accretion is occurring on beach fill rather than the underlying geology. This generally agrees with Bosma and Dalrymple (1997) who, utilizing the same data, found that since 1982, the shorelines south of Indian River Inlet have shown accretion rather than erosion indicating recent preventative measures (*i.e.* beach nourishment) have been beneficial.

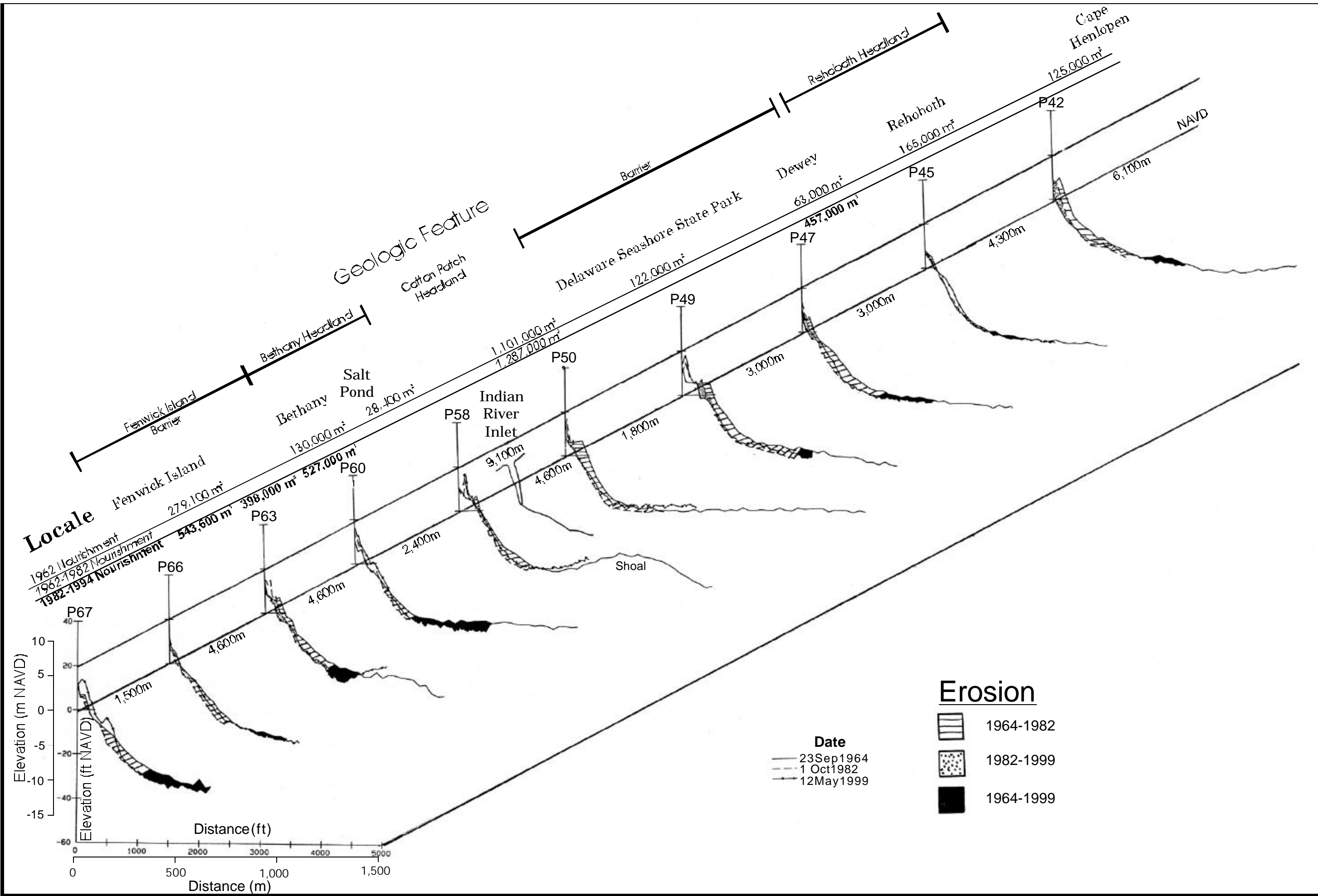


Figure 15. Erosion of the shoreface represented by beach profiles taken in 1964, 1982, and 1999.



Table 12. Shoreface rate of change by offshore contour.

Profile	0 contour			-3.0 m contour		
	1964-1982	1982-1999	1964-1999	1964-1982	1982-1999	1964-1999
	(m/yr)	(m/yr)	(m/yr)	(m/yr)	(m/yr)	(m/yr)
42	-1.62	-1.77	-1.69	-2.04	-0.94	-1.51
45	-0.48	-0.17	-0.33	0.11	1.44	0.75
47	-1.15	-0.81	-0.99	-3.09	1.13	-1.07
49	-2.00	-2.10	-2.05	-2.88	0.60	-1.22
50	-3.08	0.09	-1.56	-2.12	0.74	-0.75
58	-0.86	0.51	-0.20	-1.44	0.92	-0.31
60	0.27	0.97	0.60	-0.51	1.33	0.37
63	-1.23	-1.15	-1.19	-1.19	0.58	-0.34
66	-0.83	0.73	-0.08	-1.71	1.63	-0.11
67	-0.41	1.90	0.70	-1.61	3.41	0.80
<b>Avg.</b>	<b>-1.14</b>	<b>-0.18</b>	<b>-0.68</b>	<b>-1.65</b>	<b>1.08</b>	<b>-0.34</b>
Profile	-4.6 m contour			-6 m contour		
	1964-1982	1982-1999	1964-1999	1964-1982	1982-1999	1964-1999
	(m/yr)	(m/yr)	(m/yr)	(m/yr)	(m/yr)	(m/yr)
42	-3.54	0.26	-1.72	-5.54	1.93	-1.96
45	0.47	1.07	0.75	0.22	1.14	0.66
47	-3.73	1.40	-1.27	-3.62	0.68	-1.56
49	-3.32	0.63	-1.43	-4.49	0.63	-2.04
50	-2.25	0.68	-0.84	-3.01	1.85	-0.68
58	-1.54	0.84	-0.40	-3.83	1.74	-1.16
60	-1.42	1.07	-0.23	-2.56	1.46	-0.63
63	-2.65	0.05	-1.36	-3.18	0.19	-1.57
66	-1.81	1.06	-0.44	-2.46	1.62	-0.50
67	-3.47	3.10	-0.32	-3.06	0.71	-1.25
<b>Avg.</b>	<b>-2.33</b>	<b>1.02</b>	<b>-0.73</b>	<b>-3.15</b>	<b>1.20</b>	<b>-1.07</b>
Profile	-7.6 m contour					
	1964-1982	1982-1999	1964-1999			
	(m/yr)	(m/yr)	(m/yr)			
45	-0.94	0.61	-0.20			
47	-3.56	-0.85	-2.26			
49	-8.19	1.96	-3.33			
50	-9.60	N/A	N/A			
58	-3.87	0.93	-1.57			
60	-4.27	1.30	-1.60			
63	-2.89	-0.69	-1.84			
66	-3.33	2.03	-0.76			
67	-4.40	-0.04	-2.31			
<b>Avg.</b>	<b>-4.46</b>	<b>0.80</b>	<b>-1.64</b>			

## 4.2. Maryland

### 4.2.1. Historic Shoreline Change

In Maryland, less historical shoreline coverage exists for Fenwick Island. Coverage for 1850 to 1929 showed erosion at the MD-DE state line, then a shoreline advance along the northern half of Maryland's Fenwick Island, followed by shoreline recession on the lower half down to Ocean City Inlet (Figure 14). The 1942 shoreline is only given for the southern third of Fenwick Island. These data show significant accretion north of the inlet, most likely in response to construction of the jetties. Between 1962 and 1980, there is a general balance of erosion and advance along the Fenwick Island shoreline. The lack of significant accretion at the channel jetties is somewhat unexpected.

Linear regression of the shoreline position data at the Fenwick Island profile locations shows overall erosion of the shoreline except at profiles 1, 2 and 4 (adjacent to and north of the channel jetties) for the period 1850 to 1980 (Table 13). This accretionary trend also occurs in the analysis from 1929-1980 up to profile 9. The 1929-1980 occurred mostly after the construction of the Ocean City Inlet jetties. The remainder of the shoreline northward shows an increase in erosion rates.

### 4.2.2. Recent Shore Change

Until the major beach fill project in 1988, the main influences on the Fenwick Island shoreline were the extensive groin system and the emergency beach fill of over 800,000 m<sup>3</sup> in 1963. In 1988, about 2.1 million m<sup>3</sup> of sand was placed alongshore as part of a state/local project (Valverde *et al.*, 1999). In 1990-1991 about 2.9 million m<sup>3</sup> of sand was placed alongshore as part of a Federal project. Both nourishment projects utilized sand mined by dredge from borrow sites about 3.7 km off the south end of Ocean City and about 4 km offshore just south of the MD-DE state line.

The 1988 Maryland state nourishment project was designed to widen 13.4 km (8.35 miles) of beach to a uniform width of 67 m from its average width of 40 m. The 1991 project was one of the longest continuous beach fill projects constructed in one season in the United States. At its northern end, the project tied into a previously nourished beach in Delaware (Maryland Geological Survey, unpublished). About two-thirds of the sand used in the project was mined from "Area 2;" the remainder from "Area 3."

Table 13. Maryland historic regression analysis results.

Profile	1850-1980			1929-1980			Comments
	Rate of Change (m/yr)	R <sup>2</sup>	No. points	Rate of Change (m/yr)	R <sup>2</sup>	No. points	
1	0.9	22%	5	2.6	87%	4	North of Ocean City Inlet Jetty
2	0.4	7%	5	3.7	89%	4	
4	0.1	0%	5	2.6	87%	4	
6	-0.5	43%	5	0.6	25%	4	
8	-0.6	41%	5	0.8	35%	4	
9	-1.0	79%	5	0.2	12%	4	
10	-1.2	87%	5	-0.1	12%	4	
12	-0.9	86%	5	-0.5	24%	4	
13	-0.7	99%	5	-0.6	92%	4	
15	-0.7	86%	5	-0.1	7%	4	
17	-1.0	94%	4	-1.0	68%	3	
18	-0.8	99%	4	-1.0	100%	3	
20	-0.3	59%	4	-1.0	97%	3	
22	-0.5	32%	4	-2.2	88%	3	
24	-0.6	31%	4	-2.6	96%	3	
26	-0.5	29%	4	-2.2	89%	3	
27	-0.4	36%	4	-1.8	99%	3	
29	-0.3	32%	4	-1.5	97%	3	
30	0.1	1%	4	-1.2	71%	3	
32	-0.1	3%	4	-1.7	93%	3	
34	-0.1	1%	4	-1.7	93%	3	
36	-0.2	16%	4	-1.4	90%	3	
38	-0.4	54%	4	-1.2	94%	3	
40	-0.4	58%	4	-1.2	99%	3	
42	-0.8	96%	4	-1.0	93%	3	
44	-0.8	91%	4	-1.5	98%	3	Near MD-De Line
45	-0.7	95%	4	-1.0	97%	3	240 m North of Line
46	-0.8	89%	4	-1.4	99%	3	600 m North of Line
<b>Average</b>	<b>-0.5</b>			<b>-0.6</b>			

The federally funded second phase of the project was to provide hurricane (100 year storm) protection and extended 520 m into Delaware. About 40 percent of the sand was mined from “Area 2 ” and 60 percent from “Area 3.” The construction included a vegetated dune along most of its length (Maryland Geological Survey, unpublished).

“Area 2” was a shoal located about 3.7 km (1 mile) offshore of southern Ocean City. It was an elongated linear shoal with three crests identifiable on the 10 m isobath. The most suitable sand for beach nourishment was located on the western flank of the southern crest. The two phases of the project essentially exhausted the resource (Wells, 1994)

“Area 3” is 3 to 3.5 km (2 to 2.25 miles) offshore on a seaward extension of the Maryland-Delaware boundary. The large shoal contains medium grained sand that was very well suited for the project (Wells, 1994; Maryland Geological Survey, unpublished)

Initial monitoring Ocean City beach fills are summarized in Stauble *et al.* (1993) for selected profiles. Table 14 relates the profile number of the 1993 profiles to the street location. Analysis of the data yields several trends and identifies “hot spots” or areas of chronic beach loss. The hot spots generally are attributed to the position of shore attached linear shoals between 37<sup>th</sup> Street (profile 13) and 103<sup>rd</sup> Street (profile 32) (Figure 16). Areas where the deeper water between the shoals comes close to the shore, particularly 81<sup>st</sup> Street, are reportedly the chronic “hot spots” between “headland” shore attached shoals.

Two significant northeasters occurred in 1989 and 1991 and had a significant impact on the patterns and rates of beach change. In particular, sand was driven offshore, accentuating the “hot spot”. (Stauble *et al.*, 1993). The fate of the state-funded fill is clearly seen and primarily is due to the impacts of the March 1989 storms (Figure 17 and Figure 18). Erosion of the subaerial beach is apparent along with a parallel gain in the nearshore. The same pattern holds for the federal fill as impacted by the Halloween (“Perfect”) Storm of 1991 and a storm in January 1992 (Figure 19 and Figure 20).

Stauble *et al.* (1993) summarized volume change from the pre-State fill condition of the beach through time for Ocean City for the first 28-month period (Figure 21). The combined gains and losses included both above and below NGVD volumes. The general trend was one of accretion along the profile length at all locations. Stauble *et al.* (1993) found that, in general, the losses from the subaerial beach were balanced by gains in the nearshore so the net volume change on the 900-ft long profiles was accretionary after the beach fills. The pattern of adjustment varied alongshore as the material redistributed across the

profile. The storms in 1989 had a significant impact on the shoreline as some profiles eroded and others accreted. As of January 1992, the total project performance of both the State and Federal fills indicated that the shoreface at Ocean City has 260 m<sup>3</sup>/m of sand more than before the first fill was placed. Stauble *et al.* (1993) found that most of this material is located in the nearshore, below NGVD.

Table 14. Ocean City Beach condition on October 1995.

Profile	Street	Condition
1	S. 1st	100 Year +
2	Dorchester	100 Year +
4	3rd	100 Year +
6	10th	100 Year +
8	15th	100 Year +
9	20th	100 Year +
10	25th	100 Year +
12	32nd	100 Year +
13	37th	100 Year +
15	45th	100 Year +
17	52nd	100 Year +
18	56th	100 Year +
20	63rd	100 Year +
22	69th	100 Year +
24	74th	100 Year
26	78th	100 Year
27	81st	100 Year
29	86th	100 Year
30	92nd	100 Year +
32	100th	100 Year ?
34	112th	100 Year
36	120th	100 Year
38	124th	100 Year
40	132nd	100 Year +
42	138th	100 Year
44	146th	100 Year -

The general trend over the total profile supports the premise that areas of erosion and loss of fill are located where profiles were steepest and located near the point of connection of the shoreface-attached shoal with the shoreline. The survey lines that retained the most volume of fill were profiles that had a bar/trough configuration or were located in the lee of the shoreface-attached shoal.

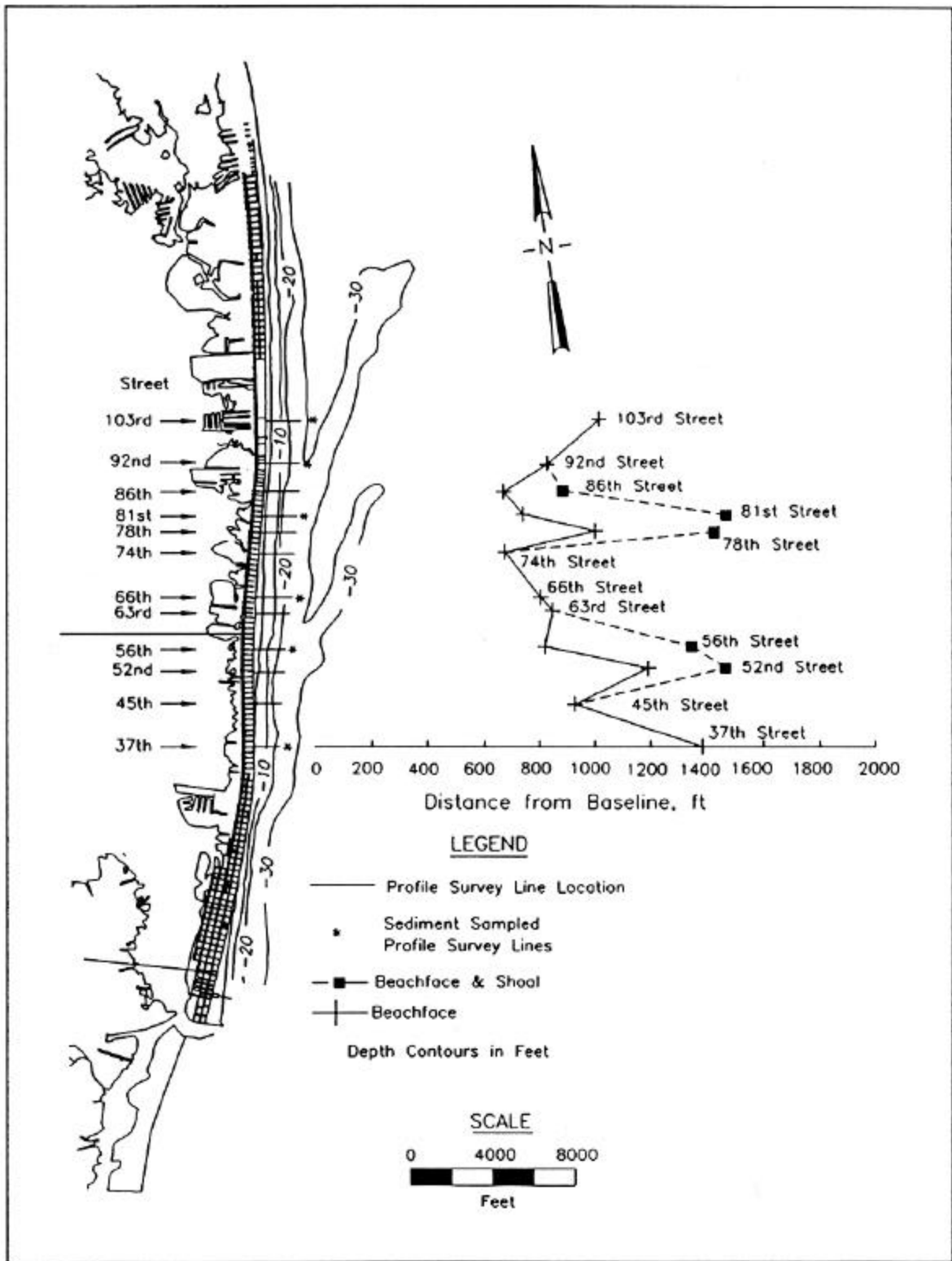


Figure 16. Alongshore variability in seaward distance of active profile envelope relative to the two shoreface-attached shoals (Stauble *et al.*, 1993).

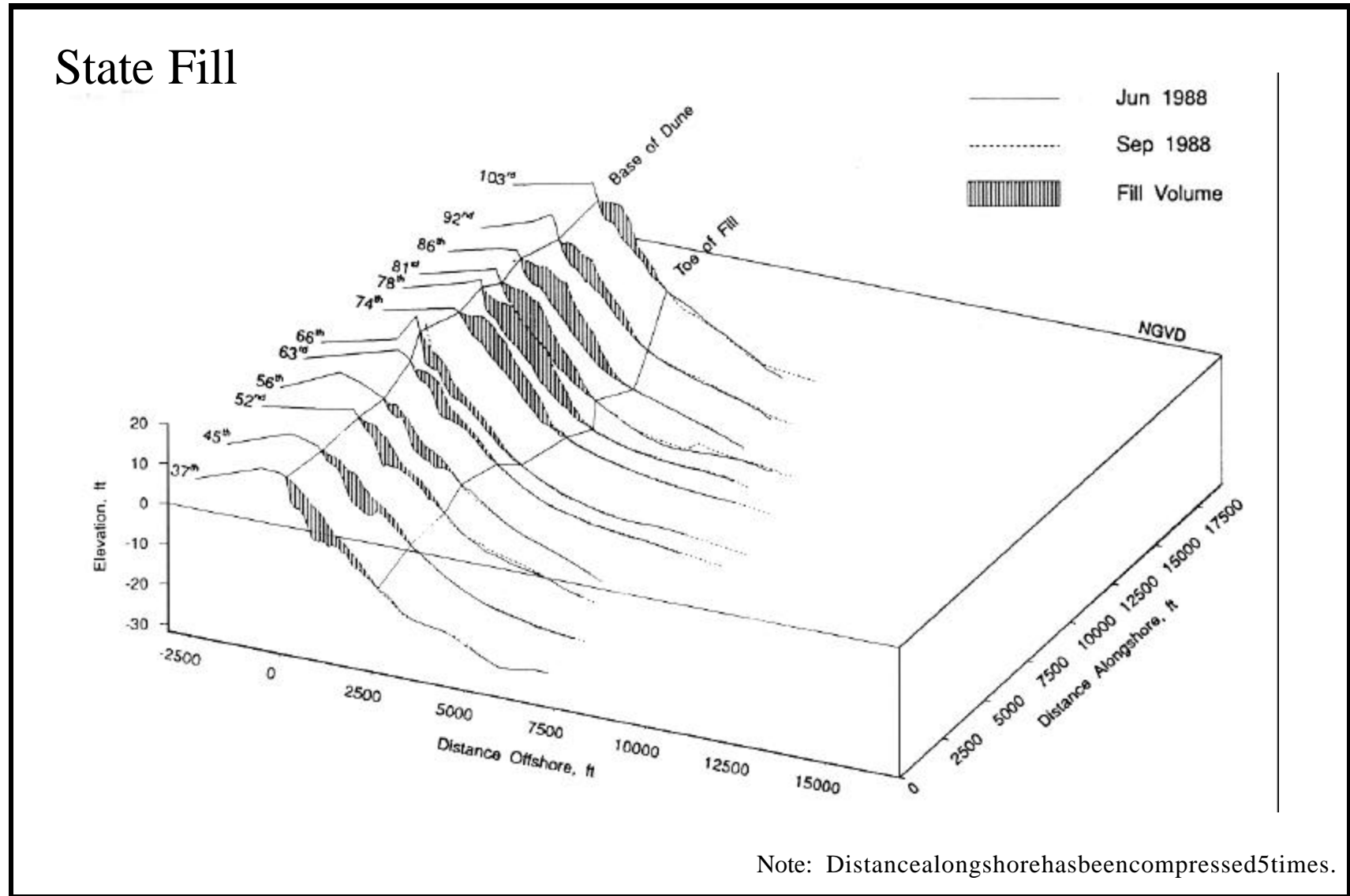


Figure 17. Three-dimensional plot of pre-and post-state fill beach profiles (Stauble *et al.*, 1993).



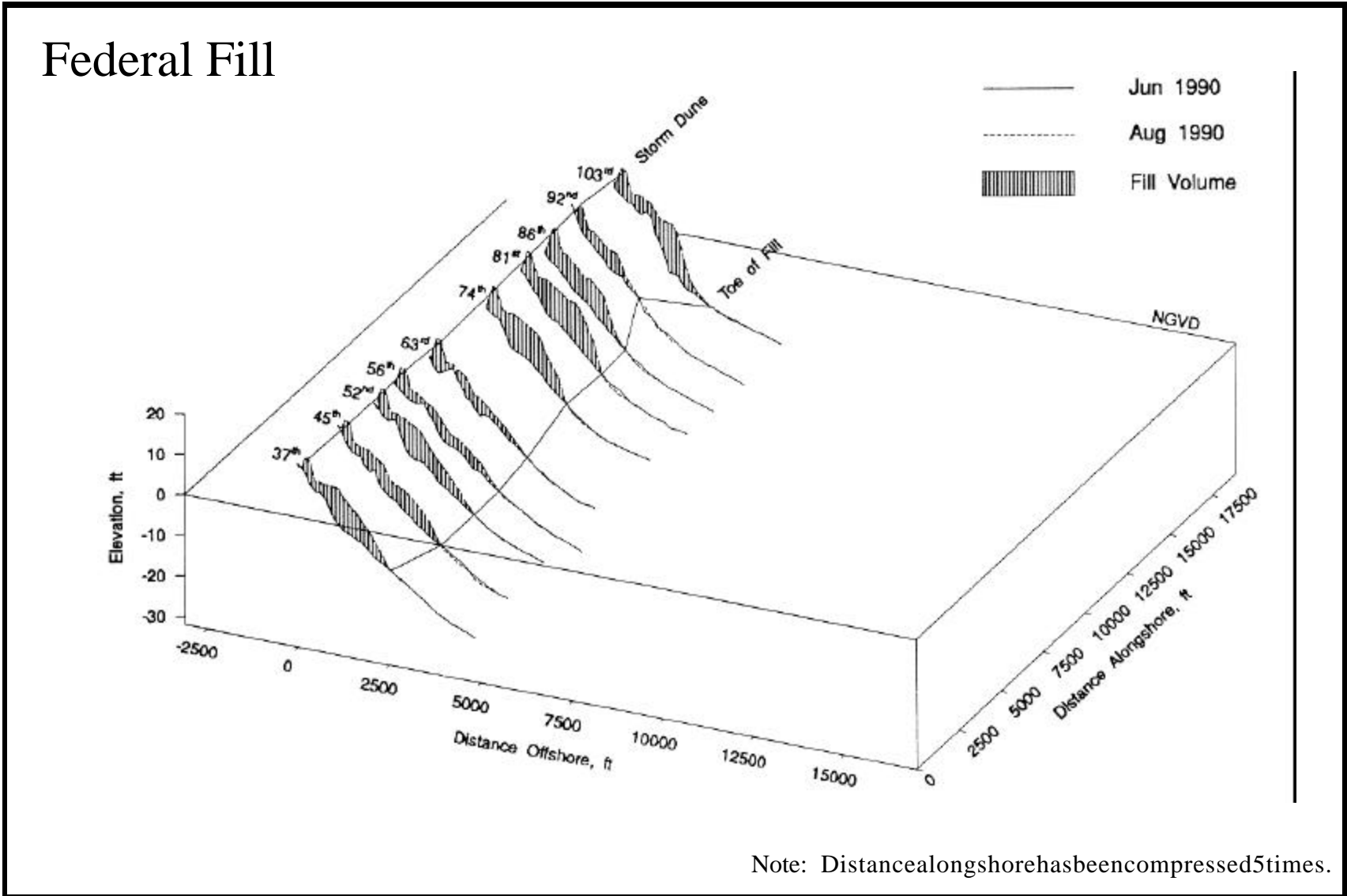
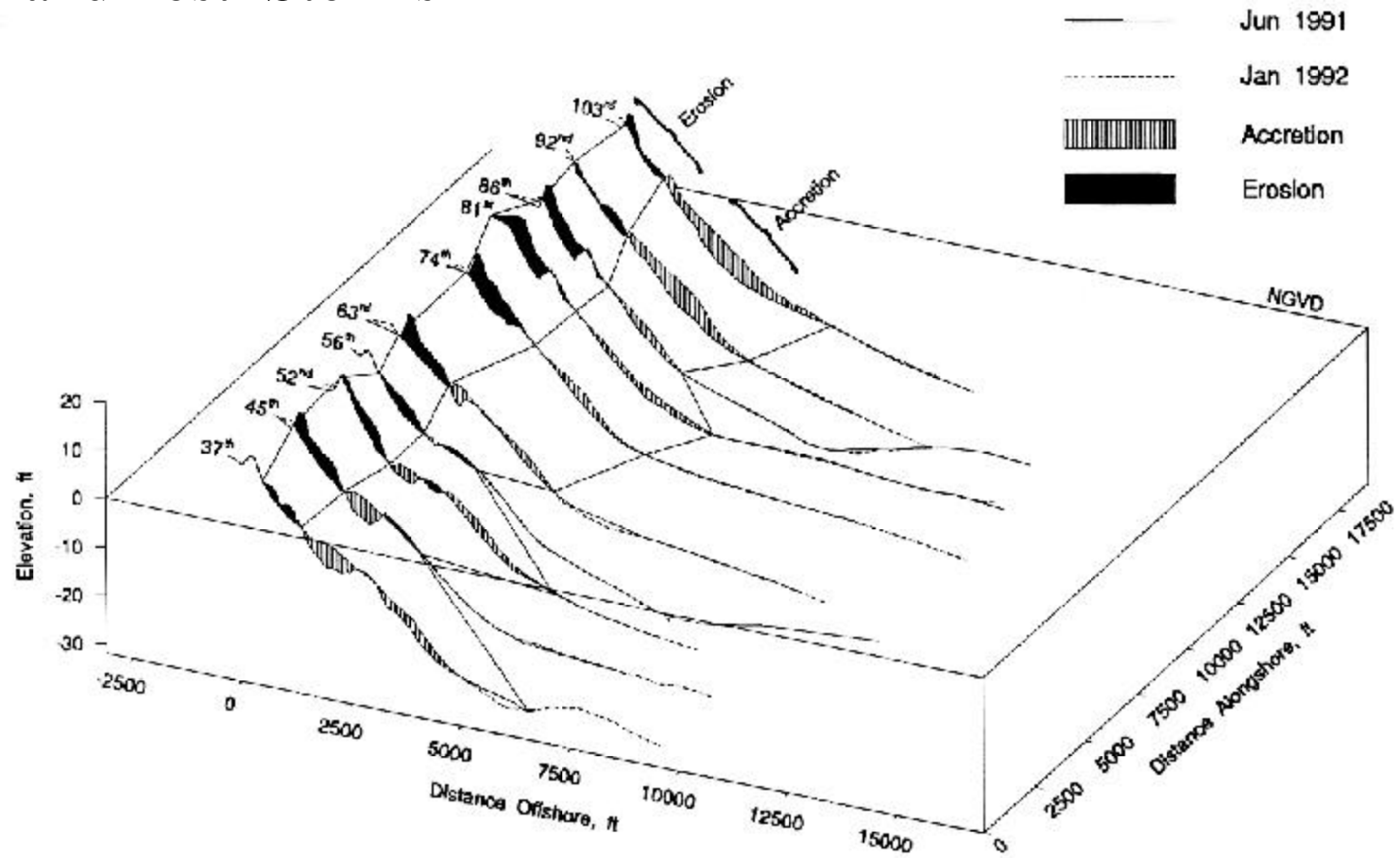


Figure 19. Three-dimensional plot of pre-and post-federal fill beach profiles (Stauble *et al.*, 1993).

# Pre- and Post- Storms



Note: Distance along shore has been compressed 5 times.

Figure 20. Three-dimensional plot of federal fill pre-and post-storm beach profiles (Stauble *et al.*, 1993).

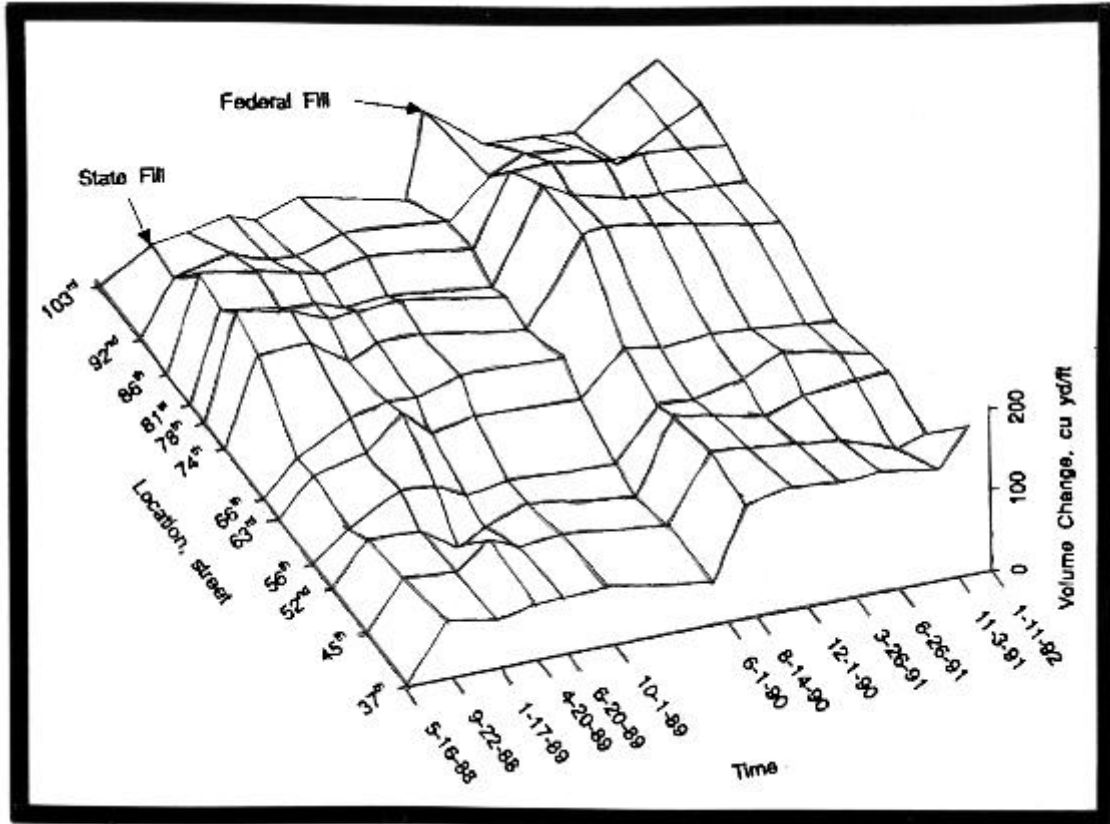


Figure 21. Percent of fill remaining above NGVD, below NGVD, and over the total profile length after the 28 month state and federal fill monitoring as measured from September 1988 to January 1992 (Stauble *et al.*, 1993).

Monitoring continues on the Ocean City beach. Summary data from project data reports are presented in Tables 14, 15, 16, and 17 for surveys between 1995 to 1997. These data show that “hot spots” continue, particularly at 81<sup>st</sup> Street and 146<sup>th</sup> Street. One must remember that the data are for major beach fills along Ocean City. To measure how the overall shoreline condition has changed, a linear regression analysis was performed (Table 18). This data is most significant for the data set extending from June 1988 to Oct 1997 between 32<sup>nd</sup> and 81<sup>st</sup> Streets (profiles 13 through 27). Although known “hot spots” occur through the reach, the net trend from June 1988 (initial pre-fill) is accretionary. This would indicate that there has been a reversal in historic rates due to anthropogenic impacts (*i.e.* beach nourishment) which initially were all erosional along this reach.

Table 15. Ocean City Beach Condition Assessment Table for May 1996.

Profile	Street	Volume Change (Oct95-May96)	Shoreline Change (Oct95-May96)	Satisfies Design Protection Level
1	S. 1st	-3 yd <sup>3</sup> /ft	-36 ft	yes
2	Dorchester	-45	-81	yes
4	3rd	-11	-35	yes
6	10th	+26	0	yes
8	15th	0	-12	yes
9	20th	-4	-20	yes
10	25th	-11	-26	yes
12	32nd	+8	-23	no
13	37th	-14	-36	yes
15	45th	+20	-16	yes
17	52nd	-2	-22	yes
18	56th	-15	-62	yes
20	63rd	+4	-38	yes
22	69th	-24	-50	yes
24	74th	-17	-14	yes
26	78th	-13	-32	marginal
27	81st	-6	-52	no
29	86th	-5	-33	yes
30	92nd	-16	-39	yes
32	100th	+27	-4	yes
34	112th	-5	-39	yes
36	120th	-9	-46	yes
38	124th	-6	-44	yes
40	132nd	-7	-28	yes
42	138th	-4	-33	yes
44	146th	-9	-83	no
45	240 m North of State Line	+37	-45	transition
46	600 m North of State Line	+21	-46	transition

Table 16. Ocean City Beach Condition Assessment in June 1997.

Profile	Street	Project Condition
4	3rd	100 yr
6	10th	>100 yr
8	15th	marginal
9	20th	100 yr
10	25th	>100 yr
12	32nd	<100 yr
13	37th	>100 yr
15	45th	>100 yr
17	52nd	>100 yr
18	56th	>100 yr
20	63rd	>100 yr
24	74th	Deficient
26	78th	Deficient
27	81st	Deficient
29	86th	<100 yr
30	92nd	>100 yr
32	104th	<100 yr
34	112th	Deficient
36	120th	<100 yr
38	124th	<100 yr
40	132nd	>100 yr
42	138th	100 yr
44	146th	Deficient

#### 4.2.3. Shoreface Retreat

Before the major beach fills along Ocean City, the historical trend from 1929 to 1980 is a higher erosion rate between the shoals (on either side of 81<sup>st</sup> Street) relative to the shore attached shoals at 37<sup>th</sup> and 103<sup>rd</sup> Streets. The longer term trend between 1850 and 1980 was still erosional but less severe. Although the “hot spot” in the area of 81<sup>st</sup> Street seems to have persisted through recent data, the actual shoreline has advanced with ongoing beach fills. Therefore, the implication is that shoreface retreat has also been arrested for the time being.

Table 17. Ocean City Beach Condition Assessment Table for October 1997.

Profile	Street	Volume Change May-Oct 1997	Condition
1	S. 1st	-13.6 cy/ft	Beyond Project Limits
2	Dorchester	+41.6	Beyond Project Limits
4	3rd	+2.3	100 yr +
6	10th	-18.6	100 yr
8	15th	-7.4	Deficient
9	20th	+6.0	100 yr
10	25th	+6.0	100 yr
12	32nd	-8.2	100 yr
13	37th	-6.8	100 yr +
15	45th	-5.2	100 yr +
17	52nd	+22.1	100 yr +
18	56th	+11.8	100 yr +
20	63rd	-10.8	100 yr +
22	69th	+8.9	100 yr +
24	74th	-1.0	Deficient
26	78th	+6.3	Deficient
27	81st	-3.4	Deficient
29	86th	-7.3	Deficient
30	92nd	-0.7	100 yr +
32	100th	+0.9	100 yr -
34	112th	+1.8	Deficient
36	120th	+3.1	100 yr
38	124th	-3.4	100 yr
40	132nd	+0.0	100 yr +
42	138th	-11.9	100 yr
44	146th	-9.2	Deficient

Table 18. Maryland recent regression analysis results.

Profile	R <sup>2</sup>	Rate of Change (m/yr)	No. points	Dates Spanned
1	100%	-6.2	2	Feb 1994 - Oct 1997
4	53%	2.1	3	Feb 1994 - Oct 1997
8	79%	-3.1	3	Feb 1994 - Oct 1997
10	76%	-0.3	3	Feb 1994 - Oct 1997
13	87%	4.2	5	June 1988 - Oct 1997
17	75%	4.2	5	June 1988 - Oct 1997
20	75%	4.2	5	June 1988 - Oct 1997
24	87%	3.5	5	June 1988 - Oct 1997
27	83%	2.5	5	June 1988 - Oct 1997
30	90%	4.5	5	June 1988 - Oct 1997
34	71%	5.2	3	Feb 1994 - Oct 1997
38	15%	1.1	3	Feb 1994 - Oct 1997
44	95%	4.9	3	Feb 1994 - Oct 1997

### 4.3. Wave Analysis

Maa and Kim (2000) have evaluated the regional wave environment for the purpose of evaluating the potential impacts of mining Fenwick Shoal and Isle of Wight Shoal which are located on the north and south sides of the MD-DE boundary respectively (Figure 7). Their analysis of present conditions shows the impacts of the shore attached-shoals on waves that reach the shoreline between Ocean City Inlet on the south to Bethany Beach to the north. This region is exposed primarily to waves from the east northeast through the southeast. A significant high frequency deep water wave condition for each of these directions is wave period of 10 s and wave height of 2 m. The results of Maa and Kim's analysis of the transformation that would be experienced by these wave conditions are shown in Figure 22. In Maryland, the highest rates of erosion occurred midway between Ocean City Inlet and the Maryland-Delaware state line. This same area was shown to be an erosional "hot spot" by a study performed on profile data taken between 1988 and 1992.

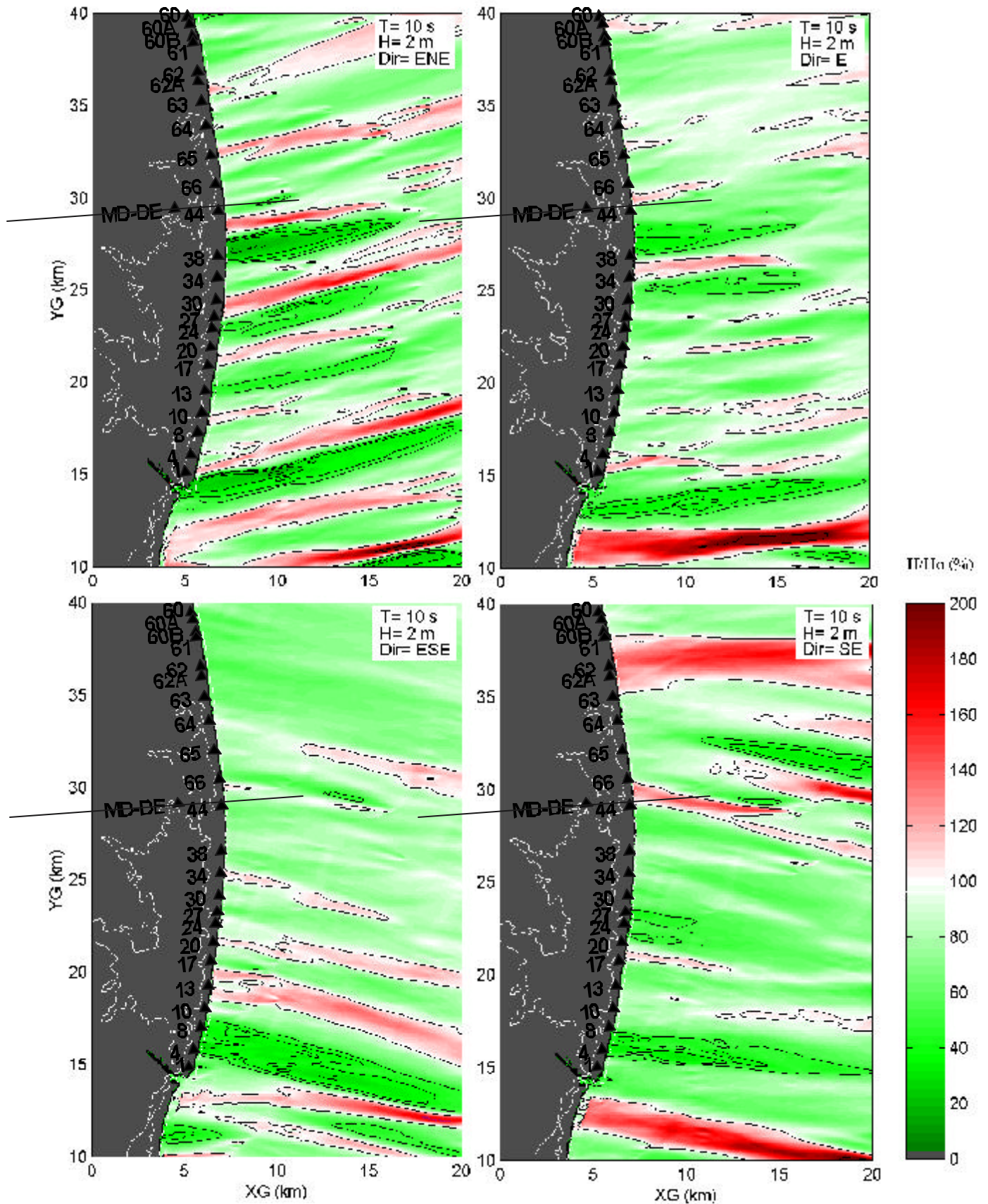


Figure 22. Normalized wave height distribution offshore of Delaware and Maryland in the vicinity of the proposed dredging sites (Maa and Kim, 2000).

## 5. CONCLUSION

The ocean shore of Delaware and Maryland is a highly utilized resource. Much of it has been modified with bulkheads, groins, jetties around two inlets, and several substantial episodes of beach nourishment in a continuing effort to maintain the viability of the beach as a recreational, residential, and commercial attraction. The long term history of the shore is one of retreat. Storm waves are the most obvious agent of shoreline erosion, but continuing sea-level rise is a major contributing factor. The jetties at Ocean City, Maryland, and Indian River Inlet, Delaware had predictable major impacts on longshore sediment transport.

It appears that the cumulative magnitude of beach nourishment in some locations appears to have modified the local processes. While the actual shoreline has continued to retreat, sand removed from the (formerly) subaerial beach has remained in the subaqueous nearshore. There it has modified the natural beach profile. The new longer, thus “flatter,” profile has the potential to dissipate more wave energy and provide some protection to the high beach. This beneficial consequence of the long program of nourishment would not be visible without an organized program of monitoring the shore and profiling the beach. The progressively positive influence of successive beach nourishment projects suggests that future nourishment projects have a relatively high likelihood of success, assuming the rate of sea-level rise does not accelerate and other factors remain relatively constant.

Sites of chronically greater rates of shoreline erosion (“hot spots”) are related to patterns of wave refraction governed by the regional wave climate and the location of offshore shoals. Modification of those shoals by sand mining will alter the specific patterns of wave refraction but might not have significant impact on the shoreline situation. This is especially true if residual sand from beach nourishment winds up in the nearshore where it has the potential to cause larger waves to break farther offshore. Knowing this, nourishment projects could be designed to modify both the active recreational beach and the generally invisible but important nearshore.

This study focused on shoreline change which is only part of the story. Perhaps the most intriguing aspect of this study was the nature of shoreface retreat in light of the mobile linear ridges and ongoing beach nourishment projects. In particular, the Delaware profile data set should be analyzed further to better detail the offshore profile changes. We suggest future efforts toward this understanding. If Maryland profile data became available, the offshore area could be assessed as well.

## 6. REFERENCES

- Anders, F. J. and M. R. Byrnes, 1991. Accuracy of shoreline change rates as determined from maps and aerial photos. *Shore and Beach*, 59: 17-26.
- Beach-Net Website, 2000. <http://www.beach-net.com/aerialphotos/>
- Belknap, D.F. and J.C. Kraft, 1985. Influence of antecedent geology on stratigraphic preservation potential and evolution of Delaware's barrier systems. *Mar. Geo.* 63:235-262
- Bosma, K.F. and Dalrymple, R.A., 1997. Beach Profile Analysis Along the Delaware Atlantic Coastline. University of Delaware, Newark, Delaware, 165pp.
- Carr, A.P., Blackley, M.W.L., and King, H.L., 1982. Spatial and seasonal aspects of beach stability. *Earth Surface Processes Landforms* 7:267-282.
- Clausner, J.E., Gerbert, J.A., Rambo, A.T., and Watson, K.D., 1991. Sand bypassing at Indian River Inlet, Delaware. *Proceedings Coastal Sediments '91*, American Society of Civil Engineers, NY, pp 1177-1191.
- Crowell, M., Leatherman, S. P., and Buckley, M. K., 1991. Historical shoreline change: Error analysis and mapping accuracy. *Journal of Coastal Research*, 7(3): 839-852.
- Crowell, M., B. C. Douglas, and S. P. Leatherman, 1997. On forecasting U.S. shoreline positions: A test of algorithms. *Journal of Coastal Research*, 13(4): 1245-1255.
- Dean, R.G. and Perlin, M., 1977. Coastal engineering study of Ocean City Inlet, Maryland. *Proceedings Coastal Sediments '77*, American Society of Civil Engineers, NY, pp 520-542.
- Delaware Geological Survey, 1988. Texture of beach sands - Atlantic coast of Delaware. An Initial Report of SEASIP. July 12, 1988.
- Dick, J.E. and Dalrymple, R.A., 1983. Coastal Engineering Study of Bethany Beach, Delaware. Ocean Engineering Research Report No. CE 83-38, University of Delaware, Newark, Delaware 19716.
- Dolan, R., M. S. Fenster, and S. J. Holme, 1991. Temporal analysis of shoreline recession and accretion. *Journal of Coastal Research*, 7(3): 723-744.
- Dolan R., B. P. Hayden, and J. Heywood, 1978. A new photogrammetric method for determining shoreline erosion. *Coastal Engineering*, 2: 21-39.
- Dolan, R., P. May, and S. May, 1980. The reliability of shoreline change measured from aerial photographs. *Shore and Beach*, 48: 22-29.
- Dubois, R.N., 1988. Seasonal Changes in Beach Topography and Beach Volume in Delaware. *Marine Geology* 81:79-96.
- Elliott, I. and D. Clarke, 1989. Temporal and spatial bias in the estimation of shoreline rate-of-change statistics from beach survey information. *Coastal Management*, 17: 129-156.
- Ellis, M. Y. (ed.), 1978. *Coastal Mapping Handbook*. U. S. Department of the Interior, Geological Survey; U. s. Department of Commerce, National Ocean Service; U. S. Government Printing Office, Washington, D. C., 199p.
- Everts, C. H., J. P. Battley, Jr., and P. N. Gibson, 1983. Shoreline Movements: Report 1: Cape Henry, Virginia to Cape Hatteras, North Carolina, 1849-1989. Technical Report CERC-83-, Report 1. U. S. Army Corps of Engineers.
- Fenster, M.S., Dolan, R., and Elder, J.F., 1993. A new method for predicting shoreline positions from historical data. *Journal of Coastal Research*, 9(1): 147-171.

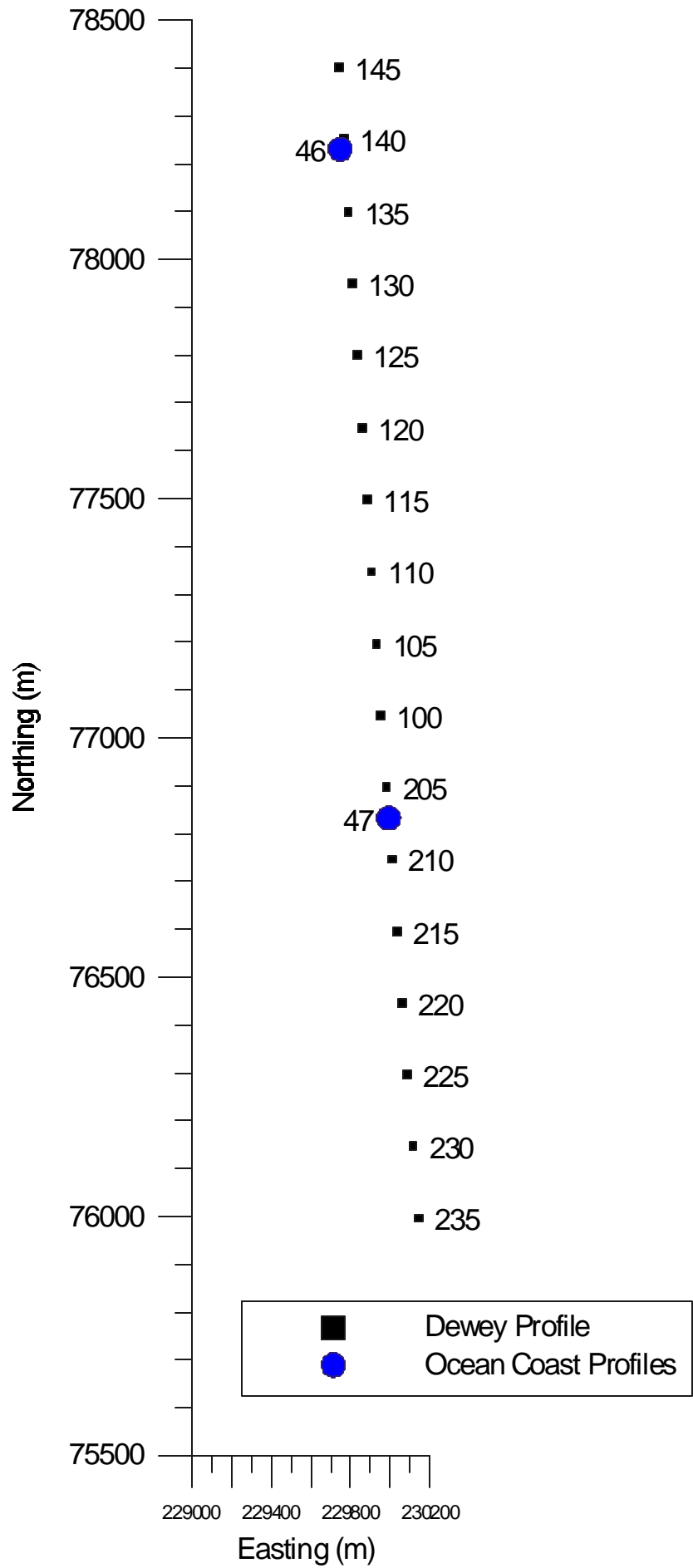
- Foster, E. R. and R. J. Savage, 1989. Methods of historical shoreline analysis, *In: Magoon, O. T., H. Converse, D. Miner, L. T. Tobin, and D. Clark (eds.), Coastal Zone '89*, American Society of Civil Engineers, 5: 4434-4448.
- Gebert, J., Watson, K., and Rambo, A. Q992. 57 years of coast engineering practice at a problem inlet: Indian River Inlet, Delaware. *Coastal Eng. Practice*, ASCE:1-17
- Grosskopf, W.G. and Resio, D.T., 1988. Storm hindcast for Ocean City, Maryland. Draft report to the USAED, Baltimore, Offshore Coastal Technologies, Inc.
- Hayes, M.O. and Boothroyd, J.C., 1969. Storms as modifying agents in the coastal environment. Coastal Research Group, Coastal Environments NE Massachusetts and New Hampshire. University of Massachusetts Department of Geology, Amherst, Massachusetts, pp.245-265.
- House Document No. 105-144, 1997. Beach Nourishment Project. Communication from The Acting Assistant Secretary (Civil Works), the Department of the Army. U.S. Government Printing Office, Washington, 381 pp.
- Kraft, J.C. and John, C.J., 1976. The Geological Structure of the Shorelines of Delaware. University of Delaware, Newark College of Marine Studies, Sea Grant, Report No. DEL-SG-14-76.
- Kraft, J.C., 1971. Sedimentary facies patterns and geologic history of a Holocene marine transgression. *Geological Soc. of Am. Bull.* 82:2131-2158.
- Kraft, J.C., 1977. Late Quaternary paleogeographic changes in the coastal environments of Delaware, Middle Atlantic Bight, related to the archaeological settings. *In: (eds. W.S. Newman and B. Salwen) Amerinds and Their Paleoenvironments in Easter North America. Annals of the New York Academy of Sciences* 288: 35-69.
- Lacey, E.M. and Peck, J.A., 1998. Long-term beach profile variations along the south shore of Rhode Island, USA. *Journal of Coastal Research*, 14(4): 1255-1264.
- Larson, M. and N. C. Kraus, 1994. temporal and spatial scales of beach profile change, Duck, North Carolina. *Marine Geology*, 115: 75-94.
- Leatherman, S. P., 1983. Shoreline mapping: a comparison of techniques. *Shore and Beach*, 51: 28-33.
- Louis Berger Group, 1999. Environmental Report: Use of Federal Offshore Sand Resources for Beach and Coastal Restoration in New Jersey, Maryland, Delaware, and Virginia. OCS Study 99-0036, U. S. Department of the Interior, Minerals Management Service, Office of International Activities and Marine Minerals.
- Maa J. P.-Y and S. C. Kim, 2000. Potential Modifications to Waves Due to Dredging and Other Oceanographic Considerations. Part 4 of Environmental Survey of Potential Sand Resource Sites Offshore Delaware and Maryland. Final Contract Report. Virginia Institute of Marine Science, Gloucester Point, VA.
- Maryland Geological Survey Website, 2000. <http://mgs.dnr.md.gov/goals.html>
- McBeth, F. H., 1956. A method of shoreline delineation. *Photogrammetric Engineering*, 22:400-405.
- McBride, R.A., 1999. Spatial and temporal distribution of historical and active tidal inlets: Delmarva Peninsula and New Jersey, USA. *In: Proceedings Coastal Sediments 1999*: 1505-1521.
- McBride, R.A. and Moslow, T.F., 1991. Origin, evolution, and distribution of shoreface sand ridges, Atlantic inner shelf, USA. *Marine Geology* 97: 57-85.
- Morton, R., 1978. Analysis of sequential shoreline changes., *In: Tanner W. F. (ed.) Standards for Measuring Shoreline Changes*, Report of Workshop, published jointly by Coastal Research and the Department of Geology, Florida State University, 43-48.

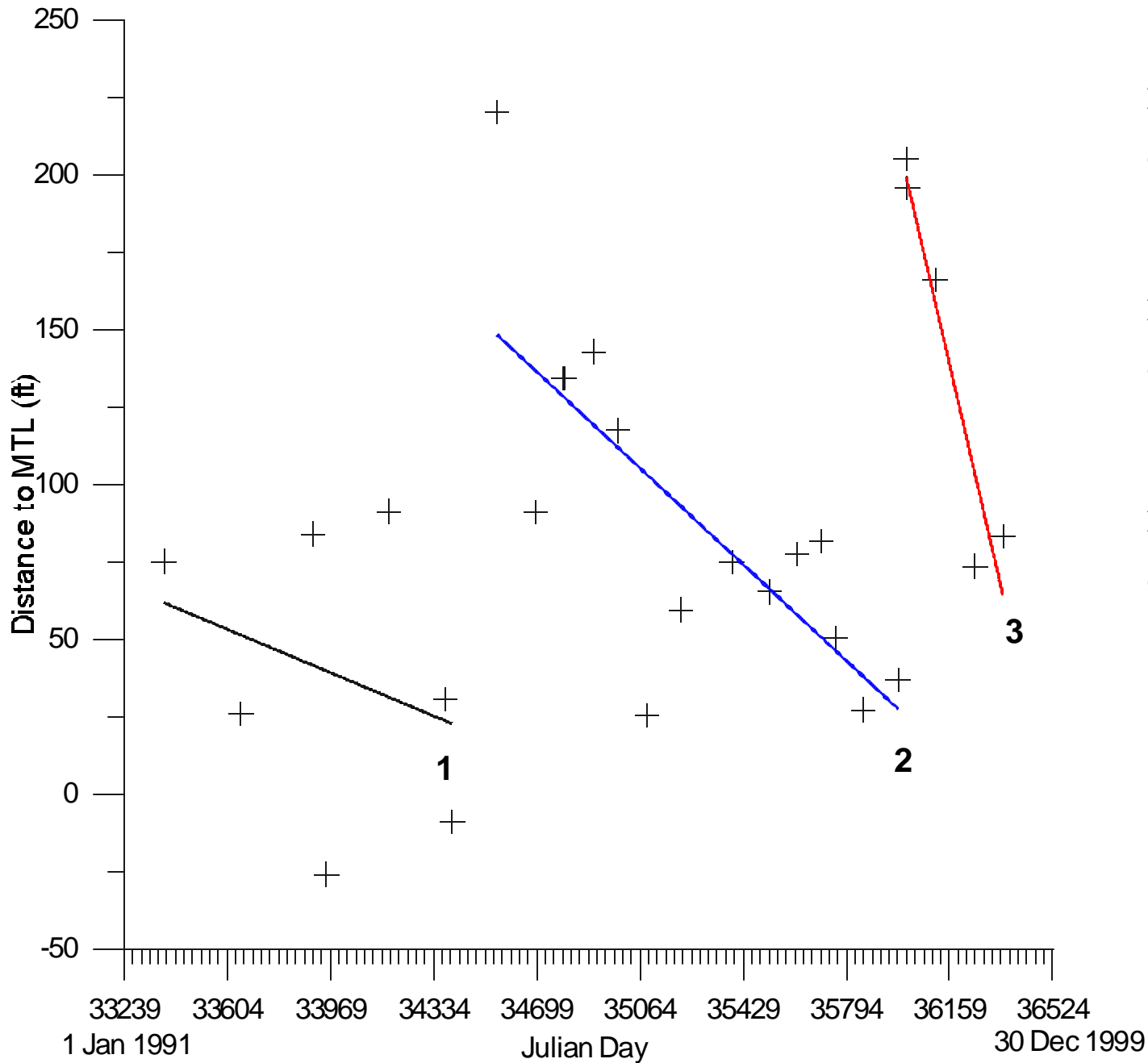
- Morton, R.A. and Speed, F.M., 1998. Evaluation of shorelines and legal boundaries controlled by water levels on sand beaches. *Journal of Coastal Research*, 14(4): 1373-1384.
- NOAA, 1989. Tide Tables. U.S. Department of Commerce, National Oceanic and Atmospheric Administration.
- Ramsey, K.W., Leathers, D.J., Wells, D.V., and Talley, J.H., 1998. Summary Report: The Coastal Storms of January 27-29 and February 4-6, 1998, Delaware and Maryland. Open File Report No. 40, Delaware Geological Survey, University of Delaware, Newark, DE, 43p.
- Shalowitz, A. L., 1964. *Shore and Sea Boundaries*, v. 2. U. S. Department of Commerce, Publication 10-1, U. S. Government Printing Office, Washington, D. C., 749p.
- Smith, G. L., and G. A. Zarillo, 1990. Calculating long-term shoreline recession rates using aerial photographic and beach profiling techniques. *Journal of Coastal Research*, 6(1): 111-120.
- Smith, E.R., 1988. *Case Histories of Corps Breakwater and Jetty Structures*. Technical Report REMR-CO-3. Coastal Engineering Research Center, Dept. of the Army, Waterways Experiment Station, Corps of Engineers, Vicksburg, Mississippi.
- Stafford, D. B., 1971. *An aerial photographic technique for beach erosion surveys in North Carolina*. CERC Tech Memorandum No 36, 115p.
- Stauble, D.K., Garcia, A.W., Kraus, N.C., Grosskopf, W.G., and Bass, G.P., 1993. Beach Nourishment Project Response and Design Evaluation: Ocean City, Maryland; Report 1 - 1988-1992. Technical Report CERC-93-13.
- Swift D.J.P. and M. Field, 1981. Evolution of a classic sand ridge field, Maryland sector, North America inner shelf. *Sedimentology* 28: 462-482.
- U. S. Army Corps of Engineers, Philadelphia District, 1996. Rehoboth Beach/Dewey Beach Interim Feasibility Study: Final Feasibility Report and Final Environmental Impact Statement. U.S. Army Corps of Engineers, Philadelphia, Pennsylvania, 146pp. and appendices A-G.
- Valverde, H.R., A.C. Trembanis, and O.H. Pilkey, 1999. Summary of beach nourishment episodes on the U.S. East Coast barrier islands. *J. Coast. Res.* 15(4): 1100-1118.
- Wells, D. V., 1994. Non-Energy Resources and Shallow Geological Framework of the Inner Continental Margin off Ocean City, Maryland. Coastal and Estuarine Geology Open File Report No. 16, Maryland Geological Survey, Baltimore.



# APPENDIX 1

## Dewey Beach regression analysis results





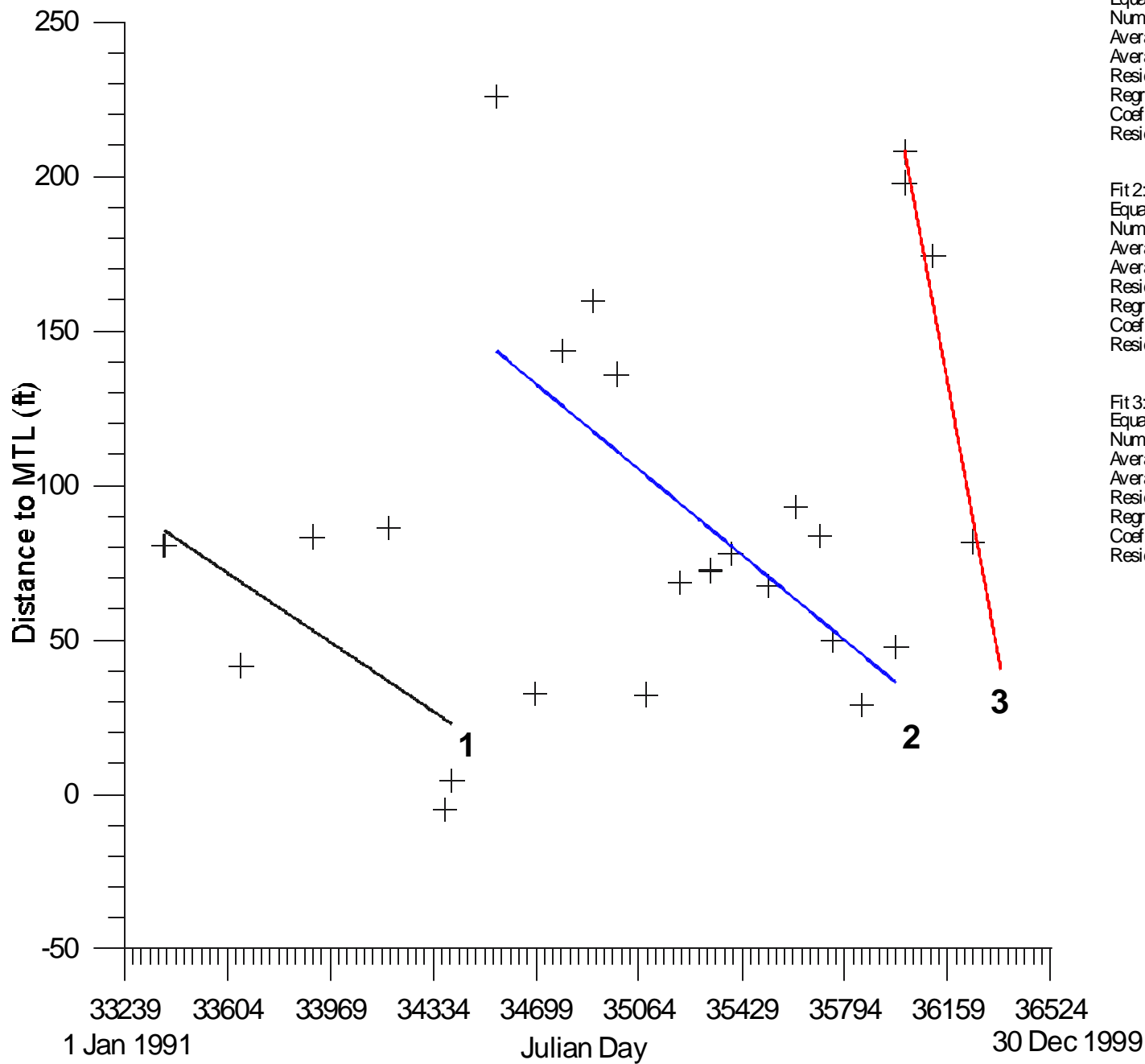
Fit Results

Fit 1: Linear 1991-1994  
 Equation  $Y = -0.03832196554 * X + 1340.97898$   
 Number of data points used = 7  
 Average X = 33978.3  
 Average Y = 38.8643  
 Residual sum of squares = 11568.7  
 Regression sum of squares = 1241  
 Coef of determination, R-squared = 0.0968792  
 Residual mean square, sigma-hat-sq d = 2313.75

Fit 2: Linear 1994-1998  
 Equation  $Y = -0.08514258571 * X + 3090.696809$   
 Number of data points used = 14  
 Average X = 35289.7  
 Average Y = 86.0393  
 Residual sum of squares = 16582.4  
 Regression sum of squares = 20140.8  
 Coef of determination, R-squared = 0.548449  
 Residual mean square, sigma-hat-sq d = 1381.87

Fit 3: Linear 1998-1999  
 Equation  $Y = -0.3949489617 * X + 14419.89925$   
 Number of data points used = 5  
 Average X = 36144.4  
 Average Y = 144.706  
 Residual sum of squares = 1310.83  
 Regression sum of squares = 14217.6  
 Coef of determination, R-squared = 0.915585  
 Residual mean square, sigma-hat-sq d = 436.942

**Dewey  
Profile 100**



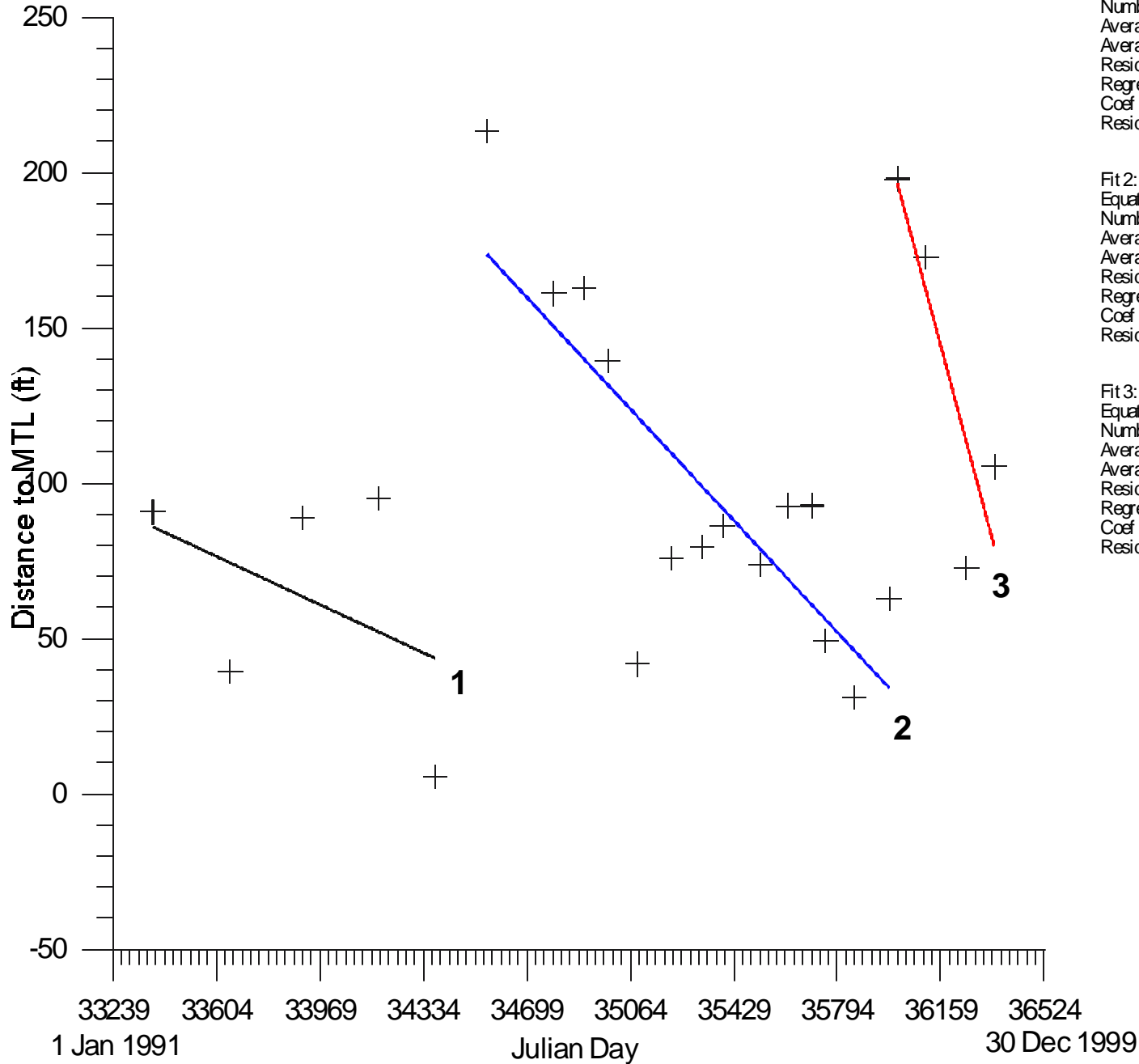
Fit Results

Fit 1: Linear 1991-1994  
 Equation  $Y = -0.06136329187 * X + 2133.745718$   
 Number of data points used = 6  
 Average X = 33982  
 Average Y = 48.4983  
 Residual sum of squares = 5332.81  
 Regression sum of squares = 3179.76  
 Coef of determination, R-squared = 0.373537  
 Residual mean square, sigma-hat-sq d = 1333.2

Fit 2: Linear 1994-1998  
 Equation  $Y = -0.07573638731 * X + 2760.812286$   
 Number of data points used = 15  
 Average X = 35291.6  
 Average Y = 87.954  
 Residual sum of squares = 27538.9  
 Regression sum of squares = 15940.8  
 Coef of determination, R-squared = 0.366626  
 Residual mean square, sigma-hat-sq d = 2118.38

Fit 3: Linear 1998-1999  
 Equation  $Y = -0.2820025969 * X + 10357.17293$   
 Number of data points used = 3  
 Average X = 36041.3  
 Average Y = 193.423  
 Residual sum of squares = 62.3253  
 Regression sum of squares = 530.806  
 Coef of determination, R-squared = 0.894922  
 Residual mean square, sigma-hat-sq d = 62.3253

**Dewey  
 Profile 105**



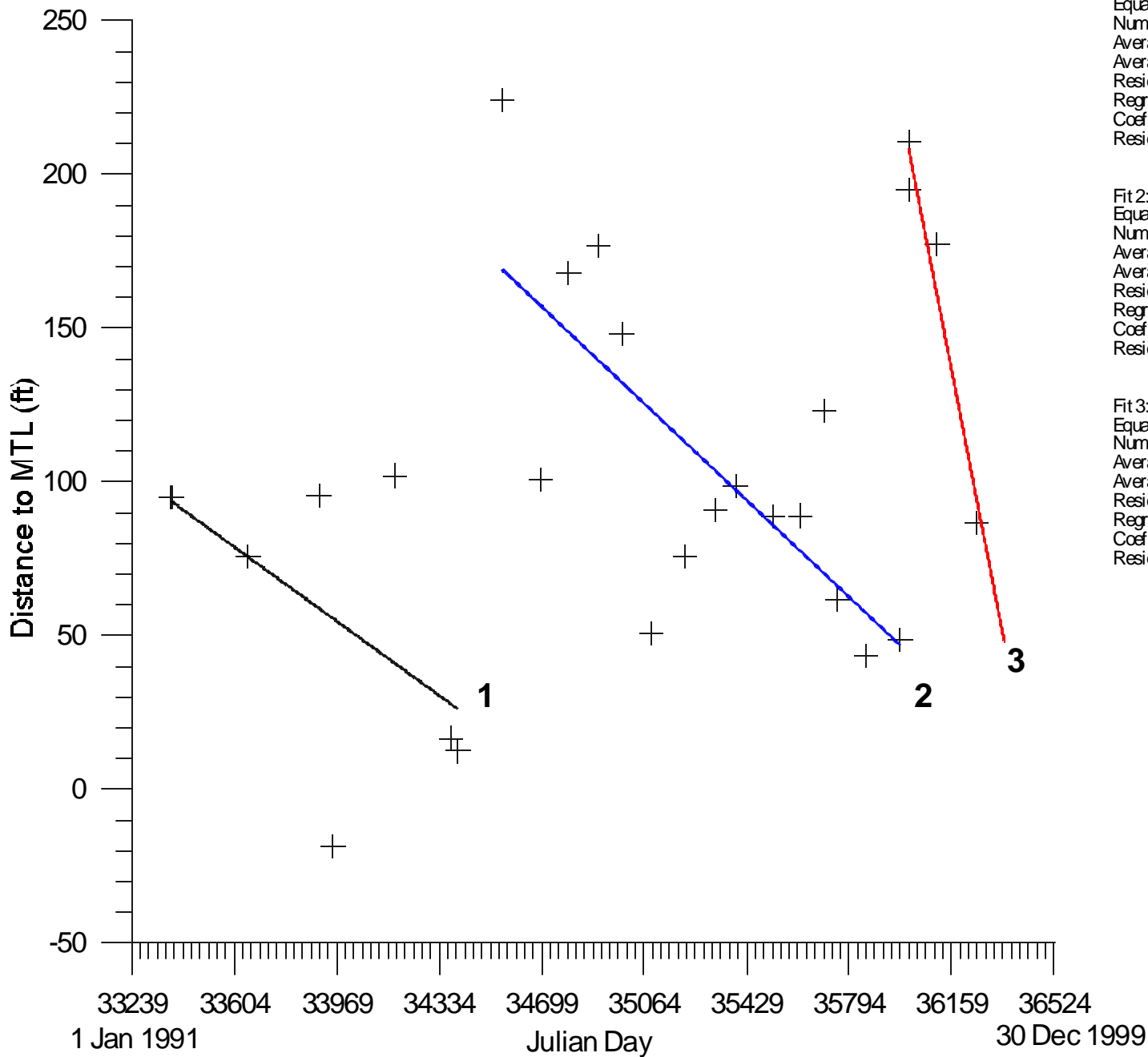
Fit Results

Fit 1: Linear 1991-1994  
 Equation  $Y = -0.04248044283 * X + 1503.944547$   
 Number of data points used = 5  
 Average X = 33898.2  
 Average Y = 63.934  
 Residual sum of squares = 5197.04  
 Regression sum of squares = 1143.72  
 Coef of determination, R-squared = 0.180376  
 Residual mean square, sigma-hat-sq d = 1732.35

Fit 2: Linear 1994-1998  
 Equation  $Y = -0.09839249662 * X + 3573.942274$   
 Number of data points used = 14  
 Average X = 35334.2  
 Average Y = 97.3207  
 Residual sum of squares = 12879.4  
 Regression sum of squares = 23212.5  
 Coef of determination, R-squared = 0.64315  
 Residual mean square, sigma-hat-sq d = 1073.28

Fit 3: Linear 1998-1999  
 Equation  $Y = -0.3419366914 * X + 12508.47255$   
 Number of data points used = 5  
 Average X = 36144.4  
 Average Y = 149.376  
 Residual sum of squares = 2428.55  
 Regression sum of squares = 10657  
 Coef of determination, R-squared = 0.81441  
 Residual mean square, sigma-hat-sq d = 809.517

**Dewey  
Profile 110**



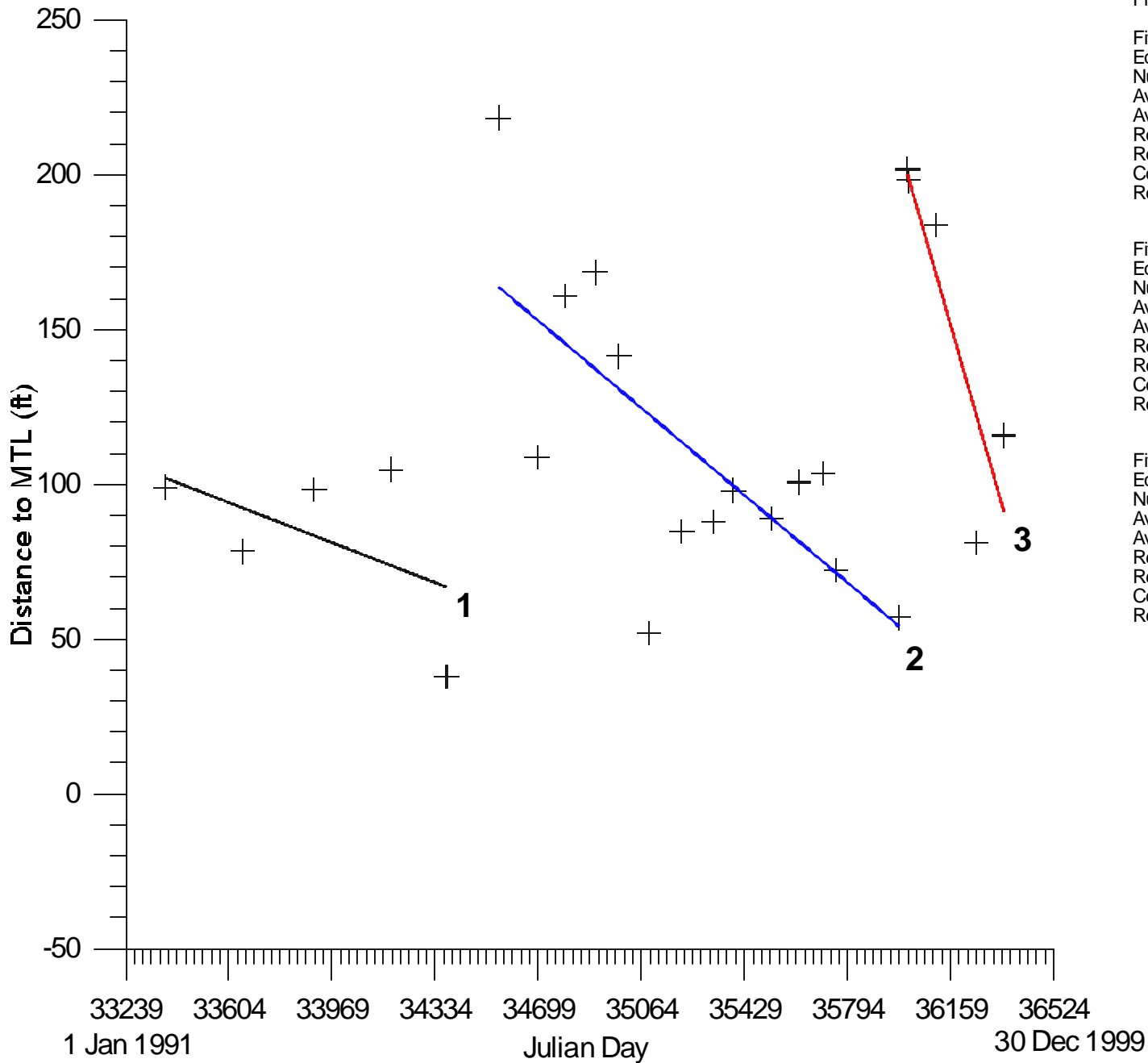
Fit Results

Fit 1: Linear 1991-1994  
 Equation  $Y = -0.06617705462 * X + 2302.655727$   
 Number of data points used = 7  
 Average X = 33978.3  
 Average Y = 54.0729  
 Residual sum of squares = 10884.2  
 Regression sum of squares = 3700.75  
 Coef of determination, R-squared = 0.253738  
 Residual mean square, sigma-hat-sq d = 2176.83

Fit 2: Linear 1994-1998  
 Equation  $Y = -0.08625917913 * X + 3150.124446$   
 Number of data points used = 15  
 Average X = 35291.6  
 Average Y = 105.9  
 Residual sum of squares = 18224.8  
 Regression sum of squares = 20678.1  
 Coef of determination, R-squared = 0.531532  
 Residual mean square, sigma-hat-sq d = 1401.9

Fit 3: Linear 1998-1999  
 Equation  $Y = -0.4707844957 * X + 17159.6477$   
 Number of data points used = 4  
 Average X = 36093.5  
 Average Y = 167.388  
 Residual sum of squares = 537.088  
 Regression sum of squares = 8717.25  
 Coef of determination, R-squared = 0.941964  
 Residual mean square, sigma-hat-sq d = 268.544

**Dewey  
Profile 115**



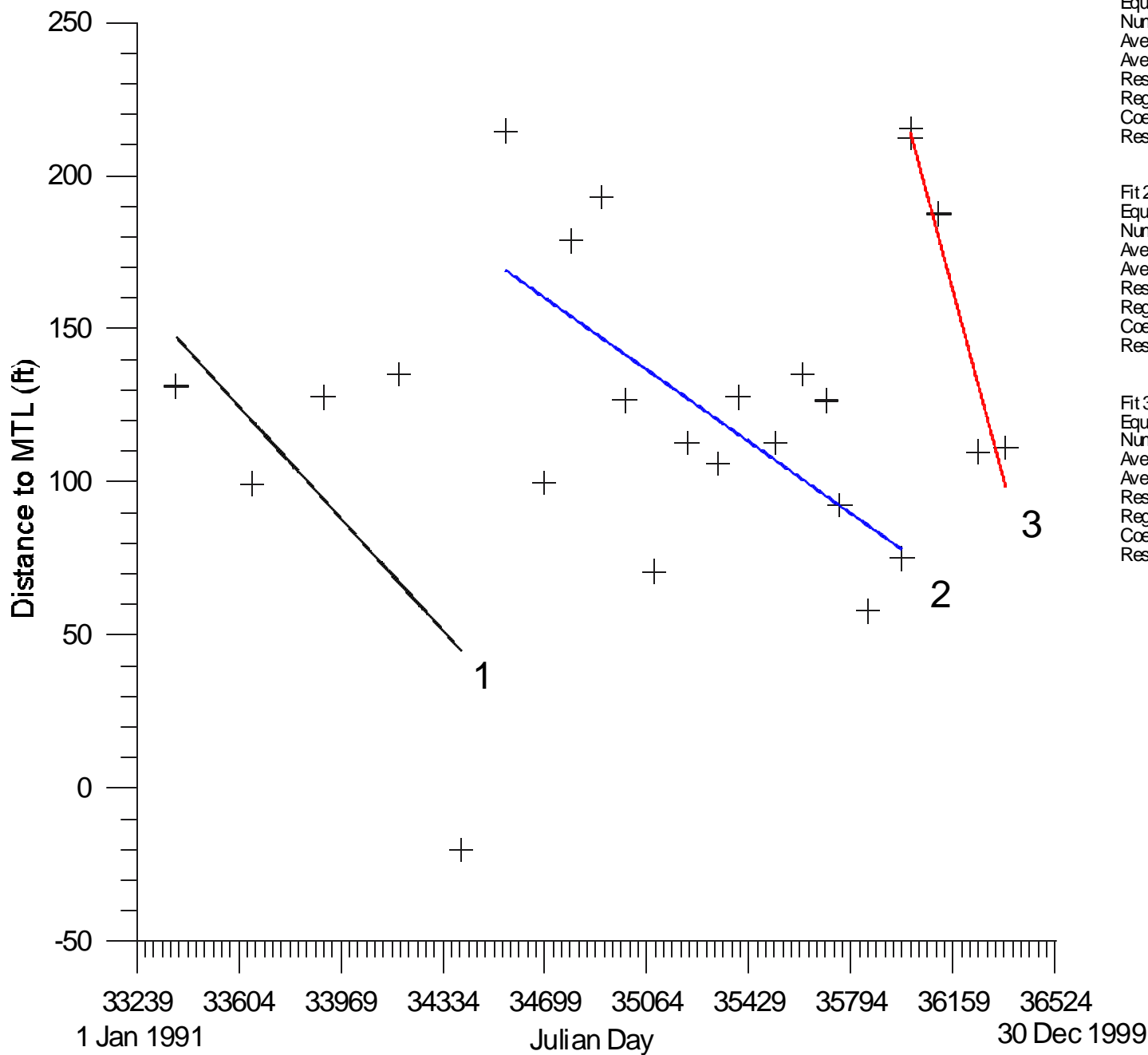
Fit Results

Fit 1: Linear 1991-1994  
 Equation  $Y = -0.0353747593 * X + 1282.794666$   
 Number of data points used = 5  
 Average X = 33898.2  
 Average Y = 83.654  
 Residual sum of squares = 2211.64  
 Regression sum of squares = 793.099  
 Coef of determination, R-squared = 0.26395  
 Residual mean square, sigma-hat-sq'd = 737.212

Fit 2: Linear 1994-1998  
 Equation  $Y = -0.07727811391 * X + 2834.353004$   
 Number of data points used = 14  
 Average X = 35251.5  
 Average Y = 110.184  
 Residual sum of squares = 13558.1  
 Regression sum of squares = 14579.8  
 Coef of determination, R-squared = 0.518155  
 Residual mean square, sigma-hat-sq'd = 1129.84

Fit 3: Linear 1998-1999  
 Equation  $Y = -0.3192940211 * X + 11696.76882$   
 Number of data points used = 5  
 Average X = 36144.4  
 Average Y = 156.078  
 Residual sum of squares = 2574.15  
 Regression sum of squares = 9292.34  
 Coef of determination, R-squared = 0.783074  
 Residual mean square, sigma-hat-sq'd = 858.051

**Dewey  
 Profile 120**



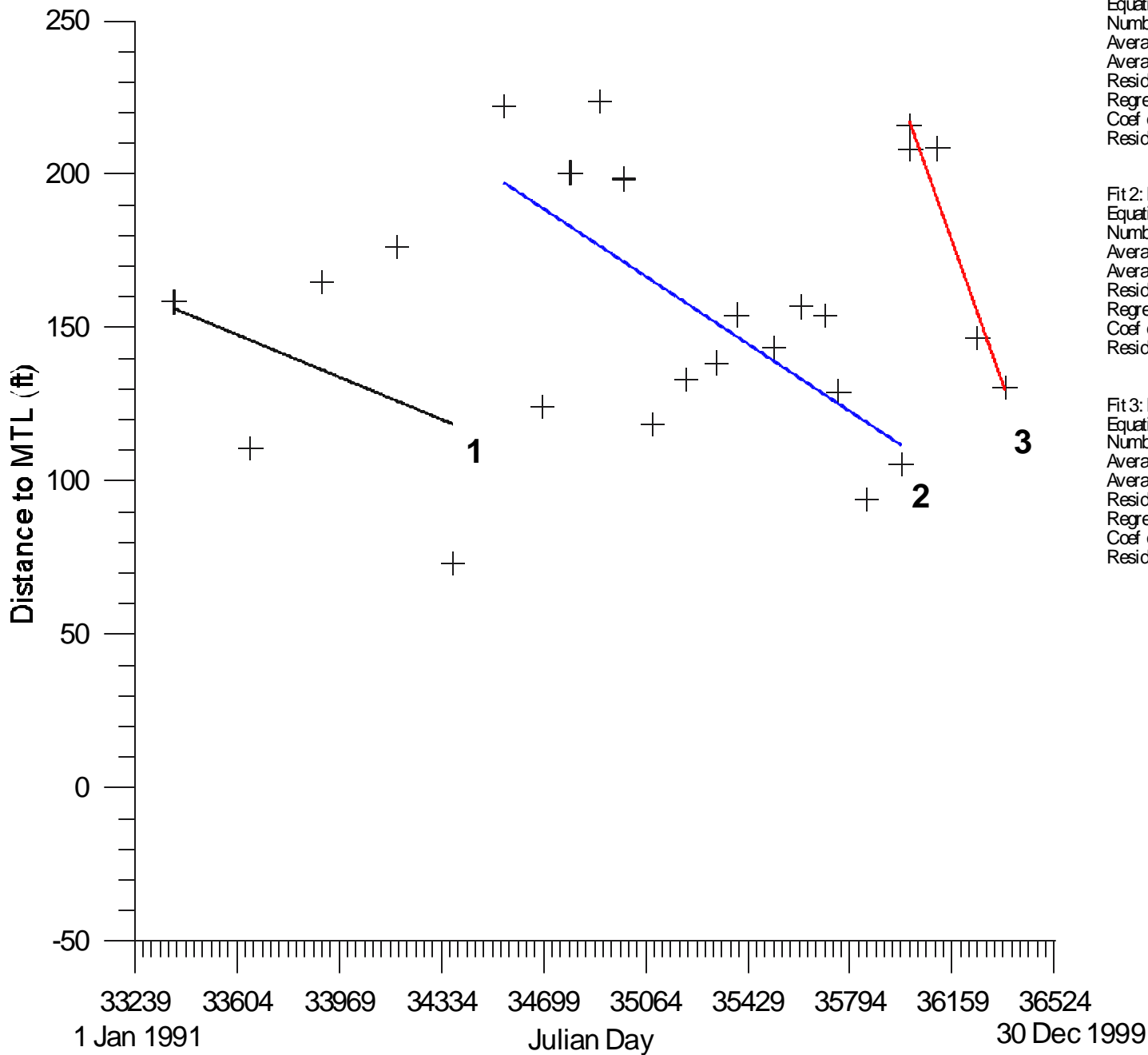
Fit Results

Fit 1: Linear 1991-1994  
 Equation  $Y = -0.1003954077 * X + 3498.455665$   
 Number of data points used = 5  
 Average X = 33903.4  
 Average Y = 94.71  
 Residual sum of squares = 10582.2  
 Regression sum of squares = 6643.4  
 Coef of determination, R-squared = 0.38567  
 Residual mean square, sigma-hat-sq d = 3527.41

Fit 2: Linear 1994-1998  
 Equation  $Y = -0.06424379819 * X + 2389.237762$   
 Number of data points used = 15  
 Average X = 35291.6  
 Average Y = 121.971  
 Residual sum of squares = 16365.6  
 Regression sum of squares = 11470  
 Coef of determination, R-squared = 0.412062  
 Residual mean square, sigma-hat-sq d = 1258.89

Fit 3: Linear 1998-1999  
 Equation  $Y = -0.3394543771 * X + 12436.69279$   
 Number of data points used = 5  
 Average X = 36144.4  
 Average Y = 167.318  
 Residual sum of squares = 711.042  
 Regression sum of squares = 10502.8  
 Coef of determination, R-squared = 0.936593  
 Residual mean square, sigma-hat-sq d = 237.014

**Dewey  
Profile 130**



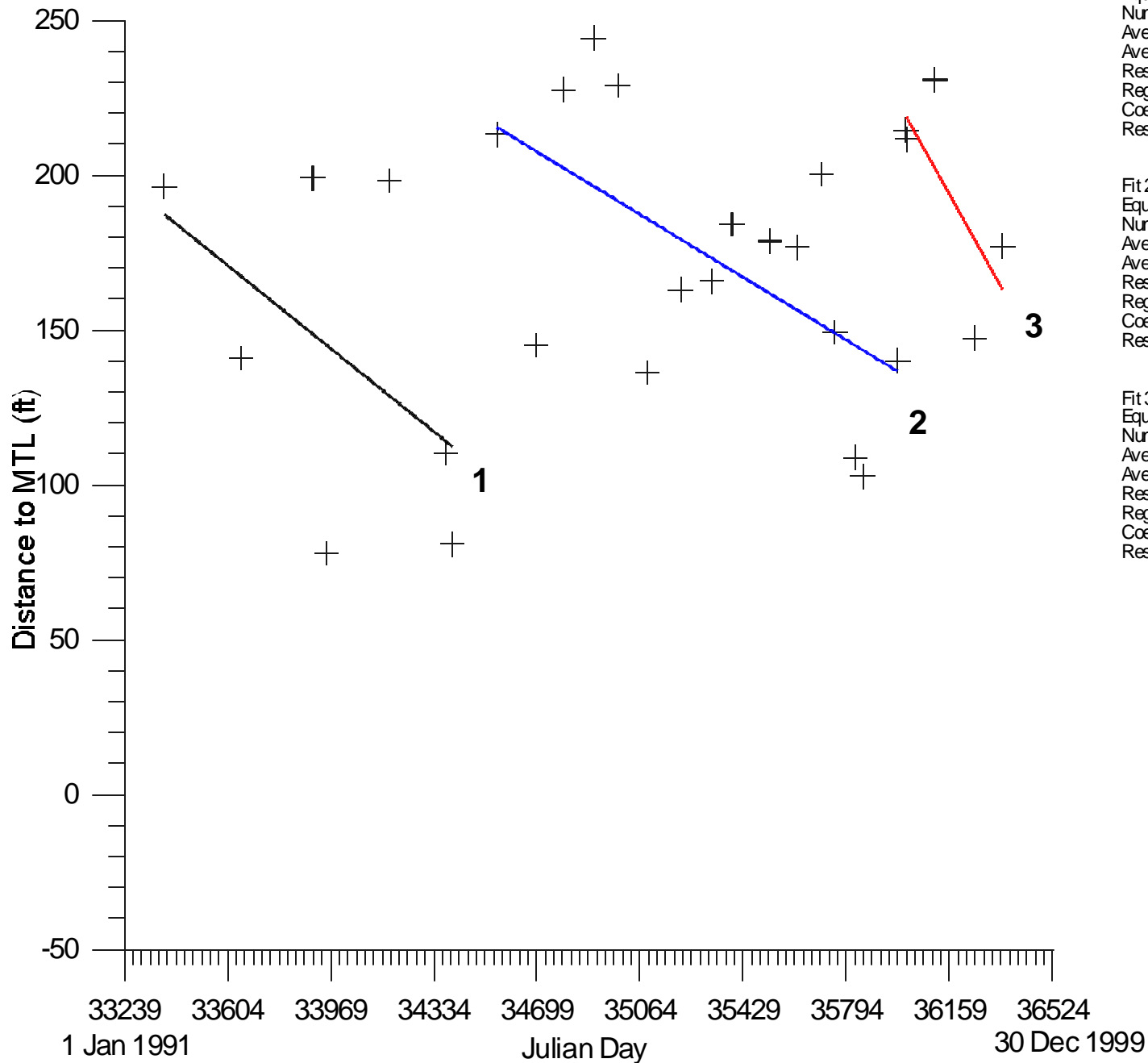
Fit Results

Fit 1: Linear 1991-1994  
 Equation  $Y = -0.0378067786 * X + 1418.197742$   
 Number of data points used = 5  
 Average X = 33898.2  
 Average Y = 136.616  
 Residual sum of squares = 6657.27  
 Regression sum of squares = 905.899  
 Coef of determination, R-squared = 0.119778  
 Residual mean square, sigma-hat-sq/d = 2219.09

Fit 2: Linear 1994-1998  
 Equation  $Y = -0.0603099876 * X + 2281.457019$   
 Number of data points used = 15  
 Average X = 35291.6  
 Average Y = 153.021  
 Residual sum of squares = 13034.8  
 Regression sum of squares = 10108.3  
 Coef of determination, R-squared = 0.436774  
 Residual mean square, sigma-hat-sq/d = 1002.68

Fit 3: Linear 1998-1999  
 Equation  $Y = -0.2616474282 * X + 9638.503951$   
 Number of data points used = 4  
 Average X = 36093.5  
 Average Y = 194.732  
 Residual sum of squares = 429.354  
 Regression sum of squares = 2692.58  
 Coef of determination, R-squared = 0.862472  
 Residual mean square, sigma-hat-sq/d = 214.677

**Dewey  
 Profile 135**



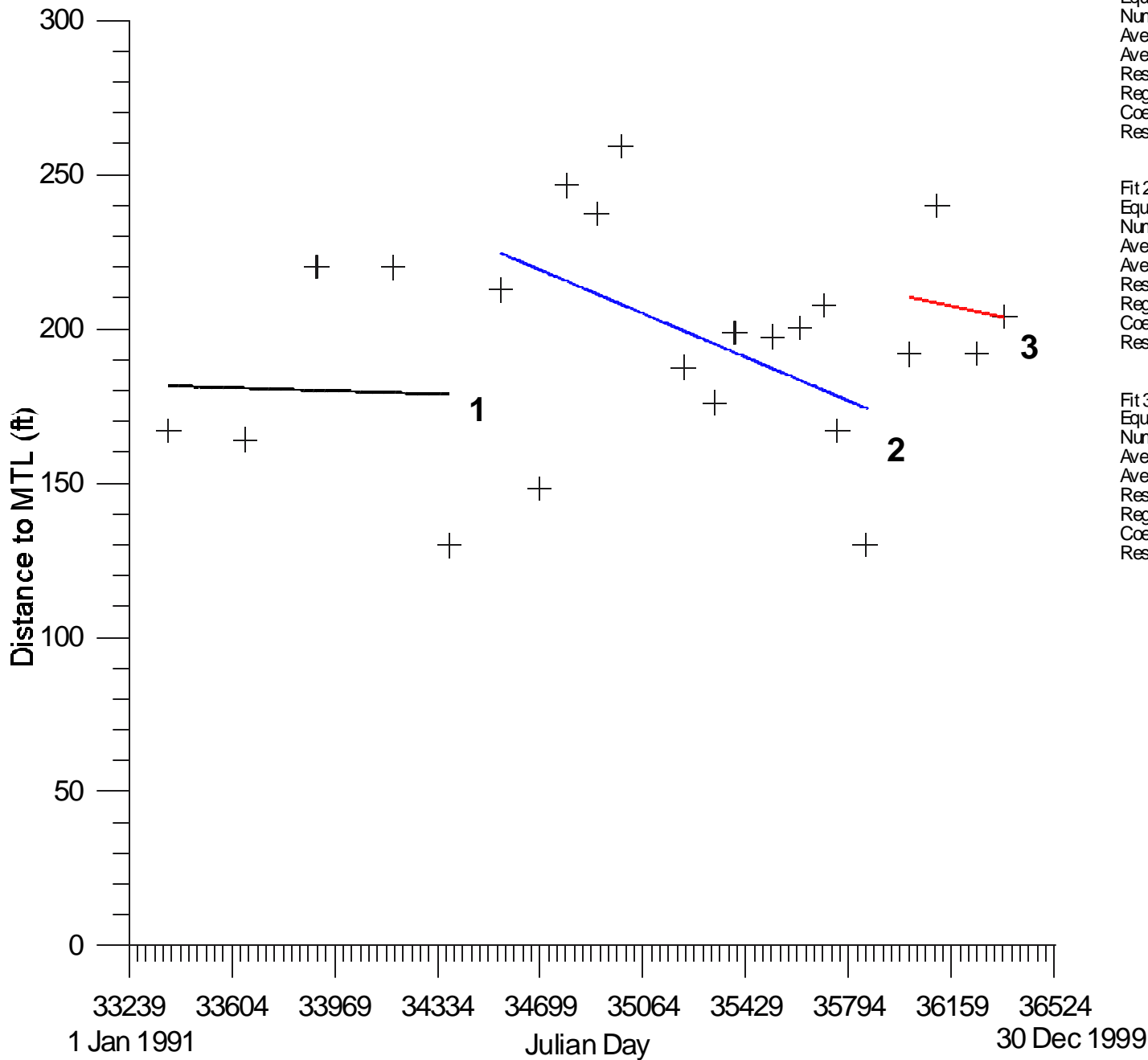
Fit Results

Fit 1: Linear 1991-1994  
 Equation  $Y = -0.07353263802 * X + 2641.870127$   
 Number of data points used = 7  
 Average X = 33978.3  
 Average Y = 143.367  
 Residual sum of squares = 13664.1  
 Regression sum of squares = 4569.15  
 Coef of determination, R-squared = 0.250594  
 Residual mean square, sigma-hat-sq d = 2732.82

Fit 2: Linear 1994-1998  
 Equation  $Y = -0.05554241722 * X + 2134.856581$   
 Number of data points used = 16  
 Average X = 35325.1  
 Average Y = 172.814  
 Residual sum of squares = 17276.9  
 Regression sum of squares = 9405.48  
 Coef of determination, R-squared = 0.352498  
 Residual mean square, sigma-hat-sq d = 1234.06

Fit 3: Linear 1998-1999  
 Equation  $Y = -0.735 * X + 26678.94$   
 Number of data points used = 2  
 Average X = 36008  
 Average Y = 213.06  
 Residual sum of squares = 1.32349E-023  
 Regression sum of squares = 4.3218  
 Coef of determination, R-squared = 1  
 Residual mean square, sigma-hat-sq d = 0

**Dewey  
Profile 140**



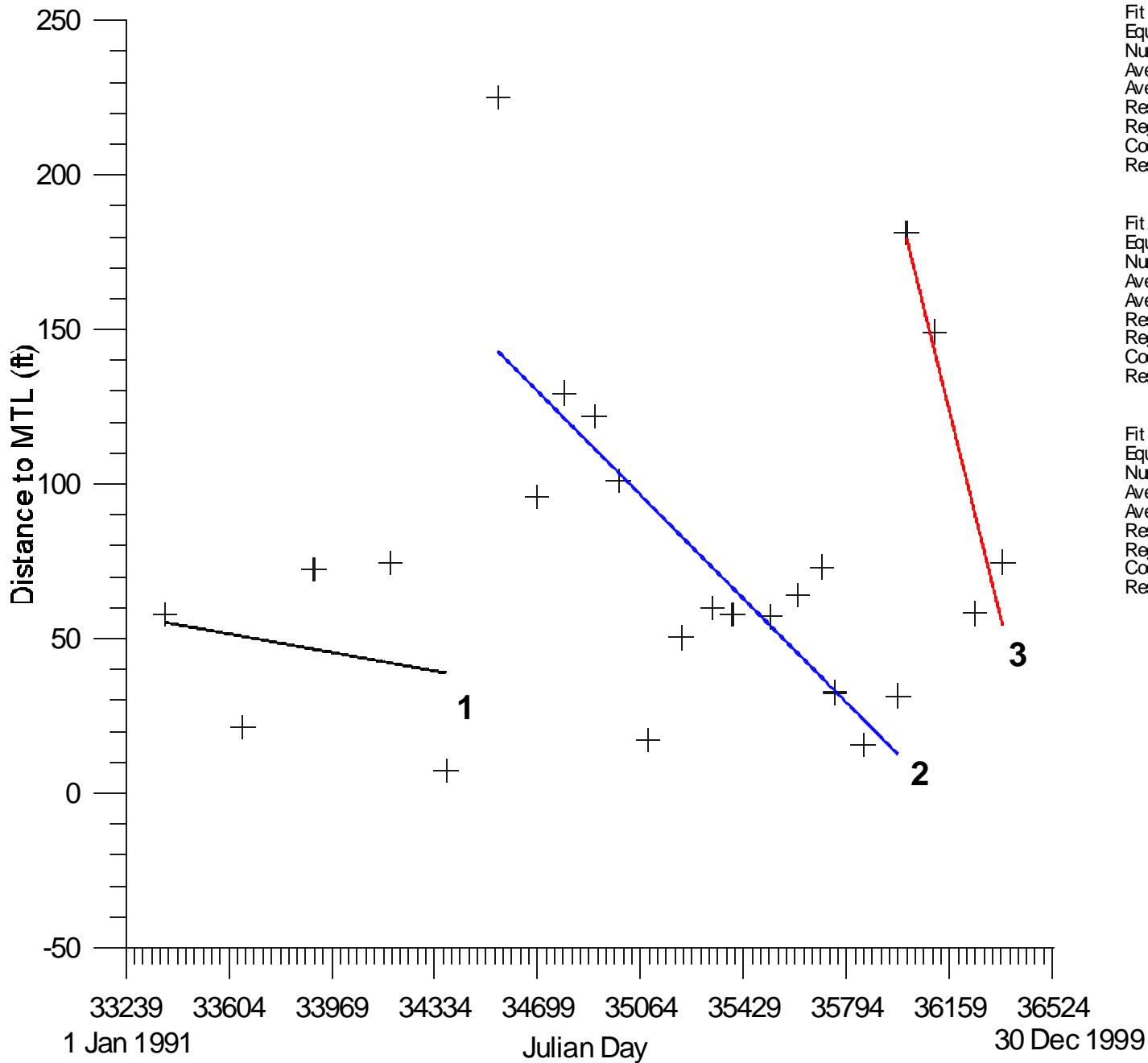
#### Fit Results

Fit 1: Linear 1991-1994  
 Equation  $Y = -0.002786080657 * X + 274.5231193$   
 Number of data points used = 5  
 Average X = 33898.2  
 Average Y = 180.08  
 Residual sum of squares = 6140.51  
 Regression sum of squares = 4.91958  
 Coef of determination, R-squared = 0.000800527  
 Residual mean square, sigma-hat-sq d = 2046.84

Fit 2: Linear 1994-1998  
 Equation  $Y = -0.03875425808 * X + 1563.799058$   
 Number of data points used = 13  
 Average X = 35254.4  
 Average Y = 197.542  
 Residual sum of squares = 13212.8  
 Regression sum of squares = 3380.24  
 Coef of determination, R-squared = 0.203715  
 Residual mean square, sigma-hat-sq d = 1201.16

Fit 3: Linear 1998-1999  
 Equation  $Y = -0.01953812273 * X + 913.8097423$   
 Number of data points used = 4  
 Average X = 36179  
 Average Y = 206.94  
 Residual sum of squares = 1525.31  
 Regression sum of squares = 25.6543  
 Coef of determination, R-squared = 0.0165409  
 Residual mean square, sigma-hat-sq d = 762.653

## Dewey Profile 145



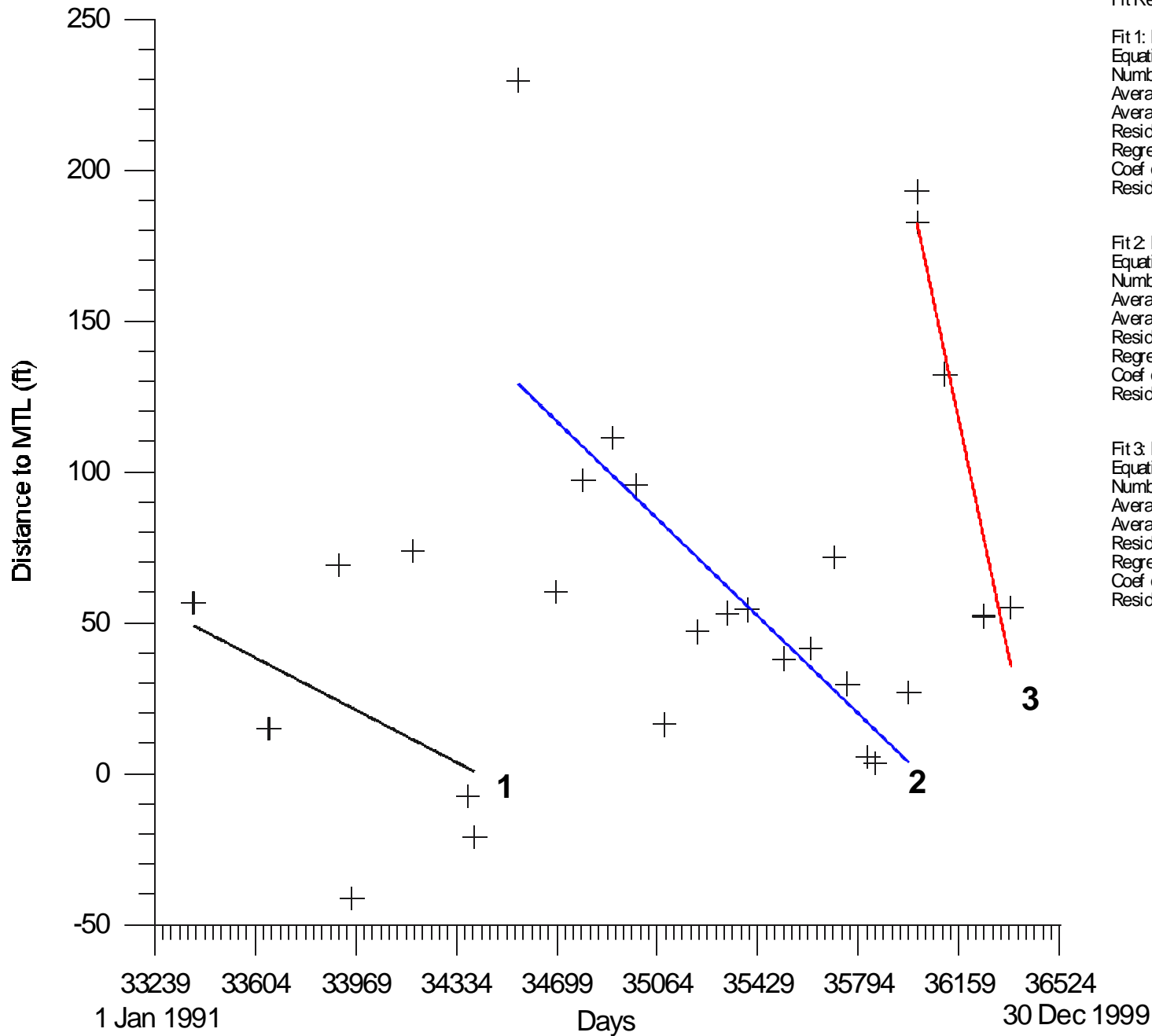
Fit Results

Fit 1: Linear 1991-1994  
 Equation  $Y = -0.01642978008 * X + 603.6672569$   
 Number of data points used = 5  
 Average X = 33898.4  
 Average Y = 46.724  
 Residual sum of squares = 3591.74  
 Regression sum of squares = 170.95  
 Coef of determination, R-squared = 0.0454328  
 Residual mean square, sigma-hat-sq/d = 1197.25

Fit 2: Linear 1994-1998  
 Equation  $Y = -0.09190342717 * X + 3318.940324$   
 Number of data points used = 15  
 Average X = 35291.6  
 Average Y = 75.5213  
 Residual sum of squares = 17401.9  
 Regression sum of squares = 23472.7  
 Coef of determination, R-squared = 0.574262  
 Residual mean square, sigma-hat-sq/d = 1338.61

Fit 3: Linear 1998-1999  
 Equation  $Y = -0.3677220145 * X + 13420.00758$   
 Number of data points used = 5  
 Average X = 36144.4  
 Average Y = 128.916  
 Residual sum of squares = 1507.05  
 Regression sum of squares = 12324.9  
 Coef of determination, R-squared = 0.891045  
 Residual mean square, sigma-hat-sq/d = 502.35

**Dewey  
 Profile 205**



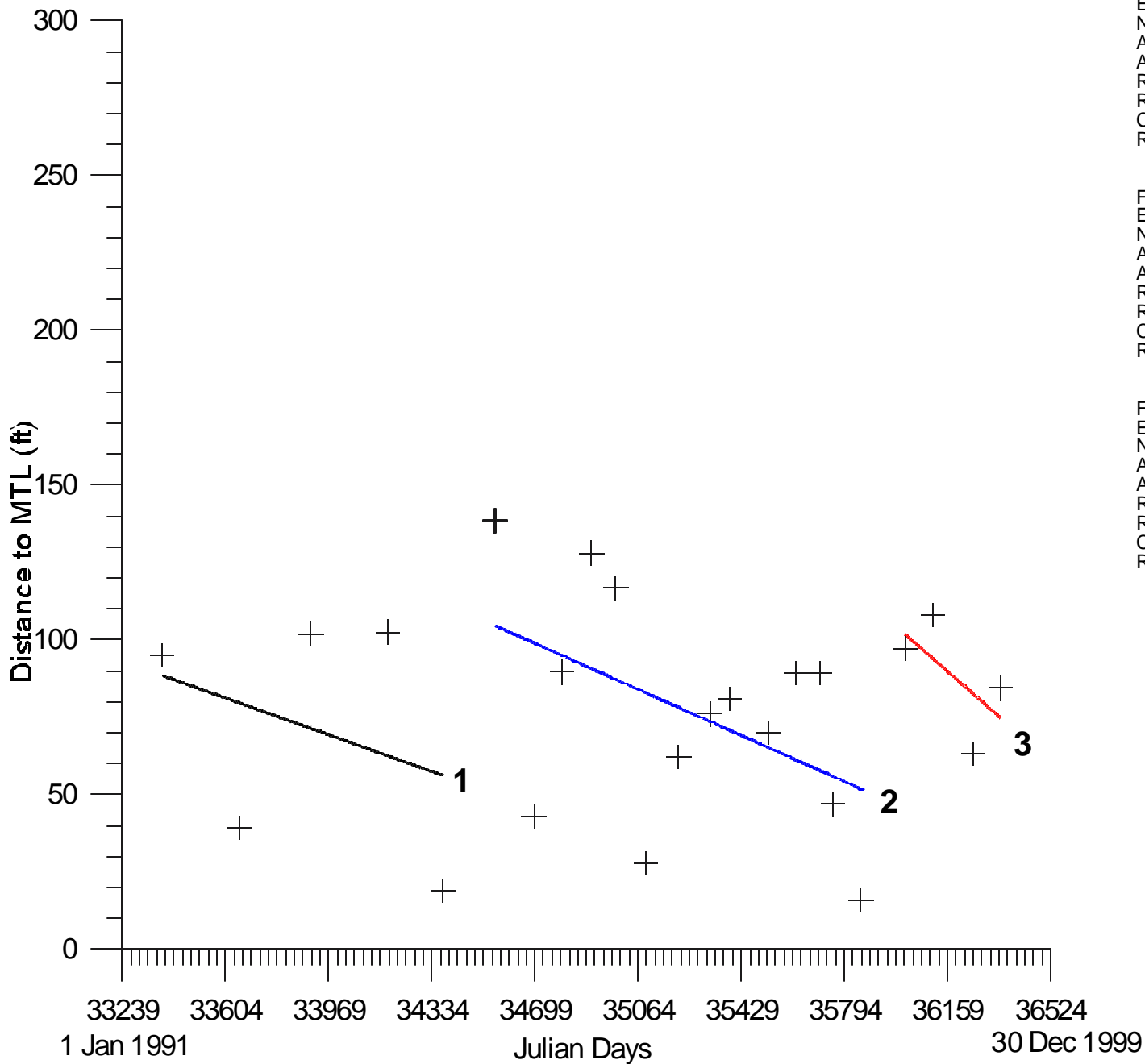
Fit Results

Fit 1: Linear 1991-1994  
 Equation  $Y = -0.04748294111 * X + 1634.091437$   
 Number of data points used = 7  
 Average X = 33978.4  
 Average Y = 20.6957  
 Residual sum of squares = 10953.1  
 Regression sum of squares = 1903.78  
 Coef of determination, R-squared = 0.148075  
 Residual mean square, sigma-hat-sq d = 2190.62

Fit 2: Linear 1994-1998  
 Equation  $Y = -0.0685140609 * X + 3188.110266$   
 Number of data points used = 16  
 Average X = 35325.1  
 Average Y = 61.34  
 Residual sum of squares = 21511  
 Regression sum of squares = 23886.7  
 Coef of determination, R-squared = 0.526166  
 Residual mean square, sigma-hat-sq d = 1536.5

Fit 3: Linear 1998-1999  
 Equation  $Y = -0.4312834185 * X + 15711.48839$   
 Number of data points used = 5  
 Average X = 36144.4  
 Average Y = 123.008  
 Residual sum of squares = 1183.43  
 Regression sum of squares = 16953.9  
 Coef of determination, R-squared = 0.934751  
 Residual mean square, sigma-hat-sq d = 394.478

**Dewey  
Profile 210**



Fit Results

Fit 1: Linear 1991-1994  
 Equation  $Y = -0.03247997294 * X + 1172.647115$   
 Number of data points used = 5  
 Average X = 33898.4  
 Average Y = 71.628  
 Residual sum of squares = 5571.82  
 Regression sum of squares = 668.092  
 Coef of determination, R-squared = 0.107067  
 Residual mean square, sigma-hat-sq'd = 1857.27

Fit 2: Linear 1994-1998  
 Equation  $Y = -0.0407371152 * X + 1512.394316$   
 Number of data points used = 14  
 Average X = 35242.6  
 Average Y = 76.7107  
 Residual sum of squares = 13128.3  
 Regression sum of squares = 3776.63  
 Coef of determination, R-squared = 0.223404  
 Residual mean square, sigma-hat-sq'd = 1094.02

Fit 3: Linear 1998-1999  
 Equation  $Y = -0.1545231664 * X + 5671.292165$   
 Number of data points used = 3  
 Average X = 36122.7  
 Average Y = 89.5033  
 Residual sum of squares = 399.562  
 Regression sum of squares = 695.374  
 Coef of determination, R-squared = 0.635082  
 Residual mean square, sigma-hat-sq'd = 399.562

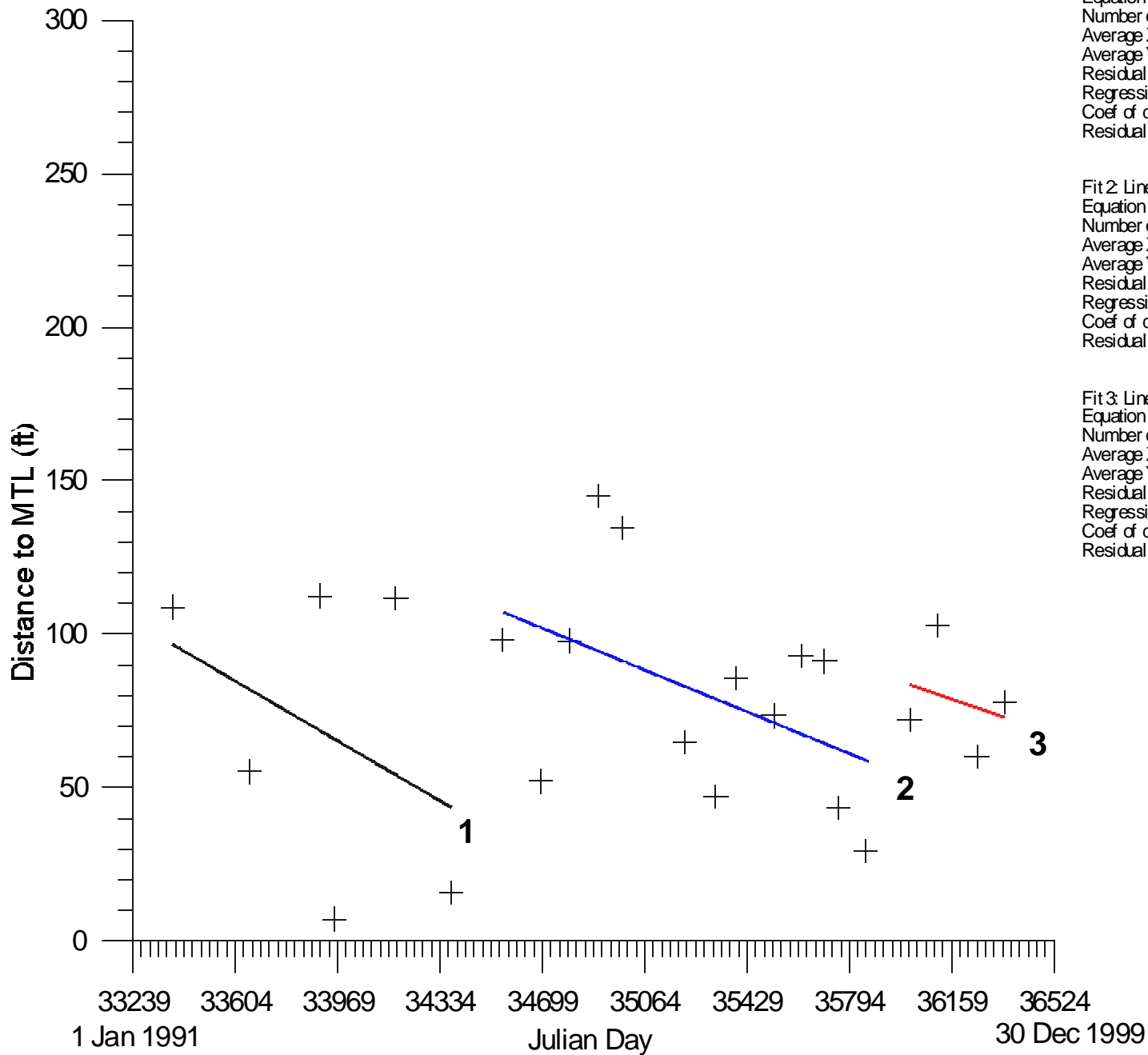
**Dewey  
Profile 225**

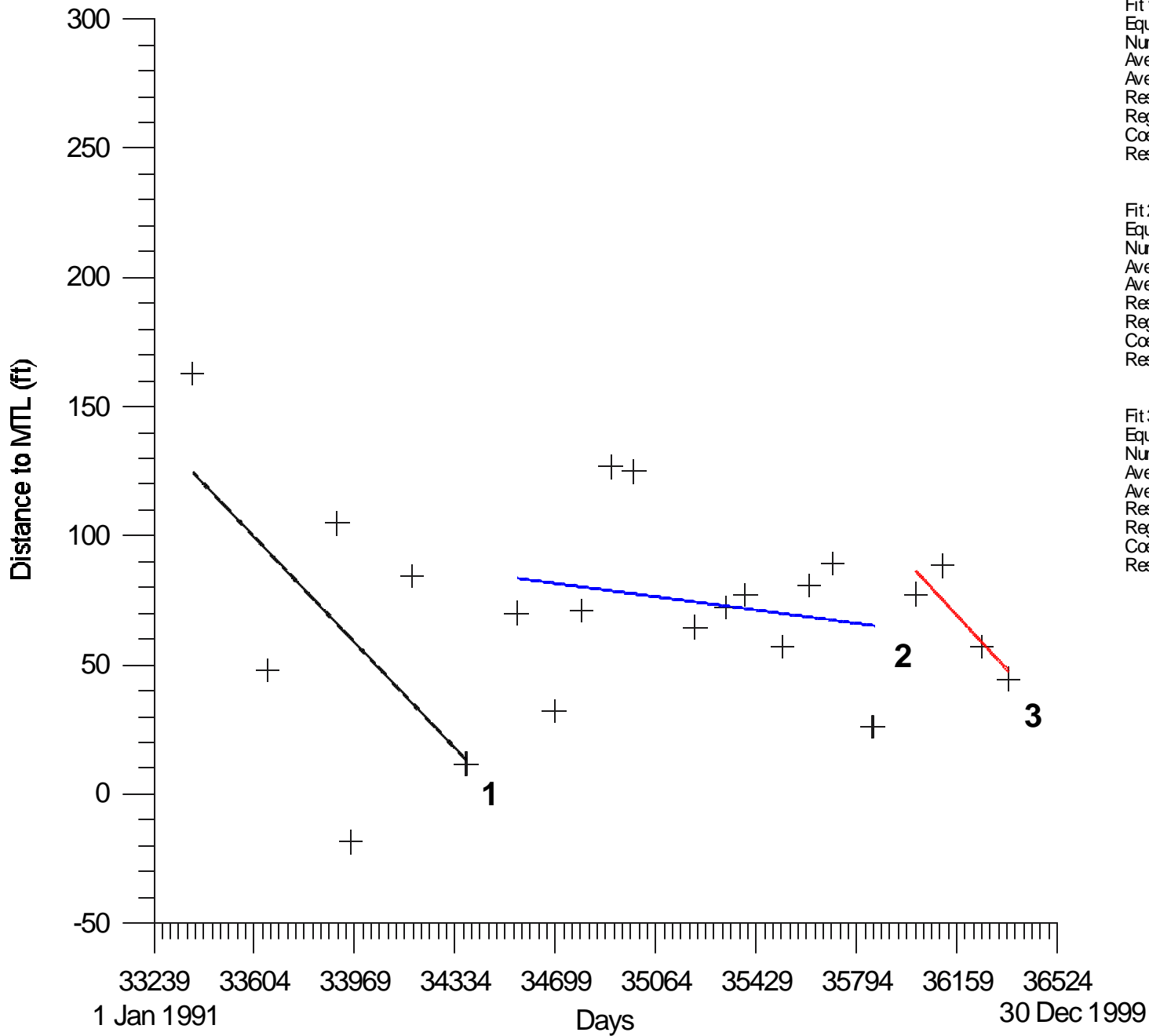
Fit Results

Fit 1: Linear 1991-1994  
Equation  $Y = -0.05343838141 * X + 1880.485303$   
Number of data points used = 6  
Average X = 33908  
Average Y = 68.4967  
Residual sum of squares = 10317.6  
Regression sum of squares = 1816.37  
Coef of determination, R-squared = 0.149692  
Residual mean square, sigma-hat-sq d = 2579.41

Fit 2: Linear 1994-1998  
Equation  $Y = -0.03728635724 * X + 1395.761425$   
Number of data points used = 13  
Average X = 35254.4  
Average Y = 81.2538  
Residual sum of squares = 11037.2  
Regression sum of squares = 3129.02  
Coef of determination, R-squared = 0.220879  
Residual mean square, sigma-hat-sq d = 1003.38

Fit 3: Linear 1998-1999  
Equation  $Y = -0.03154752693 * X + 1219.622977$   
Number of data points used = 4  
Average X = 36179  
Average Y = 78.265  
Residual sum of squares = 914.712  
Regression sum of squares = 66.8845  
Coef of determination, R-squared = 0.0681386  
Residual mean square, sigma-hat-sq d = 457.356





Fit Results

Fit 1: Linear 1991-1994  
 Equation  $Y = -0.1119870987 * X + 3862.785208$   
 Number of data points used = 6  
 Average X = 33908  
 Average Y = 65.5267  
 Residual sum of squares = 13695.8  
 Regression sum of squares = 7976.87  
 Coef of determination, R-squared = 0.368061  
 Residual mean square, sigma-hat-sq d = 3423.96

Fit 2: Linear 1994-1998  
 Equation  $Y = -0.0140890509 * X + 570.4250604$   
 Number of data points used = 12  
 Average X = 35212.8  
 Average Y = 74.3108  
 Residual sum of squares = 9734.82  
 Regression sum of squares = 393.08  
 Coef of determination, R-squared = 0.0388116  
 Residual mean square, sigma-hat-sq d = 973.482

Fit 3: Linear 1998-1999  
 Equation  $Y = -0.093646873 * X + 3457.098111$   
 Number of data points used = 3  
 Average X = 36122.7  
 Average Y = 74.3233  
 Residual sum of squares = 243.998  
 Regression sum of squares = 255.398  
 Coef of determination, R-squared = 0.511414  
 Residual mean square, sigma-hat-sq d = 243.998

**Dewey  
Profile 240**